



**HAL**  
open science

**Response to light stimuli in the marine diatom  
Phaeodactylum tricornutum: Involvement of  
bHLH-PAS proteins in the circadian clock and plastid  
physiology**

Alessandro Manzotti

► **To cite this version:**

Alessandro Manzotti. Response to light stimuli in the marine diatom *Phaeodactylum tricornutum*: Involvement of bHLH-PAS proteins in the circadian clock and plastid physiology. Biochemistry, Molecular Biology. Sorbonne Université, 2022. English. NNT : 2022SORUS232 . tel-04562734v2

**HAL Id: tel-04562734**

**<https://theses.hal.science/tel-04562734v2>**

Submitted on 29 Apr 2024

**HAL** is a multi-disciplinary open access archive for the deposit and dissemination of scientific research documents, whether they are published or not. The documents may come from teaching and research institutions in France or abroad, or from public or private research centers.

L'archive ouverte pluridisciplinaire **HAL**, est destinée au dépôt et à la diffusion de documents scientifiques de niveau recherche, publiés ou non, émanant des établissements d'enseignement et de recherche français ou étrangers, des laboratoires publics ou privés.

Sorbonne Université

Ecole doctorale Complexité du Vivant - ED515

UMR7141 - Biologie du chloroplaste et perception de la lumière chez les micro-algues

Response to light stimuli in the marine diatom  
*Phaeodactylum tricornutum* :  
Involvement of bHLH-PAS proteins  
in the circadian clock and plastid physiology

Par Alessandro Manzotti

Thèse de doctorat de Biologie

Dirigée par Angela Falciatore

Date de soutenance : 28 avril 2022

Devant un jury composé de :

Prof. Maria Mittag, rapportrice

Friedrich Schiller University, Jena

Prof. Wim Vyverman, rapporteur

Ghent University

Dr. François-Yves Bouget, examinateur

Laboratoire d'Océanographie Microbienne, CNRS, Sorbonne Université

Dr. Alessandra Rogato, examinatrice

Institute of Bioscience and BioResources, Naples, CNR

Dr. Angela Falciatore, directrice de recherche, directrice de thèse

Institut de Biologie Physico-Chimique, CNRS, Sorbonne Université

Dr. Jean-Pierre Bouly, maître de conférences, co-encadrant de thèse

Institut de Biologie Physico-Chimique, CNRS, Sorbonne Université

Membre invitée:

Prof. Eva Farré

Michigan State University









# Remerciements

Tant de personnes ont rendu cette thèse possible et je les remercie toutes du fond du cœur.

Merci à Angela, de m'avoir accueilli dans ton laboratoire il y a plus de quatre ans, alors que j'étais encore un étudiant en master perdu dans cette grande ville. Merci de m'avoir appris la valeur de la ténacité, de la persévérance et, pourquoi pas, même de l'entêtement. Merci pour toute l'énergie que tu mets dans ce que tu fais. En d'autres termes, merci de m'avoir appris l'importance d'avoir la *capa tosta*.

Merci à Jean-Pierre pour les longues discussions scientifiques et non scientifiques, au labo comme au pub. Merci pour ton ubiquité et ta capacité à toujours gérer tous les problèmes et imprévus avec la maîtrise d'un jongleur, merci pour tous les moments de défoulement et toutes les fois où tu as su me faire voir les difficultés sous le bon angle. Merci d'être un ami avant même d'être un collègue. Merci pour toutes les clopes, les bières, les whisky... bref, merci pour tout.

Thank of course to all the people that are part of my thesis committee: Maria Mittag, Wim Vyverman, François-Yves Bouget, Eva Farré and Alessandra Rogato, I hope you will enjoy the reading.

Merci à Marianne et Soizic, pour les innombrables fois où vous m'avez aidé et dépanné et pour m'avoir appris tant de choses sur la vie de laboratoire. Votre professionnalisme a été un exemple à suivre et m'a permis de grandir énormément. Merci à Carole, qui a commencé cette aventure du doctorat avec moi et qui la termine avec moi. Merci pour toutes les chansonnettes sifflées dans les couloirs et qui rentrent dans la tête pour ne plus en sortir, merci pour les memes, les rires et ta capacité à tout affronter avec une sérieuse légèreté.

Merci à tous les autres membres de l'UMR7141, un formidable groupe de chercheur.euse.s qui fait vivre ce laboratoire historique. Ce fut un plaisir et une joie de travailler avec vous.

Merci à Anaëlle, Anäis, Aurélian, Bashung, Camila, Coline, Dorian, Eleanor, Julie, Léa, Lorenzo, Noa, Tania... merci à tou.te.s les LUPAmi.e.s de m'avoir accueilli dans cette clique de bobos-babos-écolos parisien.ne.s. Merci d'avoir fait de Paris ma deuxième maison, merci d'être devenu.e.s ma deuxième famille (une famille un peu dysfonctionnelle, c'est vrai, mais sinon, où est le plaisir ?).

Grazie ai Ritals, ad Antonio, Arianna, Claudio, Eleonora, Flaminia, Matilde, Paolo, Seed e Stefano, gruppo matto e disperatissimo di italianø passatø per Parigi ad un momento o ad un altro. Grazie per tutte le volte che abbiamo riso e sdrammatizzato sulle nostre vite da dottorandi sull'orlo di una crisi di nervi. Vi aspetto dall'altra parte del varco, dai che manca poco.

Grazie a Marco e Luca, fratelli. Grazie per tutte le avventure, piccole e grandi. Grazie per le discussioni serissime sulle questioni più stupide e le discussioni stupidissime sulle questioni più serie. Grazie per avermi insegnato come elementi tanto diversi possono creare legami indissolubili. Grazie per aver dimostrato come si può cambiare ogni giorno senza cambiare mai davvero.

E in fine grazie a mia madre per tutti gli infiniti sacrifici che ha fatto e che continua a fare per me, anche se questo vuol dire avermi sempre lontano da casa. Sei la persona più forte e inarrestabile che conosca.

Enjoy the reading

Bonne lecture

Buona lettura

# Table of contents

<b>Chapter I: Introduction</b>	p.3
I.1 The life of phytoplankton	p.4
I.2 The kaleidoscopic world of diatoms	p.7
I.2.a General introduction on diatoms	p.7
I.2.b Phylogenesis and evolution	p.10
I.2.c Toolkit box for molecular biology in diatoms	p.13
I.2.d <i>Phaeodactylum tricornutum</i> as a diatom model	p.15
I.3 Light in the life of diatoms	p.17
I.3.a Light as an energy source: the photosynthetic apparatus in diatoms	p.17
I.3.b Photoacclimation and photoprotective mechanisms	p.21
I.3.c Light as a source of information: photo-perception	p.23
I.3.d Cell cycle progression and regulation in diatoms	p.25
I.4 Biological clocks	p.31
I.4.a Biological clocks: principles and characteristics	p.31
I.4.b Biological clocks: diversity and commonalities	p.34
I.4.c Translation Independent Oscillators: above and beyond TTFLs	p.41
I.4.d Circadian rhythmicity in Stramenopila: an overview	p.44
I.5 bHLH-PAS transcription factors in diatoms	p.45
Aims of the thesis	p.50
<b>Chapter II: The circadian clock of diatoms</b>	p.83
<b>Chapter II.a: Rhythms and clocks in marine organisms</b>	p.87
Abstract	p.88
1. Cycles of the sun and moon cause a multitude of biological rhythms	p.89
2. Other places, other rhythms: The oceans harbor multiple and diverse habitats with very different properties from land	p.91
3. Rhythms in the life of marine algae	p.94
Algal models for the elucidation of marine time-keeping mechanisms	p.96
4. Animal models for marine chronobiology	p.98
Vertical migrations in the pelagic zone	p.99
Rhythms in the deep sea	p.100
A plastic clock to time daily and tidal rhythms	p.101
Timing reproduction with an inner calendar	p.104
5. Marine rhythms and clocks under climate change	p.107
Present-day climate effects on marine rhythmicity	p.108
Temperature changes	p.108
pH changes	p.109
Oxygen concentration changes	p.109
Adaptability of rhythms and clocks to future ocean conditions	p.110
Phenotypic adaptive capacity	p.111
Evolutionary adaptation of clock and rhythms	p.111
Interspecies mismatches	p.112
6. Conclusions and outlook	p.113

Glossary: Rhythms and clocks in marine organisms	p.114
Acknowledgements	p.116
Bibliography	p.118
Supplementary Material	p.139
Supplementary Bibliography	p.140

## Chapter II.b: bHLH-PAS protein RITMO1 regulates diel biological rhythms in the marine diatom *Phaeodactylum tricorutum* p.145

Abstract and Significance	p.146
Results	p.147
Transcriptome Profiling Identifies Potential Regulators of Diurnal Rhythms in <i>P. tricorutum</i>	p.147
Rhythmic <i>bHLH1a</i> and <i>bHLH1b</i> Expression Is Adjusted in a Photoperiod Dependent Manner and Persists in Continuous Light and Continuous Dark Conditions	p.147
Cellular Localization of bHLH1a Protein	p.147
bHLH1a Regulates Pace of Diel Gene Expression	p.147
The Ectopic Overexpression of bHLH1a Results in Altered Circadian Rhythms	p.148
RITMO1-Like Proteins Are Widely Represented in the Genome of Marine Algae	p.148
Discussion	p.149
Methods	p.151
Gene Expression Analyses	p.151
Generation of the bHLH1a Transgenic Lines	p.151
Microscopic Analysis	p.151
Data Mining, Protein Sequence, and Phylogenetic Analysis	p.151
Acknowledgements	p.151
Bibliography	p.151
SI Appendix	p.152
Supplementary methods	p.152
Culture and irradiation conditions	p.152
Analysis of the rhythmic processes	p.152
RNA extraction and transcript analyses	p.153
Immunoblot analysis	p.153
bHLH1a subcellular localization	p.154
Generation of the <i>bHLH1a</i> transgenic lines	p.154
Selection of rhythmic transcripts and clustering analysis	p.154
Data mining, protein sequence and phylogenetic analysis	p.155
Cell cycle analysis	p.155
References	p.177

## Chapter II.c: Physiological rhythms in the marine diatom *Phaeodactylum tricorutum* are regulated by the circadian clock transcriptional regulator RITMO1 p.181

Abstract	p.182
Introduction	p.183
Materials and Methods	p.185
Cultures and irradiation conditions	p.185
Generation of RITMO1 Knock Out (KO) strains	p.185

Western Blot Analysis	p.185
Cellular fluorescence analysis	p.186
Analysis of the rhythmic processes	p.186
Cell cycle analysis	p.186
Analysis of photosynthetic parameters	p.187
RNA extraction and RT-qPCR analysis	p.187
<b>Results</b>	p.189
Generation of knock-out mutants for <i>P. tricornutum</i> <i>RITMO1</i> by CRISPR-Cas9	p.189
Diatoms cellular fluorescence rhythmicity is adjusted in a photoperiod-dependent manner and is not altered in knock-out mutants for <i>RITMO1</i>	p.190
<i>RITMO1</i> obliteration affects fluorescence rhythmicity under free-running conditions	p.192
<i>RITMO1</i> affects circadian fluorescence rhythmicity, without affecting growth and cell cycle progression	p.195
<i>RITMO1</i> is implicated in the circadian regulation of photosynthesis in <i>P. tricornutum</i>	p.196
<i>RITMO1</i> plays a central role in the circadian control of gene expression in diatoms	p.198
<b>Discussion</b>	p.202
<b>Acknowledgements</b>	p.205
<b>Bibliography</b>	p.206
<b>Supplementary Material</b>	p.210
<b>Chapter II.d: bHLH1b as a candidate partner of <i>RITMO1</i> in diatom circadian clock</b>	p.219
Abstract	p.220
Introduction	p.221
Materials and methods	p.223
Yeast two Hybrid (Y2H) Assay	p.223
Culture and irradiation conditions	p.223
CRISPR/Cas9 Mutagenesis	p.223
Flow cytometry and fluorescence rhythmicity analysis	p.225
Results	p.226
bHLH1b and <i>RITMO1</i> physically interact via their bHLH fold	p.226
Generation of <i>bHLH1b</i> KO mutants	p.228
<i>bHLH1b</i> mutations affect free-run fluorescence oscillations	p.230
Conclusions	p.232
Bibliography	p.234
<b>Chapter III: bHLH2 is a light-intensity dependent modulator of photosynthesis and growth in the marine diatom <i>Phaeodactylum tricornutum</i></b>	p.239
Abstract	p.241
Introduction	p.242
Analysis of photosynthesis via 2 chlorophyll fluorescence	p.243
Methods	p.247
Generation of <i>bHLHRNAi</i> lines	p.247
On plate colony screening	p.247
Liquid culture and irradiation conditions	p.248
ΦPSII analysis via chlorophyll fluorescence	p.248

relative Electron Transfer Rate	p.249
Evaluation of PSI redox state	p.249
Lincomycin treatment	p.249
RNA extraction and RT-qPCR analysis	p.249
Subcellular localization prediction	p.250
Generation of <i>bHLH2</i> Knock-Out (KO) strains	p.250
<b>Results and Discussion</b>	p.251
Generation of RNAi transgenic lines targeting <i>bHLH</i> genes	p.251
<i>bHLH2</i> RNAi lines are affected in photosynthetic capacity in a light intensity dependent way	p.252
Effects of antisense RNAi on <i>bHLH2</i> transcription	p.255
<i>bHLH2</i> RNAi lines show a deficit in electron transfer at the thylakoid chain level	p.256
Response of photosynthesis upon transition to high light is affected in <i>bHLH2</i> RNAi lines	p.256
<i>bHLH2</i> RNAi lines are not affected in response to photoinhibition	p.259
Photosynthetic activity represses <i>bHLH2</i> expression	p.260
Preliminary characterization of <i>bHLH2</i> KO mutants	p.263
<b>Conclusion</b>	p.266
<b>Bibliography</b>	p.268

<b>Chapter IV: Conclusions and perspectives</b>	p.273
Bibliography	p.282

# List of Figures and Tables

## Chapter I

Figure 1. Chlorophyll distribution in the world ocean	p.5
Figure 2. Diatom characteristics and morphological diversity	p.8
Figure 3. The eukaryotic Tree of Life	p.10
Figure 4. The evolution of diatoms	p.12
Figure 5. The photosynthetic Linear Electron Transfer in diatoms	p.18
Figure 6. Diatom cell cycle and cyclins	p.27
Figure 7. Main characteristics of biological rhythms	p.32
Figure 8. Circadian TTFL networks in model organisms	p.36
Figure 9. Architecture of circadian clock systems	p.43

## Chapter II.a

Figure 1. Complex rhythms emerge from solar and lunar cycles in marine ecosystems	p.90
Figure 2. Overview of the diverse marine habitats and discussed exemplary organisms	p.92
Figure 3. Established and emerging marine microalgal model systems for chronobiology	p.94
Figure 4. Climate change effects on timing and how they could impact on species interactions and ecosystems	p.110
Table 1. Characterized regulators, central clock system components and rhythmic outputs of marine algal models	p.98
Table 2. Overview of a comprehensive selection of different marine animals studied for their rhythms	p.104
Table S1. Examples of biological rhythms characterized in marine algae	p.139

## Chapter II.b

Figure 1. Diurnal expression of rhythmic <i>P. tricornutum</i> genes	p.148
Figure 2. bHLH1a localizes in the nucleus, and its overexpression alters rhythmic diel gene expression	p.149
Figure 3. bHLH1a overexpression alters circadian rhythms of cellular fluorescence	p.150
Figure 4. bHLH-PAS protein family structure and phylogeny	p.150

Figure S1. nCounter expression analysis of genes maintaining rhythmic expression in D:D condition and 16L:8D condition in Wt cells	p.157
Figure S2. nCounter expression analysis of representative genes with altered rhythmic expression in Wt cells in D:D condition compared to 16L:8D condition	p.158
Figure S3. Diel expression patterns of <i>bHLH1a</i> and <i>bHLH1b</i> genes under Fe-depletion conditions in 12L:12D photoperiods	p.159
Figure S4. Analysis of selected rhythmic gene expression profiles in L:D and D:D in Wt and bHLH1a OE1 cells	p.160
Figure S5. Cell cycle progression dynamics of Wt <i>P. tricornutum</i>	p.161
Figure S6. Diurnal oscillations of chlorophyll fluorescence (FL3-A parameter) in Wt and bHLH1a OE lines	p.162
Figure S7. Analysis of <i>bHLH1a</i> gene expression in continuous blue light	p.163
Figure S8. Circadian oscillation of chlorophyll fluorescence in Wt and bHLH1a OE lines	p.164
Figure S9. Analysis of rhythmicity in Wt and bHLH1a OE lines under blue L:L	p.165
Figure S10. Growth rate of Wt and bHLH1a OE lines grown in blue L:L	p.166
Figure S11. Circadian oscillation of chlorophyll fluorescence in Wt and a transgenic control line (pNAT) under blue (L:L)	p.167
Table S1. Accession codes and sequence probes used in the nCounter analysis	p.168
Table S2. Calculated periods, phases, amplitudes and relative amplitude errors of the Wt and bHLH1a OE lines growing in 16L:8D	p.171
Table S3. Calculated periods, phases, amplitudes and relative amplitude errors of the Wt and bHLH1a OE lines growing in L:L	p.172
Table S4. Accession numbers of the proteins utilized in the bHLH-PAS phylogenetic analysis	p.173
Table S5. List of the oligonucleotides used in this work	p.176

## Chapter II.c

Figure 1. Generation of knock-out (KO) mutants for <i>P. tricornutum</i> RITMO1	p.189
Figure 2. Fluorescence rhythmicity of wild-type and ritmo1 knock-out mutants under different light:dark cycles	p.191
Figure 3. Characterization of fluorescence rhythmicity of wild-type <i>P. tricornutum</i> cells after the transition from L:D cycles to free running conditions	p.192
Figure 4. Effects of RITMO1 mutation on cellular fluorescence in free running	p.194

Figure 5. Re-entrainment of Wt, KO1, KO3 and OE1 cultures adapted to continuous light (L:L) to L:D cycles	p.195
Figure 6. Analysis of the effect of RITMO1 obliteration and overexpression on growth capacity and cell cycle progression	p.196
Figure 7. Analysis of the effect of RITMO1 mutation and overexpression on different photosynthetic parameters under periodic L:D cycles and free running conditions	p.197
Figure 8. Analysis of the expression of selected genes by qRT-PCR in Wt, OE1 and KO3 lines under periodic L:D cycles and free running conditions	p.201
Figure S1. Sequence analysis of the KO mutants in the <i>RITMO1</i> gene	pp.210-211
Figure S2. Characterisation of growth profile in <i>P. tricornutum</i> grown under 16L:8D cycles	p.212
Figure S3. Effects of <i>RITMO1</i> mutation on cellular fluorescence in L:L 25 $\mu\text{mol photons m}^{-2} \text{s}^{-1}$	p.213
Figure S4. Time-resolved analysis of growth in free-run cultures	p.214
Table S1. List of the sgRNAs used for CRISPR-Cas9 mutagenesis of the <i>RITMO1</i>	p.215
Table S2. Growth capacity of <i>P. tricornutum</i> Wt cells in the different conditions used throughout this study	p.216
Table S3. Characterisation of cellular fluorescence rhythmicity in Wt, CTR, KO1, KO3 and OE1 lines in L:D	p.217
Table S4. Characterisation of cellular fluorescence rhythmicity in Wt, CTR, KO1, KO3 and OE1 lines in L:L	p.218
Table S5. List of the oligonucleotides used in this work	p.219

## Chapter II.d

Figure 1. Genomic arrangement of <i>RITMO1</i> and <i>bHLH1b</i> loci	p.221
Figure 2. Results of the Yeast two Hybrid assay (Y2H)	p.227
Figure 3. Generation of <i>bHLH1b</i> KO mutants	p.228
Figure 4. Characterisation of <i>bHLH1b</i> KO mutants	p.230
Figure 5. Effects of bHLH1b mutation on cellular fluorescence	p.231
Table 1. List of the oligonucleotides used in this work	p.224
Table 2. sgRNA used for <i>bHLH1b</i> KOs generation	p.224
Table 3. Characterisation of cellular fluorescence rhythmicity of bHLH1b mutants in L:L	p.230



## Chapter III

Figure 1. Principles of chlorophyll fluorescence analysis of PSII activity	p.243
Figure 2. Use of P700 redox state to localize perturbations in the plastid electron transfer chain	p.245
Figure 3. Screening on plate based on chlorophyll fluorescence	p.251
Figure 4. On plate screening of phleomycin resistant control	p.252
Figure 5. <i>bHLH2</i> RNAi lines are affected in photosynthesis and growth	p.253
Figure 7. Gene expression of <i>bHLH2</i> under the different continuous light irradiations	p.255
Figure 8. <i>bHLH2</i> RNAi lines show a defect in electron transfer located upstream of PSI	p.257
Figure 9. Response to light intensity transition is affected in <i>bHLH2</i> RNAi lines	p.258
Figure 10. <i>bHLH2</i> RNAi lines are not affected in photoinhibition	p.259
Figure 11. Expression profiles of <i>bHLH2</i> from publicly available transcriptomic data	p.261
Figure 12. <i>bHLH2</i> expression in the dark	p.262
Figure 13. Mutants on <i>bHLH2</i> gene induced by CRISPR/Cas9	p.263
Figure 14. Sequence alignment of the KO mutants for <i>bHLH2</i> gene	p.264
Figure 15. Response to light intensity transition in <i>bHLH2</i> KO lines	p.265
Table. 1 Primers used for the construction of the RNAi cassettes	p.247
Table 2. List of the oligonucleotides used in this work	p.250
Table 3. gRNAs used for <i>bHLH2</i> KOs generation	p.250
Table 4. Summary results of on plate screening	p.252
Table 5. Summary results of the RLC analysis	p.258

# Table of abbreviations

ALAN: Artificial Light At Night	MTOC: Micro Tubules Organising Centre
BCP: Biological Carbon Pump	Mya: Million years ago
bHLH: basic Helix Loop Helix domain	NPP : Net Primary Production
BP: Before Present	NPQ: Non Photochemical Quenching
CBBC: Calvin Benson Bassham Cycle	OE: Over-Expressing transgenic line
CCM: Carbon Concentrating Mechanism	OMZ: Oxygen Minimum Zones
CET: Cyclic Electron Transfer	OUC: Ornithine-Urea Cycle
D:D: continuous dark	PAS: <i>Per Arnt Sim</i> domain
DVM: Diel Vertical Migration	PQ: PlastoQuinone
EET: Electron Energy Transfer	PS: Photo System
EGT: Endosymbiont Gene Transfer	PTO: Post-Translational Oscillator
eToL: eukaryote Tree of Life	qE: energy (heat) dependent component of NPQ
ETR: Electron Transfer Rate	qI: photoinhibition component of NPQ
FCP: Fucoxanthin Chlorophyll binding Protein	qT: state transition component of NPQ
FD: Ferredoxin	RC: Reaction Center
FFC: FRQ-FRH Complex	rETR: relative Electron Transfer Rate
FLD: Flavodoxin	RNAi: RNA interference
Fx: Fucoxanthin	ROS: Reactive Oxygen Species
Gt C : Giga Ton of carbon	SAR: Stramenopila Alveolata Rhizaria
HGT: Horizontal Gene Transfer	SDV: Silica Deposition Vesicles
KD: Knock-Down transgenic line	TCA: TriCarboxylic Acid cycle
KO: Knock-Out mutant	TF: Transcription Factor
L:D: light dark cycles	TIO: Transcription-Independent Oscillator
L:L: continuous light	TTFL: Translational Feedback Loops
LET: Linear Electron Transfer	XC: Xanthophylls Cycle
LGM: Last Glacial Maximum	Y2H: Yeast two Hybrid assay
LHC: Light Harvesting Complex	ZT: <i>Zeitgeber</i> Time
LOV: Light Oxygen Voltage domain	
MC: alternative of MTOC	
MT: Micro Tubules	



*The winds, the sea, and the moving tides are what they are. If there is wonder and beauty and majesty in them, science will discover these qualities. If they are not there, science cannot create them. If there is poetry [...] about the sea, it is not because I deliberately put it there, but because no one could write truthfully about the sea and leave out the poetry.*

Rachel Carson<sup>1</sup>

---

<sup>1</sup> From Rachel Carson's acceptance of the National Book Award for Nonfiction, 1952 ("Rachel Carson Excerpts Continued - Rachel Carson - U.S. Fish and Wildlife Service,")



# Chapter I:

## Introduction

This introduction chapter is organized in five main sub-parts: in the first one, the life of phytoplankton in the oceans and their role in the biogeochemical cycles at planetary level are briefly presented.

The second part focuses on the general presentation of diatoms, the group of algae on which this thesis work focuses. Their cell biology, their physiology and their role in the global ecological context are described. Particular attention is given to the description of the model species *Phaeodactylum tricorutum* that has been the subject of study during my thesis.

The third section gives an overview on light-dependent or light-regulated biological processes in diatoms. These processes include photosynthetic activity, photoacclimation, photoperception and cell division.

An in-depth description of biological rhythmicity and biological clocks is presented in the fourth section. The molecular architecture and function of biological timekeepers is given, with a comparative depiction of their molecular components in different taxa.

Finally, the fifth part represents an overview of transcription factors in diatoms. Particular space is dedicated to the transcription factors of the bHLH-PAS family, on which I have focused my research in *P. tricorutum*.

# I.1 The life of phytoplankton

*"How inappropriate to call this planet 'Earth' when it is quite clearly 'Ocean'".*<sup>2</sup> With skill and poetry, the renowned science fiction author and undersea explorer Arthur Charles Clarke perfectly synthesized the vastness of the ocean and its importance for all lifeforms. The world ocean covers approximately 70% of the surface of our planet and has a variety of habitats and environmental conditions comparable to, if not greater than, that of dry land. Life has emerged in the oceans, which are today home to an endless variety of living organisms of all shapes and sizes ranging from the smallest bacteria to the blue whale. Still, the vast majority of life underwater is represented by microbes, with around 70% of the marine biomass being represented by bacteria and protists (Bar-On et al., 2018). These microorganisms, along with microscopic free floating animals, are collectively called plankton and represent the beating heart of the trophic web of the oceans (Pierella Karlusich et al., 2020). Meta-genomic analysis of samples extracted in the wild reveal that the number of eukaryotic planktonic species ranges between the hundreds of thousands to the tens of millions (de Vargas et al., 2015). Of this teeming and kaleidoscopic microscopic biodiversity, only a few thousand species have been classified to date, leaving to our imagination the wonders yet to be discovered below the surface of water.

The photosynthetic fraction of these organisms is called phytoplankton, also commonly referred to as microalgae, a term that encompasses a variety of unicellular organisms that are extremely diverse and also phylogenetically very distant from each other (Blaby-Haas and Merchant, 2019; Keeling, 2013; Nowack and Weber, 2018). Phytoplankton proliferation is inextricably reliant on light irradiation, which is the source

of energy for photosynthesis and the metabolism of these organisms. Because of this, phytoplankton is fundamentally found only in the photic zone, the most superficial fraction of the water column where the sun's rays can penetrate (approximately up to 200 m depth). Yet, by converting solar energy and atmospheric CO<sub>2</sub> into organic matter, phytoplankton is of critical importance for the bio-geo-physical processes that regulate the functioning of the biosphere (Pierella Karlusich et al., 2020). Eukaryotic marine algae and prokaryotic cyanobacteria are indeed accounted for circa 45% of the global Net Primary Production (NPP) or, in other words, for half of the total flux of carbon fixation from the atmosphere to organic compounds (Field et al., 1998). If terrestrial plants are commonly called the lung of the earth, phytoplankton can rightfully be honored with the same title.

Remarkably, while contributing so much to NPP on a planetary scale, phytoplankton contribute with only one Gigatonne of carbon (Gt C, where 1 Gt C = 10<sup>15</sup> g of carbon) to the global living biomass, a tiny fraction in comparison to the estimated 470 Gt of higher terrestrial plants (Bar-On et al., 2018). This seemingly paradoxical disproportion is possibly explained by the high reproduction turnover of these organisms. Despite representing a relatively small fraction of the global biomass at any given moment, many more generations follow in a short space of time in comparison to slow-growing, slowly reproducing multicellular organisms as plants. As these organisms die, they generate organic matter which precipitates on the seabed. Dead organic matter transported to the deep ocean by gravitational sinking is sequestered on timescales of thousands of years before being recirculated to the surface via the slow natural

---

<sup>2</sup> See (Rozwadowski, 2010)

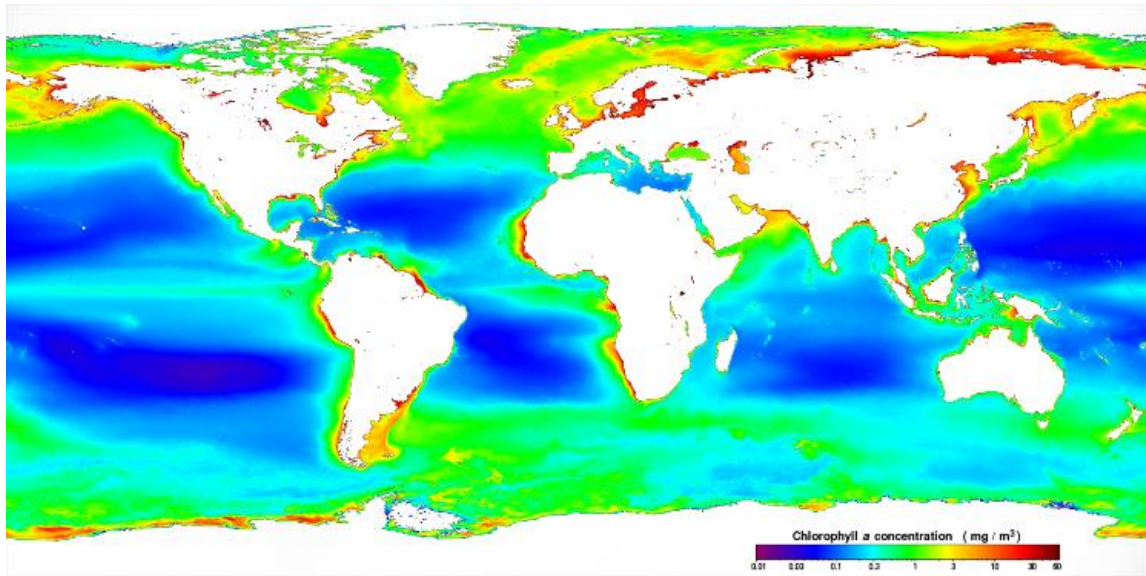


Figure 1. Chlorophyll distribution in the world ocean

Global distribution of chlorophyll in the oceans detected via Moderate Resolution Imaging Spectroradiometer by the Aqua MODIS Satellite (NASA). The image represents the composite of Chlorophyll concentration over a period ranging from July 4, 2002 and December 31, 2018. Image retrieved from the OceanColor Web tool, NASA (<https://oceancolor.gsfc.nasa.gov/>)

movements of deep-water masses. A fraction of this sedimented primary production (~0.3% of marine NPP) will eventually form the major long-lasting reservoirs of carbon that will persist for millions of years in the form of sedimentary rocks (Zhang et al., 2018). This myriad of photosynthetic organisms inhabiting the photic zone also becomes the prey of heterotrophic grazers, viruses and microbial decomposers, thus representing the base that supports the entire marine trophic web. (Bar-On et al., 2018; Zhang et al., 2018). The rapid rate of reproduction of planktonic phototrophs also means that, in marine ecosystems, primary producers can sustain a population of consumers five times higher in terms of biomass, a ratio between trophic levels opposite to that found on dry lands (Bar-On et al., 2018). This flux of CO<sub>2</sub> from the atmosphere to the oceans through photosynthetic fixation, trophic web functioning and sinking of dead matter is named Biological Carbon Pump (BCP). Its ecological relevance is evident when we consider that, thanks to BCP, oceans are held

responsible for the reabsorption of about 26% of anthropogenic CO<sub>2</sub> emitted since the industrial revolution (while land vegetation stocked 34% of it and the remaining fraction represents the net atmospheric increase of CO<sub>2</sub>) (Le Quéré et al., 2018).

In order to thrive to this extent, phytoplankton necessarily had to adapt to the light environment of the oceans, an environment that is anything but constant and uniform. Due to the spectral properties of water, light intensity quickly decreases in the first meters of the water column, so that direct light irradiation is orders of magnitude lower in the uppermost layers of seawater than on land (Depauw et al., 2012). In addition, water absorbs light extremely unevenly depending on its wavelength, with red light being completely extinguished in the very first meters, while blue light manages to penetrate much deeper. In this way, the light profile of the water column is very different from that which can be found on land, where the air absorbs the different wavelengths more



uniformly. Moreover, because of this phenomenon, the chromatic profile of light changes extremely rapidly as a function of depth, making the marine environment highly inhomogeneous and mainly dominated by green/blue light after the first few meters below the surface (Depauw et al., 2012; Stomp et al., 2007). In addition to the physical properties of water, other factors intervene in making the oceans an ever-changing environment. Atmospheric conditions, water movements (*e.g.* tides, and streams) and light scattering caused by coloured inorganic and organic suspended matter are all factors that play a role in characterizing the underwater light field (Kirk, 2011; Stomp et al., 2007). Even the scattering and absorption of light by the living phytoplankton itself can contribute substantially to the attenuation of irradiation. In nutrient rich waters (like estuaries) or during seasonal algal blooms, the algae can reach concentrations sufficient to cause self-shading to limit their own growth (Kirk, 2011).

Light quality and intensity perceived by marine organisms also dynamically change in function of time. The rotation of the Earth imposes the well-known constant ~24 hours cycles of light and dark since the beginning of life. Day length (photoperiod) also varies along the year as a function of latitude as a consequence of the revolution of the Earth around the sun and the inclination of its rotation axis, generating additional seasonal 365 days cycles. Finally, it should not be forgotten that reflected light from the moon, although not a relevant energy source for photosynthetic activity, is nevertheless a highly important source of information on the

environment. The ~24.8 hours periodicity of moonrise and moonset in combination with the ~29.5 days period of moon phases create a complex, but cyclical and predictable, pattern of illumination of the earth's surface intertwined with solar rhythms (Andreatta and Tessmar-Raible, 2020). To note, lunar cycles also play a crucial role in the environmental dynamics of coastal environments, as they are responsible for tidal rhythms and associated processes (*e.g.* the cyclic immersion of intertidal zones), profoundly shaping life in these ecosystems which are among the most productive and biodiverse in a marine context (Cahonn, 1999).

Light is not the only fundamental factor for the life of phytoplankton. Equally crucial is the availability of nutrients such as carbon, nitrogen, phosphorus, silicon or iron, (Speight and Henderson, 2010). The scarcity of these elements is one of the main limiting factors for the proliferation of phytoplankton, especially far from the coasts, where instead the runoff of elements from the mainland or upwelling phenomena of deep waters can lead to a local increase in the availability of nutrients (Lassiter et al., 2006; Speight and Henderson, 2010, Fig.1). If we add to this the fact that other factors such as salinity or temperature are part of the dynamic landscape of biotic and abiotic elements that regulate life in the oceans (Mann and Lazier, 2009) it is clear that, in order to proliferate, phytoplankton must be able to respond quickly and efficiently to all these stimuli in order to maximize their fitness. Among the various groups of phytoplankton, diatoms clearly emerge as one of the most successful.

# I.2 The kaleidoscopic world of diatoms

## I.2.a General introduction on diatoms

Diatoms are unicellular photosynthetic eukaryotes representing one of the most abundant, diversified and widely distributed groups of phytoplankton. Far from being relegated to oceanic environments, these cosmopolitan algae are distributed at all latitudes and in all types of habitats and can be found in any body of water, whether saltwater or freshwater, as well in soil moist (Falciatore et al., 2020). Diatoms are particularly relevant in polar regions (both arctic and antarctic), where they represent the most abundant group of photosynthetic eukaryotes (Malviya et al., 2016). In these regions, diatoms have also adapted to thrive and prosper in the apparently lifeless ice cap, where they reach such high concentrations to discolor the ice brown (Thomas and Dieckmann, 2002). Diatoms account for around 40% of marine carbon fixation, or 25% of the global NPP (Nelson et al., 1995; Tréguer et al., 2018), which is comparable to that of all terrestrial rainforests combined (Field et al., 1998). Estimations of diatom biodiversity are still uncertain, with the number of possible different species projected to be as high as 200,000 (Mann and Droop, 1996), although more recent studies consider this figure to be closer to 100,000 different taxonomic units (Malviya et al., 2016).

The life modes of diatoms are extremely varied. Depending on the species, they can live on the seabed (benthonic) or in suspension near the surface (pelagic or planktonic), they can appear as single isolated cells or grouped in colonies and in some cases they can establish close relationships of symbiotic interdependence with other microorganisms (Foster et al., 2011).

From a metabolic point of view, diatoms can be exclusive autotrophs (i.e.

totally dependent on photosynthetic activity for the production of carbohydrates) or mixotrophs (i.e. able to combine photosynthesis with the uptake of organic carbon sources dissolved in the environment) as in the case of *Phaeodactylum tricorutum* (Villanova et al., 2017) and also facultative heterotrophs as in the case of *Cyclotella cryptica* (Pahl et al., 2010). Although almost all diatoms are as mentioned photosynthetic, there are also known cases of species in which the plastid has lost its photosynthetic ability. These algae belong to the genera *Nitzschia* and *Hantzschia* and since most of the phylogenetically close species are photosynthetic, the loss of photosynthesis has clearly happened recently (Kamikawa et al., 2017).

Diatoms exhibit a rich variety of cellular and metabolic processes due in part to their complex evolutionary history and their composite genome, an assemblage of genes derived from different sources (the heterotrophic ancestor, photosynthetic symbionts, and prokaryotic donors, see Paragraph I.2.b). This genetic mosaic gives diatoms a variety of biological traits and processes that contribute in large part to their evolutionary success.

One of the most noteworthy characteristics of diatoms is their chiseled cell wall, called frustule (Fig.2), impregnated with hydrated glass ( $\text{SiO}_2 \cdot n\text{H}_2\text{O}$ , Kröger and Poulsen, 2008). Silicon is dissolved in marine waters mainly in the form of monomeric orthosilicic acid  $\text{Si}(\text{OH})_4$ , which is converted to organic silica mainly by diatoms and, to a minor extent, by other protists like radiolarians and silicoflagellates (Tréguer et al., 1995). Due to these features, diatoms play a prominent role in oceanic biogeochemical

cycles of silica (Nelson et al., 1995; Tréguer et al., 1995). An estimate of 200-280 Tmol of biogenic silica is fixed each year by diatoms via their cell wall, of which approximately 50% precipitates to the seabed by gravitational sinking (Nelson et al., 1995). The importance of diatoms in the biogeochemical cycle of silica becomes glaring when we consider that,

according to projections, Si dissolved in the ocean passes through diatom biomineralization an average of about 39 times before being deposited to the seafloor (Tréguer et al., 1995). Once precipitated, the glassy cell walls of diatoms can generate vast deposits of siliceous sands, also called diatomaceous earth or diatomite.

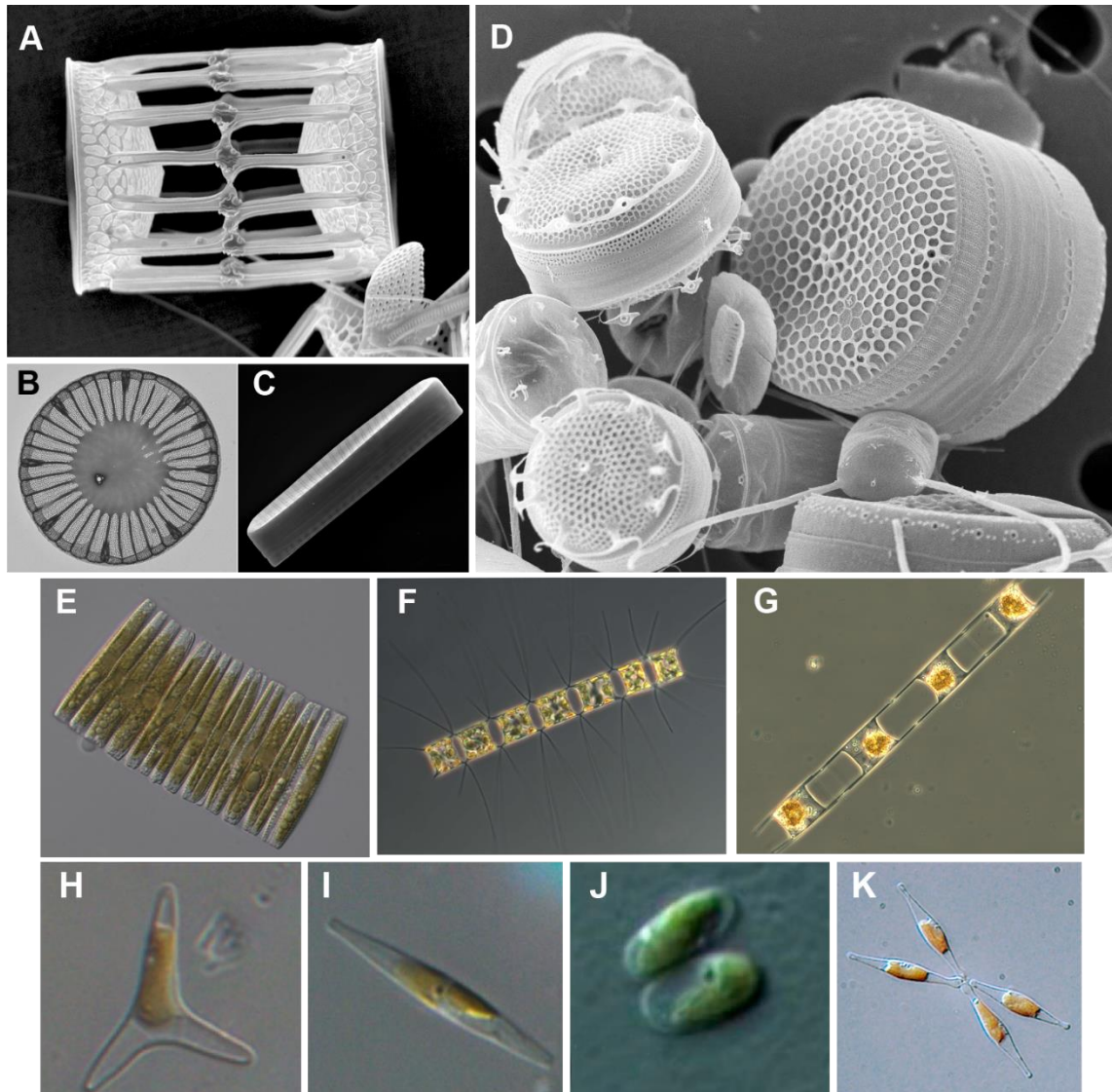


Figure 2. Diatom characteristics and morphological diversity

Examples of different diatoms showing their morphological diversity. (A) Scanning Electron Microscopy (SEM) micrograph of *Skeletonema marinoi*. (B) Transmission Electron Microscopy micrograph of *Cyclotella atomus*. (C) SEM micrograph of *Fragilariopsis cylindrus*. (D) SEM micrograph of a mix of diatom species of the genus *Thalassiosira*. Light microscopy micrographs of (E) *Fragilariopsis kerguelensis*, (F) *Chaetoceros* sp., (G) *Hemiaulus haukii* and (H-K) *Phaeodactylum tricornutum* in its three different morphotypes: tridiate (H), fusiform (I and K) and oval (J). Images were kindly provided by Diana Sarno and Marina Montesor (Stazione Zoologica Anton Dohrn, Napoli, Italy)

Diatom frustule is composed of two parts, the smaller *hypotheca* and the slightly bigger *epitheca*, capable of overlapping in a manner often compared to the two halves of a Petri dish. Each one of these two halves will become the *epitheca* of the daughter cells after cell division, causing a progressive reduction in cell size generation after generation, in a phenomenon called MacDonald-Pfitzer rule (Macdonald, 1869; Pfitzer, 1869). In many diatoms, restoration of the original cell size involves sexual reproduction and the generation of an enlarged zygote named auxospore. The generation of this auxospore is induced by the reaching of a lower bound cell size threshold. It has also been shown that the artificial, abrupt reduction of cell size induces sexual reproduction, demonstrating that this process is not dependent on the age of the population (Chepurnov et al., 2004). Still, the molecular mechanisms involved in the perception of cell volume remain non clarified (for a general review on sexual reproduction in diatoms, see (Mann, 2011; Montresor et al., 2016). To note, centric and pennate diatoms show different mating strategies, the former being mostly homothallic (hence, self-fertile and not showing mating types) and the latter being heterothallic (hence requiring the coupling of cells of different mating-types for inducing meiosis, (Chepurnov et al., 2004)

The tri-dimensional structure of the *thecae* (Fig.2) is characterized by regular patterns of pores of variable dimension, whose geometry and spatial distribution is species-specific and under strict genetic control. Indeed, the biomineralization of silica and its regular deposition in diatom cell wall involve a variety of well characterized proteins including silaffins, frustulins, silacidins, pleuralins and cingulins (for a detailed overview on frustule structure, composition and morphogenesis see (Babenko et al., 2022). The biomineralization of silica occurs in large intracellular vesicles also named Silica

Deposition Vesicles (SDV)(Heintze et al., 2020).

The diatom glass armor performs several fundamental functions for the cell, including protection against mechanical shocks and against grazers like copepods (Hamm et al., 2003; Pančić et al., 2019). In addition, the porous frustule can also function as a natural filter possibly capable of blocking the passage of viruses and bacteria potentially dangerous to the alga (Losic et al., 2006). The periodic nanostructure of silica may also perform the function of a photonic crystal, capable of redirecting and redistributing light incident on the cell wall towards the interior of the cell (Goessling et al., 2018). The optical coupling between the frustule and the plastid could consequently allow an increase in photosynthetic efficiency, although to which extent remains an open question.

Another of the metabolic characteristics of diatoms is the fact that they possess a fully functional ornithine-urea cycle (OUC). This metabolic pathway was initially considered as a peculiarity of metazoans (animals) where it performs the task of ammonium disposal in urea, less toxic and more easily eliminated by the body (Mommensen and Walsh, 1989). The fact that genes involved in this metabolic cycle are found in brown algae and *Haptophyta* (another group of protists phylogenetically related to *Stramenopila*) suggests that OUC was inherited from their common ancestor (A. E. Allen et al., 2011). Unlike in *Metazoa*, the OUC does not perform a function of ammonium detoxification and amino acid catabolism. On the contrary, its main function is to capture the ammonium dissolved in the environment and to fix it in organic compounds, allowing the storage of the nitrogen in the form of arginine, ornithine and proline, the main osmolytes of diatoms (accounting for 70% of carbon and nitrogen accumulated in metabolites (A. E. Allen et al.,

2011)). The OUC is therefore functional, in diatoms, to the rapid response to episodic cases of high availability of nitrogen (A. E. Allen et al., 2011), normally a limiting element in oceanic habitats (Falkowski et al., 2008, 1998). Since proline represents the main

precursor of polyamines (essentials for biomineralization of silica (Lin and Lin, 2018; Sumper and Kröger, 2004), OUC may also play a function in the production of the frustule (A. E. Allen et al., 2011).

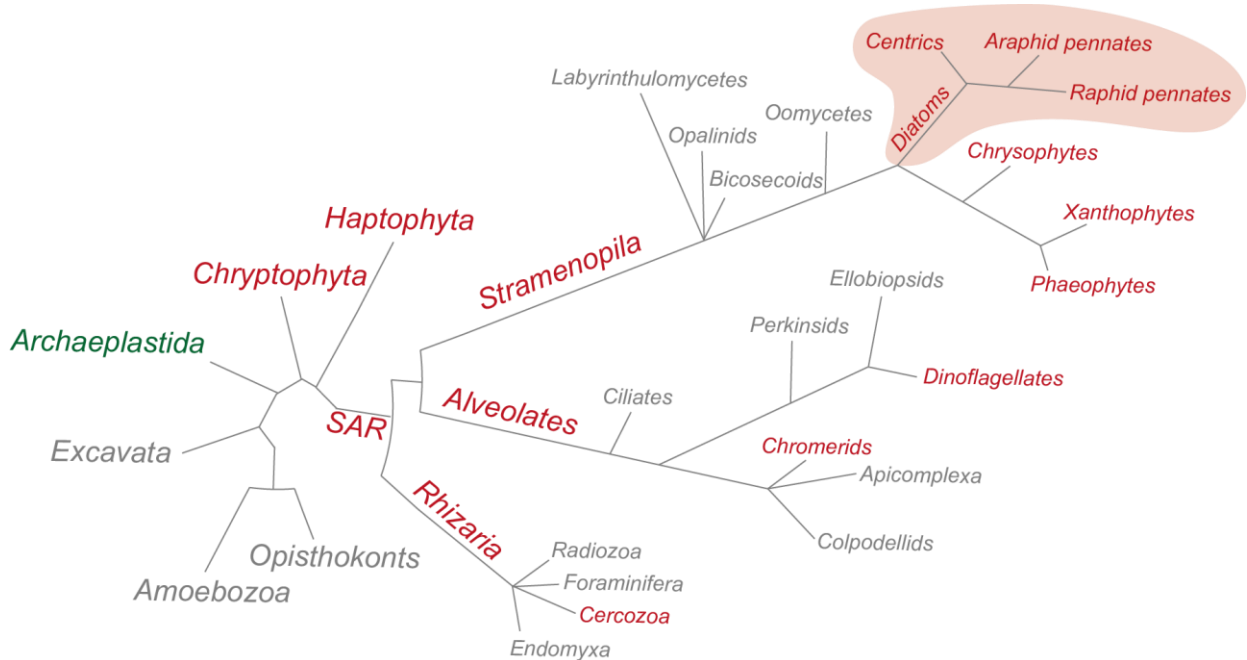


Figure 3. The eukaryotic Tree of Life

Phylogenetic tree representing the eukaryotic Tree of Life including all major supergroups. Red color highlights supergroups and taxa containing known examples of photosynthetic organisms with a plastid derived from a secondary endosymbiotic event with a red algal host. The Archaeplastida group, containing primary endosymbiotic phototrophs (including red and green algae and land plants) is highlighted in green. The Stramenopila Alveolata Rhizaria (SAR) supergroup is represented in detail to show the major taxa included in this branch and their relative phylogenetic position. Light red area highlights the position of diatoms within the Stramenopila. The tree is based on Dorrell and Smith 2011 and Burki *et al.* 2020.

## I.2.b Phylogenesis and evolution

In order to fully understand the biology of diatoms and the reasons for their ecological success, it is essential to know their evolutionary history and their position on the eukaryote Tree of Life (eToL, Fig.3). Diatoms are photosynthetic protists belonging to the Stramenopiles group, also referred to as Heterokonts. Stramenopiles fall in the larger SAR supergroup, a branch of the eToL which takes its name from the three subgroups that compose: *Stramenopila* themselves, *Alveolata* and *Rhizaria*, which derive from a single

common ancestor (Burki et al., 2020). Besides diatoms, several other organisms of utmost importance for marine ecosystems belong to SARs, such as *foraminifera*, *radiozoa* (both belonging to *Rhizaria*) and dinoflagellates (a mixed group of photosynthetic and heterotrophic unicellular organisms belonging to Alveolates). Of interest, dinoflagellates are the only family of microorganisms capable of competing with diatoms in terms of biodiversity abundance in oceanic ecosystems (Pierella Karlusich et al., 2020).

Stramenopiles encompass both unicellular heterotrophs (such as the water molds oomycetes) and a variety of photosynthetic organisms, including the multicellular brown algae *Phaeophyceae*, the unicellular *Eustigmatophyceae* and, obviously, diatoms (*Bacillariophyta*, Blaby-Haas and Merchant, 2019; Burki et al., 2020; Keeling, 2013). Diatoms first appeared ~190.4 millions of years ago (Mya, Fig.3 and Fig.4), close to the transition between the Triassic and Jurassic periods (Nakov et al., 2018). Diatoms are commonly divided into two main groups, clearly distinguishable by their shape: centric diatoms (*Coscinodiscophyceae*) with radial symmetry, the most ancient, and the fusiform, bilaterally symmetrical pennate diatoms (evolutionarily more recent and derived from centric, Kooistra et al., 2007). The separation of these two groups can be traced back to approximately 150 Mya by means of comparative taxon phylogeny (Nakov et al., 2018). Pennate diatoms can in turn be subdivided in raphid (*Bacillariophyceae*) or araphid (*Fragilariophyceae*) according to the presence or absence of a raphe, a longitudinal slit through the cell wall that is involved in motility and first appeared ~120 Mya (Nakov et al., 2018). The raphe is aligned with actin-myosin complexes responsible for the secretion of mucilaginous secretions used by these microalgae to actively slide on their substrate (Poulsen et al., 1999). To date, raphid diatoms are the most abundant, diversified and cosmopolitan. This ecological success is believed to be due in part to the evolutionary advantage given by the ability of active movement (Nakov et al., 2018).

Undoubtedly, one of the most extraordinary aspects of diatom evolutionary history is the complex origin of their plastid. Photosynthesis arose at least 3.5 billion years ago in bacteria as anoxygenic photosynthesis. The subsequent evolution of oxygenic photosynthesis in cyanobacteria promoted the generation of O<sub>2</sub> in the atmosphere (Nowack and Weber, 2018). Subsequently, a

photosynthetic cyanobacterium (endosymbiont) was engulfed by a heterotrophic eukaryote host, giving rise to the progenitor of eukaryotic plastids and to the evolution of the *Archaeplastida* group, which includes *Rhodophyta*, *Glaucophyta* green algae (*Chlorophyta*) and *Viridiplantae* (land plants, Fig.4, Keeling, 2013). This event of primary endosymbiosis is considered to be monophyletic and dates back to almost one billion years ago (Baldauf, 2008; Keeling, 2013). The only known example of independent primary endosymbiosis of a photosynthetic prokaryote is given by the amoeboids of the genus *Paulinella*, that engulfed a cyanobacterium between 65 and 90 Mya (Delaye et al., 2016). Hence, the entire diversity of plastids found in the eToL can be considered to have a single common origin. However, diatoms are not directly related to *Archaeplastida* and belong, as seen, to a distinct branch of the eToL (Fig.3). Phylogenetic and comparative genomics studies suggest that diatoms' ancestors acquired their photosynthetic organelle by means of secondary endosymbiosis, the process of engulfment and retention of a primary eukaryotic algae. In detail, the analysis of host genes transferred into the diatom genome suggests that they underwent at least two serial secondary endosymbiotic events of this kind with, in order, a green and then a red algae (Fig.4, Dorrell et al., 2017; Dorrell and Smith, 2011; Moustafa et al., 2009). The details and timing of this process and the real contribution of the green and red algal symbiont to diatom genomes remain debated (e.g. see Dorrell et al., 2017; Moustafa et al., 2009; Strasser et al., 2021). Still, it is important to keep in mind that secondary (and tertiary) endosymbiosis processes are responsible for plastid acquisition by all other non-*Archaeplastida* phototrophs, including other members of the SAR (e.g. dinoflagellates), but also photosynthetic haptophytes and excavata (for a detailed state of the art on the subject, see

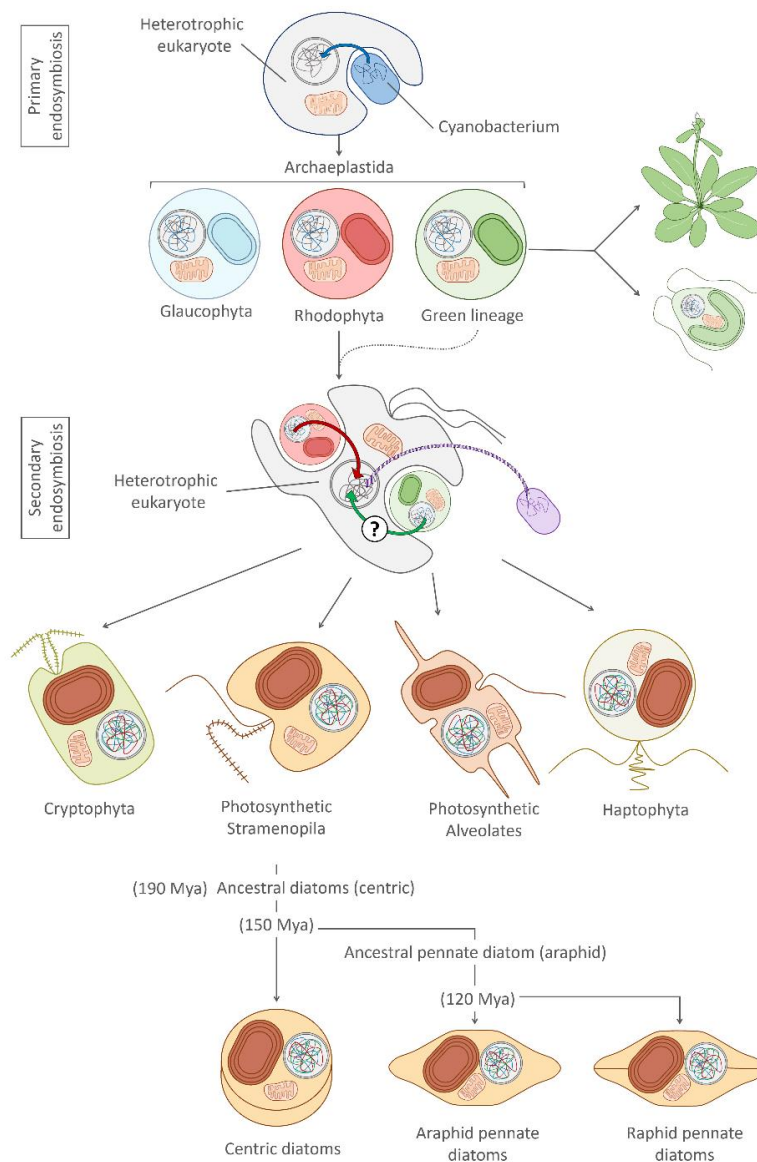


Figure 4. The evolution of diatoms

Schematic representation of the main evolutionary events that led to the emergence of diatoms. The monophyletic primary endosymbiotic engulfment of a cyanobacterium (in blue) by a heterotrophic eukaryotic host led to the apparition of the *Archaeplastida*. The blue arrow shows the transfer of part of the cyanobacterium genes to the nucleus of the host. This supergroup contains *Glaucophyta* (light blue), red algae (Rhodophyta, light red) and the photosynthetic organisms of the green lineage that include green algae as well as land plants. Secondary endosymbiotic event of a red algal led to the acquisition of plastids in the photosynthetic *Stramenopila* ancestors of diatoms, as well as in variety of organisms including *Chryptopyta*, *Haptophyta* and part of the photosynthetic *Alveolata* (which altogether form the *Chromalveolata* group). The cryptic secondary endosymbiosis with a green alga predating the engulfment of the *Rhodophyta* endosymbiont is also represented. The evolutionary details of these endosymbiotic event are still disputed (see Stiller et al 2014). Endosymbiotic gene transfer of the red and green algae to the nucleus of the eukaryotic host is represented by the red and green arrows. The horizontal gene transfer from bacteria (in purple) is also represented. The time of emergence of centric diatoms from the *Stamenopila* ancestor, as well as the time of separation of araphid pennate diatoms from centric ones is reported accordingly to Nakov 2018. The time of evolution of the raphe and consequent emergence of raphid pennate diatoms is equally reported. Mya: millions of years ago.



(Burki et al., 2020; Dorrell et al., 2017; Nowack and Weber, 2018; Stiller et al., 2014)). The secondary endosymbiosis origin of diatom plastid is further supported by the fact that diatom chloroplasts are bounded by a total of four membranes, the two innermost deriving from the envelope of the plastid of the primary alga and the outer ones descending from the plasma membrane of the endosymbiont plus the phagotrophic membrane of the host cell (Kroth and Strotmann, 1999). In addition, the phenomenon of endosymbiosis left obvious marks in the genetic makeup of diatoms, as a portion of the endosymbiont genes were transferred into the nucleus of the acceptor host (Moustafa et al., 2009). Such a process is termed Endosymbiont Gene Transfer (EGT) and is estimated to be responsible for a significant proportion of the protein-coding genes in diatoms (about 16% according to (Moustafa et al., 2009), of which a portion is derived from the endosymbiont red alga and a portion from the green alga cryptic symbiont (Dorrell et al., 2017; Moustafa et al., 2009).

Horizontal Gene Transfer (HGT) from prokaryotes donors is another process that has largely contributed to the complexity of the genomes of diatoms (Vancaester et al., 2020) and of other SAR protists (Chan et al., 2012; Nosenko and Bhattacharya, 2007). Also named lateral gene transfer, HGT is the transfer of genetic information between different species by a process of direct passage and integration of genetic material. In diatoms, bacterial HGT contributed to an average of 3-5% of the genetic pool through multiple transfer events spanned over time and with different prokaryotic donors (Vancaester et al., 2020). The genes obtained by these

processes contribute to processes such as cobalamin uptake, cold tolerance and metabolism of carbon and nitrogen (Vancaester et al., 2020). Notably, several enzymes and metabolic shunts associated with ornithine-urea cycle in diatoms are supposed to derive from HGT from bacterial donors (A. E. Allen et al., 2011). The integration of viral genomic material, although observed, has occurred to a lesser extent in diatom genomes than what has been observed in other eukaryotes (Hongo et al., 2021).

Regarding the more general characteristics of diatom genomes, they show variable ploidy. In fact, some of them are characterized by a diploid genome with limited divergence between the two haplotypes (e.g. *P. tricornutum* (Bowler et al., 2008) and *Thalassiosira pseudonana* (Armbrust, 2004)), in others the two haplotypes show a strong divergence (e.g. *Fistulifera solaris* (T. Tanaka et al., 2015)) while still others are allopolyploid, as in the case of *Fragilariopsis cylindrus* (Mock et al., 2017). Diatom genes are usually short (<2,500 bp) and with one intron, only 20% of them possessing two or more introns (Basu et al., 2017). Despite the low complexity of gene structure, alternative splicing remains possible, with for example 15% of the genes of *P. tricornutum* undergoing this process (Rastogi et al., 2018). Diatoms have also been shown to transcribe non-protein-coding RNAs such as long intergenic non-coding RNAs (lincRNAs (Basu et al., 2017)), small non-coding RNA (sRNAs, (Rogato et al., 2014) and RNAs transcribed from the antisense strand of protein coding genes (NATs: Natural Antisense Transcripts (Cruz de Carvalho and Bowler, 2020)).

### I.2.c Toolkit box for molecular biology in diatoms

Our ability to understand the complexity of the processes that govern life in the ocean depends irrevocably on the

availability of model organisms capable of representing the enormous variety of taxa that inhabit it and of genetic manipulation



techniques essential for their study. For this reason, the scientific community has made great efforts to fill these gaps, leading to the increasing availability of manipulation techniques in an ever-increasing number of organisms, most notably of protists (Faktorová et al., 2020). Concerning diatoms, the characterization of their cellular physiology and molecular biology has seen a major propulsion in the past two decades thanks to the development of molecular and genomic resources, as well as genetic manipulation techniques. Over time, the community of diatomists has therefore chosen and adopted a variety of different species to characterize according to the different focus of interest of the research. Recently, this variegation of study models has been reflected in the genomic and transcriptomic sequencing of several reference species, each chosen for its physiological and metabolic peculiarities or ecological relevance: *e.g.* *T. pseudonana* (Armbrust, 2004) and *P. tricornutum* (Bowler et al., 2008), chosen as first reference models for centric and pennate diatoms respectively; *T. oceanica* (Lommer et al., 2012) as a model for the adaptation to iron-limited environments; *Pseudo-nitzschia multistriata* (Basu et al., 2017) chosen for its well characterised sexual reproduction and meiosis; *F. cylindrus* (Mock et al., 2017) chosen as an ecological model for its adaptation to the cold water and distribution in the antarctic ocean; *S. robusta* as a reference for the adaptation to a benthic life-style and its rhythmic physiology (Bilcke et al., 2021a, 2021b); *Pseudo-nitzschia multiseries* (Basu et al., 2017) and *Skeletonema costatum* (Ogura et al., 2018) for their health relevance as toxic algae; *F. solaris* (T. Tanaka et al., 2015) and *Cyclotella cryptica* (Traller et al., 2016) for their mixotrophic metabolism and for their interest in biotechnological applications.

In addition to genomic and transcriptomic information, different nuclear transformation strategies are available for different species (Falcatore et al., 2020). *P.*

*tricornutum*, for example, can be transformed by biolistic bombardment (Apt et al., 1996; Falcatore et al., 1999; Siaux et al., 2007), and nuclear electroporation (Huang and Daboussi, 2017; Niu et al., 2012; Zhang and Hu, 2014). Similarly, nuclear transformation is also available for the centric diatom model *T. pseudonana* (Poulsen et al., 2006) and for less developed models such as *Cylindrotheca fusiformis* (Fischer et al., 1999; Poulsen and Kröger, 2005), *Chaetoceros spp.* (Miyagawa-Yamaguchi et al., 2011), *Fistulifera spp.* (Muto et al., 2013), *Navicula saprophila* and *C. cryptica* (Dunahay et al., 1995). Biolistic bombardment and electroporation can lead to the integration of multiple copies of exogenous DNA into the genome, adding an additional layer of variability between transgenic lines (Karas et al., 2015; Sharma et al., 2018).

Bacterial conjugation (the passage of plasmids from an *Escherichia coli* bacterial donor to the target cells via a conjugation pilum) is another method that has been proven to be efficient in both *P. tricornutum* and *T. pseudonana* (Karas et al., 2015). The advantage of this technique is that it allows the introduction of an episomal transgene vector in the form of a plasmid into the cell without integration into the genome (episomal vector), differently from what happens by microparticle bombardment or electroporation. This avoids the random integration of exogenous DNA that could consequently interrupt endogenous sequences either in coding or regulatory regions (*e.g.* promoters) and ensures greater genetic uniformity among mutants (George et al., 2020). Furthermore, since the vector is maintained inside the cells by antibiotic resistance, the conjugation system also allows the reversibility of the transformation, since the culture in the absence of antibiotics leads to the elimination of the episome. A final advantage of this technique is that it allows one to control the number of copies of the vector,

since the episome usually occurs in a single copy for each cell.

It is possible to modulate the expression of genes of interest by coupling the transgene to a large variety of different promoters. These promoters can be constitutive (constantly expressed at a stable level, as in the case of the Histone 4 promoter), light responsive (as in the case of the promoter of the Fucoxanthin-Chlorophyll binding Protein FCPb) or even inducible by nutrient availability cues (as in the case of the Nitrate Reductase NR promoter, activated by the presence of NO<sub>3</sub> in the culture medium) (Apt et al., 1996; Falciatore et al., 1999; Hempel et al., 2009; Poulsen et al., 2006; Siaux et al., 2007). Transformation also allows the expression of proteins coupled with Human influenza hemagglutinin (HA), fluorescent protein moieties or other tags (Siaux et al., 2007) and the expression of reporter genes like aequorin and fluorescent proteins (Falciatore et al., 2000; Karas et al., 2015; Poulsen et al., 2006; Siaux et al., 2007; Zaslavskaja et al., 2001b, 2001a). Gene expression can also be manipulated via gene knockdown silencing through RNAi (De Riso et al., 2009) and artificial miRNAs (Kaur and Spillane, 2015).

#### 1.2.d *Phaeodactylum tricornutum* as a diatom model

Given the very high diversity of species, life strategies, and complex evolutionary history, the selection of models is particularly challenging in diatoms. Historically, the earliest and best characterized models in molecular biology were *Thalassiosira pseudonana* (the first diatom whose genome has ever been sequenced (Armbrust, 2004)) and *Phaeodactylum tricornutum* (Bowler et al., 2008), chosen as reference species for centric/planktonic diatoms and pennate diatoms, respectively. *P. tricornutum* can occur in three distinct morphotypes: oval, fusiform, and triradiate. Although the three-horned form is the one

Targeted gene editing for gene function obliteration is also established in diatoms, using domesticated Transcription activator-like effector nucleases TALENs (Daboussi et al., 2014) and CRISPR/Cas9 (Nymark et al., 2016). Recent works have also implemented the direct biolistic bombardment of the Cas9 ribonucleoprotein in *P. tricornutum* cells. This innovation allows the transient and well regulated mutagenic activity of the CRISPR/Cas9 method, avoiding all the possible side effects of the random genomic insertion of the Cas9 vector and of the persistent activity of the protein after the transformation (Serif et al., 2018).

To conclude, the possibility of expressing exogenous genes in the chloroplast after transformation by electroporation has been demonstrated (Xie et al., 2014), as well as targeted mutagenesis of plastid genes by homologous recombination (Materna et al., 2009). Nevertheless, these techniques of chloroplast transformation remain unrefined and poorly used by the community of diatomists because of the limited reproducibility of the available protocols (Kroth et al., 2018).

that gives the species its Linnean name, the most common morphotype under laboratory conditions in liquid cultures is the fusiform one (de Martino et al., 2007). Even though the genus *Phaeodactylum* is not of ecological prominence (Armbrust, 2004; Malviya et al., 2016), this has been isolated in a variety of environments. In fact, this species can be found at tropical latitudes as well as near the Arctic Circle and at all longitudes (de Martino et al., 2007). This characteristic, as well as the availability in the laboratory of different ecotypes with various origins, make it of particular interest for the study of adaptation to the environment. Recent sequencing of the

genomes of the ten *P. tricornutum* ecotypes was made available (Rastogi et al., 2020) and showed relatively low genetic diversity among different accessions. All my thesis work has been carried out on *P. tricornutum*, chosen for being the diatom species for which the characterisation of molecular and cellular biology and physiology is most advanced. This makes it an ideal point of access for the acquisition of knowledge that can be translated to other diatom species in the future. In addition *P. tricornutum* possess a small genome (27.4 Mb) and its gene pool (in particular of the set of transcription factors) has been studied in detail (Ait-Mohamed et al., 2020; Bowler et al., 2008; Rastogi et al., 2018; Rayko et al., 2010). Finally, a variety of techniques of genetic manipulation is available for this alga (see previous paragraph for details). The wild type strain used as reference for all my work is *Pt1*, an ecotype from

temperate regions (Blackpool, UK, 54°N). *Pt1* was also the ecotype chosen for the first *P. tricornutum* genome sequencing project (Bowler et al., 2008).

Also, *P. tricornutum* has the peculiarity of being the only known diatom species which does not peremptorily require silicon uptake nor the synthesis of the frustule (de Martino et al., 2007). The analysis of *P. tricornutum* genome perfectly reflects the mixed and highly complex origin of diatom genetic heritage. Genome annotation predicts a total of ~12,200 genes, ~9% of which show no homologous sequences in any other organism, 12% are shared only with diatoms, 4% genes originated from independent HGT events with prokaryotes, 3% are derived from the red algal ancestor of the plastid and 9% are related to genes specific of the green lineage of the *Archaeplastida* (Bowler and Falciatore, 2019; Rastogi et al., 2018).

## I.3 Light in the life of diatoms

### I.3.a Light as an energy source: the photosynthetic apparatus in diatoms

For phototrophic organisms such as diatoms, light is the main energy source for sustaining cellular metabolism. The conversion of light energy into electrochemical potential occurs, as known, at the level of the thylakoid membrane of the chloroplast. Given the peculiar evolutionary history of the plastid of *Stramenopila* (presented in Paragraph I.2.b), a description of this organelle is indispensable for understanding the characteristics of photosynthesis in diatoms. As already aforementioned, diatom chloroplasts are bounded by four membranes deriving from the plastid and the plasma membrane of the endosymbiont plus the phagotrophic membrane of the host cell. These four membranes are at the center of a well-regulated traffic of proteins synthesized in the cytoplasm and targeted to the chloroplast. This protein traffic is necessary since only a fraction of the proteins active in the chloroplast are coded in the genome of the organelle, while the large part has been transferred to the nuclear genome. The nuclear-encoded proteins targeted to the plastid are characterized by a bipartite N terminal signal sequence constituted of a signaling peptide followed by a chloroplast transit peptide (Kilian and Kroth, 2004). The presence of a conserved amino acid sequence (ASAFAP) at the level of this targeting sequence (Kilian and Kroth, 2004) allows a bona fide identification of the plastid targeted proteins in diatoms (Gschloessl et al., 2008). Furthermore, unlike the better characterized green line plastids, diatom thylakoids are not divisible into grana and thylakoid plastids, but are stacked in groups of three thylakoids spanning the entire length of the organelle (Flori et al., 2016; A. Tanaka et al., 2015).

Another characteristic of diatoms is the fact that they lack lutein and  $\alpha$ -carotene, the carotenoids typically present in *Archaeplastida* (Grossman et al., 2004). Still, diatoms are able to synthesize other compounds of the carotenoid family, specifically  $\beta$ -carotene, diatoxanthin, diadinoxanthin and fucoxanthin (Fx). The latter represents one of the most abundant pigments in these algae and is a major harvester of light (Bertrand, 2010; Dambek et al., 2012; Kuczynska et al., 2015). Notably, the characteristic brownish/golden color of diatoms and related algae (*e.g. Phaeophyceae*) is caused by the accumulation of large quantities of Fx. Beside carotenoids, diatoms also produce chlorophylls a (chl a) and c (chl c) which, together with Fx, are responsible for the capture of photons and their funneling to the photosynthetic apparatus (Kuczynska et al., 2015). The proper and efficient functioning of these molecules is ensured by their binding with special proteins of the thylakoid membrane called LHC (Light Harvesting Complexes) or, alternatively, FCP (Fucoxanthin Chlorophyll binding Proteins) (Lang and Kroth, 2001; Lepetit et al., 2007). The precise spatial arrangement of pigments in the LHCs ensures efficient and rapid energy transfer from the Fx to the chl (Wang et al., 2019). In addition, Fx has a broader absorption spectrum than chl which allows it to efficiently capture light for photosynthesis even at depths where blue and green light are predominant (Wang et al., 2019).

In the next paragraphs I will give an overview of the photosynthetic apparatus in diatoms. Due to the vastness of the subject and the fact that this process has been historically studied mainly in plants and green algae, general information on photosynthesis valid

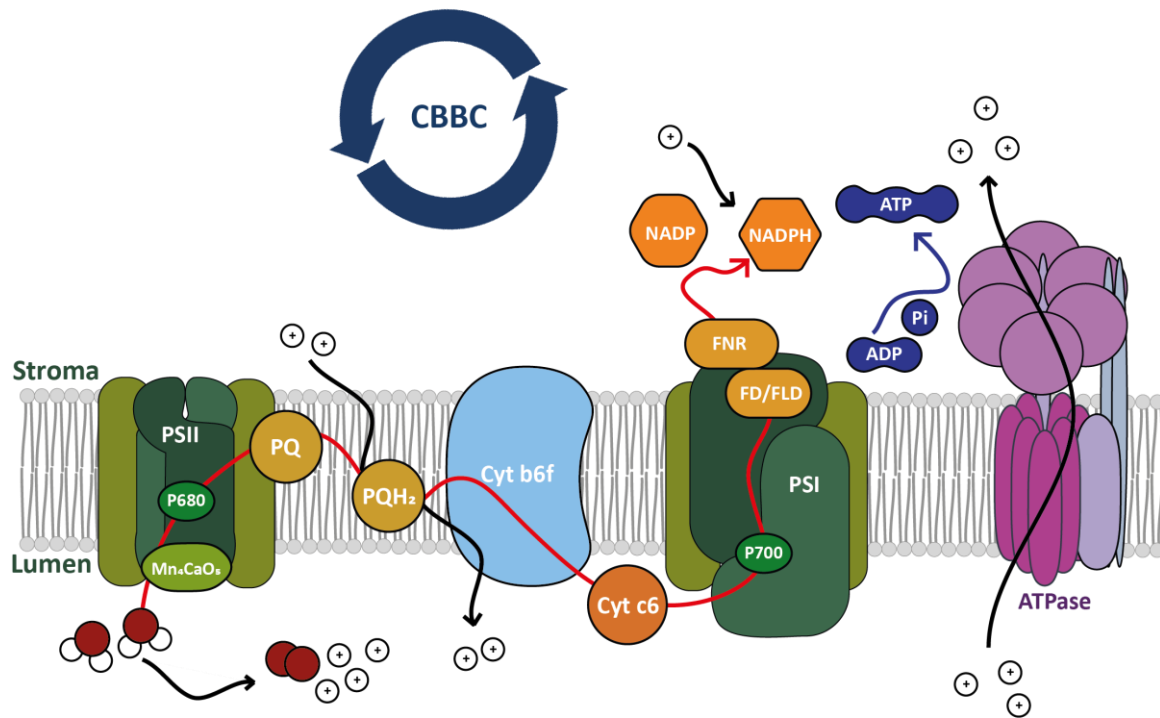


Figure 5. The photosynthetic Linear Electron Transfer in diatoms

Graphical representation of the photosynthetic Linear Electron Transfer (LET) at the level of the thylakoid and of the main protein complexes involved in the process. The red arrow highlights the path followed by electrons along the LET from a molecule of water to the NADPH molecule. Black arrows highlight proton release due to water oxidation and their movements across the thylakoid membrane. The representation is based on Allen et al. 2011 and adapted so to include specificities of the photosynthetic apparatus of diatoms. Abbreviations: Photosystem (PS), oxidised mobile plastoquinone (PQ), reduced mobile plastoquinone (PQH<sub>2</sub>), cytochrome b6f (Cyt b6f), soluble cytochrome c6 (Cyt c6) ferredoxin (FD), flavodoxin (FLD), flavodoxin(ferredoxin)-NADPH reductase (FNR), ATP synthase (ATPase), Calvin Benson Bassham Cycle (CBBC). P680 and P700 indicate the chlorophyll a special pair of PSII and PSI respectively, while Mn<sub>4</sub>CaO<sub>n</sub> indicate the Oxygen Evolving Complex at the luminal side of PSII.

also for diatoms are all derived from a small number of generalist publications (J. F. Allen et al., 2011; Eberhard et al., 2008; Taiz et al., 2015). Where the photosynthetic machinery of diatoms diverges from that of the *Archaeplastida*, bibliographic references will be punctually provided. A schematic representation of the photosynthetic machinery in diatoms is reported in Fig.5.

The capture of light by the LHC is only the first step of the photosynthetic process. These antenna complexes are located at the periphery of two protein systems (photosystem I, PSI, and photosystem II, PSII) where the actual conversion of light energy into oxidoreductive potential occurs

through the excitation of an electron. In short, photosynthesis can be described as the transport of electrons along a succession of molecular actors at the level of the thylakoid and against the oxidoreductive gradient in a process powered by light energy. The journey of these electrons begins at the level of the PSII. The peripheral antenna complexes capture the energy of a photon through their pigment and then funnel it via excitation energy transfer (EET) towards a pair of chl a molecules placed at the heart of PSII (the so called special pair or Reaction Center RC). The special pair of chl a is associated to two homologous proteins, D1 and D2, that form the core of PSII. Also, the special pair presents a peak of excitability at 680 nm, the reason

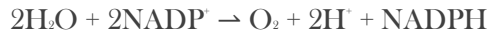
why the PSII is also called P680. Once excited directly by incident light or via EET from the peripheral antennae, the RC becomes a good reducer and passes an electron to a chain of electron carriers (pheophytin and a non-mobile plastoquinone QA). The final consequence of the excited electron transfer within the PSII is the reduction of a mobile plastoquinone (QB or PQ). In order to recover the lost electron and to be excitable again, PSII is able to oxidize water molecules thanks to the Oxygen Evolving Complex (OEC), located on the lumen side of the thylakoid membrane. By oxidizing two molecules of H<sub>2</sub>O the OEC is able to reduce four times the P680<sup>+</sup> cation, generating a molecule of O<sub>2</sub> as a byproduct and releasing four protons (H<sup>+</sup>) in the lumen of the thylakoid. This process is also called photolysis of water or water splitting, and is made possible by a metalloenzyme core containing four atoms of Mn and one of Ca, coordinated with oxygen atoms.

After the uptake of two electrons plus two protons coming from the stromal side of the membrane, the reduced PQ (PQH<sub>2</sub>) is released within the thylakoid membrane where it is able to move freely due to its hydrophobic nature. The electrons transported by PQH<sub>2</sub> are picked up by the second protein complex of the photosynthetic chain, cytochrome b6f (Cyt b6f), which transfers them to a new, mobile transporter, this time located at the level of the thylakoid lumen. In green algae, as well as in plants, this soluble electron transporter is predominantly a plastocyanin, a molecule containing copper. In case this element is scarce in the environment, plastocyanin can be replaced by an alternative transporter, cytochrome c6, which binds electrons at the level of an iron atom coordinated to a heme group. However, in most diatoms cytochrome c6 is the only soluble transporter used. To date, only a restricted number of species such as *Thalassiosira oceanica*, adapted to live in marine environments particularly poor in

iron, produces a plastocyanin in addition to the cytochrome c6 (Peers and Price, 2006). A second consequence of the oxidation of PQH<sub>2</sub> at the level of Cyt b6f, in addition to the reduction of the soluble transporter, is the release of a proton in the thylakoid lumen which is added to the four released during the photolysis of water.

The soluble electron carrier brings the electrons to PSI. Exactly like PSII, also PSI has a special pair of chl a which can be excited directly by light or by EET from peripheral antennas. In this case, however, the excitability peak of the RC is at 700 nm and not at 680 nm. Also in this case, once excited, the chlorophylls of the special pair release an energized electron and the P700<sup>+</sup> is "recharged" via reduction by the soluble carrier. Once energized, the electron again passes through a chain of carriers associated with PSI protein complex (in order: chl A<sub>s</sub>, chl A<sub>i</sub>, phyloquinone and Iron-Sulfur complex Fx). The final electron acceptor in PSI is, in *Archaeplastida*, an iron-containing molecule called ferredoxin (FD). In diatoms, FD can be replaced by an alternative electron acceptor, flavodoxin (FLD), in case of iron deficiency in the habitat. Indeed, FLD binds electrons via a flavin group that does not require any metal moiety, thus reducing iron dependence in these algae (Groussman et al., 2015; La Roche et al., 1996; Raven and Raven, 2019). Through the enzyme flavodoxin(ferredoxin)-NADP(H) reductase (FNR), the electron is shifted from flavodoxin/ferredoxin to its final acceptor, a molecule of Nicotinamide Adenine Dinucleotide Phosphate (NADP<sup>+</sup>) which is reduced to NADPH after the reception of two electrons and a proton sequestered from the stroma. NADPH is the principal reducing agent of the cell, used for a plethora of biochemical processes including lipid and nucleic acid biosynthesis and the Calvin Benson Bassham cycle described later in this section. Globally, the entire photosynthetic process just described can be summarized as a

passage of electrons from water to NADPH according to the formula:



This transport of electrons through PSII, PQ, Cyt b6f, cytochrome c6 and PSI is also called Linear Electron Transfer (LET, Fig.5).

Importantly, in diatoms PSII and PSI turn out to be structurally isolated. PSII, in particular, is localized at the level of the central thylakoid, while PSI is placed at the level of the two outer thylakoids of the stack of three, together with the Cyt b6f (Flori et al., 2017). Since the thylakoids are in continuity, this configuration does not prevent the transfer of electrons from PSII to PSI via the mobile carrier PQH<sub>2</sub> (Flori et al., 2017). The advantage of the segregation between PSII and PSI is that it avoids the direct thermodynamic energy transfer (spillover) from PSII to PSI bypassing the intermediate complexes (Flori et al., 2017). Energy spillover is observable in red algae, where it can cause a relevant drop in the efficiency of photosynthesis (Biggins and Bruce, 1989).

Anyhow, the generation of reducing potential in the form of NADPH is only the first result of photosynthesis. Indeed, the accumulation of positive charges in the lumen of the thylakoid thanks to the photolysis of water at the level of the OEC, the activity of the Cyt b6f complex and the reduction of PQ and of NADP<sup>+</sup> generates an electrochemical transmembrane potential. By exploiting this energetic potential, letting the protons move from the thylakoid lumen to the stroma, the ATPase complex phosphorylates ADP to obtain ATP. ATP will be then used as the energetic token used to power the metabolic processes of the cell, primarily the fixation of carbon in the form of sugars.

An important feature of the diatom chloroplast is its connection with the mitochondrion, so that the lumen of the two organelles, although functionally different, is in continuity (Bailleul et al., 2015). As in all

photosynthetic organisms, the ratio of NADPH to ATP generated by the operation of the LET in the thylakoid is unbalanced with respect to the energy requirements of the cell with, in particular, a surplus of reducing potential with respect to ATP produced (Bailleul et al., 2015). In order to balance the NADPH/ATP ratio, *Viridiplantae* have developed a series of redox processes ancillary to LET such as cyclic electron transport (CET) around the PSI or water-water cycles, which are however of minor importance in diatoms (Bailleul et al., 2015). In these algae this metabolic imbalance is resolved by the direct exchange of ATP, NADP(H) and O<sub>2</sub> between mitochondria and chloroplasts. This mechanism of ATP/NADPH ratio increase is also called meta-cyclic electron flow given the substitutive role with respect to CET (Bailleul et al., 2015; Zhou et al., 2020).

One of the main metabolic processes using the ATP and NADPH generated by the electron transfer machinery is the Calvin Benson Bassham Cycle (CBBC), sometimes called the dark phase of photosynthesis. This pathway is realized at the level of the stroma and consists, in short, in the fixation of CO<sub>2</sub> in the form of carbohydrates. Once the carbon accumulates as CO<sub>2</sub> or HCO<sub>3</sub><sup>-</sup>, it is moved to the stroma at the level of the pyrenoid. Pyrenoids are large aggregates of Ribulose-1,5-bisphosphate carboxylase-oxygenase (RuBisCO). The RuBisCO combines CO<sub>2</sub> molecules and a five-carbon sugar (ribulose 1,5 diphosphate) to form two molecules of a three-carbon product (3-phosphoglycerate, PGA), a process also called carboxylation. The reduction of PGA, involving NADPH and ATP (reduction phase of the CBBC) leads to the formation of glyceraldehyde 3-phosphate (G3P, two molecules generated per each CO<sub>2</sub> molecule entering the CBBC). For each 3 CO<sub>2</sub> entering in the CBBC, one excess molecule of G3P is produced and later used for the biosynthesis of sucrose, while the five remaining G3P molecules are on the contrary

reconverted to ribulose 1,5 diphosphate to restart the process.

To conclude, it is useful to consider how the concentration of dissolved  $\text{CO}_2$  in the oceans in the form of  $\text{HCO}_3^-$  (10-30  $\mu\text{M}$ ) is insufficient to saturate the enzymatic activity of RuBisCO at the pyrenoid level (Matsuda et al., 2017). For this reason, diatoms, like other photosynthetic organisms, have evolved carbon-concentrating mechanisms (CCM) to maximize  $\text{CO}_2$  concentration at the level of the thylakoid stroma to maximize CBBC efficiency (Tsuji et al., 2017). The CCM includes the use of a variety of bicarbonate active transporters (at least ten have been identified in model species) phylogenetically related to the ones found in *Metazoa*. In addition, CCM relies on the presence of

multiple Carbonic Anhydrases (CA) enzymes able to convert  $\text{CO}_2$  to  $\text{HCO}_3^-$  and vice versa. Diatoms use CAs to favor the diffusive uptake of  $\text{CO}_2$  at the cell surface by converting  $\text{HCO}_3^-$  to  $\text{CO}_2$  in the extracellular environment and the sequestration of carbon by transforming  $\text{CO}_2$  back to  $\text{HCO}_3^-$  once it has entered the cytosol. Finally, dedicated CA enzymes in the pyrenoid convert  $\text{HCO}_3^-$  to increase the local  $\text{CO}_2$  concentration improving RuBisCO activity (Matsuda et al., 2017; Tsuji et al., 2017; Young and Hopkinson, 2017). Finally, a C4-like photosynthesis, a pathway described in plants (Sage, 2004) has been proposed to be present in diatoms (Kroth et al., 2008). Still, the existence of C4-like photosynthesis in diatoms is controversial and has yet to be clarified in diatoms.

### I.3.b Photoacclimation and photoprotective mechanisms

If on the one hand light is indispensable for the activation of photosynthesis, on the other hand excessive irradiation can be harmful to the chloroplast. In strong light, in fact, the excitation of the chlorophylls of the special pair can be too fast to allow a proper uptake of electrons by the acceptors downstream of the chain. The inability of the RC chlorophylls to yield the excited electron leads to the formation of the triplet excited state of the chlorophyll ( $^3\text{Chl}^*$ ), which can in turn interact with  $\text{O}_2$  generating the highly reactive singlet oxygen form ( $^1\text{O}_2$ ) (Müller et al., 2001).  $^1\text{O}_2$  in turn generates additional reactive oxygen species (ROS) such as superoxide oxygen ( $\text{O}_2^{\cdot-}$ ), hydrogen peroxide ( $\text{H}_2\text{O}_2$ ) and hydroxyl radical ( $\text{OH}^{\cdot}$ ), which can damage membrane lipids, hence representing a relevant threat for the cell. Given that the uptake processes downstream of PSI are extremely rapid and difficult to saturate, the generation of  $^3\text{Chl}^*$  and subsequent production of ROS are primarily attributable to overexcitation of PSII.

In order to optimize the use of light to fuel photosynthesis without it becoming dangerous, diatoms, like all other photosynthetic organisms, put into practice a series of strategies to adapt their photosynthetic apparatus according to the intensity of radiation. These phenomena are called photoacclimation (Dubinsky and Stambler, 2009). In case of weak light, plastids accumulate a greater amount of pigments so as to maximize the optical density of the cell and increase the capacity of photon absorption. On the contrary, in case of high light, the content per cell of pigments functional to the absorption of photons such as chl and Fx decreases so as to reduce the tendency to over excite the photosystems (Anning et al., 2000; Dubinsky and Stambler, 2009; Pniewski and Piasecka-Jędrzejak, 2020). The net amount of photosystems present on thylakoids also decreases (Dubinsky and Stambler, 2009; Taddei et al., 2018), but in return the expression of associated proteins remains high to compensate for the higher turnover of photosystem degradation in high light (Dubinsky and Stambler, 2009). To



counteract the increased production of ROS, cells also produce more antioxidant enzymes such as catalases, peroxidases, or superoxide dismutases (Dubinsky and Stambler, 2009). At high photon fluxes the cells also increase the amount of RuBisCO subunits per photosystem (Dubinsky and Stambler, 2009), which causes the photosynthetic activity and carbon fixation rate to saturate at higher light intensities (Anning et al., 2000; Schellenberger Costa et al., 2013a; Taddei et al., 2018). The increased energy availability at high light normally results in increased growth rates compared to what is observed at low light (Anning et al., 2000; Brand and Guillard, 1981, 1981; Pniewski and Piasecka-Jędrzejak, 2020), at least until the light stress becomes excessive (Brand and Guillard, 1981).

To avoid the occurrence of  $^3\text{Chl}^*$  and its subsequent risks, photosynthetic organisms possess a variety of defensive processes that avoid overexcitation of the RC in PSII. Because these phenomena lead to a de-excitation of chlorophyll (which also occurs alternatively as a result of normal activation of LET in the photochemical process) these mechanisms take the name Non-Photochemical Quenching (NPQ) of chlorophyll fluorescence. The mechanisms of NPQ can be distinguished by the timing of activation and relaxation following the end of excess light irradiation (Eberhard et al., 2008).

A first, slow component of NPQ is the so-called photoinhibition (or qI), which consists in the degradation of the protein D1 of PSII that, as seen in the previous paragraph, interacts with the special pair of chlorophylls. The reversion of qI occurs through the resynthesis of functional forms of the D1 protein and the replacement of the damaged copy with the new one, a process that can take several minutes or even hours. In *Archaeplastida*, another form of slow NPQ is the state transition (qT), which involves the displacement of a portion of the peripheral antennas of PSII toward PSI, so as to balance

the excitation between the two photosystems and reduce the pressure on PSII. In diatoms, however, no form of qT has ever been observed, a fact that can be explained given the spatial segregation between the two photosystems in different thylakoid regions (Flori et al., 2017).

As for the fast components of NPQ, this photoprotective system is related to the dissipation of excess energy in the form of heat, it responds rapidly to changes in light intensity and is commonly called qE. In qE, a main role is played by the de-epoxidation of xanthophylls (*i.e.* oxygen containing carotenoids) in a reversible process named Xanthophyll Cycle (XC). In plants and green algae, the XC consists of the pH-dependent conversion from violaxanthin, with two epoxide groups, first to antheraxanthin (one epoxide group) and then to zeaxanthin (no epoxide). The de-epoxy xanthophylls are believed to favor the relaxation of chlorophyll by both directly absorbing the excess energy (that will be then released as heat) or by acting as allosteric regulators of the LHC (Müller et al., 2001). In particular, they might cause a conformational switch of the LHC that eases the autonomous de-excitation of chl via heat dissipation. In diatoms, the violaxanthin-zeaxanthin cycle is present, but an additional XC involving the de-epoxidation of diadinoxanthin (one epoxide) to diatoxanthin (no epoxide) (Lohr and Wilhelm, 1999) is the main contributor to the high photoprotective capacity of these algae (Blommaert et al., 2021). Interestingly, in *Archaeplastida*, the synthesis of de-epoxidized xanthophylls by the enzyme violaxanthin de-epoxidase (VDE) is strictly dependent on excessive acidification of the thylakoid lumen, one of the consequences of overloading the photosynthetic chain. In contrast, in diatoms, diatoxanthin epoxidation is repressed upon acidification of the thylakoid, but once the diatoxanthin concentration rises up NPQ capacity becomes independent on proton gradient (Goss et al., 2006).

Also, diatom fast NPQ relies on specific members of the LHC family specialized in photoprotection, the LHCXs, which act as qE effectors. This family of proteins has undergone a major expansion in diatoms. *P. tricornutum* genome for example contains 4 genes encoding for LHCX antennae (Taddei et al., 2016), a number that increases to 11 in the polar diatom *Fragilariopsis cylindrus* (Mock et al., 2017). LHCX genes are regulated in response to a variety of environmental signals, including light and nutrient deficiency (Taddei et al., 2016). In *P. tricornutum* a down regulation or obliteration of one of these proteins, LHCX1, affects significantly NPQ photoprotective capacity (Bailleul et al., 2010; Buck et al., 2019; Giovagnetti et al., 2022). LHCX proteins are phylogenetically related to LHCSR proteins from green algae, which are also involved in NPQ induction (Bailleul et al., 2010). The photoprotective effect of LHCSRs is activated following the protonation of some of their residues on the luminal side and the consequent conformational change of the protein (Ballottari et al., 2016). The photoprotection mediated by LHCSR proteins is induced by the excessive acidification of the thylakoid lumen. However, diatom LHCX proteins do not present all the amino acids responsible for this process in the green lineage and lost a large portion of the C-terminal end immersed in the thylakoid

lumen, suggesting a different mode of activation (Bailleul et al., 2010; Giovagnetti et al., 2022). Still, it has been proved in some diatoms that the acidification of the thylakoid is necessary to induce the activation of the xanthophyll cycle and, therefore, of a component of NPQ (Chukhutsina et al., 2014; Goss et al., 2006). This suggests the existence of a proton concentration sensing system in the thylakoid. Although the details of LHCX protein activation remain to be elucidated, recent investigations have identified an amino acid domain containing a tryptophan near the site of interaction with xanthophylls that is involved in qE generation (Buck et al., 2021).

As a concluding remark, it is useful to note that the oxidation status of the PQ pool is involved in the regulation of LHCX gene expression (encoded in the nucleus) and in xanthophyll neosynthesis (Lepetit et al., 2013). The control of nuclear gene expression according to the level of PQ oxidation (also called retrograde signaling) is a phenomenon already observed in the past in *Archaeplastida* (Kleine et al., 2009), but the details of how this process occurs are still unclear in diatoms. In any case, this phenomenon makes evident the presence of a tight crosstalk between the plastid and the nucleus as well as their interdependence in phenomena of regulation of physiology.

### I.3.c Light as a source of information: photo-perception

Given the highly variability and dynamic of the photic environment in oceans, light represents a fundamental source of information for aquatic life. Light quality underwater changes in function of multiple parameters, such as water turbidity, depth, daytime and season among others. Organisms evolved a variety of proteins able to perceive light, the photoreceptors, of which most are composed of a non-protein moiety (the chromophore) associated with an amino acid

backbone. The activation of the photoreceptor is induced by the conformational changes in the tridimensional structure of the protein after the chromophore interacts with a photon of the correct wavelength. These proteins can therefore be categorized depending on the wavelength they are sensitive to, the nature of their chromophore and the protein domain composition (Jaubert et al., 2017).

Diatoms, in particular, possess a rich set of photoreceptors capable of detecting light throughout the whole visible spectrum (Jaubert et al., 2017). Red and Far-Red radiation is perceived by phytochromes which, in diatoms, show a structure similar to that of their bacterial counterpart and are commonly named DPH. Moreover, DPHs absorb at longer wavelengths of red and far-red light, compared to plant phytochrome (PHY). In *P. tricornutum*, it has been also shown that far-red light is the wavelength inducing signal transduction propagation (Fortunato et al., 2016). Photosynthetic organisms absorb light predominantly in red and blue, while reflecting most of the far-red. This means that the greater the density of phototrophs in the vicinity, the smaller the R:FR ratio. In terrestrial plants it has been thoroughly characterized how the ratio between irradiation in the red and far-red (R:FR ratio) sensed through phytochromes plays an essential role in the perception of surrounding phototrophs. Specifically, phytochromes play a central role in shade avoidance processes (Pierik and de Wit, 2014). Phytochromes of marine algae, including diatoms, could play a similar role in determining the presence of neighbor phototrophs and therefore the perception of cell density in the surrounding environment. However, the density of microalgae per unit volume remains very low overall, even during reproductive blooms, making this an unlikely possibility. It is important to recall that long wavelength light is quickly absorbed in the water column, making it tricky to hypothesize the possible biological role of these receptors in diatom biology. It is not to be excluded that red light perception might play a role in the regulation of biological rhythmicity, as it has already been largely demonstrated in plants (Devlin and Kay, 2000; Somers et al., 1998). Still, no direct evidence for such a function has been found yet.

Diatom genomes also show the presence of putative photoreceptors of the rhodopsin (RHO) family. Although no

characterisation of their function and absorption properties has been carried out, diatom RHOs could act as detectors of intermediate wavelengths (centered in the blue-green) or as photoreceptors that function as transmembrane ion pumps as in other organisms (Jaubert et al., 2017). Notably, diatom RHOs show high similarity to bacterial xanthorhodopsin, suggesting that their genes were acquired by HGT (Strauss, 2012).

Since blue light dominates below the sea surface and is the most penetrating in the water column, it is not surprising that diatoms (like other groups of phytoplankton) have multiple receptors for this wavelength (Jaubert et al., 2017). Photoreceptors of the Cryptochrome Photolyase Family (CPF) belong to this class of blue detectors. CPF proteins non covalently bind flavin adenine dinucleotide (FAD) as chromophore. FAD is reduced upon photon absorption, causing a conformational modification of the CPF protein and determining its capacity to interact with other protein partners. As their name suggests, CPFs include Photolyase proteins (PL), enzymes involved in blue light-activated DNA repair upon UV damage like cyclobutane pyrimidine dimer (CPD PLs) or (6-4) pyrimidine-pyrimidone photoproducts (6-4 PLs). Still, not all CPFs conserved this DNA repair activity, as in the case of plant cryptochromes which serve as blue light photoreceptors. Concerning diatoms, these algae possess animal like CPF 6-4 photolyases (Coesel et al., 2009), plant-like CRYs (CryP, only distantly related to canonical plant cryptochromes (Juhas et al., 2014) and several CRY-DASH (Drosophila Arabidopsis Synechocystis Human) proteins (Coesel et al., 2009; Fortunato et al., 2015). The latter are CPF proteins found in eukaryotes as well as in prokaryotes, whose function has not been fully characterized yet (Fortunato et al., 2015; Jaubert et al., 2022).

Contrary to green algae and plants, blue-detecting phototropins, containing LOV

and kinase domains, cannot be found in diatoms. On the contrary, diatoms possess other blue light photoreceptors with LOV domains known as aureochromes. Originally identified in the *Xanthophyta Vaucheria frigida* (Takahashi et al., 2007), photoreceptors of the aureochrome family are found only in *Stramenopila* and in the *Raphidophyta Heterosigma akashiwo* (Ji et al., 2017). Aureochromes consist of a light-sensing LOV domain associated with a bZIP domain involved in DNA binding and regulation of gene expression (Kroth et al., 2017; Mann et al., 2020). Specifically, it has been shown in *P. tricornutum* that approximately 75% of the genes respond to the transition from red to blue light by rapid (few minutes) down-regulation or up-regulation (Mann et al., 2020). This response is almost completely suppressed in KO mutants of *aureochrome 1a*, indicating the broad-spectrum impact that these blue receptors may have on gene transcription, possibly inducing a cascade of reactions mediated by other transcription factors. The role of aureochromes in gene regulation has recently been characterized in the *Eustigmatophyceae Nannochloropsis oceanica*, in which these photoreceptors appear to play an important role in fatty acid metabolism (Poliner et al., 2022).

Blue light photoreceptors can regulate the physiology of diatoms in response to environmental stimuli. First of all, blue light

### I.3.d Cell cycle progression and regulation in diatoms

Diatoms are characterized by a high growth rate both under laboratory conditions and in natural environments (Sarhou et al., 2005; Spilling and Markager, 2008). Such a growth capacity plays an important role in the ecological success of these algae both at low latitudes and in polar environments (*e.g.* Lafond et al., 2019; Smayda, 1980; Spilling and Markager, 2008). Understanding how diatoms regulate their cell division and how it

plays a pivotal role in the regulation of photoacclimation and photosynthesis (Schellenberger Costa et al., 2013a; Valle et al., 2014) which is mediated by the above-mentioned photoreceptors. Indeed, in *P. tricornutum* CryP, CPF1 and aureochromes 1a and 1b are all involved in the expression of the protein complexes responsible of light harvesting and photoprotection (Coesel et al., 2009; Mann et al., 2020, 2017; Schellenberger Costa et al., 2013a, 2013b), see Paragraph I.3.a). Moreover, blue light is also central in the modulation of cell cycle progression and circadian rhythmicity. Cryptochromes are known to play a role in the circadian clock in animals (Kume et al., 1999; Putker et al., 2021), as well as in plants (Somers et al., 1998) and (potentially) in other secondary endosymbiont algae (Brunelle et al., 2007). In mammalian cells, the cryptochromes mCRY1 and mCRY2 are involved in the repression of CLOCK and BMAL1, positive elements of the transcriptional feedback loop of the circadian oscillator (Kume et al., 1999). Notably, the animal-like CPF1 of *P. tricornutum* is able to repress CLOCK:BMAL in simian *mCRY1* knockout cells, thus complementing the function of the lost endogenous cryptochrome (Coesel et al., 2009). This result suggests that CPF1 might play a similar role in the circadian oscillator in diatoms, although no evidence in this direction has been collected so far.

responds to environmental stimuli is essential to understanding their ecological success. The first studies on diatom cell division long precede the advent of molecular biology and date back to the end of the 19th century, with the pioneering studies of Robert Lauterborn (Lauterborn, 1896; Pickett-Heaps, 1991). The use of molecular analysis and advanced microscopy techniques (in particular transmission electron microscopy) have more

recently allowed us to characterize in more detail the fascinating complexity of cell division in these microalgae.

As in all other eukaryotes, the mitotic cycle of diatoms includes a precise succession of phases. The S phase (for DNA Synthesis) is the one in which takes place the replication of genomic material to be redistributed to daughter cells; the M phase (for Mitosis), where the actual duplication of the nucleus in two copies, the redistribution in them of the genome copies and, to end, the division of the mother cell in two daughters (cytokinesis). The S phase and M phase are separated by two G phases (for Gap) in which the cell performs its normal metabolic functions, grows and prepares for division. These two G phases are called G1 (which is between M and S) and G2 (between S and M), respectively.

Such a complex process as the cell cycle has to be regulated by a refined molecular machinery. In eukaryotes, this machinery involves proteins called cyclins (CYC) and the CYC dependent protein kinases (CDK), proteins that are highly conserved throughout the eukaryotic kingdom (De Martino et al., 2009; Huysman et al., 2014b). The function of CDKs is to regulate the activity and stability of target proteins involved in the cell cycle by means of their phosphorylation. The cyclins, for their part, determine the substrate specificity of CDKs and make them active by inducing their conformational change. A classic example of a process regulated by cyclin-CDK complexes is the entry into S-phase associated with the Rb (retinoblastoma) protein and E2F-DP transcription factors, a mechanism conserved in all eukaryotes except yeast (Giacinti and Giordano, 2006). G1-phase-specific cyclin-CDK complexes induce phosphorylation of Rb, thereby interfering with its interaction with E2F-DP. Freed from the inhibitory interaction

of Rb, the E2F-DP complex can initiate transcription of genes involved in genome duplication. In *P. tricornutum* it is hypothesized that the complex formed by the CDKA1 and dsCYC2 proteins is involved in this G1-S transition (Huysman et al., 2013, 2014b). It is also important to note that the proper activation of CDK proteins does not only involve cyclins. Phosphorylation of CDKs by CDK Associated Kinases (CAKs) also plays a central role (Kaldis, 1999). Equally, the timely proteolysis of CYCs, CDKs and their targets is regulated by appropriate E3 ubiquitin ligase complexes, the Skp1/Cullin/F-box complex (SCF) and the anaphase-promoting complex (APC). *P. tricornutum* has been shown to have conserved the genes coding for these complexes (Huysman et al., 2014a).

Remarkably, comparative genomic studies demonstrated that canonical cyclins underwent an important process of duplication in diatoms with a consecutive expansion of this gene family, with a total of 13 canonical cyclin coding genes found in *P. tricornutum* (Bowler et al., 2008; Huysman et al., 2010, 2014b). In addition to the canonical cyclins, diatom also evolved a complex set of unique cyclins called diatom specific cyclins (dsCYC) (Huysman et al., 2010). Different CYCs and CDKs are expressed during well determined moments of the cell cycle and regulate the transition through the aforementioned checkpoints, so that each phase of the cell cycle can be associated to a defined set of CYCs and CDKs (De Martino et al., 2009; Huysman et al., 2010, 2014b). The follow up of the expression of these proteins (*e.g.* via reverse transcription quantitative PCR) can be used as a proxy to follow the progression of cells through the different phases of cell cycle (Huysman et al., 2010, Fig.6).

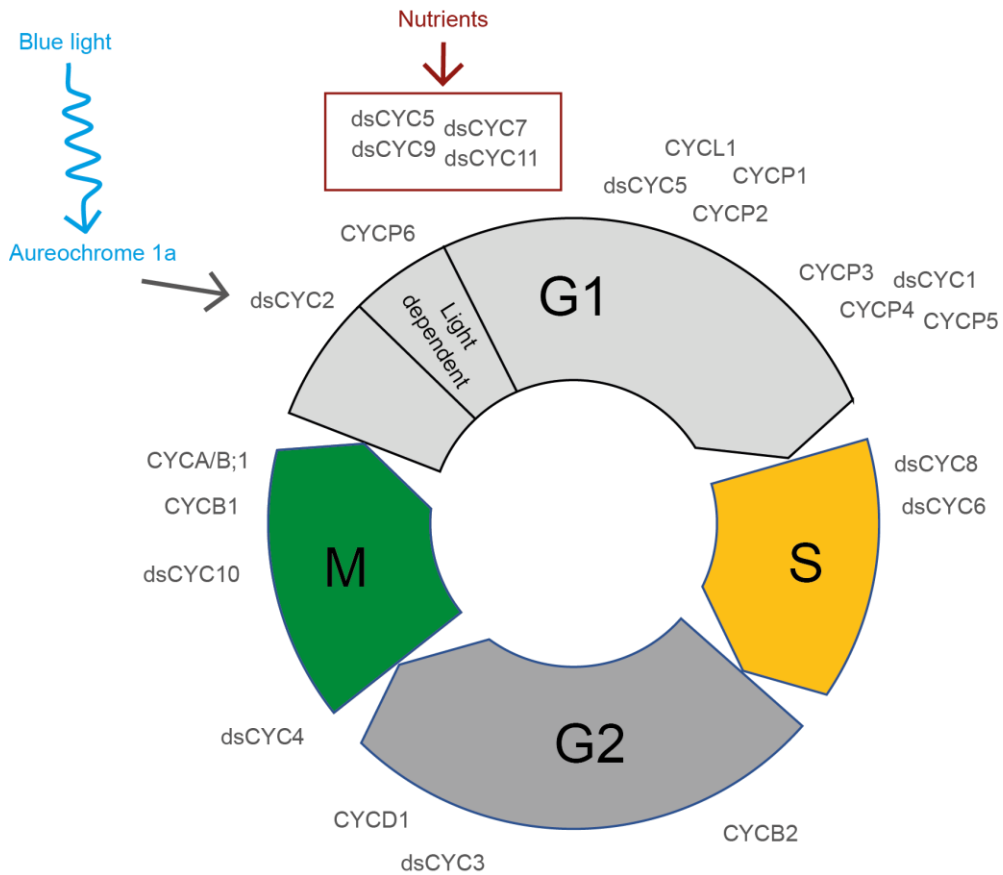


Figure 6. Diatom cell cycle and cyclins

Schematic representation of the cell cycle. Arrows indicate the different phases (G1: Gap1, S: Synthesis of genome copy, G2: Gap2, M: Mitosis). The different cyclins possibly involved in the regulation of diatom cell cycle advancement are loosely arranged to correspond to the time of the cycle in which they are expressed, following (Huysman et al., 2010). Nutrients responsive cyclins are highlighted in red. Blue light dependent expression of dsCYC2, mediated by the photoreceptor aureochrome 1a in *Phaeodactylum tricornutum* is highlighted in blue. Light dependent segment of G1 phase is equally shown. Image based on (Bilcke et al., 2021; Huysman et al., 2010, 2013).

It has been proposed that this expansion allows diatoms to respond promptly to environmental conditions and adapt cell division accordingly (Huysman et al., 2014b). Indeed, the progress of the cell cycle is strictly regulated by so-called checkpoints that ensure the correctness of the genetic material before its distribution among the daughter cells as well as the proper accumulation of energy resources essential for the completion of mitosis. These checkpoints can be located in the G1 phase (before the G1-S transition) or during the G2 phase (for the G2-M transition). In diatoms, light exposure plays a major role in controlling the transition from one phase of the cycle to another (Huysman et al., 2013; Vaultot et al., 1986). We can distinguish between light-dependent

and light-independent phases of the cell cycle, which can be studied by inducing a forced arrest of cell division via a prolonged dark treatment, after which the cells will tend to synchronize in the same phase (Gillard et al., 2008; Huysman et al., 2010; Vaultot et al., 1986). In some diatom species, the exposure to prolonged dark induces only part of the cultures to stop cell cycle progression in G1, while the remaining fraction arrests in G2 phase (Brzezinski et al., 1990). The centric diatom *Thalassiosira weissflogii* is an example of species showing similar responses to dark (Ashworth et al., 2013; Vaultot et al., 1986). These results suggest the existence of two light-dependent checkpoints in G1 and G2 respectively. In other species the dark treatment causes an almost complete

synchronization of cultures only in G1 phase, as it happens in *P. tricornutum* (Huysman et al., 2010) or *S. robusta* (Gillard et al., 2008). The G1 light-dependent progression has been dissected in *P. tricornutum* (Huysman et al., 2013), while the G2 light-dependent checkpoint observed in other species remains uncharacterised. Specifically, the diatom specific cyclin dsCYC2 has been demonstrated to be involved in the gating of cell division in response to light exposure in *P. tricornutum*. dsCYC2 ensures the proper transition from G1 to S phase to the extent that downregulation of dsCYC2 causes reduced growth capacity in *P. tricornutum* (Huysman et al., 2013). In *P. tricornutum*, light dependency of dsCYC2 is ensured by the blue light-sensitive photoreceptor aureochrome 1a (Fig.6). As reported, aureochromes act both as photoreceptors via their LOV domain and as DNA binding transcription factors via their bZIP fold. Upon light irradiation, *P. tricornutum* aureochrome 1a dimers bind dsCYC2 promoter along with homodimers of bZIP10 transcription factor and induce its expression (Huysman et al., 2013). A similar blue-light dependent regulation of dsCYC2 expression and G1 progression has been recently described in the benthic pennate diatom *S. robusta*, suggesting a possible conservation of this mechanism (Bilcke et al., 2021b).

Nutrient availability is another factor affecting diatom cell cycle and population dynamics, a principle valid for other marine microorganisms. Various dsCYC genes have been found to be differentially expressed under conditions including phosphate depletion (dsCYC5, dsCYC7, and dsCYC10), and the presence of silica (dsCYC9, Fig.6, Bowler et al., 2008; Huysman et al., 2010, 2013; Sapiel et al., 2009). In oceanic ecosystems, the elements that represent the main limiting factors for planktonic proliferation are nitrogen, phosphorus, iron and, in part, silicon (Falkowski et al., 2008, 1998). The depletion of these nutrients causes

a slowdown if not an arrest of cell division in diatoms. A prime example is given by nitrogen, an element fundamental for the biosynthesis of amino acids as well as pigments and other biomolecules and for overall diatom growth (Valenzuela et al., 2012). Nitrogen limitation and starvation have been shown to stop cell cycle progression at the G1 phase in diatoms (Huysman et al., 2014b; Vaulot et al., 1987).

The last step of cell division is, as already mentioned, cytokinesis. The cytokinesis patterns of diatoms exhibit features intermediate to those seen in other organisms. They possess a unique microtubule (MT)-organizing center (MTOC), also called the MT center, similar to those that can be found in animals and yeasts but absent in plants (De Martino et al., 2009; Pickett-Heaps and Tippit, 1978). Pennate diatoms lack animal-like centrioles, which are however present in microgametes of centric diatoms (De Martino et al., 2009). Also, diatom MTOC differs from its counterpart in brown algae (*Stramenopila*) that have an animal-like centrosome containing two centrioles. This diversity highlights the extreme evolutionary malleability of cell division mechanisms and organization even in phylogenetically closely related organisms (De Martino et al., 2009). During cytokinesis, the division of the mother cell in the two daughters occurs thanks to a longitudinal cleavage furrow that spans across the cell. The new Golgi apparatus, endoplasmic reticulum, mitochondria and plastids all align to this furrow ready to split to the two new cells, implying a major synchronization of the duplication of these organelles with the cell cycle and an important intracellular membrane trafficking (A. Tanaka et al., 2015). Of particular relevance, is the timing and regulation of chloroplast(s) division along the cell cycle. Diatoms display a considerable variability in the number of chloroplasts depending on the species. They can be indeed classified in five different groups: monoplastidic, diplastidic,

tetraplastidic, oligoplastidic, and polyplastidic species (Mann and Droop, 1996). In diatoms, with the exception of polyplastidic species, the development and division of the chloroplast is tightly coordinated with cell cycle progression (Gillard et al., 2008; Huysman et al., 2010). This synchronization is clearly of cardinal importance to ensure an equitable redistribution of plastids among daughter cells and has been extensively studied in pennate diatoms, in particular in the model species *Seminavis robusta* (Gillard et al., 2008) and *Phaeodactylum tricornutum* (Huysman et al., 2010). When synchronized under prolonged dark, the cells begin DNA synthesis 4 hours upon re-illumination and cytokinesis starts after 9-12 hours when first cells begin to display the longitudinal division furrow (Gillard et al., 2008). Cytological observations and analysis of the transcriptional profile of these algae also showed that chloroplast division precedes nuclear and cellular division, thus ensuring the correct and orderly succession of division processes (Gillard et al., 2008; Huysman et al., 2010). Given this fine synchronization between cell cycle and chloroplast division, the optical properties of the plastid can be used as a proxy for the progress of cell division. One of the methods that can be used for this purpose is the analysis of chlorophyll fluorescence per cell by flow-cytometry (Annunziata et al., 2019; Hunsperger et al., 2016; Ragni and d'Alcalà, 2007) (described in more detail throughout this thesis). Such a coordination of plastid biogenesis and cell division obviously requires fine-tuning of gene expression and a dedicated set of proteins. Some of these are conserved and shared with plants and other algae, being a relic of the cell division mechanism of the host prokaryote that gave rise to the plastid. Among these, the FtsZ protein is the best known in plants (TerBush et al., 2013) and several FtsZ copies have been found in diatoms (Ait-Mohamed et al., 2020; Gillard et al., 2008). Analysis of FtsZ genes expression can be used as a tool to follow the temporal

progression of chloroplast division (Gillard et al., 2008).

In the natural environment diatoms (like other groups of phytoplankton) can display a “bloom and bust” life cycle. When they encounter favorable environmental conditions of light, temperature, nutrient availability (often linked to fluvial runoff of onshore deposits and upwelling of nutrient-rich deep water in proximity of the coast (Lassiter et al., 2006)) they undergo a rapid acceleration of the mitotic rate and a consequent exponential increase in cell concentration, to such a degree that these “flowering” phenomena are easily observed from space (Anderson et al., 2011; Gross, 2012; Raitos et al., 2008). These blooms are followed by a population collapse likely due to a combination of abiotic and biotic factors, including predation by grazers, depletion of nutrient resources and the action of viral pathogens (Gross, 2012; Smetacek, 2012; Vincent et al., 2021). These algal bloom events are not only of utmost importance for the functioning of marine trophic networks, but also represent a phenomenon of major importance for public health issues. In fact, toxic microalgae blooms are well known and extensively studied and can represent a significant danger to humans and marine life, including those of the diatom genus *Pseudo-nitzschia* (Walsh, 2008).

Notably, structure and composition of oceanic microbial communities show seasonal patterns, also due to the response to seasonal cyclic phenomena such as the availability of nutrients and other physical and chemical parameters of the water (Gilbert et al., 2012; Lambert et al., 2019; Marquardt et al., 2016) and, possibly, day length. Photoperiod perception and photoperiodism have already been long studied in different terrestrial organisms (Pittendrigh and Minis, 1964) and the primary role of endogenous molecular clocks (see below) in regulating these phenomena is well known in terrestrial organisms (Farré and Weise, 2012). For this,



one of the dominant hypotheses is that also the molecular clocks of microalgae have a leading role in the control of blooming phenomena in response to the correct photoperiod (Lambert

et al., 2019). Still, how and to what extent this is true remain unanswered questions.

# I.4 Biological clocks

## I.4.a Biological clocks: principles and characteristics

For every living organism, the ability to adapt to its environment and its changes is the basis of evolutionary success. However, some of the environmental stimuli to which they have to respond are not unpredictable and follow a precise rhythmicity linked to precise geophysical processes: the day/night cycles due to the rotation of the earth on its axis (with the consequent rhythmic oscillations of temperature), the succession of seasons due to the revolution of our planet around the sun, the tides and the cycles of illumination due to the light reflected from the moon linked to the rhythms of our satellite. Being able to anticipate these changes and prepare metabolism and physiology in advance to best respond to these changes is therefore a huge fitness advantage (Johnson and Golden, 1999; Ouyang et al., 1998; Sanchez et al., 2011). For this reason, a large variety of prokaryotic and eukaryotic organisms have developed molecular timekeeping machinery that allows them to generate endogenous rhythms that oscillate with the same frequency of the environmental rhythms and thus regulate cellular as well as organism-wide activity. Given their timekeeping function, these molecular mechanisms are commonly referred to as biological clocks<sup>3</sup>

We can describe such an oscillator as a system that tends, in a regular manner, to move away from equilibrium before moving back to it (Dunlap, 1999). The rhythmic activity of such a mechanism (and of the processes it regulates downstream) can be assimilated to a sinusoidal function (Fig.7) and is characterized by a series of parameters such as: the amplitude of oscillation, *i.e.* the difference between the value of the system at

the equilibrium and the value assumed at its maximum deviation from the equilibrium itself; the phase, which for simplicity can be described here as the relative position of the peak of oscillation relative to the reference system (in the case of a biological clock, for example, it can be the moment of maximum activity of a daily cyclic process with respect to the time of the day); and the period, *i.e.* the time interval between two peaks of oscillation.

Depending on the length of the oscillations (and therefore, the environmental cycles they are synchronized with) biological clocks can be divided in: circadian (“approximately daily”) when they follow solar 24hrs cycles; tidal (24,8hrs) and semitidal (12,4hrs) when they follow the course of tides; lunar (29,5 days) or semilunar (14,8 days) in the case they are synchronized with cycles of moon illumination phases; circannual when they oscillate following the 365 days earth revolution. The discipline that studies biological rhythmicity and the cellular and molecular processes that govern them is also called chronobiology. Although biological clocks are composed of different molecular “gears” depending on the phylum considered, they all share common features. Before entering in the description of the different molecular clocks known today, it is useful to describe which are these common characteristics. A first important feature of biological clocks is their “three-level” structure. They are in fact composed of the proper molecular oscillator called the core clock. At a second level, a series of mechanisms of perception of environmental stimuli (input pathways). Finally the output pathways are the set of biological processes controlled by the core clock and that are

---

<sup>3</sup> The use of the term biological clocks has become mainstream during the 1960 Cold Spring Harbor

Symposium of Quantitative Biology, titled “Biological Clocks.”(Cold Spring Harbour, 1960)

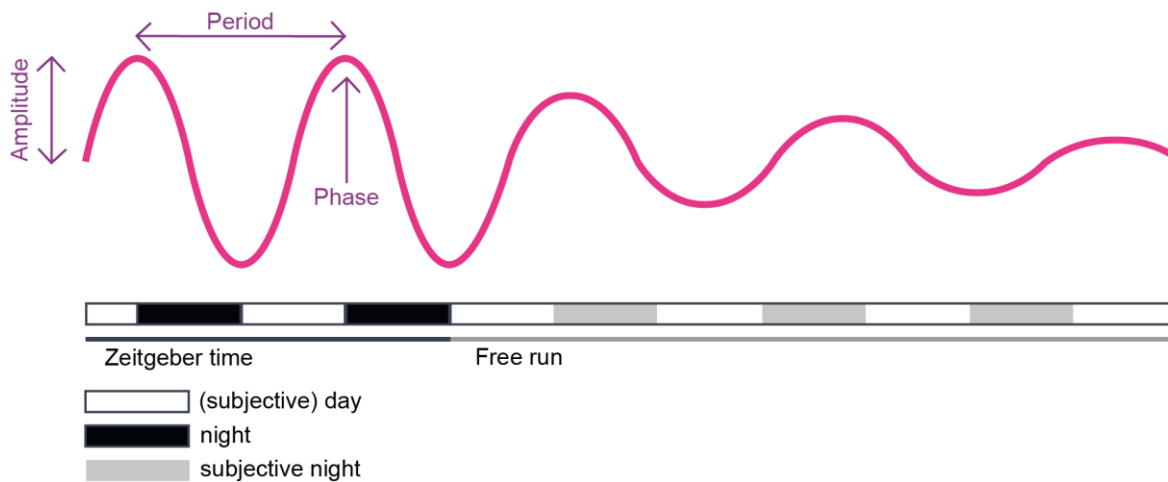


Figure 7. Main characteristics of biological rhythms

Schematic representation of a generic rhythmic biological process. Oscillations can be modelled to a cosine function with a period equivalent to that of the environmental cycles in *Zeitgeber* time (*i.e.* in presence of rhythmic external cues). Two headed arrows highlight the main parameters that can be used to describe rhythmic oscillations: amplitude, phase (in this case, the acrophase, *i.e.* the peak of the oscillation), and period (the time separating two points with the same phase). Following release to free run, the oscillations persist if the process is regulated by a circadian clock, but can show a progressive damping of the oscillation amplitude over time (*e.g.* Ould *et al.*, 2018). The period in free run, although close to that observed in *Zeitgeber* Time, can shorten or lengthen (as in the example shown in the figure). In the figure, light has been chosen as an example of rhythmic cue: white boxes represent light periods (days) in the *Zeitgeber* time and in free run; black boxes represent dark periods (nights) under *Zeitgeber* time; gray boxes represent subjective dark periods after release to continuous light. Other environmental cues (*e.g.* temperature cycles) can exert a similar synchronization of the biological activity.

rhythmic in response to the cyclic activity of the latter (Dunlap, 1999; Wijnen and Young, 2006). Focusing on the core clock, such a mechanism can be achieved by negative feedback loops in which a set of positive elements induces the synthesis of negative elements which, in turn, acts as a brake by blocking the synthesis or activity of the positive ones (Dunlap, 1999). The core clock is taken to mean the minimal set of molecular causes (hence proteins and regulatory DNA sequences) sufficient to operate circadian cycles (Dunlap, 1999).

The input pathways are involved in the second common feature of biological clocks, that is their ability to synchronize with the external environment through the perception of periodic cues detected by specific receptors (principle commonly named “entrainment”). The primary function of entrainment is to ensure that endogenous

biological oscillations constantly adapt to external conditions, ensuring for example that cellular physiology synchronizes to light/dark transitions and vice versa even when these vary over the course of the year with the passing of the seasons (Webb *et al.*, 2019). A classic example of entrainment in humans is given by the readaptation of biological rhythms following sudden geographical displacements (jet lag recovery) (Leloup and Goldbeter, 2013; Roenneberg *et al.*, 2007). The factors capable of synchronizing the endogenous clock are commonly called *Zeitgebers* (from the German “timegivers”) a term coined by Jürgen Aschoff, one of the founders of chronobiology (Aschoff, 1954). The most obvious *Zeitgeber* involved in the synchronization of the clock is undoubtedly light, an indicator of the passage of the day-night cycle. However, the temperature cycles associated with the alternation of day and night represent a time giver of primary importance

in the synchronization of biological activity (Eckardt, 2005). Small temperature oscillations (less than 2°C) have been shown to be sufficient to affect the entrainment of a variety of organisms as different as fungi, plants and animals (Rensing and Ruoff, 2002). Still, the molecular actors involved in the sensing of these cues and in the downstream synchronization of the endogenous oscillator have to be clarified. *Zeitgebers* can also be represented by factors other than simple physical stimuli from the environment. For example, metabolic inputs (food in the case of animals or sugars produced by the cyclic activity of photosynthesis in autotrophs) also play a relevant role in synchronizing the rhythmicity of the organism (Carneiro and Araujo, 2012; Haydon et al., 2017, 2013). Significantly, in the case of social animals, the interaction with peers can also promote a synchronization of activity and behavior at the level of the group in a mechanism that can even override the synchronization mediated by physical environmental stimuli (Fuchikawa et al., 2016; Levine et al., 2002). Importantly, the synchronization of biological activity with the environment also allows for the temporal separation of conflicting physiological processes. A classic example of this temporal separation is found, for example, in nitrogen-fixing cyanobacteria. In these organisms the clock regulates the differential expression of the enzyme nitrogenase (inhibited by oxygen) during the night, when oxygenic photosynthesis is not active (Kondo and Ishiura, 2000; Mitsui et al., 1986).

The ability to synchronize the oscillations of the circadian clock with the external cues via the input pathway is also at the basis of the third common characteristic of circadian clocks, namely the aforementioned anticipation of environmental cycles. In other words, the predictability of environmental cycles and the fact that the endogenous timekeeper oscillates on their same frequency allows the clock to prepare the physiological response to a phenomenon before it occurs

(for example the preparation of metabolism to the arrival of sunlight in phototrophic organisms (Dodd et al., 2014, 2005)). Typically, the appearance of a biological response before an environmental stimulus and not in direct response to it is strong evidence of its regulation by an endogenous clock (Harmer et al., 2000). However, it is important to remember that when *Zeitgebers* act on input pathways outside the expected time window and/or if they are too intense (e.g. high light irradiation) they can affect the overt rhythms in a positive or negative way, overriding the activity of the clock and inducing/repressing a specific rhythmic process out of time. In this case, the organism uncouples its activity from the endogenous oscillator and responds directly to the stimulus, in a phenomenon called clock masking (Aschoff, 1999; Redlin, 2001). On one side, masking effects show that clocks do not control physiology in an inflexible manner and that some sort of flexible and adaptive response to the environment is possible. On the other side, small "disturbances" in the rhythmic environment will not have major effects on the timing of an activity, ensuring some degree of rigidity in the system.

The fourth characteristic of endogenous clocks is persistence, probably the most relevant for the study of biological rhythms. Persistence consists in the ability of oscillators to maintain their rhythmic activity even after the organism is moved to a "free run" study condition, *i.e.* in which the environment is constant and all the rhythmicity of *Zeitgebers* is eliminated (e.g. continuous light or continuous darkness, Fig7). Crucially, free-run oscillations should have a frequency close to that observed before the transition (e.g., approximately 24-hour rhythms in the case of circadian clocks). This phenomenon is due to the nature of the feedback loop that composes the core clock, self-sustained by the activity of its components only, with no need for an external factor to activate the oscillation. The presence of external rhythmic *Zeitgebers* and

their consequent action on the input pathways are involved only in the synchronization of the core mechanism with the environment, without being indispensable to its operation. Since the dawn of chronobiology, free-run persistence has been considered an ideal study condition to dissect the characteristics of biological clocks (Sweeney and Hastings, 1958). In addition, persistence allows one to discriminate between processes that are properly endogenously regulated (which persist in free run) from those that under normal conditions oscillate only in direct response to environmental inputs (which immediately lose all oscillations in a constant environment). In the case of the rhythms of 24 hours, all processes that show oscillations under photoperiodic conditions are defined as diel (or, interchangeably, daily), but only those which persist upon release to continuous environment can be properly defined as circadian (Leming et al., 2014; Rund et al., 2011). In particular, the seminal studies that led to the identification of genes of endogenous clocks were based on the characterization of mutants exhibiting altered persistence of rhythmicity under free-running conditions (Konopka and Benzer, 1971).

To conclude, a last characteristic common to biological oscillators is temperature compensation, or the maintenance of a constant periodicity of oscillation even when the environmental temperature varies. Temperature compensation is a characteristic of endogenous clocks that has been known for a long time and already characterized in the first

half of the 20th century in animal (Brown and Webb, 1948; Pittendrigh, 1954; Wahl, 1932) as well as algal models (Bruce and Pittendrigh, 1956; Hastings and Sweeney, 1957). Biochemical processes dependent on protein activity speed up as the temperature rises as a matter of thermodynamic efficiency of enzymatic reactions (Copeland, 2000). If this were to happen in timekeeping systems it would result in their total loss of functionality outside of an optimal temperature range, and circadian clocks have evolved to avoid this problem (Eckardt, 2006).

To date, biological processes with tidal, lunar and seasonal/circumannual rhythmicity regulated by endogenous clocks have been observed (Andreatta and Tessmar-Raible, 2020; Gwinner, 2012). However, the best known and best characterized endogenous clocks are undoubtedly those of circadian nature, with an oscillation period of about 24 hours (Wijnen and Young, 2006). The greater knowledge accumulated on the oscillators with this frequency is obviously due to the possibility to more easily follow biological activity in free run for several cycles of clock activity in controlled conditions. This is obviously more prohibitive in the case of clocks that oscillate on frequencies of several weeks or even months. For this reason and for the fact that my thesis work has focused mainly on the characterization of circadian rhythmicity, in the next paragraph I will give an overview only on this type of clocks. A more extensive description of biological rhythms in the marine environment is given in the review presented in Chapter II.a.

#### I.4.b Biological clocks: diversity and commonalities

The field of chronobiology was recently brought to the attention of the general public thanks to the award of the 2017 Nobel Prize in Physiology and Medicine to Jeffrey C. Hall, Michael Rosbash and Michael W. Young for their discoveries of molecular

mechanisms controlling the circadian rhythm (The Nobel Assembly at Karolinska Institutet, 2017). In the 1980s, the three Nobel laureates launched the first pioneering studies on the molecular players of the endogenous clock of the fruit fly *Drosophila melanogaster*

(Bargiello et al., 1984; Zehring et al., 1984), working on the mutants generated a decade before by Seymour Benzer and Ronald Konopka (Konopka and Benzer, 1971). These studies laid the foundation for the future characterization of circadian clocks in metazoans and other organisms, as well as the methodological framework on which modern molecular chronobiology is based (Peschel and Helfrich-Förster, 2011; Wijnen and Young, 2006).

In eukaryotes, biological oscillators are so-called Transcriptional Translational Feedback Loops (TTFL), in which the positive and negative elements are proteins (notably transcription factors, TFs) capable of regulating their own gene expression and that of target genes (representing the outputs). The structure of the central oscillator of animals has been largely characterized and described thanks to studies in fruit flies and murine models (Fig.8A and Fig.8B). In *D. melanogaster*, the bHLH-PAS Clock (CLK) and Cycle (CYC) proteins interact to form a heterodimer that represents the positive element of TTFL, capable of inducing the expression of a number of target genes that also include the negative elements of the clock, in this case the Timeless (TIM) and Period (PER) nuclear localized proteins (Peschel and Helfrich-Förster, 2011). Light obviously plays a crucial role in fruit fly entrainment, in particular through the photoreceptor cryptochrome that, activated by blue light, induces the degradation of the negative elements TIM and PER, thus releasing the brake on the expression of CLK and CYC (Peschel and Helfrich-Förster, 2011; Stanewsky et al., 1998; Yang et al., 1998). In mammals, only some of the components found in *Drosophila* retain their function in the circadian clock. Also in this case, the positive element is given by heterodimers of bHLH-PAS transcription factors (no more CLK/CYC, but their homologues CLOCK/BMAL1 and NPAS2/BMAL1) (Hirayama et al., 2007; Huang et al., 2012;

Takahashi, 2017a). Negative elements induced by bHLH-PAS proteins again include a homolog of PER, which however in this case associates not with a homolog of TIM, but with mammalian cryptochromes which lose their function as direct light sensors (Takahashi, 2017a; Tamaru et al., 2015; Wijnen and Young, 2006). Light entrainment in mammal clocks is more dependent on visual perception and activation of cAMP-dependent signal transduction pathways induced by neural signaling (Gau et al., 2002; Shearman et al., 1997; Wijnen and Young, 2006). This divergence makes it clear that even organisms that are (relatively) evolutionarily close may exhibit substantial differences in the molecular players involved in the central oscillator, while retaining its basic structure. Lest we forget, the central feedback loop acts in close association with other peripheral TTFLs that refine the mechanisms of expression and repression of positive and negative core elements (loops composed of the VRI and PDP1 proteins in *D. melanogaster* and ROR $\alpha$  and REV-ERB $\alpha$  in mammals). A complete overview of the functioning of animal clocks can be found in Peschel and Helfrich-Förster, 2011 (*D. melanogaster*) and Takahashi, 2017b (mammals), but what described above shows how the core clock, although reducible to a TTFL, can actually have a much more complex and baroque architecture.

Fungi are organisms relatively close to animals in phylogenetic terms, being part of the same phylum, *Opisthokonta* and are classically organisms widely used in molecular biology. This is why some of the earliest and most important studies of the characterization of circadian clocks were developed in fungi. In particular, the model organism most applied in chronobiology is the filamentous fungus *Neurospora crassa*, belonging to the *Ascomycota* (Davis, 2000). *N. crassa* has a long history as a model organism in genetics (Beadle and Tatum, 1941) and shows a rhythmic daily production of spores for

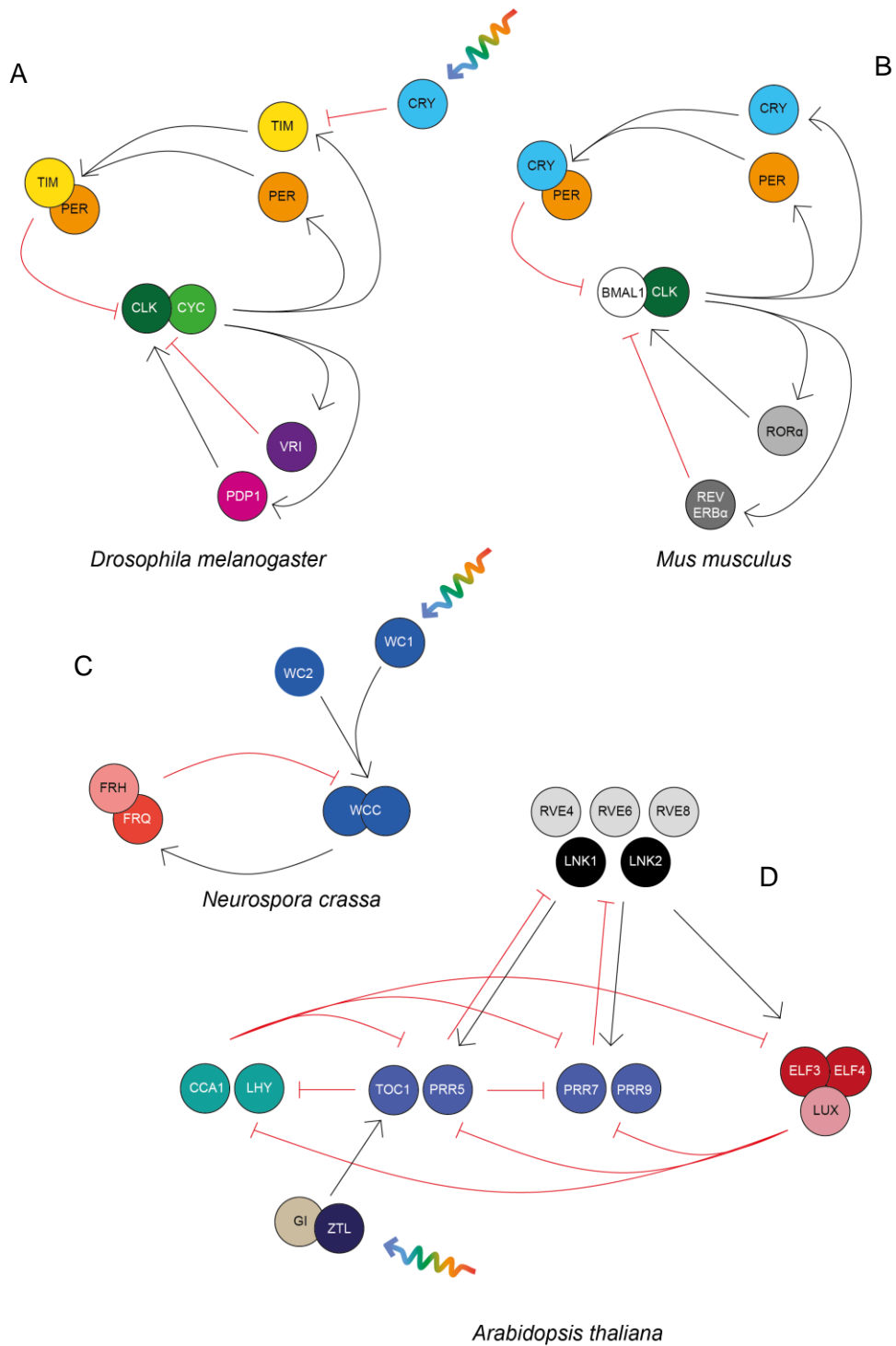


Figure 8. Circadian TTFL networks in model organisms

Simplified schematic representation of the TTFL networks at the base of circadian regulation in different organisms: insects (*Drosophila melanogaster*, A), mammals (*Mus musculus*, B), fungi (*Neurospora crassa*, C) and plants (*Arabidopsis thaliana*, D). Circles represent the different regulatory proteins reported in the text. Black arrows represent positive regulation (induction of expression or activation of protein function). Red blunt lines represent negative regulation (repression of induction, induction of protein degradation or repression of protein function). Rainbow arrow highlight light dependent activity of photoreceptors. Images are based on Saini et al 2019 (panels A-C) and Creux 2019 (panel D). Protein names abbreviations are reported in the main text.

asexual reproduction (macroconidia) (Baker et al., 2012). This rhythmicity, in particular, has an endogenous regulation being able to persist even in free run in a temperature-independent manner (Pittendrigh et al., 1959). As in animals, the endogenous timekeeper of *N. crassa* is based on a TTFL, although composed of completely different proteins (Fig.8C). In particular, the positive element of *N. crassa* TTFL are two GATA-family transcription factors, *white-collar* (WC-1 and WC-2), that heterodimerize thanks to the physical interaction of their LOV domains (of the PAS domain family) forming the so called WCC (White-Collar Complex) (Cheng et al., 2002). The WCC induces the expression, among others, of the main negative element of the clock, the *frequency* (FRQ) protein (Crosthwaite et al., 1997). Upon expression, FRQ proteins form homodimers (Cheng, 2001) that in turn interact with FRH (FRQ interacting RNA helicase) forming the FRQ-FRH Complex (FFC) (Cheng et al., 2005). FFC interacts with WCC, favouring the phosphorylation of WC proteins and the consequent destabilization of the WCC and its dissociation from the *frq* promoter (Hong et al., 2008; Schafmeier et al., 2005) hence closing the loop. Concerning the light entrainment of *N. crassa* timekeeper, this occurs primarily through the WC-1 protein. In fact, it does not only play the role of a transcription factor, but is also a photoreceptor activated by blue light. This sensitivity to light is related to its LOV domain, which is capable of binding the chromophore flavin adenine dinucleotide (Chen et al., 2010). In particular, the stability of WCC (and the consequent functioning of the positive arm of TTFL) is implemented by irradiation in the blue light of WC-1 (Crosthwaite et al., 1997). Overall, this dual function of WC-1 demonstrates how the division of the clock into different components (input, core, and output) is not rigid and that the same molecular actor can intervene on multiple levels of clock regulation (in this case photo perception and core TTFL).

Despite the interest and scientific efforts expended in characterizing the animal and fungal clock, the history of chronobiology dates back to far before the introduction of the fruit fly and *N. crassa* as model organisms. From the beginning, chronobiology has been a discipline inextricably linked to the study of photosynthetic organisms. The first scientific reports of rhythmic biological phenomena date back to the 18th century, with the famous observations made by Jean-Jacques d'Ortous de Mairan, who noted that cyclic daily leaf movements in heliotrope plants continue after transferring the plants to constant darkness (D'Ortous de Mairan, 1729). Similarly, the first studies of genetics applied to chronobiology were carried out on plant models, with the work of Erwin Bünning, first to demonstrate that period length is heritable in bean plants (Bünning, 1936, 1935; Kuhlman et al., 2018).

Similar to the animal clock, the clock of higher plants is controlled by a central mechanism based on feedback loops using transcription factors (Fig.8D). The plant central circadian oscillator has a high level of complexity, being composed of multiple loops that follow one another and intertwine over the 24 hours and depend on the expression of specific proteins at different times of the day. At the beginning of light phase MYB-like transcription factors CIRCADIAN CLOCK ASSOCIATED1 (CCA1) and LATE ELOGATED HYPOCOTYL (LHY) are expressed and repress the afternoon PSEUDO-RESPONSE REGULATOR (PRR) genes, including TIMING OF CAB EXPRESSION1 (PRR1/TOC1), PRR5, PRR7, and PRR9 (Alabadi et al., 2001; Farré et al., 2005; Kamioka et al., 2016). PRR TFs in turn repress the expression of the morning genes creating a double repressor loop (Creux and Harmer, 2019). The correctly timed expression of PRR proteins in the afternoon (and the consequent override of the inhibitory action of CCA1 and LHY) is guaranteed by the mid-day expression of other MYB-like proteins, REVEILLE (RVE) RVE4, RVE6



and RVE8 that interact with NIGHT LIGHT INDUCIBLE AND CLOCK REGULATED (LNK1 and LNK2) to induce the expression of PRR TFs (Farinas and Mas, 2011; Rawat et al., 2011). The 24-hour regulatory cycle is closed by the late-day expression of the evening regulatory transcriptional complex proteins, EARLY FLOWERING ELF3 and ELF4, and LUX ARRHYTHMO (LUX). These proteins repress genes expressed in the morning and afternoon to complete the feedback loop in the network (Huang and Nusinow, 2016).

As in *Drosophila* circadian systems, blue light and its perception through photoreceptors of the cryptochrome family play a central function in entrainment processes also in plants. This is evidenced by alterations in the persistence of free-running oscillations in CRY1 cryptochrome mutants (Gould et al., 2013; Somers et al., 1998). In addition to cryptochromes, plants have also co-opted other photoreceptors in clock regulation, as in the case of the red sensing phytochrome (Somers et al., 1998) or the blue light receptor of the LOV ZEITLUPE family (ZTP) that when activated contributes to the stabilization of TOC1 via the interaction with GIGANTEA (GI) (Kim et al., 2007; Más et al., 2003)

It is important to note that many terrestrial plants are able to perceive the length of the day (photoperiod) and exploit it as a seasonal indicator. Through the perception of day length, plants are able to correctly time processes such as flowering, dormancy, and bud break so as to induce them in the appropriate moment of the year (a phenomenon called photoperiodism). Links between the circadian clock and photoperiodism have been widely studied, especially in correlation to flowering in response to short and long days (Creux and Harmer, 2019). FLOWERING LOCUS T (FT) family proteins, which are highly conserved in angiosperms, play a central role

in regulating flowering (Andrés and Coupland, 2012). FT expression is induced by the transcription factor CONSTANS (CO), which in turn is induced by a protein complex formed by GI and FKF1 (FLAVIN-BINDING KELCH REPEAT, F-box 1, a protein related to ZTL). The GI-FKF1 complex is stabilized by blue light and thus represents a central link in the mechanism that regulates the interaction between light input, central clock and flowering (Imaizumi et al., 2005; Song et al., 2015). Also, the obliteration of central genes of the plant circadian clock can lead to relevant alterations in photoperiodic flowering, as in the case of the evening complex component ELF3 (Zagotta et al., 1996) or PRR genes (Nakamichi et al., 2012). This close interdependence between day length perception and the circadian clock in plants suggests that similar links may play out in other organisms in which these mechanisms are less well characterized. It is also relevant that, in contrast to plants, animal photoperiodic phenomena (which include, for example, hibernation and reproductive behaviors) do not appear to be altered by central clock mutations, suggesting that photoperiodism and circadian rhythmicity may undergo independent evolutionary pathways (Bradshaw and Holzapfel, 2007).

To conclude this comparative analysis of known TTFLs, it is important to consider what is known to date about circadian clocks in unicellular algae. Like plants, algae have been the subject of study long before the development of modern molecular chronobiology (Noordally and Millar, 2015). Historically, some of the earliest algal models to be used in chronobiology are evolutionarily very distant from land plants and are indeed secondary endosymbionts. The marine dinoflagellate *Lingulodinium polyedrum* (formerly *Gonyaulax polyedra*, belonging to the *Alveolata* family) has been extensively studied since the 1950s because of its highly rhythmic bioluminescence able to persist for weeks in free run condition (Hastings, 2007).

This has made it a perfect model for classical chronobiology and many concepts now established in the field, such as temperature compensation of circadian clocks, have been developed on this organism (Hastings and Sweeney, 1957). Another secondary endosymbiont alga that has been widely studied in chronobiology is *Euglena gracilis*, a freshwater flagellated protist belonging to the phylum *Discoba*. In *E. gracilis* the endogenous circadian control of cell division, as well as the involvement of cAMP in the regulation of cellular rhythmicity, have been well characterized (Bolige et al., 2005; Carré and Edmunds, 1993). However, due to the poor advancement of genomic sequencing of these algae and the few gene manipulation techniques available, knowledge about the molecular players involved in TTFLs of secondary endosymbionts is basically null (Noordally and Millar, 2015). Also for this reason, the only microalgae in which the molecular characterization of the circadian clock is advanced are those belonging to the green lineage, evolutionary closer to the already characterized land plants and for which more molecular and genomic resources are available.

One of the most prominent among them is *Chlamydomonas reinhardtii*. The endogenous control of its circadian rhythms of phototaxis and cell division are in fact already known since the early 70's (Bruce, 1970). The first studies on mutants with alterations of this rhythmicity in free run date from the same period (Bruce, 1974, 1972). Subsequent studies have shown that chloroplast gene expression is also under the control of the same circadian clock (Hwang et al., 1996). The creation of transgenic lines expressing a luciferase under the control of the elongation factor promoter Tu (*tufA*), a strongly rhythmic plastid gene, later allowed the high throughput identification of the genes involved in its endogenous timekeeper. This analysis was also made possible by the sequencing of *C. reinhardtii* genome (Merchant et al., 2007).

The screening of insertional mutants led to the identification of genes, named *rhythm of chloroplast* (ROC), whose mutations induce major deregulation of persistent circadian rhythms of the chloroplast luminescent *tufA* reporter (Matsuo et al., 2008). Among others, the four best known are the nuclear genes ROC15, ROC40, ROC66 and ROC75. Although they cannot be considered homologs in the strict sense, these proteins share some functional domains of several core clock components of *A. thaliana* such as CCA1 or LHY (for the Myb TF ROC40), LUX (in the case of ROC15 and ROC75) and Constans/TOC1 (as in the case of the CCT-containing ROC66) (Matsuo et al., 2008; Schulze et al., 2010). Still, this similarity does not go beyond the single domain level, plus other of the ROC proteins show no similarity for plant clock regulators (Matsuo et al., 2008). This suggests a clear differentiation of timekeeping mechanisms even between relatively close organisms is possible. This differentiation is made even clearer by the role played by the protein complex CHLAMY1. CHLAMY1 is a RNA-binding protein able to bind in a circadian fashion an UG repeated sequence located in the 3'-UTR of target mRNA (Mittag, 1996; Mittag et al., 1994; Waltenberger et al., 2001). This complex, composed of two subunits C1 and C3 (Zhao et al., 2004), has been shown to repress the activity of the target genes, most probably acting as a repressor of translation (Iliev et al., 2006; Schulze et al., 2010). Moreover, the deregulation of the expression of its two subunits has major effects on cellular rhythmicity (Iliev et al., 2006). Despite its crucial function in the circadian rhythmicity of *C. reinhardtii*, this protein complex has not been found in plant genomes, further stressing how timekeeping mechanisms can diverge very rapidly and co-opt different players in relatively short evolutionary timescales (Schulze et al., 2010). However, one of the factors that has remained conserved with respect to plants is the role of blue light in regulating endogenous rhythmicity. Indeed, *C.*

*reinhardtii* possesses 4 cryptochromes and the mutation of one of them (pCRY) has major effects on free-run phototaxis rhythmicity, indicating a role in input pathways (Müller et al., 2017).

A second green alga of major relevance in chronobiology is *Ostreococcus tauri*, the smallest free-living (non-symbiont) eukaryote described to date (Courties et al., 1994). *O. tauri* is part of the taxon *Prasinophyceae*, one of the first classes to differentiate into green algae (Leliaert et al., 2012), a fact that makes it a relevant study subject for characterizing elements of the circadian timekeeper common to other *Viridiplantae*. This unicellular alga exhibits strong rhythmicity of gene expression when exposed to cycles of light and dark (Monnier et al., 2010; Moulager et al., 2007). Equally, *O. tauri* cell division is rhythmic under photoperiod and maintains a rhythmicity of approximately 24 hours following transition into continuous light, demonstrating that this process is under the control of an endogenous clock (Moulager et al., 2007). *O. tauri* has an extremely compact and low redundant genome, with only 8000 genes (Derelle et al., 2006). This reduced genetic redundancy is also reflected in the structure of its endogenous clock. In fact, *O. tauri* has only one homologous gene of the TOC1 protein found in higher plants and one TF of the Myb family homologous of CCA1. The variety of PRR genes or a second Myb gene comparable to LHY that can be found in plants are not present in the genome of this alga (Corellou et al., 2009). In *O. tauri*, TOC1 sees a peak in expression during the end of the light period, followed by a decrease in expression level during the dark hours, when it is CCA1 that is transcribed instead (Corellou et al., 2009). The expression patterns of these two genes adapt dynamically to different photoperiods (Thommen et al., 2010) and the rhythmicity of expression persists following release into continuous light (Corellou et al., 2009). The misexpression by overexpression or

downregulation of each of these two genes induces a complete disruption of this persistence, demonstrating their cardinal role in the core oscillator (Corellou et al., 2009). The small number of components of the *O. tauri* oscillator has made this alga an excellent subject of study for the development of mathematical models to describe the clock regulation circuit (Morant et al., 2010; Ocone et al., 2013; Thommen et al., 2010; Troein et al., 2011). Some of these models predict that TOC1 acts as the positive arm of the feedback loop, while CCA1 (induced by TOC1), would represent the negative arm of the circuit and would be responsible for the repression of TOC1 (Morant et al., 2010; Thommen et al., 2010; Troein et al., 2011). However, it has also been proposed that the clock circuit of *O. tauri* is actually based on a triple repressor circuit (repressilator), in which CCA1 represses TOC1, responsible for the inhibition of a third component, not yet identified, which in turn represses CCA1 (Ocone et al., 2013). In this three-loop model, TOC1 would assume a repressor role similar to that observed in the circadian clock of higher plants. Concerning light perception, *O. tauri* possesses five proteins of the cryptochrome/photolyase family, none of which turn out to be plant-like (Heijde et al., 2010). Downregulation of one of these proteins, CPF1, causes a perturbation of the persistence of CCA1 expression rhythmicity in continuous light, suggesting its involvement in the circadian clock (Heijde et al., 2010). Furthermore, the CPF1 from *O. tauri* is capable of complementing the function of mammalian cryptochrome in repressing the activity on CLOCK and BMAL1 proteins in a cryptochrome knockout simian cell model (Heijde et al., 2010). In addition, *O. tauri* also possesses a Histidine Kinase-LOV and a Histidine Kinase-Rhodopsin photoreceptors. Downregulation as well as overexpression of LOV-HK protein induces an important deregulation of *O. tauri* free-run rhythmicity (Djouani-Tahri et al., 2011), indicating its involvement in clock inputs, whereas a

function of HK-Rhodopsin has not yet been fully characterized.

#### I.4.c Translation Independent Oscillators: above and beyond TTFLs

The mechanisms described in the previous paragraph only represent the heart of the core clocks. Although TTFLs are the best characterized timekeeping mechanism, other oscillatory systems that are not directly dependent on gene expression have been described. TTFLs appear to be interconnected to a more primitive metabolic oscillator, able to work even when transcription and translation are inhibited or inactive (Wong and O'Neill, 2018). Such oscillators are also referred to as TIO (Transcription Independent Oscillators) or PTO (Post-Translational Oscillators).

Post-translational oscillators are already present in cyanobacteria, the prokaryotes in which a circadian timekeeper has been first identified and characterized in detail (Iwasaki and Kondo, 2004). This mechanism is based on the activity of the Kai periodosome formed by the proteins KaiA, KaiB and KaiC. KaiC is capable of autophosphorylation, with KaiA favoring the process and KaiB repressing it. The Kai periodosome regulates gene expression by rhythmically modifying the supercoiling of the bacterial chromosome (Iwasaki and Kondo, 2004). This circadian clock follows autonomous cycles of phosphorylation and dephosphorylation even without gene expression. In addition, only ATP is required to assemble a working periodosome clock *in vitro* (Nakajima et al., 2005).

In eukaryotes, the ability to maintain a circadian rhythm in the absence of transcription has been known since the '60s, when it was evidenced that the giant unicellular green alga *Acetabularia* maintains rhythms in photosynthetic activity even after enucleation (Sweeney and Haxo, 1961). In addition, it has

been recently demonstrated the wide preservation of a metabolic rhythmicity in the form of cycles of cellular redox potential and ROS content, which can be tracked by following the oxidative state of the enzyme peroxiredoxin (PRX, involved in the neutralization of H<sub>2</sub>O<sub>2</sub>). Circadian cycles of the redox state of PRX were originally observed in erythrocytes (cells naturally lacking the nucleus and without transcriptional activity) (O'Neill and Reddy, 2011) and in the unicellular green alga *O. tauri* specifically treated to inhibit transcription (O'Neill et al., 2011). Subsequently, transcription-independent rhythms of PRX redox state were similarly observed in organisms spanning the entire tree of life, including prokaryotes and archaea, plus a variety of eukaryotes belonging to different phyla (Edgar et al., 2012). On the one hand, redox potential and ROS content are modulated by the circadian clock through its regulation of cellular metabolism (Putker and O'Neill, 2016). On the other hand, these factors act on timekeeping mechanisms (TTFL and TIO) through modulation of protein activity (including that of TFs) and a perturbation of these parameters can have repercussions on cellular rhythmicity (Putker and O'Neill, 2016). Therefore, it cannot be excluded that also the cellular redox potential has played an ancestral role in biological timekeeping. However, to date the functioning of PTO oscillators and their interaction with cellular redox potential and TTFLs remain largely unresolved. A simplified, schematic representation of the structure of the endogenous timekeeper including both TTFL and TIO is reported in Fig.9.

To conclude, post-translational regulators of the circadian clock, such as Casein Kinases (Lin et al., 2002; Poliner et al.,

2019; Tang et al., 2009; Uehara et al., 2019; Yang et al., 2003), protein phosphatases, protein methyltransferases and ubiquitination systems (Wong and O'Neill, 2018) are conserved in evolutionarily distant eukaryotic organisms and their inhibition or mutations causes an alteration of cellular rhythmicity (Wong and O'Neill, 2018). This led to the hypothesis that an ancestral timekeeper originated as a post-translational oscillator based on the mechanisms of phosphorylation,

stabilization, and degradation of clock proteins and of their molecular targets (Wong and O'Neill, 2018). The diversity of transcriptional oscillators found in eukaryotes can be explained by a later evolutionary divergence of the gene regulatory mechanisms controlled by the TIO, yet maintaining a common mechanism (the negative feedback loop) via the co-option of different actors depending on the phylum (Wong and O'Neill, 2018) .

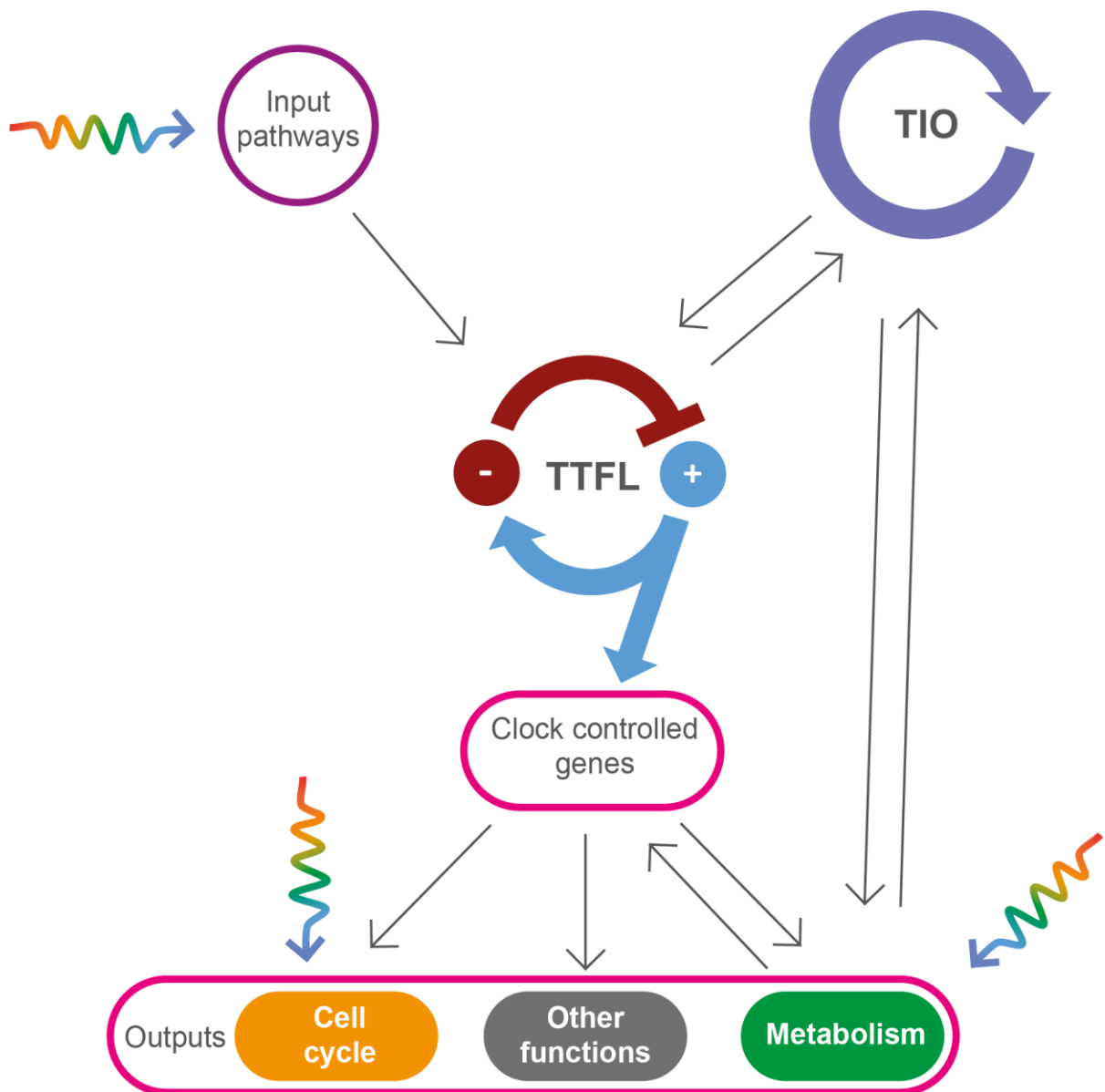


Figure 9. Architecture of circadian clock systems

Schematic and simplified architecture of a circadian clocks system. Cellular rhythmicity is synchronized with the environment by the input pathways, able to perceive external stimuli. Light (represented as a rainbow arrow) plays a major role in this entrainment process. In eukaryotes, the core oscillator is composed by a transcriptional translational feedback loop (TTFL). Positive (+) elements induce the expression of negative (-) elements that in turns repress the activity of the formers, closing the loop. The core clock regulates the timing of a variety of downstream processes, the outputs, by controlling the expression of clock controlled genes. These include cell cycle (in particular in unicellular organisms), metabolic activity and other functions such as behaviour. Light inputs can also act directly on the outputs, independently of the central oscillator, potentially causing masking effects (see main text). The persistence of circadian rhythms in absence of transcriptional/translational activity, demonstrate the possible existence of an additional TIO (Transcription Independent Oscillator) acting mainly on the post translational modification of proteins. The structure and components of the TIO remain largely unknown. Two-way arrows underlie the reciprocal influence between different components of this system (e.g. the central TTFL regulating the rhythmicity of the metabolism, whose products, like sugars, act in turn as entrainers of the timekeeper). Figure based on Wong and O'Neill, 2018.

#### I.4.d Circadian rhythmicity in *Stramenopila*: an overview

Since my thesis work has largely focused on the characterization of the circadian clock of diatoms, it is useful to introduce here a quick overview of what is already known about these algae and, more generally, about the phylum *Stramenopila* to which they belong.

As in the other taxa described above, the characterization of biological rhythmicity in *Stramenopila* dates back well before the era of molecular biology. Notably, several species of diatoms exposed to light-dark cycles show a synchronization of cell division with light and dark inputs, both under controlled laboratory conditions (Chisholm and Brand, 1981; Gaidarenko et al., 2019; Nelson and Brand, 1979; Ostgaard and Jensen, 1982, 1982; Paasche, 1968; Ragni and d'Alcalà, 2007; Williamson, 1980) and in the case of samples from natural environment (e.g. (Chang and Carpenter, 1991; Owens et al., 1980; Smayda, 1975; Williamson, 1980). In detail, cytokinesis appears to be limited to specific times of the day, which in the case of diatoms normally corresponds to the end of the light period (e.g. Hunsperger et al., 2016; Nelson and Brand, 1979; Ragni and d'Alcalà, 2007). Such a phasing of cell division emphasizes the interdependence between cell cycle advancement and light irradiation described in Paragraph I.3.d. In some diatoms, cell division oscillations observed under light and dark cycles show persistence after release in continuous light (Ostgaard and Jensen, 1982), indicating a clock influence in regulating the timing of cell division. Still, in literature, the persistence of rhythmic divisions was not unequivocally found in all studies and all species, including models like *T. pseudonana* or *P. tricornutum* (Chisholm and Brand, 1981; Ragni and d'Alcalà, 2007). It is important to note that the synchronization of cell division with external light and dark cycles may result from a metabolic response of the cells, which need to accumulate sufficient

energy to sustain cell division. Consequently, the regulation of the rhythmicity of cell division can be either under the direct control of the clock, either an indirect consequence of the clock's control of metabolism or a simple direct response to environmental rhythmic stimuli.

To date, studies on this class of organisms in molecular chronobiology are still limited and have focused mainly (but not only) on some models of diatoms (*P. tricornutum* mainly) and of *Eustigmatophyceae*, a group of algae that includes some species of high biotechnological interest such as the unicellular algae *Nannochloropsis* spp. Both diatoms and *Eustigmatophyceae* algae show rhythmic gene expression under light dark photoperiod (Chauton et al., 2013; Poliner et al., 2015; Smith et al., 2016) and persistent oscillations in transcription in free run have also been observed (Oeltjen et al., 2004; Poliner et al., 2019). This regulation of expression may, potentially, underlie the multiple circadian processes observed in *Stramenopila*. These include: rhythms in cell division, observed in *Nannochloropsis* (Poliner et al., 2019), but also in the diatom *Skeletonema costatum* (Ostgaard and Jensen, 1982) and multicellular brown algae (Makarov et al., 1995); diel oscillations in cellular fluorescence associated with pigment content (Ostgaard and Jensen, 1982; Owens et al., 1980; Ragni and d'Alcalà, 2007); photosynthetic rate and associated metabolic processes like carbon fixation (Brand, 1982; Nultsch et al., 1984; Palmer et al., 1964; Schmid and Dring, 1992); migration of benthic diatoms in sediments (Fischer et al., 1977; Palmer and Round, 1967).

All of the above suggest the possible existence of an endogenous oscillator responsible for self-sustained cycles of gene expression and circadian rhythmicity in these organisms. However, none of the

*Stramenopila* species sequenced (Armbrust, 2004; Bowler et al., 2008; Vieler et al., 2012) shows conservation of any known central component of characterized eukaryotic or prokaryotic clocks. *Stramenopila* possess SHQKYF- and MYB-related family transcription factors, a family to which belong some components of the plant clock (LHY and RVEs), as well as bHLH-PAS proteins with a structure partially similar to that of CLK, CYC, BMAL1 and NPAS2 of the animal central oscillator (Rayko et al., 2010; Thiriet-Rupert et al., 2016). Moreover, the divergence of the amino acid sequence is such that a conservation of function cannot be easily assumed. Moreover, the possibility that the TTFL of *Stramenopila* uses components that are completely different from those of *Archaeplastida* or animals cannot be excluded given the complex evolutionary history of these organisms and the high divergence of transcriptional oscillators in eukaryotes.

On the other hand, *Stramenopila* have conserved some proteins involved in post-translational regulation and input pathways of the timekeeping mechanism. For example, the inhibition of Casein Kinases alters the persistence of transcriptional rhythms in *Nannochloropsis* spp. (Poliner et al., 2019) in a way similar to what is seen in other phyla (Lin et al., 2002; Uehara et al., 2019). In addition, CPF1 cryptochromes in *P. tricornutum* and *Nannochloropsis gaditana*

show rhythmic expression under photoperiodic light/dark cycles (Coesel et al., 2009; Poliner et al., 2015; Smith et al., 2016). Moreover, as already mentioned in Paragraph I.3.c, the heterologous expression of *P. tricornutum* CPF1 in simian cells is able to complement the function of mutated endogenous CRYs in repressing CLOCK/BMAL1 activity, suggesting that this protein might perform a similar activity on diatom bHLH-PAS proteins. Still, this interaction has not been investigated yet. It is crucial to consider that cryptochrome exert a function in clock synchronization of evolutionarily distant organisms throughout the diversity of eTOL branches (Gould et al., 2013; Peschel and Helfrich-Förster, 2011; Somers et al., 1998; Stanewsky et al., 1998; Takahashi, 2017a). In addition, all the photoreceptors described in *Stramenopila* (Paragraph I.3.c) may play a role in input pathways but functional studies are missing on this front. Moreover, aureochromes do not simply act as photoreceptors but also as transcription factors (Kroth et al., 2017; Mann et al., 2020), implying a possible direct involvement in the TTFL as both light sensors and transcriptional regulators. None of this hypothesis has been tested yet. Globally, at the time of the beginning of my thesis the characterization of TTFL of diatoms and more generally of *Stramenopila* was still a largely unexplored field.



# I.5 bHLH-PAS transcription factors in diatoms

Overall, approximately 2% of the diatom proteome is predicted to encode for transcription factors, TFs (Rayko et al., 2010). This value is comparable to what can be observed in other evolutionarily distant unicellular algae (e.g. 2,1% in *C. reinhardtii* as for (Rayko et al., 2010). For comparison, in multicellular organisms where the level of complexity is increased due to cellular differentiation in different tissues, this value can be considerably higher (in *A. thaliana* 5,9% of the proteome is dedicated to TFs (Rayko et al., 2010; Riechmann et al., 2000)). In the case of *P. tricornutum*, the genes predicted to encode transcription factors total about 200, with the number varying slightly according to predictions (Rayko et al., 2010; Thiriet-Rupert et al., 2016). Among these, a relevant number is given by the Heat Shock Factors, the most numerous family followed by the Myb, bZIP and Zn finger factors that have undergone considerable expansion in diatoms (Rayko et al., 2010; Thiriet-Rupert et al., 2016).

Among the multitude of transcription factor families that can be found in diatoms, the basic-Helix-Loop-Helix (bHLH) family is of particular interest. The common element of these proteins, as their name indicates, is the presence of a highly conserved domain of 50-60 amino acids composed of a strand of 10-15 basic residues (basic region) followed by about forty amino acids that are structured in two amphipathic  $\alpha$ -helices separated by an amorphous loop of variable length (the Helix-Loop-Helix region, (Jones, 2004; Murre, 2019; Pires and Dolan, 2010a). These proteins act as homodimers or heterodimers, with the two alpha helices representing the main dimerization interface. The DNA binding function, crucial for any transcription factor, is instead performed mainly by the

basic stretch located upstream of the HLH motif (Jones, 2004). The basic region is specifically tailored to interact with five- to seven-base DNA sequences. In general, the recognized sequences can be of the type CANN(N)TG (E boxes, where N corresponds to any nucleotide) (Carroll et al., 2018), CACNNG (N-boxes) (Paroush, 1994) or ACGTG/GCGTG (typically recognized by bHLH-PAS animal proteins which I will discuss below).

The relatively small bHLH domain is located in the amino terminal region of the protein and can associate with a variety of other downstream domains that determine the functionality of the protein and the specificity of dimerization (Ledent and Vervoort, 2001; Murre, 2019). These additional domains include leucine zipper motifs, Collier/Olf-1/EBF (COE) domains and PAS domains (Ledent and Vervoort, 2001). Although the  $\alpha$  Helices of the bHLH domain represent the primary dimerisation interface at the level of the N terminus, the PAS folds act as additional surface of interaction and define the partner of choice (Kewley et al., 2004; Taylor and Zhulin, 1999). In bHLH-PAS proteins, the choice of the dimerization partner is in particular defined by the presence of the PAS domain, so that these proteins can homo/heterodimerize only with another member of the same family (Kewley et al., 2004; Michaud et al., 2000; Pongratz et al., 1998).

The first characterisation of these transcription factors dates back to 1989, when they were first identified in murine cells (Murre et al., 1989b, 1989a). Since, bHLH proteins were identified in the major eukaryotic phyla, including *Metazoa*, *Archaeplastida*, and fungi (Ledent and Vervoort, 2001; Murre, 2019; Pires and

Dolan, 2010b). Their functions are as diverse as the organisms where they can be found. Both bHLH TFs acting as transcriptional activators (*e.g.* (Jang et al., 2017) and as transcriptional repressors (*e.g.* (Kageyama et al., 2000) have been characterized. In animals they are involved in immune response, neurogenesis, myogenesis, and heart development (Jones, 2004; Massari and Murre, 2000; Murre, 2019, p. 201). In yeast they play a central role in glycolysis and phosphate uptake (Robinson, 2000). Finally, plant bHLH transcription factors have been shown to modulate secondary metabolism pathways, epidermal development, and responses to environmental light stimuli, such as in the case of processes like shade avoidance, photomorphogenesis, other processes regulated by photoreceptors and the regulation of the circadian clock (Castillon et al., 2007; Farré and Weise, 2012; Pires and Dolan, 2010a; Ramsay and Glover, 2005). In plants in particular, bHLH factors have undergone an important phenomenon of duplication and increase in gene copies, becoming the second most abundant and diverse families of transcription factors, while in unicellular *Archaeplastida* the number of copies of bHLH factors is far smaller (Pires and Dolan, 2010a, 2010b). Given the role played by plant bHLH factors in development and cell differentiation, it has been proposed that the amplification of this gene family occurred concomitantly with the transition from unicellularity to multicellularity, playing a crucial role in this evolutionary process (Pires and Dolan, 2010b).

*P. tricornutum*, in addition to TFs only containing the bHLH fold, also possess three factors associating PAS folds to the bHLH domain, proteins on which my thesis work focused. Before describing the bHLH-PAS proteins, it is essential to introduce the characteristics and functions of PAS domains. The PAS fold is an ubiquitously distributed functional domain that can be found in all eukaryotes as well as in archaea and

prokaryotes and takes its name from the first three proteins in which it was identified, the *Drosophila melanogaster* *Period* (PER) and *Single-minded* (SIM) and the mammalian *Aryl hydrocarbon Receptor Nuclear Transporter* (ARNT) (Henry and Crosson, 2011; Möglich et al., 2009; Taylor and Zhulin, 1999). It consists of 100-130 amino acids generating a five or six stranded  $\beta$ -sheet divided in two halves connected by an  $\alpha$ -helix and flanked by a variable number of additional  $\alpha$ -helices (Kewley et al., 2004; Möglich et al., 2009). PAS domains are not only found associated with bHLH DNA binding domains, but also with other functional domains such as histidine kinase, nucleotide cyclase, and response regulator domains (Henry and Crosson, 2011). All domains, therefore, are involved in signal transduction within the cell.

The PAS fold is a highly multifunctional structure, since it is in a plethora of molecular processes. The ability to interact with a chemically diverse range of metabolites is a hallmark of the PAS domain family. The chemicals bound by this domain are used either as a direct cue to initiate a cellular signaling response or represent functional cofactor moieties involved in the interaction with secondary physical or chemical signals such as gas molecules, redox potential, or photons (Henry and Crosson, 2011; Möglich et al., 2009). Among the ligands recognized by different PAS domains we count dioxin (as in ARNT proteins) (Procopio et al., 2002), metal ions (Ernst et al., 2001; Fass and Groisman, 2009), heme groups (Yoshioka et al., 2005) and various metabolites (such as malate, succinate or citrate (Henry and Crosson, 2011)).

It is important to note that PAS domains also play a central role in the activity of some photoreceptors. In fact, a specific subfamily of these protein folds (named Light-Oxygen-Voltage photoreceptor domains or LOV) is capable of binding a flavin

mononucleotide (FMN) cofactor that forms a cysteinyl-flavin C4(a) covalent adduct when activated by blue-light (Crosson et al., 2003; Purcell et al., 2007). The photoreceptive function of LOV domains was first identified in plant phototropins (Christie et al., 1999, 1998), but other LOV photoreceptors for blue light include the already mentioned LOV-HK proteins (found in prokaryotes as well as green algae (Djouani-Tahri et al., 2011)) and aureochromes, which as seen are present only in *Stramenopila* (Kroth et al., 2017).

bHLH-PAS proteins have been extensively studied in metazoans, where they are involved, for instance, in response to hypoxia and dioxin (like Hypoxia Inducible Factors and ARNTs (Jiang et al., 2001; Sonnenfeld et al., 1997; Takahata et al., 1998)), in the development of nervous system (like SIM) (Nambu et al., 1996) or in the control of circadian clock (as for CLOCK, CYCLE, NPAS2 and BMAL1, see Paragraph I.4.b for a detailed description, (Huang et al., 2012).

Even though bHLH-PAS TFs were originally thought to be uniquely present in metazoans (Kewley et al., 2004), these

proteins are not restricted to the animal kingdom, but have been recently found also in *Stramenopila* like diatoms (Rayko et al., 2010). Gene prediction analysis revealed the presence of three bHLH-PAS proteins in the model species *P. tricornutum* (bHLH1a, bHLH1b and bHLH2) out of a total of seven bHLH transcription factors (Rayko et al., 2010). A similar expansion of the bHLH family of proteins was also found in other diatoms such as *T. pseudonana* (5 paralogous bHLH genes of which 4 also contain a PAS domain, (Rayko et al., 2010)) or in *S. robusta* (13 bHLH genes of which 10 with a PAS domain (Bilcke et al., 2021a)). This is part of a more general expansion of transcription factor families observed in diatoms (Thiriet-Rupert et al., 2016). It is noteworthy that no bHLH-PAS protein has ever been described in any member of the *Viridiplantae* group. However, whereas the large majority of animal bHLH-PAS proteins contain two PAS folds, all known *Stramenopile* bHLH-PAS proteins contain only one PAS domain. Their patchy distribution among eukaryotic supergroups suggests that these domains might have fused more than once during evolution (Rayko et al., 2010).



# Aims of the thesis

As for all autotrophic organisms, the life and ecological success of diatoms depend inextricably on their ability to respond to the light environment and its dynamic changes. Adaptation to such stimuli must necessarily pass through a fine-tuning of gene expression, in a regulatory mechanism in which transcription factors clearly play a key role. Despite the ecological relevance of diatoms and their importance in marine ecosystems, however, these regulatory mechanisms remain largely unexplored to date. For this reason, I have devoted my research work to integrate genetic resources with physiological and biophysical approaches to characterize the unknown regulators controlling two light-dependent processes of crucial importance to diatoms: rhythmic cellular processes and photosynthesis. Specifically, I based all my work on the marine diatom model species *Phaeodactylum tricorutum*.

On the one hand, I have characterized the ability of this organism to synchronize their physiology with the daily rhythmic cycles of light and dark. As described in Chapter I, paragraph I.4.d and in Chapter II.a, a large number of biological processes in these algae are modulated according to these cycles, such as cell division, pigment synthesis or photosynthetic metabolism, and more. However, at the time when I began my thesis the knowledge about diatom timekeeper was still in its infancy. The identification of regulators involved in this system of timekeeping were therefore essential to better understand the nature of these processes. As presented in Chapter II.b, early results from this line of work led to the identification of the bHLH-PAS protein bHLH1a (later renamed RITMO1) as one of the most rhythmic *P. tricorutum* transcription factors (TF). Alteration of its expression by overexpression leads to a perturbation of the timing and persistence of cellular fluorescence and gene expression. Based on these results, we proposed RITMO1 as the first regulator of diel biological rhythms identified in diatoms. However, the role of this protein in a putative circadian clock system remained to be defined. Using these initial findings as an entry point, I subsequently pursued a more in-depth dissection of the rhythmic processes of *P. tricorutum* and their control by the endogenous clock.

As presented in Chapter II.c, I decided to detail how this diatom adapts its rhythmicity to different photoperiods and light intensities to understand the flexibility to respond to a range of growth conditions reflecting the variety of environmental stimuli. I also generated lines in which the RITMO1 gene was obliterated by CRISPR/Cas9 targeted mutagenesis to determine how deletion of this protein disrupts cellular rhythms. Through these transgenic lines I was able to demonstrate that the circadian clock of *P. tricorutum* regulates, through RITMO1, a plethora of processes that include cell fluorescence and cell division, photosynthetic activity and, more generally, gene expression. These studies established RITMO1 as a component of the diatom clock.

The results obtained on RITMO1 are of cardinal importance as they demonstrate for the first time the existence of a molecular circadian clock in diatoms. They also insert the first element in the puzzle represented by the architecture of this endogenous oscillator. However, circadian timekeeping mechanisms cannot rely on a single component and, as described in the previous pages, require the participation of multiple regulators capable of generating self-sustained feedback loops. For this reason, part of my work has also focused on the search for possible partners of RITMO1. As reported in chapter II.d, I was hence able to demonstrate that a second bHLH-PAS transcription factor, bHLH1b, is able to physically interact with RITMO1 in yeast cells and, if obliterated by CRISPR/Cas9, leads to phenotypic alterations similar to those observed in RITMO1 mutants.

The second light-dependent process I have focused on is photosynthesis and the regulation of plastid activity. Considerable efforts have already been conducted by the scientific community to identify and characterize the proteins involved in chloroplast activity. As secondary endosymbionts, diatoms present several peculiarities in the photosynthetic apparatus and important knowledge has been accumulated on the proteins that are directly involved in its protection to excessive light stimuli. However, the regulatory mechanisms that modulate these processes and their response to the environment still remain largely unexplored. For this reason, during my Ph.D. I participated in the validation of a screening strategy aimed at identifying transcription factors involved in the regulation of photosynthesis in *P. tricornutum*, as reported in Chapter III. This led to the characterization of transgenic lines possessing an antisense fragment for the seven *P. tricornutum* TFs possessing a bHLH domain and to the identification of significant alterations in photosynthetic activity in *bHLH2* RNAi transgenic lines. Like RITMO1 and bHLH1b, bHLH2 is a transcription factor that possesses a PAS fold and a bHLH domain. The bulk of my work therefore focused on detailed dissection of the plastid physiology of *bHLH2*RNAi lines. Such work has allowed me to demonstrate that bHLH2 is a candidate regulator of plastid response to light stimuli with *bHLH2*RNAi lines exhibiting a defect in photosynthesis and growth that is found to be dependent on light intensity. In addition, I demonstrated how the expression of bHLH2, encoded in the nucleus, is regulated in turn by photosynthetic activity in a process of retrograde signaling. Notably, before being identified in *Stramenopila*, transcription factors containing both bHLH and PAS were thought to be a peculiarity of metazoans. The work presented in this thesis clearly reveals that bHLH-PAS proteins acquired functions critical to the life of phototrophic organisms during the evolution of secondary endosymbionts.



# Bibliography

- Ait-Mohamed, O., Novák Vanclová, A.M.G., Joli, N., Liang, Y., Zhao, X., Genovesio, A., Tirichine, L., Bowler, C., Dorrell, R.G., 2020. PhaeoNet: A Holistic RNAseq-Based Portrait of Transcriptional Coordination in the Model Diatom *Phaeodactylum tricornutum*. *Front. Plant Sci.* 11, 590949. <https://doi.org/10.3389/fpls.2020.590949>
- Alabadi, D., Oyama, T., Yanovsky, M.J., Harmon, F.G., Más, P., Kay, S.A., 2001. Reciprocal Regulation Between *TOC1* and *LHY/CCA1* Within the *Arabidopsis* Circadian Clock. *Science* 293, 880–883. <https://doi.org/10.1126/science.1061320>
- Allen, A.E., Dupont, C.L., Oborník, M., Horák, A., Nunes-Nesi, A., McCrow, J.P., Zheng, H., Johnson, D.A., Hu, H., Fernie, A.R., Bowler, C., 2011. Evolution and metabolic significance of the urea cycle in photosynthetic diatoms. *Nature* 473, 203–207. <https://doi.org/10.1038/nature10074>
- Allen, J.F., de Paula, W.B.M., Puthiyaveetil, S., Nield, J., 2011. A structural phylogenetic map for chloroplast photosynthesis. *Trends Plant Sci.* 16, 645–655. <https://doi.org/10.1016/j.tplants.2011.10.004>
- Anderson, C.R., Kudela, R.M., Benitez-Nelson, C., Sekula-Wood, E., Burrell, C.T., Chao, Y., Langlois, G., Goodman, J., Siegel, D.A., 2011. Detecting toxic diatom blooms from ocean color and a regional ocean model: REMOTE DETECTION OF TOXIC DIATOM BLOOMS. *Geophys. Res. Lett.* 38, n/a-n/a. <https://doi.org/10.1029/2010GL045858>
- Andreatta, G., Tessmar-Raible, K., 2020. The Still Dark Side of the Moon: Molecular Mechanisms of Lunar-Controlled Rhythms and Clocks. *J. Mol. Biol.* 432, 3525–3546. <https://doi.org/10.1016/j.jmb.2020.03.009>
- Andrés, F., Coupland, G., 2012. The genetic basis of flowering responses to seasonal cues. *Nat. Rev. Genet.* 13, 627–639. <https://doi.org/10.1038/nrg3291>
- Anning, T., MacIntyre, H.L., Pratt, S.M., Sammes, P.J., Gibb, S., Geider, R.J., 2000. Photoacclimation in the marine diatom *Skeletonema costatum*. *Limnol. Oceanogr.* 45, 1807–1817. <https://doi.org/10.4319/lo.2000.45.8.1807>
- Annunziata, R., Ritter, A., Fortunato, A.E., Manzotti, A., Cheminant-Navarro, S., Agier, N., Huysman, M.J.J., Winge, P., Bones, A.M., Bouget, F.-Y., Cosentino Lagomarsino, M., Bouly, J.-P., Falcatore, A., 2019. bHLH-PAS protein RITMO1 regulates diel biological rhythms in the marine diatom *Phaeodactylum tricornutum*. *Proc. Natl. Acad. Sci.* 116, 13137–13142. <https://doi.org/10.1073/pnas.1819660116>
- Apt, K.E., Grossman, A.R., Kroth-Pancic, P.G., 1996. Stable nuclear transformation of the diatom *Phaeodactylum tricornutum*. *Mol. Gen. Genet.* MGG 252, 572–579. <https://doi.org/10.1007/BF02172403>
- Armbrust, E.V., 2004. The Genome of the Diatom *Thalassiosira Pseudonana*: Ecology, Evolution, and Metabolism. *Science* 306, 79–86. <https://doi.org/10.1126/science.1101156>
- Aschoff, J., 1999. Masking and parametric effects of high-frequency light-dark cycles. *Jpn. J. Physiol.* 49, 11–18. <https://doi.org/10.2170/jjphysiol.49.11>
- Aschoff, J., 1954. Zeitgeber der tierischen Tagesperiodik. *Naturwissenschaften* 41, 49–56. <https://doi.org/10.1007/BF00634164>
- Ashworth, J., Coesel, S., Lee, A., Armbrust, E.V., Orellana, M.V., Baliga, N.S., 2013. Genome-wide diel growth state transitions in the diatom *Thalassiosira pseudonana*. *Proc. Natl. Acad. Sci.* 110, 7518–7523. <https://doi.org/10.1073/pnas.1300962110>
- Babenko, I., Friedrich, B.M., Kröger, N., 2022. Structure and Morphogenesis of the Frustule, in: Falcatore, A., Mock, T. (Eds.), *The Molecular Life of Diatoms*. Springer International Publishing, Cham, pp. 287–312. [https://doi.org/10.1007/978-3-030-92499-7\\_11](https://doi.org/10.1007/978-3-030-92499-7_11)
- Bailleul, B., Berne, N., Murik, O., Petroutsos, D., Prihoda, J., Tanaka, A., Villanova, V., Bligny, R., Flori, S., Falconet, D., Krieger-Liszkay, A., Santabarbara, S., Rappaport, F., Joliot, P., Tirichine, L., Falkowski, P.G., Cardol, P., Bowler, C., Finazzi, G., 2015. Energetic coupling between plastids and mitochondria drives CO<sub>2</sub> assimilation in diatoms. *Nature* 524, 366–369. <https://doi.org/10.1038/nature14599>



- Bailleul, B., Rogato, A., de Martino, A., Coesel, S., Cardol, P., Bowler, C., Falciatore, A., Finazzi, G., 2010. An atypical member of the light-harvesting complex stress-related protein family modulates diatom responses to light. *Proc. Natl. Acad. Sci.* 107, 18214–18219. <https://doi.org/10.1073/pnas.1007703107>
- Baker, C.L., Loros, J.J., Dunlap, J.C., 2012. The circadian clock of *Neurospora crassa*. *Ederation Eur. Microbiol. Soc. Rev.* 35, 95–110. <https://doi.org/10.1111/j.1574-6976.2011.00288.x>
- Baldauf, S.L., 2008. An overview of the phylogeny and diversity of eukaryotes. *J. Syst. Evol.* 46, 11.
- Ballottari, M., Truong, T.B., De Re, E., Erickson, E., Stella, G.R., Fleming, G.R., Bassi, R., Niyogi, K.K., 2016. Identification of pH-sensing Sites in the Light Harvesting Complex Stress-related 3 Protein Essential for Triggering Non-photochemical Quenching in *Chlamydomonas reinhardtii*. *J. Biol. Chem.* 291, 7334–7346. <https://doi.org/10.1074/jbc.M115.704601>
- Bargiello, T.A., Jackson, F.R., Young, M.W., 1984. Restoration of circadian behavioural rhythms by gene transfer in *Drosophila*. *Nature* 312, 752–754. <https://doi.org/10.1038/312752a0>
- Bar-On, Y.M., Phillips, R., Milo, R., 2018. The biomass distribution on Earth. *Syst. Biol.* 6. <https://doi.org/10.1073/pnas.1711842115>
- Basu, S., Patil, S., Mapleson, D., Russo, M.T., Vitale, L., Fevola, C., Maumus, F., Casotti, R., Mock, T., Caccamo, M., Montresor, M., Sanges, R., Ferrante, M.I., 2017. Finding a partner in the ocean: molecular and evolutionary bases of the response to sexual cues in a planktonic diatom. *New Phytol.* 215, 140–156. <https://doi.org/10.1111/nph.14557>
- Beadle, G.W., Tatum, E.L., 1941. Genetic Control of Biochemical Reactions in *Neurospora*. *Proc. Natl. Acad. Sci.* 27, 499–506. <https://doi.org/10.1073/pnas.27.11.499>
- Bertrand, M., 2010. Carotenoid biosynthesis in diatoms. *Photosynth. Res.* 106, 89–102. <https://doi.org/10.1007/s11120-010-9589-x>
- Biggins, J., Bruce, D., 1989. Regulation of excitation energy transfer in organisms containing phycobilins. *Photosynth. Res.* 20, 1–34. <https://doi.org/10.1007/BF00028620>
- Bilcke, G., Osuna-Cruz, C.M., Silva, M.S., Poulsen, N., Bulankova, P., Vyverman, W., Veylder, L.D., Vandepoele, K., 2021a. Diurnal transcript profiling of the diatom *Seminavis robusta* reveals adaptations to a benthic lifestyle. *Plant J.* 107. <https://doi.org/10.1111/tjpi.15291>
- Bilcke, G., Van Craenenbroeck, L., Castagna, A., Osuna-Cruz, C.M., Vandepoele, K., Sabbe, K., De Veylder, L., Vyverman, W., 2021b. Light intensity and spectral composition drive reproductive success in the marine benthic diatom *Seminavis robusta*. *Sci. Rep.* 11, 17560. <https://doi.org/10.1038/s41598-021-92838-0>
- Blaby-Haas, C.E., Merchant, S.S., 2019. Comparative and Functional Algal Genomics. *Annu. Rev. Plant Biol.* 70, 605–638. <https://doi.org/10.1146/annurev-arplant-050718-095841>
- Blommaert, L., Chafai, L., Bailleul, B., 2021. The fine-tuning of NPQ in diatoms relies on the regulation of both xanthophyll cycle enzymes. *Sci. Rep.* 11, 12750. <https://doi.org/10.1038/s41598-021-91483-x>
- Bolige, A., Hagiwara, S., Zhang, Y., Goto, K., 2005. Circadian G2 Arrest as Related to Circadian Gating of Cell Population Growth in *Euglena*. *Plant Cell Physiol.* 46, 931–936. <https://doi.org/10.1093/pcp/pci100>
- Bowler, C., Allen, A.E., Badger, J.H., Grimwood, J., Jabbari, K., Kuo, A., Maheswari, U., Martens, C., Maumus, F., Otiillar, R.P., Rayko, E., Salamov, A., Vandepoele, K., Beszteri, B., Gruber, A., Heijde, M., Katinka, M., Mock, T., Valentin, K., Verret, F., Berges, J.A., Brownlee, C., Cadoret, J.-P., Chiovitti, A., Choi, C.J., Coesel, S., De Martino, A., Detter, J.C., Durkin, C., Falciatore, A., Fournet, J., Haruta, M., Huysman, M.J.J., Jenkins, B.D., Jiroutova, K., Jorgensen, R.E., Joubert, Y., Kaplan, A., Kröger, N., Kroth, P.G., La Roche, J., Lindquist, E., Lommer, M., Martin-Jézéquel, V., Lopez, P.J., Lucas, S., Mangogna, M., McGinnis, K., Medlin, L.K., Montsant, A., Secq, M.-P.O., Napoli, C., Obornik, M., Parker, M.S., Petit, J.-L., Porcel, B.M., Poulsen, N., Robison, M., Rychlewski, L., Rynearson, T.A., Schmutz, J., Shapiro, H., Siaut, M., Stanley, M., Sussman, M.R., Taylor, A.R., Vardi, A., von Dassow, P.,

- Vyverman, W., Willis, A., Wyrwicz, L.S., Rokhsar, D.S., Weissenbach, J., Armbrust, E.V., Green, B.R., Van de Peer, Y., Grigoriev, I.V., 2008. The Phaeodactylum genome reveals the evolutionary history of diatom genomes. *Nature* 456, 239–244. <https://doi.org/10.1038/nature07410>
- Bowler, C., Falciatore, A., 2019. Phaeodactylum tricornutum. *Trends Genet.* 35, 706–707. <https://doi.org/10.1016/j.tig.2019.05.007>
- Bradshaw, W.E., Holzapfel, C.M., 2007. Evolution of Animal Photoperiodism. *Annu. Rev. Ecol. Evol. Syst.* 38, 1–25. <https://doi.org/10.1146/annurev.ecolsys.37.091305.110115>
- Brand, L.E., 1982. Persistent diel rhythms in the chlorophyll fluorescence of marine phytoplankton species. *Mar. Biol.* 69, 253–262. <https://doi.org/10.1007/BF00397491>
- Brand, L.E., Guillard, R.R.L., 1981. The effects of continuous light and light intensity on the reproduction rates of twenty-two species of marine phytoplankton. *J. Exp. Mar. Biol. Ecol.* 50, 119–132. [https://doi.org/10.1016/0022-0981\(81\)90045-9](https://doi.org/10.1016/0022-0981(81)90045-9)
- Brown, F., Webb, M., 1948. Temperature Relations of an Endogenous Daily Rhythmicity in the Fiddler Crab, *Uca*. *Physiol. Zool.* 21. <https://doi.org/10.1086/physzool.21.4.30152016>
- Bruce, V.G., 1974. RECOMBINANTS BETWEEN CLOCK MUTANTS OF *CHLAMYDOMONAS REINHARDI*. *Genetics* 77, 221–229. <https://doi.org/10.1093/genetics/77.2.221>
- Bruce, V.G., 1972. Mutants of the biological clock in *Chlamydomonas reinhardi*. *Genetics* 70, 537–548. <https://doi.org/10.1093/genetics/70.4.537>
- Bruce, V.G., 1970. The biological clock in *Chlamydomona reinhardtii*. *J. Protozool.* 17, 328–334. <https://doi.org/10.1111/j.1550-7408.1970.tb02380.x>
- Bruce, V.G., Pittendrigh, C.S., 1956. TEMPERATURE INDEPENDENCE IN A UNICELLULAR “CLOCK.” *Proc. Natl. Acad. Sci.* 42, 676–682. <https://doi.org/10.1073/pnas.42.9.676>
- Brunelle, S.A., Hazard Starr, A., Sotka, E.E., Van Dolah, F.M., 2007. Characterization Of A Dinoflagellate Cryptochrome Blue-Light Receptor With A Possible Role In Circadian Control Of The Cell Cycle. *J. Phycol.* 43, 509–518. <https://doi.org/10.1111/j.1529-8817.2007.00339.x>
- Brzezinski, M., Olson, R.J., Chisholm, S.W., 1990. Silicon availability and cell-cycle progression in marine diatoms. *Mar. Ecol. Prog. Ser.* 67, 83–96.
- Buck, J.M., Kroth, P.G., Lepetit, B., 2021. Identification of sequence motifs in Lhcx proteins that confer qE-based photoprotection in the diatom *Phaeodactylum tricornutum*. *Plant J.* 108, 1721–1734. <https://doi.org/10.1111/tpj.15539>
- Buck, J.M., Sherman, J., Bártulos, C.R., Serif, M., Halder, M., Henkel, J., Falciatore, A., Lavaud, J., Gorbunov, M.Y., Kroth, P.G., Falkowski, P.G., Lepetit, B., 2019. Lhcx proteins provide photoprotection via thermal dissipation of absorbed light in the diatom *Phaeodactylum tricornutum*. *Nat. Commun.* 10, 4167. <https://doi.org/10.1038/s41467-019-12043-6>
- Bünning, E., 1936. Die Endogene Tagesrhythmik Als Grundlage Der Photoperiodischen Reaktion, *Berichte der Deutschen Botanischen. Gesellschaft* 57, 590–607.
- Bünning, E., 1935. Zur kenntis der erblichen tagesperiodiztat bei den primarblättern von *Phaseolus multiflorus*. *Jahrb. Für Wiss. Bot.* 81.
- Burki, F., Roger, A.J., Brown, M.W., Simpson, A.G.B., 2020. The New Tree of Eukaryotes. *Trends Ecol. Evol.* 35, 43–55. <https://doi.org/10.1016/j.tree.2019.08.008>
- Cahonn, L.B., 1999. The role of benthic microalgae in neritic ecosystems, in: *The Role of Benthic Microalgae in Neritic Ecosystems*. CRC Press, p. 40.
- Carneiro, B.T.S., Araujo, J.F., 2012. Food entrainment: major and recent findings. *Front. Behav. Neurosci.* 6. <https://doi.org/10.3389/finbeh.2012.00083>

- Carré, I.A., Edmunds, L.N., 1993. Oscillator control of cell division in *Euglena*: cyclic AMP oscillations mediate the phasing of the cell division cycle by the circadian clock. *J. Cell Sci.* 104, 11. <https://doi.org/10.1242/jcs.104.4.1163>
- Carroll, P.A., Freie, B.W., Mathsyaraja, H., Eisenman, R.N., 2018. The MYC transcription factor network: balancing metabolism, proliferation and oncogenesis. *Front. Med.* 12, 412–425. <https://doi.org/10.1007/s11684-018-0650-z>
- Castillon, A., Shen, H., Huq, E., 2007. Phytochrome Interacting Factors: central players in phytochrome-mediated light signaling networks. *Trends Plant Sci.* 12, 514–521. <https://doi.org/10.1016/j.tplants.2007.10.001>
- Chan, C.X., Bhattacharya, D., Reyes-Prieto, A., 2012. Endosymbiotic and horizontal gene transfer in microbial eukaryotes: Impacts on cell evolution and the tree of life. *Mob. Genet. Elem.* 2, 101–105. <https://doi.org/10.4161/mge.20110>
- Chang, J., Carpenter, E., 1991. Species-specific phytoplankton growth rates via diel DNA synthesis cycles. V. Application to natural populations in Long Island Sound. *Mar. Ecol. Prog. Ser.* 78, 115–122. <https://doi.org/10.3354/meps078115>
- Chauton, M.S., Winge, P., Brembu, T., Vadstein, O., Bones, A.M., 2013. Gene Regulation of Carbon Fixation, Storage, and Utilization in the Diatom *Phaeodactylum tricornutum* Acclimated to Light/Dark Cycles. *Plant Physiol.* 161, 1034–1048. <https://doi.org/10.1104/pp.112.206177>
- Chen, C.-H., Dunlap, J.C., Loros, J.J., 2010. *Neurospora* illuminates fungal photoreception. *Fungal Genet. Biol.* 47, 922–929. <https://doi.org/10.1016/j.fgb.2010.07.005>
- Cheng, P., 2001. Coiled-coil domain-mediated FRQ-FRQ interaction is essential for its circadian clock function in *Neurospora*. *EMBO J.* 20, 101–108. <https://doi.org/10.1093/emboj/20.1.101>
- Cheng, P., He, Qun, He, Qiyang, Wang, L., Liu, Y., 2005. Regulation of the *Neurospora* circadian clock by an RNA helicase. *Genes Dev.* 19, 234–241. <https://doi.org/10.1101/gad.1266805>
- Cheng, P., Yang, Y., Gardner, K.H., Liu, Y., 2002. PAS Domain-Mediated WC-1/WC-2 Interaction Is Essential for Maintaining the Steady-State Level of WC-1 and the Function of Both Proteins in Circadian Clock and Light Responses of *Neurospora*. *Mol. Cell. Biol.* 22, 517–524. <https://doi.org/10.1128/MCB.22.2.517-524.2002>
- Chepurnov, V.A., Mann, D.G., Sabbe, K., Vyverman, W., 2004. Experimental Studies on Sexual Reproduction in Diatoms, in: *International Review of Cytology*. Elsevier, pp. 91–154. [https://doi.org/10.1016/S0074-7696\(04\)37003-8](https://doi.org/10.1016/S0074-7696(04)37003-8)
- Chisholm, S.W., Brand, L.E., 1981. Persistence of cell division phasing in marine phytoplankton in continuous light after entrainment to light: Dark cycles. *J. Exp. Mar. Biol. Ecol.* 51, 107–118. [https://doi.org/10.1016/0022-0981\(81\)90123-4](https://doi.org/10.1016/0022-0981(81)90123-4)
- Christie, J.M., Reymond, P., Powell, G.K., Bernasconi, P., Raibekas, A.A., Liscum, E., Briggs, W.R., 1998. *Arabidopsis* NPH1: A Flavoprotein with the Properties of a Photoreceptor for Phototropism. *Science* 282, 1698–1701. <https://doi.org/10.1126/science.282.5394.1698>
- Christie, J.M., Salomon, M., Nozue, K., Wada, M., Briggs, W.R., 1999. LOV (light, oxygen, or voltage) domains of the blue-light photoreceptor phototropin (nph1): Binding sites for the chromophore flavin mononucleotide. *Proc. Natl. Acad. Sci.* 96, 8779–8783. <https://doi.org/10.1073/pnas.96.15.8779>
- Chukhutsina, V.U., Büchel, C., van Amerongen, H., 2014. Disentangling two non-photochemical quenching processes in *Cyclotella meneghiniana* by spectrally-resolved picosecond fluorescence at 77K. *Biochim. Biophys. Acta BBA - Bioenerg.* 1837, 899–907. <https://doi.org/10.1016/j.bbabi.2014.02.021>
- Coesel, S., Mangogna, M., Ishikawa, T., Heijde, M., Rogato, A., Finazzi, G., Todo, T., Bowler, C., Falciatore, A., 2009. Diatom PtCPF1 is a new cryptochrome/photolyase family member with

- DNA repair and transcription regulation activity. *EMBO Rep.* 10, 655–661. <https://doi.org/10.1038/embor.2009.59>
- Cold Spring Harbour, 1960. Cold Spring Harbor Symposium of Quantitative Biology (No. XXV), Biological clocks. New York, NY.
- Copeland, R.A., 2000. *Enzymes: A Practical Introduction to Structure, Mechanism, and Data Analysis*. Wiley-VCH.
- Corellou, F., Schwartz, C., Motta, J.-P., Djouani-Tahri, E.B., Sanchez, F., Bouget, F.-Y., 2009. Clocks in the Green Lineage: Comparative Functional Analysis of the Circadian Architecture of the Picoeukaryote *Ostreococcus*. *Plant Cell* 21, 3436–3449. <https://doi.org/10.1105/tpc.109.068825>
- Courties, C., Vaquer, A., Troussellier, M., Lautier, J., 1994. Smallest eukaryotic organism. *Nature*, 6487 370, 255. <https://doi.org/10.1038/370255a0>
- Creux, N., Harmer, S., 2019. Circadian Rhythms in Plants. *Cold Spring Harb. Perspect. Biol.* 11, a034611. <https://doi.org/10.1101/cshperspect.a034611>
- Crosson, S., Rajagopal, S., Moffat, K., 2003. The LOV Domain Family: Photoresponsive Signaling Modules Coupled to Diverse Output Domains. *Biochemistry* 42, 2–10. <https://doi.org/10.1021/bi026978l>
- Crosthwaite, S.K., Dunlap, J.C., Loros, J.J., 1997. *Neurospora wc-1* and *wc-2*: Transcription, Photoresponses, and the Origins of Circadian Rhythmicity. *Science* 276, 763–769. <https://doi.org/10.1126/science.276.5313.763>
- Cruz de Carvalho, M.H., Bowler, C., 2020. Global identification of a marine diatom long noncoding natural antisense transcripts (NATs) and their response to phosphate fluctuations. *Sci. Rep.* 10, 14110. <https://doi.org/10.1038/s41598-020-71002-0>
- Daboussi, F., Leduc, S., Maréchal, A., Dubois, G., Guyot, V., Perez-Michaut, C., Amato, A., Falcitore, A., Juillerat, A., Beurdeley, M., Voytas, D.F., Cavarec, L., Duchateau, P., 2014. Genome engineering empowers the diatom *Phaeodactylum tricorutum* for biotechnology. *Nat. Commun.* 5, 3831. <https://doi.org/10.1038/ncomms4831>
- Dambek, M., Eilers, U., Breitenbach, J., Steiger, S., Buchel, C., Sandmann, G., 2012. Biosynthesis of fucoxanthin and diadinoxanthin and function of initial pathway genes in *Phaeodactylum tricorutum*. *J. Exp. Bot.* 63, 5607–5612. <https://doi.org/10.1093/jxb/ers211>
- Davis, G.H., 2000. *Neurospora: contributions of a model organism*, Oxford University Press. ed.
- De Martino, A., Amato, A., Bowler, C., 2009. Mitosis in diatoms: rediscovering an old model for cell division. *BioEssays* 31, 874–884. <https://doi.org/10.1002/bies.200900007>
- de Martino, A., Meichenin, A., Shi, J., Pan, K., Bowler, C., 2007. Genetic and phenotypic characterization of *Phaeodactylum tricorutum* (Bacillariophyceae) accessions <sup>1</sup>. *J. Phycol.* 43, 992–1009. <https://doi.org/10.1111/j.1529-8817.2007.00384.x>
- De Riso, V., Raniello, R., Maumus, F., Rogato, A., Bowler, C., Falcitore, A., 2009. Gene silencing in the marine diatom *Phaeodactylum tricorutum*. *Nucleic Acids Res.* 37, e96–e96. <https://doi.org/10.1093/nar/gkp448>
- de Vargas, C., Audic, S., Henry, N., Decelle, J., Mahe, F., Logares, R., Lara, E., Berney, C., Le Bescot, N., Probert, I., Carmichael, M., Poulain, J., Romac, S., Colin, S., Aury, J.-M., Bittner, L., Chaffron, S., Dunthorn, M., Engelen, S., Flegontova, O., Guidi, L., Horak, A., Jaillon, O., Lima-Mendez, G., Luke, J., Malviya, S., Morard, R., Mulot, M., Scalco, E., Siano, R., Vincent, F., Zingone, A., Dimier, C., Picheral, M., Searson, S., Kandels-Lewis, S., Tara Oceans Coordinators, Acinas, S.G., Bork, P., Bowler, C., Gorsky, G., Grimsley, N., Hingamp, P., Iudicone, D., Not, F., Ogata, H., Pesant, S., Raes, J., Sieracki, M.E., Speich, S., Stemann, L., Sunagawa, S., Weissenbach, J., Wincker, P., Karsenti, E., Boss, E., Follows, M., Karp-Boss, L., Krzic, U., Reynaud, E.G., Sardet, C., Sullivan, M.B., Velayoudon, D., 2015. Eukaryotic plankton diversity in the sunlit ocean. *Science* 348, 1261605–1261605. <https://doi.org/10.1126/science.1261605>

- Delaye, L., Valadez-Cano, C., Pérez-Zamorano, B., 2016. How Really Ancient Is *Paulinella Chromatophora*? PLoS Curr. <https://doi.org/10.1371/currents.tol.e68a099364bb1a1e129a17b4c06b0c6b>
- Depauw, F.A., Rogato, A., Ribera d'Alcala, M., Falciatore, A., 2012. Exploring the molecular basis of responses to light in marine diatoms. *J. Exp. Bot.* 63, 1575–1591. <https://doi.org/10.1093/jxb/ers005>
- Derelle, E., Ferraz, C., Rombauts, S., Rouze, P., Worden, A.Z., Robbens, S., Partensky, F., Degroeve, S., Echeynie, S., Cooke, R., Saeys, Y., Wuyts, J., Jabbari, K., Bowler, C., Panaud, O., Piegou, B., Ball, S.G., Ral, J.-P., Bouget, F.-Y., Piganeau, G., De Baets, B., Picard, A., Delseny, M., Demaille, J., Van de Peer, Y., Moreau, H., 2006. Genome analysis of the smallest free-living eukaryote *Ostreococcus tauri* unveils many unique features. *Proc. Natl. Acad. Sci.* 103, 11647–11652. <https://doi.org/10.1073/pnas.0604795103>
- Devlin, P.F., Kay, S.A., 2000. Cryptochromes Are Required for Phytochrome Signaling to the Circadian Clock but Not for Rhythmicity. *Plant Cell* 12, 11. <https://doi.org/10.1105/tpc.12.12.2499>
- Djouani-Tahri, E.B., Christie, J.M., Sanchez-Fernandin, S., Sanchez, F., Bouget, F.-Y., Corellou, F., 2011. A eukaryotic LOV-histidine kinase with circadian clock function in the picoalga *Ostreococcus*. *Plant J.* 65, 578–588.
- Dodd, A.N., Kusakina, J., Hall, A., Gould, P.D., Hanaoka, M., 2014. The circadian regulation of photosynthesis. *Photosynth. Res.* 119, 181–190. <https://doi.org/10.1007/s11120-013-9811-8>
- Dodd, A.N., Salathia, N., Hall, A., Kévei, E., Tóth, R., Nagy, F., Hibberd, J.M., Millar, A.J., Webb, A.A.R., 2005. Plant Circadian Clocks Increase Photosynthesis, Growth, Survival, and Competitive Advantage. *Sci. New Ser.* 309, 630–633. <http://10.1126/science.1115581>
- Dorrell, R.G., Gile, G., McCallum, G., Méheust, R., Baptiste, E.P., Klinger, C.M., Brillet-Guéguen, L., Freeman, K.D., Richter, D.J., Bowler, C., 2017. Chimeric origins of ochrophytes and haptophytes revealed through an ancient plastid proteome. *eLife* 6, e23717. <https://doi.org/10.7554/eLife.23717>
- Dorrell, R.G., Smith, A.G., 2011. Do Red and Green Make Brown?: Perspectives on Plastid Acquisitions within Chromalveolates. *Eukaryot. Cell* 10, 856–868. <https://doi.org/10.1128/EC.00326-10>
- D'Ortus de Mairan, J.-J.D., 1729. Observation botanique. *Histoire de L'Academie Royale des Sciences.*
- Dubinsky, Z., Stambler, N., 2009. Photoacclimation processes in phytoplankton: mechanisms, consequences, and applications. *Aquat. Microb. Ecol.* 56, 163–176. <https://doi.org/10.3354/ame01345>
- Dunahay, T.G., Jarvis, E.E., Roessler, P.G., 1995. Genetic Transformation Of The Diatoms *Cyclotella cryptica* And *Navicula saprophila*. *J. Phycol.* 31, 1004–1012. <https://doi.org/10.1111/j.0022-3646.1995.01004.x>
- Dunlap, J.C., 1999. Molecular Bases for Circadian Clocks. *Cell* 96, 271–290. [https://doi.org/10.1016/S0092-8674\(00\)80566-8](https://doi.org/10.1016/S0092-8674(00)80566-8)
- Eberhard, S., Finazzi, G., Wollman, F.-A., 2008. The Dynamics of Photosynthesis. *Annu. Rev. Genet.* 42, 463–515. <https://doi.org/10.1146/annurev.genet.42.110807.091452>
- Eckardt, N.A., 2006. A Wheel within a Wheel: Temperature Compensation of the Circadian Clock. *Plant Cell* 18, 1105–1108. <https://doi.org/10.1105/tpc.106.043356>
- Eckardt, N.A., 2005. Temperature Entrainment of the *Arabidopsis* Circadian Clock. *Plant Cell* 17, 645–647. <https://doi.org/10.1105/tpc.104.031336>
- Edgar, R.S., Green, E.W., Zhao, Y., van Ooijen, G., Olmedo, M., Qin, X., Xu, Y., Pan, M., Valekunja, U.K., Feeney, K.A., Maywood, E.S., Hastings, M.H., Baliga, N.S., Mellow, M., Millar, A.J., Johnson, C.H., Kyriacou, C.P., O'Neill, J.S., Reddy, A.B., 2012. Peroxiredoxins

- are conserved markers of circadian rhythms. *Nature* 485, 459–464. <https://doi.org/10.1038/nature11088>
- Ernst, R.K., Guina, T., Miller, S.I., 2001. Salmonella typhimurium outer membrane remodeling: role in resistance to host innate immunity. *Microbes Infect.* 3, 1327–1334. [https://doi.org/10.1016/S1286-4579\(01\)01494-0](https://doi.org/10.1016/S1286-4579(01)01494-0)
- Faktorová, D., Nisbet, R.E.R., Fernández Robledo, J.A., Casacuberta, E., Sudek, L., Allen, A.E., Ares, M., Aresté, C., Balestreri, C., Barbrook, A.C., Beardslee, P., Bender, S., Booth, D.S., Bouget, F.-Y., Bowler, C., Breglia, S.A., Brownlee, C., Burger, G., Cerutti, H., Cesaroni, R., Chiurillo, M.A., Clemente, T., Coles, D.B., Collier, J.L., Cooney, E.C., Coyne, K., Docampo, R., Dupont, C.L., Edgcomb, V., Einarsson, E., Elustondo, P.A., Federici, F., Freire-Beneitez, V., Freyria, N.J., Fukuda, K., García, P.A., Girguis, P.R., Gomaa, F., Gornik, S.G., Guo, J., Hampl, V., Hanawa, Y., Haro-Contreras, E.R., Hehenberger, E., Highfield, A., Hirakawa, Y., Hopes, A., Howe, C.J., Hu, I., Ibañez, J., Irwin, N.A.T., Ishii, Y., Janowicz, N.E., Jones, A.C., Kachale, A., Fujimura-Kamada, K., Kaur, B., Kaye, J.Z., Kazana, E., Keeling, P.J., King, N., Klobutcher, L.A., Lander, N., Lassadi, I., Li, Z., Lin, S., Lozano, J.-C., Luan, F., Maruyama, S., Matute, T., Miceli, C., Minagawa, J., Moosburner, M., Najle, S.R., Nanjappa, D., Nimmo, I.C., Noble, L., Novák Vanclová, A.M.G., Nowacki, M., Nuñez, I., Pain, A., Piersanti, A., Pucciarelli, S., Pyrih, J., Rest, J.S., Rius, M., Robertson, D., Ruaud, A., Ruiz-Trillo, I., Sigg, M.A., Silver, P.A., Slamovits, C.H., Jason Smith, G., Sprecher, B.N., Stern, R., Swart, E.C., Tsaousis, A.D., Tsy-pin, L., Turkewitz, A., Turnšek, J., Valach, M., Vergé, V., von Dassow, P., von der Haar, T., Waller, R.F., Wang, L., Wen, X., Wheeler, G., Woods, A., Zhang, H., Mock, T., Worden, A.Z., Lukeš, J., 2020. Genetic tool development in marine protists: emerging model organisms for experimental cell biology. *Nat. Methods* 17, 481–494. <https://doi.org/10.1038/s41592-020-0796-x>
- Falciatore, A., Casotti, R., Leblanc, C., Abrescia, C., Bowler, C., 1999. Transformation of Nonselectable Reporter Genes in Marine Diatoms. *Mar. Biotechnol.* 1, 239–251. <https://doi.org/10.1007/PL00011773>
- Falciatore, A., D’Alcalà, M.R., Croot, P., Bowler, C., 2000. Perception of Environmental Signals by a Marine Diatom. *Science* 288, 2363–2366. <https://doi.org/10.1126/science.288.5475.2363>
- Falciatore, A., Jaubert, M., Bouly, J.-P., Bailleul, B., Mock, T., 2020. Diatom Molecular Research Comes of Age: Model Species for Studying Phytoplankton Biology and Diversity. *Plant Cell* 32, 547–572. <https://doi.org/10.1105/tpc.19.00158>
- Falkowski, P.G., Barber, R.T., Smetacek, V., 1998. Biogeochemical Controls and Feedbacks on Ocean Primary Production. *Sci. New Ser.* 281, 200–206. <https://doi.org/10.1126/science.281.5374.200>
- Falkowski, P.G., Fenchel, T., Delong, E.F., 2008. The Microbial Engines That Drive Earth’s Biogeochemical Cycles. *Science* 320, 1034–1039. <https://doi.org/10.1126/science.1153213>
- Farinas, B., Mas, P., 2011. Functional implication of the MYB transcription factor RVE8/LCL5 in the circadian control of histone acetylation: Role of RVE8/LCL5 in the circadian clock. *Plant J.* 66, 318–329. <https://doi.org/10.1111/j.1365-313X.2011.04484.x>
- Farré, E.M., Harmer, S.L., Harmon, F.G., Yanovsky, M.J., Kay, S.A., 2005. Overlapping and Distinct Roles of PRR7 and PRR9 in the Arabidopsis Circadian Clock. *Curr. Biol.* 15, 47–54. <https://doi.org/10.1016/j.cub.2004.12.067>
- Farré, E.M., Weise, S.E., 2012. The interactions between the circadian clock and primary metabolism. *Curr. Opin. Plant Biol.* 15, 293–300. <https://doi.org/10.1016/j.pbi.2012.01.013>
- Fass, E., Groisman, E.A., 2009. Control of Salmonella pathogenicity island-2 gene expression. *Curr. Opin. Microbiol.* 12, 199–204. <https://doi.org/10.1016/j.mib.2009.01.004>
- Field, C.B., Behrenfeld, M.J., Randerson, J.T., Falkowski, P.G., 1998. Primary Production of the Biosphere: Integrating Terrestrial and Oceanic Components. *Science* 281, 237–240. <https://doi.org/10.1126/science.281.5374.237>

- Fischer, H., Gröning, C., Köster, C., 1977. Vertical migration rhythm in freshwater diatoms. *Hydrobiologia* 56, 259–263. <https://doi.org/10.1007/BF00017513>
- Fischer, H., Robl, I., Sumper, M., Kroger, N., 1999. Targeting and covalent modification of cell wall and membrane proteins heterologously expressed in the diatom *Cylindrotheca fusiformis* (Bacillariophyceae). *J. Phycol.* 35, 113–120. <https://doi.org/10.1046/j.1529-8817.1999.3510113.x>
- Flori, S., Jouneau, P.-H., Bailleul, B., Gallet, B., Estrozi, L.F., Moriscot, C., Bastien, O., Eicke, S., Schober, A., Bártulos, C.R., Maréchal, E., Kroth, P.G., Petroustos, D., Zeeman, S., Breyton, C., Schoehn, G., Falconet, D., Finazzi, G., 2017. Plastid thylakoid architecture optimizes photosynthesis in diatoms. *Nat. Commun.* 8, 15885. <https://doi.org/10.1038/ncomms15885>
- Flori, S., Jouneau, P.-H., Finazzi, G., Maréchal, E., Falconet, D., 2016. Ultrastructure of the Periplastidial Compartment of the Diatom *Phaeodactylum tricorutum*. *Protist* 167, 254–267. <https://doi.org/10.1016/j.protis.2016.04.001>
- Fortunato, A.E., Annunziata, R., Jaubert, M., Bouly, J.-P., Falciatore, A., 2015. Dealing with light: The widespread and multitasking cryptochrome/photolyase family in photosynthetic organisms. *J. Plant Physiol.* 172, 42–54. <https://doi.org/10.1016/j.jplph.2014.06.011>
- Fortunato, S.A.V., Vervoort, M., Adamski, M., Adamska, M., 2016. Conservation and divergence of bHLH genes in the calcsponge *Sycon ciliatum*. *EvoDevo* 7, 23. <https://doi.org/10.1186/s13227-016-0060-8>
- Foster, R.A., Kuypers, M.M.M., Vagner, T., Paerl, R.W., Musat, N., Zehr, J.P., 2011. Nitrogen fixation and transfer in open ocean diatom–cyanobacterial symbioses. *ISMEJ.* 5, 1484–1493. <https://doi.org/10.1038/ismej.2011.26>
- Fuchikawa, T., Eban-Rothschild, A., Nagari, M., Shemesh, Y., Bloch, G., 2016. Potent social synchronization can override photic entrainment of circadian rhythms. *Nat. Commun.* 7, 11662. <https://doi.org/10.1038/ncomms11662>
- Gaidarenko, O., Sathoff, C., Staub, K., Huesemann, M.H., Vernet, M., Hildebrand, M., 2019. Timing is everything: Diel metabolic and physiological changes in the diatom *Cyclotella cryptica* grown in simulated outdoor conditions. *Algal Res.* 42, 101598. <https://doi.org/10.1016/j.algal.2019.101598>
- Gau, D., Lemberger, T., von Gall, C., Kretz, O., Le Minh, N., Gass, P., Schmid, W., Schibler, U., Korf, H.W., Schütz, G., 2002. Phosphorylation of CREB Ser142 Regulates Light-Induced Phase Shifts of the Circadian Clock. *Neuron* 34, 245–253. [https://doi.org/10.1016/S0896-6273\(02\)00656-6](https://doi.org/10.1016/S0896-6273(02)00656-6)
- George, J., Kahlke, T., Abbriano, R.M., Kuzhiumparambil, U., Ralph, P.J., Fabris, M., 2020. Metabolic Engineering Strategies in Diatoms Reveal Unique Phenotypes and Genetic Configurations With Implications for Algal Genetics and Synthetic Biology. *Front. Bioeng. Biotechnol.* 8, 513. <https://doi.org/10.3389/fbioe.2020.00513>
- Giacinti, C., Giordano, A., 2006. RB and cell cycle progression. *Oncogene* 25, 5220–5227. <https://doi.org/10.1038/sj.onc.1209615>
- Gilbert, J.A., Steele, J.A., Caporaso, J.G., Steinbrück, L., Reeder, J., Temperton, B., Huse, S., McHardy, A.C., Knight, R., Joint, I., Somerfield, P., Fuhrman, J.A., Field, D., 2012. Defining seasonal marine microbial community dynamics. *ISME J.* 6, 298–308. <https://doi.org/10.1038/ismej.2011.107>
- Gillard, J., Devos, V., Huysman, M.J.J., De Veylder, L., D’Hondt, S., Martens, C., Vanormelingen, P., Vannerum, K., Sabbe, K., Chepurnov, V.A., Inzé, D., Vuylsteke, M., Vyverman, W., 2008. Physiological and Transcriptomic Evidence for a Close Coupling between Chloroplast Ontogeny and Cell Cycle Progression in the Pennate Diatom *Seminavis robusta*. *Plant Physiol.* 148, 1394–1411. <https://doi.org/10.1104/pp.108.122176>
- Giovagnetti, V., Jaubert, M., Shukla, M.K., Ungerer, P., Bouly, J.-P., Falciatore, A., Ruban, A.V., 2022. Biochemical and molecular properties of LHCX1, the essential regulator of dynamic

- photoprotection in diatoms. *Plant Physiol.* 188, 509–525. <https://doi.org/10.1093/plphys/kiab425>
- Goessling, J.W., Su, Y., Cartaxana, P., Maibohm, C., Rickelt, L.F., Trampe, E.C.L., Walby, S.L., Wangpraseurt, D., Wu, X., Ellegaard, M., Kühl, M., 2018. Structure-based optics of centric diatom frustules: modulation of the *in vivo* light field for efficient diatom photosynthesis. *New Phytol.* 219, 122–134. <https://doi.org/10.1111/nph.15149>
- Goss, R., Ann Pinto, E., Wilhelm, C., Richter, M., 2006. The importance of a highly active and  $\Delta$ pH-regulated diatoxanthin epoxidase for the regulation of the PS II antenna function in diadinoxanthin cycle containing algae. *J. Plant Physiol.* 163, 1008–1021. <https://doi.org/10.1016/j.jplph.2005.09.008>
- Gould, P.D., Domijan, M., Greenwood, M., Tokuda, I.T., Rees, H., Kozma-Bognar, L., Hall, A.J., Locke, J.C., 2018. Coordination of robust single cell rhythms in the *Arabidopsis* circadian clock via spatial waves of gene expression. *eLife* 7, e31700. <https://doi.org/10.7554/eLife.31700>
- Gould, P.D., Ugarte, N., Domijan, M., Costa, M., Foreman, J., MacGregor, D., Rose, K., Griffiths, J., Millar, A.J., Finkenstädt, B., Penfield, S., Rand, D.A., Halliday, K.J., Hall, A.J.W., 2013. Network balance *via* CRY signalling controls the *Arabidopsis* circadian clock over ambient temperatures. *Mol. Syst. Biol.* 9, 650. <https://doi.org/10.1038/msb.2013.7>
- Gross, M., 2012. The mysteries of the diatoms. *Curr. Biol.* 22, R581–R585. <https://doi.org/10.1016/j.cub.2012.07.041>
- Grossman, A.R., Lohr, M., Im, C.S., 2004. *Chlamydomonas reinhardtii* in the Landscape of Pigments. *Annu. Rev. Genet.* 38, 119–173. <https://doi.org/10.1146/annurev.genet.38.072902.092328>
- Grossman, R.D., Parker, M.S., Armbrust, E.V., 2015. Diversity and Evolutionary History of Iron Metabolism Genes in Diatoms. *PLOS ONE* 10, e0129081. <https://doi.org/10.1371/journal.pone.0129081>
- Gschloessl, B., Guermeur, Y., Cock, J.M., 2008. HECTAR: A method to predict subcellular targeting in heterokonts. *BMC Bioinformatics* 9, 393. <https://doi.org/10.1186/1471-2105-9-393>
- Gwinner, E., 2012. Circannual Rhythms: Endogenous Annual Clocks in the Organization of Seasonal Processes, Springer-Verlag. ed. Berlin.
- Hamm, C.E., Merkel, R., Springer, O., Jurkojc, P., Maier, C., Prechtel, K., Smetacek, V., 2003. Architecture and material properties of diatom shells provide effective mechanical protection. *Nature* 421, 841–843. <https://doi.org/10.1038/nature01416>
- Harmer, S.L., Hogenesch, J.B., Straume, M., Chang, H.-S., Han, B., Zhu, T., Wang, X., Kreps, J.A., Kay, S.A., 2000. Orchestrated Transcription of Key Pathways in *Arabidopsis* by the Circadian Clock. *Science* 290, 2110–2113. <https://doi.org/10.1126/science.290.5499.2110>
- Hastings, J.W., 2007. The *Gonyaulax* Clock at 50: Translational Control of Circadian Expression. *Cold Spring Harb. Symp. Quant. Biol.* 72, 141–144. <https://doi.org/10.1101/sqb.2007.72.026>
- Hastings, J.W., Sweeney, B.M., 1957. On the mechanism of temperature independence in a biological clock. *Proc. Natl. Acad. Sci.* 43, 804–811. <https://doi.org/10.1073/pnas.43.9.804>
- Haydon, M.J., Mielczarek, O., Frank, A., Román, Á., Webb, A.A.R., 2017. Sucrose and Ethylene Signaling Interact to Modulate the Circadian Clock. *Plant Physiol.* 175, 947–958. <https://doi.org/10.1104/pp.17.00592>
- Haydon, M.J., Mielczarek, O., Robertson, F.C., Hubbard, K.E., Webb, A.A.R., 2013. Photosynthetic entrainment of the *Arabidopsis thaliana* circadian clock. *Nature* 502, 689–692. <https://doi.org/10.1038/nature12603>
- Heijde, M., Zabulon, G., Corellou, F., Ishikawa, T., Brazard, J., Usman, A., Sanchez, F., Plaza, P., Martin, M., Falciatore, A., Todo, T., Bouget, F.-Y., Bowler, C., 2010. Characterization of two members of the cryptochrome/photolyase family from *Ostreococcus tauri* provides



- insights into the origin and evolution of cryptochromes: Cryptochrome/photolyase family members in *Ostreococcus tauri*. *Plant Cell Environ.* 33, 1614–1626. <https://doi.org/10.1111/j.1365-3040.2010.02168.x>
- Heintze, C., Formanek, P., Pohl, D., Hauptstein, J., Rellinghaus, B., Kröger, N., 2020. An intimate view into the silica deposition vesicles of diatoms. *BMC Mater.* 2, 11. <https://doi.org/10.1186/s42833-020-00017-8>
- Hempel, F., Bullmann, L., Lau, J., Zauner, S., Maier, U.G., 2009. ERAD-Derived Preprotein Transport across the Second Outermost Plastid Membrane of Diatoms. *Mol. Biol. Evol.* 26, 1781–1790. <https://doi.org/10.1093/molbev/msp079>
- Henry, J.T., Crosson, S., 2011. Ligand-Binding PAS Domains in a Genomic, Cellular, and Structural Context. *Annu. Rev. Microbiol.* 65, 261–286. <https://doi.org/10.1146/annurev-micro-121809-151631>
- Hirayama, J., Sahar, S., Grimaldi, B., Tamaru, T., Takamatsu, K., Nakahata, Y., Sassone-Corsi, P., 2007. CLOCK-mediated acetylation of BMAL1 controls circadian function. *Nature* 450, 1086–1090. <https://doi.org/10.1038/nature06394>
- Hong, C.I., Ruoff, P., Loros, J.J., Dunlap, J.C., 2008. Closing the circadian negative feedback loop: FRQ-dependent clearance of WC-1 from the nucleus. *Genes Dev.* 22, 3196–3204. <https://doi.org/10.1101/gad.1706908>
- Hongo, Y., Kimura, K., Takaki, Y., Yoshida, Y., Baba, S., Kobayashi, G., Nagasaki, K., Hano, T., Tomaru, Y., 2021. The genome of the diatom *Chaetoceros tenuissimus* carries an ancient integrated fragment of an extant virus. *Sci. Rep.* 11, 22877. <https://doi.org/10.1038/s41598-021-00565-3>
- Huang, H., Nusinow, D.A., 2016. Into the Evening: Complex Interactions in the Arabidopsis Circadian Clock. *Trends Genet.* 32, 674–686. <https://doi.org/10.1016/j.tig.2016.08.002>
- Huang, N., Chelliah, Y., Shan, Y., Taylor, C.A., Yoo, S.-H., Partch, C., Green, C.B., Zhang, H., Takahashi, J.S., 2012. Crystal Structure of the Heterodimeric CLOCK:BMAL1 Transcriptional Activator Complex. *Science* 337, 7. <https://doi.org/10.1126/science.1222804>
- Huang, W., Daboussi, F., 2017. Genetic and metabolic engineering in diatoms. *Philos. Trans. R. Soc. B Biol. Sci.* 372, 20160411. <https://doi.org/10.1098/rstb.2016.0411>
- Hunsperger, H.M., Ford, C.J., Miller, J.S., Cattolico, R.A., 2016. Differential Regulation of Duplicate Light-Dependent Protochlorophyllide Oxidoreductases in the Diatom *Phaeodactylum tricorutum*. *PLOS ONE* 11, e0158614. <https://doi.org/10.1371/journal.pone.0158614>
- Huysman, M.J., Martens, C., Vandepoele, K., Gillard, J., Rayko, E., Heijde, M., Bowler, C., Inzé, D., 2010. Genome-wide analysis of the diatom cell cycle unveils a novel type of cyclins involved in environmental signaling. *Genome Biol.* 11, 19.
- Huysman, M.J.J., Fortunato, A.E., Matthijs, M., Costa, B.S., Vanderhaeghen, R., Van den Daele, H., Sachse, M., Inzé, D., Bowler, C., Kroth, P.G., Wilhelm, C., Falciatore, A., Vyverman, W., De Veylder, L., 2013. AUREOCHROME1a-Mediated Induction of the Diatom-Specific Cyclin *dsCYC2* Controls the Onset of Cell Division in Diatoms (*Phaeodactylum tricorutum*). *Plant Cell* 25, 215–228. <https://doi.org/10.1105/tpc.112.106377>
- Huysman, M.J.J., Martens, C., Vyverman, W., De Veylder, L., 2014a. Protein degradation during the diatom cell cycle: Annotation and transcriptional analysis of SCF and APC/C ubiquitin ligase genes in *Phaeodactylum tricorutum*. *Mar. Genomics* 14, 39–46. <https://doi.org/10.1016/j.margen.2013.09.001>
- Huysman, M.J.J., Vyverman, W., De Veylder, L., 2014b. Molecular regulation of the diatom cell cycle. *J. Exp. Bot.* 65, 2573–2584. <https://doi.org/10.1093/jxb/ert387>
- Hwang, S., Kawazoe, R., Herrin, D.L., 1996. Transcription of *tufA* and other chloroplast-encoded genes is controlled by a circadian clock in *Chlamydomonas*. *Proc. Natl. Acad. Sci.* 93, 996–1000. <https://doi.org/10.1073/pnas.93.3.996>

- Iliev, D., Voytsekh, O., Schmidt, E.-M., Fiedler, M., Nykytenko, A., Mittag, M., 2006. A Heteromeric RNA-Binding Protein Is Involved in Maintaining Acrophase and Period of the Circadian Clock. *Plant Physiol.* 142, 797–806. <https://doi.org/10.1104/pp.106.085944>
- Imaizumi, T., Schultz, T.F., Harmon, F.G., Ho, L.A., Kay, S.A., 2005. FKF1 F-Box Protein Mediates Cyclic Degradation of a Repressor of *CONSTANS* in *Arabidopsis*. *Science* 309, 293–297. <https://doi.org/10.1126/science.1110586>
- Iwasaki, H., Kondo, T., 2004. Circadian Timing Mechanism in the Prokaryotic Clock System of Cyanobacteria. *J. Biol. Rhythms* 19, 436–444. <https://doi.org/10.1177/0748730404269060>
- Jang, S., An, G., Li, H.-Y., 2017. Rice Leaf Angle and Grain Size Are Affected by the OsBULL1 Transcriptional Activator Complex. *Plant Physiol.* 173, 688–702. <https://doi.org/10.1104/pp.16.01653>
- Jaubert, M., Bouly, J.-P., Ribera d'Alcalà, M., Falciatore, A., 2017. Light sensing and responses in marine microalgae. *Curr. Opin. Plant Biol.* 37, 70–77. <https://doi.org/10.1016/j.pbi.2017.03.005>
- Jaubert, M., Duchêne, C., Kroth, P.G., Rogato, A., Bouly, J.-P., Falciatore, A., 2022. Sensing and Signalling in Diatom Responses to Abiotic Cues, in: *The Molecular Life of Diatoms*.
- Ji, N., Li, L., Lin, L., Lin, S., 2017. Identification and expression analysis of blue light receptor aureochrome in the harmful alga *Heterosigma akashiwo* (raphidophyceae). *Harmful Algae* 61, 71–79. <https://doi.org/10.1016/j.hal.2016.11.016>
- Jiang, H., Guo, R., Powell-Coffman, J.A., 2001. The *Caenorhabditis elegans* hif-1 gene encodes a bHLH-PAS protein that is required for adaptation to hypoxia. *Proc. Natl. Acad. Sci.* 98, 7916–7921. <https://doi.org/10.1073/pnas.141234698>
- Johnson, C.H., Golden, S.S., 1999. Circadian Programs in Cyanobacteria: Adaptiveness and Mechanism. *Annu. Rev. Microbiol.* 53, 389–409. <https://doi.org/10.1146/annurev.micro.53.1.389>
- Jones, S., 2004. An overview of the basic helix-loop-helix proteins. *Genome Biol.* 6.
- Juhas, M., von Zadow, A., Spexard, M., Schmidt, M., Kottke, T., Büchel, C., 2014. A novel cryptochrome in the diatom *Phaeodactylum tricorutum* influences the regulation of light-harvesting protein levels. *FEBS J.* 281, 2299–2311. <https://doi.org/10.1111/febs.12782>
- Kageyama, R., Ohtsuka, T., Tomita, K., 2000. The bHLH Gene *Hes1* Regulates Differentiation of Multiple Cell Types. *Mol. Cells* 10, 1–7. <https://doi.org/10.1007/s10059-000-0001-0>
- Kaldis, P., 1999. The cdk-activating kinase (CAK): from yeast to mammals. *Cell. Mol. Life Sci. CMLS* 55, 284–296. <https://doi.org/10.1007/s000180050290>
- Kamikawa, R., Moog, D., Zauner, S., Tanifuji, G., Ishida, K.-I., Miyashita, H., Mayama, S., Hashimoto, T., Maier, U.G., Archibald, J.M., Inagaki, Y., 2017. A Non-photosynthetic Diatom Reveals Early Steps of Reductive Evolution in Plastids. *Mol. Biol. Evol.* 34, 2355–2366. <https://doi.org/10.1093/molbev/msx172>
- Kamioka, M., Takao, S., Suzuki, T., Taki, K., Higashiyama, T., Kinoshita, T., Nakamichi, N., 2016. Direct Repression of Evening Genes by CIRCADIANT CLOCK-ASSOCIATED1 in the *Arabidopsis* Circadian Clock. *Plant Cell* 28, 696–711. <https://doi.org/10.1105/tpc.15.00737>
- Karas, B.J., Diner, R.E., Lefebvre, S.C., McQuaid, J., Phillips, A.P.R., Noddings, C.M., Brunson, J.K., Valas, R.E., Deerinck, T.J., Jablanovic, J., Gillard, J.T.F., Beerli, K., Ellisman, M.H., Glass, J.I., Hutchison III, C.A., Smith, H.O., Venter, J.C., Allen, A.E., Dupont, C.L., Weyman, P.D., 2015. Designer diatom episomes delivered by bacterial conjugation. *Nat. Commun.* 6, 6925. <https://doi.org/10.1038/ncomms7925>
- Kaur, S., Spillane, C., 2015. Reduction in Carotenoid Levels in the Marine Diatom *Phaeodactylum tricorutum* by Artificial MicroRNAs Targeted Against the Endogenous Phytoene Synthase Gene. *Mar. Biotechnol.* 17, 1–7. <https://doi.org/10.1007/s10126-014-9593-9>

- Keeling, P.J., 2013. The Number, Speed, and Impact of Plastid Endosymbioses in Eukaryotic Evolution. *Annu. Rev. Plant Biol.* 64, 583–607. <https://doi.org/10.1146/annurev-arplant-050312-120144>
- Kewley, R.J., Whitelaw, M.L., Chapman-Smith, A., 2004. The mammalian basic helix-loop-helix/PAS family of transcriptional regulators. *Int. J. Biochem. Cell Biol.* 36, 189–204. [https://doi.org/10.1016/S1357-2725\(03\)00211-5](https://doi.org/10.1016/S1357-2725(03)00211-5)
- Kilian, O., Kroth, P.G., 2004. Identification and characterization of a new conserved motif within the presequence of proteins targeted into complex diatom plastids: Protein targeting into diatom plastids. *Plant J.* 41, 175–183. <https://doi.org/10.1111/j.1365-313X.2004.02294.x>
- Kim, W.-Y., Fujiwara, S., Suh, S.-S., Kim, J., Kim, Y., Han, L., David, K., Putterill, J., Nam, H.G., Somers, D.E., 2007. ZEITLUPE is a circadian photoreceptor stabilized by GIGANTEA in blue light. *Nature* 449, 356–360. <https://doi.org/10.1038/nature06132>
- Kirk, J.T.O., 2011. Light and photosynthesis in aquatic ecosystems, 3rd Editio. ed, Cambridge University Press. Cambridge Univ. Press. <https://doi.org/10.1017/S0025315400044180>
- Kleine, T., Voigt, C., Leister, D., 2009. Plastid signalling to the nucleus: messengers still lost in the mists? *Trends Genet.* 25, 185–192. <https://doi.org/10.1016/j.tig.2009.02.004>
- Kondo, T., Ishiura, M., 2000. The circadian clock of cyanobacteria. *BioEssays* 22, 10–15. [https://doi.org/10.1002/\(SICI\)1521-1878\(200001\)22:1<10::AID-BIES4>3.0.CO;2-A](https://doi.org/10.1002/(SICI)1521-1878(200001)22:1<10::AID-BIES4>3.0.CO;2-A)
- Konopka, R.J., Benzer, S., 1971. Clock Mutants of *Drosophila melanogaster*. *Proc. Natl. Acad. Sci.* 68, 2112–2116. <https://doi.org/10.1073/pnas.68.9.2112>
- Kooistra, W.H.C.F., Gersonde, R., Medlin, L.K., Mann, D.G., 2007. The Origin and Evolution of the Diatoms: Their Adaptation to a Planktonic Existence, in: *Evolution of Primary Producers in the Sea*. Elsevier, pp. 207–249. <https://doi.org/10.1016/B978-012370518-1/50012-6>
- Kröger, N., Poulsen, N., 2008. Diatoms—From Cell Wall Biogenesis to Nanotechnology. *Annu. Rev. Genet.* 42, 83–107. <https://doi.org/10.1146/annurev.genet.41.110306.130109>
- Kroth, P., Strotmann, H., 1999. Diatom plastids: Secondary endocytobiosis, plastid genome and protein import. *Physiol. Plant.* 107, 136–141. <https://doi.org/10.1034/j.1399-3054.1999.100118.x>
- Kroth, P.G., Bones, A.M., Daboussi, F., Ferrante, M.I., Jaubert, M., Kolot, M., Nymark, M., Río Bártulos, C., Ritter, A., Russo, M.T., Serif, M., Winge, P., Falciatore, A., 2018. Genome editing in diatoms: achievements and goals. *Plant Cell Rep.* 37, 1401–1408. <https://doi.org/10.1007/s00299-018-2334-1>
- Kroth, P.G., Chiovitti, A., Gruber, A., Martin-Jezequel, V., Mock, T., Parker, M.S., Stanley, M.S., Kaplan, A., Caron, L., Weber, T., Maheswari, U., Armbrust, E.V., Bowler, C., 2008. A Model for Carbohydrate Metabolism in the Diatom *Phaeodactylum tricoratum* Deduced from Comparative Whole Genome Analysis. *PLoS ONE* 3, e1426. <https://doi.org/10.1371/journal.pone.0001426>
- Kroth, P.G., Wilhelm, C., Kottke, T., 2017. An update on aureochromes: Phylogeny - mechanism - function. *J. Plant Physiol.* 217, 20–26. <https://doi.org/10.1016/j.jplph.2017.06.010>
- Kuczynska, P., Jemiola-Rzeminska, M., Strzalka, K., 2015. Photosynthetic Pigments in Diatoms. *Mar. Drugs* 13, 5847–5881. <https://doi.org/10.3390/md13095847>
- Kuhlman, S.J., Craig, L.M., Duffy, J.F., 2018. Introduction to Chronobiology. *Cold Spring Harb. Perspect. Biol.* 10, a033613. <https://doi.org/10.1101/cshperspect.a033613>
- Kume, K., Zylka, M.J., Sriram, S., Shearman, L.P., Weaver, D.R., Jin, X., Maywood, E.S., Hastings, M.H., Reppert, S.M., 1999. mCRY1 and mCRY2 Are Essential Components of the Negative Limb of the Circadian Clock Feedback Loop. *Cell* 98, 193–205. [https://doi.org/10.1016/S0092-8674\(00\)81014-4](https://doi.org/10.1016/S0092-8674(00)81014-4)
- La Roche, J., Boyd, P.W., McKay, R.M.L., Geider, R.J., 1996. Flavodoxin as an in situ marker for iron stress in phytoplankton. *Nature* 382, 802–805. <https://doi.org/10.1038/382802a0>

- Lafond, A., Leblanc, K., Quéguiner, B., Moriceau, B., Leynaert, A., Cornet, V., Legras, J., Ras, J., Parenteau, M., Garcia, N., Babin, M., Tremblay, J.-É., 2019. Late spring bloom development of pelagic diatoms in Baffin Bay. *Elem. Sci. Anthr.* 7, 44. <https://doi.org/10.1525/elementa.382>
- Lambert, S., Tragin, M., Lozano, J.-C., Ghiglione, J.-F., Vaulot, D., Bouget, F.-Y., Galand, P.E., 2019. Rhythmicity of coastal marine picoeukaryotes, bacteria and archaea despite irregular environmental perturbations. *ISME J.* 13, 388–401. <https://doi.org/10.1038/s41396-018-0281-z>
- Lang, M., Kroth, P.G., 2001. Diatom Fucoxanthin Chlorophyll a/c-binding Protein (FCP) and Land Plant Light-harvesting Proteins Use a Similar Pathway for Thylakoid Membrane Insertion. *J. Biol. Chem.* 276, 7985–7991. <https://doi.org/10.1074/jbc.M006417200>
- Lassiter, A.M., Wilkerson, F.P., Dugdale, R.C., Hogue, V.E., 2006. Phytoplankton assemblages in the CoOP-WEST coastal upwelling area. *Deep Sea Res. Part II Top. Stud. Oceanogr.* 53, 3063–3077. <https://doi.org/10.1016/j.dsr2.2006.07.013>
- Lauterborn, R., 1896. Untersuchungen über bau: kernteilung und bewegung der diatomeen, Engelmann. ed. Leipzig.
- Le Quéré, C., Andrew, R.M., Friedlingstein, P., Sitch, S., Hauck, J., Pongratz, J., Pickers, P.A., Korsbakken, J.I., Peters, G.P., Canadell, J.G., Arneeth, A., Arora, V.K., Barbero, L., Bastos, A., Bopp, L., Chevallier, F., Chini, L.P., Ciais, P., Doney, S.C., Gkritzalis, T., Goll, D.S., Harris, I., Haverd, V., Hoffman, F.M., Hoppema, M., Houghton, R.A., Hurtt, G., Ilyina, T., Jain, A.K., Johannessen, T., Jones, C.D., Kato, E., Keeling, R.F., Goldewijk, K.K., Landschützer, P., Lefèvre, N., Lienert, S., Liu, Z., Lombardozi, D., Metzl, N., Munro, D.R., Nabel, J.E.M.S., Nakaoka, S., Neill, C., Olsen, A., Ono, T., Patra, P., Peregon, A., Peters, W., Peylin, P., Pfeil, B., Pierrot, D., Poulter, B., Rehder, G., Resplandy, L., Robertson, E., Rocher, M., Rödenbeck, C., Schuster, U., Schwinger, J., Séférian, R., Skjelvan, I., Steinhoff, T., Sutton, A., Tans, P.P., Tian, H., Tilbrook, B., Tubiello, F.N., van der Laan-Luijkx, I.T., van der Werf, G.R., Viovy, N., Walker, A.P., Wiltshire, A.J., Wright, R., Zaehle, S., Zheng, B., 2018. Global Carbon Budget 2018. *Earth Syst. Sci. Data* 10, 2141–2194. <https://doi.org/10.5194/essd-10-2141-2018>
- Ledent, V., Vervoort, M., 2001. The Basic Helix-Loop-Helix Protein Family: Comparative Genomics and Phylogenetic Analysis. *Genome Res.* 11, 754–770. <https://doi.org/10.1101/gr.177001>
- Leliaert, F., Smith, D.R., Moreau, H., Herron, M.D., Verbruggen, H., Delwiche, C.F., De Clerck, O., 2012. Phylogeny and Molecular Evolution of the Green Algae. *Crit. Rev. Plant Sci.* 31, 1–46. <https://doi.org/10.1080/07352689.2011.615705>
- Leloup, J.-C., Goldbeter, A., 2013. Critical phase shifts slow down circadian clock recovery: Implications for jet lag. *J. Theor. Biol.* 333, 47–57. <https://doi.org/10.1016/j.jtbi.2013.04.039>
- Leming, M.T., Rund, S.S., Behura, S.K., Duffield, G.E., O'Tousa, J.E., 2014. A database of circadian and diel rhythmic gene expression in the yellow fever mosquito *Aedes aegypti*. *BMC Genomics* 15, 1128. <https://doi.org/10.1186/1471-2164-15-1128>
- Lepetit, B., Sturm, S., Rogato, A., Gruber, A., Sachse, M., Falciatore, A., Kroth, P.G., Lavaud, J., 2013. High Light Acclimation in the Secondary Plastids Containing Diatom *Phaeodactylum tricorutum* is Triggered by the Redox State of the Plastoquinone Pool. *Plant Physiol.* 161, 853–865. <https://doi.org/10.1104/pp.112.207811>
- Lepetit, B., Volke, D., Szabó, M., Hoffmann, R., Garab, G., Wilhelm, C., Goss, R., 2007. Spectroscopic and Molecular Characterization of the Oligomeric Antenna of the Diatom *Phaeodactylum tricorutum*. *Biochemistry* 46, 9813–9822. <https://doi.org/10.1021/bi7008344>

- Levine, J.D., Funes, P., Dowse, H.B., Hall, J.C., 2002. Resetting the Circadian Clock by Social Experience in *Drosophila melanogaster*. *Science* 298, 2010–2012. <https://doi.org/10.1126/science.1076008>
- Lin, H.-Y., Lin, H.-J., 2018. Polyamines in Microalgae: Something Borrowed, Something New. *Mar. Drugs* 17, 1. <https://doi.org/10.3390/md17010001>
- Lin, J.-M., Kilman, V.L., Keegan, K., Paddock, B., Emery-Le, M., Rosbash, M., Allada, R., 2002. A role for casein kinase 2 $\alpha$  in the *Drosophila* circadian clock. *Nature* 420, 816–820. <https://doi.org/10.1038/nature01235>
- Lohr, M., Wilhelm, C., 1999. Algae displaying the diadinoxanthin cycle also possess the violaxanthin cycle. *Proc. Natl. Acad. Sci.* 96, 8784–8789. <https://doi.org/10.1073/pnas.96.15.8784>
- Lommer, M., Specht, M., Roy, A.-S., Kraemer, L., Andreson, R., Gutowska, M.A., Wolf, J., Bergner, S.V., Schilhabel, M.B., Klostermeier, U.C., Beiko, R.G., Rosenstiel, P., Hippler, M., LaRoche, J., 2012. Genome and low-iron response of an oceanic diatom adapted to chronic iron limitation. *Genome Biol.* 13, R66. <https://doi.org/10.1186/gb-2012-13-7-r66>
- Losic, D., Rosengarten, G., Mitchell, J.G., Voelcker, N.H., 2006. Pore Architecture of Diatom Frustules: Potential Nanostructured Membranes for Molecular and Particle Separations. *J. Nanosci. Nanotechnol.* 6, 982–989. <https://doi.org/10.1166/jnn.2006.174>
- Macdonald, J.D., 1869. On the structure of the Diatomaceous frustule, and its genetic cycle. *Ann. Mag. Nat. Hist.* 3, 1–8. <https://doi.org/10.1080/00222936908695866>
- Makarov, V.N., Schoschina, E.V., Lüning, K., 1995. Diurnal and circadian periodicity of mitosis and growth in marine macroalgae. I. Juvenile sporophytes of Laminariales (Phaeophyta). *Eur. J. Phycol.* 30, 261–266. <https://doi.org/10.1080/09670269500651031>
- Malviya, S., Scalco, E., Audic, S., Vincent, F., Veluchamy, A., Poulain, J., Wincker, P., Iudicone, D., de Vargas, C., Bittner, L., Zingone, A., Bowler, C., 2016. Insights into global diatom distribution and diversity in the world's ocean. *Proc. Natl. Acad. Sci.* 113, E1516–E1525. <https://doi.org/10.1073/pnas.1509523113>
- Mann, D.G., 2011. Size and Sex, in: Seckbach, J., Kociolek, P. (Eds.), *The Diatom World, Cellular Origin, Life in Extreme Habitats and Astrobiology*. Springer Netherlands, Dordrecht, pp. 145–166. [https://doi.org/10.1007/978-94-007-1327-7\\_6](https://doi.org/10.1007/978-94-007-1327-7_6)
- Mann, D.G., Droop, S.J.M., 1996. Biodiversity, biogeography and conservation of diatoms. *Hydrobiologia* 336, 19–32. <https://doi.org/10.1007/BF00010816>
- Mann, K.H., Lazier, J.R.N., 2009. *Dynamics of marine ecosystems: biological-physical interactions in the oceans*, 3. ed., [Nachdr.] ed. Blackwell Publ, Malden, Mass.
- Mann, M., Serif, M., Jakob, T., Kroth, P.G., Wilhelm, C., 2017. PtAUREO1a and PtAUREO1b knockout mutants of the diatom *Phaeodactylum tricornutum* are blocked in photoacclimation to blue light. *J. Plant Physiol.* 217, 44–48. <https://doi.org/10.1016/j.jplph.2017.05.020>
- Mann, M., Serif, M., Wrobel, T., Eisenhut, M., Madhuri, S., Flachbart, S., Weber, A.P.M., Lepetit, B., Wilhelm, C., Kroth, P.G., 2020. The Aureochrome Photoreceptor PtAUREO1a Is a Highly Effective Blue Light Switch in Diatoms. *iScience* 23, 101730. <https://doi.org/10.1016/j.isci.2020.101730>
- Marquardt, M., Vader, A., Stübner, E.I., Reigstad, M., Gabrielsen, T.M., 2016. Strong Seasonality of Marine Microbial Eukaryotes in a High-Arctic Fjord (Isfjorden, in West Spitsbergen, Norway). *Appl. Environ. Microbiol.* 82, 1868–1880. <https://doi.org/10.1128/AEM.03208-15>
- Más, P., Kim, W.-Y., Somers, D.E., Kay, S.A., 2003. Targeted degradation of TOC1 by ZTL modulates circadian function in *Arabidopsis thaliana*. *Nature* 426, 567–570. <https://doi.org/10.1038/nature02163>
- Massari, M.E., Murre, C., 2000. Helix-Loop-Helix Proteins: Regulators of Transcription in Eucaryotic Organisms. *Mol. Cell. Biol.* 20, 429–440. <https://doi.org/10.1128/MCB.20.2.429-440.2000>

- Materna, A.C., Sturm, S., Kroth, P.G., Lavaud, J., 2009. First induced plastid genome mutations in an alga with secondary plastids: Psba mutations in the diatom *Phaeodactylum tricornutum* (Bacillariophyceae) reveal consequences on the regulation of photosynthesis. *J. Phycol.* 45, 838–846. <https://doi.org/10.1111/j.1529-8817.2009.00711.x>
- Matsuda, Y., Hopkinson, B.M., Nakajima, K., Dupont, C.L., Tsuji, Y., 2017. Mechanisms of carbon dioxide acquisition and CO<sub>2</sub> sensing in marine diatoms: a gateway to carbon metabolism. *Philos. Trans. R. Soc. B Biol. Sci.* 372, 20160403. <https://doi.org/10.1098/rstb.2016.0403>
- Matsuo, T., Okamoto, K., Onai, K., Niwa, Y., Shimogawara, K., Ishiura, M., 2008. A systematic forward genetic analysis identified components of the *Chlamydomonas* circadian system. *Genes Dev.* 22, 918–930. <https://doi.org/10.1101/gad.1650408>
- Merchant, S.S., Prochnik, S.E., Vallon, O., Harris, E.H., Karpowicz, S.J., Witman, G.B., Terry, A., Salamov, A., Fritz-Laylin, L.K., Maréchal-Drouard, L., Marshall, W.F., Qu, L.-H., Nelson, D.R., Sanderfoot, A.A., Spalding, M.H., Kapitonov, V.V., Ren, Q., Ferris, P., Lindquist, E., Shapiro, H., Lucas, S.M., Grimwood, J., Schmutz, J., Cardol, P., Cerutti, H., Chanfreau, G., Chen, C.-L., Cognat, V., Croft, M.T., Dent, R., Dutcher, S., Fernández, E., Fukuzawa, H., González-Ballester, D., González-Halphen, D., Hallmann, A., Hanikenne, M., Hippler, M., Inwood, W., Jabbari, K., Kalanon, M., Kuras, R., Lefebvre, P.A., Lemaire, S.D., Lobanov, A.V., Lohr, M., Manuell, A., Meier, I., Mets, L., Mittag, M., Mittelmeier, T., Moroney, J.V., Moseley, J., Napoli, C., Nedelcu, A.M., Niyogi, K., Novoselov, S.V., Paulsen, I.T., Pazour, G., Purton, S., Ral, J.-P., Riaño-Pachón, D.M., Riekhof, W., Rymarquis, L., Schroda, M., Stern, D., Umen, J., Willows, R., Wilson, N., Zimmer, S.L., Allmer, J., Balk, J., Bisova, K., Chen, C.-J., Elias, M., Gendler, K., Hauser, C., Lamb, M.R., Ledford, H., Long, J.C., Minagawa, J., Page, M.D., Pan, J., Pootakham, W., Roje, S., Rose, A., Stahlberg, E., Terauchi, A.M., Yang, P., Ball, S., Bowler, C., Dieckmann, C.L., Gladyshev, V.N., Green, P., Jorgensen, R., Mayfield, S., Mueller-Roeber, B., Rajamani, S., Sayre, R.T., Brokstein, P., Dubchak, I., Goodstein, D., Hornick, L., Huang, Y.W., Jhaveri, J., Luo, Y., Martínez, D., Ngau, W.C.A., Otiillar, B., Poliakov, A., Porter, A., Szajkowski, L., Werner, G., Zhou, K., Grigoriev, I.V., Rokhsar, D.S., Grossman, A.R., 2007. The *Chlamydomonas* Genome Reveals the Evolution of Key Animal and Plant Functions. *Science* 318, 245–250. <https://doi.org/10.1126/science.1143609>
- Michaud, J.L., DeRossi, C., May, N.R., Holdener, B.C., Fan, C.-M., 2000. ARNT2 acts as the dimerization partner of SIM1 for the development of the hypothalamus. *Mech. Dev.* 90, 253–261. [https://doi.org/10.1016/S0925-4773\(99\)00328-7](https://doi.org/10.1016/S0925-4773(99)00328-7)
- Mitsui, A., Kumazawa, S., Takahashi, A., Ikemoto, H., Cao, S., Arai, T., 1986. Strategy by which nitrogen-fixing unicellular cyanobacteria grow photoautotrophically. *Nature* 323, 720–722. <https://doi.org/10.1038/323720a0>
- Mittag, M., 1996. Conserved circadian elements in phylogenetically diverse algae. *Proc. Natl. Acad. Sci.* 93, 14401–14404. <https://doi.org/10.1073/pnas.93.25.14401>
- Mittag, M., Lee, D.H., Hastings, J.W., 1994. Circadian expression of the luciferin-binding protein correlates with the binding of a protein to the 3' untranslated region of its mRNA. *Proc. Natl. Acad. Sci.* 91, 5257–5261. <https://doi.org/10.1073/pnas.91.12.5257>
- Miyagawa-Yamaguchi, A., Okami, T., Kira, N., Yamaguchi, H., Ohnishi, K., Adachi, M., 2011. Stable nuclear transformation of the diatom *Chaetoceros* sp.: Transformation of *Chaetoceros* sp. *Phycol. Res.* 59, 113–119. <https://doi.org/10.1111/j.1440-1835.2011.00607.x>
- Mock, T., Otiillar, R.P., Strauss, J., McMullan, M., Paajanen, P., Schmutz, J., Salamov, A., Sanges, R., Toseland, A., Ward, B.J., Allen, A.E., Dupont, C.L., Frickenhaus, S., Maumus, F., Veluchamy, A., Wu, T., Barry, K.W., Falciatore, A., Ferrante, M.I., Fortunato, A.E., Glöckner, G., Gruber, A., Hipkin, R., Janech, M.G., Kroth, P.G., Leese, F., Lindquist, E.A., Lyon, B.R., Martin, J., Mayer, C., Parker, M., Quesneville, H., Raymond, J.A., Uhlig, C., Valas, R.E., Valentin, K.U., Worden, A.Z., Armbrust, E.V., Clark, M.D., Bowler, C., Green,

- B.R., Moulton, V., van Oosterhout, C., Grigoriev, I.V., 2017. Evolutionary genomics of the cold-adapted diatom *Fragilariopsis cylindrus*. *Nature* 541, 536–540. <https://doi.org/10.1038/nature20803>
- Möglich, A., Ayers, R.A., Moffat, K., 2009. Structure and Signaling Mechanism of Per-ARNT-Sim Domains. *Structure* 17, 1282–1294. <https://doi.org/10.1016/j.str.2009.08.011>
- Mommsen, T.P., Walsh, P.J., 1989. Evolution of Urea Synthesis in Vertebrates: The Piscine Connection. *Science* 243, 72–75. <https://doi.org/10.1126/science.2563172>
- Monnier, A., Liverani, S., Bouvet, R., Jesson, B., Smith, J.Q., Mosser, J., Corellou, F., Bouget, F.-Y., 2010. Orchestrated transcription of biological processes in the marine picoeukaryote *Ostreococcus* exposed to light/dark cycles. *BMC Genomics* 11, 192. <https://doi.org/10.1186/1471-2164-11-192>
- Montresor, M., Vitale, L., D'Alelio, D., Ferrante, M.I., 2016. Sex in marine planktonic diatoms: insights and challenges. *Perspect. Phycol.* 3, 61–75. <https://doi.org/10.1127/pip/2016/0045>
- Morant, P.-E., Thommen, Q., Pfeuty, B., Vandermoere, C., Corellou, F., Bouget, F.-Y., Lefranc, M., 2010. A robust two-gene oscillator at the core of *Ostreococcus tauri* circadian clock. *Chaos Interdiscip. J. Nonlinear Sci.* 20, 045108. <https://doi.org/10.1063/1.3530118>
- Moulager, M., Monnier, A., Jesson, B., Bouvet, R., Mosser, J., Schwartz, C., Garnier, L., Corellou, F., Bouget, F.-Y., 2007. Light-Dependent Regulation of Cell Division in *Ostreococcus*: Evidence for a Major Transcriptional Input. *Plant Physiol.* 144, 1360–1369. <https://doi.org/10.1104/pp.107.096149>
- Moustafa, A., Beszteri, B., Maier, U.G., Bowler, C., Valentin, K., Bhattacharya, D., 2009. Genomic Footprints of a Cryptic Plastid Endosymbiosis in Diatoms. *Science* 324, 1724–1726. <https://doi.org/10.1126/science.1172988>
- Müller, N., Wenzel, S., Zou, Y., Künzel, S., Sasso, S., Weiß, D., Prager, K., Grossman, A., Kottke, T., Mittag, M., 2017. A Plant Cryptochrome Controls Key Features of the *Chlamydomonas* Circadian Clock and Its Life Cycle. *Plant Physiol.* 174, 185–201. <https://doi.org/10.1104/pp.17.00349>
- Müller, P., Li, X.-P., Niyogi, K.K., 2001. Non-Photochemical Quenching. A Response to Excess Light Energy. *Plant Physiol.* 125, 1558–1566. <https://doi.org/10.1104/pp.125.4.1558>
- Murre, C., 2019. Helix-loop-helix proteins and the advent of cellular diversity: 30 years of discovery. *Genes Dev.* 33, 6–25. <https://doi.org/10.1101/gad.320663.118>
- Murre, C., McCaw, P.S., Baltimore, D., 1989a. A new DNA binding and dimerization motif in immunoglobulin enhancer binding, daughterless, MyoD, and myc proteins. *Cell* 56, 777–783. [https://doi.org/10.1016/0092-8674\(89\)90682-X](https://doi.org/10.1016/0092-8674(89)90682-X)
- Murre, C., McCaw, P.S., Vaessin, H., Caudy, M., Jan, L.Y., Jan, Y.N., Cabrera, C.V., Buskin, J.N., Hauschka, S.D., Lassar, A.B., Weintraub, H., Baltimore, D., 1989b. Interactions between heterologous helix-loop-helix proteins generate complexes that bind specifically to a common DNA sequence. *Cell* 58, 537–544. [https://doi.org/10.1016/0092-8674\(89\)90434-0](https://doi.org/10.1016/0092-8674(89)90434-0)
- Muto, M., Fukuda, Y., Nemoto, M., Yoshino, T., Matsunaga, T., Tanaka, T., 2013. Establishment of a Genetic Transformation System for the Marine Pennate Diatom *Fistulifera* sp. Strain JPCD DA0580—A High Triglyceride Producer. *Mar. Biotechnol.* 15, 48–55. <https://doi.org/10.1007/s10126-012-9457-0>
- Nakajima, M., Imai, K., Ito, H., Nishiwaki, T., Murayama, Y., Iwasaki, H., Oyama, T., Kondo, T., 2005. Reconstitution of Circadian Oscillation of Cyanobacterial KaiC Phosphorylation in Vitro. *Science* 308, 414–415. <https://doi.org/10.1126/science.1108451>
- Nakamichi, N., Kiba, T., Kamioka, M., Suzuki, T., Yamashino, T., Higashiyama, T., Sakakibara, H., Mizuno, T., 2012. Transcriptional repressor PRR5 directly regulates clock-output pathways. *Proc. Natl. Acad. Sci.* 109, 17123–17128. <https://doi.org/10.1073/pnas.1205156109>

- Nakov, T., Beaulieu, J.M., Alverson, A.J., 2018. Accelerated diversification is related to life history and locomotion in a hyperdiverse lineage of microbial eukaryotes (Diatoms, Bacillariophyta). *New Phytol.* 219, 462–473. <https://doi.org/10.1111/nph.15137>
- Nambu, J.R., Chen, W., Hu, S., Crews, S.T., 1996. The *Drosophila melanogaster* similar bHLH-PAS gene encodes a protein related to human hypoxia-inducible factor 1 $\alpha$  and *Drosophila* single-minded. *Gene* 172, 249–254. [https://doi.org/10.1016/0378-1119\(96\)00060-1](https://doi.org/10.1016/0378-1119(96)00060-1)
- Nelson, D.M., Brand, L.E., 1979. Cell Division periodicity in 13 species of phytoplankton. *J. Phycol.* 67–75.
- Nelson, D.M., Tréguer, P., Brzezinski, M.A., Leynaert, A., Quéguiner, B., 1995. Production and dissolution of biogenic silica in the ocean: Revised global estimates, comparison with regional data and relationship to biogenic sedimentation. *Glob. Biogeochem. Cycles* 9, 359–372. <https://doi.org/10.1029/95GB01070>
- Niu, Y.-F., Yang, Z.-K., Zhang, M.-H., Zhu, C.-C., Yang, W.-D., Liu, J.-S., Li, H.-Y., 2012. Transformation of diatom *Phaeodactylum tricorutum* by electroporation and establishment of inducible selection marker. *BioTechniques* 52, 1–3. <https://doi.org/10.2144/000113881>
- Noordally, Z.B., Millar, A.J., 2015. Clocks in Algae. *Biochemistry* 54, 171–183. <https://doi.org/10.1021/bi501089x>
- Nosenko, T., Bhattacharya, D., 2007. Horizontal gene transfer in chromalveolates. *BMC Evol. Biol.* 7, 173. <https://doi.org/10.1186/1471-2148-7-173>
- Nowack, E.C.M., Weber, A.P.M., 2018. Genomics-Informed Insights into Endosymbiotic Organelle Evolution in Photosynthetic Eukaryotes. *Annu. Rev. Plant Biol.* 69, 51–84. <https://doi.org/10.1146/annurev-arplant-042817-040209>
- Nultsch, W., Ruffer, U., Pfau, J., 1984. Circadian rhythms in the chromatophore movements of *Dictyota dichotoma*. *Mar. Biol.* 81, 217–222. <https://doi.org/10.1007/BF00393215>
- Nymark, M., Sharma, A.K., Sparstad, T., Bones, A.M., Winge, P., 2016. A CRISPR/Cas9 system adapted for gene editing in marine algae. *Sci. Rep.* 6, 24951. <https://doi.org/10.1038/srep24951>
- Ocone, A., Millar, A.J., Sanguinetti, G., 2013. Hybrid regulatory models: a statistically tractable approach to model regulatory network dynamics. *Bioinformatics* 29, 910–916. <https://doi.org/10.1093/bioinformatics/btt069>
- Oeltjen, A., Marquardt, J., Rhiel, E., 2004. Differential circadian expression of genes *fcp2* and *fcp6* in *Cyclotella cryptica*. *Int. Microbiol.* 7, 6.
- Ogura, A., Akizuki, Y., Imoda, H., Mineta, K., Gojobori, T., Nagai, S., 2018. Comparative genome and transcriptome analysis of diatom, *Skeletonema costatum*, reveals evolution of genes for harmful algal bloom. *BMC Genomics* 19, 765. <https://doi.org/10.1186/s12864-018-5144-5>
- O’Neill, J.S., Reddy, A.B., 2011. Circadian clocks in human red blood cells. *Nature* 469, 498–503. <https://doi.org/10.1038/nature09702>
- O’Neill, J.S., van Ooijen, G., Dixon, L.E., Troein, C., Corellou, F., Bouget, F.-Y., Reddy, A.B., Millar, A.J., 2011. Circadian rhythms persist without transcription in a eukaryote. *Nature* 469, 554–558. <https://doi.org/10.1038/nature09654>
- Ostgaard, K., Jensen, A., 1982. Diurnal and circadian rhythms in the turbidity of growing *Skeletonema costatum* cultures. *Mar. Biol.* 66, 261–268. <https://doi.org/10.1007/BF00397031>
- Ouyang, Y., Andersson, C.R., Kondo, T., Golden, S.S., Johnson, C.H., 1998. Resonating circadian clocks enhance fitness in cyanobacteria. *Proc. Natl. Acad. Sci.* 95, 8660–8664. <https://doi.org/10.1073/pnas.95.15.8660>
- Owens, T.G., Falkowski, P.G., Whitledge, T.E., 1980. Diel periodicity in cellular chlorophyll content in marine diatoms. *Mar. Biol.* 59, 71–77. <https://doi.org/10.1007/BF00405456>



- Paasche, E., 1968. Marine Plankton Algae Grown with Light-Dark Cycles.. II. *Ditylum brightwellii* and *Nitzschia turgidula*. *Physiol. Plant.* 21, 66-77. <https://doi.org/10.1111/j.1399-3054.1968.tb07231.x>
- Pahl, S.L., Lewis, D.M., Chen, F., King, K.D., 2010. Heterotrophic growth and nutritional aspects of the diatom *Cyclotella cryptica* (Bacillariophyceae): Effect of some environmental factors. *J. Biosci. Bioeng.* 109, 235-239. <https://doi.org/10.1016/j.jbiosc.2009.08.480>
- Palmer, J.D., Livingston, L., Zussy, Fr.D., 1964. A Persistent Diurnal Rhythm in Photosynthetic Capacity. *Nature* 203, 1087-1088. <https://doi.org/10.1038/2031087a0>
- Palmer, J.D., Round, F.E., 1967. PERSISTENT, VERTICAL-MIGRATION RHYTHMS IN BENTHIC MICROFLORA. VI. THE TIDAL AND DIURNAL NATURE OF THE RHYTHM IN THE DIATOM *HANTZSCHIA VIRGATA*. *Biol. Bull.* 132, 44-55. <https://doi.org/10.2307/1539877>
- Pančić, M., Torres, R.R., Almeda, R., Kiørboe, T., 2019. Silicified cell walls as a defensive trait in diatoms. *Proc. R. Soc. B Biol. Sci.* 286, 20190184. <https://doi.org/10.1098/rspb.2019.0184>
- Paroush, Z., 1994. Groucho is required for *Drosophila* neurogenesis, segmentation, and sex determination and interacts directly with hairy-related bHLH proteins. *Cell* 79, 805-815. [https://doi.org/10.1016/0092-8674\(94\)90070-1](https://doi.org/10.1016/0092-8674(94)90070-1)
- Peers, G., Price, N.M., 2006. Copper-containing plastocyanin used for electron transport by an oceanic diatom. *Nature* 441, 341-344. <https://doi.org/10.1038/nature04630>
- Peschel, N., Helfrich-Förster, C., 2011. Setting the clock - by nature: Circadian rhythm in the fruitfly *Drosophila melanogaster*. *FEBS Lett.* 585, 1435-1442. <https://doi.org/10.1016/j.febslet.2011.02.028>
- Pfitzer, E., 1869. Über den Bau und die Zellteilung der Diatomeen. *Bot. Ztg.* 27, 774-776.
- Pickett-Heaps, J., 1991. Cell Division in Diatoms, in: *International Review of Cytology*. Elsevier, pp. 63-108. [https://doi.org/10.1016/S0074-7696\(08\)60497-0](https://doi.org/10.1016/S0074-7696(08)60497-0)
- Pickett-Heaps, J.D., Tippit, D.H., 1978. The diatom spindle in perspective. *Cell* 14, 455-467. [https://doi.org/10.1016/0092-8674\(78\)90232-5](https://doi.org/10.1016/0092-8674(78)90232-5)
- Pierella Karlusich, J.J., Ibarbalz, F.M., Bowler, C., 2020. Phytoplankton in the *Tara* Ocean. *Annu. Rev. Mar. Sci.* 12, 233-265. <https://doi.org/10.1146/annurev-marine-010419-010706>
- Pierik, R., de Wit, M., 2014. Shade avoidance: phytochrome signalling and other aboveground neighbour detection cues. *J. Exp. Bot.* 65, 2815-2824. <https://doi.org/10.1093/jxb/ert389>
- Pires, N., Dolan, L., 2010a. Origin and Diversification of Basic-Helix-Loop-Helix Proteins in Plants. *Mol. Biol. Evol.* 27, 862-874. <https://doi.org/10.1093/molbev/msp288>
- Pires, N., Dolan, L., 2010b. Early evolution of bHLH proteins in plants. *Plant Signal. Behav.* 5, 911-912. <https://doi.org/10.4161/psb.5.7.12100>
- Pittendrigh, C.S., 1954. On temperature independence in the clock system controlling emergence time in *Drosophila*. *Proc. Natl. Acad. Sci.* 40, 1018-1029. <https://doi.org/10.1073/pnas.40.10.1018>
- Pittendrigh, C.S., Bruce, V.G., Rosensweig, N.S., Rubin, M.L., 1959. Growth Patterns in *Neurospora*: A Biological Clock in *Neurospora*. *Nature* 184, 169-170. <https://doi.org/10.1038/184169a0>
- Pittendrigh, C.S., Minis, D.H., 1964. The Entrainment of Circadian Oscillations by Light and Their Role as Photoperiodic Clocks. *Am. Nat.* 98, 261-294. <https://doi.org/10.1086/282327>
- Pniewski, F., Piasecka-Jędrzejak, I., 2020. Photoacclimation to Constant and Changing Light Conditions in a Benthic Diatom. *Front. Mar. Sci.* 7, 381. <https://doi.org/10.3389/fmars.2020.00381>
- Poliner, E., Busch, A.W.U., Newton, L., Kim, Y.U., Clark, R., Gonzalez-Martinez, S.C., Jeong, B., Montgomery, B.L., Farré, E.M., 2022. Aureochromes maintain polyunsaturated fatty acid content in *Nannochloropsis oceanica*. *Plant Physiol.* kiac052. <https://doi.org/10.1093/plphys/kiac052>

- Poliner, E., Cummings, C., Newton, L., Farré, E.M., 2019. Identification of circadian rhythms in *Nannochloropsis* species using bioluminescence reporter lines. *Plant J.* 99, 112–127. <https://doi.org/10.1111/tpj.14314>
- Poliner, E., Panchy, N., Newton, L., Wu, G., Lapinsky, A., Bullard, B., Zienkiewicz, A., Benning, C., Shiu, S., Farré, E.M., 2015. Transcriptional coordination of physiological responses in *Nannochloropsis oceanica* CCMP 1779 under light/dark cycles. *Plant J.* 83, 1097–1113. <https://doi.org/10.1111/tpj.12944>
- Pongratz, I., Antonsson, C., Whitelaw, M.L., Poellinger, L., 1998. Role of the PAS Domain in Regulation of Dimerization and DNA Binding Specificity of the Dioxin Receptor. *Mol. Cell. Biol.* 18, 4079–4088. <https://doi.org/10.1128/MCB.18.7.4079>
- Poulsen, N., Chesley, P.M., Kröger, N., 2006. Molecular genetic manipulation of the diatom *Thalassiosira pseudonana* (Bacillariophyceae). *J. Phycol.* 42, 1059–1065. <https://doi.org/10.1111/j.1529-8817.2006.00269.x>
- Poulsen, N., Kröger, N., 2005. A new molecular tool for transgenic diatoms: Control of mRNA and protein biosynthesis by an inducible promoter-terminator cassette. *FEBS J.* 272, 3413–3423. <https://doi.org/10.1111/j.1742-4658.2005.04760.x>
- Poulsen, N.C., Spector, I., Spureck, T.P., Schultz, T.F., Wetherbee, R., 1999. Diatom gliding is the result of an actin-myosin motility system. *Cell Motil. Cytoskeleton* 44, 23–33. [https://doi.org/10.1002/\(SICI\)1097-0169\(199909\)44:1<23::AID-CM2>3.0.CO;2-D](https://doi.org/10.1002/(SICI)1097-0169(199909)44:1<23::AID-CM2>3.0.CO;2-D)
- Procopio, M., Lahm, A., Tramontano, A., Bonati, L., Pitea, D., 2002. A model for recognition of polychlorinated dibenzo-*p*-dioxins by the aryl hydrocarbon receptor: A model for PCDD - AhR recognition. *Eur. J. Biochem.* 269, 13–18. <https://doi.org/10.1046/j.0014-2956.2002.02619.x>
- Purcell, E.B., Siegal-Gaskins, D., Rawling, D.C., Fiebig, A., Crosson, S., 2007. A photosensory two-component system regulates bacterial cell attachment. *Proc. Natl. Acad. Sci.* 104, 18241–18246. <https://doi.org/10.1073/pnas.0705887104>
- Putker, M., O’Neill, J.S., 2016. Reciprocal Control of the Circadian Clock and Cellular Redox State - a Critical Appraisal. *Mol. Cells* 39, 6–19. <https://doi.org/10.14348/molcells.2016.2323>
- Putker, M., Wong, D.C.S., Seinkmane, E., Rzechorzek, N.M., Zeng, A., Hoyle, N.P., Chesham, J.E., Edwards, M.D., Feeney, K.A., Fischer, R., Peschel, N., Chen, K., Vanden Oever, M., Edgar, R.S., Selby, C.P., Sancar, A., O’Neill, J.S., 2021. CRYPTOCHROMES confer robustness, not rhythmicity, to circadian timekeeping. *EMBO J.* 40. <https://doi.org/10.15252/emboj.2020106745>
- Rachel Carson Excerpts Continued - Rachel Carson - U.S. Fish and Wildlife Service [WWW Document], n.d. URL [https://www.fws.gov/refuge/Rachel\\_Carson/about/rachelcarsonexcerpts2.html#RC4](https://www.fws.gov/refuge/Rachel_Carson/about/rachelcarsonexcerpts2.html#RC4) (accessed 2.25.22).
- Ragni, M., d’Alcalà, M.R., 2007. Circadian variability in the photobiology of *Phaeodactylum tricornutum*: pigment content. *J. Plankton Res.* 29, 141–156. <https://doi.org/10.1093/plankt/fbm002>
- Raitsos, D.E., Lavender, S.J., Maravelias, C.D., Haralabous, J., Richardson, A.J., Reid, P.C., 2008. Identifying four phytoplankton functional types from space: An ecological approach. *Limnol. Oceanogr.* 53, 605–613. <https://doi.org/10.4319/lo.2008.53.2.0605>
- Ramsay, N.A., Glover, B.J., 2005. MYB-bHLH-WD40 protein complex and the evolution of cellular diversity. *Trends Plant Sci.* 10, 63–70. <https://doi.org/10.1016/j.tplants.2004.12.011>
- Rastogi, A., Maheswari, U., Dorrell, R.G., Vieira, F.R.J., Maumus, F., Kustka, A., McCarthy, J., Allen, A.E., Kersey, P., Bowler, C., Tirichine, L., 2018. Integrative analysis of large scale transcriptome data draws a comprehensive landscape of *Phaeodactylum tricornutum* genome and evolutionary origin of diatoms. *Sci. Rep.* 8, 4834. <https://doi.org/10.1038/s41598-018-23106-x>

- Rastogi, A., Vieira, F.R.J., Deton-Cabanillas, A.-F., Veluchamy, A., Cantrel, C., Wang, G., Vanormelingen, P., Bowler, C., Piganeau, G., Hu, H., Tirichine, L., 2020. A genomics approach reveals the global genetic polymorphism, structure, and functional diversity of ten accessions of the marine model diatom *Phaeodactylum tricornutum*. *ISME J.* 14, 347–363. <https://doi.org/10.1038/s41396-019-0528-3>
- Raven, J.A., Raven, J.A., 2019. Iron in Diatoms, in: Seckbach, J., Gordon, R. (Eds.), *Diatoms: Fundamentals and Applications*. Wiley, pp. 213–224. <https://doi.org/10.1002/9781119370741.ch9>
- Rawat, R., Takahashi, N., Hsu, P.Y., Jones, M.A., Schwartz, J., Salemi, M.R., Phinney, B.S., Harmer, S.L., 2011. REVEILLE8 and PSEUDO-REPOSE REGULATOR5 Form a Negative Feedback Loop within the Arabidopsis Circadian Clock. *PLoS Genet.* 7, e1001350. <https://doi.org/10.1371/journal.pgen.1001350>
- Rayko, E., Maumus, F., Maheswari, U., Jabbari, K., Bowler, C., 2010. Transcription factor families inferred from genome sequences of photosynthetic stramenopiles. *New Phytol.* 188, 52–66. <https://doi.org/10.1111/j.1469-8137.2010.03371.x>
- Redlin, U., 2001. Neural basis and biological function of masking by light in mammals: suppression of melatonin and locomotor activity. *Chronobiol. Int.* 18, 737–758. <https://doi.org/10.1081/CBI-100107511>
- Rensing, L., Ruoff, P., 2002. TEMPERATURE EFFECT ON ENTRAINMENT, PHASE SHIFTING, AND AMPLITUDE OF CIRCADIAN CLOCKS AND ITS MOLECULAR BASES. *Chronobiol. Int.* 19, 807–864. <https://doi.org/10.1081/CBI-120014569>
- Riechmann, J.L., Heard, J., Martin, G., Reuber, L., Jiang, C.-Z., Keddie, J., Adam, L., Pineda, O., Ratchliffe, O.J., Samaha, R.R., Creelman, R., Pilgrim, M., Broun, P., Zhang, J.Z., Ghandehari, D., Sherman, B.K., Yu, G., 2000. *Arabidopsis* Transcription Factors: Genome-Wide Comparative Analysis Among Eukaryotes. *Science* 290, 2105–2110. <https://doi.org/10.1126/science.290.5499.2105>
- Robinson, K.A., 2000. SURVEY AND SUMMARY: *Saccharomyces cerevisiae* basic helix-loop-helix proteins regulate diverse biological processes. *Nucleic Acids Res.* 28, 1499–1505. <https://doi.org/10.1093/nar/28.7.1499>
- Roenneberg, T., Kumar, C.J., Merrow, M., 2007. The human circadian clock entrains to sun time. *Curr. Biol.* 17, R44–R45. <https://doi.org/10.1016/j.cub.2006.12.011>
- Rogato, A., Richard, H., Sarazin, A., Voss, B., Cheminant Navarro, S., Champeimont, R., Navarro, L., Carbone, A., Hess, W.R., Falcatore, A., 2014. The diversity of small non-coding RNAs in the diatom *Phaeodactylum tricornutum*. *BMC Genomics* 15, 698. <https://doi.org/10.1186/1471-2164-15-698>
- Rozwadowski, H.M., 2010. Ocean's Depths. *Environ. Hist.* 15, 520–525. <https://doi.org/10.1093/envhis/emq055>
- Rund, S.S.C., Hou, T.Y., Ward, S.M., Collins, F.H., Duffield, G.E., 2011. Genome-wide profiling of diel and circadian gene expression in the malaria vector *Anopheles gambiae*. *Proc. Natl. Acad. Sci.* 108, E421–E430. <https://doi.org/10.1073/pnas.1100584108>
- Sage, R.F., 2004. The evolution of C<sub>4</sub> photosynthesis. *New Phytol.* 161, 341–370. <https://doi.org/10.1111/j.1469-8137.2004.00974.x>
- Sanchez, A., Shin, J., Davis, S.J., 2011. Abiotic stress and the plant circadian clock. *Plant Signal. Behav.* 6, 223–231. <https://doi.org/10.4161/psb.6.2.14893>
- Sapriel, G., Quinet, M., Heijde, M., Jourdain, L., Tanty, V., Luo, G., Le Crom, S., Lopez, P.J., 2009. Genome-Wide Transcriptome Analyses of Silicon Metabolism in *Phaeodactylum tricornutum* Reveal the Multilevel Regulation of Silicic Acid Transporters. *PLoS ONE* 4, e7458. <https://doi.org/10.1371/journal.pone.0007458>
- Sarthou, G., Timmermans, K.R., Blain, S., Tréguer, P., 2005. Growth physiology and fate of diatoms in the ocean: a review. *J. Sea Res.* 53, 25–42. <https://doi.org/10.1016/j.seares.2004.01.007>

- Schafmeier, T., Haase, A., Káldi, K., Scholz, J., Fuchs, M., Brunner, M., 2005. Transcriptional Feedback of *Neurospora* Circadian Clock Gene by Phosphorylation-Dependent Inactivation of Its Transcription Factor. *Cell* 122, 235–246. <https://doi.org/10.1016/j.cell.2005.05.032>
- Schellenberger Costa, B., Jungandreas, A., Jakob, T., Weisheit, W., Mittag, M., Wilhelm, C., 2013a. Blue light is essential for high light acclimation and photoprotection in the diatom *Phaeodactylum tricornutum*. *J. Exp. Bot.* 64, 483–493. <https://doi.org/10.1093/jxb/ers340>
- Schellenberger Costa, B., Sachse, M., Jungandreas, A., Bartulos, C.R., Gruber, A., Jakob, T., Kroth, P.G., Wilhelm, C., 2013b. Aureochrome 1a Is Involved in the Photoacclimation of the Diatom *Phaeodactylum tricornutum*. *PLoS ONE* 8, e74451. <https://doi.org/10.1371/journal.pone.0074451>
- Schmid, R., Dring, M.J., 1992. Circadian rhythm and fast responses to blue light of photosynthesis in *Ectocarpus* (Phaeophyta, Ectocarpales). *Planta* 187, 14. <https://doi.org/10.1007/BF00201624>
- Schulze, T., Prager, K., Dathe, H., Kelm, J., Kiessling, P., Mittag, M., 2010. How the green alga *Chlamydomonas reinhardtii* keeps time. *Protoplasma* 244, 3–14. <https://doi.org/10.1007/s00709-010-0113-0>
- Serif, M., Dubois, G., Finoux, A.-L., Teste, M.-A., Jallet, D., Daboussi, F., 2018. One-step generation of multiple gene knock-outs in the diatom *Phaeodactylum tricornutum* by DNA-free genome editing. *Nat. Commun.* 9, 3924. <https://doi.org/10.1038/s41467-018-06378-9>
- Sharma, A.K., Nymark, M., Sparstad, T., Bones, A.M., Winge, P., 2018. Transgene-free genome editing in marine algae by bacterial conjugation – comparison with biolistic CRISPR/Cas9 transformation. *Sci. Rep.* 8, 14401. <https://doi.org/10.1038/s41598-018-32342-0>
- Shearman, L.P., Zylka, M.J., Weaver, D.R., Kolakowski, L.F., Reppert, S.M., 1997. Two period Homologs: Circadian Expression and Photic Regulation in the Suprachiasmatic Nuclei. *Neuron* 19, 1261–1269. [https://doi.org/10.1016/S0896-6273\(00\)80417-1](https://doi.org/10.1016/S0896-6273(00)80417-1)
- Siaut, M., Heijde, M., Mangogna, M., Montsant, A., Coesel, S., Allen, A., Manfredonia, A., Falciatore, A., Bowler, C., 2007. Molecular toolbox for studying diatom biology in *Phaeodactylum tricornutum*. *Gene* 406, 23–35. <https://doi.org/10.1016/j.gene.2007.05.022>
- Smayda, T.J., 1980. Phytoplankton species succession., in: *The Physiological Ecology of Phytoplankton*. Oxford, pp. 493–570.
- Smayda, T.J., 1975. Phased cell division in natural populations of the marine diatom *Ditylum brightwellii* and the potential significance of diel phytoplankton behavior in the sea. *Deep Sea Res. Oceanogr. Abstr.* 22, 151–165. [https://doi.org/10.1016/0011-7471\(75\)90055-8](https://doi.org/10.1016/0011-7471(75)90055-8)
- Smetacek, V., 2012. Making sense of ocean biota: How evolution and biodiversity of land organisms differ from that of the plankton. *J. Biosci.* 37, 589–607. <https://doi.org/10.1007/s12038-012-9240-4>
- Smith, S.R., Gillard, J.T.F., Kustka, A.B., McCrow, J.P., Badger, J.H., Zheng, H., New, A.M., Dupont, C.L., Obata, T., Fernie, A.R., Allen, A.E., 2016. Transcriptional Orchestration of the Global Cellular Response of a Model Pennate Diatom to Diel Light Cycling under Iron Limitation. *PLoS Genet.* 12, e1006490. <https://doi.org/10.1371/journal.pgen.1006490>
- Somers, D.E., Devlin, P.F., Kay, S.A., 1998. Phytochromes and Cryptochromes in the Entrainment of the *Arabidopsis* Circadian Clock. *Sci. New Ser.* 282, 1488–1490. <https://doi.org/10.1126/science.282.5393.1488>
- Song, Y.H., Shim, J.S., Kinmonth-Schultz, H.A., Imaizumi, T., 2015. Photoperiodic Flowering: Time Measurement Mechanisms in Leaves. *Annu. Rev. Plant Biol.* 66, 441–464. <https://doi.org/10.1146/annurev-arplant-043014-115555>
- Sonnenfeld, M., Ward, M., Nystrom, G., Mosher, J., Stahl, S., Crews, S., 1997. The *Drosophila tango* gene encodes a bHLH-PAS protein that is orthologous to mammalian Arnt and controls CNS midline and tracheal development. *Development* 124, 4571–4582. <https://doi.org/10.1242/dev.124.22.4571>

- Speight, M., Henderson, P., 2010. *Marine Ecology: Concepts and Applications*, 1st ed. Wiley Blackwell.
- Spilling, K., Markager, S., 2008. Ecophysiological growth characteristics and modeling of the onset of the spring bloom in the Baltic Sea. *J. Mar. Syst.* 73, 323–337. <https://doi.org/10.1016/j.jmarsys.2006.10.012>
- Stanewsky, R., Kaneko, M., Emery, P., Beretta, B., Wager-Smith, K., Kay, S.A., Rosbash, M., Hall, J.C., 1998. The cryb Mutation Identifies Cryptochrome as a Circadian Photoreceptor in *Drosophila*. *Cell* 95, 681–692. [https://doi.org/10.1016/S0092-8674\(00\)81638-4](https://doi.org/10.1016/S0092-8674(00)81638-4)
- Stiller, J.W., Schreiber, J., Yue, J., Guo, H., Ding, Q., Huang, J., 2014. The evolution of photosynthesis in chromist algae through serial endosymbioses. *Nat. Commun.* 5, 5764. <https://doi.org/10.1038/ncomms6764>
- Stomp, M., Huisman, J., Stal, L.J., Matthijs, H.C.P., 2007. Colorful niches of phototrophic microorganisms shaped by vibrations of the water molecule. *ISME J.* 1, 271–282. <https://doi.org/10.1038/ismej.2007.59>
- Strassert, J.F.H., Irisarri, I., Williams, T.A., Burki, F., 2021. A molecular timescale for eukaryote evolution with implications for the origin of red algal-derived plastids. *Nat. Commun.* 12, 1879. <https://doi.org/10.1038/s41467-021-22044-z>
- Strauss, J., 2012. A genomic analysis using RNA-Seq to investigate the adaptation of the psychrophilic diatom *Fragilariopsis cylindrus* to the polar environment. University of East Anglia, Norwich, UK.
- Sumper, M., Kröger, N., 2004. Silica formation in diatoms: the function of long-chain polyamines and silaffins. *J Mater Chem* 14, 2059–2065. <https://doi.org/10.1039/B401028K>
- Sweeney, B.M., Hastings, J.W., 1958. Rhythmic Cell Division in Populations of *Gonyaulax polyedra*. *J. Protozool.* 5, 217–224.
- Sweeney, B.M., Haxo, F.T., 1961. Persistence of a Photosynthetic Rhythm in Enucleated *Acetabularia*. *Sci. New Ser.* 134, 1361–1363.
- Taddei, L., Chukhutsina, V.U., Lepetit, B., Stella, G.R., Bassi, R., van Amerongen, H., Bouly, J.-P., Jaubert, M., Finazzi, G., Falciatore, A., 2018. Dynamic Changes between Two LHCX-Related Energy Quenching Sites Control Diatom Photoacclimation. *Plant Physiol.* 177, 953–965. <https://doi.org/10.1104/pp.18.00448>
- Taddei, L., Stella, G.R., Rogato, A., Bailleul, B., Fortunato, A.E., Annunziata, R., Sanges, R., Thaler, M., Lepetit, B., Lavaud, J., Jaubert, M., Finazzi, G., Bouly, J.-P., Falciatore, A., 2016. Multisignal control of expression of the LHCX protein family in the marine diatom *Phaeodactylum tricornutum*. *J. Exp. Bot.* 67, 3939–3951. <https://doi.org/10.1093/jxb/erw198>
- Taiz, L., Zeiger, E., Moller, I.M., Murphy, A., 2015. *Plant physiology and development*, 6th ed. Sinauer Associates, Oxford University Press.
- Takahashi, F., Yamagata, D., Ishikawa, M., Fukamatsu, Y., Ogura, Y., Kasahara, M., Kiyosue, T., Kikuyama, M., Wada, M., Kataoka, H., 2007. AUREOCHROME, a photoreceptor required for photomorphogenesis in stramenopiles. *Proc. Natl. Acad. Sci.* 104, 19625–19630. <https://doi.org/10.1073/pnas.0707692104>
- Takahashi, J.S., 2017a. Transcriptional architecture of the mammalian circadian clock. *Nat. Rev. Genet.* 18, 164–179. <https://doi.org/10.1038/nrg.2016.150>
- Takahata, S., Sogawa, K., Kobayashi, A., Ema, M., Mimura, J., Ozaki, N., Fujii-Kuriyama, Y., 1998. Transcriptionally Active Heterodimer Formation of an Arnt-like PAS Protein, Arnt3, with HIF-1a, HLF, and Clock. *Biochem. Biophys. Res. Commun.* 248, 789–794. <https://doi.org/10.1006/bbrc.1998.9012>
- Tamaru, T., Hattori, M., Honda, K., Nakahata, Y., Sassone-Corsi, P., van der Horst, G.T.J., Ozawa, T., Takamatsu, K., 2015. CRY Drives Cyclic CK2-Mediated BMAL1 Phosphorylation to Control the Mammalian Circadian Clock. *PLOS Biol.* 13, e1002293. <https://doi.org/10.1371/journal.pbio.1002293>

- Tanaka, A., De Martino, A., Amato, A., Montsant, A., Mathieu, B., Rostaing, P., Tirichine, L., Bowler, C., 2015. Ultrastructure and Membrane Traffic During Cell Division in the Marine Pennate Diatom *Phaeodactylum tricornutum*. *Protist* 166, 506–521. <https://doi.org/10.1016/j.protis.2015.07.005>
- Tanaka, T., Maeda, Y., Veluchamy, A., Tanaka, Michihiro, Abida, H., Maréchal, E., Bowler, C., Muto, M., Sunaga, Y., Tanaka, Masayoshi, Yoshino, T., Taniguchi, T., Fukuda, Y., Nemoto, M., Matsumoto, M., Wong, P.S., Aburatani, S., Fujibuchi, W., 2015. Oil Accumulation by the Oleaginous Diatom *Fistulifera solaris* as Revealed by the Genome and Transcriptome. *Plant Cell* 27, 162–176. <https://doi.org/10.1105/tpc.114.135194>
- Tang, C.-T., Li, S., Long, C., Cha, J., Huang, G., Li, L., Chen, S., Liu, Y., 2009. Setting the pace of the *Neurospora* circadian clock by multiple independent FRQ phosphorylation events. *Proc. Natl. Acad. Sci.* 106, 10722–10727. <https://doi.org/10.1073/pnas.0904898106>
- Taylor, B.L., Zhulin, I.B., 1999. PAS Domains: Internal Sensors of Oxygen, Redox Potential, and Light. *Microbiol. Mol. Biol. Rev.* 63, 479–506. <https://doi.org/10.1128/MMBR.63.2.479-506.1999>
- TerBush, A.D., Yoshida, Y., Osteryoung, K.W., 2013. FtsZ in chloroplast division: structure, function and evolution. *Curr. Opin. Cell Biol.* 25, 461–470. <https://doi.org/10.1016/jceb.2013.04.006>
- The Nobel Assembly at Karolinska Institutet, 2017. The 2017 Nobel Prize in Physiology or Medicine [WWW Document]. [www.nobelprize.org](http://www.nobelprize.org) URL <https://www.nobelprize.org/prizes/medicine/2017/press-release/>
- Thiriet-Rupert, S., Carrier, G., Chénais, B., Trottier, C., Bougaran, G., Cadoret, J.-P., Schoefs, B., Saint-Jean, B., 2016. Transcription factors in microalgae: genome-wide prediction and comparative analysis. *BMC Genomics* 17, 282. <https://doi.org/10.1186/s12864-016-2610-9>
- Thomas, D.N., Dieckmann, G.S., 2002. Antarctic Sea Ice—a Habitat for Extremophiles. *Science* 295, 641–644. <https://doi.org/10.1126/science.1063391>
- Thommen, Q., Pfeuty, B., Morant, P.-E., Corellou, F., Bouget, F.-Y., Lefranc, M., 2010. Robustness of Circadian Clocks to Daylight Fluctuations: Hints from the Picoeucaryote *Ostreococcus tauri*. *PLoS Comput. Biol.* 6, e1000990. <https://doi.org/10.1371/journal.pcbi.1000990>
- Traller, J.C., Cokus, S.J., Lopez, D.A., Gaidarenko, O., Smith, S.R., McCrow, J.P., Gallaher, S.D., Podell, S., Thompson, M., Cook, O., Morselli, M., Jaroszewicz, A., Allen, E.E., Allen, A.E., Merchant, S.S., Pellegrini, M., Hildebrand, M., 2016. Genome and methylome of the oleaginous diatom *Cyclotella cryptica* reveal genetic flexibility toward a high lipid phenotype. *Biotechnol. Biofuels* 9, 258. <https://doi.org/10.1186/s13068-016-0670-3>
- Tréguer, P., Bowler, C., Moriceau, B., Dutkiewicz, S., Gehlen, M., Aumont, O., Bittner, L., Dugdale, R., Finkel, Z., Iudicone, D., Jahn, O., Guidi, L., Lasbleiz, M., Leblanc, K., Levy, M., Pondaven, P., 2018. Influence of diatom diversity on the ocean biological carbon pump. *Nat. Geosci.* 11, 27–37. <https://doi.org/10.1038/s41561-017-0028-x>
- Tréguer, P., Nelson, D.M., Van Bennekom, A.J., DeMaster, D.J., Leynaert, A., Quéguiner, B., 1995. The Silica Balance in the World Ocean: A Reestimate. *Science* 268, 375–379. <https://doi.org/10.1126/science.268.5209.375>
- Troein, C., Corellou, F., Dixon, L.E., van Ooijen, G., O'Neill, J.S., Bouget, F.-Y., Millar, A.J., 2011. Multiple light inputs to a simple clock circuit allow complex biological rhythms: Multiple light inputs to a simple clock circuit. *Plant J.* 66, 375–385. <https://doi.org/10.1111/j.1365-313X.2011.04489.x>
- Tsuji, Y., Nakajima, K., Matsuda, Y., 2017. Molecular aspects of the biophysical CO<sub>2</sub>-concentrating mechanism and its regulation in marine diatoms. *J. Exp. Bot.* 68, 3763–3772. <https://doi.org/10.1093/jxb/erx173>
- Uehara, T.N., Mizutani, Y., Kuwata, K., Hirota, T., Sato, A., Mizoi, J., Takao, S., Matsuo, H., Suzuki, T., Ito, S., Saito, A.N., Nishiwaki-Ohkawa, T., Yamaguchi-Shinozaki, K., Yoshimura, T.,

- Kay, S.A., Itami, K., Kinoshita, T., Yamaguchi, J., Nakamichi, N., 2019. Casein kinase 1 family regulates PRR5 and TOC1 in the Arabidopsis circadian clock. *Proc. Natl. Acad. Sci.* 116, 11528–11536. <https://doi.org/10.1073/pnas.1903357116>
- Valenzuela, J., Mazurie, A., Carlson, R.P., Gerlach, R., Cooksey, K.E., Peyton, B.M., Fields, M.W., 2012. Potential role of multiple carbon fixation pathways during lipid accumulation in *Phaeodactylum tricornutum*. *Biotechnol. Biofuels* 5, 40. <https://doi.org/10.1186/1754-6834-5-40>
- Valle, K.C., Nymark, M., Aamot, I., Hancke, K., Winge, P., Andresen, K., Johnsen, G., Brembu, T., Bones, A.M., 2014. System Responses to Equal Doses of Photosynthetically Usable Radiation of Blue, Green, and Red Light in the Marine Diatom *Phaeodactylum tricornutum*. *PLoS ONE* 9, e114211. <https://doi.org/10.1371/journal.pone.0114211>
- Vancaester, E., Depuydt, T., Osuna-Cruz, C.M., Vandepoele, K., 2020. Comprehensive and Functional Analysis of Horizontal Gene Transfer Events in Diatoms. *Mol. Biol. Evol.* 37, 3243–3257. <https://doi.org/10.1093/molbev/msaa182>
- Vaulot, D., Olson, R.J., Chisholm, S.W., 1986. Light and dark control of the cell cycle in two marine phytoplankton species. *Exp. Cell Res.* 167, 38–52. [https://doi.org/10.1016/0014-4827\(86\)90202-8](https://doi.org/10.1016/0014-4827(86)90202-8)
- Vaulot, D., Olson, R.J., Merkel, S., Chisholm, S.W., 1987. Cell-cycle response to nutrient starvation in two phytoplankton species, *Thalassiosira weissflogii* and *Hymenomonas carterae*. *Mar. Biol.* 95, 625–630. <https://doi.org/10.1007/BF00393106>
- Vieler, A., Wu, G., Tsai, C.-H., Bullard, B., Cornish, A.J., Harvey, C., Reza, I.-B., Thornburg, C., Achawanantakun, R., Buehl, C.J., Campbell, M.S., Cavalier, D., Childs, K.L., Clark, T.J., Deshpande, R., Erickson, E., Armenia Ferguson, A., Handee, W., Kong, Q., Li, X., Liu, B., Lundback, S., Peng, C., Roston, R.L., Sanjaya, Simpson, J.P., TerBush, A., Warakanont, J., Zäuner, S., Farre, E.M., Hegg, E.L., Jiang, N., Kuo, M.-H., Lu, Y., Niyogi, K.K., Ohlrogge, J., Osteryoung, K.W., Shachar-Hill, Y., Sears, B.B., Sun, Y., Takahashi, H., Yandell, M., Shiu, S.-H., Benning, C., 2012. Genome, Functional Gene Annotation, and Nuclear Transformation of the Heterokont Oleaginous Alga *Nannochloropsis oceanica* CCMP1779. *PLoS Genet.* 8, e1003064. <https://doi.org/10.1371/journal.pgen.1003064>
- Villanova, V., Fortunato, A.E., Singh, D., Bo, D.D., Conte, M., Obata, T., Jouhet, J., Fernie, A.R., Marechal, E., Falcioratore, A., Pagliardini, J., Le Monnier, A., Poolman, M., Curien, G., Petroustos, D., Finazzi, G., 2017. Investigating mixotrophic metabolism in the model diatom *Phaeodactylum tricornutum*. *Philos. Trans. R. Soc. B Biol. Sci.* 372, 20160404. <https://doi.org/10.1098/rstb.2016.0404>
- Vincent, F., Sheyn, U., Porat, Z., Schatz, D., Vardi, A., 2021. Visualizing active viral infection reveals diverse cell fates in synchronized algal bloom demise. *Proc. Natl. Acad. Sci.* 118, e2105198118. <https://doi.org/10.1073/pnas.2105198118>
- Wahl, O., 1932. Neue Untersuchungen über das Zeitgedächtnis der Bienen [Further investigations on the temporal memory of bees]. *Z. Für Vgl. Physiol.* 16.
- Walsh, P.J. (Ed.), 2008. *Oceans and human health*. Elsevier, Amsterdam ; Boston.
- Waltenberger, H., Schneid, C., Grosch, J.O., Bareiss, A., Mittag, M., 2001. Identification of target mRNAs for the clock-controlled RNA-binding protein Chlamy 1 from *Chlamydomonas reinhardtii*. *Mol. Genet. Genomics* 265, 180–188. <https://doi.org/10.1007/s004380000406>
- Wang, W., Yu, L.-J., Xu, C., Tomizaki, T., Zhao, S., Umena, Y., Chen, X., Qin, X., Xin, Y., Suga, M., Han, G., Kuang, T., Shen, J.-R., 2019. Structural basis for blue-green light harvesting and energy dissipation in diatoms. *Science* 363, eaav0365. <https://doi.org/10.1126/science.aav0365>
- Webb, A.A.R., Seki, M., Satake, A., Caldana, C., 2019. Continuous dynamic adjustment of the plant circadian oscillator. *Nat. Commun.* 10, 550. <https://doi.org/10.1038/s41467-019-08398-5>

- Wijnen, H., Young, M.W., 2006. Interplay of Circadian Clocks and Metabolic Rhythms. *Annu. Rev. Genet.* 40, 409–448. <https://doi.org/10.1146/annurev.genet.40.110405.090603>
- Williamson, C.E., 1980. Phased cell division in natural and laboratory populations of marine planktonic diatoms. *J. Exp. Mar. Biol. Ecol.* 43, 271–279. [https://doi.org/10.1016/0022-0981\(80\)90052-0](https://doi.org/10.1016/0022-0981(80)90052-0)
- Wong, D.C., O’Neill, J.S., 2018. Non-transcriptional processes in circadian rhythm generation. *Curr. Opin. Physiol.* 5, 117–132. <https://doi.org/10.1016/j.cophys.2018.10.003>
- Xie, W.-H., Zhu, C.-C., Zhang, N.-S., Li, D.-W., Yang, W.-D., Liu, J.-S., Sathishkumar, R., Li, H.-Y., 2014. Construction of Novel Chloroplast Expression Vector and Development of an Efficient Transformation System for the Diatom *Phaeodactylum tricornutum*. *Mar. Biotechnol.* 16, 538–546. <https://doi.org/10.1007/s10126-014-9570-3>
- Yang, Y., Cheng, P., He, Q., Wang, L., Liu, Y., 2003. Phosphorylation of FREQUENCY Protein by Casein Kinase II Is Necessary for the Function of the *Neurospora* Circadian Clock. *Mol. Cell. Biol.* 23, 6221–6228. <https://doi.org/10.1128/MCB.23.17.6221-6228.2003>
- Yang, Z., Emerson, M., Su, H.S., Sehgal, A., 1998. Response of the Timeless Protein to Light Correlates with Behavioral Entrainment and Suggests a Nonvisual Pathway for Circadian Photoreception. *Neuron* 21, 215–223. [https://doi.org/10.1016/S0896-6273\(00\)80528-0](https://doi.org/10.1016/S0896-6273(00)80528-0)
- Yoshioka, S., Kobayashi, K., Yoshimura, H., Uchida, T., Kitagawa, T., Aono, S., 2005. Biophysical Properties of a *c*-Type Heme in Chemotaxis Signal Transducer Protein DcrA. *Biochemistry* 44, 15406–15413. <https://doi.org/10.1021/bi0513352>
- Young, J.N., Hopkinson, B.M., 2017. The potential for co-evolution of CO<sub>2</sub>-concentrating mechanisms and Rubisco in diatoms. *J. Exp. Bot.* 68, 3751–3762. <https://doi.org/10.1093/jxb/erx130>
- Zagotta, M.T., Hicks, K.A., Jacobs, C.I., Young, J.C., Hangarter, R.P., Meeks-Wagner, D.R., 1996. The Arabidopsis ELF3 gene regulates vegetative photomorphogenesis and the photoperiodic induction of flowering. *Plant J.* 10, 691–702. <https://doi.org/10.1046/j.1365-313X.1996.10040691.x>
- Zaslavskaja, L.A., Lippmeier, J.C., Kroth, P.G., Grossman, A.R., Apt, K.E., 2001a. Transformation of the diatom *Phaeodactylum tricornutum* (Bacillariophyceae) with a variety of selectable marker and reporter genes. *J. Phycol.* 36, 379–386. <https://doi.org/10.1046/j.1529-8817.2000.99164.x>
- Zaslavskaja, L.A., Lippmeier, J.C., Shih, C., Ehrhardt, D., Grossman, A.R., Apt, K.E., 2001b. Trophic Conversion of an Obligate Photoautotrophic Organism Through Metabolic Engineering. *Science* 292, 2073–2075. <https://doi.org/10.1126/science.160015>
- Zehring, W.A., Wheeler, D.A., Reddy, P., Konopka, R.J., Kyriacou, C.P., Rosbash, M., Hall, J.C., 1984. P-element transformation with period locus DNA restores rhythmicity to mutant, arrhythmic *Drosophila melanogaster*. *Cell* 39, 369–376. [https://doi.org/10.1016/0092-8674\(84\)90015-1](https://doi.org/10.1016/0092-8674(84)90015-1)
- Zhang, C., Dang, H., Azam, F., Benner, R., Legendre, L., Passow, U., Polimene, L., Robinson, C., Suttle, C.A., Jiao, N., 2018. Evolving paradigms in biological carbon cycling in the ocean. *Nat. Sci. Rev.* 5, 481–499. <https://doi.org/10.1093/nsr/nwy074>
- Zhang, C., Hu, H., 2014. High-efficiency nuclear transformation of the diatom *Phaeodactylum tricornutum* by electroporation. *Mar. Genomics* 16, 63–66. <https://doi.org/10.1016/j.margen.2013.10.003>
- Zhao, B., Schneid, C., Iliev, D., Schmidt, E.-M., Wagner, V., Wollnik, F., Mittag, M., 2004. The Circadian RNA-Binding Protein CHLAMY 1 Represents a Novel Type Heteromer of RNA Recognition Motif and Lysine Homology Domain-Containing Subunits. *Eukaryot. Cell* 3, 815–825. <https://doi.org/10.1128/EC.3.3.815-825.2004>



Zhou, L., Gao, S., Wu, S., Han, D., Wang, H., Gu, W., Hu, Q., Wang, J., Wang, G., 2020. PGRL1 overexpression in *Phaeodactylum tricornutum* inhibits growth and reduces apparent PSII activity. *Plant J.* 103, 1850–1857. <https://doi.org/10.1111/tpj.14872>





*Time is more complex near the sea than in any other place, for in addition to the circling of the sun and the turning of the seasons, the waves beat out the passage of time on the rocks and the tides rise and fall as a great clepsydra.*

John Steinbeck - Tortilla Flat



# Chapter II:

## The circadian clock of diatoms

This second chapter is devoted to my study of circadian rhythmic processes in diatoms and, more precisely, in *Phaeodactylum tricorutum*. The text is divided into four sections (subchapters II.a to II.d) as follows.

The first subchapter is devoted to a general description of rhythmic phenomena in the oceans and endogenous clocks in the organisms that inhabit them. The text presented is a review written for the journal *Annual Reviews of Marine Science* of which I am co-first author. This paper was written in collaboration with the research group of Kristin Teßmar-Raible, of the Max Perutz Laboratory at the University of Vienna, leaders in the characterization of lunar rhythms in marine animal models. The review provides an in-depth overview of the biological and ecological questions in which my research work has been embedded: the oceans are a complex and highly dynamic environment characterized by a series of rhythmic phenomena with different periodicity (tidal, diurnal, lunar and seasonal). Organisms must adapt to them in order to maximize their fitness and ensure evolutionary success. The text provides an overview of rhythmic biological processes in animals and eukaryotic algae, as well as of the endogenous molecular mechanisms that regulate such rhythmicity. This first subchapter completes what has already been introduced on biological rhythmic processes in Chapter I and places them in the marine ecological context. This first subchapter also delves into how environmental changes (natural and anthropogenic) can affect endogenous clocks and rhythmic biological phenomena. At the time of the completion of this manuscript, the review is under peer review.

The following three subchapters provide a description of the experimental work I performed to characterize biological rhythmicity in my model organism of choice, *P. tricorutum*. As in other photosynthetic organisms, a fine response to light stimuli is of paramount importance to *P. tricorutum*. For this, the daily rhythmic stimuli of light and dark have a major influence on the biology of this diatom on multiple levels: gene expression, metabolism, and cell division are the most prominent examples of processes synchronized with the external photocycles. Through my Ph.D. work, I contributed to discover how two bHLH-PAS proteins, bHLH1a and bHLH1b, play a role in regulating these processes by participating in the endogenous timekeeper machinery of *P. tricorutum*.

Subchapter II.b contains a first publication I co-authored in which the influence of bHLH1a (renamed RITMO1) on the transcriptional profile of *P. tricorutum* is described for the first time by using lines overexpressing this protein. In this work, my main contribution consisted in the refinement of a protocol for the analysis of cellular fluorescence rhythms by flow cytometry. This technique allowed to demonstrate that *P. tricorutum* presents diurnal oscillations in the content of fluorescent pigments per-cell, oscillations that persist after the release of the cultures in continuous light. The

novelty of this work consisted in clearly demonstrating that *P. tricornutum* presents an endogenous oscillator that controls cellular physiology and in identifying by transcriptomic exploration of the rhythmic TF the first possible regulator of these rhythms. In addition, phylogenetic analysis revealed a wide distribution of RITMO1-like proteins in the genomes of diatoms, suggesting a possible conservation of function in these phototrophs.

The following subchapter II.c presents a detailed investigation of *P. tricornutum* rhythmicity in response to different environmental photoperiods and light irradiance intensities. The role of RITMO1 has also been investigated through the generation of KO mutant lines. Obliteration of this protein leads to a major alteration in the persistence of the rhythms of in cellular fluorescence in cells released under continuous light, thus confirming that RITMO1 plays a role in the circadian clock machinery. More importantly, through a time-resolved analysis of the expression levels of a set of rhythmic genes, I was able to demonstrate how obliteration of RITMO1 eliminates the persistence of the transcriptional oscillations exhibited by the wild type line in free run conditions. This suggests that RITMO1 represents indeed a central transcriptional regulator in the pacemaker of *P. tricornutum* and allows to propose it as a central clock component of this alga. To conclude, by exploiting a technique based on chlorophyll fluorescence analysis, I was also able to demonstrate that the circadian clock exerts control over the photosynthetic machinery in *P. tricornutum*, as mutation of RITMO1 results in a loss of the oscillations in free-running maximal photosynthetic capacity.

Finally, subchapter II.d provides a preliminary characterization of the bHLH1b protein in the circadian clock of *P. tricornutum*. The analysis by Yeast Two Hybrid (Y2H) assay indicates that RITMO1 and bHLH1b can physically interact at the level of their bHLH domain, corroborating their co-implantation in the same molecular process. Furthermore, KO mutants for this protein show altered cellular fluorescence rhythmicity similar to that presented by RITMO1 mutants, although to a lesser extent, suggesting a similar implication in endogenous clock regulation. These assays represent the first effort aimed at molecular dissection of the circadian clock in diatoms, as well as the first characterization of the function of bHLH-PAS proteins in these algae.







# Chapter II.a:

## Rhythms and clocks in marine organisms

N. Sören Häfker<sup>1,2\*</sup>, Gabriele Andreatta<sup>1,2\*</sup>, Alessandro Manzotti<sup>3\*</sup>, Angela Falciatore<sup>3 @</sup>, Florian Raible<sup>1,2 @</sup>, and Kristin Tessmar-Raible<sup>1,2 @</sup>

<sup>1</sup>Max Perutz Labs, University of Vienna, Vienna BioCenter, Dr. Bohr-Gasse 9/4, 1030 Vienna, Austria

<sup>2</sup>Research Platform “Rhythms of Life”, University of Vienna, Vienna BioCenter, Dr. Bohr-Gasse 9/4, A-1030 Vienna, Austria

<sup>3</sup>Laboratoire de Biologie du chloroplaste et perception de la lumière chez les micro-algues, UMR7141, CNRS, Sorbonne Université, Institut de Biologie Physico-Chimique, Paris, 75005, France

\*equal contribution

@ contacts:

[angela.falciatore@ibpc.fr](mailto:angela.falciatore@ibpc.fr)

[florian.raible@univie.ac.at](mailto:florian.raible@univie.ac.at)

[kristin.tessmar@mfpl.ac.at](mailto:kristin.tessmar@mfpl.ac.at)

Keywords: endogenous oscillators, environmental cycles, climate change, circadian, circatidal, circalunar, circannual, algae, animals

This chapter has been written upon invitation by Annual Reviews of Marine science and is currently under peer-review.

I was responsible for the conception and editing of paragraph 3, *Rhythms in the life of marine algae*, as well as for the conception and editing of Figures 2 and 3, Tables 1 and 2 and Table Supplementary S1.

# Abstract

The regular movements of waves and tides are obvious representations of the oceans' rhythmicity. But the rhythms of marine life span across ecological niches and time scales, including short (in the range of hours) and long periods (in the range of days and months). These rhythms regulate physiology and behavior of individuals, as well as their interactions with each other and the environment. This review highlights examples of rhythmicity in marine animals and algae that represent important groups of marine life and different habitats. The examples cover ecologically highly relevant species and a growing number of laboratory model systems that are used to disentangle key mechanistic principles. The review introduces fundamental concepts of chronobiology, such as the distinction between rhythmic and endogenous oscillator-driven processes. It also addresses the relevance of studying diverse rhythms and oscillators, as well as their interconnection, for better predictions of how species will respond to environmental perturbations, including climate change. As the review aims to address scientists from the diverse fields of marine biology, ecology and molecular chronobiology, which all have their own scientific terms, we provide a term glossary at the end of the text.

# 1. Cycles of the sun and moon cause a multitude of biological rhythms

“The blue marble” is the title of a series of images produced during various NASA missions, starting with the Apollo 17 mission in 1972. The view of Earth from space (Fig. 1a) not only prominently pictures the fact that marine environments are dominating Earth, but is also a reminder that as part of the solar system, our planet is exposed to regular astronomical and geophysical cycles. The most relevant of these are the rhythmic impacts of sun and moon, which shape physico-chemical cycles that organisms have been exposed to since the dawn of life. Adaptations to these cycles have therefore likely been a fundamental aspect for survival. The relative positions of sun, moon and earth results in cycles with a complexity of different period lengths, ranging from tidal periods in the range of 12 hours, over diel and monthly periods to annual/seasonal cycles (Fig. 1g,h). Furthermore, these cycles differ depending on geographic location (Fig. 1b-f).

Life is commonly assumed to have originated in the marine environment, and thus in an ecosphere dominated by periodicity on these different time scales. A broad number of species indeed make use of distinct cycles generated by sun and moon to adjust their behavior and physiology, as detailed below. In chronobiology, the regular re-occurrence of a distinct physiological, behavioral or cellular event is referred to as a “biological rhythm”. Periodicities of these rhythms approximate those of the underlying natural cycles (Fig. 1g,h). An important conceptual distinction concerns the question of how biological rhythms are elicited: on the one hand, biological rhythms can result from direct organismal responses to environmental cycles. On the other hand, biological rhythms are often caused by endogenously driven

cellular/molecular oscillators, also referred to as inner “clocks” or “calendars”. Such endogenous oscillators, in turn, are synchronized to the respective environmental cycles by a process called “entrainment”. Endogenous oscillators allow organisms to anticipate predictable changes in their environment, and therefore adjust their behavior and physiology before the actual changes occur (Dodd et al. 2014). In many scenarios, this ability is likely advantageous for the fitness of a species (Dodd et al. 2005; Johnson & Golden 1999; Krittika & Yadav 2020; Ouyang et al. 1998; Sanchez et al. 2011). The general mechanistic principle of such oscillators are positive-negative feedback loops, using different cell-biological processes. So far, circadian clocks in land organisms are the only clocks understood in molecular mechanistic detail. Whereas animals, plants and fungi all rely on transcriptional/translational feedback loops (TTFLs) for their central clock machinery, and phosphorylation/de-phosphorylation cycles play critical roles, the exact molecular factors in these three groups are not homologous, or only to a limited extent (Brenna & Albrecht 2020; Narasimamurthy & Virshup 2021; Saini et al. 2019; Yan et al. 2021; Yildirim et al. 2022). Furthermore, also non-TTFL-based ~24hr oscillatory systems exist. Even though these were originally uncovered in the marine alga *Acetabularia* (Sweeney et al. 1967), they are mainly investigated in terrestrial systems (Edgar et al. 2012), and knowledge on their molecular mechanisms remains scarce. The understanding of other oscillatory systems (e.g. circatidal,

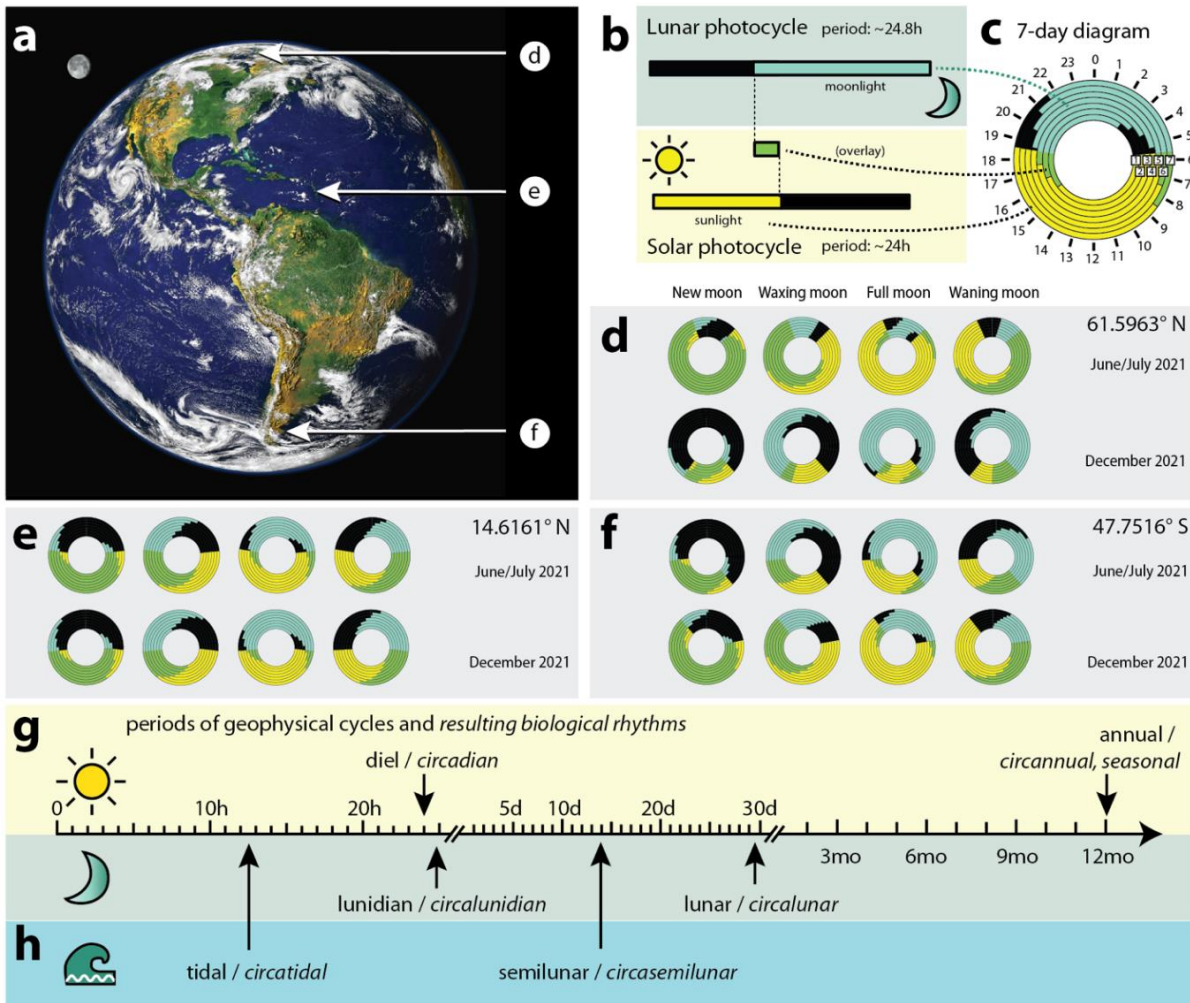


Figure 1. Complex rhythms emerge from solar and lunar cycles in marine ecosystems.

(a) Earth and moon as seen from space; arrows highlight coordinates used in panels d-f ; (b, c) Summary of weekly solar and lunar photocycles, with the perimeter indicating hours of the day, and concentric circles representing consecutive days (1-7). The daily cycles of solar light cause the well-known diel light cycle of ~24 hours. The gradual shifts of moonrise and moonset cause an independent – lunidian – photocycle, with an average period of ~24.8h. (d-f) Exemplary 7-day diagrams covering one month (new moon, waxing moon, full moon, waning moon) around summer (top) and winter (bottom) solstices on three distinct coastal locations of different latitude, illustrating the complexity of superimposed solar and lunar light cycles; (g) overview over the period lengths of major natural cycles and in italics the associated (endogenous) biological rhythms generated by the solar (top) and lunar (bottom) photocycles; (h) period lengths of major natural cycles and associated biological rhythms generated by the lunar gravitational cycles. Tidal cycles have a basic period length of half a lunar day (~12.4h), while the mutual constellation of moon, earth and sun also causes a longer cycle (semilunar, ~14.8 days, spring tides).

circalunar, circannual) is less advanced and particularly for the interplay between solar and lunar timing systems, marine systems have been helping significantly to advance our understanding (see below).

If or not a rhythm is endogenous, needs to be experimentally determined: a hallmark of inner oscillators is a “free-running” biological rhythm even under environmental conditions that do not provide regular cues for the entrainment of the investigated rhythm. The individual cases highlighted in the following sections argue that molecular oscillators are likely present across a diverse array of marine species and period lengths. By contrast, most of our molecular and cellular knowledge about the molecular

sensors and timing systems still stems from terrestrial model systems. We will outline below that such models have natural limitations for marine chronobiology; in turn, chronobiological research in marine organisms can help to understand phenomena still present in non-marine species. To cover at least a part of the marine species diversity, this review focuses on animals and the polyphyletic group of eukaryotic algae. Chronobiological research on these groups has particularly advanced during recent years, they represent different levels of marine environments (Fig. 2) and the food web, and the comparative overview also begins to address biodiversity and evolution of timekeepers in eukaryotic organisms.

## 2. Other places, other rhythms: The oceans harbor multiple and diverse habitats with very different properties from land

As outlined in the preceding section, the regular cycles of sun and moon produce the principle physical framework that generates regular environmental cycles, but the exact nature of these cycles depends on the habitat and its chemo-physical properties. This aspect is particularly relevant when considering the rhythmic biological processes present in terrestrial vs. marine environments and across the diversity of marine habitats (Fig.2). Temperature is a prominent cyclic cue for terrestrial organisms, both for diel and annual cycles (Buhr et al. 2010; Chen et al. 2015; Watson & Smallman 1971; Yocum et al. 2016). In marine environments, however, temperature rhythms (on daily and yearly scales) are mainly restricted to tidal habitats and uppermost surface layers (d’Alcalà et al.

2004). At which exact depth temperature changes rhythmically differs between locations and depends on water currents and mixing, which can even vary between days (Moum 2021). Moreover, temperature can be quite strongly off-set from photoperiod (Häfker et al. 2018b): for instance, Mediterranean seawater at the Gulf of Naples in 50-70m depths is warmest between October-December and cooler throughout the rest of the year (d’Alcalà et al. 2004). Furthermore, seasonal temperature cycles and the timing of sea ice break-up/formation in polar regions are typically delayed relative to the photoperiod cycle (Kahru et al. 2010; Wallace et al. 2010). As we will discuss in section 5, the fact that temperature is a less predictable cue in marine environments, but at the same time

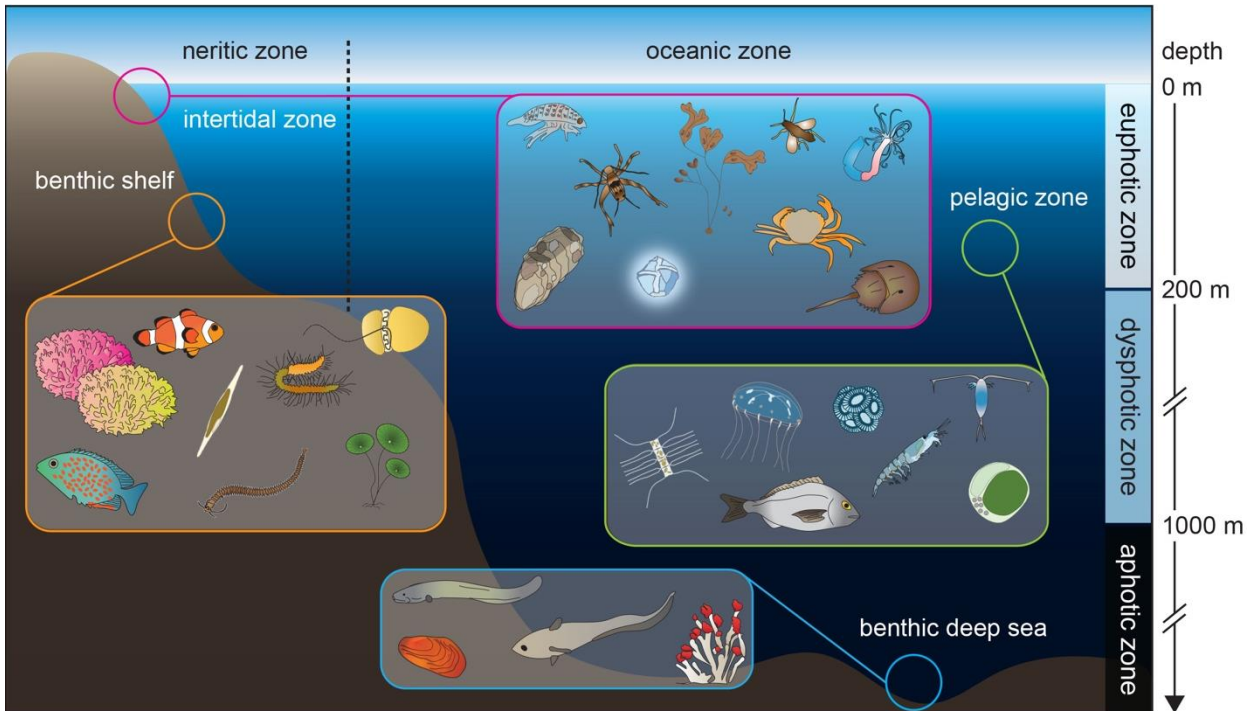


Figure 2. Overview of the diverse marine habitats and discussed exemplary organisms.

Important subdivisions of marine habitats include open waters (pelagic) vs. sea floor (benthic), as well as nearshore shelf seas (neritic) vs. the open ocean (oceanic). Temporary air exposure defines the intertidal zone. Differences in light penetrance further separate euphotic (typically 0-200m depth), dysphotic (200-1000m depth) and aphotic (>1000m) zones. Each of these zones exhibits different combinations of rhythmic factors relevant to its inhabitants.

strongly influences biomass production, also has significant consequences for the effects of climate change on marine ecosystems.

Light is another cyclic cue that is of relevance for the rhythmicity of organisms, and its penetrance is an important factor for the definition of marine habitats (Fig. 2). In those accessible by light, the outlined astronomical photocycles (Fig. 1) define basic patterns of rhythmicity that can be used by marine organisms. However, position, especially water depth, as well as distance to coast, strongly impact on the overall amount and spectral quality (Austin & Petzold 1986). Moreover, the biological rhythmicity itself can have secondary effects on light. For instance, seasonal phytoplankton blooms significantly affect light penetrance to deeper habitats. In addition, many marine organisms do not only move (actively or passively) horizontally, but also in depth, and thereby between habitats.

Such vertical migrations can span across several hundred meters within a single day (Brierley 2014; van Haren 2007). For planktonic organisms, this phenomenon, known as diel vertical migration (DVM), is likely under circadian clock control (Häfker et al. 2017). Besides plankton, many other marine organisms exhibit vertical migrations, including top predators like fish, squids and whales (Chambault et al. 2021; Christiansen et al. 2019; Gilly et al. 2006; Sims et al. 2005). How are the entrainment mechanisms of any potential endogenous oscillator adapted to the drastic environmental changes that occur during such vertical migrations?

Besides light or temperature, additional cues such as salinity, mechanical forces, pressure or magnetic field changes (Aguzzi et al. 2011; Hewson-Browne 1973) can provide a rhythmic framework unparalleled on land. Taken together, it is therefore obvious that research on terrestrial

model systems can only provide limited mechanistic insights into the chronobiology of marine species. In order to understand more about these mechanisms, biological analyses on marine species amenable to functional molecular investigations need to be interconnected with long-term measurements of environmental parameters. For instance, systematic long-term quantification of light

conditions in a benthic habitat and corresponding laboratory experiments with molecular read-outs have unraveled a new role of UVA-light for seasonal adjustments (Veedin Rajan et al. 2021).



### 3. Rhythms in the life of marine algae

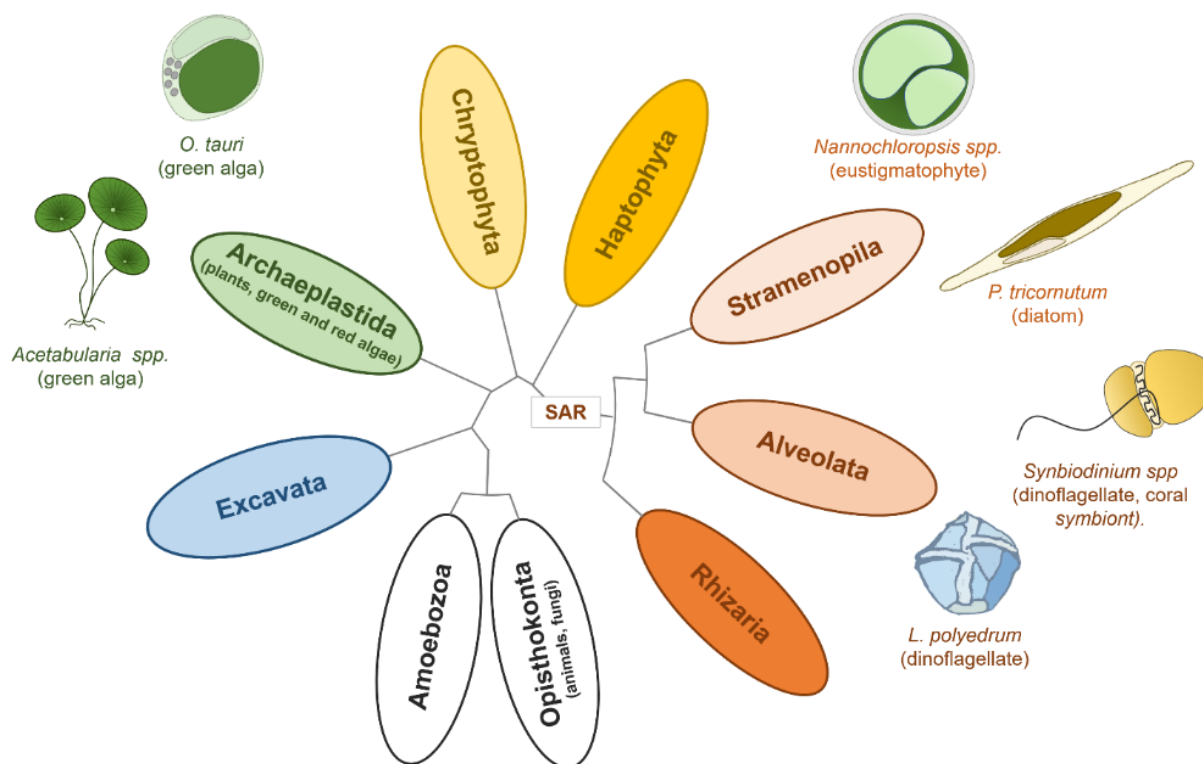


Figure 3. Established and emerging marine microalgal model systems for chronobiology.

Evolutionary position of established and emerging marine microalgal model systems in the eukaryotic tree of life. The groups including microalgae are reported in colors. SAR clade, including *Stramenopila*, *Alveolata*, and *Rhizaria*, is highlighted. Adapted from (Brodie et al. 2017).

The word “alga” subsumes highly diverse photosynthetic species widely distributed in the photic zone (Fig. 2). Derived by a series of endosymbiotic events (Blaby-Haas & Merchant 2019; Brodie et al. 2017; Keeling 2013), algae are positioned throughout the major groups of the eukaryotic tree of life (Fig. 3). A crucial ecological role in the marine environment is played by phytoplankton, also known as microalgae, which produce at least 50% of the world’s oxygen and primary organic biomass (Pierella Karlusich et al. 2020).

A variety of biological rhythms have been described in algae. Strong diurnal and circadian regulation of gene expression has been described under laboratory conditions in different taxa (e.g. (Corellou et al. 2009;

Poliner et al. 2019; Sorek et al. 2013), Suppl.Table 1) and diurnal rhythmicity of gene expression has been recently found in plankton communities from the natural environment (Coesel et al. 2021; Kolody et al. 2019). Rhythmic cell division is well documented for algae (e.g. (Chisholm & Brand 1981; Moulager et al. 2007; Sweeney & Hastings 1958), and Suppl.Table 1), as in plants (Fung-Uceda et al. 2018) and animals (Matsuo 2003), suggesting that this circadian function is critical for environmental adaptations. For algae, light not only serves as environmental information source, but is also the primary source of energy for photosynthesis. Consistent with this notion, endogenous daily rhythms of photosynthetic activity and related processes have been described in most algae (e.g. (Brand 1982;

Hastings et al. 1961; Ragni & d'Alcalà 2007), Supp. Table 1), suggesting that the tight temporal control of energy metabolism by a circadian clock is advantageous for algae, as previously shown for plants (Dodd et al. 2005). Photosynthesis may, in turn, represent an input for the regulation of the algal circadian clock itself as already shown in plants (Haydon et al. 2017) and similar to food cues in animals (Asher & Sassone-Corsi 2015).

Periodic changes in algal photosynthetic metabolism also impacts on symbiotic associations with animal partners. These associations supply the heterotroph host with organic products of photosynthesis to match energy needs, and are especially relevant in waters where nutrient levels are low (Muller et al. 2009). In corals that facultatively host the photosynthetic dinoflagellate *Symbiodinium sp.*, the dinoflagellate's photosynthesis follows endogenously-regulated circadian rhythms (Sorek & Levy 2012). These persist during association with the coral hosts, unlike other circadian processes such as cell division and motility that are rhythmic only in free living algae (Sorek et al. 2013). In turn, the aposymbiotic anemone *Aiptasia diaphana* shows dominant circatidal transcriptional dynamics, but these change to predominantly circadian patterns when anemones are associated with the symbiont (Sorek et al. 2018).

In different algae, the circadian clock also contributes to the regulation of population behavior (Supp. Table 1). Phytoplankton exhibits diurnal vertical migrations (Sournia 1975), but on a much smaller scale compared to zooplankton (see also section 4 below). Endogenous rhythms of bioluminescence (Hastings & Sweeney 1957) and cellular aggregation (Hastings & Sweeney 1957; Roenneberg et al. 1989; Roenneberg & Morse 1993) have also been described.

In addition, algae also exhibit moon-related cycles. Migratory rhythms in intertidal

sediments synchronized with diurnal and tidal cycles have been reported in different diatom species (Mitbavkar & Anil 2004; Round & Palmer 1966) and semidiurnal (12-h) gene expression periodicity has been documented in the diatom *Seminavis robusta* (Bilcke et al. 2021), likely reflecting adaptations to the tides in coastal ecosystems. Sexual reproduction is another process tangled with moon rhythms in algae. Multicellular algae have long been known to show synchronous gamete release patterns following lunar or semilunar periodicity (Andersson et al. 1994; Brawley & Johnson 1992).

Rhythmicity in algae also extends to cycles of longer period length: Composition and dynamics of phytoplanktonic populations exhibit strong seasonal patterns. Different taxa show seasonal bursts (algal blooms) in a specific area, generally interspersed with periods of apparent absence from the water column. External cues such as nutrients, light or predators (Reynolds 2006), photoperiodic variations or temperature changes (Lambert et al. 2019) can act as important drivers of community dynamics. In certain cases, there is even evidence for endogenous control on an annual scale, like in kelp (belonging to Stramenopiles) where growth was shown to be under circannual control (Lüning 1991; Schaffelke & Lüning 1994; tom Dieck 1991). Moreover, the activation of resting cysts of the dinoflagellate *Alexandrium* appears to follow an internal, circannual timing system (Matrai et al. 2005). The discovery of biannual patterns of sexual reproduction in the marine diatom *Pseudo-nitzschia multistriata* (D'Alelio et al. 2010) additionally highlights the robust long-term organization of the phytoplanktonic life cycle. Research into the dissection of the mechanisms that orchestrate algal rhythmicity on different timescales is not only scientifically promising, but also of tremendous relevance for ocean ecosystems.

## Algal models for the elucidation of marine time-keeping mechanisms

As outlined above, a variety of ecologically crucial biological rhythms have been described in algae. By contrast, far less information is available on the underlying algal timekeepers. Below, we briefly summarize the available knowledge on the molecular clock of these models (Fig. 3, Table 1). Important insights into algal timing systems were derived from research on the pykoekaryote *Ostreococcus tauri*, the smallest known free-living marine eukaryote (Courties et al. 1994). The small genome of this green alga (13Mbp, (Derelle et al. 2006)) harbors a minimal timekeeper that is formed by only two transcription factors: TOC1 and CCA1 (Corellou et al. 2009). Both factors are homologous to central circadian clock components of land plants (Creux & Harmer 2019) and of the fresh water green alga *Chlamydomonas reinhardtii* (Schulze et al. 2010). CCA1 is also conserved in the thermoacidophilic red alga *Cyanidioschyzon merolae* (Miyagishima et al. 2014). This indicates that critical TTF components might have a common origin in Archaeplastida.

Regarding the SAR (*Stramenopila*, *Alveolata*, *Rhizaria*) supergroup, information on the circadian clock is emerging from the study of diatoms, prominent aquatic microalgae evolved by secondary endosymbiosis (Falciatore et al. 2020). Remarkably, the genomes of these algae lack clear homologues of bacteria, plants or animal circadian clock components, with the exception of cryptochromes and casein kinases (see below) (Farré 2020; Poliner et al. 2019). A survey for rhythmic transcription factors of the diatom *Phaeodactylum tricorntum* (Pt) identified proteins with bHLH and PAS domains as putative circadian clock components (Annunziata et al. 2019), reminiscent of animal circadian clocks that

make use of bHLH-PAS domain transcription factors (Gekakis 1998). The additional presence of RITMO1-like proteins in other Stramenopiles (e.g. *Nannochloropsis*, *Ectocarpus*), as well as in Alveolates (Annunziata et al. 2019; Farré 2020; Thiriet-Rupert et al. 2016), is consistent with a circadian function of these transcription factors among the SAR. Another putative regulator of the diatom circadian clock is the blue-light sensor animal-like cryptochrome/photolyase 1 of *P. tricorntum* (*Pt*-CPF1). This protein and its *O. tauri* ortholog can function as transcriptional repressors in mammalian cell culture by interacting with the mammalian core circadian clock components CLOCK:BMAL (Coesel et al. 2009; Heijde et al. 2010). This suggests a conserved involvement of cryptochrome/photolyase in circadian TTF processes of animals and algae. However, while *Ot*-CPF1 is functionally involved in the maintenance of the *O. tauri* circadian clock, this alga misses bHLH-PAS transcription factors, as do other Archaeplastida (Heijde et al. 2010), pointing at possible limitations in the interpretation of heterologous cell culture studies.

Studies in algae have also contributed to reveal the existence of transcription-independent oscillators (TIOs). Initial insights derived from enucleated unicellular green alga *Acetabularia spp.* (Mergenhagen & Schweiger 1975; Sweeney & Haxo 1961), were followed by the discovery of endogenous bioluminescence rhythmicity in the dinoflagellate *Lingulodinium polyedrum* (formerly *Gonyaulax polyedra*) (Hastings 2007; Morse et al. 1989a,b). In this alga, luciferase bioluminescence is regulated via a transcription-independent mechanism relying on an RNA-binding protein named Circadian-Controlled Translational Regulator (CCTR).

CCTR represses the translation of luciferin binding protein (LBP) in a circadian fashion, by rhythmically binding a target sequence in the 3'UTR of the respective mRNA (Mittag et al. 1994). Moreover, work on *O. tauri* identified rhythmic oxidation of peroxiredoxin (PRX) (Bouget et al. 2014; O'Neill et al. 2011). PRX rhythms persist in constant darkness, a condition under which *O. tauri* transcription stops. PRX rhythms were found to be conserved across many kingdoms of life, including cyanobacteria, archaea, fungi and animals (Edgar et al. 2012; O'Neill et al. 2011). Given the role of PRX in the detoxification of Reactive Oxygen Species (ROS) by-products of cellular metabolism, it has been proposed that the evolutionary origin of circadian timekeeping might be linked to diel cycles of redox stress, and that more species-specific TTFL clockworks evolved independently later in the different eukaryotic lineages (Edgar et al. 2012).

As in other organisms, the circadian clock of algae is entrained by cyclic

environmental signals. Physiological analyses provide evidence that blue and red light play an important role in the entrainment (e.g. (Poliner et al. 2019; Roenneberg & Hastings 1988)). Diverse blue-light absorbing proteins have been identified in the genome of algal model systems, and their involvement in circadian regulation has been demonstrated in some species. By contrast, red/far red light-sensitive phytochromes have only been found in some diatom species (Fortunato et al. 2016), possibly due to the strong attenuation of long wavelengths underwater.

In addition to light, fundamental concepts on the temperature compensation of the circadian oscillators arose from early studies on the bioluminescence of *L. polyedrum* (Hastings & Sweeney 1957). More recent studies on circadian clock features of *Nannochloropsis spp.* (Poliner et al. 2019) and of coral-symbiotic algae (Sorek & Levy 2012) support this notion. The pathways implicated in these mechanisms, however, remain to be elucidated.



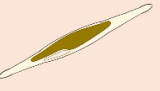


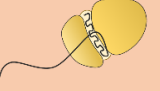
Marine algal models	Photoreceptors and modulators	Clock components	Rhythmic circadian biomarkers	References
 <i>Ostreococcus tauri</i> (green alga, mamiellophyceae)	CPF1 Cry-DASH LOV-HK ot-HKR CK	Evidences for <i>TTFL</i> CCA1/TOC1 Evidences for <i>TIO</i>	gene expression (LUC reporter), endogenous fluorescence, cell division, magnesium fluxes, PRX redox state	Heijde et al. 2009; Luck et al. 2019; Djouani-Tahri et al. 2011; Corellou et al. 2009; Moulager et al. 2007; Feeney et al. 2016; Le Bihan et al. 2015; O'Neill et al. 2011; Derelle et al. 2006; Lozano et al. 2014; van Ooijen et al. 2011, 2013
 <i>Acetabularia</i> spp. (green alga, ulvophyceae)	ARI ARII	Evidences for <i>TIO</i>	chloroplast migration, photosynthesis, oxygen production	Tsunoda et al. 2006; Wada et al. 2011; Sweeney et al. 1961; Koop et al. 1978; Neuhaus et al. 1986; Leebens-Mack et al. 2019
 <i>Phaeodactylum tricornutum</i> (diatom)	CPF1 CryP Cry-DASHs AUREOs RHO DPH CK	Evidences for <i>TTFL</i> bHLH/PAS (RITMO1)	photosynthesis, cellular fluorescence, pigment synthesis, gene expression	Coesel et al. 2009; Fortunato et al. 2016; König et al. 2017; Mann et al. 2020; Palmer et al. 1964; Ragni et al. 2007; Annunziata et al. 2019; Bowler et al. 2008; Falciatore et al. 2020
 <i>Nannochloropsis</i> spp. (eustigmatophyte)	AUREOs CPF Cry-DASH CK	Evidences for <i>TTFL</i> bHLH/PAS	gene expression (LUC reporter), photosynthesis, pigment synthesis, cell division	Vieler et al. 2012; Wang et al. 2014; Braun et al. 2014; Poliner et al. 2018; Poliner et al. 2019; Farré 2020
 <i>Lingulodinium polyedrum</i> (formely <i>Gonyaulax polyedra</i> , dinoflagellate)	CRYs Cry-DASH putative red light sensor CCTR protein phosphorylation	Evidences for <i>TIO</i>	cell division, swimming, aggregation, endogenous bioluminescence, photosynthesis	Roenneberg et al. 1997, 1988, 1989, 1993; Hastings et al. 1957, 1958, 2007; Sweeney 1958; Mittag et al. 1994; Johnson et al. 1984; Morse et al. 1989; Mackenzie et al. 2011; Comolli et al. 2003; Beauchemin et al. 2012
 <i>Symbiodinium</i> spp. (dinoflagellate, coral symbiont)	CRYs RHO putative red light sensor		cell division, motility, gene expression, photosynthesis, oxygen production, pigment synthesis	Fitt 1983; Sorek et al. 2012a, 2012b, 2013, 2014; Liu et al. 2018; Aranda et al. 2016; Lin et al. 2015; Shoguchi et al. 2013

Table 1. Characterized regulators, central clock system components and rhythmic outputs of marine algal models.

Components for which a role in circadian rhythm regulation has been demonstrated are reported in green, while putative regulators for which an empirical characterization is missing are reported in red. Background colors refer to the supergroups of Fig.3. Abbreviations: CPF, Cryptochrome Photolyase Family; CRY-DASH, Cryptochrome-DASH; LOV-HK, LOV-Histidine Kinase, ot-HKR, *Ostreococcus tauri* Rhodopsin Histidine Kinase; CK, casein Kinase; ARI and ARII, *Acetabularia* Rhodopsin I and II; CryP, Plant-like cryptochrome; AUREO, Aureochrome; RHO, Rhodopsin; DPH, Diatom Phytochrome; CCTR, Circadian-Controlled Translational Regulator; TIO, transcription-independent oscillator; CCA1, Circadian Clock Associated 1; TOC1, Timing of CAB expression 1; bHLH-PAS, basic Helix–Loop–Helix/Per-ARNT-SIM protein; LUC, luciferase; PRX, peroxiredoxin. Table adapted from (Noordally & Millar 2015). Although not directly related to algae chronobiology, in the “references” column we are reporting additional useful works concerning genomic and mutagenesis/transgenesis resources in the respective model organisms.

# 4. Animal models for marine chronobiology

In this section we present examples of prominent rhythmic phenomena, as well as animal models that have helped to start disentangling a variety of marine biological timers. We especially cover the naturally

highly relevant interplay of solar and lunar timing cues.

## Vertical migrations in the pelagic zone

As mentioned above, one of the Earth's largest regular biomass movements is the diel vertical migration (DVM) of marine plankton (Brierley 2014). This very heterogeneous group of species represents a key component of the ocean food network. Commonly, zooplankton migrates to the water surface at dusk, returning to depths at dawn, thought to represent the balance between feeding needs and predator avoidance (Fortier et al. 2001; Pearre 2003; van Haren & Compton 2013).

Although solar light represents the main reported stimulus synchronizing DVM (Kaartvedt 2010; van Haren & Compton 2013), moonlight also affects its rhythm, especially during polar nights, when periodicity shifts from the solar-cycle (24 hrs) to the lunidian-cycle (24.8hrs) (Gilly et al. 2006; Kaartvedt 2010; Last et al. 2016, 2020). Solar and lunar eclipses (Strömberg et al. 2002; Tarling et al. 1999), as well as other phenomena, presumably influencing local light intensities (i.e. storms and clouds) have been shown to also affect the dynamics of vertical migrations (Omand et al. 2021). Of note, DVMs persist during the darkest part of the polar night (Berge et al. 2009, 2015; Last et al. 2020), and in the deep sea (van Haren & Compton 2013), suggesting the existence of an endogenous oscillator coordinating these migration events.

Among the marine models that are used to investigate the molecular mechanisms of DVM are the Northern and Antarctic krill (Cohen et al. 2021; Piccolin et al. 2020) and the copepod *Calanus finmarchicus* (Häfker et al. 2017). Studies on these organisms are consistent with an involvement of the conventional circadian clock in DVM regulation (Biscontin et al. 2017; Häfker et al. 2017; Teschke et al. 2011). Putative core circadian clock genes of both krill and *Calanus* species show a diel/circadian transcriptional oscillation both in the field, laboratory LD and DD conditions (Häfker et al. 2017; Teschke et al. 2011). Transcriptional dynamics (including core circadian clock gene expression) showed ~24hr rhythms even under the polar “midnight sun” in *C. finmarchicus*, but also several ultradian patterns (including circatidal frequencies) in ice-covered areas (Hüppe et al. 2020; Payton et al. 2020). Consistently, DVM rhythms of the Antarctic krill (*Euphausia superba*) shifted from ~24 hrs in LD to ~12 hrs in DD (Piccolin et al. 2020). ~50% of the krill transcriptome oscillated with a ~24 hrs rhythm in LD, while under DD conditions, the dominant molecular signature exhibited frequencies of ~12-15 hrs (~40% of the transcripts) (Biscontin et al. 2019). Taken together, these data indicate a possible plastic nature of a circatidal/circadian/circalunidian clock in

zooplankton and/or polar species (for more details see below).

Whereas DVMs occur at any latitude, another type of vertical migration, yet with annual period, occurs mostly in temperate and polar regions, and is typically associated with diapausing strategies. In copepods, a facultative diapause occurs during times of low productivity in autumn/winter. Individuals migrate to large depths, where they will spend several months (Baumgartner & Tarrant 2017; Lenz & Roncalli 2019). Despite several phenotypic and (high-throughput) gene expression studies (Aruda et al. 2011; Baumgartner & Tarrant 2017; Christie et al. 2016; Clark et al. 2013; Häfker et al. 2018b; Lenz & Roncalli 2019; Roncalli et al. 2018; Schründer et al. 2013; Tarrant et al. 2016) the underlying mechanisms are still unclear. This includes the question if endogenous oscillator(s) or direct environmental/physiological cues are responsible for this annual rhythm. Similarly, seasonal-dependent signatures have been identified in the transcriptome of the Antarctic krill *E. superba*, when the species enters winter quiescence, a state of metabolic reduction (Höring et al. 2021), but the driving forces remain to be determined. Considering the key position of copepods and krill in pelagic food webs, understanding the factors

## Rhythms in the deep sea

The deep sea had long been considered an arrhythmic environment with low and steady biological rates due to darkness, average temperatures below 4 °C, high pressure, and limited food availability or driven by “spontaneous” hydrothermal vent activity, caused by plate tectonics. Chronobiological studies require either long(er)-term or repeated measurements, while ensuring that those measurements do not distort the results. Indeed, sample collection takes several hours to just bring on board, while camera observations will generate

and mechanisms driving their diel and seasonal rhythms is highly relevant (see also section 5 for a discussion on adaptability).

The regular migrations of zooplankton communities often drive similar phenomena in their mesopelagic and epipelagic predators, such as fish and sharks. Indeed, DVMs have been documented in the European hake *Merluccius merluccius* (De Pontual et al. 2012), the glacier lanternfish *Benthosema glaciale* (Dypvik et al. 2012a,b), the Pacific cod *Gadus macrocephalus* (Nichol et al. 2013), the Japanese eel *Anguilla japonica* (Chow et al. 2015), the jumbo squid *Dosidicus gigas* (Gilly et al. 2006) and the deepwater bluntnose sixgill shark *Hexanchus griseus* (Coffey et al. 2020). Modern strategies, including pop-up satellite transmitters and machine learning approaches, facilitate the assessment of diel, seasonal, or other migratory dynamics in larger animals like eels (Chang et al. 2020), bigeye thresher (*Alopias superciliosus*) (Coelho et al. 2015), whale sharks (Andrzejaczek et al. 2021), and sperm whales (Chambault et al. 2021).

There are many rhythms and possible endogenous oscillators that critically determine the interaction within and across marine species that await mechanistic analyses.

unnatural light exposure. This has complicated studies about possible temporal components in deep sea life.

However, evidence for environmental rhythms, such as seabed currents with periodic changes in velocity and direction, as well as temperature changes are emerging (Wagner et al. 2007). Deep sea tidal changes (“internal tides”) occur when coastal/surface tides propagate vertically across water layers with different properties (often cold and warm, respectively), along the water column (Garrett

2003). The advance of observatory technology and long-term infrastructure investments identified tidal (Cuvelier et al. 2017), diel, lunar (Mercier et al. 2011) and seasonal rhythms in different categories of animal life, covering behavior, growth rates, abundance and reproduction (Aguzzi et al. 2011; Baillon et al. 2014).

Molecularly, circatidal oscillations in melatonin levels from isolated pineal glands and retinae were observed in deep-sea fish (Wagner et al. 2007). Transcriptome sequencing from vent crabs and mussels started to set up resource to understand the molecular mechanism underlying the adaptation to the extreme hydrothermal vent habitat, including conventional animal core

circadian clock genes (Hui et al. 2017; Zheng et al. 2017). Such transcriptomic sequencing combined with repeated deep-sea on-site organism fixation and behavioral observations under red light allowed the identification of correlational tidal signatures in the behavior and transcriptome of the gill tissue of the vent mussel *Bathymodiolus azoricus* (Mat et al. 2020). Of note, the putative core circadian clock genes *period*, *timeless* and *cry1* (a *dCry/L-Cry* ortholog) exhibited ~tidal rhythms in field samples (Mat et al. 2020), suggesting plasticity of the ~24hr oscillator. Similarly, putative core circadian clock genes showed daily and/or tidal oscillations in the Arctic scallop *Chlamys islandica* during equinox and polar night (Perrigault et al. 2020).

## A plastic clock to time daily and tidal rhythms

In the marine environment, behavior and physiology are often synchronized with relatively short environmental cycles (in the range of hours), which comprise tidal (~12.4 hrs), diel (~24 hrs), and lunidian (~24.8 hrs) cycles, including the examples raised above, but also many others (Fig. 1g,h, Table 1,2 and (Andreatta & Tessmar-Raible 2020; Rock et al. 2022).

Tidal variations at the coast cause remarkably regular, but cause drastic changes in immersion, temperature, salt concentrations, oxygen and food availability, etc. As it is of utmost importance for organisms to not be “surprised” by those environmental changes, circatidal clock mechanisms to anticipate the imminent tidal variation are of high adaptive advantage (Rock et al. 2022). Circatidal locomotor rhythms have been described in a variety of animal taxa, such as crustaceans (Mehta & Lewis 2000; Naylor 1996; Palmer 1991; Williams 1998); insects (Evans 1976; Foster & Moreton 1981; Satoh 2017; Satoh et al. 2006, 2008); *Limulus* (Chabot et al. 2016; Chabot &

Watson 2010), polychaetes (Last et al. 2009), acoel worms (Arboleda et al. 2018), limpets (Schnytzner et al. 2018), and fish (Pülmanns et al. 2018). Valve opening activity rhythms in the oyster *Crassostrea gigas* shifted from a predominantly circadian (~24 hrs) to a circatidal pattern (~12.4 hrs) during constant lab condition in darkness, suggesting a control by both the environment, as well as an endogenous circatidal oscillator (Perrigault & Tran 2017). Diel and tidal rhythms have also been documented in the amphipod *Parhyale hawaiiensis* (Hunt 2016; Ramos et al. 2019), and the starlet sea anemone *Nematostella vectensis* (Hendricks et al. 2012; Oren et al. 2015; Tarrant et al. 2019). Dominance of either circadian or circatidal activity rhythms in *Nematostella* depends on light conditions (blue/green light versus red light/DD, respectively) (Leach & Reitzel 2020).

The mechanisms underlying circatidal oscillators have been debated as evidence for different models exists. Indeed, circatidal rhythms could rely on a) a unimodal circatidal clock (~12.4 hrs) which coexists



independently from the circadian clock (Naylor 2010), and does not even require to interact with the latter (Williams 1998) the superposition of two unimodal antiphase circalunidian (~24.8 hrs) clocks (Palmer 1995, 2000) a single bimodal clock orchestrating both circadian and circatidal rhythms (~24 hrs/~12.4 hrs) (Enright 1976; Tran et al. 2020).

Analyses of the plasticity of the conventional circadian oscillator and possible other oscillatory mechanisms in the diel/lunidian/tidal range have thus been of particular interest. Functional molecular investigations of the isopod *Eurydice pulchra* revealed an at least partial dissociation of circadian and circatidal oscillations (Zhang et al. 2013) and predominantly circatidal rhythms in metabolic dynamics were uncovered (O'Neill et al. 2015). Similarly, in the cricket *Apteronomobius asahinai* several genes involved in metabolic processes cycled in the transcriptome predominantly in a circatidal fashion, yet presumptive core circadian clock genes showed no evident rhythmicity (Sato & Terai 2019). Furthermore, RNAi-mediated downregulation of the core circadian clock genes *period* and *clock* in the cricket revealed impaired circadian, but not circatidal rhythms in this species (Takekata et al. 2012, 2014), in line with RNAi experiments targeting the *period* gene in *E. pulchra* (Zhang et al. 2013). These findings suggest that if molecular overlaps between circadian and circatidal oscillators exist, they might only be partial.

Dominant circadian signatures have been observed in mussels both at the transcript and protein levels under natural and simulated tidal environment (Connor & Gracey 2011; Elowe & Tomanek 2021). Oyster classical circadian clock genes showed circatidal expression in the field, a signature maintained under dark-dark (DD) conditions, but became diel in animals exposed to light-dark (LD) cycles under lab conditions (Tran

et al. 2020). This is very similar to observations of transcriptional core circadian clock gene oscillations in the Antarctic krill under different conditions, where the changes also matched with changes in diel-vertical migration behavior and metabolism (Piccolin et al. 2020).

Although these findings do not resolve the circatidal oscillator riddle, they indicate a plastic clock machinery which 1) times in the range of hours, and 2) differentially integrates environmental cues (e.g. light, tides). Independent input pathways might modulate the period length of the endogenous oscillator(s) by acting on different molecular loops of what at present is all considered the “conventional circadian clock”. These loops could resonate either with circadian or circatidal frequency, depending on the dominant environmental input. Additionally, such a scenario might be confined to specific cells, with others maintaining a classical circadian period. Finally, it is possible that the ticking of a still elusive metabolic oscillator is at the core of circatidal rhythms, directly or indirectly modulating oscillations of conventional core circadian clock genes.

Evidence that at least the conventional circadian clock can function individually in cells of marine organisms is well documented for the chromatophores of the annelid *Platynereis dumerilii*. These cells oscillate on molecular and phenotypic level independently of the worms' central head oscillator (Arboleda et al. 2019). Moreover, work on the integration of solar and lunar light cues for the exact timing of spawning hour shed further insight on the plasticity of the conventional circadian clock in *P. dumerilii*. At least in mature worms this clock can change its period length depending on exposure to either naturalistic sunlight or a combination of naturalistic (full/waning) moonlight and sunlight. This circadian/circalunidian plasticity allows the worms to spawn exactly at the darkness window between sunset and

moonrise, the exact time of which changes across the month (Zurl et al. 2021). Functional genetic analyses demonstrate that the combination of two light receptors, L-CRY and r-Opn1, is critical for the correct interpretation of light valence (i.e. sun- or moonlight) and moon phase (Zurl et al. 2021). Of note, light-dependent plasticity of ~24h clock period length has long been observed across a wide range of aquatic and terrestrial organisms, including humans (Aschoff 1960, 1965), but its biological relevance had remained unclear. Studies under more naturalistic conditions, including those on marine organisms, will provide a better understanding of oscillators that time specific hours.

Plasticity of the ~24hr clock not within the same individual, but between different

individuals builds the basis for the marine midge *Chunio marinus* to adapt its hour of adult emergence to local tidal regimes. In order to find the best substrate for zygote deposition, *C. marinus* emerges at the lowest low tide (Neumann 1966, 1968, 1988). However, the exact hours of the lowest low tide vary predictably along the coast. Polymorphisms in the *CaMKII.1* gene cause differential splicing and subsequent functional differences of the  $[Ca^{2+}]$ -dependent kinase. Those variances result in different circadian clock periods and ultimately in distinct emergence times, which match the local tidal conditions (Kaiser et al. 2016).

In summary, evidence for plasticity of ~24hr oscillators exists that could be sufficient to explain rhythms in the tidal, diel and lunidian range.

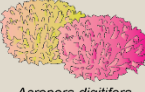












Marine animal models	Photoreceptors and modulators with functionally-tested roles in chronobiology	Putative core ~24h clock components	Rhythmic biomarkers	References
 <i>Acropora digitifera</i> <i>Acropora millepora</i>		<i>cry 1-3, clk 1-3, clk-like, bmal/cyc, pdp1-like 1-3, tim/tmo</i>	diel, lunar and seasonal spawning, lunar phase-dependent transcriptional oscillation, lunar transcriptional oscillation in the field and LL, diel, lunar and seasonal transcriptional oscillation	Levy et al. 2007; Shoguchi et al. 2013; Brady et al. 2011, 2016; Rosenberg et al. 2017; Wuitchik et al. 2019
 <i>Nematostella vectensis</i>	<i>CK1δ/ε</i> (circadian timing)	<i>clk, tim/tmo, cry1a, cry1b, cry2, bmal/cyc</i>	circadian locomotor activity, diel transcriptional oscillation, diel melatonin and serotonin variation, chromatin accessibility in LD and DD, circadian bacterial community abundance, circadian O <sub>2</sub> consumption, circatidal locomotor activity, diel variation in body length, plastic circadian/circatidal locomotor activity	Hendricks et al. 2012; Tarrant et al. 2019; Reitzel et al. 2010, 2013; Peres et al. 2014; Oren et al. 2015; Maas et al. 2016; Leach et al. 2018, 2019; Leach & Reitzel, 2019, 2020; Reuven et al. 2021; Renfer et al. 2010; Ikmi et al. 2014; Renfer & Technau, 2017; Weizman et al. 2019
 <i>Clityia hemisphaerica</i>	<i>Opsin 9, MIHR</i> (light-dependent timing)		light-dependent oocyte maturation and spawning	Quiroga-Artigas et al. 2018; 2020 Takeda et al. 2018
 <i>Platynereis dumerilii</i>	<i>l-cry</i> (sunlight and moonlight discriminator), <i>r-Opn1</i> (moonlight detection in circadian/circalunidian timing), <i>c-Opn1</i> (seasonality), <i>CK1δ/ε</i> (circadian but not circa(semi)lunar timing, <i>Gα-Opn1</i> (not involved), <i>pt-cry</i> (not involved)	<i>bmal, clk, tr-cry</i> (in vitro assay for positive and negative circadian clock loop transcription), <i>per, tim, pdp1, vri, tmo</i>	(semi)monthly/circa(semi)lunar spawning, (semi)monthly epitoky entry, plastic circadian/circalunidian swarming, circadian activity rhythm, circadian and lunar transcriptional oscillation, circalunar transcriptional and protein oscillation, circadian pigment dispersion, diel swimming behavior	Zantke et al. 2013; Arboleda et al. 2019; Poehn et al. 2021; Zurl et al. 2021; Andreatta et al. 2020; Tosches et al. 2014; Tsukamoto et al. 2017; Ayers et al. 2018
 <i>Crassostrea gigas</i>		<i>bmal, per, clk, cry1, cry2, tim, ror, rev-erb</i>	plastic circadian/circatidal valve opening activity semilunar, lunar, annual valve opening activity plastic circadian/circatidal transcriptional oscillation	Tran et al. 2011, 2020; Mat et al. 2012, 2016; Bernard et al. 2016; Perrigault & Tran, 2017; Payton et al. 2017a,b; Wu et al. 2018; Payton & Tran, 2019; Zhang et al. 2012; Peñaloza et al. 2021; Feng et al. 2019
 <i>Bathymodiolus azoricus</i>		<i>bmal, per, clk, tim, tmo, cry1a, cry1b, cry2</i>	circatidal transcriptional oscillation, diel transcriptional oscillation	Mat et al. 2020
 <i>Eurydice pulchra</i>	<i>CK1δ/ε</i> (circadian and circatidal timing)	<i>clk, cry2, bmal1, per, tim</i> (in vitro assay for positive and negative circadian clock loop transcription)	circatidal swimming activity, circadian pigment dispersion, ~12h transcriptional oscillation, ~12h O <sub>2</sub> consumption and enzymatic activity, semilunar activity and O <sub>2</sub> consumption	Hastings, 1981; Zhang et al. 2013; O'Neill et al. 2015
 <i>Clunio marinus</i> <i>Clunio tsushimensis</i>	<i>CaMKII.1</i> (circadian timing)	<i>clk, cyc</i> (in vitro assay for positive circadian clock loop transcription), <i>tim, tim2, per, cry2, vri, pdp1, rev-erb/eip75b</i>	circadian and circa(semi)lunar eclosion, circasimilunar imaginal disc development, lunar changes in shielding pigment transparency	Kaiser et al. 2011, 2012, 2016; Neumann and Spindler, 1991; Fleissner et al. 2008; Neumann, 1988, 1995; Kaiser and Haeckel, 2012
 <i>Apteronemobius asahinae</i>		<i>per, clk</i> (circadian but not circatidal timing), <i>tim, cyc, cry1, cry2</i>	plastic circadian/circatidal locomotor activity, plastic circadian/circatidal transcriptional oscillation	Satoh et al. 2008; Takekata et al. 2012, 2014; Satoh & Terao, 2019; Satoh et al. 2021
 <i>Calanus finmarchicus</i>	<i>CK1δ/ε</i> (circadian timing)	<i>clk, cyc, per1, per2, tim, cry1, cry2, vri</i>	circadian vertical migration circadian O <sub>2</sub> consumption annual vertical migration and diapause, circadian transcriptional oscillation, plastic circadian/ultradian transcriptional oscillation	Lenz et al. 2014; Häfker et al. 2017; Payton et al. 2020, 2021, 2022; Hüppe et al. 2020; Porter et al. 2017; Christie et al. 2013; Häfker et al. 2018a,b
 <i>Euphausia superba</i>	<i>cry1</i> (in vitro assay for light-sensitivity in circadian clock resetting)	<i>clk, cyc, cry2, per, tim1</i> (in vitro assay for positive and negative circadian clock loop transcription)	plastic circadian/circatidal vertical migration, plastic circadian/circatidal transcriptional oscillation, seasonal O <sub>2</sub> consumption, quiescence and transcriptional oscillation, seasonal changes in body length in LD and DD, seasonal O <sub>2</sub> consumption, seasonal changes in enzymatic activity in LD and DD, plastic circadian/circatidal O <sub>2</sub> consumption, circatidal enzymatic activity	Kaartvedt, 2010; Teschke et al. 2011; Biscontin et al. 2017, 2019; Horing et al. 2018, 2021; Piccolin et al. 2020; Huang et al. 2020; Meyer et al. 2017; Biscontin et al. 2016; Piccolin et al. 2018; De Pittà et al. 2013
 <i>Amphiprion ocellaris</i> <i>Amphiprion percula</i>		<i>bmal1, clocka, cry1b, per1b, per2, per3</i>	diel locomotor activity, diel transcriptional oscillation lunar, semilunar, trient-lunar spawning	Tan et al. 2018; Schalm et al. 2021; Mitchell et al. 2021a,b; Madhu & Madhu, 2007; Seymour et al. 2018
 <i>Siganus guttatus</i> <i>Siganus argenteus</i> <i>Siganus canaliculatus</i>		<i>Cry1a, Cry1b, Cry2, Cry3, Per1, Per2a, Per2b, Per3, Clock1a, Clock1b, Bmal1, Bmal2</i>	diel and lunar spawning rhythms, diel transcriptional oscillation, lunar phase-dependent and circalunar transcriptional oscillation, diel hormone levels, lunar phase-dependent hormone levels	Rahman et al. 2003; 2004a,b; Park et al. 2007a,b; Sugama et al. 2008; Fukushiro et al. 2011; Kashiwagi et al. 2013; Takeuchi et al. 2018; Jiang et al. 2019

Table 2. Overview of a comprehensive selection of different marine animals studied for their rhythms.

In this table we included a collection of the animal models that provided some of the major advances in marine chronobiology, both considering phenotypic/behavioral and molecular aspects. Box colors distinguish different phylogenetic groups (beige = cnidarians; light green = spiralian; light blue = ecdysozoans; light orange = chordates, more specifically vertebrates). In the second column, we focused on the photoreceptors and modulators of biological rhythms (but not part of the core molecular oscillators) that have been functionally validated (in green), using *in vivo* (i.e. mutagenesis, RNAi), *in vitro* (cell culture-based assays), or pharmacological approaches (agonists/antagonists). In the column “putative core ~24h clock components”, we focused on the genes characterized by clear orthology with known core circadian clock genes in animals (being this machinery well characterized in flies and mammals), and we distinguish between functionally-validated players (green, see above for the experimental evidence considered) or only putatively involved in the circadian oscillator of that species (red). Although not directly related to animal chronobiology, in the “references” column we are reporting additional useful works concerning genomic and mutagenesis/transgenesis resources in the respective model organisms.

## Timing reproduction with an inner calendar

Below we briefly focus on ~monthly and ~semimonthly cycles (Andreatta & Tessmar-Raible 2020). In animals, circasemilunar (semimonthly)/circalunar (monthly) rhythms have been well documented (Table 2, (Andreatta & Tessmar-Raible 2020; Raible et al. 2017; Tessmar-Raible et al. 2011). For several species ranging from annelids (*Platynereis dumerilii*, *Typosyllis prolifera*), molluscs (e.g. *Haliotis asinina*), crustaceans (e.g. *Eurydice pulchra*), insects (e.g. *Clunio marinus/tsushimensis*, *Pontomyia oceana*) to fishes (e.g. *Fundulus heteroclitus/grandis*, *Oncorhynchus mykiss*) they have been shown to persist in the absence of (semi)monthly cues and hence be controlled by endogenous oscillators (Kaiser & Neumann 2021). For some, the entraining stimuli are known, and for members of annelids, insects and fishes evidence for temperature compensation has been provided (Kaiser & Neumann 2021).

Here, we consider lunar and semilunar rhythms (and their underlying oscillators) as output modifications of the same mechanisms, because it has been shown that both periods can variably occur within the same insect and worm lab strains, depending on the entraining light conditions (Kaiser et al.

2021; Poehn et al. 2021). Importantly, this does, however, not necessarily imply the same oscillatory mechanisms across species.

Circa(semi)lunar clocks might rely on: 1) oscillators with a ~15/~30 day periodicity; 2) rhythms generated by the superposition of a circadian and a circatidal or circalunidian clocks (beat hypothesis); 3) ~15/~30 circadian cycles counter mechanism (frequency demultiplication hypothesis) (Kaiser & Neumann 2021). The latter two mechanism imply that each circadian clock change would also influence the (semi)monthly oscillator, while an independent circa(semi)lunar oscillator would provide more flexibility for independent adjustments of diel and monthly timing. Many correlational studies on transcript, and some on protein, level exist (reviewed in detail in (Andreatta & Tessmar-Raible 2020), but mechanistic molecular insight still remains largely open.

The first knock-out studies on an organism with a circa(semi)lunar oscillator, the marine annelid *P. dumerilii*, suggests that the worms’ cryptochrome L-Cry is critical to provide the organism with information if a given light comes from the sun or moon, and as such functions as a natural light interpreter

or valence detector (Poehn et al. 2021). Depending on light intensity and/or spectrum *Pdu-L-Cry* assumes distinct biochemical “moonlight” and “sunlight” states that coincide with distinct subcellular (stable nuclear versus cytoplasmic/nuclear degradation, respectively) localizations. Biochemically, *L-Cry* only reaches its full “moonlight” state under at least 6hrs of naturalistic moonlight, allowing it not only to discriminate between sun and moonlight, but also moon phases (Poehn et al. 2021). This enables the system to work independently of photoperiods and is in line with classical work that showed that nocturnal light duration, not its exact timing is relevant (Hauenschild 1960). Interestingly, the specific biochemically “moonlight state” properties of *L-Cry* are not present in its ortholog *dCry* of the diurnal/crepuscular insect *Drosophila melanogaster*, which does not possess a moon-controlled (semi)monthly oscillator (Zurl et al.

2021). It will be attractive to test cryptochromes of other species with moonlight-controlled rhythms for their biochemical and cellular properties. This is particularly interesting for corals due to the long-standing proposal of the involvement of a cryptochrome in lunar light-controlled spawning synchronization (Levy et al. 2007). Reef-building corals have been extensively studied for their extremely precise spawning, often occurring only once per year (Babcock et al. 1986), highlighting the required complex coordination of diel, monthly and annual cues (Wuitchik et al. 2019). While this complex multi-timer coordination is likely widespread, the reefs’ ecological relevance makes corals critical model systems to study the anthropogenic impacts on the timing of fundamental physiological and behavioral aspects of marine organisms (Fogarty & Marhaver 2019).

## 5. Marine rhythms and clocks under climate change

In this section, we review past and present effects of climate change on biological rhythms, and elaborate how climate effects on rhythms and timing systems can affect fitness, species interactions and ecosystem functioning. We discuss how organismic plasticity and genetic adaptability of timing system might favorably impact on species survival in an environment, whose cyclic conditions change (Häfker & Tessmar-Raible 2020).

Artificial light at night (ALAN) is another important and historically unprecedented anthropogenic environmental stressor. Nocturnal light pollution by e.g. human settlements can affect various aspects of biological rhythmicity in marine habitats (Ayalon et al. 2020; Berge et al. 2020; Duarte et al. 2019). ALAN is not directly connected to ‘climate change’ and for conciseness, we will not cover ALAN here, but refer to other reviews that address this important topic in appropriate detail (e.g. (Davies et al. 2014; Hölker et al. 2021).

### Changes of marine rhythms in the past

Earth has gone through numerous climate changes. It is difficult to deduce how biological rhythms responded to such changes, as fossils do not provide temporal information. They might, however, provide information about lifestyles (e.g. diurnal vs. nocturnal based on eye size) or – if sufficient DNA is recoverable – about putative clock genes and their sequence evolution. One famous example comes from nocturnal mammals, which, likely after the decline of dinosaurs, occupied new temporal niches in all environments, including the oceans. The spread of activity across the day-night cycle allowed for a higher diversity (Gerkema et al. 2013; Maor et al. 2017).

The last major change in environmental conditions was the warming after the last glacial maximum (LGM) 20,000 years before present (BP) and the associated retreat of the polar ice caps. Population analysis in the marine midge *Clunio marinus* showed that the species’ habitat-specific, genetically encoded circadian and circa(semi)lunar rhythmicity (see section 4)

likely evolved between the LGM and 8,000 BP from a single population that spread throughout the European coast (Kaiser et al. 2010). Along the European Atlantic coast these midges have adapted to different temporal niches, characterized by the monthly and diel combination of the lowest low tides optimal for adult emergence and zygote deposition (Kaiser et al. 2016, 2021).

Other evidence for favorable plasticity in timing stems from the Arctic/northern Atlantic *Calanus* complex. The boreal copepod *Calanus finmarchicus* maintained its population size throughout the LGM, while its Arctic congener *C. glacialis* experienced an ~1000-fold increase in population size since the LGM (Provan et al. 2009; Weydmann et al. 2018). This was likely due to increased availability of shelf habitats which *C. glacialis* prefers. Although it is not possible to proof past changes in copepod rhythmicity, it is likely that since the last ice age species of the *Calanus* complex experienced major latitudinal shifts and thus adapted to

changes in light conditions (e.g. photoperiod) and other rhythmic cues.

Thus, the rhythms and endogenous oscillators of marine organisms can adapt to

environmental changes. However, it remains unclear how much time is required for such adaptations and how they affect and are affected by population sizes. Likely, the answer is species-specific.

## Present-day climate effects on marine rhythmicity

Since the end of the 18<sup>th</sup> century, earth's climate has been experiencing major changes, at least partially caused by anthropogenic CO<sub>2</sub> emissions (IPCC 2014). These affect marine life through at least three major implications: (1) increase in water temperatures and associated decrease in polar sea ice cover, (2) decreasing water pH, due to

the uptake of atmospheric CO<sub>2</sub> and (3) expansion of marine oxygen minimum zones (Fig.4). While various studies addressed the impacts of this 'deadly trio' on e.g. physiology, ecosystem composition and fluxes, effects on biological rhythms and possible inner timing systems have been addressed to a much smaller extend.

## Temperature changes

Warming of tropical waters affects the synchronized mass spawning of reef-forming corals. Gamete maturation and release in these cnidarians show seasonal, lunar & diel coordination that is also reflected in corresponding rhythmic transcriptome changes (Hoadley et al. 2011; Oldach et al. 2017; Wuitchik et al. 2019) and circadian rhythmicity (Oren et al. 2015; Sorek et al. 2014). The seasonal phase of coral spawning is set primarily by a summer increase in water temperature (Keith et al. 2016). Besides desynchronization by artificial light (Ayalon et al. 2020), the overall increase in ocean temperature has been suggested to cause temporal desynchronization of gamete release in Red Sea corals. This implies that increasing temperatures do not only threaten coral reefs through direct effects (e.g. bleaching), but likely also by the disturbance of (reproductive) rhythms (Fig.4).

Increasing temperatures also result in a decline of polar sea ice cover and earlier ice break-up in spring/summer. Polar phytoplankton blooms start with the ice break-up and their peaks have shifted up to 50 days forward in one decade (Kahru et al. 2010). The reduction in Antarctic sea ice has been

connected to a decline in the stock of the Antarctic krill *Euphausia superba* (Atkinson et al. 2019; Meyer et al. 2017). In winter, krill larvae find shelter from predation at the underside of the sea ice and perform a 'reverse' DVM, sinking into the water column after sunset and drifting with the water current to find new under-ice food patches (Meyer et al. 2017). The decrease in krill stocks could thus be at least in part due to a loss of larval daytime refuge and consequently higher predation pressure in open water habitats. Polar phytoplankton growth is strong near the ice edge due to the seeding by algae released from the melting ice. As the ice edge retreats further poleward, so do the associated blooms. Together with the aforementioned forward shift of bloom timing, this could increase migration distance and impair the timing of seasonal latitudinal migrations that benefit from polar productivity (Jenouvrier et al. 2009). Baleen whales that visit boreal/polar regions in summer apparently show some adaptive plasticity in migratory timing, but it is unclear what the underlying mechanisms are and whether they can keep pace with the ongoing shifts in productivity, both on a latitudinal (Ramp et al. 2015; Visser et al. 2011) and temporal scale (Kahru et al. 2010)

(Fig.4). Warming in general has resulted in latitudinal distribution shift in a variety of marine species that, in an attempt to stay within their thermal niche, move closer towards the poles and thereby into habitats

## pH changes

Effects of ocean acidification on rhythms and clocks have so far hardly been investigated. A recent study found altered timing and synchronization in coral spawning under a combination of increased temperature and reduced pH (Lieberman et al. 2021). Furthermore, reports of altered circadian clocks gene expression in fish at reduced pH-levels suggest a response by the circadian clock that regulates diel rhythms of osmoregulation in marine fishes (Jesus et al. 2017; Schunter et al. 2016). Ocean acidification can also impact on chemical detection and brain functioning in fish (Dixson et al. 2010; Schunter et al. 2018), and could thus impair rhythm entrainment

## Oxygen concentration changes

Oxygen minimum zones (OMZs) in the world's ocean are expanding both vertically and horizontally. Many species cannot inhabit OMZs while others are closely associated with them. Thus, the expansion of these zones can have profound effects on species, as shown for the depth distribution of the vertically migrating jumbo squid *Dosidicus gigas*, and other eastern Pacific top-predators (Rosa & Seibel 2008; Stramma et al. 2012). Similar to vertical distribution shift caused by OMZs, ocean warming can also affect vertical habitat usage due to downward shifts of thermoclines (Howard et al. 2020; Jorda et al. 2020). Vertical distribution shifts alter the experienced diel rhythms of light and other parameters (temperature, oxygen, pressure) (Fig.4). This could affect the entrainment of circadian clock systems, that can regulate DVM (Häfker et al. 2017), as well as potential photoperiod-based seasonal timing (Häfker et al. 2018a; Teuber et al. 2013). Altered diel and

with more extreme rhythmic environmental conditions (Atkinson et al. 2019; Beaugrand et al. 2003; Chivers et al. 2017; Kaartvedt & Titelman 2018; Melle et al. 2014; Sundby et al. 2016; Villarino et al. 2020).

through chemical cues (e.g. pheromones) used to synchronize reproduction (Baghel & Pati 2015; Watson et al. 2003) and egg release (Caballes & Pratchett 2017; Tankersley et al. 2002). Reduced pH-levels were further shown to influence DNA methylation and chromatin condensation in corals and marine fish and could thereby also affect both, circadian (de Lima & Göndör 2018; Weizman et al. 2019) and circannual timing mechanisms (Stevenson & Lincoln 2017). While the potential effects of acidification on biological clocks have long been overlooked, they clearly warrant detailed investigation.

seasonal vertical distribution patterns could further impact CO<sub>2</sub> sequestration to deep waters (Brun et al. 2019; Jónasdóttir et al. 2015). Additionally, horizontal OMZ spreading leads to latitudinal shifts of species specifically adapted to these zones, while species intolerant to low oxygen levels are forced to shift their habitat as well (Seibel et al. 2014; Stramma et al. 2012; Zeidberg & Robison 2007). The induced latitudinal shifts will again alter the light conditions the species encounter and could thus impair diel and/or seasonal timing (Fig.4).



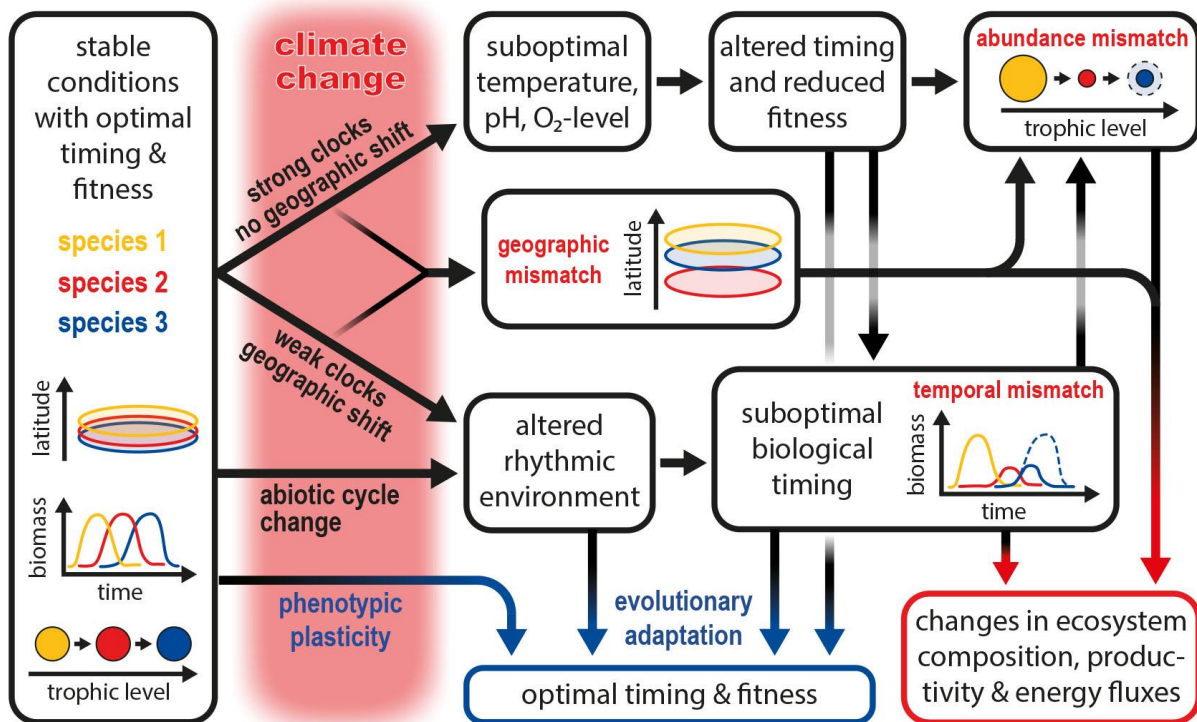


Figure 4. Climate change effects on timing and how they could impact on species interactions and ecosystems.

Changes in abiotic factors (here temperature, pH, oxygen) and/or the rhythmic environment create suboptimal conditions, forcing responses that can differ between species. A simplified 3 species system illustrates mismatches with the species 2 (red, intermediate trophic level) most severely affected. Dashed lines indicate potential of species 3 (blue, higher trophic level), if species 2 was not affected. The enlarged cycle for species 1 (yellow, lower trophic level) in the abundance mismatch scenario illustrates the reduced top-down control by species 2. In the more complex natural environment other species may compensate for, benefit from or suffer under some of the interspecies mismatches.

Generally, present-day temperature changes are especially pronounced at high latitudes (Cohen et al. 2014; Ducklow et al. 2007) and ocean acidification will also disproportionately affect these regions due to

higher CO<sub>2</sub> solubility in cold water (Fabry et al. 2009; Yamamoto-Kawai et al. 2009). Hence, it is likely that present and future changes in marine rhythms will be especially pronounced in polar habitats (Tougeron 2021).

### Adaptability of rhythms and clocks to future ocean conditions

Climatic conditions continue to change and marine organisms will have to respond either by adapting to them or by avoiding them through distribution shifts. Changes can affect a species' rhythmic environment, as well as a species' ability to respond to such changes (Fig.4). It is also

important to distinguish rhythms that are direct responses to environmental changes and those that are generated by endogenous timing systems, as the responses to ecological changes will differ significantly, e.g. due to temperature compensation.

## Phenotypic adaptive capacity

As discussed above, climate change can cause major latitudinal distribution shifts in marine species, e.g. due to increasing temperatures or expanding OMZs. However, individual adaptive capacity and photoperiodic range for clock functioning (diel rhythmicity, seasonal photoperiodism) are adjusted to a given habitat (Bradshaw & Holzapfel 2001; Höring et al. 2018; Schneck & Barreto 2020; Schwarzenberger et al. 2021) and could hinder occupation of new higher latitude habitats with different environmental cycles (Huffeldt 2020; Kaartvedt & Titelman 2018; Saikkonen et al. 2012; Sundby et al. 2016). If species are unable to adjust their timing systems to the altered environment or cannot shift their distribution due to rigid timing systems, they face suboptimal environmental conditions and, as a consequence, likely reduced fitness and abundance (Deutsch et al. 2015; Hughes et al. 2019) (Fig.4). Furthermore, if a species does not shift its distribution, temperature can directly affect photoperiodic seasonal timing, thus altering species phenology in spite of unchanged light conditions (Hairston & Kearns 1995; Watson & Smallman 1971) (Fig.4). Generally, whether species exhibit distribution shifts or not will depend on the relative selection pressure exerted by the light environment relative to other environmental factors (Tougeron 2021).

## Evolutionary adaptation of clock and rhythms

Speed of evolutionary adaptation depends on several factors including overall population size, connectivity of populations, generation time and selection pressure. Many of these factors differ strongly between marine and terrestrial habitats. Gene flow is typically considered to be stronger in the oceans due to the interconnection of water masses, reproduction through broadcast spawning and larval dispersal via currents. The zooplankton

Phenotypic rhythm/clock adaptability to altered environments is difficult to predict. Classical as well as recent work shows that circadian period can be plastic, for instance depending on ambient light intensities (see section 4, (Aschoff 1960; Zurl et al. 2021)), and photoperiods (Pfeuty et al. 2012; Piccolin et al. 2018).

In contrast, circadian clock genes peak at the same time under field photoperiods of 16h (56°N) and almost 24h (79°N) in the boreal copepod *C. finmarchicus* (Häfker et al. 2018a,b). However, a significant fraction of the *C. finmarchicus* transcriptome, including presumptive core circadian clock genes, showed semidiurnal cycling under midnight sun conditions at 82.5°N (Hüppe et al. 2020; Payton et al. 2020), either due to the different light conditions or due to entrainment by tidal food cues. A possible adaptation to extreme photoperiods might also be the ~tidal period of core circadian clock gene transcript oscillations in the brain of the Antarctic krill (*E. superba*) under constant (darkness) conditions, which shifted to a ~24hr period under light/dark cycles (Piccolin et al. 2020). It is further possible that latitudinal light changes could be compensated for behaviorally through vertical distribution adjustments.

species *C. finmarchicus* and *E. superba* both have enormous overall population sizes and inhabit vast areas of the northern Atlantic and Southern Ocean, respectively. Nevertheless, *C. finmarchicus* and its congener *C. glacialis* show at best weak genetic differentiation among populations (Provan et al. 2009; Unal & Bucklin 2010; Weydmann et al. 2018) and for *E. superba* there seems to be no genetic differentiation at all (Deagle et al. 2015).

While high overall population size should increase the probability for the emergence of favorable alleles and rhythmic phenotypes, the high connectivity of habitats could hinder the genetic adaptation of rhythmicity to a new local regime as it occurred in e.g. the midge *C. marinus* (Kaiser et al. 2010, 2021). Low genetic differentiation among populations could be a trait of highly abundant species (e.g. *E. superba*, *Calanus*), while stronger differentiation may be found between populations of less conspicuous species (Peijnenburg & Goetze 2013). This would mean that species of high abundance and ecological relevance could struggle most to adapt their rhythmicity due to the high marine connectivity hindering genetic differentiation. Understanding the timing systems and adaptability of such keystone species is thus of particular importance.

Potentially rapid evolution of new chronotypes in response to environmental

## Interspecies mismatches

Both, generation times and timing mechanisms are species-specific and circadian clocks can show mechanistic differences between species, even when closely related (Menegazzi et al. 2017; Tomioka & Matsumoto 2015). It is thus likely that phenotypic adaptive capacity and time needed to evolve chronobiological adaptations will strongly differ between species. This is even more probable, if species use different timing mechanisms, as suggested for seasonal (Baumgartner & Tarrant 2017; Goldman et al. 2004), but also lunar rhythms (Kaiser & Neumann 2021). Furthermore, as suboptimal timing results in a loss in fitness and likely reduced abundance (Dodd et al. 2005; Horn et al. 2019; Spoelstra et al. 2016; Yerushalmi & Green 2009), species with proper timing can still be affected through e.g. trophic interactions with suboptimally timed species (Fig.4). Moreover, latitudinal shifts can

changes could occur through hybridization (Kaiser et al. 2010; Strelkov et al. 2007). *C. marinus* parents from populations with differing diel emergence timing produce offspring with intermediate timing rhythms (Neumann 1967). Although less studied, hybridization in marine environments seems to be just as common as in terrestrial ecosystems (Gardner 1997) and has been reported from numerous species like fish and bivalves (Montanari et al. 2016; Zbawicka et al. 2019). However, even for closely related species (e.g. *Calanus* complex) hybridization is not necessarily a given (Choquet et al. 2017, 2021) and it can furthermore be hindered by temporal reproductive isolation (Niehoff et al. 2002). Thus, determining the hybridization potential among closely related species and the rhythms of hybrid offspring could provide valuable insights on their adaptability to climate change.

separate trophic interactors or lead to encounters between species that were previously separated (Chivers et al. 2017; Kaartvedt & Titelman 2018; Thorne & Nye 2021) (Fig.4). If species adjust their seasonal timing based on environmental cues (e.g. temperature, food availability, light intensity/spectrum, photoperiod) and/or endogenous timing systems (circannual clock, hourglass timer) this can cause mismatches in response to climate change (Beaugrand et al. 2003; Durant et al. 2019; Edwards & Richardson 2004; Régnier et al. 2019) (Fig.4). For example, the onset of Arctic phytoplankton bloom is gradually shifting to earlier dates (Kahru et al. 2010), but seasonal reproduction of the copepod *C. glacialis*, which depends on the bloom as a food source, could not adapt to changed bloom timing, resulting in a seasonal mismatch with low copepod abundance (Søreide et al. 2010).

Control of *Calanus* seasonal diapause is not properly understood, but it is thought to rely on endogenous cues like lipid content, circannual clocks (Baumgartner & Tarrant 2017; Conover 1965; Fulton 1973) and/or photoperiod (Häfker et al. 2018b).

At lower latitudes, seasonal mismatches affecting a given species could be compensated by other species becoming more abundant (Atkinson et al. 2015), but high latitude systems are often centered on a limited number of highly abundant species, which show precisely adjusted seasonal timing

due to the shorter productive period (Falk-Petersen et al. 2009). Thus, temporal mismatches might become more prominent in temperate/polar seas with high seasonality, which also harbor many of the most important commercial fisheries. Some models suggest that changes of high latitude habitats towards possibly longer productive periods (due to higher temperatures) and smaller species with shorter generation lengths could result in increased productivity (Feng et al. 2017; Renaud et al. 2018). However, such models typically lack considerations of climate effects on the organisms' timing systems.

## 6. Conclusions and outlook

Marine environments are characterized by numerous environmental cycles, and biological rhythms are central in shaping species interactions as well as ecosystem functioning and productivity. Periods span from diel vertical migrations of pelagic organisms, to the seasonal productivity rhythms of temperate and polar latitudes, to moon-synchronized reproductions that results in sudden burst of food abundance. Biological rhythms are important for coastal organisms to those at the bottom of the deep sea. Many of these rhythms are under the control of endogenous timing mechanisms and the (emerging) model species highlighted in this review have helped to identify general principles of oscillators functioning of relevance not just for marine habitats. Marine models have also helped to uncover fundamental insights, that still require further understanding, such as the existence of a ~24hr metabolic oscillator, the remarkable diversification of circadian clock systems in polyphyletic algae and plasticity of the "conventional" core circadian clock in animals or the decoding of solar versus lunar light input. It will be of increasing importance to discriminate between truly endogenous oscillator-driven rhythms and organismal

rhythms that directly follow environmental changes. The impact of changing environmental cues on both types of rhythms is very different- e.g. due to the presence/absence of temperature-compensation, responses to environmental cues as entrainment factors versus rhythm drivers. Environmental changes will - either directly or indirectly - affect marine rhythms and timing systems, but to which extent they can adapt to changes, and the time needed for this, are still hardly explored. Effects of climate change on marine rhythms could result in major ecosystem restructuring and changes in productivity that could also affect fishery yields and marine CO<sub>2</sub> storage.

It is evident that the quest for an understanding of marine rhythms must not stop at the descriptive, phenomenological level, but move to the cellular/molecular mechanistic level for which model systems can pave the way. Such investigations will be crucial to better understand and predict consequences of climate change. Yet, proper observations of environmental factors and biological systems will also be essential for the future, as particularly exemplified by the recent discovery of rhythms in the deep sea.

After all, solid observations and descriptions are the basis from which discoveries arise-

from the bottom of the deep sea to the surface of the shores.

# Glossary: Rhythms and clocks in marine organisms

aphotic zone:

below ~1000 m. Light from sun or moon is completely absent.

benthic:

associated with the sea floor

biological rhythm:

cyclic change in an organism's biology ranging from behavior to rhythms in physiology and gene expression. The term does not specify whether a rhythm is evoked by external cues or controlled by an endogenous oscillator.

central versus peripheral circadian clocks:

Animals possess circadian oscillators in (almost) all tissues. Evidence from terrestrial (mouse, *Drosophila*) and marine (*Platynereis*) models shows that these peripheral clocks are coordinated by a central brain oscillator.

conventional circadian clock:

The molecular oscillator based on a TTFL and well-defined sets of functionally tested components is the main, but not only, endogenous driving force of diel rhythms. The involved molecules are typically conserved within a given eukaryote phylum, but rarely beyond.

core (circadian) clock genes:

genes who have functionally been shown to be part of a central (circadian) oscillatory network  
As so far only the molecular mechanisms for the circadian clock are known, the term "clock genes" is often synonymously used for "circadian clock genes".

dysphotic zone:

~200-1000 m depth. Light (from sun/moon) is detectable, but insufficient for photosynthesis.

endogenous oscillator:

internal timing mechanism that is self-sustained, but can be entrained by environmental cues.

entrainment:

phase-adjustment ('synchronization') of an endogenous oscillator through environmental cues.

environmental cycle:

cyclic and predictable change of the environmental conditions affecting an organism. Cycles can be abiotic (e.g. light, temperature), but also related to biological rhythms (predation risk, food availability).

(eu)photic zone:

~0-200 m depth. There is enough light for sustained photosynthetic production.

inputs:

cues involved in the entrainment process

mismatch:

dissimilarity in the distribution, timing, abundance, etc. of two or more currently interacting species that often results in fitness reduction.

neritic:

associated with coastal shelf areas

oceanic:

shelf water or the open ocean

outputs:

biological processes whose rhythmicity is regulated by an endogenous oscillator

pelagic:

associated with the water column

persistence/free-run:

maintenance of rhythmicity in environments without time cues relevant to the tested oscillator

phytoplankton: large and highly diverse group of photosynthetic microorganisms found predominantly in aquatic environments

plasticity of oscillator:

variability in the period length of an endogenous oscillator. It can be read out on any output level (molecular, physiological or behavioral)

temperature compensation:

endogenous oscillators do not follow the Le Bel-Van 't Hoff rule, but are buffered against temperature changes.

transcriptional/translational feedback loop (TTFL):

autoregulation of genes via interactions of the translated proteins with other genes/proteins.

# Acknowledgements

We apologize to colleagues whose work could not be cited due to limitations of space. Our research is supported by the following funding sources: Falciatore lab: the Fondation Bettencourt-Schueller (Coups d'élan pour la recherche française-2018), the "Initiative d'Excellence" program (Grant "DYNAMO," ANR-11-LABX-0011-01), the ANR-DFG Grant "DiaRhythm (KR1661/20-1) and ANR Grant ClimaClock (ANR-20-CE20-0024), Raible and Tessmar-Raible labs: The research leading to these results has received funding from the European Research Council under the European Community's Seventh Framework Programme (FP7/2007-2013)/ERC Grant Agreement 260304 (F.R.) and ERC Grant Agreement 337011 (K.T.-R.); the Horizon 2020 Programme ERC Grant Agreement 81995 (K.T.-R.); the research platforms 'Rhythms of Life' (K.T.-R., F.R.) and "Single-cell genomics of stem cells" (F.R.) of the University of Vienna; the Austrian Science Fund (FWF) START award, project Y413 (K.T.-R.); the Austrian Science Fund (FWF) projects P28970 (K.T.-R.) and I2972 (F.R.); the Austrian Science Fund (FWF) grant F78 (K.T.-R., F.R.). N.S.H. was supported by a Lise-Meitner fellowship from the FWF (M2820).

# Bibliography

- Aguzzi J, Company JB, Costa C, Menesatti P, Garcia JA, et al. 2011. Activity rhythms in the deep-sea: a chronobiological approach. *Front Biosci (Landmark Ed)*. 16:131–50
- Andersson S, Kautsky L, Kalvas A. 1994. Circadian and lunar gamete release in *Fucus vesiculosus* in the atidal Baltic Sea. *Marine Ecology Progress Series*. 110:195–201
- Andreatta G, Broyart C, Borghgraef C, Vadiwala K, Kozin V, et al. 2020. Corazonin signaling integrates energy homeostasis and lunar phase to regulate aspects of growth and sexual maturation in *Platynereis*. *Proc Natl Acad Sci U S A*. 117(2):1097–1106
- Andreatta G, Tessmar-Raible K. 2020. The Still Dark Side of the Moon: Molecular Mechanisms of Lunar-Controlled Rhythms and Clocks. *J Mol Biol*. 432(12):3525–46
- Andrzejczek S, Vély M, Jouannet D, Rowat D, Fossette S. 2021. Regional movements of satellite-tagged whale sharks *Rhincodon typus* in the Gulf of Aden. *Ecol Evol*. 11(9):4920–34
- Annunziata R, Ritter A, Fortunato AE, Manzotti A, Cheminant-Navarro S, et al. 2019. bHLH-PAS protein RITMO1 regulates diel biological rhythms in the marine diatom *Phaeodactylum tricorutum*. *Proc Natl Acad Sci U S A*. 116(26):13137–42
- Aranda M, Li Y, Liew YJ, Baumgarten S, Simakov O, et al. 2016. Genomes of coral dinoflagellate symbionts highlight evolutionary adaptations conducive to a symbiotic lifestyle. *Scientific Reports*. 6(1):39734
- Arboleda E, Hartenstein V, Martinez P, Reichert H, Sen S, et al. 2018. An Emerging System to Study Photosymbiosis, Brain Regeneration, Chronobiology, and Behavior: The Marine Acoel *Symsagittifera roscoffensis*. *Bioessays*. 40(10):e1800107
- Arboleda E, Zurl M, Waldherr M, Tessmar-Raible K. 2019. Differential Impacts of the Head on *Platynereis dumerilii* Peripheral Circadian Rhythms. *Front Physiol*. 10:900
- Aruda AM, Baumgartner MF, Reitzel AM, Tarrant AM. 2011. Heat shock protein expression during stress and diapause in the marine copepod *Calanus finmarchicus*. *J Insect Physiol*. 57(5):665–75
- Aschoff J. 1960. Exogenous and Endogenous Components in Circadian Rhythms. *Cold Spring Harbor Symposia on Quantitative Biology*. 25:11–28
- Aschoff J. 1965. Circadian rhythms in man. *Science*. 148(3676):1427–32
- Asher G, Sassone-Corsi P. 2015. Time for Food: The Intimate Interplay between Nutrition, Metabolism, and the Circadian Clock. *Cell*. 161(1):84–92
- Atkinson A, Harmer RA, Widdicombe CE, McEvoy AJ, Smyth TJ, et al. 2015. Questioning the role of phenology shifts and trophic mismatching in a planktonic food web. *Progress in Oceanography*. 137:498–512
- Atkinson A, Hill SL, Pakhomov EA, Siegel V, Reiss CS, et al. 2019. Krill (*Euphausia superba*) distribution contracts southward during rapid regional warming. *Nature Clim Change*. 9(2):142–47
- Austin RW, Petzold TJ. 1986. Spectral Dependence Of The Diffuse Attenuation Coefficient Of Light In Ocean Waters. *OE*. 25(3):471–79
- Ayalon I, Rosenberg Y, Benichou JIC, Campos C  
LD, Sayco SLG, et al. 2020. Coral Gametogenesis Collapse under Artificial Light Pollution. *Current Biology*. 31(2):413–19
- Ayers T, Tsukamoto H, Gühlmann M, Veedin Rajan VB, Tessmar-Raible K. 2018. A G<sub>o</sub>-type opsin mediates the shadow reflex in the annelid *Platynereis dumerilii*. *BMC Biol*. 16(1):41



- Babcock RC, Bull GD, Harrison PL, Heyward AJ, Oliver JK, et al. 1986. Synchronous spawnings of 105 scleractinian coral species on the Great Barrier Reef. *Marine Biology*. 90(3):379–94
- Baghel KK, Pati AK. 2015. Pheromones as time cues for circadian rhythms in fish. *Biological Rhythm Research*. 46(5):659–69
- Baillon S, Hamel J-F, Mercier A. 2014. Diversity, distribution and nature of faunal associations with deep-sea pennatulacean corals in the Northwest Atlantic. *PLoS One*. 9(11):e111519
- Baumgartner MF, Tarrant AM. 2017. The Physiology and Ecology of Diapause in Marine Copepods. *Annual Review of Marine Science*. 9(1):387–411
- Beauchemin M, Roy S, Daoust P, Dagenais-Bellefeuille S, Bertomeu T, et al. 2012. Dinoflagellate tandem array gene transcripts are highly conserved and not polycistronic. *Proc Natl Acad Sci U S A*. 109(39):15793–98
- Beaugrand G, Brander KM, Alistair Lindley J, Souissi S, Reid PC. 2003. Plankton effect on cod recruitment in the North Sea. *Nature*. 426(6967):661–64
- Berge J, Cottier F, Last KS, Varpe Ø, Leu E, et al. 2009. Diel vertical migration of Arctic zooplankton during the polar night. *Biology Letters*. 5(1):69–72
- Berge J, Geoffroy M, Daase M, Cottier F, Priou P, et al. 2020. Artificial light during the polar night disrupts Arctic fish and zooplankton behaviour down to 200 m depth. *Communications Biology*. 3(1):1–8
- Berge J, Renaud PE, Darnis G, Cottier F, Last K, et al. 2015. In the dark: A review of ecosystem processes during the Arctic polar night. *Progress in Oceanography*. 139:258–71
- Bernard I, Massabuau J-C, Ciret P, Sow M, Sottolichio A, et al. 2016. In situ spawning in a marine broadcast spawner, the Pacific oyster *Crassostrea gigas*: Timing and environmental triggers. *Limnology and Oceanography*. 61(2):635–47
- Bilcke G, Osuna-Cruz CM, Silva MS, Poulsen N, Bulankova P, et al. 2021. Diurnal transcript profiling of the diatom *Seminavis robusta* reveals adaptations to a benthic lifestyle. *The Plant Journal*. 107:
- Biscontin A, Frigato E, Sales G, Mazzotta GM, Teschke M, et al. 2016. The opsin repertoire of the Antarctic krill *Euphausia superba*. *Mar Genomics*. 29:61–68
- Biscontin A, Martini P, Costa R, Kramer A, Meyer B, et al. 2019. Analysis of the circadian transcriptome of the Antarctic krill *Euphausia superba*. *Sci Rep*. 9(1):13894
- Biscontin A, Wallach T, Sales G, Grudziecki A, Janke L, et al. 2017. Functional characterization of the circadian clock in the Antarctic krill, *Euphausia superba*. *Sci Rep*. 7(1):17742
- Blaby-Haas CE, Merchant SS. 2019. Comparative and Functional Algal Genomics. *Annual Review of Plant Biology*. 70(1):605–38
- Bouget F-Y, Lefranc M, Thommen Q, Pfeuty B, Lozano J-C, et al. 2014. Transcriptional versus non-transcriptional clocks: A case study in *Ostreococcus*. *Marine Genomics*. 14:17–22
- Bowler C, Allen AE, Badger JH, Grimwood J, Jabbari K, et al. 2008. The *Phaeodactylum* genome reveals the evolutionary history of diatom genomes. *Nature*. 456(7219):239–44
- Bradshaw WE, Holzapfel CM. 2001. Genetic shift in photoperiodic response correlated with global warming. *Proc Natl Acad Sci U S A*. 98(25):14509–11
- Brady AK, Snyder KA, Vize PD. 2011. Circadian cycles of gene expression in the coral, *Acropora millepora*. *PLoS One*. 6(9):e25072
- Brady AK, Willis BL, Harder LD, Vize PD. 2016. Lunar Phase Modulates Circadian Gene Expression Cycles in the Broadcast Spawning Coral *Acropora millepora*. *Biol Bull*. 230(2):130–42
- Brand LE. 1982. Persistent diel rhythms in the chlorophyll fluorescence of marine phytoplankton species. *Marine Biology*. 69(3):253–62

- Braun R, Farré EM, Schurr U, Matsubara S. 2014. Effects of light and circadian clock on growth and chlorophyll accumulation of *Nannochloropsis gaditana*. *Journal of Phycology*. 50(3):515–25
- Brawley SH, Johnson LE. 1992. Gametogenesis, gametes and zygotes: An ecological perspective on sexual reproduction in the algae. *British Phycological Journal*. 27(3):233–52
- Brenna A, Albrecht U. 2020. Phosphorylation and Circadian Molecular Timing. *Front Physiol*. 11:612510
- Brierley AS. 2014. Diel vertical migration. *Current Biology*. 24(22):R1074–76
- Brodie J, Chan CX, De Clerck O, Cock JM, Coelho SM, et al. 2017. The Algal Revolution. *Trends in Plant Science*. 22(8):726–38
- Brun P, Stamieszkin K, Visser AW, Licandro P, Payne MR, Kiørboe T. 2019. Climate change has altered zooplankton-fuelled carbon export in the North Atlantic. *Nat Ecol Evol*. 3(3):416–23
- Buhr ED, Yoo S-H, Takahashi JS. 2010. Temperature as a Universal Resetting Cue for Mammalian Circadian Oscillators. *Science*. 330(6002):379–85
- Caballes CF, Pratchett MS. 2017. Environmental and biological cues for spawning in the crown-of-thorns starfish. *PLoS One*. 12(3):
- Chabot CC, Ramberg-Pihl NC, Watson WH. 2016. Circalunidian clocks control tidal rhythms of locomotion in the American horseshoe crab, *Limulus polyphemus*. *Mar Freshw Behav Physiol*. 49(2):75–91
- Chabot CC, Watson WH III. 2010. Circatidal rhythms of locomotion in the American horseshoe crab *Limulus polyphemus*: Underlying mechanisms and cues that influence them. *Current Zoology*. 56(5):499–517
- Chambault P, Fossette S, Heide-Jørgensen MP, Jouannet D, Vély M. 2021. Predicting seasonal movements and distribution of the sperm whale using machine learning algorithms. *Ecol Evol*. 11(3):1432–45
- Chang Y, Dall’Olmo G, Schabetsberger R. 2020. Tracking the marine migration routes of South Pacific silver eels. *Mar. Ecol. Prog. Ser.* 646:1–12
- Chen C, Buhl E, Xu M, Croset V, Rees JS, et al. 2015. *Drosophila* Ionotropic Receptor 25a mediates circadian clock resetting by temperature. *Nature*. 527(7579):516–20
- Chisholm SW, Brand LE. 1981. Persistence of cell division phasing in marine phytoplankton in continuous light after entrainment to light: Dark cycles. *Journal of Experimental Marine Biology and Ecology*. 51(2–3):107–18
- Chivers WJ, Walne AW, Hays GC. 2017. Mismatch between marine plankton range movements and the velocity of climate change. *Nature Communications*. 8:14434
- Choquet M, Hatlebakk M, Dhanasiri AKS, Kosobokova K, Smolina I, et al. 2017. Genetics redraws pelagic biogeography of *Calanus*. *Biology Letters*. 13(12):
- Choquet M, Smolina I, Hoarau G. 2021. No evidence for hybridization in *Calanus*: Reply to the comment by Parent et al. *Limnology and Oceanography*. 66(10):3603–6
- Chow S, Okazaki M, Watanabe T, Segawa K, Yamamoto T, et al. 2015. Light-Sensitive Vertical Migration of the Japanese Eel *Anguilla japonica* Revealed by Real-Time Tracking and Its Utilization for Geolocation. *PLoS One*. 10(4):e0121801
- Christiansen S, Titelman J, Kaartvedt S. 2019. Nighttime Swimming Behavior of a Mesopelagic Fish. *Frontiers in Marine Science*. 6:
- Christie AE, Fontanilla TM, Nesbit KT, Lenz PH. 2013. Prediction of the protein components of a putative *Calanus finmarchicus* (Crustacea, Copepoda) circadian signaling system using a *de novo* assembled transcriptome. *Comparative Biochemistry and Physiology Part D: Genomics and Proteomics*. 8(3):165–93

- Christie AE, Roncalli V, Lenz PH. 2016. Diversity of insulin-like peptide signaling system proteins in *Calanus finmarchicus* (Crustacea; Copepoda) - Possible contributors to seasonal pre-adult diapause. *Gen Comp Endocrinol.* 236:157-73
- Clark KAJ, Brierley AS, Pond DW, Smith VJ. 2013. Changes in seasonal expression patterns of ecdysone receptor, retinoid X receptor and an A-type allatostatin in the copepod, *Calanus finmarchicus*, in a sea loch environment: an investigation of possible mediators of diapause. *Gen Comp Endocrinol.* 189:66-73
- Coelho R, Fernandez-Carvalho J, Santos M. 2015. Habitat use and diel vertical migration of bigeye thresher shark: Overlap with pelagic longline fishing gear. *Marine Environmental Research.* 112:
- Coesel S, Mangogna M, Ishikawa T, Heijde M, Rogato A, et al. 2009. Diatom PtCPF1 is a new cryptochrome/photolyase family member with DNA repair and transcription regulation activity. *EMBO reports.* 10(6):655-61
- Coesel SN, Durham BP, Groussman RD, Hu SK, Caron DA, et al. 2021. Diel transcriptional oscillations of light-sensitive regulatory elements in open-ocean eukaryotic plankton communities. *Proc Natl Acad Sci U S A.* 118(6):e2011038118
- Coffey DM, Royer MA, Meyer CG, Holland KN. 2020. Diel patterns in swimming behavior of a vertically migrating deepwater shark, the bluntnose sixgill (*Hexanchus griseus*). *PLoS One.* 15(1):e0228253
- Cohen J, Screen JA, Furtado JC, Barlow M, Whittleston D, et al. 2014. Recent Arctic amplification and extreme mid-latitude weather. *Nature Geosci.* 7(9):627-37
- Cohen JH, Last KS, Charpentier CL, Cottier F, Daase M, et al. 2021. Photophysiological cycles in Arctic krill are entrained by weak midday twilight during the Polar Night. *PLOS Biology.* 19(10):e3001413
- Comolli JC, Fagan T, Hastings JW. 2003. A Type-1 Phosphoprotein Phosphatase from a Dinoflagellate as a Possible Component of the Circadian Mechanism. *Journal of Biological Rhythms.* 18(5):367-76
- Connor KM, Gracey AY. 2011. Circadian cycles are the dominant transcriptional rhythm in the intertidal mussel *Mytilus californianus*. *Proc Natl Acad Sci U S A.* 108(38):16110-15
- Conover RJ. 1965. Notes on the Molting Cycle, Development of Sexual Characters and Sex Ratio in *Calanus hyperboreus*. *Crustaceana.* 8(3):308-20
- Corellou F, Schwartz C, Motta J-P, Djouani-Tahri EB, Sanchez F, Bouget F-Y. 2009. Clocks in the Green Lineage: Comparative Functional Analysis of the Circadian Architecture of the Picoeukaryote *Ostreococcus*. *The Plant Cell.* 21(11):3436-49
- Courties C, Vaquer A, Troussellier M, Lautier J. 1994. Smallest eukaryotic organism. *Nature.* 370:255
- Creux N, Harmer S. 2019. Circadian Rhythms in Plants. *Cold Spring Harbor Perspectives in Biology.* 11(9):a034611
- Cuvelier D, Legendre P, Laës-Huon A, Sarradin P-M, Sarrazin J. 2017. Biological and environmental rhythms in (dark) deep-sea hydrothermal ecosystems. *Biogeosciences.* 14(12):2955-77
- d'Alcalà MR, Conversano F, Corato F, Licandro P, Mangoni O, et al. 2004. Seasonal patterns in plankton communities in a pluriannual time series at a coastal Mediterranean site (Gulf of Naples): an attempt to discern recurrences and trends. *Scientia marina.* 68(S1):65-83
- D'Alelio D, d'Alcalà MR, Dubroca L, Sarn D, Zingone A, Montresor M. 2010. The time for sex: A biennial life cycle in a marine planktonic diatom. *Limnology and Oceanography.* 55(1):106-14
- Davies TW, Duffy JP, Bennie J, Gaston KJ. 2014. The nature, extent, and ecological implications of marine light pollution. *Frontiers in Ecology and the Environment.* 12(6):347-55

- de Lima CDM, Göndör A. 2018. Circadian organization of the genome. *Science*. 359(6381):1212-13
- De Pittà C, Biscontin A, Albiero A, Sales G, Millino C, et al. 2013. The Antarctic krill *Euphausia superba* shows diurnal cycles of transcription under natural conditions. *PLoS One*. 8(7):e68652
- De Pontual H, Jolivet A, Bertignac M, Fablet R. 2012. Diel vertical migration of European hake *Merluccius merluccius* and associated temperature histories: insights from a pilot data-storage tagging (DST) experiment. *J Fish Biol*. 81(2):728-34
- Deagle BE, Faux C, Kawaguchi S, Meyer B, Jarman SN. 2015. Antarctic krill population genomics: apparent panmixia, but genome complexity and large population size muddy the water. *Molecular Ecology*. 24(19):4943-59
- Derelle E, Ferraz C, Rombauts S, Rouze P, Worden AZ, et al. 2006. Genome analysis of the smallest free-living eukaryote *Ostreococcus tauri* unveils many unique features. *Proc Natl Acad Sci U S A*. 103(31):11647-52
- Deutsch C, Ferrel A, Seibel B, Pörtner H-O, Huey RB. 2015. Climate change tightens a metabolic constraint on marine habitats. *Science*. 348(6239):1132-35
- Dixson DL, Munday PL, Jones GP. 2010. Ocean acidification disrupts the innate ability of fish to detect predator olfactory cues. *Ecology Letters*. 13(1):68-75
- Djouani-Tahri EB, Christie JM, Sanchez-Fernandin S, Sanchez F, Bouget F-Y, Corellou F. 2011. A eukaryotic LOV-histidine kinase with circadian clock function in the picoalga *Ostreococcus*. *The Plant Journal*. 65:578-88
- Dodd AN, Dalchau N, Gardner MJ, Baek S-J, Webb AAR. 2014. The circadian clock has transient plasticity of period and is required for timing of nocturnal processes in *Arabidopsis*. *New Phytologist*. 201(1):168-79
- Dodd AN, Salathia N, Hall A, Kévei E, Tóth R, et al. 2005. Plant Circadian Clocks Increase Photosynthesis, Growth, Survival, and Competitive Advantage. *Science*. 309(5734):630-33
- Duarte C, Quintanilla-Ahumada D, Anguita C, Manríquez PH, Widdicombe S, et al. 2019. Artificial light pollution at night (ALAN) disrupts the distribution and circadian rhythm of a sandy beach isopod. *Environmental Pollution*. 248:565-73
- Ducklow HW, Baker K, Martinson DG, Quetin LB, Ross RM, et al. 2007. Marine pelagic ecosystems: the West Antarctic Peninsula. *Philosophical Transactions of the Royal Society B: Biological Sciences*. 362(1477):67-94
- Durant JM, Molinero J-C, Ottersen G, Reygondeau G, Stige LC, Langangen Ø. 2019. Contrasting effects of rising temperatures on trophic interactions in marine ecosystems. *Sci Rep*. 9(1):1-9
- Dypvik E, Klevjer TA, Kaartvedt S. 2012a. Inverse vertical migration and feeding in glacier lanternfish (*Benthosema glaciale*). *Mar Biol*. 159(2):443-53
- Dypvik E, Røstad A, Kaartvedt S. 2012b. Seasonal variations in vertical migration of glacier lanternfish, *Benthosema glaciale*. *Mar Biol*. 159(8):1673-83
- Edgar RS, Green EW, Zhao Y, van Ooijen G, Olmedo M, et al. 2012. Peroxiredoxins are conserved markers of circadian rhythms. *Nature*. 485(7399):459-64
- Edwards M, Richardson AJ. 2004. Impact of climate change on marine pelagic phenology and trophic mismatch. *Nature*. 430(7002):881-84
- Elowe C, Tomanek L. 2021. Circadian and circatidal rhythms of protein abundance in the California mussel (*Mytilus californianus*). *Mol Ecol*. 30(20):5151-63
- Enright JT. 1976. Plasticity in an isopod's clockworks: Shaking shapes form and affects phase and frequency. *J. Comp. Physiol*. 107(1):13-37

- Evans WG. 1976. Circadian and circatidal locomotory rhythms in the intertidal beetle *Thalassotrechus barbarae* (Horn): Carabidae. *Journal of Experimental Marine Biology and Ecology*. 22(1):79-90
- Fabry VJ, McClintock JB, Mathis JT, Grebmeier J. 2009. Ocean Acidification at High Latitudes:: The Bellwether. *Oceanography*. 22(4):160-71
- Falciatore A, Jaubert M, Bouly J-P, Bailleul B, Mock T. 2020. Diatom Molecular Research Comes of Age: Model Species for Studying Phytoplankton Biology and Diversity. *The Plant Cell*. 32(3):547-72
- Falk-Petersen S, Mayzaud P, Kattner G, Sargent JR. 2009. Lipids and life strategy of Arctic *Calanus*. *Marine Biology Research*. 5(1):18-39
- Farré EM. 2020. The brown clock: circadian rhythms in stramenopiles. *Physiologia Plantarum*. 169(3):430-41
- Feeney KA, Hansen LL, Putker M, Olivares-Yañez C, Day J, et al. 2016. Daily magnesium fluxes regulate cellular timekeeping and energy balance. *Nature*. 532(7599):375-79
- Feng D, Li Q, Yu H. 2019. RNA Interference by Ingested dsRNA-Expressing Bacteria to Study Shell Biosynthesis and Pigmentation in *Crassostrea gigas*. *Mar Biotechnol (NY)*. 21(4):526-36
- Feng Z, Ji R, Ashjian C, Campbell R, Zhang J. 2017. Biogeographic responses of the copepod *Calanus glacialis* to a changing Arctic marine environment. *Glob Change Biol*. e159-70
- Fitt WK, Trench RK. 1983. The relation of diel patterns of cell division to diel patterns of motility in the symbiotic dinoflagellate *Symbiodinium microadriaticum* Freudenthal in culture. *New Phytologist*. 94(3):421-32
- Fleissner G, Schuchardt K, Neumann D, Bali G, Falkenberg G, Fleissner G. 2008. A lunar clock changes shielding pigment transparency in larval ocelli of *Clunio marinus*. *Chronobiol Int*. 25(1):17-30
- Fogarty ND, Marhaver KL. 2019. Coral spawning, unsynchronized. *Science (New York, N.Y.)*. 365(6457):987-88
- Fortier M, Fortier L, Hattori H, Saito H, Legendre L. 2001. Visual predators and the diel vertical migration of copepods under Arctic sea ice during the midnight sun. *Journal of Plankton Research*. 23(11):1263-78
- Fortunato AE, Jaubert M, Enomoto G, Bouly J-P, Raniello R, et al. 2016. Diatom Phytochromes Reveal the Existence of Far-Red-Light-Based Sensing in the Ocean. *The Plant Cell*. 28(3):616-28
- Foster WA, Moreton RB. 1981. Synchronization of activity rhythms with the tide in a saltmarsh collembolan *Anurida maritima*. *Oecologia*. 50(2):265-70
- Fukushiro M, Takeuchi T, Takeuchi Y, Hur S-P, Sugama N, et al. 2011. Lunar phase-dependent expression of cryptochrome and a photoperiodic mechanism for lunar phase-recognition in a reef fish, goldlined spinefoot. *PLoS One*. 6(12):e28643
- Fulton J. 1973. Some Aspects of the Life History of *Calanus plumchrus* in the Strait of Georgia. *J. Fish. Res. Bd. Can*. 30(6):811-15
- Fung-Uceda J, Lee K, Seo PJ, Polyn S, De Veylder L, Mas P. 2018. The Circadian Clock Sets the Time of DNA Replication Licensing to Regulate Growth in *Arabidopsis*. *Developmental Cell*. 45(1):101-113.e4
- Gardner JPA. 1997. Hybridization in the Sea. In *Advances in Marine Biology*, Vol. 31, eds. JHS Blaxter, AJ Southward, pp. 1-78. Academic Press
- Garrett C. 2003. Ocean science. Enhanced: internal tides and ocean mixing. *Science*. 301(5641):1858-59
- Gekakis N. 1998. Role of the CLOCK Protein in the Mammalian Circadian Mechanism. *Science*. 280(5369):1564-69

- Gerkema MP, Davies WIL, Foster RG, Menaker M, Hut RA. 2013. The nocturnal bottleneck and the evolution of activity patterns in mammals. *Proceedings of the Royal Society B: Biological Sciences*. 280(1765):20130508–20130508
- Gilly WF, Markaida U, Baxter CH, Block BA, Boustany A, et al. 2006. Vertical and horizontal migrations by the jumbo squid *Dosidicus gigas* revealed by electronic tagging. *Marine Ecology Progress Series*. 324:1–17
- Goldman B, Gwinner E, Karsch FJ, Saunders D, Zucker I, Gall GF. 2004. Circannual Rhythms and Photoperiodism. In *Chronobiology: Biological Timekeeping*, eds. JC Dunlap, JJ Loros, PJ DeCoursey, pp. 107–42. Sunderland, MA: Sinauer
- Häfker NS, Meyer B, Last KS, Pond DW, Hüppe L, Teschke M. 2017. Circadian Clock Involvement in Zooplankton Diel Vertical Migration. *Current Biology*. 27(14):2194–2201.e3
- Häfker NS, Teschke M, Hüppe L, Meyer B. 2018a. *Calanus finmarchicus* diel and seasonal rhythmicity in relation to endogenous timing under extreme polar photoperiods. *Marine Ecology Progress Series*. 603:79–92
- Häfker NS, Teschke M, Last KS, Pond DW, Hüppe L, Meyer B. 2018b. *Calanus finmarchicus* seasonal cycle and diapause in relation to gene expression, physiology, and endogenous clocks. *Limnology and Oceanography*. 63(6):2815–38
- Häfker NS, Tessmar-Raible K. 2020. Rhythms of behavior: are the times changin'?. *Curr Opin Neurobiol*. 60:55–66
- Hairston NG, Kearns CM. 1995. The interaction of photoperiod and temperature in diapause timing: a copepod example. *The Biological Bulletin*. 189:42–48
- Hastings JW. 2007. The *Gonyaulax* Clock at 50: Translational Control of Circadian Expression. *Cold Spring Harbor Symposia on Quantitative Biology*. 72(1):141–44
- Hastings JW, Astrachan L, Sweeney BM. 1961. A Persistent Daily Rhythm in Photosynthesis. *The Journal of General Physiology*. 45(1):69–76
- Hastings JW, Sweeney BM. 1957. On the mechanism of temperature independence in a biological clock. *Proc Natl Acad Sci U S A*. 43:804–11
- Hastings M. 1981. Semi-Lunar Variations of Endogenous Circa-Tidal Rhythms of Activity and Respiration In the Isopod *Eurydice pulchra*
- Hauenschild C. 1960. Lunar periodicity. *Cold Spring Harb Symp Quant Biol*. 25:491–97
- Haydon MJ, Mielczarek O, Frank A, Román Á, Webb AAR. 2017. Sucrose and Ethylene Signaling Interact to Modulate the Circadian Clock. *Plant Physiology*. 175(2):947–58
- Heijde M, Zabulon G, Corellou F, Ishikawa T, Brazard J, et al. 2010. Characterization of two members of the cryptochrome/photolyase family from *Ostreococcus tauri* provides insights into the origin and evolution of cryptochromes. *Plant, Cell & Environment*. 33(10):1614–26
- Hendricks WD, Byrum CA, Meyer-Bernstein EL. 2012. Characterization of circadian behavior in the starlet sea anemone, *Nematostella vectensis*. *PLoS One*. 7(10):e46843
- Hewson-Browne RC. 1973. Magnetic effects of sea tides. *Physics of the Earth and Planetary Interiors*. 7(2):167–86
- Hoadley KD, Szmant AM, Pyott SJ. 2011. Circadian Clock Gene Expression in the Coral *Favia fragum* over Diel and Lunar Reproductive Cycles. *PLoS One*. 6(5):e19755
- Hölker F, Bolliger J, Davies TW, Giavi S, Jechow A, et al. 2021. 11 Pressing Research Questions on How Light Pollution Affects Biodiversity. *Frontiers in Ecology and Evolution*. 9:896
- Höring F, Biscontin A, Harms L, Sales G, Reiss CS, et al. 2021. Seasonal gene expression profiling of Antarctic krill in three different latitudinal regions. *Mar Genomics*. 56:100806
- Höring F, Teschke M, Suberg L, Kawaguchi S, Meyer B. 2018. Light regime affects the seasonal cycle of Antarctic krill (*Euphausia superba*): impacts on growth, feeding, lipid metabolism, and maturity. *Can. J. Zool*. 96(11):1203–13

- Horn M, Mitesser O, Hovestadt T, Yoshii T, Rieger D, Helfrich-Förster C. 2019. The Circadian Clock Improves Fitness in the Fruit Fly, *Drosophila melanogaster*. *Front. Physiol.* 10:1374
- Howard EM, Penn JL, Frenzel H, Seibel BA, Bianchi D, et al. 2020. Climate-driven aerobic habitat loss in the California Current System. *Science Advances.* 6(20):eaay3188
- Huang Y, Bian C, Liu Z, Wang L, Xue C, et al. 2020. The First Genome Survey of the Antarctic Krill (*Euphausia superba*) Provides a Valuable Genetic Resource for Polar Biomedical Research. *Mar Drugs.* 18(4):E185
- Huffeldt NP. 2020. Photic Barriers to Poleward Range-shifts. *Trends in Ecology & Evolution*
- Hughes AR, Hanley TC, Moore AF, Ramsay-Newton C, Zerebecki RA, Sotka EE. 2019. Predicting the sensitivity of marine populations to rising temperatures. *Frontiers in Ecology and the Environment.* 17(1):17–24
- Hui M, Song C, Liu Y, Li C, Cui Z. 2017. Exploring the molecular basis of adaptive evolution in hydrothermal vent crab *Austinograea alayseae* by transcriptome analysis. *PLoS One.* 12(5):e0178417
- Hunt BJ. 2016. Advancing molecular crustacean chronobiology through the characterisation of the circadian clock in two malacostracan species, *Euphausia superba* and *Parhyale hawaiiensis*. PhD thesis. University of Leicester
- Hüppe L, Payton L, Last K, Wilcockson D, Ershova E, Meyer B. 2020. Evidence for oscillating circadian clock genes in the copepod *Calanus finmarchicus* during the summer solstice in the high Arctic. *Biology Letters.* 16(7):20200257
- Ikmi A, McKinney SA, Delventhal KM, Gibson MC. 2014. TALEN and CRISPR/Cas9-mediated genome editing in the early-branching metazoan *Nematostella vectensis*. *Nat Commun.* 5:5486
- IPCC. 2014. Climate Change 2014: Synthesis Report. Contribution of Working Groups I, II and III to the Fifth Assessment Report of the Intergovernmental Panel on Climate Change. Geneva, Switzerland: IPCC
- Jenouvrier S, Caswell H, Barbraud C, Holland M, Strøeve J, Weimerskirch H. 2009. Demographic models and IPCC climate projections predict the decline of an emperor penguin population. *Proc Natl Acad Sci U S A.* 106(6):1844–47
- Jesus TF, Moreno JM, Repolho T, Athanasiadis A, Rosa R, et al. 2017. Protein analysis and gene expression indicate differential vulnerability of Iberian fish species under a climate change scenario. *PLoS One.* 12(7):e0181325
- Jiang B, Du JJ, Li Y-W, Ma P, Hu Y-Z, Li A-X. 2019. Transcriptome analysis provides insights into molecular immune mechanisms of rabbitfish, *Siganus oramin* against *Cryptocaryon irritans* infection. *Fish Shellfish Immunol.* 88:111–16
- Johnson CH, Golden SS. 1999. Circadian programs in cyanobacteria: adaptiveness and mechanism. *Annu Rev Microbiol.* 53:389–409
- Johnson CH, Roeber JF, Hastings JW. 1984. Circadian Changes in Enzyme Concentration Account for Rhythm of Enzyme Activity in *Gonyaulax*. *Science.* 223(4643):1428–30
- Jónasdóttir SH, Visser AW, Richardson K, Heath MR. 2015. Seasonal copepod lipid pump promotes carbon sequestration in the deep North Atlantic. *Proc Natl Acad Sci U S A.* 112(39):12122–26
- Jorda G, Marbà N, Bennett S, Santana-Garcon J, Agusti S, Duarte CM. 2020. Ocean warming compresses the three-dimensional habitat of marine life. *Nat Ecol Evol.* 4(1):109–14
- Kaartvedt S. 2010. Chapter Nine - Diel Vertical Migration Behaviour of the Northern Krill (*Meganctiphanes norvegica* Sars). In *Advances in Marine Biology*, Vol. 57, ed. GA Tarling, pp. 255–75. Academic Press

- Kaartvedt S, Titelman J. 2018. Planktivorous fish in a future Arctic Ocean of changing ice and unchanged photoperiod. *ICES Journal of Marine Science*. 75(7):2312–18
- Kahru M, Brotas V, Manzano-Sarabia M, Mitchell BG. 2010. Are phytoplankton blooms occurring earlier in the Arctic? *Global Change Biology*. 17(4):1733–39
- Kaiser TS, Haeseler A von, Tessmar-Raible K, Heckel DG. 2021. Timing strains of the marine insect *Clunio marinus* diverged and persist with gene flow. *Molecular Ecology*. 30:11264–80
- Kaiser TS, Heckel DG. 2012. Genetic architecture of local adaptation in lunar and diurnal emergence times of the marine midge *Clunio marinus* (Chironomidae, Diptera). *PLoS One*. 7(2):e32092
- Kaiser TS, Neumann J. 2021. Circalunar clocks—Old experiments for a new era. *BioEssays*. 43(8):2100074
- Kaiser TS, Neumann D, Heckel DG. 2011. Timing the tides: genetic control of diurnal and lunar emergence times is correlated in the marine midge *Clunio marinus*. *BMC Genet*. 12:49
- Kaiser TS, Neumann D, Heckel DG, Berendonk TU. 2010. Strong genetic differentiation and postglacial origin of populations in the marine midge *Clunio marinus* (Chironomidae, Diptera). *Molecular Ecology*. 19(14):2845–57
- Kaiser TS, Poehn B, Szkiba D, Preussner M, Sedlazeck FJ, et al. 2016. The genomic basis of circadian and circalunar timing adaptations in a midge. *Nature*. 540(7631):69–73
- Kashiwagi T, Park Y-J, Park J-G, Imamura S, Takeuchi Y, et al. 2013. Moonlight affects mRNA abundance of arylalkylamine N-acetyltransferase in the retina of a lunar-synchronized spawner, the goldlined spinefoot. *J Exp Zool A Ecol Genet Physiol*. 319(9):505–16
- Keeling PJ. 2013. The Number, Speed, and Impact of Plastid Endosymbioses in Eukaryotic Evolution. *Annual Review of Plant Biology*. 64(1):583–607
- Keith SA, Maynard JA, Edwards AJ, Guest JR, Bauman AG, et al. 2016. Coral mass spawning predicted by rapid seasonal rise in ocean temperature. *Proceedings of the Royal Society B: Biological Sciences*. 283(1830):20160011
- Kolody BC, McCrow JP, Allen LZ, Aylward FO, Fontanez KM, et al. 2019. Diel transcriptional response of a California Current plankton microbiome to light, low iron, and enduring viral infection. *The ISME Journal*. 13(11):2817–33
- Konig S, Eisenhut M, Brüggen A, Kurz S, Weber APM, Bichel C. 2017. The Influence of a Cryptochrome on the Gene Expression Profile in the Diatom *Phaeodactylum tricorutum* under Blue Light and in Darkness. *Plant and Cell Physiology*. 58(11):1914–23
- Koop H-U, Schmid R, Heunert H-H, Milthaler B. 1978. Chloroplast migration: A new circadian rhythm in *Acetabularia*. *Protoplasma*. 97(2–3):301–10
- Krittika S, Yadav P. 2020. Circadian clocks: an overview on its adaptive significance. *Biological Rhythm Research*. 51(7):1109–32
- Lambert S, Tragin M, Lozano J-C, Ghiglione J-F, Vaultot D, et al. 2019. Rhythmicity of coastal marine picoeukaryotes, bacteria and archaea despite irregular environmental perturbations. *The ISME Journal*. 13(2):388–401
- Last KS, Bailhache T, Kramer C, Kyriacou CP, Rosato E, Olive PJW. 2009. Tidal, daily, and lunar-day activity cycles in the marine polychaete *Nereis virens*. *Chronobiol Int*. 26(2):167–83
- Last KS, Häfker NS, Hendrick VJ, Meyer B, Tran D, Piccolin F. 2020. Biological Clocks and Rhythms in Polar Organisms. In *POLAR NIGHT Marine Ecology: Life and Light in the Dead of Night*, eds. J Berge, G Johnsen, JH Cohen, pp. 217–40. Cham: Springer International Publishing
- Last KS, Hobbs L, Berge J, Brierley AS, Cottier F. 2016. Moonlight Drives Ocean-Scale Mass Vertical Migration of Zooplankton during the Arctic Winter. *Current Biology*. 26(2):244–51



- Le Bihan T, Hindle M, Martin SF, Barrios-Llerena ME, Krahmer J, et al. 2015. Label-free quantitative analysis of the casein kinase 2-responsive phosphoproteome of the marine minimal model species *Ostreococcus tauri*. *PROTEOMICS*. 15(23-24):4135-44
- Leach WB, Carrier TJ, Reitzel AM. 2019. Diel patterning in the bacterial community associated with the sea anemone *Nematostella vectensis*. *Ecol Evol*. 9(17):9935-47
- Leach WB, Macrander J, Peres R, Reitzel AM. 2018. Transcriptome-wide analysis of differential gene expression in response to light:dark cycles in a model cnidarian. *Comp Biochem Physiol Part D Genomics Proteomics*. 26:40-49
- Leach WB, Reitzel AM. 2019. Transcriptional remodelling upon light removal in a model cnidarian: losses and gains in gene expression. *Mol Ecol*. 28(14):3413-26
- Leach WB, Reitzel AM. 2020. Decoupling behavioral and transcriptional responses to color in an eyeless cnidarian. *BMC Genomics*. 21(1):361
- Leebens-Mack JH, Barker MS, Carpenter EJ, Deyholos MK, Gitzendanner MA, et al. 2019. One thousand plant transcriptomes and the phylogenomics of green plants. *Nature*. 574(7780):679-85
- Lenz PH, Roncalli V. 2019. Diapause within the context of life-history strategies in calanid copepods (Calanoida: Crustacea). *Biological Bulletin*. 237(2):170-79
- Lenz PH, Roncalli V, Hassett RP, Wu L-S, Cieslak MC, et al. 2014. *De novo* assembly of a transcriptome for *Calanus finmarchicus* (Crustacea, Copepoda)--the dominant zooplankter of the North Atlantic Ocean. *PLoS One*. 9(2):e88589
- Levy O, Appelbaum L, Leggat W, Gothlif Y, Hayward DC, et al. 2007. Light-responsive cryptochromes from a simple multicellular animal, the coral *Acropora millepora*. *Science*. 318(5849):467-70
- Liberman R, Fine M, Benayahu Y. 2021. Simulated climate change scenarios impact the reproduction and early life stages of a soft coral. *Marine Environmental Research*. 163:105215
- Lin S, Cheng S, Song B, Zhong X, Lin X, et al. 2015. The *Symbiodinium kawagutii* genome illuminates dinoflagellate gene expression and coral symbiosis. *Science*. 350(6261):691-94
- Liu H, Stephens TG, González-Pech RA, Beltran VH, Lapeyre B, et al. 2018. *Symbiodinium* genomes reveal adaptive evolution of functions related to coral-dinoflagellate symbiosis. *Communications Biology*. 1(1):95
- Lozano J-C, Schatt P, Botebol H, Vergé V, Lesuisse E, et al. 2014. Efficient gene targeting and removal of foreign DNA by homologous recombination in the picoeukaryote *Ostreococcus*. *The Plant Journal*. 78(6):1073-83
- Luck M, Velázquez Escobar F, Glass K, Sabotke M-I, Hagedorn R, et al. 2019. Photoreactions of the Histidine Kinase Rhodopsin Ot-HKR from the Marine Picoalga *Ostreococcus tauri*. *Biochemistry*. 58(14):1878-91
- Lüning K. 1991. Circannual Growth Rhythm in a Brown Alga, *Pterygophora californica*. *Botanica Acta*. 104(2):157-62
- Maas AE, Jones IT, Reitzel AM, Tarrant AM. 2016. Daily cycle in oxygen consumption by the sea anemone *Nematostella vectensis* Stephenson. *Biol Open*. 5(2):161-64
- Mackenzie TDB, Morse D. 2011. Circadian photosynthetic reductant flow in the dinoflagellate *Lingulodinium* is limited by carbon availability: Circadian O<sub>2</sub> production is sink-limited. *Plant, Cell & Environment*. 34(4):669-80
- Madhu K, Madhu R. 2007. Influence of lunar rhythm on spawning of clown anemonefish *Amphiprion percula* under captive condition in Andaman and Nicobar islands. *Journal of the Marine Biological Association of India*. 49(1):58-64

- Mann M, Serif M, Wrobel T, Eisenhut M, Madhuri S, et al. 2020. The Aureochrome Photoreceptor PtAUREO1a Is a Highly Effective Blue Light Switch in Diatoms. *iScience*. 23(11):101730
- Maor R, Dayan T, Ferguson-Gow H, Jones KE. 2017. Temporal niche expansion in mammals from a nocturnal ancestor after dinosaur extinction. *Nat Ecol Evol*. 1(12):1889-95
- Mat AM, Massabuau J-C, Ciret P, Tran D. 2012. Evidence for a plastic dual circadian rhythm in the oyster *Crassostrea gigas*. *Chronobiol Int*. 29(7):857-67
- Mat AM, Perrigault M, Massabuau J-C, Tran D. 2016. Role and expression of *cry1* in the adductor muscle of the oyster *Crassostrea gigas* during daily and tidal valve activity rhythms. *Chronobiol Int*. 33(8):949-63
- Mat AM, Sarrazin J, Markov GV, Apremont V, Dubreuil C, et al. 2020. Biological rhythms in the deep-sea hydrothermal mussel *Bathymodiolus azoricus*. *Nat Commun*. 11(1):3454
- Matrai P, Thompson B, Keller M. 2005. Circannual excystment of resting cysts of *Alexandrium spp.* from eastern Gulf of Maine populations. *Deep Sea Research Part II: Topical Studies in Oceanography*. 52(19-21):2560-68
- Matsuo T. 2003. Control Mechanism of the Circadian Clock for Timing of Cell Division *in Vivo*. *Science*. 302(5643):255-59
- Mehta TS, Lewis RD. 2000. Quantitative tests of a dual circalunidian clock model for tidal rhythmicity in the sand beach isopod *Cirolana cookii*. *Chronobiol Int*. 17(1):29-41
- Melle W, Runge J, Head E, Plourde S, Castellani C, et al. 2014. The North Atlantic Ocean as habitat for *Calanus finmarchicus*: Environmental factors and life history traits. *Progress in Oceanography*. 129(Part B):244-84
- Menegazzi P, Dalla Benetta E, Beauchamp M, Schlichting M, Steffan-Dewenter I, Helfrich-Förster C. 2017. Adaptation of Circadian Neuronal Network to Photoperiod in High-Latitude European Drosophilids. *Current Biology*. 27(6):833-39
- Mercier A, Sun Z, Baillon S, Hamel J-F. 2011. Lunar Rhythms in the Deep Sea: Evidence from the Reproductive Periodicity of Several Marine Invertebrates. *Journal of Biological Rhythms*. 26:82-86
- Mergenhausen D, Schweiger HG. 1975. Circadian rhythm of oxygen evolution in cell fragments of *Acetabularia mediterranea*. *Experimental Cell Research*. 92(1):127-30
- Meyer B, Freier U, Grimm V, Groeneveld J, Hunt BPV, et al. 2017. The winter pack-ice zone provides a sheltered but food-poor habitat for larval Antarctic krill. *Nature Ecology & Evolution*. 1(12):1853-61
- Mitbavkar S, Anil AC. 2004. Vertical migratory rhythms of benthic diatoms in a tropical intertidal sand flat: influence of irradiance and tides. *Marine Biology*. 145(1):
- Mitchell LJ, Cheney KL, Lührmann M, Marshall J, Michie K, Cortesi F. 2021a. Molecular Evolution of Ultraviolet Visual Opsins and Spectral Tuning of Photoreceptors in Anemonefishes (Amphiprioninae). *Genome Biol Evol*. 13(10):evab184
- Mitchell LJ, Tettamanti V, Rhodes JS, Marshall NJ, Cheney KL, Cortesi F. 2021b. CRISPR/Cas9-mediated generation of biallelic F0 anemonefish (*Amphiprion ocellaris*) mutants. *PLoS One*. 16(12):e0261331
- Mittag M, Lee DH, Hastings JW. 1994. Circadian expression of the luciferin-binding protein correlates with the binding of a protein to the 3' untranslated region of its mRNA. *Proc Natl Acad Sci U S A*. 91(12):5257-61
- Miyagishima S, Fujiwara T, Sumiya N, Hirooka S, Nakano A, et al. 2014. Translation-independent circadian control of the cell cycle in a unicellular photosynthetic eukaryote. *Nature Communications*. 5(1):3807

- Montanari SR, Hobbs J-PA, Pratchett MS, van Herwerden L. 2016. The importance of ecological and behavioural data in studies of hybridisation among marine fishes. *Rev Fish Biol Fisheries*. 26(2):181-98
- Morse D, Milos PM, Roux E, Hastings JW. 1989a. Circadian regulation of bioluminescence in *Gonyaulax* involves translational control. *Proc Natl Acad Sci U S A*. 86(1):172-76
- Morse D, Pappenheimer AM, Hastings JW. 1989b. Role of a luciferin-binding protein in the circadian bioluminescent reaction of *Gonyaulax polyedra*. *Journal of Biological Chemistry*. 264(20):11822-26
- Moullager M, Monnier A, Jesson B, Bouvet R, Mosser J, et al. 2007. Light-Dependent Regulation of Cell Division in *Ostreococcus*: Evidence for a Major Transcriptional Input. *Plant Physiology*. 144(3):1360-69
- Moum JN. 2021. Variations in Ocean Mixing from Seconds to Years. *Ann Rev Mar Sci*. 13:201-26
- Muller EB, Kooijman SALM, Edmunds PJ, Doyle FJ, Nisbet RM. 2009. Dynamic energy budgets in syntrophic symbiotic relationships between heterotrophic hosts and photoautotrophic symbionts. *Journal of Theoretical Biology*. 259(1):44-57
- Narasimamurthy R, Virshup DM. 2021. The phosphorylation switch that regulates ticking of the circadian clock. *Mol Cell*. 81(6):1133-46
- Naylor E. 1996. Crab Clockwork: The Case for Interactive Circatidal and Circadian Oscillators Controlling Rhythmic Locomotor Activity of *Carcinus Maenas*. *Chronobiology International*. 13(3):153-61
- Naylor E. 2010. *Chronobiology of Marine Organisms*. Cambridge: Cambridge University Press
- Neuhaus G, Neuhaus-Url G, de Groot EJ, Schweiger H-G. 1986. High yield and stable transformation of the unicellular green alga *Acetabularia* by microinjection of SV40 DNA and pSV2neo. *The EMBO Journal*. 5(7):1437-44
- Neumann D. 1966. Die lunare und tägliche Schlüpfperiodik der Mücke *Chunio* - Steuerung und Abstimmung auf die Gezeitenperiodik. *Zeitschrift für Vergleichende Physiologie*. 53(1):1-61
- Neumann D. 1967. Genetic adaptation in emergence time of *Chunio* populations to different tidal conditions. *Helgolander Wiss. Meeresunters*. 15(1):163-71
- Neumann D. 1968. Die Steuerung einer semilunaren Schlüpfperiodik mit Hilfe eines künstlichen Gezeitenzyklus. *Zeitschrift für Vergleichende Physiologie*. 60(1):63-78
- Neumann D. 1988. The Timing of Reproduction to Distinct Spring Tide Situations in the Intertidal Insect *Chunio*. In *Behavioral Adaptation to Intertidal Life*, eds. G Chelazzi, M Vannini, pp. 45-54. Boston, MA: Springer US
- Neumann D. 1995. Physiological clocks of insects-ecophysiology of reproductive activities controlled by lunar cycles. *Naturwissenschaften*. 82(7):310-20
- Neumann D, Spindler K. 1991. Circasemilunar control of imaginal disc development in *Chunio marinus*: Temporal switching point, temperature-compensated developmental time and ecdysteroid profile
- Nichol DG, Kotwicki S, Zimmermann M. 2013. Diel vertical migration of adult Pacific cod *Gadus macrocephalus* in Alaska. *J Fish Biol*. 83(1):170-89
- Niehoff B, Madsen S, Hansen B, Nielsen T. 2002. Reproductive cycles of three dominant *Calanus* species in Disko Bay, West Greenland. *Marine Biology*. 140(3):567-76
- Noordally ZB, Millar AJ. 2015. Clocks in Algae. *Biochemistry*. 54(2):171-83
- Oldach MJ, Workentine M, Matz MV, Fan T-Y, Vize PD. 2017. Transcriptome dynamics over a lunar month in a broadcast spawning acroporid coral. *Mol Ecol*. 26(9):2514-26
- Omand MM, Steinberg DK, Stamieszkin K. 2021. Cloud shadows drive vertical migrations of deep-dwelling marine life. *Proc Natl Acad Sci U S A*. 118(32):e2022977118

- O'Neill JS, Lee KD, Zhang L, Feeney K, Webster SG, et al. 2015. Metabolic molecular markers of the tidal clock in the marine crustacean *Eurydice pulchra*. *Current Biology*. 25(8):R326-27
- O'Neill JS, van Ooijen G, Dixon LE, Troein C, Corellou F, et al. 2011. Circadian rhythms persist without transcription in a eukaryote. *Nature*. 469(7331):554-58
- Oren M, Tarrant AM, Alon S, Simon-Blecher N, Elbaz I, et al. 2015. Profiling molecular and behavioral circadian rhythms in the non-symbiotic sea anemone *Nematostella vectensis*. *Scientific Reports*. 5:11418
- Ouyang Y, Andersson CR, Kondo T, Golden SS, Johnson CH. 1998. Resonating circadian clocks enhance fitness in cyanobacteria. *Proc Natl Acad Sci U S A*. 95(15):8660-64
- Palmer J. 1995. Review of the Dual-Clock Control of Tidal Rhythms and the Hypothesis that the Same Clock Governs Both Circatidal and Circadian Rhythms. *Chronobiol. Int*. 12(5):299-310
- Palmer JD. 1991. Contributions made to chronobiology by studies of fiddler crab rhythms. *Chronobiol Int*. 8(2):110-30
- Palmer JD. 2000. The clocks controlling the tide-associated rhythms of intertidal animals. *BioEssays*. 22(1):32-37
- Palmer JD, Livingston L, Zusy FrD. 1964. A Persistent Diurnal Rhythm in Photosynthetic Capacity. *Nature*. 203(4949):1087-88
- Park J-G, Park Y-J, Sugama N, Kim S-J, Takemura A. 2007a. Molecular cloning and daily variations of the Period gene in a reef fish *Siganus guttatus*. *J Comp Physiol A Neuroethol Sens Neural Behav Physiol*. 193(4):403-11
- Park Y-J, Park J-G, Hiyakawa N, Lee Y-D, Kim S-J, Takemura A. 2007b. Diurnal and circadian regulation of a melatonin receptor, MT1, in the golden rabbitfish, *Siganus guttatus*. *Gen Comp Endocrinol*. 150(2):253-62
- Payton L, Hüppe L, Noirot C, Hoede C, Last KS, et al. 2021. Widely rhythmic transcriptome in *Calanus finmarchicus* during the high Arctic summer solstice period. *iScience*. 24(1):
- Payton L, Noirot C, Hoede C, Hüppe L, Last K, et al. 2020. Daily transcriptomes of the copepod *Calanus finmarchicus* during the summer solstice at high Arctic latitudes. *Sci Data*. 7(1):415
- Payton L, Noirot C, Last KS, Grigor J, Hüppe L, et al. 2022. Annual transcriptome of a key zooplankton species, the copepod *Calanus finmarchicus*. *Ecology and Evolution*. 12(2):e8605
- Payton L, Perrigault M, Bourdineaud J-P, Marcel A, Massabuau J-C, Tran D. 2017a. Trojan Horse Strategy for Non-invasive Interference of Clock Gene in the Oyster *Crassostrea gigas*. *Mar Biotechnol (NY)*. 19(4):361-71
- Payton L, Sow M, Massabuau J-C, Ciret P, Tran D. 2017b. How annual course of photoperiod shapes seasonal behavior of diploid and triploid oysters, *Crassostrea gigas*. *PLoS One*. 12(10):e0185918
- Payton L, Tran D. 2019. Moonlight cycles synchronize oyster behaviour. *Biol Lett*. 15(1):20180299
- Pearre S. 2003. Eat and run? The hunger/satiation hypothesis in vertical migration: History, evidence and consequences
- Peijnenburg KTCA, Goetze E. 2013. High evolutionary potential of marine zooplankton. *Ecology and Evolution*. 3(8):2765-81
- Peñaloza C, Gutierrez AP, Eöry L, Wang S, Guo X, et al. 2021. A chromosome-level genome assembly for the Pacific oyster *Crassostrea gigas*. *Gigascience*. 10(3):giab020
- Peres R, Reitzel AM, Passamaneck Y, Afeche SC, Cipolla-Neto J, et al. 2014. Developmental and light-entrained expression of melatonin and its relationship to the circadian clock in the sea anemone *Nematostella vectensis*. *Evodevo*. 5:26

- Perrigault M, Andrade H, Bellec L, Ballantine C, Camus L, Tran D. 2020. Rhythms during the polar night: evidence of clock-gene oscillations in the Arctic scallop *Chlamys islandica*. *Proceedings of the Royal Society B: Biological Sciences*. 287(1933):20201001
- Perrigault M, Tran D. 2017. Identification of the Molecular Clockwork of the Oyster *Crassostrea gigas*. *PLoS One*. 12(1):e0169790
- Pfeuty B, Thommen Q, Corellou F, Djouani-Tahri EB, Bouget F-Y, Lefranc M. 2012. Circadian clocks in changing weather and seasons: Lessons from the picoalga *Ostreococcus tauri*. *BioEssays*. 34(9):781-90
- Piccolin F, Meyer B, Biscontin A, De Pittà C, Kawaguchi S, Teschke M. 2018. Photoperiodic modulation of circadian functions in Antarctic krill *Euphausia superba* Dana, 1850 (Euphausiacea). *Journal of Crustacean Biology*. 38(6):707-15
- Piccolin F, Pitzschler L, Biscontin A, Kawaguchi S, Meyer B. 2020. Circadian regulation of diel vertical migration (DVM) and metabolism in Antarctic krill *Euphausia superba*. *Scientific Reports*. 10(1):16796
- Pierella Karlusich JJ, Ibarbalz FM, Bowler C. 2020. Phytoplankton in the *Tara* Ocean. *Annual Review of Marine Science*. 12(1):233-65
- Poehn B, Krishnan S, Zurl M, Coric A, Rokvic D, et al. 2021. A Cryptochrome adopts distinct moon- and sunlight states and functions as moonlight interpreter in monthly oscillator entrainment. *bioRxiv*. 2021.04.16.439809
- Poliner E, Cummings C, Newton L, Farré EM. 2019. Identification of circadian rhythms in *Nannochloropsis* species using bioluminescence reporter lines. *The Plant Journal*. 99(1):112-27
- Poliner E, Farré EM, Benning C. 2018. Advanced genetic tools enable synthetic biology in the oleaginous microalgae *Nannochloropsis* sp. *Plant Cell Reports*. 37(10):1383-99
- Porter ML, Steck M, Roncalli V, Lenz PH. 2017. Molecular Characterization of Copepod Photoreception. *Biol Bull*. 233(1):96-110
- Provan J, Beatty GE, Keating SL, Maggs CA, Savidge G. 2009. High dispersal potential has maintained long-term population stability in the North Atlantic copepod *Calanus finmarchicus*. *Proceedings of the Royal Society B: Biological Sciences*. 276(1655):301-7
- Pülmanns N, Castellanos-Galindo GA, Krumme U. 2018. Tidal-diel patterns in feeding and abundance of armed snook *Centropomus armatus* from macrotidal mangrove creeks of the tropical eastern Pacific Ocean. *J Fish Biol*. 93(5):850-59
- Quiroga Artigas G, Lapébie P, Leclère L, Bauknecht P, Uveira J, et al. 2020. A G protein-coupled receptor mediates neuropeptide-induced oocyte maturation in the jellyfish *Clytia*. *PLoS Biol*. 18(3):e3000614
- Quiroga Artigas G, Lapébie P, Leclère L, Takeda N, Deguchi R, et al. 2018. A gonad-expressed opsin mediates light-induced spawning in the jellyfish *Clytia*. *Elife*. 7:e29555
- Ragni M, d'Alcalà MR. 2007. Circadian variability in the photobiology of *Phaeodactylum tricornutum*: pigment content. *Journal of Plankton Research*. 29(2):141-56
- Rahman MS, Kim B-H, Takemura A, Park C-B, Lee Y-D. 2004a. Effects of moonlight exposure on plasma melatonin rhythms in the seagrass rabbitfish, *Siganus canaliculatus*. *J Biol Rhythms*. 19(4):325-34
- Rahman MS, Kim B-H, Takemura A, Park C-B, Lee Y-D. 2004b. Influence of light-dark and lunar cycles on the ocular melatonin rhythms in the seagrass rabbitfish, a lunar-synchronized spawner. *J Pineal Res*. 37(2):122-28
- Rahman MS, Morita M, Takemura A, Takano K. 2003. Hormonal changes in relation to lunar periodicity in the testis of the forktail rabbitfish, *Siganus argenteus*. *Gen Comp Endocrinol*. 131(3):302-9

- Raible F, Takekata H, Tessmar-Raible K. 2017. An Overview of Monthly Rhythms and Clocks. *Front Neurol.* 8:189
- Ramos AP, Gustafsson O, Labert N, Salecker I, Nilsson D-E, Averof M. 2019. Analysis of the genetically tractable crustacean *Parhyale hawaiiensis* reveals the organisation of a sensory system for low-resolution vision. *BMC Biology.* 17(1):67
- Ramp C, Delarue J, Palsbøll PJ, Sears R, Hammond PS. 2015. Adapting to a Warmer Ocean—Seasonal Shift of Baleen Whale Movements over Three Decades. *PLoS One.* 10(3):e0121374
- Régnier T, Gibb FM, Wright PJ. 2019. Understanding temperature effects on recruitment in the context of trophic mismatch. *Sci Rep.* 9(1):1–13
- Reitzel AM, Behrendt L, Tarrant AM. 2010. Light entrained rhythmic gene expression in the sea anemone *Nematostella vectensis*: the evolution of the animal circadian clock. *PLoS One.* 5(9):e12805
- Reitzel AM, Tarrant AM, Levy O. 2013. Circadian clocks in the cnidaria: environmental entrainment, molecular regulation, and organismal outputs. *Integr Comp Biol.* 53(1):118–30
- Renaud PE, Daase M, Banas NS, Gabrielsen TM, Søreide JE, et al. 2018. Pelagic food-webs in a changing Arctic: a trait-based perspective suggests a mode of resilience. *ICES Journal of Marine Science.* 75(6):1871–81
- Renfer E, Amon-Hassenzahl A, Steinmetz PRH, Technau U. 2010. A muscle-specific transgenic reporter line of the sea anemone, *Nematostella vectensis*. *Proc Natl Acad Sci U S A.* 107(1):104–8
- Renfer E, Technau U. 2017. Meganuclease-assisted generation of stable transgenics in the sea anemone *Nematostella vectensis*. *Nat Protoc.* 12(9):1844–54
- Reuven S, Rinsky M, Brekhlman V, Malik A, Levy O, Lotan T. 2021. Cellular pathways during spawning induction in the starlet sea anemone *Nematostella vectensis*. *Sci Rep.* 11(1):15451
- Reynolds C. 2006. *Ecology of Phytoplankton.* Cambridge Univ. Press.
- Rock A, Wilcockson D, Last KS. 2022. Towards an Understanding of Circatidal Clocks. *Frontiers in Physiology.* 13:830107
- Roenneberg T, Colfax GN, Hastings JW. 1989. A Circadian Rhythm of Population Behavior in *Gonyaulax polyedra*. *Journal of Biological Rhythms.* 4(2):89–104
- Roenneberg T, Deng T-S. 1997. Photobiology of the *Gonyaulax* circadian system. I. Different phase response curves for red and blue light. *Planta.* 202(4):494–501
- Roenneberg T, Hastings JW. 1988. Two photoreceptors control the circadian clock of a unicellular alga. *Naturwissenschaften.* 75(4):206–7
- Roenneberg T, Morse D. 1993. Two circadian oscillators in one cell. *Nature.* 362(6418):362–64
- Roncagli V, Cieslak MC, Sommer SA, Hopcroft RR, Lenz PH. 2018. *De novo* transcriptome assembly of the calanoid copepod *Neocalanus flemingeri*: A new resource for emergence from diapause. *Mar Genomics.* 37:114–19
- Rosa R, Seibel BA. 2008. Synergistic effects of climate-related variables suggest future physiological impairment in a top oceanic predator. *Proc Natl Acad Sci U S A.* 105:20776–80
- Rosenberg Y, Doniger T, Harii S, Sinniger F, Levy O. 2017. Canonical and cellular pathways timing gamete release in *Acropora digitifera*, Okinawa, Japan. *Mol Ecol.* 26(10):2698–2710
- Round FE, Palmer JD. 1966. Persistent, vertical-migration rhythms in benthic microflora.: II. Field and Laboratory Studies On Diatoms From The Banks Of The River Avon. *J. Mar. Biol. Ass. U.K.* 46(1):191–214
- Saikkonen K, Taulavuori K, Hyvönen T, Gundel PE, Hamilton CE, et al. 2012. Climate change-driven species' range shifts filtered by photoperiodism. *Nature Clim. Change.* 2(4):239–42

- Saini R, Jaskolski M, Davis SJ. 2019. Circadian oscillator proteins across the kingdoms of life: structural aspects. *BMC Biol.* 17:13
- Sanchez A, Shin J, Davis SJ. 2011. Abiotic stress and the plant circadian clock. *Plant Signal Behav.* 6(2):223-31
- Satoh A. 2017. Constant light disrupts the circadian but not the circatidal rhythm in mangrove crickets. *Biological Rhythm Research.* 48(3):459-63
- Satoh A, Momoshita H, Hori M. 2006. Circatidal rhythmic behaviour in the coastal tiger beetle *Callytron inspecularis* in Japan. *Biological Rhythm Research.* 37(2):147-55
- Satoh A, Takasu M, Yano K, Terai Y. 2021. *De novo* assembly and annotation of the mangrove cricket genome. *BMC Res Notes.* 14(1):387
- Satoh A, Terai Y. 2019. Circatidal gene expression in the mangrove cricket *Apteronemobius asahinai*. *Sci Rep.* 9(1):3719
- Satoh A, Yoshioka E, Numata H. 2008. Circatidal activity rhythm in the mangrove cricket *Apteronemobius asahinai*. *Biol Lett.* 4(3):233-36
- Schaffelke B, Lüning K. 1994. A circannual rhythm controls seasonal growth in the kelps *Laminaria hyperborea* and *L. digitata* from Helgoland (North Sea). *European Journal of Phycology.* 29(1):49-56
- Schalm G, Bruns K, Drachenberg N, Geyer N, Foulkes NS, et al. 2021. Finding Nemo's clock reveals switch from nocturnal to diurnal activity. *Sci Rep.* 11(1):6801
- Schneck DT, Barreto FS. 2020. Phenotypic Variation in Growth and Gene Expression Under Different Photoperiods in Allopatric Populations of the Copepod *Tigriopus californicus*. *The Biological Bulletin.* 238(2):106-18
- Schnytzer Y, Simon-Blecher N, Li J, Ben-Asher HW, Salmon-Divon M, et al. 2018. Tidal and diel orchestration of behaviour and gene expression in an intertidal mollusc. *Scientific Reports.* 8(1):1-13
- Schründer S, Schnack-Schiel SB, Auel H, Sartoris FJ. 2013. Control of Diapause by Acidic pH and Ammonium Accumulation in the Hemolymph of Antarctic Copepods. *PLoS One.* 8(10):e77498
- Schulze T, Prager K, Dathe H, Kelm J, Kiessling P, Mittag M. 2010. How the green alga *Chlamydomonas reinhardtii* keeps time. *Protoplasma.* 244:3-14
- Schunter C, Welch MJ, Nilsson GE, Rummer JL, Munday PL, Ravasi T. 2018. An interplay between plasticity and parental phenotype determines impacts of ocean acidification on a reef fish. *Nat Ecol Evol.* 2(2):334-42
- Schunter C, Welch MJ, Ryu T, Zhang H, Berumen ML, et al. 2016. Molecular signatures of transgenerational response to ocean acidification in a species of reef fish. *Nature Clim Change.* 6(11):1014-18
- Schwarzenberger A, Handke NH, Romer T, Wacker A. 2021. Geographic clines in *Daphnia magna*'s circadian clock gene expression: Local adaptation to photoperiod. *Zoology.* 144:125856
- Seibel BA, Häfker NS, Trübenbach K, Zhang J, Tessier SN, et al. 2014. Metabolic suppression during protracted exposure to hypoxia in the jumbo squid, *Dosidicus gigas*, living in an oxygen minimum zone. *The Journal of Experimental Biology.* 217(14):2555-68
- Seymour JR, Barbasch TA, Buston PM. 2018. Lunar cycles of reproduction in the clown anemonefish *Amphiprion percula*: individual-level strategies and population-level patterns. *Marine Ecology Progress Series.* 594:193-201
- Shoguchi E, Shinzato C, Kawashima T, Gyoja F, Mungpakdee S, et al. 2013a. Draft Assembly of the *Symbiodinium minutum* Nuclear Genome Reveals Dinoflagellate Gene Structure. *Current Biology.* 23(15):1399-1408

- Shoguchi E, Tanaka M, Shinzato C, Kawashima T, Satoh N. 2013b. A genome-wide survey of photoreceptor and circadian genes in the coral, *Acropora digitifera*. *Gene*. 515(2):426–31
- Sims DW, Southall EJ, Tarling GA, Metcalfe JD. 2005. Habitat-specific normal and reverse diel vertical migration in the plankton-feeding basking shark. *Journal of Animal Ecology*. 74(4):755–61
- Søreide JE, Leu E, Berge J, Graeve M, Falk-Petersen S. 2010. Timing of blooms, algal food quality and *Calanus glacialis* reproduction and growth in a changing Arctic. *Global Change Biology*. 16:3154–63
- Sorek M, Díaz-Almeyda EM, Medina M, Levy O. 2014. Circadian clocks in symbiotic corals: The duet between *Symbiodinium* algae and their coral host. *Marine Genomics*. 14:47–57
- Sorek M, Levy O. 2012. Influence of the Quantity and Quality of Light on Photosynthetic Periodicity in Coral Endosymbiotic Algae. *PLoS One*. 7(8):e43264
- Sorek M, Schnytzer Y, Waldman Ben-Asher H, Caspi VC, Chen C-S, et al. 2018. Setting the pace: host rhythmic behaviour and gene expression patterns in the facultatively symbiotic cnidarian *Aiptasia* are determined largely by *Symbiodinium*. *Microbiome*. 6(1):83
- Sorek M, Yacobi YZ, Roopin M, Berman-Frank I, Levy O. 2013. Photosynthetic circadian rhythmicity patterns of *Symbiodinium*, the coral endosymbiotic algae. *Proceedings of the Royal Society B: Biological Sciences*. 280(1759):20122942
- Sournia A. 1975. Circadian periodicities in natural populations of marine phytoplankton. *Advances in marine biology*. 12:325–89
- Spoelstra K, Wikelski M, Daan S, Loudon ASI, Hau M. 2016. Natural selection against a circadian clock gene mutation in mice. *Proc Natl Acad Sci U S A*. 113(3):686–91
- Stevenson TJ, Lincoln GA. 2017. Epigenetic Mechanisms Regulating Circannual Rhythms. In *Biological Timekeeping: Clocks, Rhythms and Behaviour*, ed. V Kumar, pp. 607–23. New Delhi: Springer India
- Stramma L, Prince ED, Schmidtko S, Luo J, Hoolihan JP, et al. 2012. Expansion of oxygen minimum zones may reduce available habitat for tropical pelagic fishes. *Nature Clim Change*. 2(1):33–37
- Strelkov P, Nikula R, Väinölä R. 2007. *Macoma balthica* in the White and Barents Seas: properties of a widespread marine hybrid swarm (Mollusca: Bivalvia). *Molecular Ecology*. 16(19):4110–27
- Strömberg J-O, Spicer JJ, Liljebladh B, Thomasson MA. 2002. Northern krill, *Meganyctiphanes norvegica*, come up to see the last eclipse of the millennium? *J. Mar. Biol. Assoc. U.K.* 82(5):919–20
- Sugama N, Park J-G, Park Y-J, Takeuchi Y, Kim S-J, Takemura A. 2008. Moonlight affects nocturnal *Period2* transcript levels in the pineal gland of the reef fish *Siganus guttatus*. *J Pineal Res*. 45(2):133–41
- Sundby S, Drinkwater KF, Kjesbu OS. 2016. The North Atlantic Spring-Bloom System—Where the Changing Climate Meets the Winter Dark. *Frontiers in Marine Science*. 3:00028
- Sweeney BM, Hastings JW. 1958. Rhythmic Cell Division in Populations of *Gonyaulax polyedra*. *The Journal of Protozoology*. 5(3):217–24
- Sweeney BM, Haxo FT. 1961. Persistence of a Photosynthetic Rhythm in Enucleated *Acetabularia*. *Science*. 134(3487):1361–63
- Sweeney BM, Tuffli CF, Rubin RH. 1967. The Circadian Rhythm in Photosynthesis in *Acetabularia* in the Presence of Actinomycin D, Puromycin, and Chloramphenicol. *J Gen Physiol*. 50(3):647–59



- Takeda N, Kon Y, Quiroga Artigas G, Lapébie P, Barreau C, et al. 2018. Identification of jellyfish neuropeptides that act directly as oocyte maturation-inducing hormones. *Development*. 145(2):dev156786
- Takekata H, Matsuura Y, Goto SG, Satoh A, Numata H. 2012. RNAi of the circadian clock gene *period* disrupts the circadian rhythm but not the circatidal rhythm in the mangrove cricket. *Biology Letters*. 8(4):488-91
- Takekata H, Numata H, Shiga S, Goto SG. 2014. Silencing the circadian clock gene *Clock* using RNAi reveals dissociation of the circatidal clock from the circadian clock in the mangrove cricket. *J Insect Physiol*. 68:16-22
- Takeuchi Y, Kabutomori R, Yamauchi C, Miyagi H, Takemura A, et al. 2018. Moonlight controls lunar-phase-dependency and regular oscillation of clock gene expressions in a lunar-synchronized spawner fish, Goldlined spinefoot. *Sci Rep*. 8(1):6208
- Tan MH, Austin CM, Hammer MP, Lee YP, Croft LJ, Gan HM. 2018. Finding Nemo: hybrid assembly with Oxford Nanopore and Illumina reads greatly improves the clownfish (*Amphiprion ocellaris*) genome assembly. *Gigascience*. 7(3):1-6
- Tankersley RA, Bullock TM, Forward RB, Rittschof D. 2002. Larval release behaviors in the blue crab *Callinectes sapidus*: role of chemical cues. *Journal of Experimental Marine Biology and Ecology*. 273(1):1-14
- Tarling GA, Buchholz F, Matthews JBL. 1999. The effect of a lunar eclipse on the vertical migration behaviour of *Meganycitiphanes norvegica* (Crustacea: Euphausiacea) in the Ligurian Sea. *J PLANKTON RES*. 21(8):1475-88
- Tarrant AM, Baumgartner MF, Lysiak NSJ, Altin D, Størseth TR, Hansen BH. 2016. Transcriptional Profiling of Metabolic Transitions during Development and Diapause Preparation in the Copepod *Calanus finmarchicus*. *Integr Comp Biol*. 56(6):1157-69
- Tarrant AM, Helm RR, Levy O, Rivera HE. 2019. Environmental entrainment demonstrates natural circadian rhythmicity in the cnidarian *Nematostella vectensis*. *J Exp Biol*. 222(21):jeb205393
- Teschke M, Wendt S, Kawaguchi S, Kramer A, Meyer B. 2011. A Circadian Clock in Antarctic Krill: An Endogenous Timing System Governs Metabolic Output Rhythms in the Euphausiid Species *Euphausia superba*. *PLoS One*. 6(10):e26090
- Tessmar-Raible K, Raible F, Arboleda E. 2011. Another place, another timer: Marine species and the rhythms of life. *Bioessays*. 33(3):165-72
- Teuber L, Schukat A, Hagen W, Auel H. 2013. Distribution and Ecophysiology of Calanoid Copepods in Relation to the Oxygen Minimum Zone in the Eastern Tropical Atlantic. *PLoS One*. 8(11):e77590
- Thiriet-Rupert S, Carrier G, Chénais B, Trottier C, Bougaran G, et al. 2016. Transcription factors in microalgae: genome-wide prediction and comparative analysis. *BMC Genomics*. 17(1):282
- Thorne LH, Nye JA. 2021. Trait-mediated shifts and climate velocity decouple an endothermic marine predator and its ectothermic prey. *Sci Rep*. 11(1):18507
- tom Dieck I. 1991. Circannual Growth Rhythm and Photoperiodic Sorus Induction in the Kelp *Laminaria Setchellii* (Phaeophyta). *Journal of Phycology*. 27(3):341-50
- Tomioka K, Matsumoto A. 2015. Circadian molecular clockworks in non-model insects. *Current Opinion in Insect Science*. 7:58-64
- Tosches MA, Bucher D, Vopalensky P, Arendt D. 2014. Melatonin signaling controls circadian swimming behavior in marine zooplankton. *Cell*. 159(1):46-57
- Tougeron K. 2021. How Constraining are Photic Barriers to Poleward Range-Shifts? *Trends in Ecology & Evolution*. 36(6):478-79

- Tran D, Nadau A, Durrieu G, Ciret P, Parisot J-P, Massabuau J-C. 2011. Field chronobiology of a molluscan bivalve: how the moon and sun cycles interact to drive oyster activity rhythms. *Chronobiol Int.* 28(4):307-17
- Tran D, Perrigault M, Ciret P, Payton L. 2020. Bivalve mollusc circadian clock genes can run at tidal frequency. *Proceedings of the Royal Society B: Biological Sciences.* 287(1918):20192440
- Tsukamoto H, Chen I-S, Kubo Y, Furutani Y. 2017. A ciliary opsin in the brain of a marine annelid zooplankton is ultraviolet-sensitive, and the sensitivity is tuned by a single amino acid residue. *J Biol Chem.* 292(31):12971-80
- Tsunoda SP, Ewers D, Gazzarrini S, Moroni A, Gradmann D, Hegemann P. 2006. H<sup>+</sup>-Pumping Rhodopsin from the Marine Alga *Acetabularia*. *Biophysical Journal.* 91(4):1471-79
- Unal E, Bucklin A. 2010. Basin-scale population genetic structure of the planktonic copepod *Calanus finmarchicus* in the North Atlantic Ocean. *Progress in Oceanography.* 87(1):175-85
- van Haren H. 2007. Monthly periodicity in acoustic reflections and vertical motions in the deep ocean. *Geophysical Research Letters.* 34(12):L12603
- van Haren H, Compton TJ. 2013. Diel Vertical Migration in Deep Sea Plankton Is Finely Tuned to Latitudinal and Seasonal Day Length. *PLoS One.* 8(5):e64435
- van Ooijen G, Dixon LE, Troein C, Millar AJ. 2011. Proteasome Function Is Required for Biological Timing throughout the Twenty-Four Hour Cycle. *Current Biology.* 21(10):869-75
- van Ooijen G, Hindle M, Martin SF, Barrios-Llerena M, Sanchez F, et al. 2013. Functional Analysis of Casein Kinase 1 in a Minimal Circadian System. *PLoS One.* 8(7):e70021
- Veedin Rajan VB, Häfker NS, Arboleda E, Poehn B, Gosssenreiter T, et al. 2021. Seasonal variation in UVA light drives hormonal and behavioural changes in a marine annelid via a ciliary opsin. *Nat Ecol Evol.* 5(2):204-18
- Vieler A, Wu G, Tsai C-H, Bullard B, Cornish AJ, et al. 2012. Genome, Functional Gene Annotation, and Nuclear Transformation of the Heterokont Oleaginous Alga *Nannochloropsis oceanica* CCMP1779. *PLoS Genetics.* 8(11):e1003064
- Villarino E, Irigoien X, Villate F, Iriarte A, Uriarte I, et al. 2020. Response of copepod communities to ocean warming in three time-series across the North Atlantic and Mediterranean Sea. *Marine Ecology Progress Series.* 636:47-61
- Visser F, Hartman KL, Pierce GJ, Valavanis VD, Huisman J. 2011. Timing of migratory baleen whales at the Azores in relation to the North Atlantic spring bloom. *Marine Ecology Progress Series.* 440:267-79
- Wada T, Shimono K, Kikukawa T, Hato M, Shinya N, et al. 2011. Crystal Structure of the Eukaryotic Light-Driven Proton-Pumping Rhodopsin, *Acetabularia* Rhodopsin II, from Marine Alga. *Journal of Molecular Biology.* 411(5):986-98
- Wagner HJ, Kemp K, Mattheus U, Priede IG. 2007. Rhythms at the bottom of the deep sea: Cyclic current flow changes and melatonin patterns in two species of demersal fish. *Deep-Sea Research Part I: Oceanographic Research Papers.* 54(11):1944-56
- Wallace MI, Cottier FR, Berge J, Tarling GA, Griffiths C, Brierley AS. 2010. Comparison of zooplankton vertical migration in an ice-free and a seasonally ice-covered Arctic fjord: An insight into the influence of sea ice cover on zooplankton behavior. *Limnol. Oceanogr.* 55(2):831-45
- Wang D, Ning K, Li J, Hu J, Han D, et al. 2014. *Nannochloropsis* Genomes Reveal Evolution of Microalgal Oleaginous Traits. *PLoS Genetics.* 10(1):e1004094
- Watson GJ, Bentley MG, Gaudron SM, Hardege JD. 2003. The role of chemical signals in the spawning induction of polychaete worms and other marine invertebrates. *Journal of Experimental Marine Biology and Ecology.* 294(2):169-87

- Watson NHF, Smallman BN. 1971. The role of photoperiod and temperature in the induction and termination of an arrested development in two species of freshwater cyclopoid copepods. *Can. J. Zool.* 49(6):855-62
- Weizman EN, Tannenbaum M, Tarrant AM, Hakim O, Levy O. 2019. Chromatin dynamics enable transcriptional rhythms in the cnidarian *Nematostella vectensis*. *PLOS Genetics.* 15(11):e1008397
- Weydmann A, Przyłucka A, Lubośny M, Walczyńska KS, Serrão EA, et al. 2018. Postglacial expansion of the Arctic keystone copepod *Calanus glacialis*. *Mar Biodiv.* 48(2):1027-35
- Williams BG. 1998. The lack of circadian timing in two intertidal invertebrates and its significance in the circatidal/circalunidian debate. *Chronobiology International.* 15(3):205-18
- Wu C, Jiang Q, Wei L, Cai Z, Chen J, et al. 2018. A Rhodopsin-Like Gene May Be Associated With the Light-Sensitivity of Adult Pacific Oyster *Crassostrea gigas*. *Front Physiol.* 9:221
- Wuitchik DM, Wang D, Pells TJ, Karimi K, Ward S, Vize PD. 2019. Seasonal temperature, the lunar cycle and diurnal rhythms interact in a combinatorial manner to modulate genomic responses to the environment in a reef-building coral. *Molecular Ecology.* 28(16):3629-41
- Yamamoto-Kawai M, McLaughlin FA, Carmack EC, Nishino S, Shimada K. 2009. Aragonite Undersaturation in the Arctic Ocean: Effects of Ocean Acidification and Sea Ice Melt. *Science.* 326(5956):1098-1100
- Yan J, Kim YJ, Somers DE. 2021. Post-Translational Mechanisms of Plant Circadian Regulation. *Genes (Basel).* 12(3):325
- Yerushalmi S, Green RM. 2009. Evidence for the adaptive significance of circadian rhythms. *Ecology Letters.* 12(9):970-81
- Yildirim E, Curtis R, Hwangbo D-S. 2022. Roles of peripheral clocks: lessons from the fly. *FEBS Lett.* 596(3):263-93
- Yocum GD, Rinehart JP, Yocum IS, Kemp WP, Greenlee KJ. 2016. Thermoperiodism Synchronizes Emergence in the Alfalfa Leafcutting Bee (Hymenoptera: Megachilidae). *Environmental Entomology.* 45(1):245-51
- Zantke J, Ishikawa-Fujiwara T, Arboleda E, Lohs C, Schipany K, et al. 2013. Circadian and circalunar clock interactions in a marine annelid. *Cell Rep.* 5(1):99-113
- Zbawicka M, Gardner JPA, Wenne R. 2019. Cryptic diversity in smooth-shelled mussels on Southern Ocean islands: connectivity, hybridisation and a marine invasion. *Frontiers in Zoology.* 16(1):32
- Zeidberg LD, Robison BH. 2007. Invasive range expansion by the Humboldt squid, *Dosidicus gigas*, in the eastern North Pacific. *Proc Natl Acad Sci U S A.* 104:12946-48
- Zhang G, Fang X, Guo X, Li L, Luo R, et al. 2012. The oyster genome reveals stress adaptation and complexity of shell formation. *Nature.* 490(7418):49-54
- Zhang L, Hastings MH, Green EW, Tauber E, Sladek M, et al. 2013. Dissociation of Circadian and Circatidal Timekeeping in the Marine Crustacean *Eurydice pulchra*. *Curr Biol.* 23(19):1863-73
- Zheng P, Wang M, Li C, Sun X, Wang X, et al. 2017. Insights into deep-sea adaptations and host-symbiont interactions: A comparative transcriptome study on *Bathymodiolus mussels* and their coastal relatives. *Mol Ecol.* 26(19):5133-48
- Zurl M, Poehn B, Rieger D, Krishnan S, Rokvic D, et al. 2021. Two light sensors decode moonlight versus sunlight to adjust a plastic circadian/circalunidian clock to moon phase. *bioRxiv.* 2021.04.16.440114

# Supplementary Material

	Cell division	Gene expression	Photosynthesis and related processes (pigment synthesis, carbon assimilation, O <sub>2</sub> evolution...)	Behaviours (gamete release, migration, motility) and other processes		
	<i>Ostreococcus tauri</i> , un ● ○ ○ ○ ○ ○ Moulager, 2007 <i>Ulva pseudocurvata</i> , mc ● ○ ○ ○ ○ ○ Titlyanov, 1996 <i>Porphyra umbilicalis</i> , mc ● ○ ○ ○ ○ ○ Lüning, 1997 <i>Nannochloropsis spp.</i> , un ● ○ ○ ○ ○ ○ Braun, 2014 <i>Skeletonema costatum</i> , un ● ○ ○ ○ ○ ○ Ostgaard, 1982 <i>Pterygophora californica</i> , mc ● ○ ○ ○ ○ ○ Makarov, 1995 <i>Lingulodinium poliedrum</i> , un ● ○ ○ ○ ○ ○ Sweeney, 1958 <i>Symbiodinium microadriaticum</i> , un ● ○ ○ ○ ○ ○ Fitt, 1983 <i>Karenia brevis</i> , un ● ○ ○ ○ ○ ○ Brunelle, 2007 <i>Coccolitophores, various spp.</i> , un ● ○ ○ ○ ○ ○ Chisholm, 1981 <i>Euglena gracilis</i> , un ● ○ ○ ○ ○ ○ Edmunds, 1966; Carré, 1993; Hagiwara, 2002; Bolige, 2005	<i>Ostreococcus tauri</i> , un ● ○ ○ ○ ○ ○ Corellou, 2009; Monnier, 2010 <i>Grateloupia turuturu</i> , mc ● ○ ○ ○ ○ ○ Goulard, 2004 <i>Nannochloropsis spp.</i> , un ● ○ ○ ○ ○ ○ Poliner, 2019 <i>Phaeodactylum tricornutum</i> , un ● ○ ○ ○ ○ ○ Annunziata, 2019 <i>Symbiodinium spp.</i> , un ● ○ ○ ○ ○ ○ Sorek, 2013, 2014 <i>Bigelowiella natans (plastid)</i> , un ● ○ ○ ○ ○ ○ Suzuki, 2016	<i>Acetabularia spp.</i> , un ● ○ ○ ○ ○ ○ Sweeney, 1961; Schweiger, 1964; Driessche, 1966 <i>Ulva ssp.</i> , mc ● ○ ○ ○ ○ ○ Koop, 1978 <i>Bryopsis maxima</i> , mc ● ○ ○ ○ ○ ○ Britz, 1976, Okada, 1978 <i>Kappaphycus alvarezii</i> , mc ● ○ ○ ○ ○ ○ Granborn, 2001 <i>Grateloupia turuturu</i> , mc ● ○ ○ ○ ○ ○ Goulard, 2004 <i>Phaeodactylum tricornutum</i> , un ● ○ ○ ○ ○ ○ Palmer, 1964; Ragni, 2007; Annunziata, 2019 <i>Various diatom spp.</i> , un ● ○ ○ ○ ○ ○ Brand, 1982 <i>Dictyota dichotom</i> , mc ● ○ ○ ○ ○ ○ Nultsch, 1984 <i>Ectocarpus siliculosus</i> , mc ● ○ ○ ○ ○ ○ Schmid, 1992 <i>Lingulodinium poliedrum</i> , un ● ○ ○ ○ ○ ○ Hastings, 1961; Samuelsson, 1983 <i>Symbiodinium spp.</i> , un ● ○ ○ ○ ○ ○ Mackenzie, 2011; Sorek, 2012a, 2012b, 2013, 2014 <i>Various dinoflagellate species</i> , un ● ○ ○ ○ ○ ○ Brand, 1982 <i>Emiliana huxleyi</i> , un ● ○ ○ ○ ○ ○ Brand, 1982 <i>Euglena gracilis</i> , un ● ○ ○ ○ ○ ○ Lonergan, 1978, 1979	<i>Ostreococcus tauri</i> , un ● ○ ○ ○ ○ ○ O'Neill, 2011; Feeney, 2016 <i>Ulva spp.</i> , mc ○ ○ ● ○ ○ ○ Tal, 2011 <i>Enteromorpha intestinalis</i> , mc ○ ○ ○ ● ○ ○ Christie, 1962 <i>Various diatom species</i> , un ● ● ○ ○ ○ ○ Palmer, 1967, Fischer, 1977; Happey-Wood, 1988 <i>Fucus vesiculosus</i> , mc ○ ○ ○ ● ○ ○ Andresson, 1994 <i>Dyctiota diemensis</i> , mc ○ ● ○ ○ ○ ○ Sweeney, 1987 <i>Various species of Kelp</i> , mc ○ ○ ○ ○ ● ○ Dieck, 1991; Lüning, 1991; Schaffelke 1994 <i>Lingulodinium poliedrum</i> , un ● ○ ○ ○ ○ ○ Hastings, 1957; Roenneberg, 1989, 1993 <i>Symbiodinium microadriaticum</i> , un ● ○ ○ ○ ○ ○ Fitt, 1983 <i>Alexandrium fundyense</i> , un ○ ○ ○ ○ ● ○ Matrai, 2005 <i>Euglena proxima</i> , un ○ ● ○ ○ ○ ○ Kingston, 1999 <i>Natural mixed populations</i> ○ ● ○ ○ ○ ○ Barnett, 2020; Haro, 2019	● daily rhythm ● tidal rhythm ● lunar rhythm ● semilunar rhythm ● circannual rhythm	Phylogenetic group: <i>Archaeplastida</i> ; <i>Stramenopila</i> ; <i>Alveolata</i> ; <i>Rhizaria</i> ; <i>Haptophyta</i> ; <i>Excavata</i>

Supplementary Table 1: Examples of biological rhythms characterized in marine algae. The table only lists rhythms for which evidence of an endogenous oscillator exist. uc: unicellular; mc: multicellular

# Supplementary Bibliography

- Andersson S, Kautsky L, Kalvas A. 1994. Circadian and lunar gamete release in *Fucus vesiculosus* in the atidal Baltic Sea. *Marine Ecology Progress Series*. 110:195-201
- Annunziata R, Ritter A, Fortunato AE, Manzotti A, Cheminant-Navarro S, et al. 2019. bHLH-PAS protein RITMO1 regulates diel biological rhythms in the marine diatom *Phaeodactylum tricorutum*. *Proc Natl Acad Sci U S A*. 116(26):13137-42
- Barnett A, Méléder V, Dupuy C, Lavaud J. 2020. The Vertical Migratory Rhythm of Intertidal Microphytobenthos in Sediment Depends on the Light Photoperiod, Intensity, and Spectrum: Evidence for a Positive Effect of Blue Wavelengths. *Frontiers in Marine Science*. 7:212
- Bolige A, Hagiwara S, Zhang Y, Goto K. 2005. Circadian G2 Arrest as Related to Circadian Gating of Cell Population Growth in *Euglena*. *Plant and Cell Physiology*. 46(6):931-36
- Brand LE. 1982. Persistent diel rhythms in the chlorophyll fluorescence of marine phytoplankton species. *Marine Biology*. 69(3):253-62
- Braun R, Farré EM, Schurr U, Matsubara S. 2014. Effects of light and circadian clock on growth and chlorophyll accumulation of *Nannochloropsis gaditana*. *Journal of Phycology*. 50(3):515-25
- Britz SJ, Briggs WR. 1976. Circadian Rhythms of Chloroplast Orientation and Photosynthetic Capacity in *Ulva*. *Plant Physiology*. 58(1):22-27
- Brunelle SA, Hazard Starr A, Sotka EE, Van Dolah FM. 2007. Characterization Of A Dinoflagellate Cryptochrome Blue-Light Receptor With A Possible Role In Circadian Control Of The Cell Cycle. *Journal of Phycology*. 43:509-18
- Carré IA, Edmunds LN. 1993. Oscillator control of cell division in *Euglena*: cyclic AMP oscillations mediate the phasing of the cell division cycle by the circadian clock. *Journal of Cell Science*. 104:11
- Chisholm SW, Brand LE. 1981. Persistence of cell division phasing in marine phytoplankton in continuous light after entrainment to light: Dark cycles. *Journal of Experimental Marine Biology and Ecology*. 51(2-3):107-18
- Christie AO, Evans LV. 1962. Periodicity in the Liberation of Gametes and Zoospores of *Enteromorpha intestinalis* Link. *Nature*. 193:193-94
- Corellou F, Schwartz C, Motta J-P, Djouani-Tahri EB, Sanchez F, Bouget F-Y. 2009. Clocks in the Green Lineage: Comparative Functional Analysis of the Circadian Architecture of the Picoeukaryote *Ostreococcus*. *The Plant Cell*. 21(11):3436-49
- Edmunds LN. 1966. Studies on synchronously dividing cultures of *Euglena gracilis* Klebs (strain Z). III. Circadian Components Of Cell Division. *Journal of cell physiology*. 67:35-44
- Feeney KA, Hansen LL, Putker M, Olivares-Yañez C, Day J, et al. 2016. Daily magnesium fluxes regulate cellular timekeeping and energy balance. *Nature*. 532(7599):375-79
- Fischer H, Gröning C, Köster C. 1977. Vertical migration rhythm in freshwater diatoms. *Hydrobiologia*. 56(3):259-63
- Fitt WK, Trench RK. 1983. The relation of diel patterns of cell division to diel patterns of motility in the symbiotic dinoflagellate *Symbiodinium microadriaticum* Freudenthal in culture. *New Phytologist*. 94(3):421-32
- Goulard F, Lüning K, Jacobsen S. 2004. Circadian rhythm of photosynthesis and concurrent oscillations of transcript abundance of photosynthetic genes in the marine red alga *Grateloupia turuturu*. *European Journal of Phycology*. 39(4):431-37

- Granbom M, Pedersén M, Kadel P, Lüning K. 2001. Circadian rhythm of photosynthetic oxygen evolution in *Kappaphycus alvarezii* (Rhodophyta): dependence on light quantity and quality. *Journal of Phycology*. 37(6):1020-25
- Hagiwara S, Bolige A, Zhang Y, Takahashi M, Yamagishi A, Goto K. 2002. Gating of Photoinduction of Commitment to Cell-cycle Transitions in Relation to Photoperiodic Control of Cell Reproduction in *Euglena*. *Photochemistry and Photobiology*. 76(1):105-15
- Happey-Wood CM, Jones P. 1988. Rhythms of vertical migration and motility in intertidal benthic diatoms with particular reference to *Pleurosigma angulatum*. *Diatom research*. 3(1):83-93
- Haro S, Bohórquez J, Lara M, Garcia-Robledo E, González CJ, et al. 2019. Diel patterns of microphytobenthic primary production in intertidal sediments: the role of photoperiod on the vertical migration circadian rhythm. *Scientific Reports*. 9(1):13376
- Hastings JW, Astrachan L, Sweeney BM. 1961. A Persistent Daily Rhythm in Photosynthesis. *The Journal of General Physiology*. 45(1):69-76
- Hastings JW, Sweeney BM. 1957. On the mechanism of temperature independence in a biological clock. *Proc Natl Acad Sci U S A*. 43:804-11
- Kingston MB. 1999. Effect of light on vertical migration and photosynthesis of *Euglena proxima* (Euglenophyta). *Journal of Phycology*. 35(2):245-53
- Koop H-U, Schmid R, Heunert H-H, Milthaler B. 1978. Chloroplast migration: A new circadian rhythm in *Acetabularia*. *Protoplasma*. 97(2-3):301-10
- Loneragan TA, Sargent ML. 1978. Regulation of the Photosynthesis Rhythm in *Euglena gracilis*. *Plant Physiology*. 61:150-53
- Loneragan TA, Sargent ML. 1979. Regulation of the Photosynthesis Rhythm in *Euglena gracilis* II. Involvement of electron flow through both photosystems. *Plant Physiol*. 64(1):99-103
- Lüning K. 1991. Circannual Growth Rhythm in a Brown Alga, *Pterygophora californica*. *Botanica Acta*. 104(2):157-62
- Lüning K, Titlyanov E, Titlyanova T. 1997. Diurnal and circadian periodicity of mitosis and growth in marine macroalgae. III. The red alga *Porphyra umbilicalis*. *European Journal of Phycology*. 32(2):167-73
- Mackenzie TDB, Morse D. 2011. Circadian photosynthetic reductant flow in the dinoflagellate *Lingulodinium* is limited by carbon availability: Circadian O<sub>2</sub> production is sink-limited. *Plant, Cell & Environment*. 34(4):669-80
- Makarov VN, Schoschina EV, Lüning K. 1995. Diurnal and circadian periodicity of mitosis and growth in marine macroalgae. I. Juvenile sporophytes of Laminariales (Phaeophyta). *European Journal of Phycology*. 30(4):261-66
- Matrai P, Thompson B, Keller M. 2005. Circannual excystment of resting cysts of *Alexandrium* spp. from eastern Gulf of Maine populations. *Deep Sea Research Part II: Topical Studies in Oceanography*. 52(19-21):2560-68
- Monnier A, Liverani S, Bouvet R, Jesson B, Smith JQ, et al. 2010. Orchestrated transcription of biological processes in the marine picoeukaryote *Ostreococcus* exposed to light/dark cycles. *BMC Genomics*. 11(1):192
- Moulager M, Monnier A, Jesson B, Bouvet R, Mosser J, et al. 2007. Light-Dependent Regulation of Cell Division in *Ostreococcus*: Evidence for a Major Transcriptional Input. *Plant Physiology*. 144(3):1360-69
- Nultsch W, Rüffer U, Pfau J. 1984. Circadian rhythms in the chromatophore movements of *Dictyota dichotoma*. *Marine Biology*. 81(3):217-22
- Okada M, Inoue M, Ikeda T. 1978. Circadian rhythm in photosynthesis of the green alga *Bryopsis maxima*. *Plant and Cell Physiology*. 19(2):197-202

- O'Neill JS, van Ooijen G, Dixon LE, Troein C, Corellou F, et al. 2011. Circadian rhythms persist without transcription in a eukaryote. *Nature*. 469(7331):554–58
- Ostgaard K, Jensen A. 1982. Diurnal and circadian rhythms in the turbidity of growing *Skeletonema costatum* cultures. *Marine Biology*. 66(3):261–68
- Palmer JD, Livingston L, Zusy FrD. 1964. A Persistent Diurnal Rhythm in Photosynthetic Capacity. *Nature*. 203(4949):1087–88
- Palmer JD, Round FE. 1967. Persistent, vertical-migration rhythms in benthic microflora. VI. The tidal and diurnal nature of the rhythm in the diatom *Hantzschia virgate*. *The Biological Bulletin*. 132(1):44–55
- Poliner E, Cummings C, Newton L, Farré EM. 2019. Identification of circadian rhythms in *Nannochloropsis* species using bioluminescence reporter lines. *The Plant Journal*. 99(1):112–27
- Ragni M, d'Alcalà MR. 2007. Circadian variability in the photobiology of *Phaeodactylum tricorutum*: pigment content. *Journal of Plankton Research*. 29(2):141–56
- Roenneberg T, Colfax GN, Hastings JW. 1989. A Circadian Rhythm of Population Behavior in *Gonyaulax polyedra*. *Journal of Biological Rhythms*. 4(2):89–104
- Roenneberg T, Morse D. 1993. Two circadian oscillators in one cell. *Nature*. 362(6418):362–64
- Samuelsson G, Sweeney BM, Matlick HA, Prézelin BB. 1983. Changes in Photosystem II Account for the Circadian Rhythm in Photosynthesis in *Gonyaulax polyedra*. *Plant Physiology*. 73(2):329–31
- Schaffelke B, Lüning K. 1994. A circannual rhythm controls seasonal growth in the kelps *Laminaria hyperborea* and *L. digitata* from Helgoland (North Sea). *European Journal of Phycology*. 29(1):49–56
- Schmid R, Dring MJ. 1992. Circadian rhythm and fast responses to blue light of photosynthesis in *Ectocarpus* (Phaeophyta, Ectocarpales). *Planta*. 187:14
- Schweiger E, Wallraff HG, Schweiger HG. 1964. Endogenous Circadian Rhythm in Cytoplasm of *Acetabularia*: Influence of the Nucleus. *Science*. 146(3644):658–59
- Sorek M, Díaz-Almeyda EM, Medina M, Levy O. 2014. Circadian clocks in symbiotic corals: The duet between *Symbiodinium* algae and their coral host. *Marine Genomics*. 14:47–57
- Sorek M, Levy O. 2012a. Influence of the Quantity and Quality of Light on Photosynthetic Periodicity in Coral Endosymbiotic Algae. *PLoS One*. 7(8):e43264
- Sorek M, Levy O. 2012b. The effect of temperature compensation on the circadian rhythmicity of photosynthesis in *Symbiodinium*, coral-symbiotic alga. *Scientific Reports*. 2(1):536
- Sorek M, Yacobi YZ, Roopin M, Berman-Frank I, Levy O. 2013. Photosynthetic circadian rhythmicity patterns of *Symbiodinium*, the coral endosymbiotic algae. *Proceedings of the Royal Society B: Biological Sciences*. 280(1759):20122942
- Suzuki S, Ishida K-I, Hirakawa Y. 2016. Diurnal Transcriptional Regulation of Endosymbiotically Derived Genes in the Chlorarachniophyte *Bigeloviella natans*. *Genome Biology and Evolution*. 8(9):2672–82
- Sweeney BM. 1987. *Rhythmic Phenomena in Plants*. San Diego, Calif.: Acad. Pr. 2nd ed.
- Sweeney BM, Hastings JW. 1958. Rhythmic Cell Division in Populations of *Gonyaulax polyedra*. *The Journal of Protozoology*. 5(3):217–24
- Sweeney BM, Haxo FT. 1961. Persistence of a Photosynthetic Rhythm in Enucleated *Acetabularia*. *Science*. 134(3487):1361–63
- Tal O, Haim A, Harel O, Gerchman Y. 2011. Melatonin as an antioxidant and its semi-lunar rhythm in green macroalga *Ulva sp.* *Journal of Experimental Botany*. 62(6):1903–10

- Titlyanov EA, Titlyanova TV, Lüning K. 1996. Diurnal and circadian periodicity of mitosis and growth in marine macroalgae. II. The green alga *Ulva pseudocurvata*. *European Journal of Phycology*. 31(2):181-88
- tom Dieck I. 1991. Circannual Growth Rhythm and Photoperiodic Sorus Induction in the Kelp *Laminaria Setchellii* (Phaeophyta). *Journal of Phycology*. 27(3):341-50
- Vanden Driessche T. 1966. Circadian rhythms in *Acetabularia*: Photosynthetic capacity and chloroplast shape. *Experimental Cell Research*. 42(1):18-30





*Horloge ! dieu sinistre, effrayant, impassible,  
Dont le doigt nous menace et nous dit : « Souviens-toi !  
Les vibrantes Douleurs dans ton cœur plein d'effroi  
Se planteront bientôt comme dans une cible ;  
Le Plaisir vaporeux fuira vers l'horizon  
Ainsi qu'une sylphide au fond de la coulisse ;  
Chaque instant te dévore un morceau du délice  
A chaque homme accordé pour toute sa saison.  
Trois mille six cents fois par heure, la Seconde  
Chuchote : Souviens-toi ! - Rapide, avec sa voix  
D'insecte, Maintenant dit : Je suis Autrefois,  
Et j'ai pompé ta vie avec ma trompe immonde !  
Remember ! Souviens-toi, prodigue ! Esto memor !  
(Mon gosier de métal parle toutes les langues.)  
Les minutes, mortel folâtre, sont des gangues  
Qu'il ne faut pas lâcher sans en extraire l'or !  
Souviens-toi que le Temps est un joueur avide  
Qui gagne sans tricher, à tout coup ! c'est la loi.  
Le jour décroît ; la nuit augmente, souviens-toi !  
Le gouffre a toujours soif ; la clepsydre se vide.  
Tantôt sonnera l'heure où le divin Hasard,  
Où l'auguste Vertu, ton épouse encor vierge,  
Où le Repentir même (oh ! la dernière auberge !),  
Où tout te dira : Meurs, vieux lâche ! il est trop tard ! »*

Charles Baudelaire - L'horloge - Les Fleurs du mal



# Chapter II.b:

## bHLH-PAS protein RITMO1 regulates diel biological rhythms in the marine diatom *Phaeodactylum tricornutum*

Rossella Annunziata<sup>a,h,1</sup>, Andrés Ritter<sup>a,1,2</sup>, Antonio Emidio Fortunato<sup>a,3</sup>, Alessandro Manzotti<sup>a,c</sup>,  
Soizic Cheminant-Navarro<sup>a,c</sup>, Nicolas Agier<sup>a</sup>, Marie J. J. Huysman<sup>a,d,e</sup>, Per Wingé<sup>f</sup>, Atle M. Bones<sup>f</sup>, François-  
Yves Bouget<sup>g</sup>, Marco Cosentino Lagomarsino<sup>a</sup>, Jean-Pierre Bouly<sup>a,c</sup>, and Angela Falciatore<sup>a,c,4</sup>

<sup>a</sup>Laboratory of Computational and Quantitative Biology, Sorbonne Université, CNRS, Institut de  
Biologie Paris-Seine, F-75005 Paris, France

<sup>b</sup>Integrative Marine Ecology, Stazione Zoologica Anton Dorn, 80121 Napoli, Italy  
<sup>c</sup>Laboratoire de Biologie du chloroplaste et perception de la lumière chez les microalgues UMR7141,  
CNRS, Sorbonne Université, Institut de Biologie Physico-Chimique, 75005, Paris, France

<sup>d</sup>Department of Plant Biotechnology and Bioinformatics, Ghent University, B-9052 Ghent, Belgium

<sup>e</sup>Vlaams Instituut voor Biotechnologie Center for Plant Systems Biology, B-9052 Ghent, Belgium

<sup>f</sup>Cell Molecular Biology and Genomics Group, Department of Biology, Norwegian University of Science  
and Technology, 7491 Trondheim, Norway

<sup>g</sup>Sorbonne Université, CNRS, UMR 7621, Laboratoire d'Océanographie Microbienne, Observatoire  
Océanologique, 66650 Banyuls-sur-Mer, France

Keywords: diatom, circadian rhythms, bHLH-PAS, gene expression, cellular fluorescence



# bHLH-PAS protein RITMO1 regulates diel biological rhythms in the marine diatom *Phaeodactylum tricornutum*

Rossella Annunziata<sup>a,b,1</sup>, Andrés Ritter<sup>a,1,2</sup>, Antonio Emidio Fortunato<sup>a,3</sup>, Alessandro Manzotti<sup>a,c</sup>, Soizic Cheminant-Navarro<sup>a,c</sup>, Nicolas Agier<sup>a</sup>, Marie J. J. Huysman<sup>a,d,e</sup>, Per Winge<sup>f</sup>, Atle M. Bones<sup>f</sup>, François-Yves Bouget<sup>g</sup>, Marco Cosentino Lagomarsino<sup>a</sup>, Jean-Pierre Bouly<sup>a,c</sup>, and Angela Falciatore<sup>a,c,4</sup>

<sup>a</sup>Laboratory of Computational and Quantitative Biology, Sorbonne Université, CNRS, Institut de Biologie Paris-Seine, F-75005 Paris, France; <sup>b</sup>Integrative Marine Ecology, Stazione Zoologica Anton Dohrn, 80121 Napoli, Italy; <sup>c</sup>Laboratoire de Biologie du chloroplaste et perception de la lumière chez les microalgues UMR7141, CNRS, Sorbonne Université, Institut de Biologie Physico-Chimique, 75005, Paris, France; <sup>d</sup>Department of Plant Biotechnology and Bioinformatics, Ghent University, B-9052 Ghent, Belgium; <sup>e</sup>Vlaams Instituut voor Biotechnologie Center for Plant Systems Biology, B-9052 Ghent, Belgium; <sup>f</sup>Cell Molecular Biology and Genomics Group, Department of Biology, Norwegian University of Science and Technology, 7491 Trondheim, Norway; and <sup>g</sup>Sorbonne Université, CNRS, UMR 7621, Laboratoire d'Océanographie Microbienne, Observatoire Océanologique, 66650 Banyuls-sur-Mer, France

Edited by Susan S. Golden, University of California, San Diego, La Jolla, CA, and approved May 10, 2019 (received for review November 27, 2018)

Periodic light–dark cycles govern the timing of basic biological processes in organisms inhabiting land as well as the sea, where life evolved. Although prominent marine phytoplanktonic organisms such as diatoms show robust diel rhythms, the mechanisms regulating these processes are still obscure. By characterizing a *Phaeodactylum tricornutum* bHLH-PAS nuclear protein, hereby named RITMO1, we shed light on the regulation of the daily life of diatoms. Alteration of RITMO1 expression levels and timing by ectopic overexpression results in lines with deregulated diurnal gene expression profiles compared with the wild-type cells. Reduced gene expression oscillations are also observed in these lines in continuous darkness, showing that the regulation of rhythmicity by RITMO1 is not directly dependent on light inputs. We also describe strong diurnal rhythms of cellular fluorescence in wild-type cells, which persist in continuous light conditions, indicating the existence of an endogenous circadian clock in diatoms. The altered rhythmicity observed in RITMO1 overexpression lines in continuous light supports the involvement of this protein in circadian rhythm regulation. Phylogenetic analysis reveals a wide distribution of RITMO1-like proteins in the genomes of diatoms as well as in other marine algae, which may indicate a common function in these phototrophs. This study adds elements to our understanding of diatom biology and offers perspectives to elucidate time-keeping mechanisms in marine organisms belonging to a major, but under-investigated, branch of the tree of life.

diatom | circadian rhythms | bHLH-PAS | gene expression | cellular fluorescence

The Earth's rotation means that life evolved under a daily cycle of alternate light and dark periods. Most living organisms have developed rhythms of many fundamental biological processes, ranging from physiology to behavior, such that they occur at optimal times of the day, which can enhance fitness (1). These rhythms are the product of the coordinated action of signals from endogenous biological clocks, together with environmental and metabolic inputs (2–4). In most eukaryotes, biological rhythms are controlled by interconnected transcriptional-translational feedback loops involving transcription factors (TFs). Although this regulatory framework is conserved among eukaryotes, the regulators orchestrating these rhythms seem to have emerged several times through evolution (5, 6).

Robust diel rhythms in growth, gene expression, pigment synthesis, phototactic movements, and bioluminescence have been observed in a variety of phytoplanktonic organisms, including diatoms (7–10). Diatoms represent the most species-rich group of algae in the ocean and populate a wide range of aquatic environments (11). These algae of the Stramenopila lineage, derived by secondary endosymbiosis events (12), show peculiar genomic,

metabolic, and cellular features and have an impressive capacity to deal with environmental changes (e.g., refs. 12–16). Genome-wide analyses have also shown that 25% of the diurnal transcriptome is influenced by light–dark cycles in the centric diatom *Thalassiosira pseudonana* (17). Additional studies in the pennate diatom *Phaeodactylum tricornutum* have highlighted strong synchronization of the cell cycle with day–night cycles and a strict temporal separation of transcriptional gene networks and metabolism (18–21), as observed in other algae (22, 23). However, the molecular mechanisms orchestrating these processes are still unknown in diatoms and many other phytoplanktonic organisms, except for the green alga *Ostreococcus tauri*, which possesses a plant-like circadian clock (24). Indeed, no clear homologs of the circadian clock components discovered in bacteria, fungi, animals, or

## Significance

Most organisms experience daily light–dark changes and show rhythms of basic biological processes such that they occur at optimal times of the day. Rhythms are also observed in a multitude of marine organisms, but their molecular foundations are still largely unknown. Here, we report daily oscillations of gene expression and cell fluorescence in the diatom *Phaeodactylum tricornutum*, which persist in the absence of external timing cues. We demonstrate that the protein RITMO1, encoded by a bHLH-PAS gene, which is widely represented in algal genomes, regulates these rhythms. By demonstrating circadian regulation in the most species-rich algal group in the ocean, this study unveils critical features of diatom biology, thus advancing the field of diurnal and circadian rhythms in marine algae.

Author contributions: R.A., A.R., A.E.F., J.-P.B., and A.F. designed research; R.A., A.R., A.E.F., A.M., S.C.-N., M.J.J.H., and A.F. performed research; P.W., A.M.B., F.-Y.B., and M.C.L. contributed new reagents/analytic tools; R.A., A.R., A.E.F., N.A., M.C.L., J.-P.B., and A.F. analyzed data; and R.A., A.R., A.E.F., and A.F. wrote the paper.

This article is a PNAS Direct Submission.

This open access article is distributed under [Creative Commons Attribution-NonCommercial-NoDerivatives License 4.0 \(CC BY-NC-ND\)](https://creativecommons.org/licenses/by-nc-nd/4.0/).

Data deposition: Code set information and raw nCounter data are available from the Gene Expression Omnibus database, <https://www.ncbi.nlm.nih.gov/geo/> (Series GSE112268).

<sup>1</sup>R.A. and A.R. contributed equally to this work.

<sup>2</sup>Present addresses: Department of Plant Biotechnology and Bioinformatics, Ghent University, B-9052 Ghent, Belgium; and Vlaams Instituut voor Biotechnologie Center for Plant Systems Biology, B-9052 Ghent, Belgium.

<sup>3</sup>Present address: ImmunRise Technologies, 75005 Paris, France.

<sup>4</sup>To whom correspondence may be addressed. Email: [angela.falciatore@upmc.fr](mailto:angela.falciatore@upmc.fr).

This article contains supporting information online at [www.pnas.org/lookup/suppl/doi:10.1073/pnas.1819660116/-/DCSupplemental](http://www.pnas.org/lookup/suppl/doi:10.1073/pnas.1819660116/-/DCSupplemental).

plants have been found in the diatom genomes except for cryptochromes and casein kinases (13).

In this work, by characterizing gene transcription and cell fluorescence rhythms in *P. tricornutum*, we uncover the existence of circadian rhythms in diatoms and demonstrate the involvement of the bHLH-PAS protein bHLH1a, here named RITMO1, in the regulation of these processes. Notably, the bHLH-PAS domains feature in proteins involved in the regulation of rhythmic processes in animals (5). Phylogenetic analyses reveal a wide distribution of RITMO-like homologs in the genomes of diatoms and other marine algae. Thus, RITMO1 represents a key molecular entry point for the identification of the timekeeper components in diatoms and paves the way for a deeper understanding of marine rhythms and their evolutionary and ecological relevance.

## Results

Transcriptome Profiling Identifies Potential Regulators of Diurnal Rhythms in *P. tricornutum*. To identify potential regulators of cellular rhythmicity in *P. tricornutum*, a publicly available diurnal transcriptomic dataset (18) was analyzed. One hundred and four genes with robust diel oscillating expression were selected, including eight photoreceptors (19, 25–27), 66 TFs (28), and 30 potential output genes implicated in diel rhythmic processes (pigment synthesis, cell cycle regulation, and photosynthesis) (SI Appendix, Table S1). The transcriptional dynamics of the selected genes were further examined in a 16:8-h light:dark (L:D) photocycle for 32 h. Hierarchical clustering analysis revealed four main clusters of coexpressed genes, termed I–IV (Fig. 1 A and B). Cluster I phased at dawn, at around Zeitgeber Time 0 h (ZT: hours after illumination), suggesting a transcriptional anticipation of the light onset. This cluster comprised 18 genes including 14 TFs, mostly belonging to the Heat Shock Transcription Factor family (HSF), the two DNA repair enzymes CPD photolyases (*CPD2* and *CPD3*), and one carotenoid synthesis enzyme (*PDS1*). Cluster II phased around ZT7 and encompassed 36 genes, including the *dsCYC2* gene controlling the onset of cell division (19). Cluster II also contained 18 TFs, of which 8 were sigma factors putatively involved in the regulation of chloroplast transcription, three genes implicated in photoprotection (*LHCX1*, *Val2*, and *Zep1*), and the chlorophyll synthesis *POR1* gene. Such active transcription of genes involved in chloroplast activity during the light period has been shown previously (18, 29). The blue light sensors *Aurochrome1b* and the cryptochromes *CPF1* and *CryP-like* also belonged to cluster II and showed a strong expression following light onset in accordance with previous observations (26, 30). Cluster III phased around ZT9 and comprised 9 TFs and 10 metabolism-related genes. Finally, cluster IV phased just before dusk, at around ZT15, and included 23 TF genes, likely contributing to preparing cells for light-to-dark transition. Cluster IV also contained the *CPF4* and the far-red light sensing phytochrome (*DPH1*), the peak expression of which at the end of the light period has been observed previously (26, 31).

To explore transcription dynamics in the absence of light inputs, the expression of these rhythmic genes was further analyzed in cells exposed to continuous darkness (D:D) for 30 h. The analysis of transcript profiles revealed that around 20% of the analyzed genes showed persistent oscillating expression in D:D, although some profiles displayed reduced amplitudes and/or shifted phases of expression compared with the L:D condition (SI Appendix, Fig. S1). In particular, we identified 18 genes, including putative TFs, pigment-related enzymes, and cell cycle-related genes, showing the highest amplitudes of expression in both L:D and D:D. Conversely, the other 80% of the analyzed expression profiles did not have persistent oscillating patterns in darkness and instead had strongly reduced amplitudes or altered expression timing compared with the L:D condition (SI Appendix, Fig. S2).

Rhythmic *bHLH1a* and *bHLH1b* Expression Is Adjusted in a Photoperiod-Dependent Manner and Persists in Continuous Light and Continuous Dark Conditions. Our analysis identified two TFs—*bHLH1a* (Phatr3\_J44962) belonging to cluster IV and *bHLH1b* (Phatr3\_J44963) belonging

to cluster III—which each have a Per-ARNT-Sim (PAS) domain in conjunction with a bHLH DNA-binding domain. Because bHLH-PAS proteins have been shown to be involved in the regulation of rhythmic processes in animals (5), the expression profiles of *bHLH1a* and *bHLH1b* were further examined in *P. tricornutum* cells grown under different photoperiods. *bHLH1a* expression peaked at ZT8 in the 12L:12D photoperiod and at ZT12 in the 16L:8D photoperiod, 4 h before the end of the light period in both cases, and then gradually decreased to below detection limits at ZT0 (Fig. 1C). Transcription of *bHLH1b* appeared to start earlier than that of *bHLH1a*. In cells entrained in 12L:12D cycles, *bHLH1b* expression peaked at ZT8, whereas it peaked between ZT8 and ZT12 in 16L:8D photoperiods (Fig. 1C). Rhythmic expression was maintained in continuous light (L:L), although amplitude was reduced and period elongated for both genes. In D:D (Fig. 1C), *bHLH1a* and *bHLH1b* showed an increase in relative transcript abundance during the subjective day that was comparable to that observed in L:D, but the decrease during the subjective night was less pronounced (Fig. 1C and SI Appendix, Fig. S1). Because iron metabolism is diurnally regulated in *P. tricornutum* and iron starvation strongly affects rhythmic gene expression (32), we further examined the *bHLH1a* and *bHLH1b* expression profiles in cells grown in iron replete and deplete conditions by using public transcriptome datasets (32). In this analysis, *bHLH1a* and *bHLH1b* showed similar expression patterns in both control and iron starvation conditions, with peak expression at ZT9 in cells grown in 12L:12D photocycles (SI Appendix, Fig. S3). Together, these results demonstrate the robust control of *bHLH1a* and *bHLH1b* expression timing. Of these proteins, we decided to further investigate the possible involvement of *bHLH1a* in the regulation of *P. tricornutum* rhythms.

Cellular Localization of bHLH1a Protein. To examine bHLH1a cellular localization, we generated transgenic lines expressing bHLH1a fused to a YFP-tag at the C-terminal under the regulation of the *Lhcf2p* promoter (33). Confocal laser scanning microscopy of bHLH1a-YFP-expressing cells showed colocalized signals of YFP with the Hoechst 33342 (DNA tracker) stain in the nucleus (Fig. 2A). This confirmed the predicted *in silico* localization (SI Appendix) of bHLH1a in the nucleus of *P. tricornutum*, further supporting its possible role as a transcriptional regulator.

bHLH1a Regulates Pace of Diel Gene Expression. To explore possible functions of bHLH1a in diel rhythmicity, we generated cell lines expressing HA-tagged bHLH1a under the regulation of the *Lhcf2p* promoter, which drives gene expression 3 h after the light onset (33). Immunoblot analysis performed at ZT7 and ZT12 in a 16L:8D regime revealed three independent bHLH1a-HA overexpressing lines, hereafter named OE1, OE2, and OE3 (Fig. 2B). The ectopic protein was detected at ZT7 and ZT12 in these lines. Analysis of *bHLH1a* total transcripts, both endogenous (*bHLH1a*) and transgenic (*bHLH1a-HA*) mRNAs, also showed earlier expression in the OE lines compared with the wild type (WT) (Fig. 2C and D).

To investigate the effect of bHLH1a deregulation on diel gene expression, WT and OE lines were grown in 16L:8D photocycles and sampled for RNA analysis. The expression of selected genes exhibiting a diurnal rhythmic expression pattern (Fig. 1) was analyzed in WT and OE1 sampled every 3 h over 24 h (Fig. 2C and SI Appendix, Fig. S4A). As described above, total *bHLH1a* transcript levels were higher in the OE line compared with the WT (Fig. 2C and D), but a decrease in endogenous *bHLH1a* transcripts was also observed (Fig. 2C and D). A similar pattern was also reported for the *bHLH1b* gene while *bHLH3* showed earlier expression in OE1 compared with the WT (Fig. 2C and D). In addition to the *bHLH* genes, altered expression patterns in OE1 were also found for other putative TF genes and cell cycle regulators (SI Appendix, Fig. S4A). To test a possible function of bHLH1a in the maintenance of diurnal rhythms in the absence of light inputs, the expression of genes found to be rhythmic in the WT in D:D (SI Appendix, Fig. S1) was analyzed also in OE1. Ten



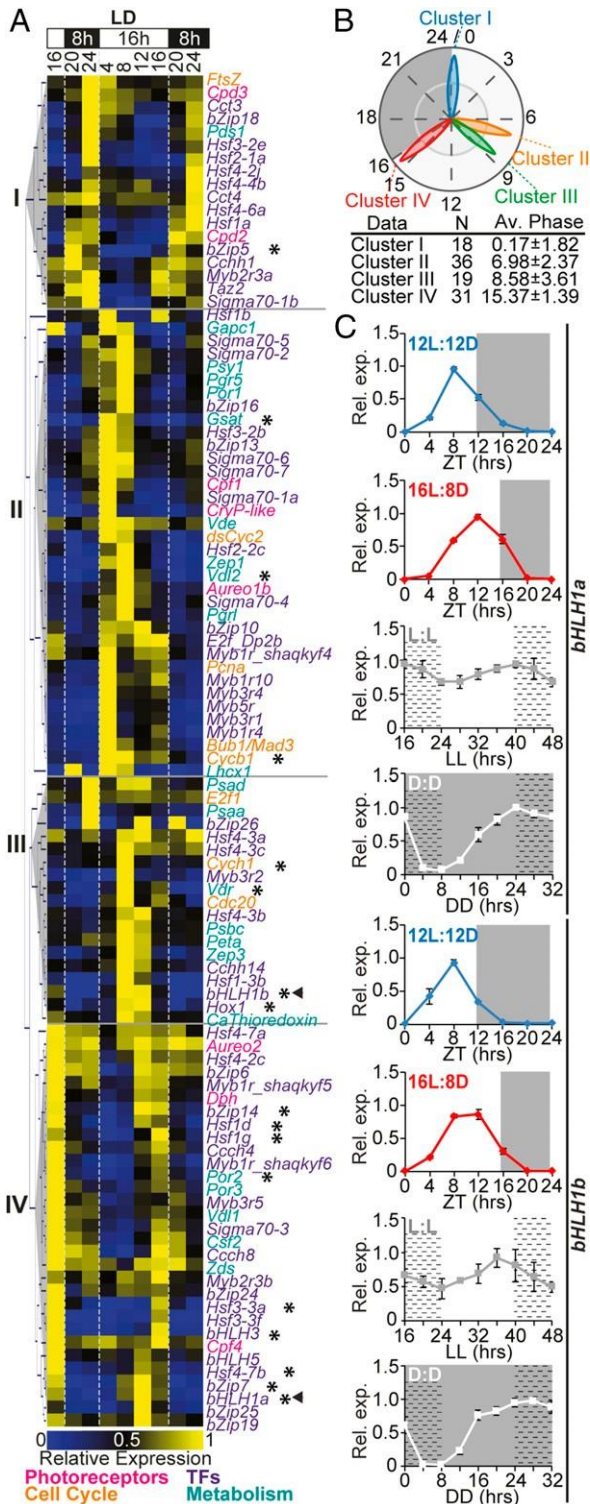
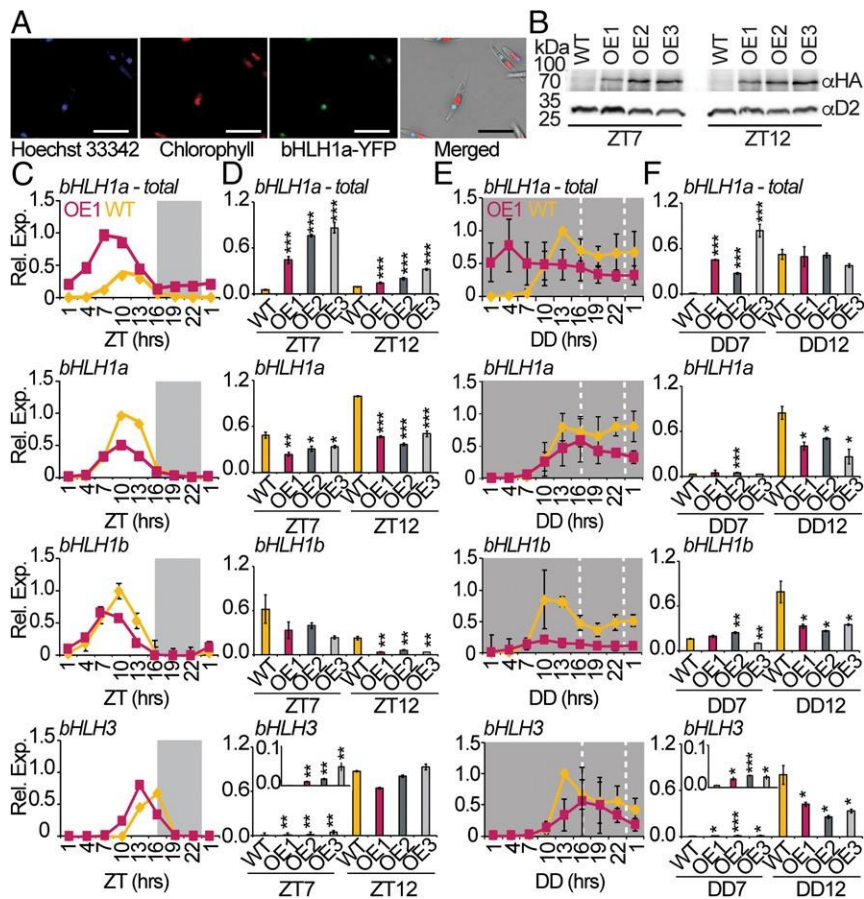


Fig. 1. Diurnal expression of rhythmic *P. tricornutum* genes. (A) Hierarchical clustering of gene expression profiles in 16L:8D, analyzed by nCounter analysis. Arrowheads highlight *bHLH1a* and *bHLH1b*; asterisks indicate the transcript profiles oscillating in D:D, shown in *SI Appendix, Fig. S1*. (B) Polar plot showing average phases of expression of the four clusters. N: number of genes within each cluster; Av. Phase: average phases ± SD. (C) *bHLH1a* and *bHLH1b* expression in 12L:12D, 16L:8D, L:L, and D:D (mean ± SEM,  $n = 3$ ). In L:L and D:D, cells entrained under 16L:8D cycles were released to continuous light or dark at ZT16. White and gray regions represent light and dark periods; dashed regions represent subjective nights in L:L and D:D. The expression value of each gene is relative to its maximum expression.

of 11 genes displayed reduced amplitudes and shifts in the phase of expression in OE1, compared with WT (Fig. 2E and *SI Appendix, Fig. S4B*). Analysis of *bHLH1a*, *bHLH1b*, and *bHLH3* in OE2 and OE3 at ZT7 and ZT12 in L:D (Fig. 2D) and at DD7 and DD12 in D:D (Fig. 2F) suggested a similar deregulation of gene expression in independent transgenic lines.

The Ectopic Overexpression of *bHLH1a* Results in Altered Circadian Rhythms. We next questioned if, beside gene expression, other physiological rhythms were regulated by *bHLH1a*. With this aim, daily cellular fluorescence was analyzed using the flow cytometer channel FL3-A that estimates chlorophyll *a* cellular content (8, 29). Cellular fluorescence displayed strong oscillations in 16L:8D grown cultures with a periodicity of ~24 h (Fig. 3A and *SI Appendix, Table S2*). Cell fluorescence in WT cultures increased during daytime to phase around ZT12 (Fig. 3A) and then started to decrease before night onset. Fluorescence progressively declined during the night period, reaching a trough in the early morning at ZT0 (Fig. 3A). In synchronized cells, the increase of FL3-A fluorescence is concomitant with the increase in the proportion of G2/M cells, and a decrease in the FL3-A relates to an increase in cell concentration (29) (*SI Appendix, Fig. S5*), likely reflecting chloroplast partitioning to daughter cells during cell division. Despite maintaining period rhythmicity in the cellular fluorescence dynamics, all three OE lines displayed less synchronized phenotypes, resulting in higher variability of waveforms among replicates compared with WT (Fig. 3A). Phase-time estimations using the FFT-NLLS method identified significant shifts of ~2 h in the maximum fluorescence timing in OE1 and OE2 compared with the WT (Fig. 3A and B and *SI Appendix, Fig. S6 and Table S2*). We then questioned if these oscillations were maintained in continuous blue light (L:L) as observed in other microalgae (24, 34). First, we found that under these conditions *bHLH1a* gene expression showed a stronger rhythmic pattern on the second subjective day (*SI Appendix, Fig. S7*), compared with the white L:L condition (Fig. 1C). WT cells also showed persistent fluorescence oscillations from LL33, with a period of ~27 h. These rhythms lasted to at least the fifth day of continuous light (Fig. 3C), supporting the hypothesis that they are self-sustained by an endogenous clock. Patterns of cell fluorescence oscillations in L:L were strongly altered in all three OE lines compared with WT (Fig. 3C and D and *SI Appendix, Figs. S8 and S9*) although similar growth rates were observed (*SI Appendix, Fig. S10*). Analysis via the Fast Fourier Transform Nonlinear Least Squares (FFT-NLLS) method showed that all lines maintained residual rhythmicity, but with a strong phase shift compared with the WT (Fig. 3C and D) and a reduced amplitude, with the OE2 being the less affected for the latter one (Fig. 3D and *SI Appendix, Figs. S8 and S9 and Table S3*). Additionally, OE lines also presented shorter periods than the WT, although OE1 lines lacked a significant difference most likely due to the variability introduced by the replicates with high relative amplitude error (*SI Appendix, Supplementary Methods, Fig. S8 C and D, and Table S3*). Fluorescence oscillations were similar between WT and an independent transgenic line expressing only the antibiotic resistance cassette (*SI Appendix, Fig. S11*), excluding a generic alteration of rhythmicity due to transgenesis. Based on these results, we named *bHLH1a* “RITMO1” (Italian word for “rhythm”) after its role as regulator of diatom diel rhythms.

RITMO1-Like Proteins Are Widely Represented in the Genome of Marine Algae. The *bHLH*-PAS proteins were thought to be restricted to the animal (Opisthokonta) lineage (35) until various sequencing projects revealed *bHLH*-PAS family members in microalgae (diatoms and *Nannochloropsis*) (36). Diatom proteins show peculiar features including a single predicted PAS domain, whereas animal *bHLH*-PAS proteins have two and an N-terminal extension that is absent in their animal counterparts (Fig. 4A). Through searching transcriptomic and genomic databases from Archaeplastida, Cryptophyta, Stramenopila, Alveolata, and basal Opisthokonta organisms (*SI Appendix, Table S4*), we discovered about 90 *bHLH*-PAS proteins. With one exception, the identified



**Fig. 2.** bHLH1a localizes in the nucleus, and its overexpression alters rhythmic diel gene expression. (A) Confocal fluorescence microscopy of *P. tricornutum* cells expressing the bHLH1a-YFP protein under the control of the *Lhcf2p* promoter. (Scale bar: 15  $\mu\text{m}$ .) (B) Immunoblot analysis of bHLH1a-HA protein at ZT7 and ZT12 in 16L:8D entrained WT and OE lines, using the anti-HA and anti-D2 (loading control) antibodies. (C) qRT-PCR analysis of *bHLH1a*, *bHLH1b*, and *bHLH3* in WT and OE1 cultures sampled in L:D every 3 h over 24 h (mean  $\pm$  SEM,  $n = 2$ ). (D) qRT-PCR analysis of the same genes at ZT7 and ZT12 in WT and OE1, OE2, and OE3 lines (mean  $\pm$  SEM,  $n = 3$ ). Inset in the *bHLH3* graph magnifies the ZT7 time point. (E) nCounter analysis of the *bHLH1a*, *bHLH1b*, and *bHLH3* over 24 h of continuous dark (D:D) in WT and OE1 lines (mean  $\pm$  SEM,  $n = 3$ ). (F) qRT-PCR analysis of the same genes at DD7 and DD12 in WT and OE1, OE2, and OE3 lines (mean  $\pm$  SEM,  $n = 3$ ). *bHLH1a-total* includes endogenous *bHLH1a* and *bHLH1a-HA* transgene transcripts; for all of the other genes, we refer to endogenous transcripts. The expression value of each gene is relative to its maximum expression. \* $P < 0.05$ , \*\* $P < 0.01$ , \*\*\* $P < 0.001$ , *t* test.

proteins showed a single predicted PAS domain, short C-terminal extensions, and N-terminal regions of variable length, similar to the predicted structure of diatom bHLH-PAS (Fig. 4A). Notably, we identified the first Archaeplastida bHLH-PAS that possesses two PAS domains like the animal proteins in *Galdieria sulphuraria* (Rhodophyta).

All of the identified sequences, including selected bHLH-PAS from Opisthokonta lineages, were used to perform a detailed phylogenetic analysis of the protein family using the bHLH and PAS domains. This analysis revealed that the majority of microalgal bHLH-PAS proteins fall into three separate clades, the first containing 9 TFs from diatoms and *Ectocarpus siliculosus*, the second comprising RITMO1 together with 35 proteins from diatoms and Alveolata (Dinoflagellata), and the third comprising 41 proteins from Alveolata (Ciliophora and Dinoflagellata) and diatoms, including bHLH1b (Fig. 4B). Interestingly, domain organization and branching positions of proteins from basal Opisthokonta (*Monosiga brevicollis*) and secondary endosymbiotic microalgae [*Guillardia theta* (Cryptophyta) and *Nannochloropsis* species (Stramenopila)] (Fig. 4B) support a possible common origin for this TF family from a heterotrophic ancestor (37) featuring single bHLH and PAS domains. However, the basal position and domain organization of the *G. sulphuraria* bHLH-PAS protein hint at a more complex scenario possibly involving endosymbiotic (horizontal) gene transfer, gene duplication/loss, and convergent evolution in the diversification of this family.

## Discussion

This study shows that diatoms integrate light signals from the environment as well as from an endogenous circadian clock to tightly regulate diel cellular activities. It also unveils the *P. tricornutum* RITMO1 protein of the bHLH-PAS transcription factor family as the first regulator of circadian rhythms to be found in these algae. RITMO1 displays robust diel expression patterns, which

are adjusted in a photoperiod-dependent manner and are unaffected by iron deficiency. As for other circadian clock-regulated genes in algae (24), the rhythmic expression of RITMO1 persists in cells exposed to continuous blue light, a dominant waveband in the ocean (27). However, RITMO1 transcription shows reduced oscillation amplitude in constant darkness, likely due to the lack of critical light time setting signals and alteration of metabolism due to the fact that photosynthesis is not dispensable in *P. tricornutum*. Thus, the RITMO1 expression timing is tightly regulated and likely subjected to multiple levels of control from different input regulators, conceivably blue light photoreceptors (27) and metabolism, as already observed for other clock genes in plants and animals (3, 4).

RITMO1 is involved in the transcriptional regulation of diel rhythms, as supported by consistent deregulation of transcript diurnal oscillations for several genes in RITMO1 OE lines in L:D, this pattern being accentuated in D:D. These results suggest, on one hand, that multiple light-driven processes participate in the regulation of daily gene expression, partially masking RITMO1's contribution to this process in cyclic environments and, on the other hand, reveal a key role for RITMO1 in the maintenance of rhythms in the absence of light-dark inputs. Furthermore, the observed down-regulation of the endogenous RITMO1 transcription in OE lines compared with the WT may reflect negative feedback regulation of RITMO1 controlling its own transcription. This would be compatible with this gene being part of a transcriptional feedback loop operating over the daily cycle (2). We also report robust oscillations of diatom cellular fluorescence in L:D cycles, as observed for gene expression. These rhythms persisted for at least five subjective days in L:L, supporting the existence of a circadian clock regulating diatom physiology. The oscillations in L:L have a period slightly longer than 24 h under free running conditions, a common feature in circadian clock-regulated processes (1, 2). The deregulation of



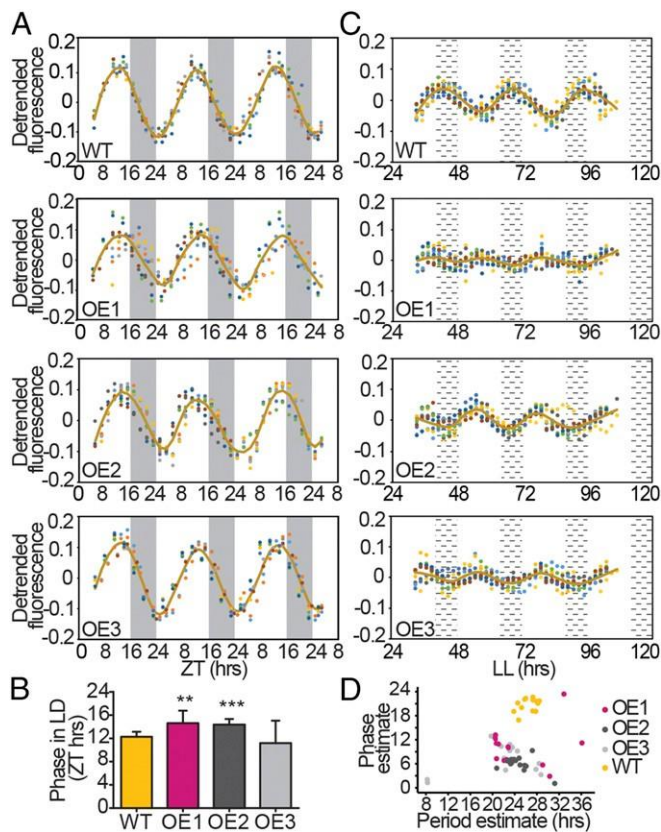


Fig. 3. bHLH1a overexpression alters circadian rhythms of cellular fluorescence. (A) Diurnal oscillation of chlorophyll fluorescence (FL3-A parameter) in WT and OE lines entrained under 16L:8D over 3 d ( $n \geq 8$ ). (B) Phase-time calculation of the FL3-A value in WT and OE lines (mean  $\pm$  SD,  $n \geq 8$ ,  $**P < 0.01$ ,  $***P < 0.001$ ,  $t$  test). (C) Circadian oscillation of chlorophyll fluorescence in representative WT and OE lines under continuous blue light (L:L) over 4 subjective days ( $n = 8$ ). (D) Plot of phase against period estimates in L:L ( $n = 15$ ). Dots of different color indicate independent replicate cultures. White and gray regions represent light and dark periods; black dashed regions represent subjective nights. Brown lines in plots represent the fitted curves (lowess fit) of the average FL3-A.

RITM01 expression in transgenic lines shifts the phase of fluorescence rhythms in L:D compared with the WT. In constant blue light (L:L), all of the independent OE lines showed altered rhythmicity if compared with the WT and a transgenic control line, with a strongly altered phase, reduced amplitude, and the period also being remarkably perturbed. Although multiple factors may account for the slight phenotypic differences observed between OE lines (e.g., chromosomal position effects on the transgenes, deregulation of other genetic or epigenetic processes due to the overexpression), the consistent deregulation of rhythmicity is coherent with a role of RITM01 in the regulation of circadian rhythms. Because all of the OE lines show a normal growth rate compared with WT, the observed altered rhythmicity is likely due to a defect in retrieving synchrony in chloroplast ontogeny and cell cycle progression, which are closely coupled in diatoms (20).

Together, our results support the hypothesis that RITM01 is one component of the still-uncharacterized endogenous circadian clock in diatoms. RITM01 contains bHLH and PAS protein domains that are also present in the CLOCK and BMAL proteins, components of the mammalian central circadian oscillator (2, 5, 38). Interestingly, previous studies have shown that the *P. tricornutum* animal-like blue light sensor Cpf1 can repress the transcriptional activity of these proteins in a heterologous mammalian cell system (25), suggesting at least partial conservation in the regulatory program generating rhythmicity in animals and diatoms.

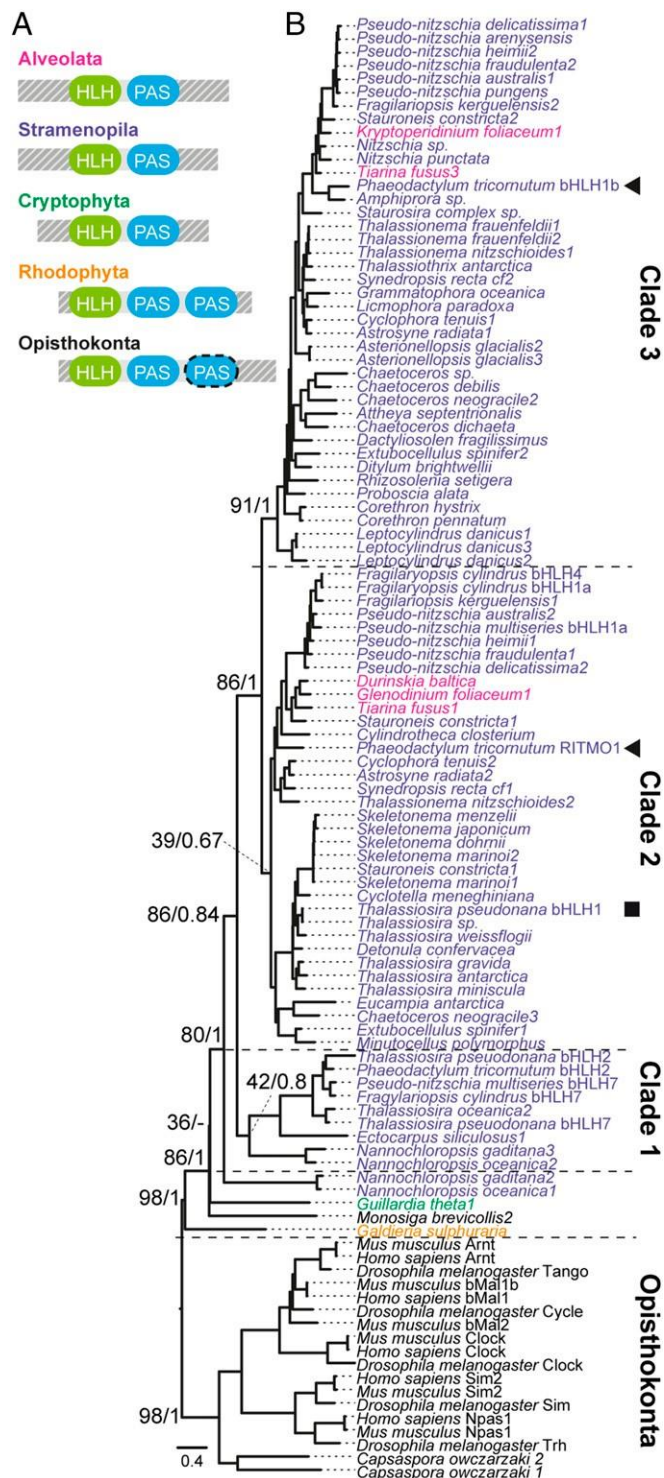


Fig. 4. bHLH-PAS protein family structure and phylogeny. (A) bHLH-PAS protein domain schematic architecture in eukaryotes. Dotted line indicates possible absence of the second PAS in some Opisthokonta species; gray patterns represent the variations in N-terminal and C-terminal length in different groups. (B) Maximum likelihood (ML) phylogenetic tree of the bHLH-PAS family (outgroup: the Opisthokonta clade) midpoint rooted. Numbers refer to bootstrap values of the basal nodes using ML (RAxML, 1,000 bootstraps) and Bayesian inference (MrBayes). Symbols indicate the position of *P. tricornutum* RITM01 and bHLH1b (arrows) and *T. pseudonana* bHLH1 (square).

We have reported several other putative TFs showing altered diel expression patterns in *RITMO1* OE cells (i.e., *bHLH1b*, *bHLH3*, *bZIP7*, *HSF1g*, *HSF4.7b*), which represent direct or indirect targets of *RITMO1* activity and possible additional components of the network generating circadian rhythms. *RITMO1* might also act downstream of signal transduction cascades activated by the diatom photoreceptors (27). Therefore, *RITMO1* now represents a key molecular entry point for the identification of other diatom timekeeper components and the input–output pathways interacting with the clock.

Biological rhythms are still poorly understood at the molecular level in many phyla of marine algae such as Stramenopila. Our phylogenetic analysis revealed a wide distribution of *RITMO1*-like bHLH-PAS proteins in diatoms, as well as in other algae. The similarities in the timing of expression between *RITMO1* and its homolog in the diatom *T. pseudonana* (*TpHLH1*) (17) suggest that these proteins may play a similar role in the regulation of cellular rhythmicity. Regulators such as *RITMO1* may have played a critical role for diatom prominence in marine ecosystems by synchronizing cellular activities in optimal temporal programs and maximizing the diatoms' ability to anticipate and adapt to cyclic environmental variations.

bHLH-PAS *RITMO1*-like proteins might have independently acquired a function in rhythm regulation by convergent evolution (6). However, the existence of this function in an ancient heterotrophic marine ancestor that subsequently acquired plastids via endosymbiosis events (12) and before colonization of land cannot be excluded. Thus, further characterization of *RITMO1*-like proteins is expected to provide insights into the evolution of biological rhythms and their significance for life in the marine environment.

- C. S. Pittendrigh, Temporal organization: Reflections of a Darwinian clock-watcher. *Annu. Rev. Physiol.* 55, 16–54 (1993).
- D. Bell-Pedersen *et al.*, Circadian rhythms from multiple oscillators: Lessons from diverse organisms. *Nat. Rev. Genet.* 6, 544–556 (2005).
- K. Greenham, C. R. McClung, Integrating circadian dynamics with physiological processes in plants. *Nat. Rev. Genet.* 16, 598–610 (2015).
- H. Reinke, G. Asher, Crosstalk between metabolism and circadian clocks. *Nat. Rev. Mol. Cell Biol.* 20, 227–241 (2019).
- J. C. Dunlap, Molecular bases for circadian clocks. *Cell* 96, 271–290 (1999).
- M. Rosbash, The implications of multiple circadian clock origins. *PLoS Biol.* 7, e62 (2009).
- M. Moulager *et al.*, Light-dependent regulation of cell division in *Ostreococcus*: Evidence for a major transcriptional input. *Plant Physiol.* 144, 1360–1369 (2007).
- M. Ragni, M. R. D'Alcala, Circadian variability in the photobiology of *Phaeodactylum tricornutum*: Pigment content. *J. Plankton Res.* 29, 141–156 (2007).
- Z. B. Noordally, A. J. Millar, Clocks in algae. *Biochemistry* 54, 171–183 (2015).
- E. Poliner, C. Cummings, L. Newton, E. M. Farré, Identification of circadian rhythms in *Nannochloropsis* species using bioluminescence reporter lines. *Plant J.*, 10.1111/tpj.14314 (2019).
- S. Malviya *et al.*, Insights into global diatom distribution and diversity in the world's ocean. *Proc. Natl. Acad. Sci. U.S.A.* 113, E1516–E1525 (2016).
- A. Moustafa *et al.*, Genomic footprints of a cryptic plastid endosymbiosis in diatoms. *Science* 324, 1724–1726 (2009).
- C. Bowler *et al.*, The *Phaeodactylum* genome reveals the evolutionary history of diatom genomes. *Nature* 456, 239–244 (2008).
- S. Flori *et al.*, Plastid thylakoid architecture optimizes photosynthesis in diatoms. *Nat. Commun.* 8, 15885 (2017).
- A. E. Allen *et al.*, Evolution and metabolic significance of the urea cycle in photosynthetic diatoms. *Nature* 473, 203–207 (2011).
- B. Bailleul *et al.*, Energetic coupling between plastids and mitochondria drives CO<sub>2</sub> assimilation in diatoms. *Nature* 524, 366–369 (2015).
- J. Ashworth *et al.*, Genome-wide diel growth state transitions in the diatom *Thalassiosira pseudonana*. *Proc. Natl. Acad. Sci. U.S.A.* 110, 7518–7523 (2013).
- M. S. Chauton, P. Winge, T. Brembu, O. Vadstein, A. M. Bones, Gene regulation of carbon fixation, storage, and utilization in the diatom *Phaeodactylum tricornutum* acclimated to light/dark cycles. *Plant Physiol.* 161, 1034–1048 (2013).
- M. J. Huysman *et al.*, AUREOCHROME1a-mediated induction of the diatom-specific cyclin *dsCYC2* controls the onset of cell division in diatoms (*Phaeodactylum tricornutum*). *Plant Cell* 25, 215–228 (2013).
- M. J. Huysman *et al.*, Genome-wide analysis of the diatom cell cycle unveils a novel type of cyclins involved in environmental signaling. *Genome Biol.* 11, R17 (2010).
- A. Volpert, S. Graff van Crevel, S. Rosenwasser, A. Vardi, Diurnal fluctuations in chloroplast GSH redox state regulate susceptibility to oxidative stress and cell fate in a bloom-forming diatom. *J. Phycol.* 54, 329–341 (2018).

## Methods

**Culture Conditions.** WT *P. tricornutum* (Pt1 8.6) cells and transgenic lines were grown in *f/2* Guillard media, as described in *SI Appendix*.

**Gene Expression Analyses.** To select genes with rhythmic expression, we used data from (18, 39). Total RNA was extracted as described in ref. 31 and analyzed by qRT-PCR and nCounter analysis as described in *SI Appendix*. Proteins were analyzed as previously described (25).

**Generation of the *bHLH1a* Transgenic Lines.** Diatom cell lines overexpressing bHLH1a-HA and bHLH1a-YFP were obtained by cotransformation of the Nourseothricin resistance plasmid (pNAT) together with the pDEST-C-HA-*bHLH1a* and the pDEST-C-YFP-*bHLH1a* plasmids, respectively. Details of vectors and transformation are provided in *SI Appendix*.

**Microscopic Analysis.** Images were produced with the confocal laser scanning microscope Leica SP8× as described in *SI Appendix*.

**Data Mining, Protein Sequence, and Phylogenetic Analysis.** Detailed information about data mining, protein sequence, and phylogenetic analysis is provided in *SI Appendix*.

**ACKNOWLEDGMENTS.** We thank M. Jaubert, L. De Veylder, R. Dorrell, and P. Oliveri for critical suggestions; D. Petroustos and G. Finazzi for support in monitoring cell physiology; G. Benvenuto for assistance in microscopy; and the Institut de Biologie Paris-Seine imaging core facility for help with flow cytometry. This work was funded by Human Frontier Science Program Grant RGY0082/2010; the Gordon and Betty Moore Foundation Grant GBMF 4966; the European Union H2020 EMBRIC Grant G.A. 654008; and the Fondation Bettencourt Schueller (A.F.). M.J.J.H. is currently an employee of the European Research Council Executive Agency. The views expressed are purely those of the writer and may not in any circumstances be regarded as stating an official position of the European Commission.

- J. M. Zones, I. K. Blaby, S. S. Merchant, J. G. Umen, High-resolution profiling of a synchronized diurnal transcriptome from *Chlamydomonas reinhardtii* reveals continuous cell and metabolic differentiation. *Plant Cell* 27, 2743–2769 (2015).
- E. Poliner *et al.*, Transcriptional coordination of physiological responses in *Nannochloropsis oceanica* CCMP1779 under light/dark cycles. *Plant J.* 83, 1097–1113 (2015).
- F. Corellou *et al.*, Clocks in the green lineage: Comparative functional analysis of the circadian architecture of the picoeukaryote *ostreococcus*. *Plant Cell* 21, 3436–3449 (2009).
- S. Coesel *et al.*, Diatom PtCPF1 is a new cryptochrome/photolyase family member with DNA repair and transcription regulation activity. *EMBO Rep.* 10, 655–661 (2009).
- A. E. Fortunato, R. Annunziata, M. Jaubert, J. P. Bouly, A. Falciatore, Dealing with light: The widespread and multitasking cryptochrome/photolyase family in photosynthetic organisms. *J. Plant Physiol.* 172, 42–54 (2015).
- M. Jaubert, J. P. Bouly, M. Ribera d'Alcala, A. Falciatore, Light sensing and responses in marine microalgae. *Curr. Opin. Plant Biol.* 37, 70–77 (2017).
- E. Rayko, F. Maumus, U. Maheswari, K. Jabbari, C. Bowler, Transcription factor families inferred from genome sequences of photosynthetic stramenopiles. *New Phytol.* 188, 52–66 (2010).
- H. M. Hunsperger, C. J. Ford, J. S. Miller, R. A. Cattolico, Differential regulation of duplicate light-dependent protochlorophyllide oxidoreductases in the diatom *Phaeodactylum tricornutum*. *PLoS One* 11, e0158614 (2016).
- A. Banerjee *et al.*, Allosteric communication between DNA-binding and light-responsive domains of diatom class I aureochromes. *Nucleic Acids Res.* 44, 5957–5970 (2016).
- A. E. Fortunato *et al.*, Diatom phytochromes reveal the existence of far-red-light-based sensing in the Ocean. *Plant Cell* 28, 616–628 (2016).
- S. R. Smith *et al.*, Transcriptional orchestration of the global cellular response of a model pennate diatom to diel light cycling under iron limitation. *PLoS Genet.* 12, e1006490 (2016).
- M. T. Russo, R. Annunziata, R. Sanges, M. I. Ferrante, A. Falciatore, The upstream regulatory sequence of the light harvesting complex *Lhcf2* gene of the marine diatom *Phaeodactylum tricornutum* enhances transcription in an orientation- and distance-independent fashion. *Mar. Genomics* 24, 69–79 (2015).
- R. Braun, E. M. Farré, U. Schurr, S. Matsubara, Effects of light and circadian clock on growth and chlorophyll accumulation of *Nannochloropsis gaditana*. *J. Phycol.* 50, 515–525 (2014).
- J. Yan, Z. Ma, X. Xu, A. Y. Guo, Evolution, functional divergence and conserved exon-intron structure of bHLH/PAS gene family. *Mol. Genet. Genomics* 289, 25–36 (2014).
- S. Thiriet-Rupert *et al.*, Transcription factors in microalgae: Genome-wide prediction and comparative analysis. *BMC Genomics* 17, 282 (2016).
- J. Brodie *et al.*, The algal revolution. *Trends Plant Sci.* 22, 726–738 (2017).
- N. Gekakis *et al.*, Role of the CLOCK protein in the mammalian circadian mechanism. *Science* 280, 1564–1569 (1998).
- R. Annunziata *et al.*, Data from “bHLH-PAS protein *RITMO1* regulates diel biological rhythms in the marine diatom *Phaeodactylum tricornutum*.” Gene Expression Omnibus. <https://www.ncbi.nlm.nih.gov/geo/query/acc.cgi?acc=GSE112268>. Deposited 23 March 2018.

## SI APPENDIX

### SUPPLEMENTARY METHODS

#### Culture and irradiation conditions

Wild-type *P. tricornutum* (Pt1 8.6; CCMP2561) cells and transgenic lines were grown in f/2 Guillard media (1). For experiments in different photoperiods, cultures were pre-adapted to the different L:D cycles for 2 weeks before starting the experiment. For L:D experiments, cells were illuminated at 40  $\mu\text{mol photons m}^{-2} \text{s}^{-1}$  of white light (Philips TL-D De Luxe Pro 950) either for 16 or 12 hours. For gene expression experiments in continuous darkness and continuous light, cells were pre-adapted in 16L:8D photocycles for 2 weeks, then transferred to D:D or L:L at the start of the experiment. For fluorescence measurement and growth analysis experiments in free running L:L conditions, cells were grown in 16L:8D cycles, then transferred to 15  $\mu\text{mol photons m}^{-2} \text{s}^{-1}$  of blue light from ZT12 onwards. Cell concentrations were measured using a MACSQuant Analyser flow cytometer (Miltenyi Biotec, Germany) by counting the cells based on the R1-A (630 nm excitation, 670-700 nm emission) versus the R1-H parameters. Growth rates ( $\mu$ ) were calculated during the exponential phase of growth over four days. Cellular fluorescence rhythmicity assays were carried out by measuring the flow cytometer FL3-A parameter (488 nm excitation, 655-730 nm emission).

#### Analysis of the rhythmic processes

For the analysis of rhythmic parameters, each FL3-A fluorescence dataset was amplitude and baseline detrended, then normalized to the maximum value. For graphical representations, data were aligned to the mean values. Fitted curves of the average FL3-A fluorescence were calculated using the lowess fit function in R (span = 0.35). Circadian period, amplitudes and phases were calculated by Fast Fourier nonlinear least square algorithm (FFT-NLLS), evaluated within a period range of 20 and 30 h using the Biodare2 tool (biodare2.ed.ac.uk, (2)). This analysis allows to formally identify differences in rhythm profiles using the Relative Amplitude Errors (RAE) as a reliable proxy for rhythmic coherence. The RAE is a measure of goodness-of-fit to a theoretical sine wave. RAE is defined as the ratio of the amplitude error to the most probable derived amplitude magnitude. The RAE value ranges from 0.0 to 1.0, with 0.0 meaning a rhythmic component has an infinite precision and with 1.0 meaning the rhythm is not significant (error exceeds the most probable amplitude magnitude) (3). For L:L analyses, periods, phases and amplitudes were estimated starting from 33 h after the last dark/light transition. To evaluate if cell lines presented altered rhythmic traits, the obtained periods and

phases were plotted against the RAE (Table S3 and Fig. S9) so to provide a measure of how well the observed outcomes are replicated by the fitted cos waves, as previously described (4). Eight to nine independent biological replicates were considered for the analysis in 16L:8D conditions (Table S2), while fifteen biological replicates were considered for the analysis in L:L conditions (Table S3). Three periods of oscillations were considered for each replicate in all period estimation analyses. Two-tailed t-test was used to determine statistical differences between mean phases, amplitudes, periods and RAEs (Fig 3, Fig. S8, Table S2 & S3).

### **RNA extraction and transcript analyses**

For qRT-PCR analysis, *RPS* and *TBP* were used as reference genes. Each independent replicate of the qRT-PCR data was normalized against the maximum expression value of each gene (*i.e.*, gene expression range lies between 0 and 1 across the time series). Average expression and standard error were then calculated and plotted. The full list of oligonucleotides used in this work can be found in Table S5. For the nCounter analysis, gene specific probes (Table S1) were designed and screened against the *P. tricornutum* annotated transcript database (JGI, genome version 2, Phatr2) for potential cross-hybridization. Total RNA extracts (100 ng) from three biological replicates were used for hybridization. Transcript levels were measured using the nCounter analysis system (Nanostring Technologies) at the UCL Nanostring Facility (London, UK) and at the Institut Curie technical platform (Paris, France) as previously described (5). Expression values were first normalized against the internal spike-in controls, then against the geometric mean of the reference genes *RPS* and *TBP*. The 12L:12D and 16L:8D experiments of Fig. 1 were analysed by qPCR, while L:L and D:D experiments were analysed by nCounter. All sequence data in this publication have been deposited in National Center for Biotechnology Information Gene Expression Omnibus (6).

### **Immunoblot analysis**

Proteins were extracted as previously described (7). Membranes were blocked with PBS-T 5% milk and incubated overnight at 4° C with  $\alpha$ -HA (Covance) (1:2000) antibody and an  $\alpha$ -D2 (1:10000) antibody used as loading control. Following incubation with HRP-conjugated 521 secondary antibodies (Promega), proteins were detected with Clarity reagents (Bio-Rad) and imaged with a G:Box camera (Syngene, UK).



### **bHLH1a subcellular localization**

bHLH1a protein sequence was scanned using two online tools for subcellular localization prediction: ELSpred (8) and DeepLoc (9). For microscopic analysis, chlorophyll autofluorescence and YFP fluorescence were excited at 510 nm and detected at 650–741 nm and 529–562 nm respectively. Hoechst 33342 (Life Technologies) was used at a final concentration of 5 µg/ml to stain nuclear DNA and stained cells were visualized by illumination at 405 nm and detection at 424–462 nm.

### **Generation of the *bHLH1a* transgenic lines**

The full length *bHLH1a* coding sequence was obtained by PCR amplification with the specific oligonucleotides *PtbHLH1a*-DraI-Fw and *PtbHLH1a*-XhoI-Rv on cDNA template using the Phusion high fidelity DNA polymerase (Thermo Fisher, USA). The PCR fragment was inserted into the pENTR1A vector (Invitrogen, USA) using the DraI/XhoI restriction sites, and recombined with the pDEST-C-HA vector or the pDEST-C-YFP vector (10) both driving expression of the transgenes under the control of the *Light harvesting complex protein family F2* promoter (*Lhcf2p*). Transgenic lines were generated as in (11). Transformed cells were tested for the presence of the transgene by PCR and qRT-PCR analysis (see Table S5 for oligonucleotide sequences).

### **Selection of rhythmic transcripts and clustering analysis**

For the selection of genes with rhythmic expression in the light-dark cycle, we used microarray data from (12). First, we identified all the genes belonging to the TFs, photoreceptors, cell cycle and metabolism-related categories (pigment synthesis and photosynthesis). Then, transcripts were ranked based on a defined t-value for each time point (mean gene expression of the replicate/(1+s.d.)) and those showing t-value  $>+0.7$  or  $<-0.7$  across the time series, were retained. The nCounter expression data was normalized against the maximum expression value of each gene, in a similar way to qRT-PCR expression data. This normalization was applied to the 3 replicates independently and for each condition (L:D and D:D) with the average expression value used for the clustering analysis. Hierarchical clustering analysis was performed with MeV 4.9 (13) using Pearson correlation. Peak analysis was performed using the MFourfit curve-fitting method defining average expression phases for each cluster (<https://biodare2.ed.ac.uk>, (2)).

For the selection of rhythmic transcripts in D:D, expression values were normalized using *RPS*, *TBP* and *ACTIN12* as reference genes. The genes with the highest values of standard

deviation from the average expression over the two time courses (16L:8D and D:D) were selected. A threshold equal to 1 was set using the published *P. tricornutum* diurnal microarray dataset (12) as background. Gene expression profiles were further empirically examined and false positives eliminated.

### **Data mining, protein sequence and phylogenetic analysis**

The *P. tricornutum* bHLH1a (Phatr3\_J44962) protein sequence was used as the query for BlastP analyses on the JGI, NCBI and MMETSP public database (14). The Pfam database was also searched for proteins possessing both the HLH and PAS domains. The retrieved sequences were analyzed using the batch search tool on the CDD (Conserved Domain Database) NCBI server to retrieve proteins presenting at least one HLH and one PAS domain only. We identified 100 HLH-PAS proteins from 71 marine algal species which were aligned using MAFFT (15), along with 22 HLH-PAS proteins from relevant metazoan (*Homo sapiens*, *Mus musculus* and *Drosophila melanogaster*) and unicellular Opisthokonta (*Monosiga brevicollis* and *Capsaspora owczarzaki*). As previously reported (16), no bHLH-PAS proteins were identified in Archaeplastida organisms, with the exception of the Rhodophyta alga *Galdieria sulphuraria*. Preliminary phylogenies were produced with MEGA 7 (17) to eliminate ambiguously aligned sequences, refining the alignment to 107 sequences and a final length of 198 aa (<5% gap per position). The best amino acid model to fit the data was estimated with ProtTest 3.4.2 (18). Phylogenetic analyses were performed with RAxML (1000 bootstraps) and MrBayes 3.2.6 (2.5 million generations, 2 runs, 25% burn-in) on the CIPRESS gateway (19). The final tree was edited in Figure Tree 1.4 ([http://tree.bio.ed.ac.uk/software/Figure tree/](http://tree.bio.ed.ac.uk/software/Figure%20tree/)). GenBank accession codes of the genes utilized in the bHLH-PAS phylogenetic analysis are reported in Table S4.

### **Cell cycle analysis**

*P. tricornutum* Wt and transgenic cells were synchronized in the G1 phase with prolonged darkness for 40h. After re-illumination, the FL3-A parameter was measured in cultures on an hourly basis for 12h using a flow cytometer (Miltenyi Biotec, Germany). At the same time, samples were harvested for cell cycle analysis. Cells were pelleted by centrifugation (4000 rpm, 15 minutes, 4°C), fixed in 70% EtOH and stored in the dark at 4°C until processing. Fixed cells were then washed three times with PBS, stained with 4',6-diamidino-2-phenylindole (at a final concentration of 1 ng/ml) on ice for 30', then washed and resuspended in PBS. After staining, samples were immediately analyzed with a MACSQuant Analyser flow cytometer (Miltenyi Biotec, Germany). For each sample 30,000 cells were analysed and G1 and G2 proportions

were inferred by calculating the 2c and 4c peak areas at 450 nm (V1-A channel) using the R software. A peak calling method was applied to the resulting histogram, based on a 1<sup>st</sup> derivative approach (20). The locations of G1 and G2 peaks were first determined using G1 and G2 reference samples and then used to identify G1 and G2 cells in the experimental samples. The area under each peak was used as a proxy for the proportion of cells in each population.

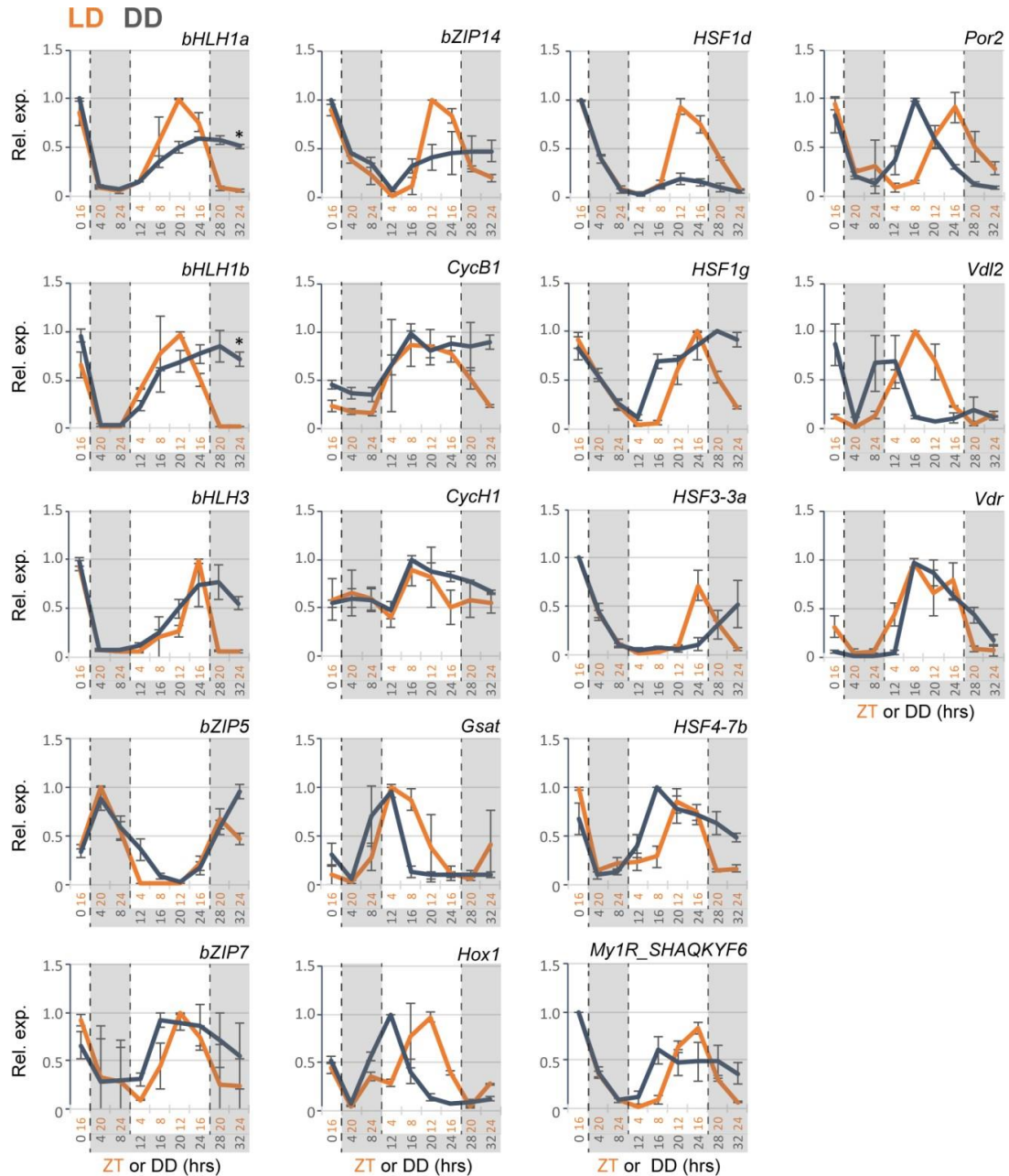


**Fig. S1. nCounter expression analysis of genes maintaining rhythmic expression in D:D condition and 16L:8D condition in Wt cells.** Data represent the average expression of biological triplicates  $\pm$ SD and are normalized using the *RPS*, *TBP* and *ACTIN12* reference genes. Expression values are given relative to the maximum expression for each gene, where ‘1’ represents the highest expression value of the time series. Results for cells grown in 16L:8D cycle are shown in orange (L:D); results for cells in constant darkness (following 16L:8D adaptation) are shown in grey (D:D). For the *bHLH1a* and *bHLH1b* profiles in D:D, the asterisks on the last time points indicate that the expression at DD32 is significantly decreased with respect to the peak of expression of each gene (DD24 for *bHLH1a* and DD28 for *bHLH1b*)(\* $P$ <0.05, t-test).



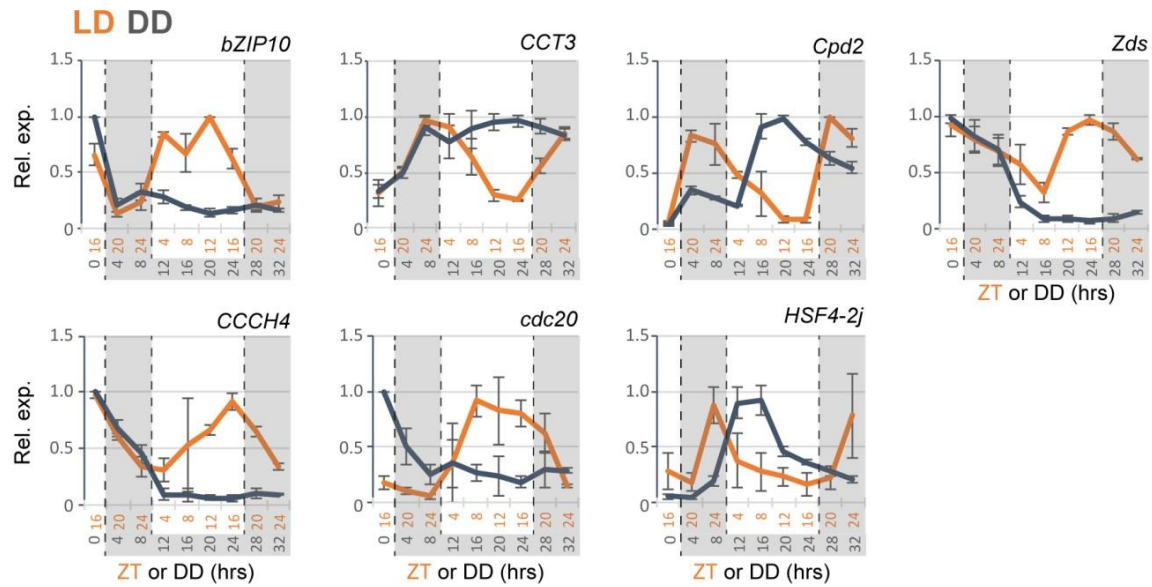


**Fig. S2. nCounter expression analysis of representative genes with altered rhythmic expression in Wt cells in D:D condition compared to 16L:8D condition.** Expression values represent the average of three biological triplicates  $\pm$ SD and are normalized using the *RPS*, *TBP* and *ACTIN12* reference genes. Expression values are given relative to the maximum expression for each gene, where ‘1’ represents the highest expression value of the time series. Results for cells grown in 16L:8D cycle are shown in orange (L:D); results for cells in constant darkness (following 16L:8D adaptation) are shown in grey (D:D).

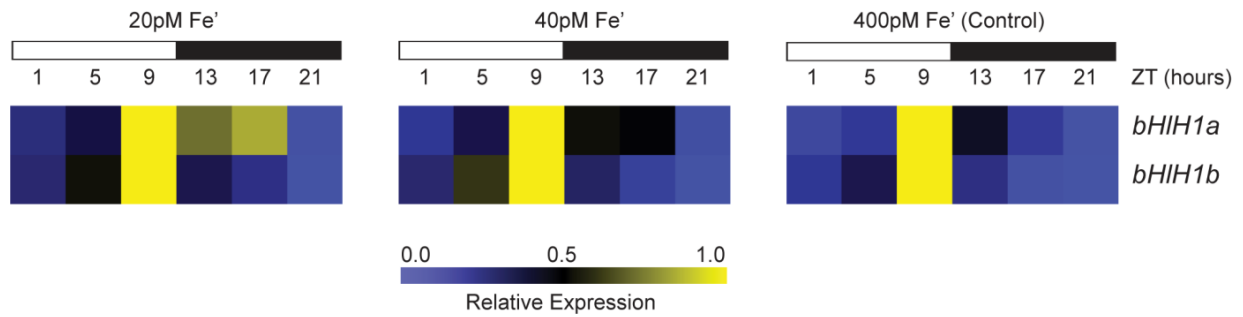


**Fig. S3. Diel expression patterns of *bHLH1a* and *bHLH1b* genes under Fe-depletion conditions in 12L:12D photoperiods.** Diel expression patterns of *bHLH1a* and *bHLH1b* in normal (400 pM Fe') and iron depletion conditions (40 and 20 pM Fe') were obtained using transcriptome data extracted from (21). Light and dark periods are represented by white and black rectangles. Expression values are given relative to the maximum expression for each gene, where '1' represents the highest expression value of the time series.

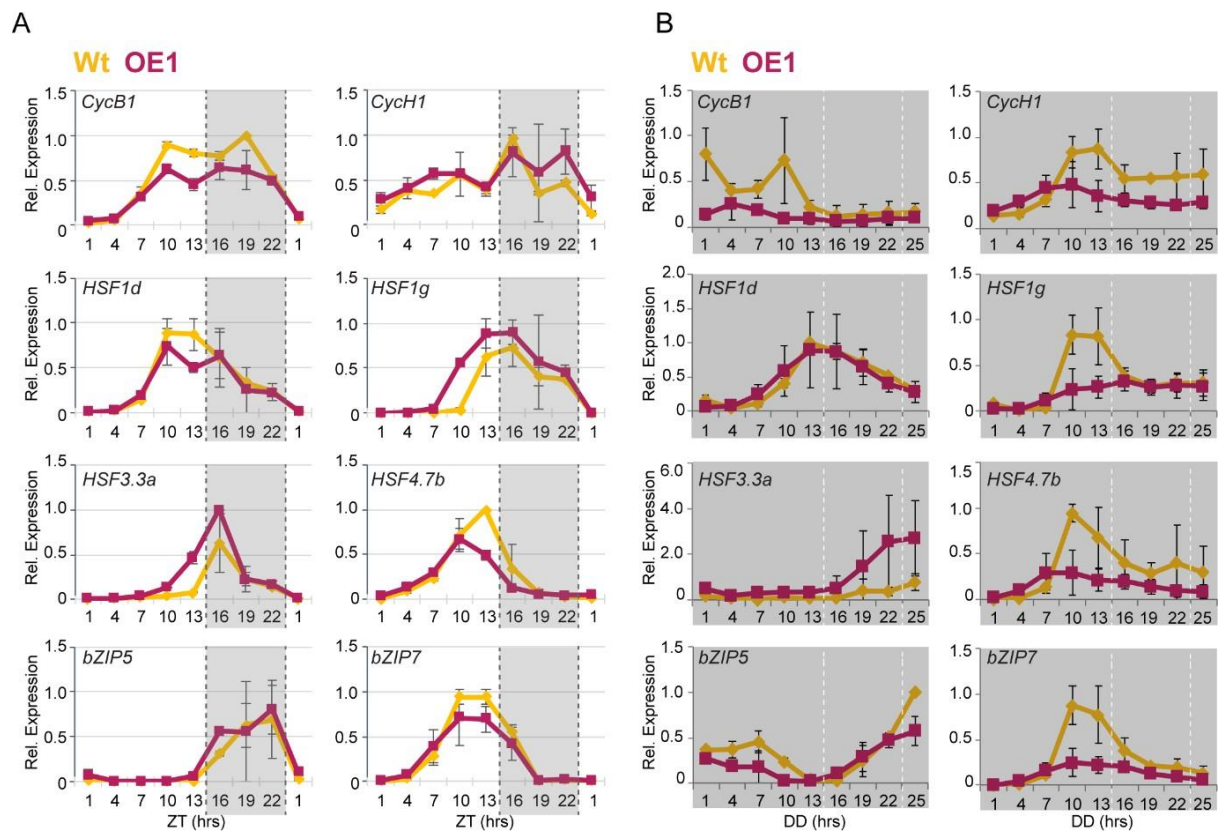


**Fig. S4. Analysis of selected rhythmic gene expression profiles in L:D and D:D in Wt and *bHLH1a* OE1 cells.** Cells were entrained in 16L:8D cycles, then kept in L:D or transferred to D:D and collected every 3 hours for 24 hours. Expression values represent the average of three biological replicates ( $n=3$ )  $\pm$  s.e.m (black bars) and have been normalized using *RPS* and *TBP* genes. A: qRT-PCR analysis; B: nCounter analysis.

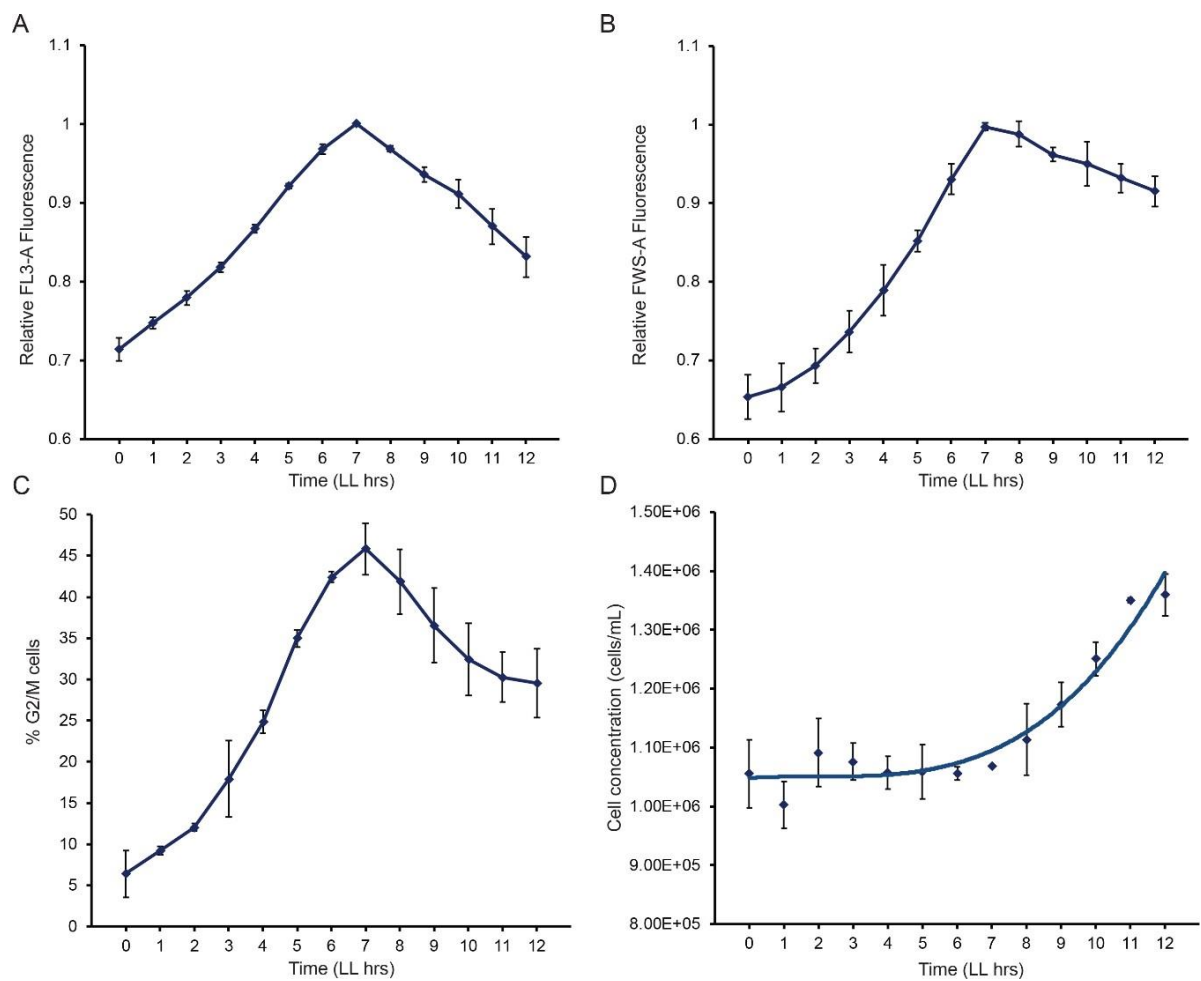


**Fig. S5. Cell cycle progression dynamics of *Wt P. tricornutum*.** A-B) Progression of chlorophyll fluorescence (FL3-A parameter) and cell size (FWS-A parameter) measured by flow cytometry each hour over 12h of illumination following dark synchronization. C) Proportion of cells in the G2 phase measured by flow cytometry each hour over 12h of illumination following dark synchronization. D) Hourly measures of cell density in re-illuminated cultures. The trend curve represents the third-degree polynomial regression. Results are representative of three biological replicates  $\pm$  s.e.m (black bars).

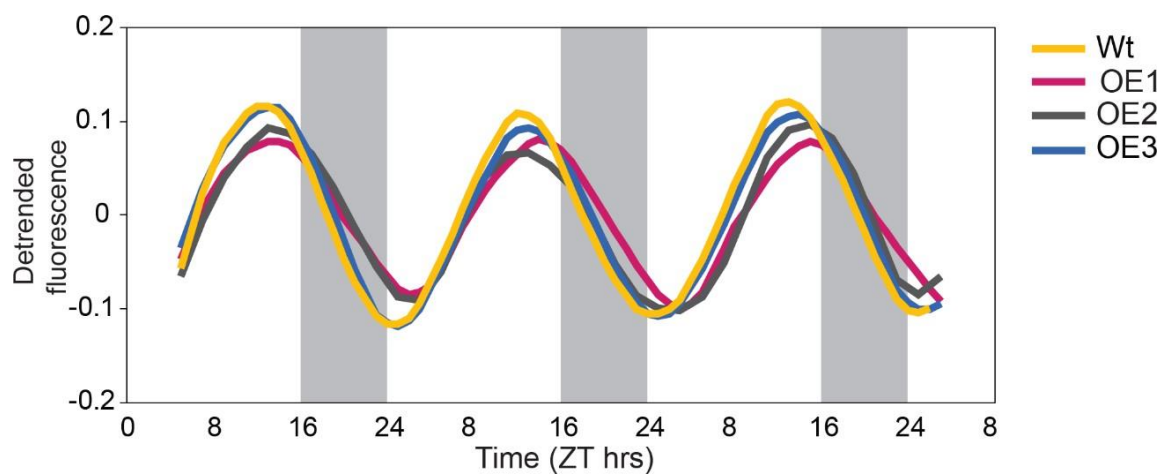


**Fig. S6 Diurnal oscillations of chlorophyll fluorescence (FL3-A parameter) in Wt and *bHLH1a* OE lines.** Lowess fitted curves of the mean FL3-A values in Wt and OE lines entrained under 16L:8D over 3 days ( $n \geq 8$ ).

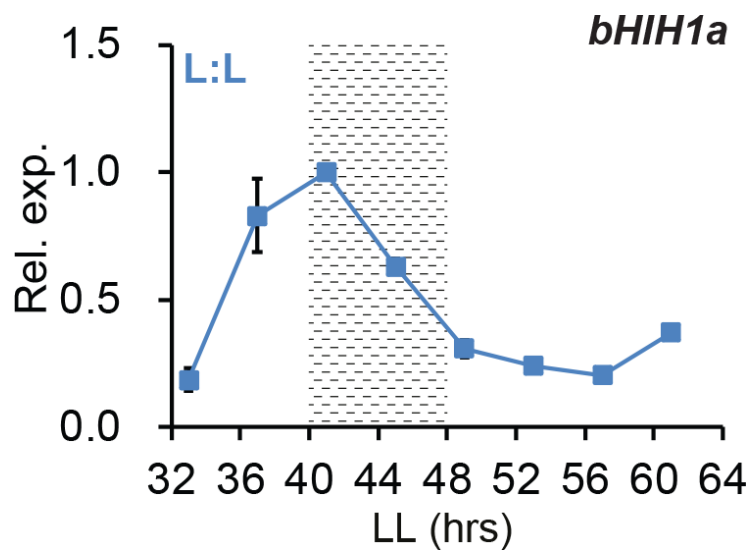


**Fig. S7. Analysis of *bHLH1a* gene expression in continuous blue light.** Cells were entrained in 16L:8D cycles, then transferred to constant blue light (L:L) and sampled every 4 hours for 28 hours. *bHLH1a* gene expression was analysed by qRT-PCR starting from L:L33. Expression values represent the average of two biological replicates (n=2)  $\pm$  s.e.m (black bars) and have been normalized using *RPS* and *TBP* genes. Dotted region represents the subjective night in L:L.

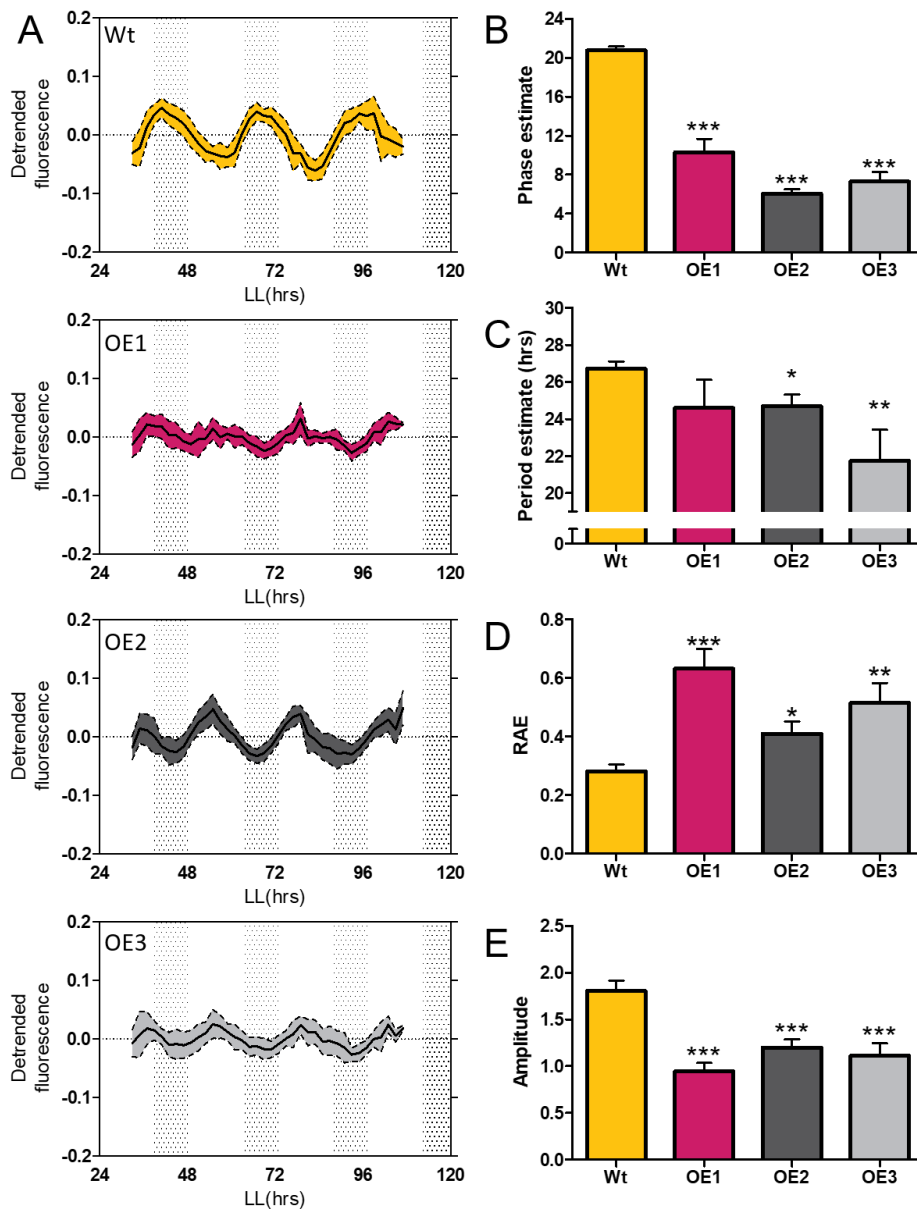


**Fig. S8. Circadian oscillation of chlorophyll fluorescence in Wt and *bHLH1a* OE lines.** A) Solid lines represent the average diurnal FL3-A fluorescence oscillation under continuous blue light (L:L) of Wt and OE lines replicates reported in Table S3 (n=15). Colored ribbons represent the standard deviation. B) Phase, C) period, D) relative amplitude error and E) amplitude of the FL3-A oscillations in Wt and OE lines (mean  $\pm$  s.e.m., n=13 to 15, two tailed t-test between transgenic lines and *Wt*: \*P<0.05, \*\*P<0.01, \*\*\*P<0.001). The OE1 line also showed shorter average periods than the Wt, although it lacked a significant difference most likely due to the high variability introduced by the replicates with high relative amplitude error (RAE) (Table S3).

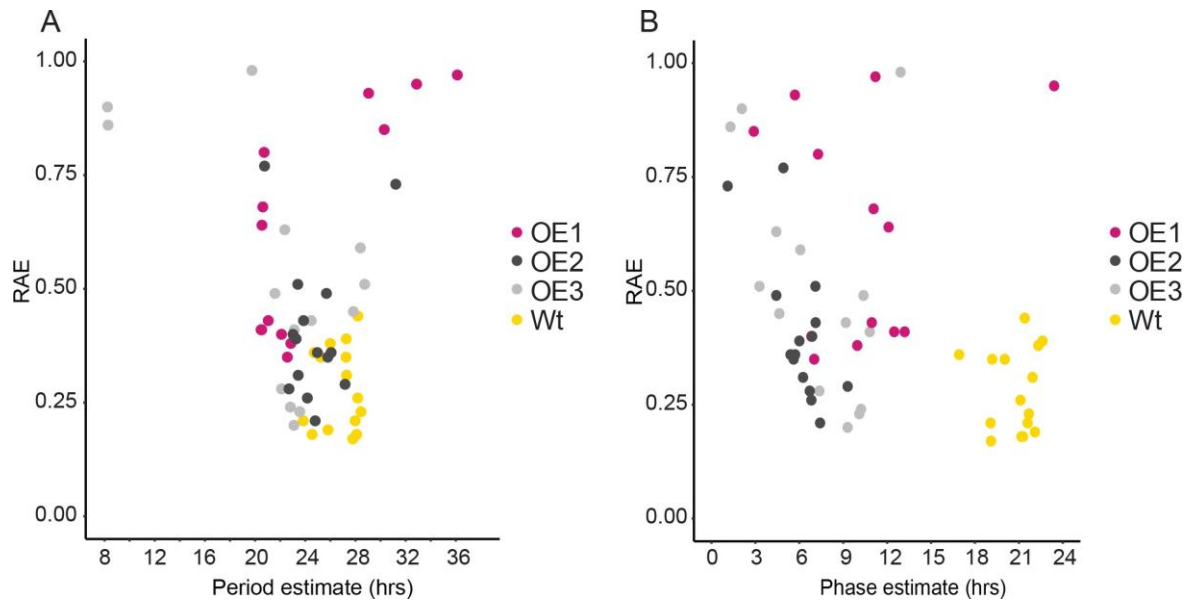


**Fig. S9. Analysis of rhythmicity in Wt and *bHLH1a* OE lines under blue L:L.** Relative amplitude error plotted against A) Period and B) Phase estimate for individual cell cultures growing in L:L (n=13 to 15, Table S3). Multiple dots of each color indicate independent replicate cultures.



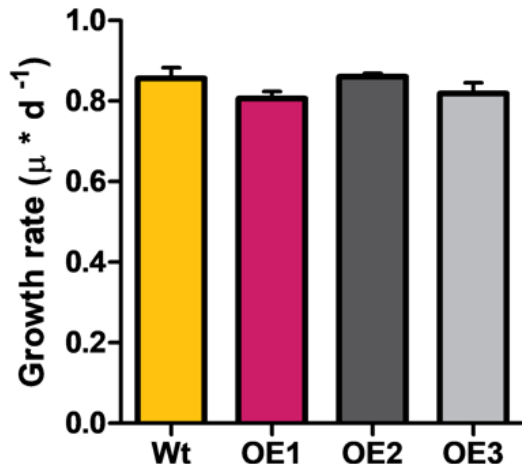


**Fig. S10. Growth rate of Wt and *bHLH1a* OE lines grown in blue L:L.** Cells were grown in 16L:8D conditions, then transferred to continuous blue light (L:L) and followed during five subjective days. Growth rates were calculated over four days. Results represent the average of three biological replicates  $\pm$  s.e.m (black bars). *p* values were calculated by comparing Wt to the indicated OE lines via two tailed t-test. No significant difference among lines was detected.

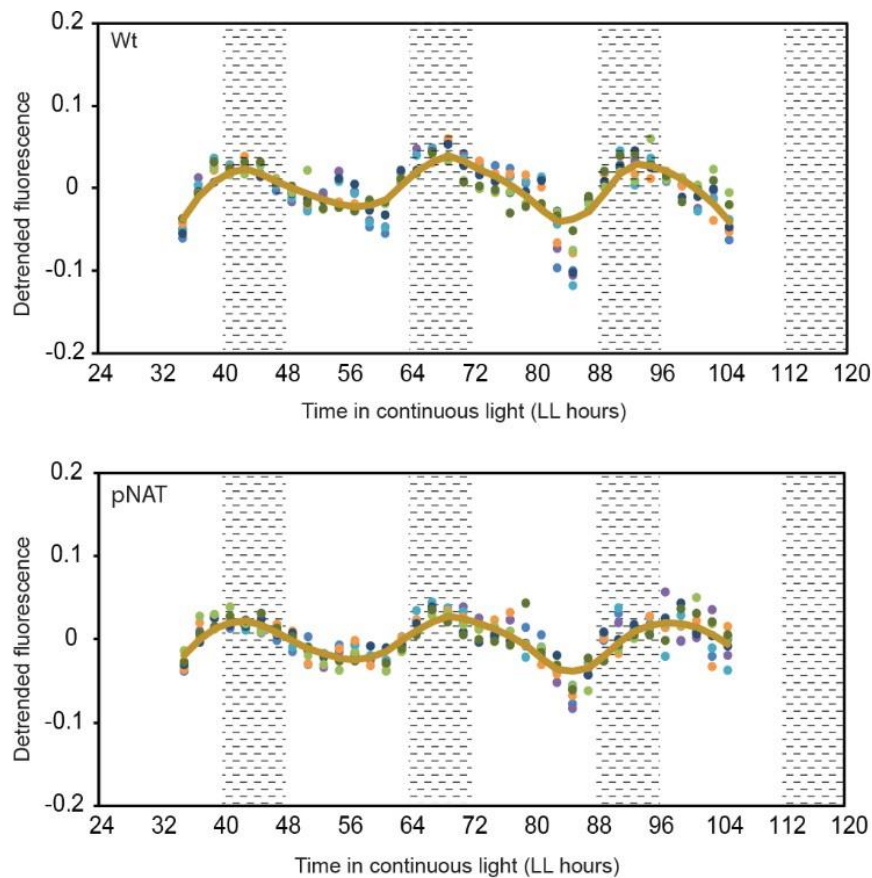


**Fig. S11. Circadian oscillation of chlorophyll fluorescence in Wt and a transgenic control line (pNAT) under blue (L:L).** Cells were grown in 16L:8D conditions, then transferred to continuous blue light (L:L) and followed during four subjective days (n=8). Colors in dots represent independent replicate cultures. White bars represent subjective days and dotted bars represent subjective nights. Brown lines in plots represent the fitted curves (lowess fit) of the average FL3-A fluorescence.

**Table S1:** Accession codes and sequence probes used in the nCounter analysis.

Category	Gene Name	NCBI Accession	Phatr3 Accession	nCounter Probe Target Sequence
Reference Gene	Actin12	XM_002182185.1	Phatr3_J29136	ATGTAAGCCTGCAGCCACTGAGGACTTGTGCTCGTAACCCCTGATTTCGATATCCAAAATGGCGCTCACTAAAAGACATCGTAGTCCAGTGCCAGTCCC
Photoreceptor	Aureo1b	#N/A	Phatr3_J49458	TTATTGCCGAGTCTGCTACTCGAGTCCGTTGTTGAAGAAATGGAGGCATAGATCAAACGAAAGGGCCAACTGGAACCTGCCGATTTTCATTGAT
Photoreceptor	Aureo2	XM_002183279.1	Phatr3_J15468	AGACGTTACTGCTACTCTCATGAACACTGCGCATGTTGACACCATTTTGGAAACAGCTCTTTATGCGCATTGCGTGACGGCAAAAATACATTGTC
TF	bHLH1a_PAS	XM_002179032.1	Phatr3_J44962	TACTTTGGTCAATATCAAGTCAAGTCTGGTACGAACAGCTCAGCATAGCCCTCGTTTTCATGTGGCGTTGGTCCATCAGACGATGACGCGAAGCTG
TF	bHLH1b_PAS	XM_002178812.1	Phatr3_J44963	AGGAATTGACTACCGTCTGTTTCAATCATTGTCATATGCAATGGGGTGGCTTATTGGAGGAAATACTGGTTCGCAACAGCTCTTTCGAATCT
TF	bHLH3	XM_002176560.1	Phatr3_J42586	ATCACTAGCAGACATTCAGATTCTATCGGGGAAAGGAGGCTTATCCCGTCACTAGTGTGTAAGTGTAGCGGTTCAAGTCTCGCTCGGAACTGC
TF	bHLH5	XM_002177858.1	Phatr3_J43365	ACCCTCTGCAGCGCAATCATTGCTCCCGCATACGACTATGGGTCGATTTCTCAATGAACGCCATTCCTTTCTCAGACCTTTCGCTCGCTGCGCT
Cell cycle	BUB1/MAD3	XM_002178639.1	Phatr3_J10954	CGTGTGCTGATGATCGGCAAAAACCGATCGTCCACTGGAAGTTTCCAGCATCTACATCAGCAAGGATCGGGAGCGATATTGCCGTGTTCTGGATG
TF	bZIP10	XM_002177776.1	Phatr3_J43744	AAGTGTGCGGAAATCGCTCGCGGAAAGAGTGTATGATGAAGAACTCAACGACGCTGATTTCTTCTCGCTCGCAACGCCCAACCCCAACACA
TF	bZIP13	XM_002181635.1	Phatr3_J47278	CGCGGGCTTCGCGTCTAAGATTGATGCGCATCACCAGACTTGAACCGAGTTAGTGGTGGAAAGATAATACACAAAGCAATGGAACGCTTG
TF	bZIP14	XM_002179477.1	Phatr3_EG02108	ATGCAGAGCTTGGAGGTCAGCTCAGGATCTCAAGCATGAGCAAAATCGTTTAAACAGATCATTAAACGAAAGAACCGGCAACATTCGGTGGGGC
TF	bZIP16	XM_002181462.1	Phatr3_J47279	CTTTTGAAGCAGTCAACAATCCGCAACATGAACAGTCCAAAGCCAGGAAAGTCGCTCGTCACTGAACGAAAGTCTCGCTCGCTCGGAAAGCGCTG
TF	bZIP18	XM_002176556.1	Phatr3_J42577	ACTTCTTATAGCGAATCCGAGCGGATTTCAAACATATAGCTCAGGCTGCTGTTTGAATCTGATCATGTCGGTGGAACTACCAAGTTGAATCTGG
TF	bZIP19	XM_002183101.1	Phatr3_J48701	CCTGCACCTTCTCAAATCAGTGTGCAACGAGTGAACAAGAAATATGGTCCGAGGCAATTAACCTACCTTTTATAGCGGTTTTCGCAATTTGGC
TF	bZIP24	XM_002184633.1	Phatr3_J49887	TTGTCACGGGGCAACAGATATCTGGAAGATCACTTCTGCCCCAAGAAAGCGGAAAGAACTCGTTCGGCTTTGCAAGCATCGCTCGCTGGGGAA
TF	bZIP25	XM_002185584.1	Phatr3_J46647	TCGTGTTACAGATGGCATCTGTACCACTCACTAGTAGAAATACGTGCATCACTGATACAGGTTATCAGCCAGTTTCGTGCTATTACTGCAAGCGG
TF	bZIP26	XM_002182641.1	Phatr3_EG02494	GATTTCTGACGACTCAAGGAGCGCAACTGTGCTGCACTCAGGAGCTTTCGGTGCAGGAAAAGTCAAGCGCTTTGAAATCGAAACCTC
TF	bZIP5_PAS	XM_002179145.1	Phatr3_J45142	CCCTGTTTCCGAACGCGCATTCGATCCGCAAAACAGCTAGCAACAACGCAATACAGTCCGAAATGATGATCGAGAAGTGGCTATTATAGATG
TF	bZIP6_PAS	XM_002184884.1	Phatr3_J50039	CGCGCAATTAATACACAATATCAGTACAGCCCAACAATCCGAAAATACGATGTCGACAGTACAGCCGAGCGGTTCAAATAATCGGCGAAC
TF	bZIP7_PAS	XM_002183297.1	Phatr3_J48800	CGTGAGACCTTGCATCGTAATCAAGGATAGAGGCAATAGCGCGATTGCGACAGCAAGCTCGTCTTCCGGGCAACAGTTAGTACCAACCGAAT
Metabolism	CaThioredoxin	XM_002184396.1	Phatr3_J49634	CTGGAGACCCCTACCGTGTAGTGTCCGTTGATTTGAAAATGTCGTTGTTTGGTTCAGCGTAGAAGACATTCCTCAGACCTCCATCTGAGTCTGAA
TF	CCCH4	XM_002181104.1	Phatr3_J13664	CATGTGCCGCTTGGAGCTCGCACAATTAACATGCTACTGGCGAAAACATTGAAAGGACATTTGATGGTCCGAAAGCCCAAGCCAACTTAAATCTCTA
TF	CCCH8	XM_002186091.1	Phatr3_J44042	TCCGAAAATATGTCGGAAGAGTCCCACTTTCGCGTATGTTCTGGCTCATACGATATTCGCGCAGGAAAGGAAAGATTGAGTTGCGGGTGAA
TF	CCHH1_CCCH20	XM_002179821.1	Phatr3_EG02317	TAACACTACAACGTTCTCAGCTAAACGGTTTGAACCATTCGCTTCTAAGAACCTATCCGACTTACATCCCCTCACTCAAGATCATAGGAGTCCAAAC
TF	CCHH14	#N/A	Phatr3_J34600	GCCAGTTTTCGCGAGGCAATCCCGTTCAATCCGCGATCTGAGTTACGAAACGCACTACATGCGGTACCAAAAAGTTTACTGATGCCGAGTTGTTTC
TF	CCT3	XM_002185983.1	Phatr3_J43850	AAACGCTCCCGCGGTTTGAATAAGAAGATTGCTACGGTTCGCGTAAAATTTAGCAGACCGCGGTTGCGCGTGAAGGGCGGATTCGTGAAACGTT
TF	CCT4	XM_002178133.1	Phatr3_J44285	TATGAATGAGTGCAGCGGAAATGAGTTTCCATCAAAACACAGAGCTAAGTGGTGCAGACCCAGCAGCCCTTCCGCCATCTCTTTCACGATAGTG
Cell cycle	cdc20	XM_002180546.1	Phatr3_J12783	TTACGACGGAATTGCTTGAAGAAATCAGAACACTTATGGGCACACAGCCGAAATATCGTCTGGGATGGAACCAACTGGTGTGAGTTGAGGCGCA
Photoreceptor	Cpd2	XM_002179343.1	Phatr3_J54342	CTGTGTCGCGCAATACGCGGCAAGTGTTCGAGCTGTAATAATGCTCTGAGATTGGCGAGTGCAGTCTATTGGAATCGCGAGTACACACT
Photoreceptor	Cpd3	XM_002180035.1	Phatr3_J51952	CTCTGATTTTCTCGATACCGCAATACGCTCAATGATGGAATCCAGCCGCTACTATCTGGAGGAAAGCAAGTCCCGTTTATCAGGTTGATGCC
Photoreceptor	Cpf1	XM_002180059.1	Phatr3_J27429	GGATGGTGCCAAAAATCCGAATCACTCTCCGATTTAGTGTGACCCCTGAATTTCCCTTCGCGCAAACTGCTGGTGGCGCGCGGTACAATTGCT
Photoreceptor	Cpf4	XM_002184521.1	Phatr3_J55091	CTCGATCCCTGTTGCGCGCAACGAGACTGCATTTCCGTAATGGTCTACCTAATGATTTGTAGACTCCATTGTCGAGGCGGTTTGAAGCAGCTG
Photoreceptor	CryP-like	XM_002178853.1	Phatr3_J34592	CACTTTATGGTGGCAACAGCGGCACTGCACGATTTGTAAGGATTACTCGAAACCGGCAACGGGATGCTGGGCGCAACTTTCGACCAAAATCA
TF	CSF2	XM_002185522.1	Phatr3_J41601	GAAACAGAAAGAAATTCGGGACGCTTATGATTTCAACAGACGAAATCGACAGGCTCATCACTTATTTGCAATTTGGGATGGAGCTTGCAGACT
Cell cycle	CYCB1	XM_002180361.1	Phatr3_J46095	TTAGAGAAATCAATCGCAATCTCGAGCTCCGAGCGTGAATAAAGTACAGCGTCACTGATACGGCGAGTTCGTCGACCGTCTCGATTTGGA
Cell cycle	CYCH1	XM_002185709.1	Phatr3_J36892	TTGCGATGGCTCGGTTTACGTTTCCATCCGACCCGAGGAGTTCGCGCAATCTCAACCATCTCGTGGATTGCTCACTCAATGGTTTGGC
Photoreceptor	Dph	XM_002179026.1	Phatr3_J54330	CAACAATCCATTAACAACAAAGAGCTGACGGAATGATCGTGCAGCTGTGCACTTGTGCAAAACGTCACAAAGGGTACCGGCAATTTGTTGTCATT
Cell cycle	dsCY2	XM_002179247.1	Phatr3_J34956	GATATTGCCGTTACCGAACCGAAATAATGACTGCTCTTCTGGCACTTGCATCTCCAAACCGCTATTGGCTTTTCAGCAATGACTGGTCTGCTGG
TF	E2F_Dp2b	XM_002181452.1	Phatr3_EG02016	TGATTTGAATAGAGCTGTGCAAGAAATGAGGTTACAAAAGCCCGGATTTATGACATTACCAACGTTTGAAGTATTGGGCTGATTTACCAAGGATAGC
Cell cycle	E2F1	XM_002176842.1	Phatr3_J43065	GTGTGGTCTCATCGAAAACGATCCAAAACACAGTCCGTTGGAAGGAGTGAAGTCTCTTCTGGCTCGCTTTTCAAGTCCGCGCAAGCAGAGAAT
Cell cycle	FtsZ	XM_002185088.1	Phatr3_J42361	GAAAAGGAGAATGAAGCAAGCGATTGCCGATGAGAGTTGCGAGAGAATGGATACCGTCACTGATGTCCAAACGACAGACTGCTCGAGATTAT
Metabolism	GapC1	XM_002182255.1	Phatr3_J22122	TGAAGGATTCCTCGGATCTCCGACGACCGTTGGTCTCCACCGACTTGAAGTGACTTGGCTCTCCATCTTTGATGCGGATCGCGTATCATGCT

Metabolism	Gsat	XM_002180931.1	Phatr3_136347	ATTCTGTTGGTCCGGCCACACACGGGTCGGGAAAAGTCAATCAAGTTCGAAGGATGTACCACGGACACGCCGATTCATTTTGGTCCAAGCCGGATCCG
TF	Hox1	XM_002184935.1	Phatr3_EG02213	AACAACATCGGTTCACATCTCGTCACTACCAGGCAAGTCCCGACAGTCCGAAGATGTACGATCTTACCAATGTTCCGGGGAACGCATTCCTCGAAG
TF	HSF1.3b	XM_002179894.1	Phatr3_135419	CTCCAGGGAACAACCTGATACCAGAGTTCCTCTATCAGCTAACAAAGATGTGACGGATAACACCCAGATATTTAATGAATGGCAAAATGGCAAGATTGA
TF	HSF1a	XM_002177362.1	Phatr3_143051	CCACCAACGTCGGATAGCTCCGACTGGGGTTCCTCAATCCCAATCAATCCAAAGCCAGCTGTGATCTTAAACGAGGATATGCGCAATGGCAAAATATAC
TF	HSF1b	XM_002181395.1	Phatr3_147181	TTGATGTGACACTTCGATGCTCGAAGAGTTCATCAACGAAACCGCAGCCACTCGTGGAGCAAGGTAGTCTTCCCTTTGACAAATAGAGCACCAGT
TF	HSF1d	XM_002178673.1	Phatr3_144750	GTCACCATTCAGCATCGGATCGGCTCCTTACGCCATTTCTCCGAAACCTCACCAGAGACTTGACTCTGAGACACAAGAAATTCOCAACCTTGATG
TF	HSF1g	XM_002177016.1	Phatr3_142514	ATAGAGAATCTGCAAGCACTAGGACCATGACGACTACTTCATCGAAGGTAGCATACAGAGAGCAAGATAGTTCCTGTGACACTCAGCATCAGGAG
TF	HSF2.1a	XM_002181681.1	Phatr3_147360	AGCCCTTGGCCGTGAATTTGGGTCGTTGTGCCTCAAGTCAACCAACCACCGCGTGGATGATCAACACGCCCTGTCAATCGCTCAAGCGTGTAGT
TF	HSF2.2c	XM_002185405.1	Phatr3_150481	GGACTGGAACTGTAAGCGGACATATTTCCGAGCGCTTCTAGCGATTTGAGCGAATCATCCCTATCTGACATTATCACTTGGCTTCCACATGGACG
TF	HSF3.2b	XM_002186124.1	Phatr3_144099	TTGACTCTCCGCGCACAGCAAGCACTTAGCGCTTTCACAGTCCCTCGGTGATCCGAGAGTCAAGTCTAGCTTTTCCACCACAACCTCTC
TF	HSF3.2e	XM_002179404.1	Phatr3_145206	TTGGAACGGGACGCTTCCCTCAGATTAGCAATCCGCAACCTTCGCTACTCTCCAAGTTCGACGATGGTAAATCTCGGACTTAGCAAGCACTACT
TF	HSF3.3a	XM_002179738.1	Phatr3_145393	CTGGGCAATCTTCGATGTAAGGTTGGCGACGCGAGTAGTCAGGAGTGGCGTAACACAGCAGCTTTGCCCTTCGACAGCAAGCGCTGTA
TF	HSF3.3f	XM_002179735.1	Phatr3_145389	CATGCCAATTGAACACCAATTCAGCCATACATGGAAGAGCTTAAGAGGTCATCTTCGACGGCGGGGAAGTTCGAAAATGCGCTCGAATTTTG
TF	HSF4.2c	XM_002182762.1	Phatr3_148361	CGACGATATACAGATTTCGCAAGTGGCGCCGACGCGGATCCATGATGATCTCGGAAAAGACTGGAGGACTCACTCAGCATTTCGCGAAA
TF	HSF4.2j	XM_002177548.1	Phatr3_143363	GTCGGCGGACGGCCCTTATCATTCAACAGCTGACAAGTTCCTTAAGGATATAGTCCGCTATATTTTCCGACGTCGGCGTGGTTCATTCAGCGGC
TF	HSF4.3a	XM_002184368.1	Phatr3_149594	CGCAACACTCGGTTCCAATGTCGCGGAAGAACCTTCCAAAGCAACCTTTGTTGAGCATAATTTACCATGACCATATGAACACCTGAGCAGGTGGATG
TF	HSF4.3b	XM_002183012.1	Phatr3_148558	CTGTCTTGAGCTTACGACAGTGGCGCGAATTTCTACGCTATGCCAATCTGAAGTGGAGCAAGACCAATATTTCTGATCCAAAATACGTTG
TF	HSF4.3c	XM_002183081.1	Phatr3_148667	AAACTGTCAGTACTGTTGACCATGTAAGAGCCGAGGATGGACGACGTTATTTCTGGGCGAGTATGGCGGTTTATGATTACCAACCCAGACC
TF	HSF4.4b	XM_002184371.1	Phatr3_155070	CCCATTCCGGTAAACCCGGTTTCCAACTTGGCGTATCCGAGCGCTAGTTTGGTAACTGCAACAGGCAATTCGCTCTTATGCGGTTGTATGA
TF	HSF4.6a	XM_002184347.1	Phatr3_149557	CTCAACACTGGCGATTGCGGTATCGCTCGTTCGCGCATCCAGTGCACGCCAACATCTGGAATCCTTCGCACTTTCCGCTCTGTCTCAATAACGGGCAC
TF	HSF4.7a	XM_002185271.1	Phatr3_EG00092	CGACATCCCGGGGGGATTTGAGATCGACGCGATAGTGTCACTTTCGCTTCAAGAGTATTTCCCAACTCTACATATCGGTGGTACGCTACTCAC
TF	HSF4.7b	XM_002184277.1	Phatr3_149596	CTCGAGTGGTGGGAACTCCTTTTCCACTCAAGCTGCAGAAATGCTTCAAAATGCTGCAAGAGCGCTACGCTCACATGATCGTGGCAGCCTCA
Metabolism	Lhx1	XM_002179724.1	Phatr3_127278	AATCTTTGAGAATCTTCAGGGTTAAGAGTGCATCCATCCCAAACTGGAGGATGGCTGGTACATGACAGAGTAAACAAACCAATCCCTTTTCAAGCGA
TF	Myb1R_SHAQKYF4	XM_002178425.1	Phatr3_144331	CGTATCTGCCGAATCGGTCTCGTGGCAATCAAGTCCACGCCCAAAAAGTCTCAAGCGCATGATCAAGGGAACACGCTTCCGACGATCGAGGA
TF	Myb1R_SHAQKYF5	XM_002181623.1	Phatr3_147256	ACGCTTCACTGGCCGAAGACTTACACGGGATTTGATCGGCAATTTTGTATGTCGGCTTGAACAGCTGTCACCGTCCACCAATTTTGGAAACCATG
TF	Myb1R_SHAQKYF6	XM_002180835.1	Phatr3_146535	TAACGACGAAGCGCAAACTCTTACCGCAAACTTGCCTCCGCGAAAAGGTTAAGACACGAAAGTTCGCCCTTGGTACAGCGTAATCTCAGTTTC
TF	Myb1R10	XM_002181361.1	Phatr3_137257	CATATCCCTCTTCGGGGCCCTCACTTCCCTGTACAAGTGAATCTTTGGGGTGAAGCGAATCTGAGAAGAAACGCTGTAAGGACGAGACTCGGTTCT
TF	Myb1R4	XM_002181410.1	Phatr3_147205	AAAGTCTGTTGAGGTTTAGACGAAAGCTTACCGCATTTGCAATGGGAACAATCCGCGAGTAGGATTCACCATATGCGATTAACATTCGGAAGCCG
TF	Myb2R3a	XM_002181911.1	Phatr3_147726	TCCATCTTCCCTTGGAGCGACTGACGACCTGTGGAGGGAGAGTATTTTGTACTGTAAGTGTGCTGATCCGCGACTCGGCAGGTAATACTC
TF	Myb2R3b	XM_002182076.1	Phatr3_EG02275	GCGCACACGGTTAAAGTATTCGGGATTCATTCACAACAGTCAATGGCTAATTTGGCTCCATCGTTCACTGGTTGACATTTGCGATCGGCCAACACT
TF	Myb3R1	XM_002182738.1	Phatr3_151016	GTATGATCTCGAGTGTCTTTGACGTTGGAAACCGCTGGCGGAAATGCCAAGCGTCTACCGGGAAGACTGATAACCGTATTAATAACTCACTATACGG
TF	Myb3R2	XM_002180449.1	Phatr3_16839	CGAATCTCATAGGACACAGGACACAATGGAAATCGATGGGCTGAGATTGCCAAGCGGCTGCCAGGACTGACGCAATGCGAATAAAGAAATCGTGGA
TF	Myb3R4	XM_002180741.1	Phatr3_136337	GACAGATCCGGAAGCGCAATTTGTAATGGATCGGCTCAATCCAGCTCGGAGCAACATTTACTCGTTGGTCACTTGGCGCAACGCTACCCGGACGT
TF	Myb3R5	XM_002184658.1	Phatr3_17959	GACGCTGTTATCTGAATTCGTTGAGCCAAACAATCCGAAAAGCAATGGACGGAGCAAGAAAGAAAGCTTTGTTGATGACAGCGCGCATGGGAAA
TF	Myb5R	XM_002185245.1	Phatr3_150365	TCAACACCATAAACGCTCGTTTCAAGCTTTGGATGTTGATGAGTGAACGCGGTTGGTTTTCATCGAGAACCAATGACCAATGAACGAGCAGAAAGATG
Cell cycle	PCNA	XM_002182225.1	Phatr3_129196	AATGACGGAACCGGTGAACTCACTTTGCCCTGCGTACCTCAACTTTTTTACCAAGCGGACTCGTGTAGTGGACAGCTCATATCTCCATGGCACCG
Metabolism	Pds1	XM_002180135.1	Phatr3_135509	AGCATGCCAAGGCACGCAATTCATTGATCCCGCAAAATGAGTATGACGCTGTTTTGACCGCATGAACTCGCTTTTGAACGAGCAACGGCCTCC
Metabolism	petA	Gi:118411009	#N/A	TCTCTGGATCAGGAGCCATAACAGGGAAAATTAECTTGTATGAGTCTTCTCGCAATTTGGTCCAACTACTAAGATATTAATCAAAATCACTACTATACGG
Metabolism	Pgr5	XM_002178672.1	Phatr3_144748	GTAACGTCGCGCTTCTGATGCTACGCTGCGCGCTTTCGCGTGGCGGGGAGCCACCGGGGTTCTTCTTTGCTTTCCCGACGAAACGACATCG
Metabolism	PgrL	XM_002177043.1	Phatr3_142543	CCACAACAAGTACGCTTCCAAATTTAGACAAGACTACGAACAACGATGCGGATCACTCTGTGATTTTGGCTTTTGGTGTCTCGCGCTCAGCGAT
Metabolism	Por1	XM_002179653.1	Phatr3_112155	TCCGGTGGTGAATTTTGAAGATCAGCAGTCCGACGAGTACGGGATCTTCTACCGCCAAAGAAATGGGAACTGAGTAGGGAAGCAGTTGGTCTTT
Metabolism	Por2	XM_002180956.1	Phatr3_113001	AATCACCATAATCCGTAAGGCGCCGCTGGTTCGCTAAATCTTCCATCTTTAATGAAGTTTATTCGGGAGGATACGTTGAGAGCAGCAAGCGCGG
Metabolism	Por3	XM_002177432.1	Phatr3_143164	CGGTTCTCAACAGGAAAAGCGGTGAGACTCATGATTCGTGATCCGACAGTGTCTATCGAGGACACCGTAGCTGGGAGCAGTACGTTCC
Metabolism	psaA	Gi:118410964	#N/A	GCTAAGAAGACGCCCAAGTAGTCCAAATACCAACCAATAAATAATGAGCTAAACCAACTGCACGACCCCTGAGTAAATGCTTAATGACGAGGTTGGATTG
Metabolism	psaD	Gi:118410999	#N/A	TTAAATGACGTAATGGGTTCCCAATGCTAAACATGCTCTTTGCGCGTAAGTATAATAAATTTTCCACTACGATGATGAGTCTCCACCAATG

Metabolism	psbC	HQ912250.1	#N/A	GGCCCAACAGGTCCTGAGGCTTCAACAAGCACAAGCATTACGTTTTAGTTCGAGATCAACGTTTAGGTGCTAATGTTTCATCAGCACAGGTCACACTG
Metabolism	Psy1	XM_002178740.1	Phatr3_EG02349	ACCTGTCTCGTGGGAATTGCGAATGGAGCGTTTGTGGCAATACGGACAAGTACAGGATGTCTTTGACCTGTGTTGCTAGATCTTCGAATCCAGTATCC
Reference Gene	Rps	XM_002178225.1	Phatr3_J10847	CTCCCGCATTTTTGCCCGGTTCCCAATTTGACCCGACAGTTGCCCGACGAAGATCTCATTGGAAACAACCTTGACAGCTTAAATTCCTCGAAGTCAACCAGG
TF	Sigma70.1a	XM_002182291.1	Phatr3_J14599	GACAATTAGGGGTATCTCGGGATCGGATTCGCTTGTGAAACCCGAGCACTGAACAATTCGGACACCCGCAACAAAATTACAAGCTGCAGCTTTACGT
TF	Sigma70.1b	XM_002182124.1	Phatr3_J3388	TTCTTGGTCATTGGAAGAAACGGCAACCACTAGGATGCTCTCGGGATCGGATTCGCTTGTGAAAGCCGAGCACTGAATAAATTCGACGTCACAAA
TF	Sigma70.2	XM_002178682.1	Phatr3_J5537	ACGTGGATTGCGATTTCGCCACTACGCCACTTACTGGTCCACCAATTCGTCAGCTTCTGCTTCCAAACCGCATCCACCGGATGTTGGGGTACCGGTA
TF	Sigma70.3	XM_002185461.1	Phatr3_J17029	TATGATGGTCTCTGATCTAAAGAGCAAATTCGTCGCTCGCTTCGGCCAGGCTGCCCTGACCGAATCAAAATTCGACTCGTGGTATCCATTGCGAAA
TF	Sigma70.4	XM_002177232.1	Phatr3_J9312	AACCCGAAAGATCTCGTACGAAAGTACGATTTGCTAGGGGACACAATCTCCGCCAGTATGCTCTTTTGGACAAAGCACACCCGAAAACGAGTCCG
TF	Sigma70.5	XM_002182854.1	Phatr3_J14908	AAGAAGCTATACAGGAAGCAGTTGGGATTGTTGGCGGGCCGAAATTTGATCCGAGCGAGGACTGCGATTCAGCACTTACCGGTAGTGGAT
TF	Sigma70.6	XM_002178042.1	Phatr3_J9855	CTGGAAAATCAATATGGAGCTATTCGGCAGACCATTGAAGAAGACTGGAAGCCAAAATCAGCTAGTCACTTCGAATCTCGGGATGTTACAGAGTGT
TF	Sigma70.7	XM_002185047.1	Phatr3_J50183	AATGATGACGCTCTCTCGCATACGGTGAACCTCGTCTGATCAAGCAAAATCGAAGCTGATCTTGGCTTTGACGTATCCATCTCCCGGAAACCCACTACT
TF	Taz2	XM_002178935.1	Phatr3_J44807	CCTAATGTAGAGACTGTAGTGGTAAAAGCGAAGCGCGACGCTCGACTATTGGACTTTACTTCATGCACAGAATTGCGTTTTGGGGACAGATGCCAC
Reference Gene	Tbp	XM_002186285.1	Phatr3_J10199	CTGATTTTTCCAGCGTAAATGTGCGTGACCGGAGTCAAGAGCACACACAACGCCAATCTGGCGGAAAAAGTTGCTACATTGGGAGCGCGTGG
Metabolism	Vde	XM_002178607.1	Phatr3_J51703	GGCGATGACGGATCATATCCCGTTCCCGCACCCGAAATCGTCTGTACCCAAAGTTGACACCAAGTCTTCGATGGACGACTCTACATCTCAGCCGGACAAA
Metabolism	Vdl1	XM_002180599.1	Phatr3_J36048	AAGGCTCTCTTTAGCAATCCGCGTGAATCAAAGGTGCTCTCTGTTGGGACGCTGCAAGGGCGGAAATCGTGTGCGACCGGTTTGGCGAATTCG
Metabolism	Vdl2	XM_002180015.1	Phatr3_J45846	ACACACCCCTTCGGCAATGAATATCCAATTTCCGGAGCCAGCAATCACTCCATGCTGGGACCAGTACGAACACATCGTAAAGTGTGACCGGTT
Metabolism	Vdr	XM_002177477.1	Phatr3_J43240	GTGCTTGGCGTCCAAACGAGCTATGATAAGTTTCCTTCGCGAAGCACTCTTCTATCCCGCTGCTCGCGTGGAGATTGTGGTACGATCCCGTTT
Metabolism	Zds	XM_002184417.1	Phatr3_J30514	CGGCGTCAACGAATCCATCCGGGACCCGCCAAGTACTCGCCGTTTTAATTCACATCTTCGCGCGAGTCTTTGGACACCGCGACGTCACGGAACTC
Metabolism	Zep1	XM_002179586.1	Phatr3_J45485	TTCCCAATGAAGTTTCTACACGGTGTCTCGGCAGTGTCTGATCGCGTGGTATCGACCAAGACTTCCCTCACACCCGCTCCAGTCTTTGGCGTGC
Metabolism	Zep3	XM_002178331.1	Phatr3_J10970	CCAAGGTTTGACCAAGATGCCCAATGGATGTTACCGTACTGGAACAACGTCGAAATTCAAACGGTTCGGTGGACCCATCCAGCTCGCTAGTAACCG

**Table S2:** Calculated periods, phases, amplitudes and relative amplitude errors of the Wt and bHLH1a OE lines growing in 16L:8D. P-values obtained via t- test between Wt and the OE lines are shown. Amp., amplitude; RAE, Relative Amplitude Error.

Data	Period	Period P value	Phase	Phase P value	Amp.	Amp. P value	RAE	RAE P value
Wt	23.9		13.44		0.1		0.15	
Wt	23.71		12.41		0.12		0.12	
Wt	23.86		11.95		0.13		0.13	
Wt	24.58		12.21		0.11		0.1	
Wt	25.71		10.32		0.12		0.21	
Wt	24.79		12.15		0.12		0.12	
Wt	24.24		12.81		0.15		0.19	
Wt	23.89		12.27		0.12		0.15	
Wt	23.64		12.89		0.11		0.19	
Wt average	24.26		12.27		0.12		0.15	
OE1	23.87		15.24		0.07		0.24	
OE1	24.53		16.17		0.07		0.23	
OE1	23.29		16.53		0.06		0.37	
OE1	23.18		18.16		0.07		0.52	
OE1	24.17		15.23		0.08		0.28	
OE1	24.67		12.19		0.14		0.09	
OE1	24.41		12.14		0.12		0.09	
OE1	23.77		13.32		0.09		0.16	
OE1 average	23.95	0.2940	14.62	0.0078	0.09	0.0042	0.24	0.0653
OE2	23.65		15.47		0.11		0.19	
OE2	24.04		14.8		0.11		0.21	
OE2	24.23		14.78		0.11		0.22	
OE2	24.18		14.98		0.11		0.23	
OE2	23.34		14.22		0.09		0.21	
OE2	22.82		15.05		0.08		0.24	
OE2	21.91		14.14		0.08		0.32	
OE2	22.42		13.71		0.07		0.38	
OE2	23.6		12.24		0.08		0.33	
OE2 average	23.35	0.0206	14.38	0.0002	0.09	0.0021	0.26	0.0007
OE3	24.14		14.05		0.13		0.13	
OE3	24.49		13.73		0.12		0.18	
OE3	24.55		12.29		0.11		0.21	
OE3	24.31		11.32		0.1		0.25	
OE3	24.43		11.19		0.11		0.23	
OE3	23.74		11.96		0.11		0.17	
OE3	23.74		11.97		0.12		0.17	
OE3	24.77		12.31		0.11		0.21	
OE3 average	24.17	0.9607	12.58	0.8640	0.11	0.3037	0.20	0.0364

**Table S3:** Calculated periods, phases, amplitudes and relative amplitude errors of the Wt and bHLH1a OE lines growing in L:L. P-values obtained via t- test between Wt and the OE lines are shown. Amp., amplitude; RAE, Relative Amplitude Error.

Data	Period	Period P value	Phase	Phase P value	Amp.	Amp. P value	RAE	RAE P value	
Wt	25.99		22.33		2.41		0.38		
Wt	25.24		20.04		1.68		0.35		
Wt	24.7		16.92		1.69		0.36		
Wt	25.81		22.1		2.43		0.19		
Wt	24.54		21.18		2.55		0.18		
Wt	23.83		19.07		2.14		0.21		
Wt	28.19		21.4		1.51		0.44		
Wt	27.27		22.62		1.59		0.39		
Wt	27.29		21.93		1.37		0.31		
Wt	28.1		21.28		1.88		0.18		
Wt	28.18		21.11		1.59		0.26		
Wt	27.25		19.18		1.21		0.35		
Wt	27.78		19.1		1.52		0.17		
Wt	27.97		21.6		1.4		0.21		
Wt	28.44		21.69		2.12		0.23		
Wt average	26.71		20.77		1.81		0.28		
OE1		FAILED Could not find cos waves that fit the data							
OE1	30.3		2.89		0.44		0.85		
OE1	29.04		5.7		0.46		0.93		
OE1	20.62		11.08		0.94		0.68		
OE1	20.72		7.28		1.12		0.8		
OE1	20.54		12.1		1.1		0.64		
OE1	20.48		12.48		1.55		0.41		
OE1	20.53		13.2		1.33		0.41		
OE1	21.05		10.95		1.09		0.43		
OE1	22.85		9.96		1.01		0.38		
OE1	22.57		7.02		1.04		0.35		
OE1	22.1		6.82		0.61		0.4		
OE1	36.12		11.2		0.72		0.97		
OE1		FAILED Could not find cos waves that fit the data							
OE1	32.87		23.41		0.86		0.95		
OE1 average	24.6	0.17	10.31	< 0,0001	0.94	< 0,0001	0.63	< 0,0001	
OE2	27.17		9.3		0.99		0.29		
OE2	24.79		7.42		1.19		0.21		
OE2	24.17		6.82		1.14		0.26		
OE2	26.06		5.4		1.25		0.36		
OE2	23.86		7.11		1.17		0.43		
OE2	25.79		5.61		1.71		0.35		
OE2	23.02		6.88		1.23		0.4		
OE2	23.4		7.1		0.88		0.51		
OE2	24.96		5.71		1.41		0.36		
OE2	23.27		6.01		1.35		0.39		
OE2	22.7		6.71		1.74		0.28		
OE2	23.44		6.26		1.56		0.31		
OE2	25.69		4.43		1.02		0.49		
OE2	31.21		1.1		0.85		0.73		
OE2	20.75		4.91		0.54		0.77		
OE2 average	24.69	0.0108	6.05	< 0,0001	1.2	0.0002	0.41	0.0118	
OE3	8.28		1.3		0.55		0.86		
OE3	8.23		2.07		0.46		0.9		
OE3	28.39		6.07		0.72		0.59		
OE3		FAILED Could not find cos waves that fit the data							
OE3	19.75		12.92		0.56		0.98		
OE3	24.48		9.18		1.73		0.43		
OE3	23.12		10.81		1.51		0.41		
OE3	22.1		7.37		2.15		0.28		
OE3	27.83		4.63		1.08		0.45		
OE3	28.74		3.28		1.2		0.51		
OE3	23.56		10.1		1.41		0.23		
OE3	23.1		9.3		1.46		0.2		
OE3	22.81		10.22		1.11		0.24		
OE3	22.37		4.43		0.86		0.63		
OE3	21.58		10.38		0.76		0.49		
OE3 average	21.74	0.0062	7.29	< 0,0001	1.11	0.0004	0.51	0.0024	

**Table S4:** Accession numbers of the proteins utilized in the bHLH-PAS phylogenetic analysis.

SPECIES	ABBREVIATION	ACCESSION	ACCESSION(AI)
Amphiprora sp., Strain CCMP467	Amph	CAMPEP_0168730192	
Asterionellopsis glacialis, Strain CCMP134	Agla2	CAMPEP_0195290872	
Asterionellopsis glacialis, Strain CCMP1581	Agla3	CAMPEP_0197142484	
Astrosyne radiata, Strain 13vi08-1A	Arad1	CAMPEP_0116831938	
Astrosyne radiata, Strain 13vi08-1A	Arad2	CAMPEP_0116837632	
Attheya septentrionalis, Strain CCMP2084	Asep	CAMPEP_0198303966	
Capsaspora owczarzakii ATCC 30864	Cowc1	XP_004345696	
Capsaspora owczarzakii ATCC 30864	Cowc2	XP_004343694	
Chaetoceros debilis, Strain MM31A-1	Cdeb	CAMPEP_0194099558	
Chaetoceros dictyota, Strain CCMP1751	Cdic	CAMPEP_0198277646	
Chaetoceros neogracile, Strain CCMP1317	Cneo2	CAMPEP_0195415676	
Chaetoceros neogracile, Strain CCMP1317	Cneo3	CAMPEP_0195453836	
Chaetoceros sp., Strain GSL56	Chae	CAMPEP_0176495412	
Corethron hystrix, Strain 308	Chys	CAMPEP_0113330172	
Corethron pennatum, Strain L29A3	Cpen	CAMPEP_0194280324	
Cyclophora tenuis, Strain ECT3854	Cten1	CAMPEP_0116540656	
Cyclophora tenuis, Strain ECT3854	Cten2	CAMPEP_0116579710	
Cyclotella meneghiniana, Strain CCMP 338	Cmen	CAMPEP_0172279412	
Cylindrotheca closterium	Cclo	CAMPEP_0113624952	
Dactyliosolen fragilissimus	Dfra	CAMPEP_0184871870	
Detonula confervacea, Strain CCMP 353	Dcon	CAMPEP_0172306268	
Ditylum brightwellii, Strain Pop2 (SS10)	Dbri	CAMPEP_0181012646	
Drosophila melanogaster	dmClock	AAC62234	FBpp0099478
Drosophila melanogaster	dmCycle	NP_524168	FBpp0074693
Drosophila melanogaster	dmSim	AAC64519	FBpp0082178
Drosophila melanogaster	dmTango	NP_731308	FBpp0081483
Drosophila melanogaster	dmTrh	AAA96754	FBpp0293065
Durinskia baltica, Strain CSIRO CS-38	Dbal	CAMPEP_0170381008	
Ectocarpus siliculosus	Esil1	Ec-02_004780 PAS domain (681) ;mRNA; f:5082087-5086119	
Eucampia antarctica, Strain CCMP1452	Eant	CAMPEP_0197830682	
Extubocellulus spinifer, Strain CCMP396	Espi1	CAMPEP_0178587872	
Extubocellulus spinifer, Strain CCMP396	Espi2	CAMPEP_0178723458	
Fragilariopsis kerguelensis, Strain L26-C5	Fkue1	CAMPEP_0170867208	
Fragilariopsis kerguelensis, Strain L26-C5	Fkue2	CAMPEP_0170907188	
Fragylariopsis cylindrus	FcbHLH1a	jgi Fracy1 204663	
Fragylariopsis cylindrus	FcbHLH4	jgi Fracy1 241747	
Fragylariopsis cylindrus	FcbHLH7	jgi Fracy1 172104	
Galdieria sulphuraria	Gsul	XP_005709404	
Glenodinium foliaceum, Strain CCAP 1116/3	Gfol1	CAMPEP_0167841300	
Grammatophora oceanica, Strain CCMP 410	Goce	CAMPEP_0194036250	



Guillardia theta CCMP2712	Gthe1	XP_005835918	
Homo sapiens	hsArnt	AAA51777	
Homo sapiens	hsbMal1	NP_1284651	
Homo sapiens	hsClock	AAB83969	
Homo sapiens	hsNpas1	AAH39016	
Homo sapiens	hsSim2	NP_5060	
Kryptoperidinium foliaceum, Strain CCMP 1326	Kfol1	CAMPEP_0176099000	
Leptocylindrus danicus var. danicus, Strain B650	Ldan1	CAMPEP_0116039394	
Leptocylindrus danicus var. danicus, Strain B651	Ldan2	CAMPEP_0116053596	
Leptocylindrus danicus, Strain CCMP1856	Ldan3	CAMPEP_0196809694	
Licmophora paradoxa, Strain CCMP2313	Lpar	CAMPEP_0202478474	
Minutocellus polymorphus, Strain RCC2270	Mpol	CAMPEP_0185804732	
Monosiga brevicollis	Mbre2	jgi Monbr1 26507	
Mus musculus	mmArnt	AAA56717	
Mus musculus	mmbMal1b	BAD26600	
Mus musculus	mmbMal2	ABC50103	
Mus musculus	mmClock	AAC53200	
Mus musculus	mmNpas1	NP_32744	
Mus musculus	mmSim2	AAA91202	
Nannochloropsis gaditana CCMP526	Ngad_2	Naga_100016g14	
Nannochloropsis gaditana CCMP526	Ngad_3	Naga_100165g4	
Nannochloropsis oceanica CCMP1779	Noce	NannoCCMP1779_9983-mRNA-1	
Nannochloropsis oceanica CCMP1779	Noce_2	NannoCCMP1779_1600-mRNA-1	
Nitzschia punctata, Strain CCMP561	Npun	CAMPEP_0178827522	
Nitzschia sp.	Nitz	CAMPEP_0113465330	
Phaeodactylum tricornutum	PtbHLH1a	jgi Phatr2 44962	Phatr3_I44962
Phaeodactylum tricornutum	PtbHLH1b	jgi Phatr2 44963	Phatr3_I44963
Phaeodactylum tricornutum	PtbHLH2	jgi Phatr2 54435	Phatr3_I54435
Proboscia alata, Strain PI-D3	Pala	CAMPEP_0194393728	
Pseudo-nitzschia arenysensis, Strain B593	Pare	CAMPEP_0116139930	
Pseudo-nitzschia australis, Strain 10249 10 AB	Paus1	CAMPEP_0168282354	
Pseudo-nitzschia australis, Strain 10249 10 AB	Paus2	CAMPEP_0168310394	
Pseudo-nitzschia delicatissima, Strain B596	Pdel1	CAMPEP_0116091770	
Pseudo-nitzschia delicatissima, Strain B596	Pdel2	CAMPEP_0116094064	
Pseudo-nitzschia fraudulenta, Strain WWA7	Pfra1	CAMPEP_0201229664	
Pseudo-nitzschia fraudulenta, Strain WWA7	Pfra2	CAMPEP_0201232896	
Pseudo-nitzschia heimii, Strain UNC1101	Phei1	CAMPEP_0197189528	
Pseudo-nitzschia heimii, Strain UNC1101	Phei2	CAMPEP_0197199168	
Pseudo-nitzschia multiseriis	PmbHLH1a	jgi Psemu1 26622	
Pseudo-nitzschia multiseriis	PmbHLH7	jgi Psemu1 228145	
Pseudo-nitzschia pungens, Strain cf. pungens	Ppun	CAMPEP_0172413298	
Rhizosolenia setigera, Strain CCMP 1694	Rset	CAMPEP_0178942232	
Skeletonema costatum, Strain 1716	Scos1	CAMPEP_0113408658	

Skeletonema dohrnii, Strain SkelB	Sdoh	CAMPEP_0195221452	
Skeletonema japonicum, Strain CCMP2506	Sjap	CAMPEP_0201725346	
Skeletonema marinoi, Strain FE7	Smar1	CAMPEP_0180846198	
Skeletonema marinoi, Strain UNC1201	Smar2	CAMPEP_0197231700	
Skeletonema menzeli, Strain CCMP793	Smen	CAMPEP_0183679140	
Stauroneis constricta, Strain CCMP1120	Scon1	CAMPEP_0119548954	
Stauroneis constricta, Strain CCMP1120	Scon2	CAMPEP_0119572288	
Staurosira complex sp., Strain CCMP2646	Stau	CAMPEP_0202487246	
Synedropsis recta cf, Strain CCMP1620	Srec1	CAMPEP_0119009808	
Synedropsis recta cf, Strain CCMP1620	Srec2	CAMPEP_0119029558	
Thalassionema frauenfeldii, Strain CCMP 1798	Tfra1	CAMPEP_0178899126	
Thalassionema frauenfeldii, Strain CCMP 1798	Tfra2	CAMPEP_0178923098	
Thalassionema nitzschioides, Strain L26-B	Tnit1	CAMPEP_0194218124	
Thalassionema nitzschioides, Strain L26-B	Tnit2	CAMPEP_0194240022	
Thalassiosira antarctica, Strain CCMP982	Tant	CAMPEP_0202006238	
Thalassiosira gravida, Strain GMP14c1	Tgra	CAMPEP_0201684800	
Thalassiosira miniscula, Strain CCMP1093	Tmin	CAMPEP_0183747574	
Thalassiosira oceanica	Toce2	EJK65393	
Thalassiosira pseudonana	TpbHLH1	jgi Thaps3 24007	
Thalassiosira pseudonana	TpbHLH2	jgi Thaps3 20899	
Thalassiosira pseudonana	TpbHLH7	jgi Thaps3 23208	
Thalassiosira sp., Strain FW	Tfw	CAMPEP_0172354094	
Thalassiosira weissflogii, Strain CCMP1010	Twei	CAMPEP_0203515806	
Thalassiothrix antarctica, Strain L6-D1	Txnt	CAMPEP_0194143228	
Tiarina fusus, Strain LIS	Tfus1	CAMPEP_0117003500	
Tiarina fusus, Strain LIS	Tfus3	CAMPEP_0117046192	

**Table S5:** List of the oligonucleotides used in this work.

Gene	Phatr3 Accession	Oligo name	Sequence	Type
<i>bHLH1a</i>	Phatr3_J44962	bHLH1a-endogenous-QFw	TTATGTCTTTCGGCGACGGG	QPCR
		bHLH1a-endogenous-QRv	AGCAACGAATGCATGCAAGG	
		bHLH1a-total-QFw	ATTCTTGGTCCCACCCGGTA	QPCR
		bHLH1a-total-QRv	ACGCCACATTGAAAAACCGAG	
		<i>Pt</i> -bHLH1a-DraI-Fw	GATTTTAAAATGAATAAGCCAGGACAGCG	Full lenght cloning
		<i>Pt</i> -bHLH1a-XhoI-Rv	TTGCTCGAGCACAGCTTCGCTGCATCGTC	
<i>bHLH1b</i>	Phatr3_J44963	bHLH1b-QFw	TGCGATCTCAACGGCTAATA	QPCR
		bHLH1b-QRv	CGAAAACGAGGCTAATTC	
<i>bHLH3</i>	Phatr3_J42586	bHLH3-QFw	CACTCTCATCATGCGGGAAT	QPCR
		bHLH3-QRv	GCGCGTTGTCTTCTCTATC	
<i>bZIP7</i>	Phatr3_J48800	bZIP7-QFw	CCTTATTGATATTCAAGATTCCAAGG	QPCR
		bZIP7-QRv	GTTTCGGAACCTGCATAGGA	
<i>bZIP5</i>	Phatr3_J45142	bZIP5-QFw	ACCGGGTACAAGAAGTCGC	QPCR
		bZIP5-QRv	GACCTCCAAGCTCTGCATT	
<i>CYCH1</i>	Phatr3_J36892	CYCH1-QFw	ATACACGACGAGCGGATAC	QPCR
		CYCH1-QRv	AACAAGACGCCGTAATCG	
<i>CYCB1</i>	Phatr3_J46095	CYCB1-QFw	TCCTGGTCCGCTACTTGAAAG	QPCR
		CYCB1-QRv	GCTGGCTGGGAAGATAACGC	
<i>HSF1d</i>	Phatr3_J44750	HSF1d-QFw	TGCTCCATCAAGATACCACCAAT	QPCR
		HSF1d-QRv	GACGACACCCGAAGCTTGTT	
<i>HSF1g</i>	Phatr3_J42514	HSF1g-QFw	AGTTCCTGTCTCAGACTCAGC	QPCR
		HSF1g-QRv	ACACTTTCGCCTCTACTGTCA	
<i>HSF3.3a</i>	Phatr3_J45393	HSF3.3a-QFw	CCTTCGAATTCCTACTGCACC	QPCR
		HSF3.3a-QRv	CGTAGCCTTCCATCCGTAGT	
<i>HSF4.7b</i>	Phatr3_J49596	HSF4.7b-QFw	GACGACACCCGAAGCTTGTT	QPCR
		HSF4.7b-QRv	ACG AAGCGATCTTGACAGT	
<i>Tbp</i>	Phatr3_J10199	Tbp-QFw	ACCGGAGTCAAGAGCACACAC	QPCR
		Tbp-QRv	CGGAATGCGCGTATACCAGT	
<i>Rps</i>	Phatr3_J10847	Rps-QFw	CGAAGTCAACCAGGAAACCAA	QPCR
		Rps-QRv	GTGCAAGAGACCCGGACATACC	

## References

1. Guillard RRL (1975) Culture of Phytoplankton for Feeding Marine Invertebrates. In *Culture of Marine Invertebrate Animals*. Smith DR and Chanley MH (Springer US).
2. Zielinski T, Moore AM, Troup E, Halliday KJ, Millar AJ (2014) Strengths and limitations of period estimation methods for circadian data. *PLoS One* 9(5):e96462.
3. Plautz JD, et al. (1997) Quantitative analysis of Drosophila period gene transcription in living animals. *J Biol Rhythms* 12:204–217.
4. Doyle MR, et al. (2002) The ELF4 gene controls circadian rhythms and flowering time in *Arabidopsis thaliana*. *Nature* 419(6902):74-77.
5. Geiss GK, et al. (2008) Direct multiplexed measurement of gene expression with color-coded probe pairs. *Nature biotechnology* 26(3):317-325.
6. Annunziata R. et al. (2019) Data from "bHLH-PAS protein RITMO1 regulates diel biological rhythms in the marine diatom *Phaeodactylum tricorutum*". Gene Expression Omnibus. Available at <https://www.ncbi.nlm.nih.gov/geo/> (Series GSE112268). Deposited March 23, 2018.
7. Coesel S, et al. (2009) Diatom PtCPF1 is a new cryptochrome/photolyase family member with DNA repair and transcription regulation activity. *EMBO Rep* 10(6):655-661.
8. Bhasin M, Raghava GP (2004) ESLpred: SVM-based method for subcellular localization of eukaryotic proteins using dipeptide composition and PSI-BLAST. *Nucleic Acids Res* 32(Web Server issue):W414-419.
9. Almagro Armenteros JJ, Sonderby CK, Sonderby SK, Nielsen H, Winther O (2017) DeepLoc: prediction of protein subcellular localization using deep learning. *Bioinformatics* 33(21):3387-3395.
10. Siaut M, et al. (2007) Molecular toolbox for studying diatom biology in *Phaeodactylum tricorutum*. *Gene* 406(1-2):23-35.
11. Falcatore A, Casotti R, Leblanc C, Abrescia C, Bowler C (1999) Transformation of Nonselectable Reporter Genes in Marine Diatoms. *Mar Biotechnol* (NY) 1(3):239-251.
12. Chauton MS, Winge P, Brembu T, Vadstein O, Bones AM (2013) Gene regulation of carbon fixation, storage, and utilization in the diatom *Phaeodactylum tricorutum* acclimated to light/dark cycles. *Plant physiology* 161(2):1034-1048.
13. Saeed AI, et al. (2003) TM4: a free, open-source system for microarray data management and analysis. *Biotechniques* 34(2):374-378.
14. Keeling PJ, et al. (2014) The Marine Microbial Eukaryote Transcriptome Sequencing Project (MMETSP): illuminating the functional diversity of eukaryotic life in the oceans through transcriptome sequencing. *PLoS Biol* 12(6):e1001889.
15. Katoh K, Standley DM (2013) MAFFT multiple sequence alignment software version 7: improvements in performance and usability. *Mol Biol Evol* 30(4):772-780.
16. Pires N, Dolan L (2010) Origin and diversification of basic-helix-loop-helix proteins in plants. *Mol Biol Evol* 27(4):862-874.
17. Kumar S, Stecher G, Tamura K (2016) MEGA7: Molecular Evolutionary Genetics Analysis Version 7.0 for Bigger Datasets. *Mol Biol Evol* 33(7):1870-1874.
18. Darriba D, Taboada GL, Doallo R, Posada D (2011) ProtTest 3: fast selection of best-fit models of protein evolution. *Bioinformatics* 27(8):1164-1165.
19. Miller MA, et al. (2015) A RESTful API for Access to Phylogenetic Tools via the CIPRES Science Gateway. *Evol Bioinform Online* 11:43-48.
20. Agier N, Fischer G (2016) A Versatile Procedure to Generate Genome-Wide Spatiotemporal Program of Replication in Yeast Species. *Methods Mol Biol* 1361:247-264.

21. Smith SR, et al. (2017) Transcriptional Orchestration of the Global Cellular Response of a Model Pennate Diatom to Diel Light Cycling under Iron Limitation. *PLoS Genet* 13(3):e1006688.





# Chapter II.c:

## Physiological rhythms in the marine diatom *Phaeodactylum tricoratum* are regulated by the circadian clock transcriptional regulator RITMO1

Alessandro Manzotti<sup>1</sup>, Raphael Monteil<sup>1</sup>, Antoine Hoguin<sup>1</sup>, Cheminant Navarro<sup>1</sup>, Danis Jallet<sup>2</sup>, Francois-Yves Bouget<sup>3</sup>, Fayza Daboussi<sup>2,4</sup>, Marianne Jaubert<sup>1</sup>, Jean-Pierre Bouly<sup>1</sup> and Angela Falciatore<sup>1\*</sup>

<sup>1</sup>Laboratoire de Biologie du Chloroplaste et perception de la lumière chez les micro-algues, UMR7141, 10 CNRS, Sorbonne Université, Institut de Biologie Physico-Chimique, Paris, 75005, France

<sup>2</sup>Toulouse Biotechnology Institute (TBI), Université de Toulouse, CNRS, INRAE, INSA, Toulouse, France

<sup>3</sup>Sorbonne Université, UMR 7621, Laboratoire d'Océanographie Microbienne, Observatoire Océanologique, Banyuls-sur-Mer, France

<sup>4</sup>Toulouse White Biotechnology (TWB), INSA, Toulouse, France  
\* corresponding author

Keywords: circadian clock, diatom, rhythms, cell division, gene expression, photosynthesis, bHLH-PAS

Manuscript in preparation



# Abstract

Circadian clocks are sophisticated molecular devices of critical importance to the lives of most organisms, as they synchronize biological processes with periodic environmental cycles. Biological rhythms have been described in a variety of marine organisms in laboratory conditions and in the natural environment. However, the timekeepers controlling marine rhythms remain largely uncharacterized, primarily due to the limited genomic resources and tools to study rhythmicity. Here we address circadian regulation in prominent phytoplanktonic organisms, diatoms, by characterizing the *Phaeodactylum tricornutum* bHLH-PAS protein RITMO1, previously proposed as a genetic regulator of diel rhythmicity. We report rhythms in critical physiological processes such as cell fluorescence, photosynthesis and gene expression which persist in continuous light conditions. These rhythms are disrupted in lines in which RITMO1 has been genetically obliterated by CRISPR/Cas9 as well as in ectopic overexpressing lines, supporting a direct role of this protein in the circadian regulation. By analysing the expression of selected genes of interest, we also show that RITMO1 plays a wide role in the circadian transcriptional regulation, acting as a component of the diatom endogenous clock oscillator. RITMO1 represents a key entry point for the molecular exploration of other components of the circadian clock system of diatoms and lays the basis for assessing the relevance of circadian regulation to the life of these organisms in the marine environment.

# Introduction

Diatoms are prominent unicellular algae found in all aquatic environments (Field et al., 1998; Pierella Karlusich et al., 2020). With an estimated number of species close to 100,000 (Malviya et al., 2016), diatoms represent the most species-rich of algae, playing a central role in trophic networks and biogeochemical cycles of the oceans (Bar-On et al., 2018). Although being photosynthetic, diatoms are not directly related to the terrestrial plants and green algae of the Archaeplastida clade, which are derived by a primary endosymbiosis event. Diatoms belong to the *Stramenopila* and acquired their plastid through multiple secondary endosymbiosis of a eukaryotic red alga and likely a green alga by a heterotrophic host (Burki et al., 2020; Keeling, 2013). Traces of the complex evolutionary history are found in their genome (Armbrust, 2004; Bowler et al., 2008) and in the peculiar gene repertoire derived by the different heterotroph and phototroph ancestors as well as by bacteria via horizontal gene transfer (Dorrell et al., 2017; Vancaester et al., 2020). Comparative analysis of several diatom genomes has also highlighted a significant portion of core diatom-specific genes and species-specific genes mostly of unknown function, which may represent relevant genetic innovations for the diatom ecological success in the marine environment (for a review, see Falcatore et al., 2020).

It is well established that diatoms are able to successfully grow in extremely variable environments and are able to cope with unpredictable light changes thanks to sophisticated acclimation mechanisms (Lepetit et al., 2022). There is also considerable evidence that diatoms have adapted their physiology and metabolism to the periodic daily changes in light and darkness, experienced by most organisms on Earth. Diatoms show robust diurnal rhythms in critical processes such as photosynthesis

(Brand, 1982), pigment synthesis (Ostgaard and Jensen, 1982; Owens et al., 1980; Ragni and d'Alcalà, 2007), gene expression (Chauton et al., 2013; Smith et al., 2016) and cell cycle progression (Chisholm and Brand, 1981; Gaidarenko et al., 2019; Nelson and Brand, 1979; Ostgaard and Jensen, 1982; Williamson, 1980) so that they occur at optimal times of the day. Recent metagenomic analyses also detected strong diurnal patterns of gene expression in natural diatom communities (Coesel et al., 2021; Kolody et al., 2019). Still, the mechanisms controlling the temporal synchronization and segregation of cellular and metabolic events during light and dark periods are still largely unknown in diatoms as well as in most phytoplanktonic organisms.

The circadian clock is a powerful timing system generating biological rhythms of 24-hour cycle, extensively characterised at the molecular level in terrestrial plants and animals. Formally defined as an endogenous oscillator generating rhythmicity, the circadian clock is entrained by periodic light changes, which represent the primary time giver (*Zeitgeber*; ZT, Roenneberg and Foster, 1997). Photoreceptors play a key role in the input pathways which synchronize the circadian clock with light (Dunlap, 1999). Although different taxa use different molecular players to generate circadian rhythms, the timekeeping system share common features. In eukaryotes, they are structured around interlocked negative transcriptional-translational feed-back loops (TTFL) that uses transcription regulatory proteins to control the expression of their cognate genes (Dunlap, 1999). This regulatory loop is self-sustained, which means that the oscillations of the endogenous clock, as well as the physiological processes it controls, are maintained after transition to a constant environment (*e.g.* in continuous light) in a

process called free-run persistence. In terrestrial plants, the circadian clock has been shown to play a crucial role in the rhythmic regulation of genes involved in photosynthesis, carbon assimilation or cell division as well as in the regulation of photoperiodic-regulated processes such as the flowering (Dodd et al., 2005; Fung-Uceda et al., 2018; Zagotta et al., 1996). In marine phytoplankton, the molecular components of the clock system have been so far elucidated only in the green alga *Ostreococcus tauri*, which contain a minimalist plant-like clock with two components, OtCCA1 and OtTOC1, (Corellou et al., 2009). The existence and the nature of an endogenous circadian oscillator in diatoms remains still enigmatic for two main reasons: Although diurnal rhythms have been described in many diatom species for many years now, the persistence of these rhythms in free-running has been little characterized and, secondly, diatom genomes lack the canonical components of the circadian systems characterised in bacteria, algae, plants or animals. Recently, however, a new regulator of cellular rhythmicity named RITMO1 has been identified in the model diatom *Phaeodactylum tricorutum*, in a survey of the most rhythmic diurnal transcription factors (Annunziata et al., 2019). RITMO1 possesses bHLH-PAS domains, also found in the animal central clock proteins (Peschel and Helfrich-Förster, 2011; Takahashi, 2017). In *P. tricorutum*, it has been shown that alteration of *RITMO1* timing and expression levels by ectopic overexpression resulted in cells with altered gene expression profiles in L:D cycles but also in continuous darkness, showing that the regulation of rhythmicity by *RITMO1* is not directly dependent on light

inputs. Initial analysis of cellular fluorescence rhythms, which in diatoms reflect synchrony in the closely coupled chloroplast ontogeny and cell cycle progression (Hunsperger et al., 2016; Ragni and d'Alcalà, 2007), also revealed that ectopic expression of RITMO1 can affect cellular rhythmicity (Annunziata et al., 2019). Although these altered phenotypes identified RITMO1 as a genetic modifier of diel rhythmicity, they did not allow to assess its direct implication in the still cryptic diatom circadian clock system as misexpression was achieved in a wild-type background, under the control of a non-constitutive promoter.

To get a more insight into the function of RITMO1 in circadian regulation of diatoms, in this study we have performed an extended characterization of light-dependent biological rhythms, by assessing features of these rhythms under different photoperiodic and light intensity conditions. We have generated and exploited knock-out (KO) mutants of *RITMO1* by CRISPR/Cas9 proteolistic bombardment to test the direct consequence of the obliteration of this protein on the circadian rhythmicity of *P. tricorutum*, in parallel with the ectopic over-expressing lines. Our analyses reveal a molecular control of temporal events in key biological processes such as cell fluorescence and photosynthetic activity and support a role of RITMO1 in this regulation. The expression analysis of selected genes of interest also demonstrated a strong transcriptional control of circadian processes in *P. tricorutum*, and establish RITMO1 as the first identified component of the transcriptional clock oscillator of diatoms.

# Materials and Methods

## Cultures and irradiation conditions

Transgenic and control lines of *P. tricornutum* used in this study have a Pt1 8.6; CCMP2561 genomic background. Cell cultures were grown in batch culture in F/2 Guillard media (Guillard, 1975) at 18°C under white light (Bridgelux BXRV-DR-1830H-3000-A-13 LEDs) of different intensities and photoperiods, as described in the text. Cells were preadapted at least two weeks to the specific growth condition before performing analysis of rhythmicity. For circadian experiments, cultures were grown in incubators with orbital agitation and were not diluted during the whole course of the cellular fluorescence analysis. Final refresh of culture was performed 3 days before the release to free-run conditions to have cultures in exponential phase of growth during the experiment and ensure minimal perturbation of physiology due to culture refreshment. Cell concentrations were measured using a Z2 Coulter Particle Count and Size Analyser (Beckman Coulter). Minimal and maximal size thresholds were set respectively to 3µm and 11µm. Growth rates were calculated during the exponential phase of growth over four days and expressed as number of divisions per day. The formula used for the calculation of divisions per day is  $division\ per\ day = \frac{\ln(c_4) - \ln(c_0)}{(4 * \ln(2))}$ , where  $c_0$  and  $c_4$  represent the culture concentrations at day 0 and day 4.

## Generation of RITMO1 Knock-Out (KO) strains

RITMO1 KO mutants were generated by biolistic delivery of the CRISPR-Cas9 ribonucleoproteins according to Serif et al., 2018. Selection of transformed lines with the riboprotein complex was accomplished by co-targeting the *APT* gene (Phatr3\_J6834) to

induce resistance to 2-fluoroadenine (2-FA). A total of three and two independent sgRNAs were co-transformed to target *RITMO1* and *APT*, respectively. The sequences of the sgRNAs and the targeted region in the genome are reported in Table ST1. A total of eight 2-FA resistant colonies were sequenced by Sanger sequencing with allele specific primers to detect biallelic mutants (Fig. S1). Of the eight colonies, four appeared to bear mutations (single nucleotide insertion, deletions or inversions of gene fragments) on the two alleles of *RITMO1* gene and were named KO1 to KO4. An additional colony showed no mutation in *RITMO1* alleles and was therefore chosen as control of the effect of proteolistic bombardment (CTR line).

## Western Blot Analysis

$1 * 10^8$  cells were pelleted, quickly frozen in liquid nitrogen and stored at -80°C until use. After thawing, pellets were added with 50 µL of lysis buffer (Tris HCl pH 6.8 50 mM, 2% sodium dodecyl sulfate (SDS) and Protease Cocktail Inhibitor solution 1x (SIGMA Aldrich), solubilized at room temperature for 30 minutes, and then centrifuged at 15,000 rpm at 4°C for 30 minutes. Total proteins were extracted and analyzed by western blot as described previously (Taddei et al., 2016). Proteins were analyzed by loading on gel equal amounts of protein (30 µg), quantified with Pierce BCA Protein Assay Kit (Thermo Fisher Scientific). RITMO1 protein was detected via purified rabbit antiserum polyclonal antibody (Agrisera Antibodies, 1:10,000 dilution in PBS 5% milk) designed against a RITMO1 specific peptide (NQDHMQDVFGAMRDMLRRPFPGE-NH<sub>2</sub>) corresponding to the amino acids from position 428 to 450. Photosystem II D2 protein was used as charge control and

detected via rabbit anti-D2 antibody (1:10,000 dilution in 5% milk PBS). Following incubation with HRP-conjugated anti-rabbit secondary secondary antibodies (Promega), proteins were detected with Clarity reagents (Bio-Rad) and a ChemiDoc imaging system (Bio-Rad) imaging system.

## Cellular fluorescence analysis

In circadian experiments, culture samples were automatically collected every 2 hours via a BVP standard ISM444 peristaltic pump (Ismatec) controlled by a FC204 fraction collector (Gilson). Previous to cytometry analysis, cells were stored at 4°C in the dark for at least 2 hours to a maximum of 24 hours. Cellular fluorescence rhythmicity analyses were performed using a MACSQuant Analyser flow cytometer (Miltenyi Biotec, Annunziata et al., 2019). B3-A parameter (488 nm excitation, 655-730 nm detection) was used to track chlorophyll fluorescence. Between 10,000 and 30,000 cells were analysed per each time point per each culture replicate and median B3-A value was used for following rhythmicity analysis.

## Analysis of the rhythmic processes

The analysis of B3-A fluorescence dataset rhythmicity was performed using the BioDare2 webtool (<https://biodare2.ed.ac.uk/>, Zielinski et al., 2014). For graphical representation, data traces were baseline detrended, normalized to the maximum value and aligned to the mean values. Data traces were first analysed using the Enright Periodogram (EPR) algorithm, which was used as an arrhythmicity test (Zielinski et al., 2014). Tracks not identified as rhythmic by EPR were used for graphical representations of average fluorescence, but were not further analysed for period, amplitude and Relative Amplitude Errors (RAE). Period, amplitude and RAE were calculated via Fast Fourier nonlinear least

square algorithm (FFT-NLLS), within a period range of 18 and 34 hours. For fluorescence traces of cells grown in photoperiod, the acrophase relative to dark onset was also calculated via the same algorithm. At least three full oscillations were considered for the analysis. RAE was used as a measure of goodness-of-fit to a theoretical sine wave of the empirical traces. RAE is defined as the ratio of the amplitude error to the most probable derived amplitude magnitude (Plautz et al., 1997). Statistical differences in rhythmicity parameters among lines were evaluated via One-way analysis of variance against Wt with Bonferroni post-test for multiple testing correction.

## Cell cycle analysis

Cell cycle analysis were performed either in *P. tricornutum* cells grown under 16L:8D cycles or on cultures synchronized in G1 phase with prolonged darkness for 40h. Under diurnal conditions, 15 mL of samples in exponential growth ( $1 \times 10^6$  to  $2 \times 10^6$  cells per mL) were collected by centrifugation (2500 rpm, 15 minutes, 4°C) every 3 hrs for 24 hours. In dark synchronised experiments, the samples were collected every 3 hrs for 30 hours after re-illumination (25  $\mu$ mol photons  $m^{-2} s^{-1}$ ). Cell pellets were fixed in cold 70% EtOH and stored for at least 24hrs in the dark at 4°C until processing. Fixed cells were then washed once in cold EtOH 70%, once in PBS and stained in the dark for 45 minutes at room temperature with DAPI (4',6-diamidino-2-phenylindole) at a final concentration of 0.5ng/ml. After staining, cells were washed with PBS and kept on ice in the dark until the flow cytometry analysis. 50,000 cells per each sample were analysed using the MACSQuant Analyser flow cytometer. V1-A channel (408 nm excitation, 450/50 nm detection) was used to evaluate the content of DAPI-stained DNA. 2c and 4c peaks were used to infer the fraction of cells in G1 and S/G2/M phases, using a dedicated R script (Agier and Fischer, 2016). The area under each peak was used as a proxy

for the proportion of cells in each phase. Two-way analysis of variance was performed to verify statistical differences among lines along the time series. Bonferroni post-test was used to compare replicate means by rows, comparing each line to Wt.

## Analysis of photosynthetic parameters

The analyses were performed on cultures (three biological replicates) adapted to 16L:8D (25  $\mu\text{mol photons m}^{-2} \text{ s}^{-1}$ ) and then either maintained in 16L:8D 25  $\mu\text{mol photons m}^{-2} \text{ s}^{-1}$  or transferred to L:L 17  $\mu\text{mol photons m}^{-2} \text{ s}^{-1}$ . For the analysis, samples were collected every 4 hours over 36 hours starting from the second free run day (LL32). 15 mL of samples in exponential growth ( $1 \times 10^6$  to  $2 \times 10^6$  cells per mL) were concentrated 10 folds in their own supernatant by centrifugation (2,500 rpm, 10 minutes). For chlorophyll fluorescence analysis, the cells were left under dim light (<5  $\mu\text{mol photons m}^{-2} \text{ s}^{-1}$ ) in order to allow full relaxation of Photosystem II (PSII) reaction centers before Rapid Light Curve (RLC) analysis (Ralph and Gademann, 2005). Samples were then exposed to one minute of dark, followed by increasing intensity steps of actinic light up to 1450  $\mu\text{mol photons m}^{-2} \text{ s}^{-1}$  to obtain the RLCs. Each light step lasted 30 seconds and illumination was performed with red LEDs. At the end of each light step, chlorophyll fluorescence was measured with a blue light measuring pulse and a 250 ms red light saturating pulse (1700  $\mu\text{mol photons m}^{-2} \text{ s}^{-1}$ ) was used to induce PSII maximal fluorescence ( $F_m'$ ). Fluorescence of light adapted PSII ( $F_s$ ) was measured just prior to saturating light application. Chlorophyll fluorescence detection was performed using a Paradigme Camera Speedzen system (Beambio). PSII quantum yield  $\phi\text{PSII}$  was calculated as  $(F_m' - F_s) / F_m'$  (Maxwell and Johnson, 2000). Non-Photochemical Quenching (NPQ) was calculated as  $(F_m' -$

$F_m) / F_m'$ , where  $F_m$  is the maximal fluorescence of dark adapted PSII (Maxwell and Johnson, 2000). NPQ values were obtained at the last 1,450  $\mu\text{mol photons m}^{-2} \text{ s}^{-1}$  light step. For each light step, the relative Electron Transfer Rate through the photosynthetic chain (rETR) was calculated as  $\phi\text{PSII} \times \text{Light intensity}$ . The RLC resulting from plotting rETR as a function of light intensity was fitted to a double exponential decay function: 
$$\text{ETR} = \text{ETR}_{max} * \left(1 - e^{-\alpha * \frac{E}{\text{ETR}_{max}}}\right) * \left(e^{-\beta * \frac{E}{\text{ETR}_{max}}}\right)$$
 following Platt et al., 1980. By RLC fitting, the maximum value of rETR (rETR<sub>max</sub>) and the angular coefficient of the function in the light limiting region ( $\alpha$ ) were calculated. Fitting was performed via Origin software version 9.1.

## RNA extraction and RT-qPCR analysis

For RNA purification,  $10^8$  cells from exponential phase cultures were filtered onto Whatman filter 589/2. Filters were then washed with 25mL of PBS 1X, cut in two to have technical replicates, flash frozen in liquid nitrogen and stored at  $-80^\circ\text{C}$  until use. RNA was extracted with TriPure Isolation Reagent (Roche) following the protocol provided by the company and further purified by an ammonium acetate precipitation. RNA purity and integrity were checked on samples by assessing the 260nm/230nm and 260nm/280nm OD ratios and by gel electrophoresis. 500ng of RNA were retro-transcribed via an oligo-dT and random primers mix using the QuantiTect Reverse Transcription Kit (Quiagen). For RT-qPCR, ribosomal protein small subunit 30S (RPS) and TATA box Binding Protein (TBP) were used as reference genes (Siaut et al., 2007). For each sample, geometrical average of Ct was used as reference to evaluate the expression of genes of interest via the  $\Delta\Delta\text{Ct}$  Livak method (Livak and Schmittgen, 2001). For each gene, data was normalized against the maximum

expression value among the different strains, so that expression values are all between 0 and 1. This normalization method allows to compare the relative gene expression among different cell lines. All RT-qPCR analyses

were performed on two biological replicates obtained in distinct experiments. All the primers used for RT-qPCR analysis are listed in Table ST5.

# Results

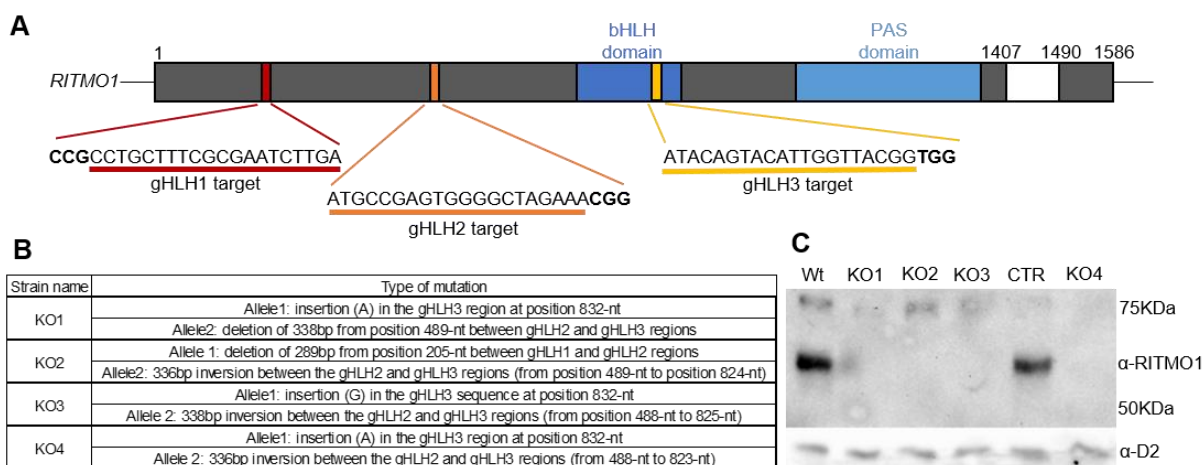


Figure 1. Generation of knock-out (KO) mutants for *P. tricornutum* RITMO1.

(A) Schematic representation of the *RITMO1* locus of *P. tricornutum* on Chromosome 5 (Phatr3\_J44962). Exons are represented as black boxes, the intron as a white box. Blue and light blue boxes represent the relative location of the bHLH and PAS domains respectively. Red, orange and yellow boxes highlight the localisation of the target sequences (underlined) of the three gRNAs used for RITMO1 CRISPR-Cas9 mutagenesis. Letters in bold represent the protospacer adjacent motif associated with each target site. (B) Description of the mutations introduced on each allele of the *RITMO1* locus on the four KO mutants as identified by Sanger sequencing. (C) Immunoblot analysis in Wt, KO and CTR lines of RITMO1 protein at ZT9 in cells adapted to 12L:12D of 25  $\mu\text{mol photons m}^{-2} \text{s}^{-1}$ . An antipeptide antibody recognizing the RITMO1 protein downstream of the targeted mutation sites (corresponding to the amino acids from position 428 to 450 in the wild-type sequence) was used for the detection of the RITMO1 protein. An  $\alpha$ -D2 antibody was used as loading control.

## Generation of knock-out mutants for the *P. tricornutum* RITMO1 by CRISPR-Cas9

In order to characterize more thoroughly the role of *P. tricornutum* RITMO1 within the diatom timekeeper machinery, we generated knock-out lines for RITMO1 by proteolistic bombardment of the CRISPR-Cas9 protein (Serif et al., 2018). A set of three RITMO1-specific sgRNAs (Fig. 1A) were co-transformed together with two sgRNAs for the endogenous counter-selectable markers *PtAPT* (*Adenine Phosphoribosyl Transferase*), whose mutation allows the selection of KO lines via the resistance to 2-fluoroadenine (2-FA) (Table S1). Four knock-out lines presenting mutations on both alleles of the RITMO1 gene were generated (Figure 1 B and Fig. S1),

hereafter named KO1-4. A line resistant to 2-FA but not presenting any mutation for RITMO1 was also generated and chosen as independent transformation control (CTR). Wild-type (Wt), Kos and CTR lines were analysed by western blot by using an antipeptide recognizing the RITMO1 protein downstream of the targeted mutation sites. The analysis shown in Fig. 1C demonstrated a loss of the RITMO1-associated band in the four mutant lines, but not in the Wt and CTR lines. The KO1 and KO3 lines were used to further analyse cellular rhythmicity, along with the previously generated RITMO1 over-expressor OE1 line (Annunziata et al., 2019).



Diatoms cellular fluorescence rhythmicity is adjusted in a photoperiod-dependent manner and is not altered in knock-out mutants for *RITMO1*

Previous studies in *P. tricornutum* (Annunziata et al., 2019; Hunsperger et al., 2016; Ragni and d'Alcalà, 2007) grown under periodic light:dark (L:D) cycles indicated that the diurnal fluorescence changes monitored by flow cytometer represent a good proxy of the chlorophyll a content in the growing chloroplast and of progression through the cell cycle. To characterise the features and robustness of diurnal and circadian processes in diatoms and the involvement of *RITMO1* in these processes, we first performed an extended characterization of cellular fluorescence changes in *P. tricornutum* cells adapted to different photoperiods and light intensities (Fig. 2). We performed this comparative analysis on Wt, CTR, KO1, KO3 and OE1 lines. In cells adapted to 16L:8D cycles of moderate light intensity (25  $\mu\text{mol photons m}^{-2}\text{s}^{-1}$ ) and showing a cell division per day (Table S2), cellular fluorescence displayed strong diurnal oscillations during the L:D, with an acrophase of fluorescence at around ZT14, hence anticipating dark transition of 2 hours (Fig. 2A and F, and Table S3). During the night period, fluorescence continued to decrease, reaching a minimum at the end of the dark. To confirm the correlation between cell fluorescence changes and cell cycle progression, cell concentration was analysed in wild-type cells all three hours over the course of three days, and the different cell cycle phased monitored by DAPI staining. We observed a strong inverse correlation between the increase in cell number after cytokinesis (Fig. S1A-C) during the night period and fluorescence signal, confirming the fluorescence as a good proxy of the cell cycle. This is also confirmed by the progressive reduction of the percentage of cells in G1 along the light period (Fig. S1D).

We further tested *P. tricornutum* responses to different photoperiods. Cells adapted to 12L:12D of 25  $\mu\text{mol photons m}^{-2}\text{s}^{-1}$  (Fig. 2B) showed oscillations, as for the 16L:8L (Fig. 2A) and a comparable division rate (Table S2). They exhibited a similar anticipation of the dark, with an acrophase of cellular fluorescence anticipating dark transition of about 1.5 h (Fig. 1F) indicating that cell rhythmicity was adjusted to the shorter photoperiod. Differently, in cells acclimated to 8L:16D photoperiod at 25  $\mu\text{mol photons m}^{-2}\text{s}^{-1}$  (Fig. 2C), the fluorescence peak occurred 2 hours after the onset of darkness (Fig. 2F). Cells showed a reduced growth (around 0.6 division/day, Table S2). To test whether the loss of night anticipation and the observed phase shift was due a metabolic control of growth and synchronization capacity due to the limiting amount of light, we repeated the analysis in 8L:16D, but applying twice the light intensity (50 instead of 25  $\mu\text{mol photons m}^{-2}\text{s}^{-1}$ ) during the light phases (Fig. 2D). This increased irradiation resulted in an increase growth of *P. tricornutum* (~1 division/day, Table S2). Under these conditions, however, no significant change of the phase was observed compared to the analysis done in the same photoperiod with lower irradiation (Fig. 2F and Table S3). Similarly, when *P. tricornutum* cells were adapted to 16L:8L with higher light intensity (75  $\mu\text{mol photons m}^{-2}\text{s}^{-1}$ , Fig. 2E), they showed an increased growth (1.5 division/day, Table S2), but a similar phase compared to cells adapted to lower irradiation (Fig. 2A and Table S3), suggesting a synchronization of cell population within L:D cycles, independently on the light intensity applied and division rate.

As clearly seen in Fig. 2 and Table S3, neither the obliteration of *RITMO1* in knock-out lines nor the deregulation of its expression in OE1 altered cellular fluorescence rhythmicity in cells adapted to different photoperiods and light intensities. All the transgenic lines showed rhythmic fluorescence trends comparable to that of the Wt and CTR

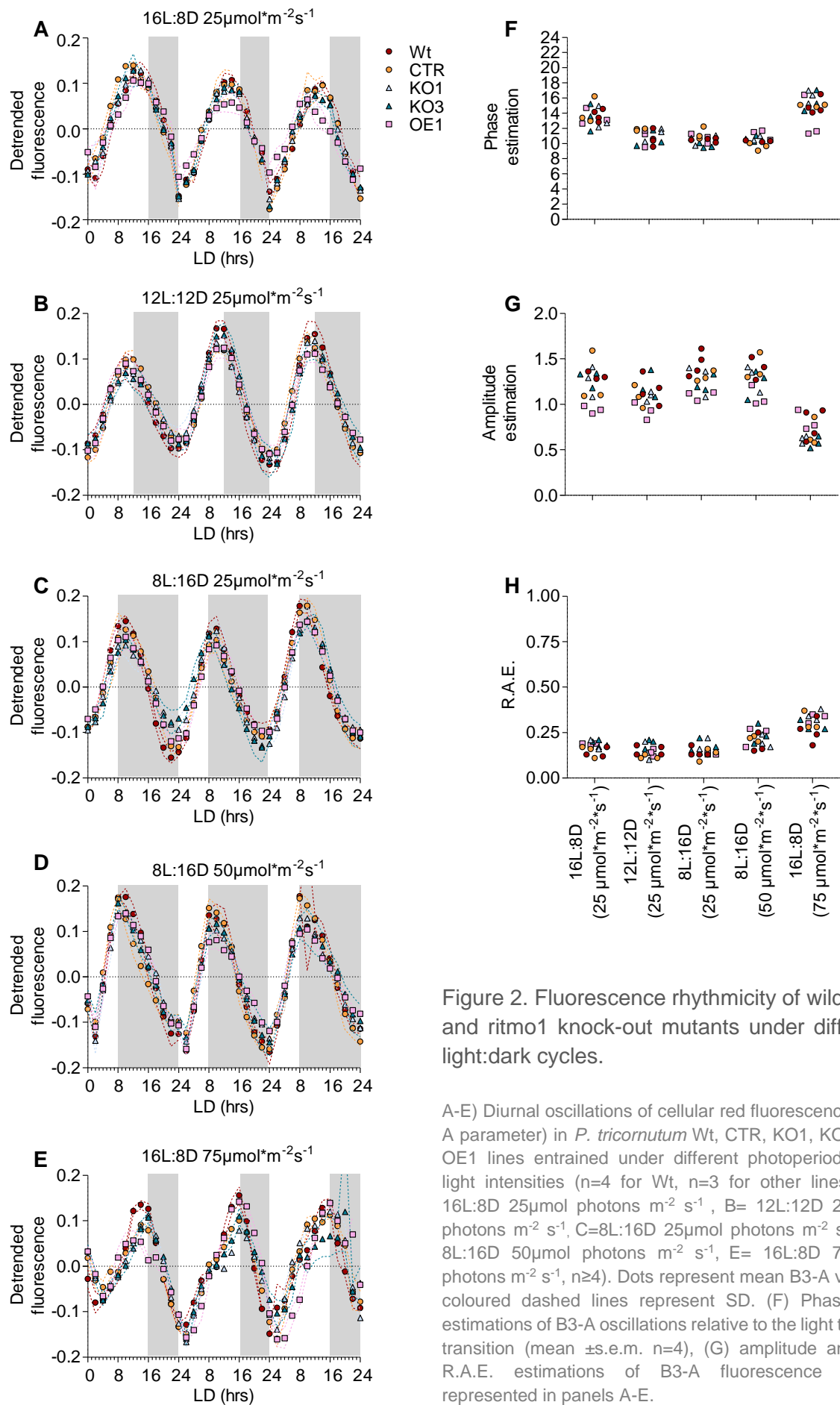


Figure 2. Fluorescence rhythmicity of wild-type and *ritmo1* knock-out mutants under different light:dark cycles.

A-E) Diurnal oscillations of cellular red fluorescence (B3-A parameter) in *P. tricornutum* Wt, CTR, KO1, KO3 and OE1 lines entrained under different photoperiods and light intensities ( $n=4$  for Wt,  $n=3$  for other lines). A= 16L:8D  $25\mu\text{mol photons m}^{-2} \text{s}^{-1}$ , B= 12L:12D  $25\mu\text{mol photons m}^{-2} \text{s}^{-1}$ , C=8L:16D  $25\mu\text{mol photons m}^{-2} \text{s}^{-1}$ , D= 8L:16D  $50\mu\text{mol photons m}^{-2} \text{s}^{-1}$ , E= 16L:8D  $75\mu\text{mol photons m}^{-2} \text{s}^{-1}$ ,  $n\geq 4$ ). Dots represent mean B3-A values, coloured dashed lines represent SD. (F) Phase-time estimations of B3-A oscillations relative to the light to dark transition (mean  $\pm$ s.e.m.  $n=4$ ), (G) amplitude and (H) R.A.E. estimations of B3-A fluorescence traces represented in panels A-E.

lines, indicating that RITMO1 does not have a major impact on cell synchronization as far as the cells are exposed to periodic L:D cycles.

### RITMO1 obliteration affects fluorescence rhythmicity under free-running conditions

Previous study in *P. tricornutum* showed that cells pre-adapted in L:D cycles and subsequently released under constant light maintain cell fluorescence rhythms for several days, suggesting a possible regulation of these rhythms by a circadian clock (Annunziata et al., 2019). To test the robustness of these rhythms, we here first analysed cellular fluorescence profiles in wild-type cells adapted to 16L:8D cycles of  $25 \mu\text{mol photons m}^{-2} \text{s}^{-1}$  and then exposed to free-run conditions either of continuous dark (Fig. 3A), or continuous light of different light intensities (5, 17 or  $25 \mu\text{mol photons m}^{-2} \text{s}^{-1}$ )

for four days (Fig 3B-D). The transition to continuous darkness resulted in the total flattening of fluorescence oscillations after the first subjective night, which is consistent with the arrest of cell cycle progression observed in *P. tricornutum* cells exposed to prolonged darkness (Huysman et al., 2010). In case of the transition to constant low light condition (from 16L:8D  $25 \mu\text{mol photons m}^{-2} \text{s}^{-1}$  to L:L of  $5 \mu\text{mol photons m}^{-2} \text{s}^{-1}$ , Fig. 3B), the cell continued to divide over the days considered for the analysis, but to a strongly reduced rate (around 0.22 division/day in L:L compared to 1 division/day before the transition (Table S2). In none of the biological replicates, the cells passed the periodicity EPR test (Materials and Methods), suggesting a possible desynchronization of the whole population under light irradiance potentially limiting for the metabolism. On the contrary, in the case of cells exposed to  $17 \mu\text{mol photons m}^{-2} \text{s}^{-1}$  L:L

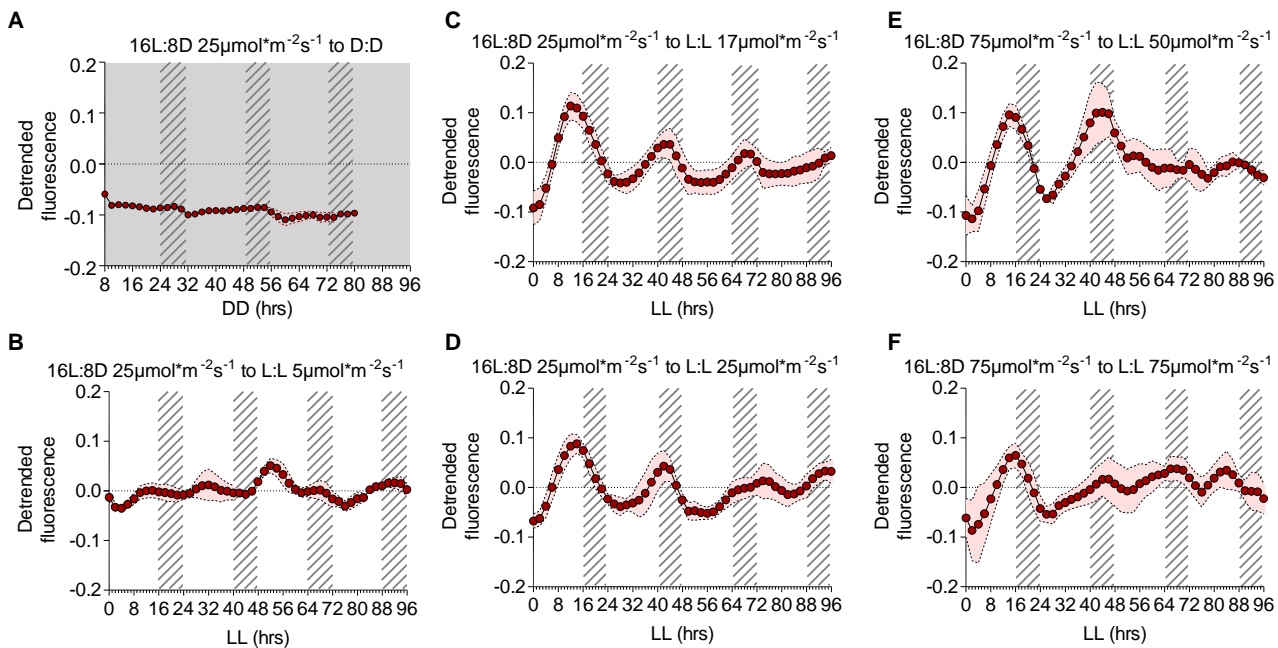


Figure 3. Characterization of fluorescence rhythmicity of wild-type *P. tricornutum* cells after the transition from L:D cycles to free running conditions.

A-D) Cellular fluorescence profiles after transition from 16L:8D  $25 \mu\text{mol photons m}^{-2} \text{s}^{-1}$  to different free-run conditions over four subjective days: A= D:D, B= L:L  $5 \mu\text{mol photons m}^{-2} \text{s}^{-1}$ , C= L:L  $17 \mu\text{mol photons m}^{-2} \text{s}^{-1}$ , D= L:L  $25 \mu\text{mol photons m}^{-2} \text{s}^{-1}$ ,  $n \geq 4$ ). (E) Cellular fluorescence profiles after transition from 16L:8D  $75 \mu\text{mol photons m}^{-2} \text{s}^{-1}$  to L:L of  $50 \mu\text{mol photons m}^{-2} \text{s}^{-1}$  ( $n=7$ ) and (F) to L:L  $75 \mu\text{mol photons m}^{-2} \text{s}^{-1}$  (L,  $n=4$ ) over four subjective days. Dots represent mean B3-A values, coloured ribbons represent SD. Gray dashed regions represent subjective nights in free-run conditions.

(Fig. 3C), and thus experiencing during the 24 h a total irradiance equivalent to that of a 16L:8D cycle, the fluorescence oscillations showed a rhythmic pattern. Oscillation persisted for at least 4 days in free run, although with a longer period, in accordance with what already reported in Annunziata et al., 2019. Similar oscillation features were observed in cells exposed in L:L to the same light of 25  $\mu\text{mol photons m}^{-2}\text{s}^{-1}$ , as used for entrainment (Fig. 3D), suggesting that the total increased irradiance due to the absence of the dark period did not affect global growth and synchronization capacity (Table S2 and 4). On the contrary, rhythmicity appeared perturbed in cells experiencing higher light intensity. In particular, in cells pre-adapted in 16L:8D of 75  $\mu\text{mol photons m}^{-2}\text{s}^{-1}$  and then exposed to continuous light of 50  $\mu\text{mol photons m}^{-2}\text{s}^{-1}$  (Fig. 3E), clear oscillations were visible during the first two days of free-run, with a first peak of fluorescence occurring at L:L14 followed by the second peak at L:L42-44, and estimated period of about 28-30 hour. After the second day, we reported a rapid damping of the fluorescence profiles that made a reliable calculation of the period impossible. In the case of cells exposed to the 75  $\mu\text{mol photons m}^{-2}\text{s}^{-1}$  in both L:D and after release to L:L (Fig. 3E), the cultures lost a consistent rhythmic profile following the end of the first subjective day. All together these data support a strong regulation of biological rhythms in diatoms by an endogenous oscillator, whose activity is potentially influenced by other light-intensity dependent metabolic and cellular processes.

We then investigated the effect of the RITMO1 mutation on free running oscillation. Differently from what reported in cells exposed to periodic L:D cycles (Fig. 2), significant effect on cellular rhythmicity was observed in all the transgenic lines, when exposed to conditions in which Wt cells exhibited strong circadian rhythms (Fig. 4). In particular, when cells were adapted to 16L:8D 25  $\mu\text{mol photons m}^{-2}\text{s}^{-1}$  and subsequently

exposed to free running light of 17  $\mu\text{mol photons m}^{-2}\text{s}^{-1}$  (Fig 4A-E), both KO lines and OE lines showed alteration of rhythmicity in free running, if compared to Wt and CTR lines. In several independent biological replica (Table S4) these lines were considered arrhythmic by using EPR algorithms estimating periodicity. When a rhythm could be calculated (Table S4), both KO1 and KO3 lines and the OE1 exhibited a significant reduction in oscillation amplitude and a trend of increase in RAE when compared to the Wt and CTR (Fig. 4 G and H and Table S4), indicating a strongly affected synchronization of the population in free running condition. In addition, both KO lines manifested a major and significant reduction in period when compared to Wt and CTR lines. Parallel time resolved analysis of cell growth in L:L (Fig. S4) confirmed an alteration of circadian period in KO3 compared to Wt. OE1 (Fig. 4E and Table S4) showed strongly altered oscillations, as for the KOs lines. Analysis of rhythmicity in cells exposed to free running condition of higher light intensity of 25  $\mu\text{mol photons m}^{-2}\text{s}^{-1}$  (Fig. S3), showed similar alteration of rhythmicity in *RITMO1* mutants compared to wild-type cells to that observed at lower irradiance (Fig 4A-E). While the increased light intensity did not have any effect on the period of the Wt and CTR lines, a small, but still significant modification was observed in the free running period of KO and OE lines (Fig. S3).

We further inquired whether obliteration of RITMO1 in KO lines or alteration of its expression in OE might have an effect on the capacity of *P. tricornutum* to dynamically respond to environmental inputs. To do so, we first desynchronized the cells by growing them to continuous light of 17  $\mu\text{mol photons m}^{-2}\text{s}^{-1}$  for two weeks and we re-exposed them to 16L:8D photoperiod of 25  $\mu\text{mol photons m}^{-2}\text{s}^{-1}$  (Fig. 5), in a mirror treatment to that reported in Fig 4. This analysis indicated that all the lines are capable of recovering rhythmic changes in

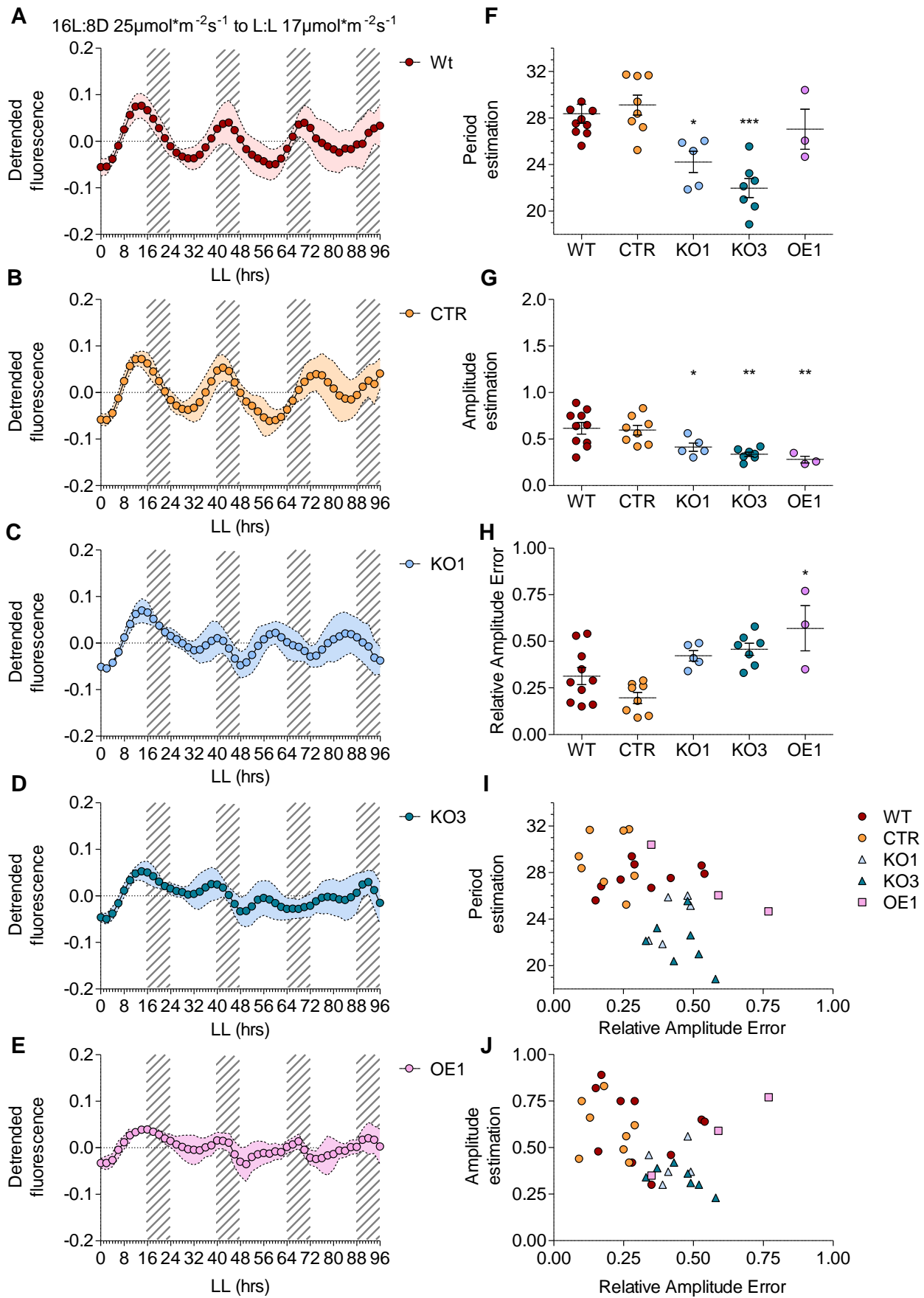


Figure 4. Effects of RITMO1 mutation on cellular fluorescence in free running.

(A-E) Cellular fluorescence profiles after transition from 16L:8D 25 $\mu$ mol photons  $m^{-2} s^{-1}$  to L:L 17 $\mu$ mol photons  $m^{-2} s^{-1}$  in Wt, CTR, KO1, KO3 and OE1 cells ( $n \geq 8$ ). Dots represent mean B3-A values, coloured ribbons represent SD. White and grey regions represent light and dark periods, grey dashed regions represent subjective nights in free-run conditions. (F-J) Period (F), amplitude (G) and R.A.E. (H) estimations of B3-A fluorescence traces represented in panels A-E that passed the EPR rhythmicity test (mean  $\pm$  s.e.m., \* $P < 0.05$ , \*\* $P < 0.01$ , \*\*\* $P < 0.001$ , One-way analysis of variance against Wt with Bonferroni post-test correction). (I) Plot of period versus R.A.E. estimates. (J) Plot of amplitude versus R.A.E. estimates.

fluorescence, visible at the population level already after the first night, with a period that is attested to 24 hours. The fact that the amplitude of these oscillations is comparable between the first light-dark cycle and the two subsequent ones analysed in the course of the experiment suggests that a treatment of 8 hours of darkness is sufficient to ensure the re-synchronization of the population. Both *RITMO1* KOs and the OE lines did not show differences compared to the Wt and CTR, hinting that the alterations of RITMO1 activity does not affect the capacity of cell cycle to re-synchronise to diel environmental cues.

*RITMO1* affects circadian fluorescence rhythmicity, without affecting growth and cell cycle progression

The alteration of cellular fluorescence rhythmicity observed in free running conditions in the *RITMO1* KO mutants compared to Wt and CTR lines opens the question of whether this effect is due to a possible role of RITMO1 in the regulation of cell growth and cell cycle progression. We therefore monitored the growth of Wt, CTR, OE1 and KO lines under L:D cycles and following L:D to L:L shift. The analysis in Fig. 6A and Table S4 indicated that mutants lines had a growth capacity comparable to that of

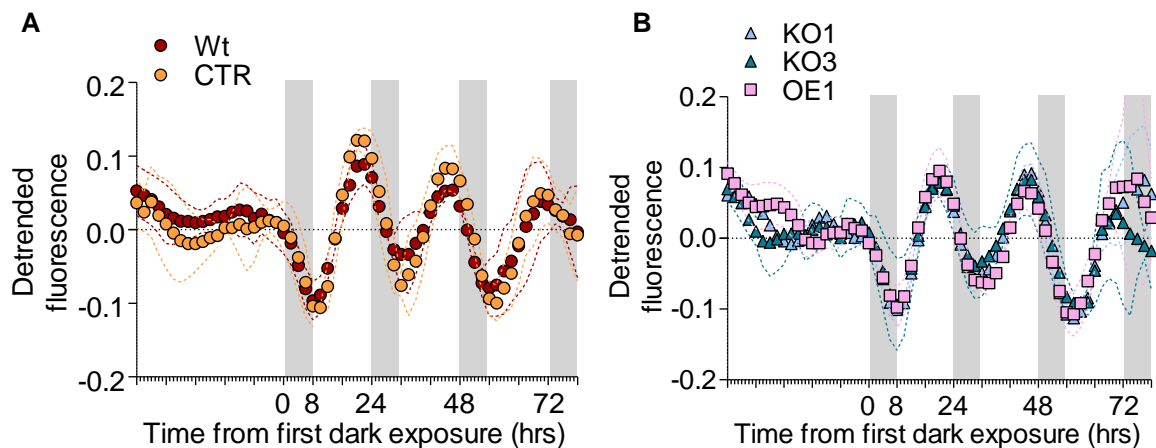


Figure 5. Re-entrainment of Wt, KO1, KO3 and OE1 cultures adapted to continuous light (L:L) to L:D cycles.

Cellular fluorescence profiles after transition from L:L 17 $\mu$ mol photons  $m^{-2} s^{-1}$  to 16L:8D 25 $\mu$ mol photons  $m^{-2} s^{-1}$  in Wt and CTR lines (A) and in KO1, KO3 and OE1 lines (B). Cells were pre-adapted to L:L for two weeks before re-entrainment to photoperiod. Dots represent mean B3-A values, coloured dashed lines represent SD ( $n=3$ ). White and grey regions represent light and dark periods.

the Wt and CTR lines in both 16L:8D and following a shift to L:L ( $17 \mu\text{mol photons m}^{-2} \text{s}^{-1}$ ). Moreover, we also tested effect on cell cycle progression by analysing the cell cycle phases of cells first synchronized with a dark treatment of 40 hours and subsequently exposed to continuous light, as previously done (Annunziata et al., 2019; Huysman et al., 2010). As shown in Fig. 6B, the 2 KO lines showed the same percentage of cells in G1 (around 80%) at the end of the dark treatment. A similar reduction of the G1 phases, corresponding to an increase of dividing cells (S/G2), was also observed following light exposure inducing cell cycle progression. The data indicate that the alterations of cell fluorescence rhythmicity observed in *P. tricornutum* in free-run in *RITMO1* KO and

OE1 are attributable to a loss of synchronization of the population associated with an alteration of a clock component, and not to a deregulation of the cell cycle.

## RITMO1 is implicated in the circadian regulation of photosynthesis in *P. tricornutum*

Adaptation of the photosynthetic apparatus to external stimuli is vital for photoautotrophic organisms and evidences in plants and algal species, including diatoms, indicate a regulation of this process by an endogenous oscillator (Brand, 1982; Dodd et al., 2014). To evaluate the involvement of RITMO1 in the rhythmic activity of the plastid, we compared the photosynthetic capacity of the Wt, KO1, KO3, and OE1 lines both in cells adapted to 16L:8D cells and following the 16L:8D to L:L transition (Fig. 7A). Samples were collected every 4 hours over 36 hours. In free running, analysis started at the second subjective day, from LL32. Different photosynthetic parameters were measured by performing a Rapid Light response Curve (RLC) (Materials and Methods, Ralph and Gademann, 2005). In 16L:8D, the four lines showed a twofold variation of the Maximal relative Electron Transfer Rate (ETRmax) (Fig. 7B) and photoprotection capacity here measured via the NPQ (Fig. 7D) over the 24 hours. Both parameters started to increase during the dark, peaked in the middle of the light and reached a minimum towards the final hours of the light period. Notably, ETRmax and NPQ peak during the light period, while the maximal

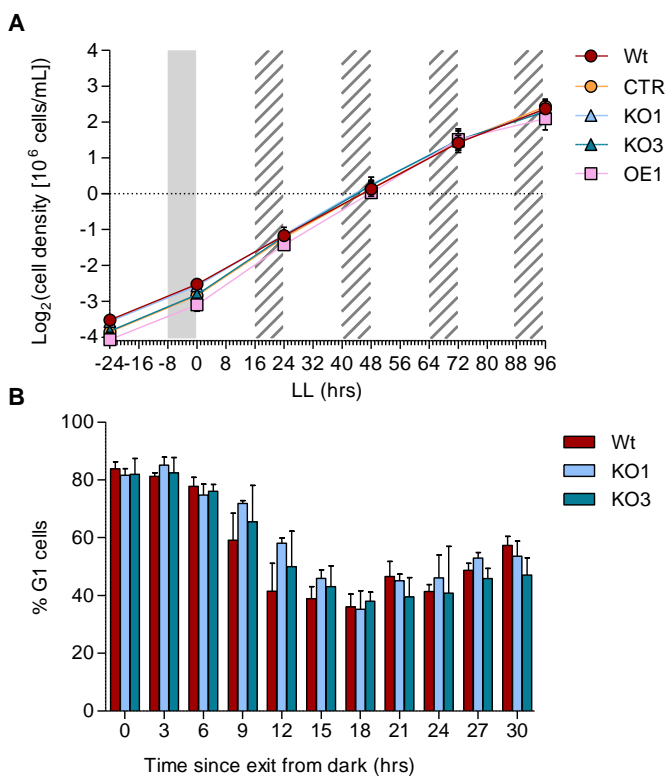


Figure 6. Analysis of the effect of RITMO1 obliteration and overexpression on growth capacity and cell cycle progression.

(A) Growth curves of Wt, CTR, KO1, KO3 and OE1 cells entrained under 16L:8D  $25 \mu\text{mol photons m}^{-2} \text{s}^{-1}$  and released to L:L  $17 \mu\text{mol photons m}^{-2} \text{s}^{-1}$ . Dots and error bars represent the mean  $\pm$  s.e.m. Log<sub>2</sub> of cell density expressed as  $10^6 \text{ cells mL}^{-1}$  ( $n=3$ ). (B) Percentage of cells in G1 phase in cultures synchronized for 48 hours in dark and subsequently exposed to  $25 \mu\text{mol photons m}^{-2} \text{s}^{-1}$  continuous light. Cell cycle was determined by flow cytometry after DAPI staining of the cellular DNA content. Columns represent mean percentage values of cells in G1 at each time point  $\pm$  s.e.m. ( $n=3$ ). Two-way analysis of variance with Bonferroni correction was used to compare cell cycle progression among lines, but no significant difference was detected.



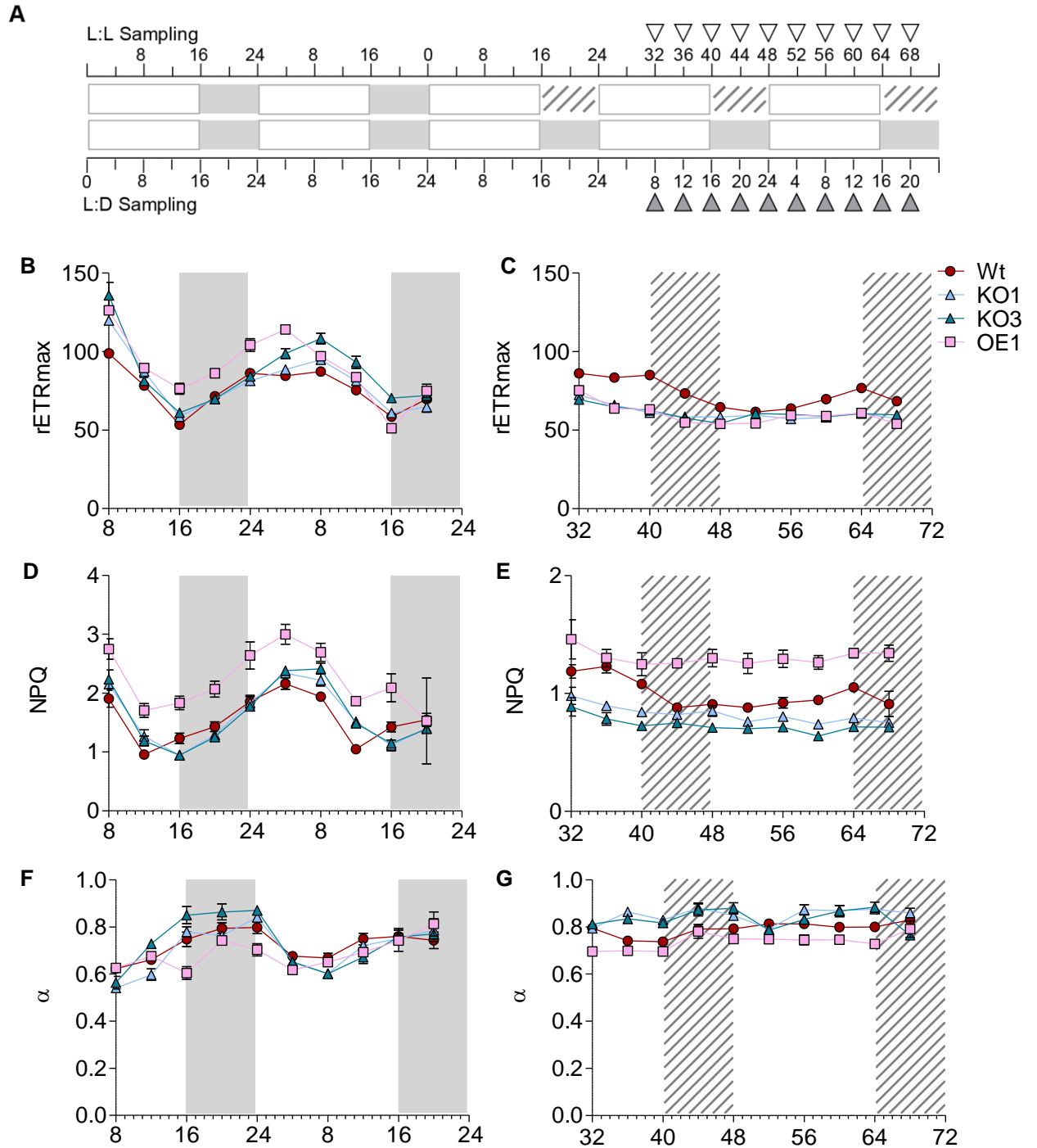


Figure 7. Analysis of the effect of RITMO1 mutation and overexpression on different photosynthetic parameters under periodic L:D cycles and free running conditions.

A) Schematic representation of sampling points for the analysis from Wt, KO1, KO3 and OE1 cells grown under 16L:8D 25 $\mu\text{mol photons m}^{-2} \text{s}^{-1}$  and released to L:L 17 $\mu\text{mol photons m}^{-2} \text{s}^{-1}$ . Samples were collected every 4 hours over 36 hours in L:D and L:L. In free running, samples were collected starting at L:L32. (B) Maximal relative Electron Transfer Rate (rETRmax), (D) non photochemical quenching (NPQ) and (F) photosynthetic rate under light limitation ( $\alpha$ ) in L:D. (C) rETRmax, (D) NPQ and (G)  $\alpha$  in cells transferred to L:L. Dots represent mean values  $\pm$  s.e.m. (n=3).



value is attained between ZT4 and ZT8 in both wild-type and the two KO lines. The light-limited initial slope ( $\alpha$ ), which is an indication of the maximum quantum yield of PSII, manifested oscillations of minor magnitude (25% of its maximum value over the course of the day), with a minimum after 4-8 hours after the beginning of the light period, followed by a progressive increase until the end of the dark phase (Fig. 7F). In L:L, the Wt lines retained an oscillation with a period of 24 and 28 hours for both ETR<sub>max</sub> and NPQ respectively, although the rhythms were attenuated compared with the 16L:8D (showing approximately a 30% variation relative to the maximum value) (Fig. 7C and E). As for the cell fluorescence, a clear shift in the phase was observed compared to the L:D, with a peak around the transition from the subjective light to the subjective dark phase. The KO mutants and the OE1 line did not show significant oscillations already after the second day in free run condition, supporting an involvement of RITMO1 in the circadian regulation of these processes. Considering the  $\alpha$  value, no major variations during the 36 hours analysed can be observed for any of the four lines considered (Fig. 7G).

## RITMO1 plays a central role in the circadian control of gene expression in diatoms

RITMO1 belongs to the bHLH-PAS family of the *P. tricornutum* transcription factors. The deregulation of its expression by ectopic overexpression generates a perturbation of gene expression rhythmicity in L:D but also in continuous dark (Annunziata et al., 2019), indicating that its activity is independent on direct light inputs. Here we further investigated the role of RITMO1 in the circadian clock system, by analysing the expression of a set of genes of interest by RT-qPCR in cells adapted to 16L:8D (25  $\mu\text{mol photons m}^{-2} \text{s}^{-1}$ ) and following a 16L:8D to L:L (17  $\mu\text{mol photons m}^{-2} \text{s}^{-1}$ ). In order to uncover

rhythms controlled by the circadian clock only, persistence in gene expression oscillation in free-run condition was analysed every 4 hours between LL32 to LL68, at the second and third subjective night and day, as done for the photosynthesis experiment (Fig. 7A). Wt, KO3 and OE1 lines were chosen for the analysis in order to compare the effect of both obliteration and overexpression of RITMO1 on expression patterns. First, the expression level of RITMO1 was analysed to check how the deregulation of the protein affects its own transcription. Because we also analysed expression in the ectopic OE line, we used two different primer sets recognized the endogenous RITMO1 mRNAs (Fig. 8A left) and also the total transcript (endogenous plus transgene) in OE lines (Fig. 8A right). As shown in Fig. 8A (left), KO3 and OE1 cells showed rhythmic profile of the endogenous RITMO1 expression in L:D comparable to that of Wt. OE1 showed a ~60 % lower expression level at the peak of expression (ZT12), as already shown in (Annunziata et al., 2019). Although less pronounced, a reduction in gene expression was observed in KO3 too, indicating that RITMO1 transcription was maintained despite the mutation of the gene by CRISPR/Cas9 and total obliteration of the full-length protein (Fig. 1). In Wt cells in free-run, RITMO1 transcript showed a clear oscillation with an increase in transcript levels before the start of the second subjective night, followed by a decline in the following hours, a minimum at LL52 and a new increase in the expression in the following hours. The peak of expression is delayed from the subjective L:D day by approximately four hours. As for the OE1 and KO lines, they both lost the oscillation observed in the Wt, with a flattened expression profile and an average transcript value in the range of that of the control line. By using a pair of primers designed to recognise the total RITMO1 mRNA in OE1 (Fig 8A right), in L:D a rhythmic pattern was still observed in OE1, but with an earlier peak of expression compared to Wt and KO lines, due to the over-expression of RITMO1 driven

by the FcpB promoter. In L:L, OE1 showed higher expression level than Wt and distinct rhythmic pattern, with an acrophase during the subjective light period. As expected, both the Wt and KO3 showed no difference in the expression pattern compared to the analysis done with the other set of primers. In addition to *RITMO1*, we also analysed other TFs transcripts (*bHLH1b*, *bHLH3* and *bZIP7*) exhibiting strong rhythmic expression in L:D cycles (Annunziata et al., 2019). All these TFs showed persistence of gene expression rhythmicity in L:L in Wt cells (Fig. 8B), which was strongly altered in both OE1 and KO3 for the *bHLH1b* and *bZIP7*. For the *bHLH3*, a minimal residual rhythmicity was still detected in KO3, although with an altered phase. In addition, we also analysed the expression of photoreceptors, potential actors in the input pathway of the diatom circadian clock (Fig. 8C). The analysis of the *aureochrome1* (*Aureo1a*) was particularly relevant. This blue light receptor also acts as light-dependent TFs controlling the expression of an important number of genes in *P. tricornutum*, including *RITMO1* (Mann et al., 2020). In our study, *Aureo1a* expression appeared rhythmic under diurnal (L:D) and free run (L:L) conditions in Wt, and this rhythmic pattern was strongly altered by *RITMO1* mutation in KO3 or OE1 in L:L. Rhythmic expression was also observed for the Red/Far-red light phytochrome photoreceptor (*DPH*) in L:D. Similarly, *DPH* showed oscillating expression at the second and third day in L:L in Wt. Minor residual oscillations were observed in OE1 and KO3 only at the second subjective day, which appeared anticipated compared to the Wt. Rhythmic patterns in L:D and at the second and third L:L were detected for the blue-light receptor *CPF1* too. KO3 and OE1 showed no alteration in L:D compared to Wt, but greatly reduced oscillation in amplitude and temporally offset by 4-8 h when compared with Wt in L:L.

We also analysed the expression of genes involved in the control of the cell cycle

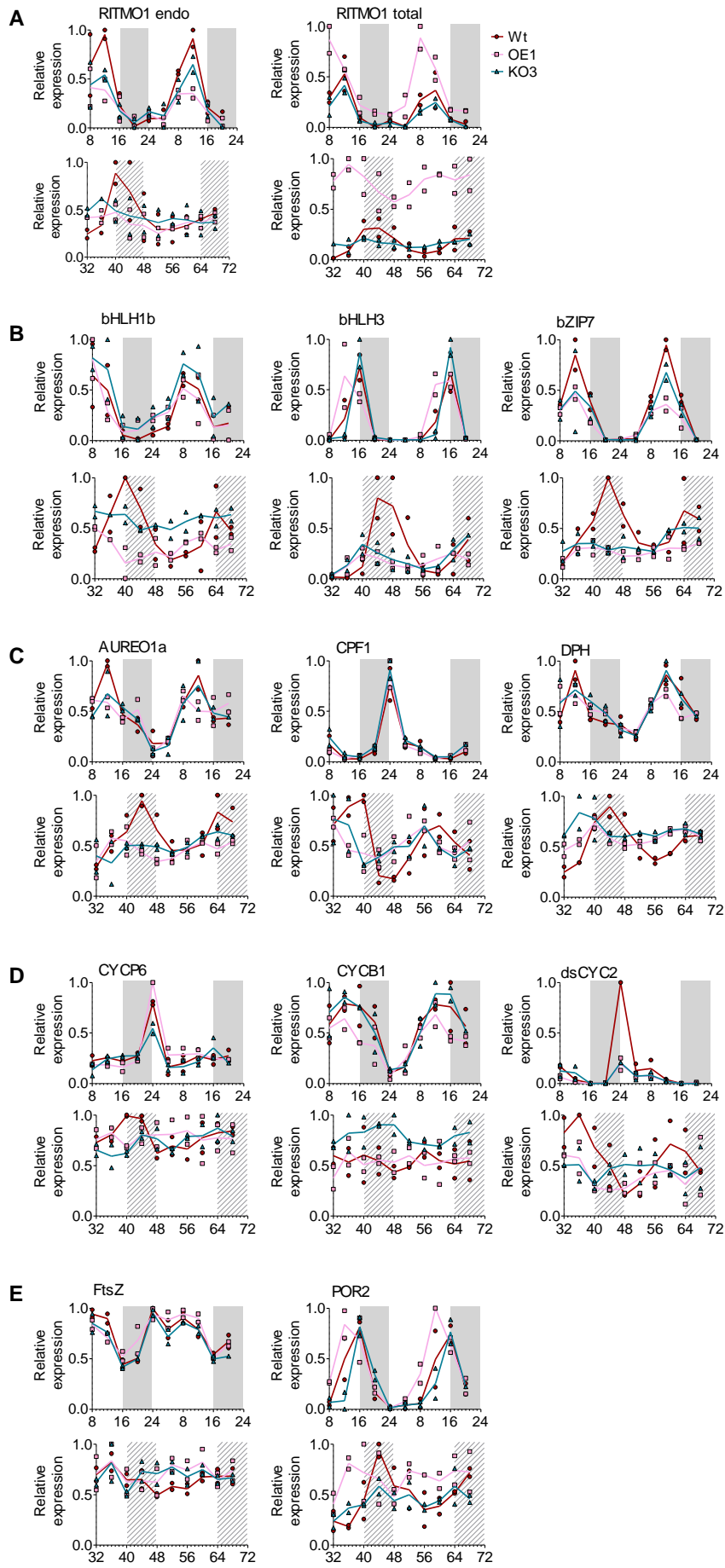
(Huysman et al., 2010, Fig. 8 D). The *CYCP6* gene, whose expression has been shown to be associated to G1 phase in synchronized culture, showed a rhythmic expression in L:D, with a peak at the end of the night period. In the OE1 and KO3, we detected some effect in the expression levels but not in the rhythmic profile in L:D compared to the Wt. Minor rhythmicity was detected in Wt in the second free running day, further reduced at the third day. Rhythmic patterns were not observed in the transgenic lines for *CYCP6*. The *CycB1* gene, considered as a marker of the G2/M phase, showed a clear rhythmic pattern in L:D, peaking at the end of the light period, which was overall unaltered in KO3 and OE1. However, the expression of *CycB1* became arrhythmic in L:L in all the lines. Finally, we also monitored expression of *dsCYC2*, a key regulator of the cell cycle onset following dark to light transition. It has been previously reported that the strong blue-light dependent regulation of *dsCYC2* is directly controlled by *Aureo1* (Huysman et al., 2013). Our study also measured a rhythmic expression of *dsCYC2* in the Wt, with a clear anticipation of its expression before the light onset (Fig. 8 D). This pattern was also confirmed by reanalysing public diurnal transcriptomic data (Chauton et al., 2013). The strong light induction, which is mediated by *Aureo1a* just after the light onset, is not detected in our analysis because of the selected sampling points. Remarkably, *dsCYC2* maintains robust oscillation also in Wt in free running. Both, the OE1 and KO3 showed a strongly reduced expression of this gene at the end of the dark period, and loss of rhythmicity in L:L, supporting an implication of *RITMO1* in both the light anticipation of *dsCYC2* expression in L:D and circadian rhythmicity in L:L conditions. Finally, we also analyzed the expression of two genes linked to chloroplast biogenesis and activity: one of the *P. tricornutum* *FtsZ* genes, putatively encoding for a key component of the chloroplast division machinery (Gillard et al., 2008; TerBush et al., 2013) and the protochlorophyllide oxidoreductase 2, *POR2*,

involved in chlorophyll biosynthesis (Hunsperger et al., 2016). For *POR2*, we observed a strong rhythmicity of the expression in both L:D and L:L, which is affected by KO deregulation in free run. On the contrary, for *FtsZ* we observed rhythmic

oscillation in L:D conditions, but not in LL, and the expression pattern is not altered in RITMO OE or KO lines, ruling out the possible regulation of *FtsZ* by an endogenous oscillator.

Figure 8. Analysis of the expression of selected genes by qRT-PCR in Wt, OE1 and KO3 lines under periodic L:D cycles and free running conditions.

For the analysis the samples were collected every 4 hours over 36 hours in cells adapted to 16L:8D cycles  $25\mu\text{mol photons m}^{-2} \text{ s}^{-1}$  and released to L:L  $25\mu\text{mol photons m}^{-2} \text{ s}^{-1}$ . In free running, samples were collected starting at LL32. Dots represents separate replicates cultures grown in independent experiments ( $n = 2$ , bold line represent the average value of gene expression per each line). (A) RITMO1 expression profiles. RITMO1-endo refers to endogenous transcripts, while RITMO1-total includes endogenous RITMO1 and RITMO-HA transgene transcripts for the OE1 line; (B) Transcription factors bHLH1b, bHLH3 and bZIP7; (C) Photoreceptors aureochrome 1a (AUREO1a), cryptochrome photolyase family (CPF1) and diatom phytochrome (DPH); (D) Expression profiles of the cyclins CYCP6, CYCB1 and dsCYC2 and (E) of the FtsZ and protochlorophyllide oxidoreductases 2 (POR2). For each line and each time point, the expression value of the genes is normalized over the geometrical average of the TBP and RPS control genes expression. Over the time course, the expression of each gene is normalised to its maximum expression over the three lines, where '1' represents the highest expression value of the time series.



# Discussion

This study provides evidences for a strong temporal regulation of biological processes by a circadian clock system in an important group of marine phytoplankton, diatoms, which are at the crossroads of several evolutionary lineages (Keeling, 2013).

Our investigation of cell fluorescence rhythmicity (Fig. 2 and Fig.3) supports the existence of a self-sustained oscillator in diatoms able to synchronize processes associated to cell division. The increase in *P. tricornutum* cell number after the fluorescence peak, begins to be observed around the transition to darkness and parallels a decrease in cell fluorescence caused by plastid splitting between daughter cells (Huysman et al., 2010). The adjustment of cell fluorescence phase according to day length as well as the anticipation of darkness suggest day length is a main driver of cell division timing. Under short days (8L:16D), cell fluorescence in *P. tricornutum* cultures still increases before the end of the light period, but the acrophase is reached in the dark, suggesting that a timekeeper restricts cell division to a window of time, more than to a specific time, as already observed in *Ostreococcus tauri* (Moulager et al., 2007). This short photoperiod effect is observed in cells showing a lower division rate, compared to that adapted to longer photoperiods, but also in cells showing a higher division rate in 8L:16D, when exposed to higher irradiance. In most organisms, cell division cycle and the circadian cycle co-exist and are somehow intertwined (Masri et al., 2013). We can therefore assume that under short photoperiods, cell separation is delayed to after the dark onset, but the activity of the circadian clock is still visible because cells maintain a 24-hour period. The circadian regulation of processes monitored by cell fluorescence is further supported by the persistence of rhythmicity under free running conditions, as previously described

(Annunziata et al., 2019). We here found that this effect is observable as long as the light intensity in free running is not limiting for the growth and, potentially, for other metabolic activities necessary to sustain cellular activities in a broad sense. During free run, *P. tricornutum* rhythms of cell fluorescence shift into a new phase and have periods longer than 24 hours at the light conditions tested, indicating that the circadian clock adjusts to its own time in the absence of periodic environmental signals.

In *P. tricornutum*, photosynthesis also appears regulated by a circadian clock (Fig. 7), supporting previous observation (Palmer et al., 1964) and also *in situ* studies reporting strong oscillations in optical properties related to photosynthetic activity and growth in natural populations along the seasons (Kheireddine and Antoine, 2014). In our study, rhythms of photosynthesis are clearly visible in light-dark and persist at least until the third day under free running conditions, although with smaller oscillations. On the other hand, we also observed that cell fluorescence oscillations, proxy of cell division and pigment synthesis, in free running conditions are strongly affected or even lost when cells experience higher light intensities (Fig. 3). Possibly, changes in the photosynthetic activity due to the absence of dark and/or higher light intensity may affect circadian clock system controlling cell fluorescence rhythmicity. Increasing evidences in multicellular plants and animals indicate that metabolic processes not only are regulated by the circadian clock, but also in turn regulate its function (Asher and Sassone-Corsi, 2015; Farré and Weise, 2012; Haydon et al., 2017; Mora-García et al., 2017), by acting in the input pathways of the clock system. Our study suggests that a regulatory cross-talk between photosynthesis and an endogenous timekeeper likely also exists in unicellular algae such as diatoms. This cross-talk deserves to be studied in more detail as this may be

particularly relevant for enabling rapid acclimatisation responses of diatoms under changing environmental condition and for regulating their growth capacity. Specifically, it will be relevant to attest the persistence of other clock-regulated processes, notably photosynthesis and gene expression, under increasing free-run light intensity. Such an analysis would allow to determine whether the masking of cellular fluorescence persistence under high light is peculiar of this phenotype or a generalised effect on clock activity. This complex network of regulation may indeed mask circadian clock activity under particular conditions, and could explain why the step wise increase of cell density under continuous light, proposed as a strong indication of cell cycle gating by a circadian clock, has been detected in some (Ostgaard and Jensen, 1982), but not all diatom species (Chisholm and Brand, 1981). A weak free-running rhythmicity of cell cycle comparable to what is shown in Fig. S4 has also been reported in *Nannochloropsis*, another *Stramenopila*, like diatoms (Poliner et al., 2019).

Our work clearly defines *RITMO1* as a component of the diatom circadian clock system. Thanks to the generation of knock-out mutants in which this protein has been genetically eliminated (Fig. 1), we observed that three circadian processes described in this study are directly affected by *RITMO1* mutation (Fig. 4, Fig. 7 and Fig. 8). The fact that mutants in the *RITMO1* gene are not affected in growth capacity after L:D to L:L transitions nor in the progression of cell cycle after dark synchronisation (Fig. 6), allows us to exclude that the altered rhythmicity of cell fluorescence is due to a direct implication of this protein in the regulation of the cell cycle machinery. Moreover, the fact that the period of cell fluorescence is independent of the rate of division in wild-type cells, but it is altered in the *RITMO1* KO lines, supports the idea that the circadian clock is a different process from the cell division cycle in diatoms. *RITMO1*-like bHLH-PAS genes have been found in all

diatoms and other *Stramenopila* for which omic sequences are available (Annunziata et al., 2019; Bilcke et al., 2021; Farré, 2020), suggesting a possible conservation of its role across this clade. Of note, an expansion of bHLH-PAS TFs showing different rhythmic expression times has been recently described in the benthic diatom *Seminavis robusta*, likely reflecting an adaptations and functional diversification of this protein family to both diurnal and tidal cycles (Bilcke et al., 2021).

The transcription analysis performed in this study support a function of *RITMO1* in the diatom central circadian transcriptional oscillator (Fig. 8). First of all, robust circadian oscillations in gene expression are detected for most, but not all, of the rhythmic genes analysed at the second and third free running day, supporting a circadian regulation of diatom transcription, as seen in most eukaryotes. The phases of these rhythms are shifted compared to the L:D, as observed for the cell fluorescence and photosynthesis and as photosynthesis they show an apparent period of 24h, indicating that the transcriptional rhythms are less affected by the physiological changes of the cells following the L:L transitions and maintain an apparent period close to the one of L:D entrainment. As for other physiological rhythms characterized in this study, the effect of *RITMO1* obliteration on rhythmic gene expression is visible in free running conditions but it's masked under diel light-dark cycles. An equally likely alternative is that the rhythmic light cues used in the study are sufficient to ensure complete masking of endogenous clock effects and rhythmic physiology is just a direct response to environmental stimuli. This suggests that other, still unidentified clock components, may perform a redundant function with respect to *RITMO1*, compensating for its mutation as long as there are periodic light cues. The redundancy of *RITMO1* function could also explain some residual cell fluorescence oscillation in KO mutants, although with shorter periods and

reduced amplitudes, observed in some replicates. A parallel can be made with the central clock component CCA1 and LHY of *Arabidopsis thaliana*, in which a single mutation results in a shortening of the circadian period in free-run, whereas a double mutation is required to induce arrhythmicity (Alabadi et al., 2002; Mizoguchi et al., 2002).

By identifying RITMO1 as a transcriptional regulator of the diatom circadian clock, this study paves the way for the molecular identification of other RITMO1-interacting components in the as yet unresolved TTFL system. Between the transcription factor analysed, other members of the bHLH family (bHLH1b and bHLH3), but also bZIP7, represent direct or indirect RITMO1-target genes and may participate in circadian clock function.

The discovery of circadian regulation of the diatom Red/Far-Red light Phytochrome DPH photoreceptor, the blue light Cryptochrome Photolyase 1 CPF1 and aureochrome 1a (Aureo1), make these proteins interesting new candidate regulators of the light-dependent rhythmic processes and possibly of the clock input pathway of diatoms. Interestingly, the absence of RITMO1 or deregulation of its expression by ectopic overexpression does not affect the ability of cells to readapt to periodic light conditions after acclimation to constant light for several weeks (Fig. 5). This suggests that RITMO1 is not directly implicated in the input pathways needed for the clock entrainment, but rather in the core clock system. Still, an effect on the free running period is observed in the mutant KO3 for RITMO1 exposed to higher light intensity in continuous light (Fig. 4 and Fig. S3), which shows a longer period length than under L:L 17  $\mu\text{mol photons m}^{-2}\text{s}^{-1}$ . Further investigations under different fluence rate and quality of light would be necessary to further assess the primary role of RITMO1 in the circadian clock system and its possible

interaction with the photic control of circadian rhythms.

Regulation by RITMO1 is also observed for the protochlorophyllide oxidoreductase 2 (*POR2*), putatively involved in chlorophyll biosynthesis (Hunsperger et al., 2016), further supporting a circadian regulation of processes of relevance for plastid function. Between the analysed genes involved in cell cycle progression or plastid division machinery (Gillard et al., 2008; Huysman et al., 2010, 2013), a clear circadian regulation has been seen only for *dsCYC2*. This gene has been described as a critical regulator of cell cycle progression of diatoms because its down-regulation clearly alter the onset of cell division (Huysman et al., 2013). *dsCYC2* has been characterized as a blue light regulated gene. Its expression is strongly and transiently induced after switching from darkness to light, thanks to the activity of the blue light-receptor Aureo1a, which also act as transcription factor on *dsCYC2* promoter. Our analysis here identifies another important level of regulation of this critical process by the circadian clock component RITMO1. This is clearly visible from the anticipation of *dsCYC2* expression before the light onset in L:D cycles, the circadian rhythmic expression in L:L and the loss of *dsCYC2* and *Aureo1a* rhythmicity in RITMO1 mutants. Interestingly, KO and OE lines also show a deregulated and lower expression of *dsCYC2* in L:D at the transition from light to dark (Fig. 8). We still do not know if this effect corresponds to a real reduction in the maximal expression of *dsCYC2* in mutants compared to Wt or only into a shift in its peak of expression, which is not detectable in our analyses because of the selected time points.

Finally, the initial generation of clock mutants also offers new opportunities to assess the importance of the circadian clock for diatom life. Based on the initial characterisation, the RITMO1 mutation does not appear to affect *P. tricornutum* growth.

However, further research with multiple clock mutants will be needed to clearly assess the role of the diatom clock on fitness. In cyanobacteria, the effect of clock mutation on fitness is only clearly seen in competition experiments between circadian period mutants and wild-type cells and when their internal rhythms match those of the environmental cycle (Ouyang et al., 1998; Woelfle et al., 2004). Similar observations are

also made with a variety of clock mutants in plants (Dodd et al., 2005; Yerushalmi et al., 2011). Further analysis of the responses to widely varying photoperiodic conditions will also be of interest, as diatoms are the dominant photosynthetic organisms in polar regions and the circadian clock is central to photoperiodic regulation in terrestrial plants and animals.

## Acknowledgements

This work has been supported by funding from the Fondation Bettencourt-Schueller (Coups d'élan pour la recherche française-2018), the "Initiative d'Excellence" program (Grant "DYNAMO," ANR-11-LABX-0011-01), the ANR-DFG Grant "DiaRhythm (KR1661/20-1) to A.F. and ANR Grant ClimaClock (ANR-20-CE20-0024) to A.F and F-Y.B.



# Bibliography

- Agier, N., Fischer, G., 2016. A Versatile Procedure to Generate Genome-Wide Spatiotemporal Program of Replication in Yeast Species, in: Devaux, F. (Ed.), *Yeast Functional Genomics, Methods in Molecular Biology*. Springer New York, New York, NY, pp. 247–264. [https://doi.org/10.1007/978-1-4939-3079-1\\_14](https://doi.org/10.1007/978-1-4939-3079-1_14)
- Alabadi, D., Yanovsky, M.J., Más, P., Harmer, S.L., Kay, S.A., 2002. Critical Role for CCA1 and LHY in Maintaining Circadian Rhythmicity in Arabidopsis. *Curr. Biol.* 12, 757–761. [https://doi.org/10.1016/S0960-9822\(02\)00815-1](https://doi.org/10.1016/S0960-9822(02)00815-1)
- Annunziata, R., Ritter, A., Fortunato, A.E., Manzotti, A., Cheminant-Navarro, S., Agier, N., Huysman, M.J.J., Winge, P., Bones, A.M., Bouget, F.-Y., Cosentino Lagomarsino, M., Bouly, J.-P., Falciatore, A., 2019. bHLH-PAS protein RITMO1 regulates diel biological rhythms in the marine diatom *Phaeodactylum tricorutum*. *Proc. Natl. Acad. Sci.* 116, 13137–13142. <https://doi.org/10.1073/pnas.1819660116>
- Armbrust, E.V., 2004. The Genome of the Diatom *Thalassiosira Pseudonana*: Ecology, Evolution, and Metabolism. *Science* 306, 79–86. <https://doi.org/10.1126/science.1101156>
- Asher, G., Sassone-Corsi, P., 2015. Time for Food: The Intimate Interplay between Nutrition, Metabolism, and the Circadian Clock. *Cell* 161, 84–92. <https://doi.org/10.1016/j.cell.2015.03.015>
- Bar-On, Y.M., Phillips, R., Milo, R., 2018. The biomass distribution on Earth. *Syst. Biol.* 6. <https://doi.org/10.1073/pnas.1711842115>
- Bilcke, G., Osuna-Cruz, C.M., Silva, M.S., Poulsen, N., Bulankova, P., Vyverman, W., Veylder, L.D., Vandepoele, K., 2021. Diurnal transcript profiling of the diatom *Seminavis robusta* reveals adaptations to a benthic lifestyle. *Plant J.* 107. <https://doi.org/10.1111/tpj.15291>
- Bowler, C., Allen, A.E., Badger, J.H., Grimwood, J., Jabbari, K., Kuo, A., Maheswari, U., Martens, C., Maumus, F., Otiillar, R.P., Rayko, E., Salamov, A., Vandepoele, K., Beszteri, B., Gruber, A., Heijde, M., Katinka, M., Mock, T., Valentin, K., Verret, F., Berges, J.A., Brownlee, C., Cadoret, J.-P., Chiovitti, A., Choi, C.J., Coesel, S., De Martino, A., Detter, J.C., Durkin, C., Falciatore, A., Fournet, J., Haruta, M., Huysman, M.J.J., Jenkins, B.D., Jiroutova, K., Jorgensen, R.E., Joubert, Y., Kaplan, A., Kröger, N., Kroth, P.G., La Roche, J., Lindquist, E., Lommer, M., Martin-Jézéquel, V., Lopez, P.J., Lucas, S., Mangogna, M., McGinnis, K., Medlin, L.K., Montsant, A., Secq, M.-P.O., Napoli, C., Obornik, M., Parker, M.S., Petit, J.-L., Porcel, B.M., Poulsen, N., Robison, M., Rychlewski, L., Rynearson, T.A., Schmutz, J., Shapiro, H., Siaut, M., Stanley, M., Sussman, M.R., Taylor, A.R., Vardi, A., von Dassow, P., Vyverman, W., Willis, A., Wyrwicz, L.S., Rokhsar, D.S., Weissenbach, J., Armbrust, E.V., Green, B.R., Van de Peer, Y., Grigoriev, I.V., 2008. The *Phaeodactylum* genome reveals the evolutionary history of diatom genomes. *Nature* 456, 239–244. <https://doi.org/10.1038/nature07410>
- Brand, L.E., 1982. Persistent diel rhythms in the chlorophyll fluorescence of marine phytoplankton species. *Mar. Biol.* 69, 253–262. <https://doi.org/10.1007/BF00397491>
- Burki, F., Roger, A.J., Brown, M.W., Simpson, A.G.B., 2020. The New Tree of Eukaryotes. *Trends Ecol. Evol.* 35, 43–55. <https://doi.org/10.1016/j.tree.2019.08.008>
- Chauton, M.S., Winge, P., Brembu, T., Vadstein, O., Bones, A.M., 2013. Gene Regulation of Carbon Fixation, Storage, and Utilization in the Diatom *Phaeodactylum tricorutum* Acclimated to Light/Dark Cycles. *Plant Physiol.* 161, 1034–1048. <https://doi.org/10.1104/pp.112.206177>
- Chisholm, S.W., Brand, L.E., 1981. Persistence of cell division phasing in marine phytoplankton in continuous light after entrainment to light: Dark cycles. *J. Exp. Mar. Biol. Ecol.* 51, 107–118. [https://doi.org/10.1016/0022-0981\(81\)90123-4](https://doi.org/10.1016/0022-0981(81)90123-4)
- Coesel, S.N., Durham, B.P., Groussman, R.D., Hu, S.K., Caron, D.A., Morales, R.L., Ribalet, F., Armbrust, E.V., 2021. Diel transcriptional oscillations of light-sensitive regulatory elements in open-ocean eukaryotic plankton communities. *Proc. Natl. Acad. Sci.* 118, e2011038118. <https://doi.org/10.1073/pnas.2011038118>

- Corellou, F., Schwartz, C., Motta, J.-P., Djouani-Tahri, E.B., Sanchez, F., Bouget, F.-Y., 2009. Clocks in the Green Lineage: Comparative Functional Analysis of the Circadian Architecture of the Picoeukaryote *Ostreococcus*. *Plant Cell* 21, 3436–3449. <https://doi.org/10.1105/tpc.109.068825>
- Dodd, A.N., Kusakina, J., Hall, A., Gould, P.D., Hanaoka, M., 2014. The circadian regulation of photosynthesis. *Photosynth. Res.* 119, 181–190. <https://doi.org/10.1007/s11120-013-9811-8>
- Dodd, A.N., Salathia, N., Hall, A., Kévei, E., Tóth, R., Nagy, F., Hibberd, J.M., Millar, A.J., Webb, A.A.R., 2005. Plant Circadian Clocks Increase Photosynthesis, Growth, Survival, and Competitive Advantage. *Sci. New Ser.* 309, 630–633. <http://10.1126/science.1115581>
- Dorrell, R.G., Gile, G., McCallum, G., Méheust, R., Bapteste, E.P., Klinger, C.M., Brillet-Guéguen, L., Freeman, K.D., Richter, D.J., Bowler, C., 2017. Chimeric origins of ochrophytes and haptophytes revealed through an ancient plastid proteome. *eLife* 6, e23717. <https://doi.org/10.7554/eLife.23717>
- Dunlap, J.C., 1999. Molecular Bases for Circadian Clocks. *Cell* 96, 271–290. [https://doi.org/10.1016/S0092-8674\(00\)80566-8](https://doi.org/10.1016/S0092-8674(00)80566-8)
- Falciatore, A., Jaubert, M., Bouly, J.-P., Bailleul, B., Mock, T., 2020. Diatom Molecular Research Comes of Age: Model Species for Studying Phytoplankton Biology and Diversity. *Plant Cell* 32, 547–572. <https://doi.org/10.1105/tpc.19.00158>
- Farré, E.M., 2020. The brown clock: circadian rhythms in stramenopiles. *Physiol. Plant.* 169, 430–441. <https://doi.org/10.1111/ppl.13104>
- Farré, E.M., Weise, S.E., 2012. The interactions between the circadian clock and primary metabolism. *Curr. Opin. Plant Biol.* 15, 293–300. <https://doi.org/10.1016/j.pbi.2012.01.013>
- Field, C.B., Behrenfeld, M.J., Randerson, J.T., Falkowski, P.G., 1998. Primary Production of the Biosphere: Integrating Terrestrial and Oceanic Components. *Science* 281, 237–240. <https://doi.org/10.1126/science.281.5374.237>
- Fung-Uceda, J., Lee, K., Seo, P.J., Polyn, S., De Veylder, L., Mas, P., 2018. The Circadian Clock Sets the Time of DNA Replication Licensing to Regulate Growth in Arabidopsis. *Dev. Cell* 45, 101–113.e4. <https://doi.org/10.1016/j.devcel.2018.02.022>
- Gaidarenko, O., Sathoff, C., Staub, K., Huesemann, M.H., Vernet, M., Hildebrand, M., 2019. Timing is everything: Diel metabolic and physiological changes in the diatom *Cyclotella cryptica* grown in simulated outdoor conditions. *Algal Res.* 42, 101598. <https://doi.org/10.1016/j.algal.2019.101598>
- Gillard, J., Devos, V., Huysman, M.J.J., De Veylder, L., D'Hondt, S., Martens, C., Vanormelingen, P., Vannerum, K., Sabbe, K., Chepurinov, V.A., Inzé, D., Vuylsteke, M., Vyverman, W., 2008. Physiological and Transcriptomic Evidence for a Close Coupling between Chloroplast Ontogeny and Cell Cycle Progression in the Pennate Diatom *Seminavis robusta*. *Plant Physiol.* 148, 1394–1411. <https://doi.org/10.1104/pp.108.122176>
- Guillard, R.R.L., 1975. . *Cult. Phytoplankton Feed. Mar. Invertebr., Cultures of Marine invertebrate Animals.* [https://doi.org/10.1007/978-1-4615-8714-9\\_3](https://doi.org/10.1007/978-1-4615-8714-9_3)
- Haydon, M.J., Mielczarek, O., Frank, A., Román, Á., Webb, A.A.R., 2017. Sucrose and Ethylene Signaling Interact to Modulate the Circadian Clock. *Plant Physiol.* 175, 947–958. <https://doi.org/10.1104/pp.17.00592>
- Hunsperger, H.M., Ford, C.J., Miller, J.S., Cattolico, R.A., 2016. Differential Regulation of Duplicate Light-Dependent Protochlorophyllide Oxidoreductases in the Diatom *Phaeodactylum tricornutum*. *PLOS ONE* 11, e0158614. <https://doi.org/10.1371/journal.pone.0158614>
- Huysman, M.J., Martens, C., Vandepoele, K., Gillard, J., Rayko, E., Heijde, M., Bowler, C., Inzé, D., 2010. Genome-wide analysis of the diatom cell cycle unveils a novel type of cyclins involved in environmental signaling. *Genome Biol.* 11, 19. <https://doi.org/10.1186/gb-2010-11-2-r17>
- Huysman, M.J.J., Fortunato, A.E., Matthijs, M., Costa, B.S., Vanderhaeghen, R., Van den Daele, H., Sachse, M., Inzé, D., Bowler, C., Kroth, P.G., Wilhelm, C., Falciatore, A., Vyverman, W., De Veylder, L., 2013. AUREOCHROME1a-Mediated Induction of the Diatom-

- Specific Cyclin *dsCYC2* Controls the Onset of Cell Division in Diatoms (*Phaeodactylum tricorutum*). *Plant Cell* 25, 215–228. <https://doi.org/10.1105/tpc.112.106377>
- Keeling, P.J., 2013. The Number, Speed, and Impact of Plastid Endosymbioses in Eukaryotic Evolution. *Annu. Rev. Plant Biol.* 64, 583–607. <https://doi.org/10.1146/annurev-arplant-050312-120144>
- Kheireddine, M., Antoine, D., 2014. Diel variability of the beam attenuation and backscattering coefficients in the northwestern Mediterranean Sea (BOUSSOLE site). *J. Geophys. Res. Oceans* 119, 5465–5482. <https://doi.org/10.1002/2014JC010007>
- Kolody, B.C., McCrow, J.P., Allen, L.Z., Aylward, F.O., Fontanez, K.M., Moustafa, A., Moniruzzaman, M., Chavez, F.P., Scholin, C.A., Allen, E.E., Worden, A.Z., Delong, E.F., Allen, A.E., 2019. Diel transcriptional response of a California Current plankton microbiome to light, low iron, and enduring viral infection. *ISME J.* 13, 2817–2833. <https://doi.org/10.1038/s41396-019-0472-2>
- Lepetit, B., Campbell, D.A., Lavaud, J., Büchel, C., Goss, R., Bailleul, B., Falciatore, A., Mock, T., 2022. Photosynthetic Light Reactions in Diatoms. II. The Dynamic Regulation of the Various Light Reaction, in: *Molecular Life of Diatoms*. Springer, pp. 423–464.
- Livak, K.J., Schmittgen, T.D., 2001. Analysis of relative gene expression data using real-time quantitative PCR and the  $2^{-\Delta\Delta CT}$  method.pdf. *METHODS* 25, 402–408. <https://doi.org/10.1006/meth.2001.1262>
- Malviya, S., Scalco, E., Audic, S., Vincent, F., Veluchamy, A., Poulain, J., Wincker, P., Iudicone, D., de Vargas, C., Bittner, L., Zingone, A., Bowler, C., 2016. Insights into global diatom distribution and diversity in the world’s ocean. *Proc. Natl. Acad. Sci.* 113, E1516–E1525. <https://doi.org/10.1073/pnas.1509523113>
- Mann, M., Serif, M., Wrobel, T., Eisenhut, M., Madhuri, S., Flachbart, S., Weber, A.P.M., Lepetit, B., Wilhelm, C., Kroth, P.G., 2020. The Aureochrome Photoreceptor PtAUREO1a Is a Highly Effective Blue Light Switch in Diatoms. *iScience* 23, 101730. <https://doi.org/10.1016/j.isci.2020.101730>
- Masri, S., Cervantes, M., Sassone-Corsi, P., 2013. The circadian clock and cell cycle: interconnected biological circuits. *Curr. Opin. Cell Biol.* 25, 730–734. <https://doi.org/10.1016/j.ceb.2013.07.013>
- Maxwell, K., Johnson, G.N., 2000. Chlorophyll fluorescence—a practical guide. *J. Exp. Bot.* 51, 659–668. <https://doi.org/10.1093/jexbot/51.345.659>
- Mizoguchi, T., Wheatley, K., Hanzawa, Y., Wright, L., Mizoguchi, M., Song, H.-R., Carré, I.A., Coupland, G., 2002. LHY and CCA1 Are Partially Redundant Genes Required to Maintain Circadian Rhythms in Arabidopsis. *Dev. Cell* 2, 629–641. [https://doi.org/10.1016/S1534-5807\(02\)00170-3](https://doi.org/10.1016/S1534-5807(02)00170-3)
- Mora-García, S., de Leone, M.J., Yanovsky, M., 2017. Time to grow: circadian regulation of growth and metabolism in photosynthetic organisms. *Curr. Opin. Plant Biol.* 35, 84–90. <https://doi.org/10.1016/j.pbi.2016.11.009>
- Moullager, M., Monnier, A., Jesson, B., Bouvet, R., Mosser, J., Schwartz, C., Garnier, L., Corellou, F., Bouget, F.-Y., 2007. Light-Dependent Regulation of Cell Division in *Ostreococcus*: Evidence for a Major Transcriptional Input. *Plant Physiol.* 144, 1360–1369. <https://doi.org/10.1104/pp.107.096149>
- Nelson, D.M., Brand, L.E., 1979. Cell Division periodicity in 13 species of phytoplankton. *J. Phycol.* 67–75. <https://doi-org.insb.bib.cnrs.fr/10.1111/j.1529-8817.1979.tb02964.x>
- Ostgaard, K., Jensen, A., 1982. Diurnal and circadian rhythms in the turbidity of growing *Skeletonema costatum* cultures. *Mar. Biol.* 66, 261–268. <https://doi.org/10.1007/BF00397031>
- Ouyang, Y., Andersson, C.R., Kondo, T., Golden, S.S., Johnson, C.H., 1998. Resonating circadian clocks enhance fitness in cyanobacteria. *Proc. Natl. Acad. Sci.* 95, 8660–8664. <https://doi.org/10.1073/pnas.95.15.8660>
- Owens, T.G., Falkowski, P.G., Whitedge, T.E., 1980. Diel periodicity in cellular chlorophyll content in marine diatoms. *Mar. Biol.* 59, 71–77. <https://doi.org/10.1007/BF00405456>
- Palmer, J.D., Livingston, L., Zusy, Fr.D., 1964. A Persistent Diurnal Rhythm in Photosynthetic Capacity. *Nature* 203, 1087–1088. <https://doi.org/10.1038/2031087a0>

- Peschel, N., Helfrich-Förster, C., 2011. Setting the clock - by nature: Circadian rhythm in the fruitfly *Drosophila melanogaster*. *FEBS Lett.* 585, 1435–1442. <https://doi.org/10.1016/j.febslet.2011.02.028>
- Pierella Karlusich, J.J., Ibarbalz, F.M., Bowler, C., 2020. Phytoplankton in the Tara Ocean. *Annu. Rev. Mar. Sci.* 12, 233–265. <https://doi.org/10.1146/annurev-marine-010419-010706>
- Platt, T., Gallegos, C.L., Harrison, W.G., 1980. Photoinhibition of photosynthesis in natural assemblages of marine phytoplankton. *J. Mar. Res.* 38, 9. <https://doi.org/10.1093/pasj/57.2.341>
- Plautz, J.D., Straume, M., Stanewsky, R., Jamison, C.F., Brandes, C., Dowse, H.B., Hall, J.C., Kay, S.A., 1997. Quantitative Analysis of *Drosophila* period Gene Transcription in Living Animals. *J. Biol. Rhythms* 12, 204–217. <https://doi.org/10.1177/074873049701200302>
- Poliner, E., Cummings, C., Newton, L., Farré, E.M., 2019. Identification of circadian rhythms in *Nannochloropsis* species using bioluminescence reporter lines. *Plant J.* 99, 112–127. <https://doi.org/10.1111/tpj.14314>
- Ragni, M., d'Alcalà, M.R., 2007. Circadian variability in the photobiology of *Phaeodactylum tricorutum*: pigment content. *J. Plankton Res.* 29, 141–156. <https://doi.org/10.1093/plankt/fbm002>
- Ralph, P.J., Gademann, R., 2005. Rapid light curves: A powerful tool to assess photosynthetic activity. *Aquat. Bot.* 82, 222–237. <https://doi.org/10.1016/j.aquabot.2005.02.006>
- Roenneberg, T., Foster, R.G., 1997. Twilight Times: Light and the Circadian System. *Photochem. Photobiol.* 66, 549–561. <https://doi.org/10.1111/j.1751-1097.1997.tb03188.x>
- Serif, M., Dubois, G., Finoux, A.-L., Teste, M.-A., Jallet, D., Daboussi, F., 2018. One-step generation of multiple gene knock-outs in the diatom *Phaeodactylum tricorutum* by DNA-free genome editing. *Nat. Commun.* 9, 3924. <https://doi.org/10.1038/s41467-018-06378-9>
- Siaut, M., Heijde, M., Mangogna, M., Montsant, A., Coesel, S., Allen, A., Manfredonia, A., Falciatore, A., Bowler, C., 2007. Molecular toolbox for studying diatom biology in *Phaeodactylum tricorutum*. *Gene* 406, 23–35. <https://doi.org/10.1016/j.gene.2007.05.022>
- Smith, S.R., Gillard, J.T.F., Kustka, A.B., McCrow, J.P., Badger, J.H., Zheng, H., New, A.M., Dupont, C.L., Obata, T., Fernie, A.R., Allen, A.E., 2016. Transcriptional Orchestration of the Global Cellular Response of a Model Pennate Diatom to Diel Light Cycling under Iron Limitation. *PLOS Genet.* 12, e1006490. <https://doi.org/10.1371/journal.pgen.1006490>
- Taddei, L., Stella, G.R., Rogato, A., Bailleul, B., Fortunato, A.E., Annunziata, R., Sanges, R., Thaler, M., Lepetit, B., Lavaud, J., Jaubert, M., Finazzi, G., Bouly, J.-P., Falciatore, A., 2016. Multisignal control of expression of the LHCX protein family in the marine diatom *Phaeodactylum tricorutum*. *J. Exp. Bot.* 67, 3939–3951. <https://doi.org/10.1093/jxb/erw198>
- Takahashi, J.S., 2017. Transcriptional architecture of the mammalian circadian clock. *Nat. Rev. Genet.* 18, 164–179. <https://doi.org/10.1038/nrg.2016.150>
- TerBush, A.D., Yoshida, Y., Osteryoung, K.W., 2013. FtsZ in chloroplast division: structure, function and evolution. *Curr. Opin. Cell Biol.* 25, 461–470. <https://doi.org/10.1016/j.ceb.2013.04.006>
- Vancaester, E., Depuydt, T., Osuna-Cruz, C.M., Vandepoele, K., 2020. Comprehensive and Functional Analysis of Horizontal Gene Transfer Events in Diatoms. *Mol. Biol. Evol.* 37, 3243–3257. <https://doi.org/10.1093/molbev/msaa182>
- Williamson, C.E., 1980. Phased cell division in natural and laboratory populations of marine planktonic diatoms. *J. Exp. Mar. Biol. Ecol.* 43, 271–279. [https://doi.org/10.1016/0022-0981\(80\)90052-0](https://doi.org/10.1016/0022-0981(80)90052-0)
- Woelfle, M.A., Ouyang, Y., Phanvijhitsiri, K., Johnson, C.H., 2004. The Adaptive Value of Circadian Clocks: An Experimental Assessment in Cyanobacteria. *Curr. Biol.* 14, 1481–1486. <https://doi.org/10.1016/j.cub.2004.08.023>
- Yerushalmi, S., Yakir, E., Green, R.M., 2011. Circadian clocks and adaptation in *Arabidopsis*. *Mol. Ecol.* 20, 1155–1165. <https://doi.org/10.1111/j.1365-294X.2010.04962.x>
- Zagotta, M.T., Hicks, K.A., Jacobs, C.I., Young, J.C., Hangarter, R.P., Meeks-Wagner, D.R., 1996. The *Arabidopsis* ELF3 gene regulates vegetative photomorphogenesis and the photoperiodic induction of flowering. *Plant J.* 10, 691–702. <https://doi.org/10.1046/j.1365-313X.1996.10040691.x>
- Zielinski, T., Moore, A., Troup, E., Halliday, K.J., Millar, A.J., 2014. Strengths and Limitations of Period Estimation Methods for Circadian Data. *PLOS ONE* 9, e96462. <https://doi.org/10.1371/journal.pone.0096462>

# Supplementary Material

## A

Reference sequence (1): bHLH1a\_allele\_1  
Identities normalized by reference length.  
Colored by: identity

	cov	pid			
1 bHLH1a_allele_1	100.0%	100.0%	1	[	1
2 bHLH1a_allele_1-K01	100.0%	100.0%			
3 bHLH1a_allele_1-K02	80.6%	68.6%			
4 bHLH1a_allele_1-K03	100.0%	99.9%			
5 bHLH1a_allele_1-K04	100.0%	100.0%			
1 bHLH1a_allele_1	100.0%	100.0%	121		248
2 bHLH1a_allele_1-K01	100.0%	100.0%			
3 bHLH1a_allele_1-K02	80.6%	68.6%			
4 bHLH1a_allele_1-K03	100.0%	99.9%			
5 bHLH1a_allele_1-K04	100.0%	100.0%			
1 bHLH1a_allele_1	100.0%	100.0%	241		368
2 bHLH1a_allele_1-K01	100.0%	100.0%			
3 bHLH1a_allele_1-K02	80.6%	68.6%			
4 bHLH1a_allele_1-K03	100.0%	99.9%			
5 bHLH1a_allele_1-K04	100.0%	100.0%			
1 bHLH1a_allele_1	100.0%	100.0%	361		480
2 bHLH1a_allele_1-K01	100.0%	100.0%			
3 bHLH1a_allele_1-K02	80.6%	68.6%			
4 bHLH1a_allele_1-K03	100.0%	99.9%			
5 bHLH1a_allele_1-K04	100.0%	100.0%			
1 bHLH1a_allele_1	100.0%	100.0%	481		600
2 bHLH1a_allele_1-K01	100.0%	100.0%			
3 bHLH1a_allele_1-K02	80.6%	68.6%			
4 bHLH1a_allele_1-K03	100.0%	99.9%			
5 bHLH1a_allele_1-K04	100.0%	100.0%			
1 bHLH1a_allele_1	100.0%	100.0%	601		720
2 bHLH1a_allele_1-K01	100.0%	100.0%			
3 bHLH1a_allele_1-K02	80.6%	68.6%			
4 bHLH1a_allele_1-K03	100.0%	99.9%			
5 bHLH1a_allele_1-K04	100.0%	100.0%			
1 bHLH1a_allele_1	100.0%	100.0%	721		840
2 bHLH1a_allele_1-K01	100.0%	100.0%			
3 bHLH1a_allele_1-K02	80.6%	68.6%			
4 bHLH1a_allele_1-K03	100.0%	99.9%			
5 bHLH1a_allele_1-K04	100.0%	100.0%			
1 bHLH1a_allele_1	100.0%	100.0%	841		960
2 bHLH1a_allele_1-K01	100.0%	100.0%			
3 bHLH1a_allele_1-K02	80.6%	68.6%			
4 bHLH1a_allele_1-K03	100.0%	99.9%			
5 bHLH1a_allele_1-K04	100.0%	100.0%			
1 bHLH1a_allele_1	100.0%	100.0%	961		1080
2 bHLH1a_allele_1-K01	100.0%	100.0%			
3 bHLH1a_allele_1-K02	80.6%	68.6%			
4 bHLH1a_allele_1-K03	100.0%	99.9%			
5 bHLH1a_allele_1-K04	100.0%	100.0%			
1 bHLH1a_allele_1	100.0%	100.0%	1081		1200
2 bHLH1a_allele_1-K01	100.0%	100.0%			
3 bHLH1a_allele_1-K02	80.6%	68.6%			
4 bHLH1a_allele_1-K03	100.0%	99.9%			
5 bHLH1a_allele_1-K04	100.0%	100.0%			
1 bHLH1a_allele_1	100.0%	100.0%	1201		1320
2 bHLH1a_allele_1-K01	100.0%	100.0%			
3 bHLH1a_allele_1-K02	80.6%	68.6%			
4 bHLH1a_allele_1-K03	100.0%	99.9%			
5 bHLH1a_allele_1-K04	100.0%	100.0%			
1 bHLH1a_allele_1	100.0%	100.0%	1321		1440
2 bHLH1a_allele_1-K01	100.0%	100.0%			
3 bHLH1a_allele_1-K02	80.6%	68.6%			
4 bHLH1a_allele_1-K03	100.0%	99.9%			
5 bHLH1a_allele_1-K04	100.0%	100.0%			
1 bHLH1a_allele_1	100.0%	100.0%	1441		1505
2 bHLH1a_allele_1-K01	100.0%	100.0%			
3 bHLH1a_allele_1-K02	80.6%	68.6%			
4 bHLH1a_allele_1-K03	100.0%	99.9%			
5 bHLH1a_allele_1-K04	100.0%	100.0%			



**B**

Reference sequence (1): bHLH1a allele\_2\_Mt  
Identities normalised by reference length.  
Colored by: Identity

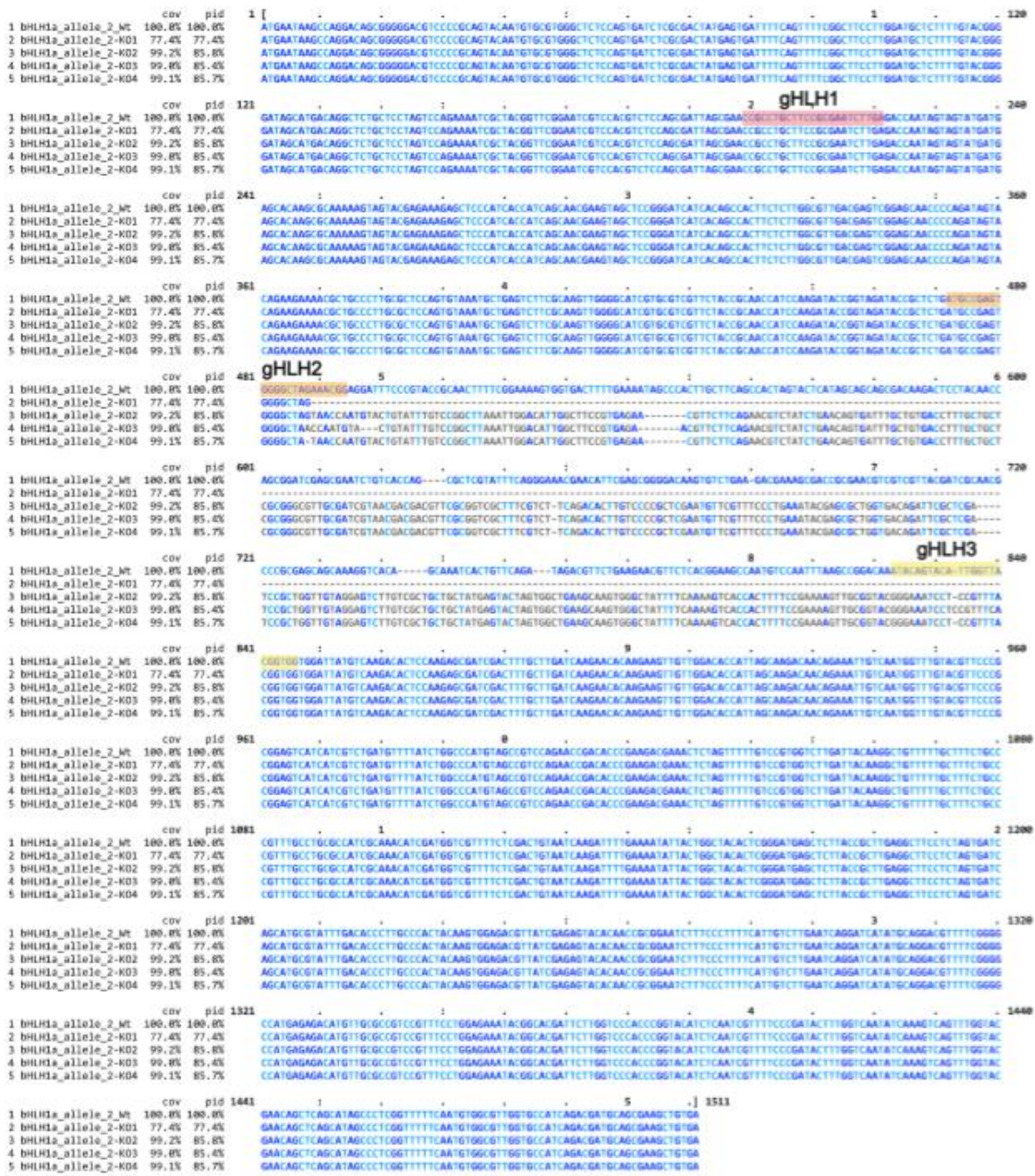


Figure S1. Sequence analysis of the KO mutants in the *RITM1* gene.

(A) Alignment of the sequence of the *RITM1* in Pt1 Wt strain (allele 1) with that of the *RITM1* KOs 1-4; (B) Alignment of the sequence of the *RITM1* in Pt1 Wt strain (allele 2) with that of the *RITM1* KOs 1-4. The alignments were generated via EBI Clustal Omega webtool and visualized via Mview. Bases are colored by identity to the Wt reference sequence. gHLH1, gHLH2 and gHLH3 gRNA target sites are highlighted in red, orange and yellow respectively

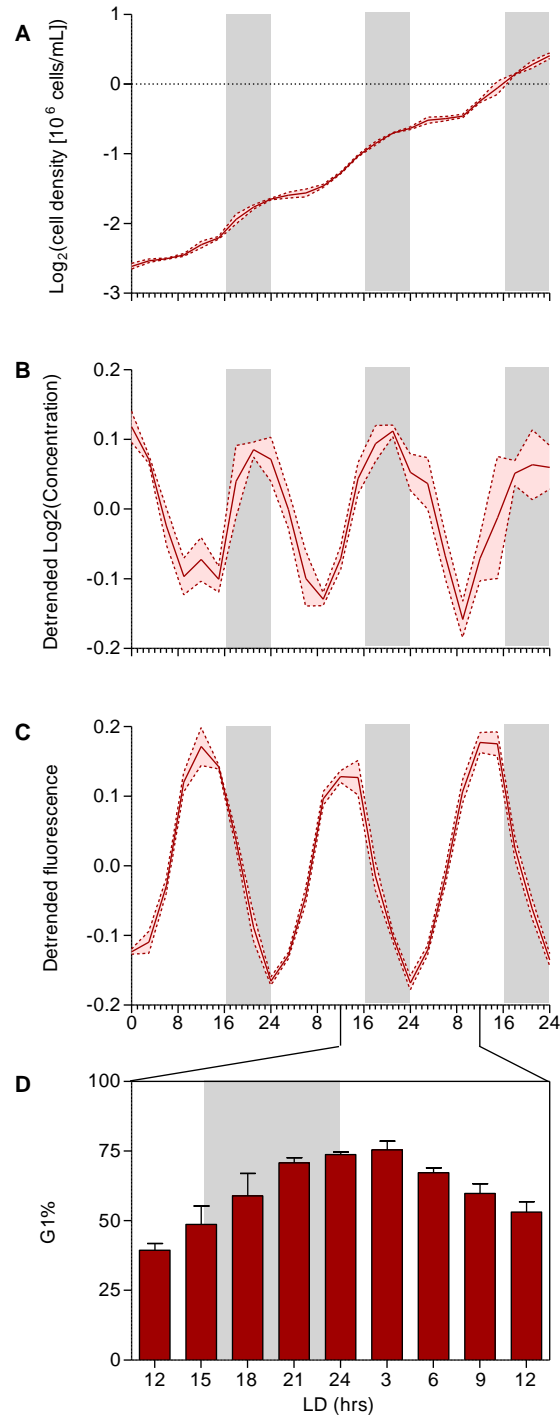


Figure S2. Characterisation of growth profile in *P. tricornutum* grown under 16L:8D cycles.

Characterisation of growth (A and B), cellular fluorescence (C) and cell cycle synchronization (D) in Wt cells entrained under 16L:8D  $25\mu\text{mol photons m}^{-2} \text{s}^{-1}$ . Samples were collected every three hours for the analysis. (A) Cell concentration plotted as  $\text{Log}_2$  of cell density expressed as  $10^6$  cells  $\text{mL}^{-1}$ . (B) Residuals after baseline detrending of the data shown in A, to extract oscillatory components. (C) Cellular fluorescence (B3-A parameter) profile of the samples reported in panel (A) and (B). Solid lines represent the average, coloured ribbons represent the SD ( $n=3$ ). (D) Percentage of cells in G1 phase in the highlighted time window. Cell cycle was determined by flow cytometry after DAPI staining of the cellular DNA content. Columns represent mean  $\pm$  s.e.m. ( $n=3$ ).

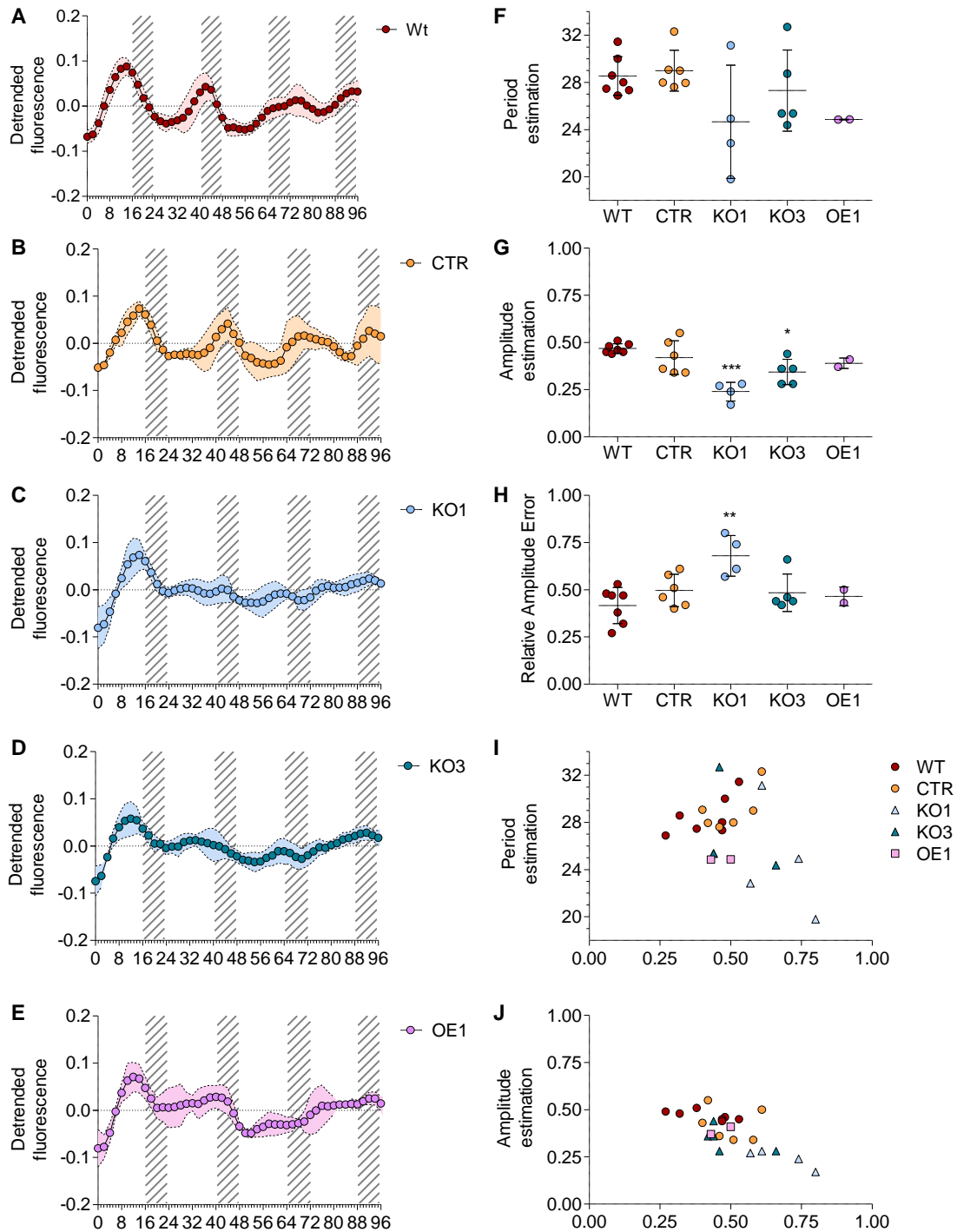


Figure S3. Effects of RITMO1 mutation on cellular fluorescence in L:L 25  $\mu\text{mol photons m}^{-2} \text{s}^{-1}$ .

(A-E) Cellular fluorescence profiles after transition from 16L:8D 25 $\mu\text{mol photons m}^{-2} \text{s}^{-1}$  to L:L 25 $\mu\text{mol photons m}^{-2} \text{s}^{-1}$  in Wt, CTR, KO1, KO3 and OE1 cells ( $n \geq 6$ ). Dots represent mean B3-A values, coloured ribbons represent SD. Gray dashed regions represent subjective nights in free-run conditions. (F-H) Period (F), amplitude (G) and R.A.E. (H) estimations of B3-A fluorescence traces represented in panels A-E that passed the EPR rhythmicity test (mean  $\pm$  s.e.m., \* $P < 0.05$ , \*\* $P < 0.01$ , \*\*\* $P < 0.001$ , t test). (I) Plot of period versus R.A.E. estimates. (J) Plot of amplitude versus R.A.E. estimates.



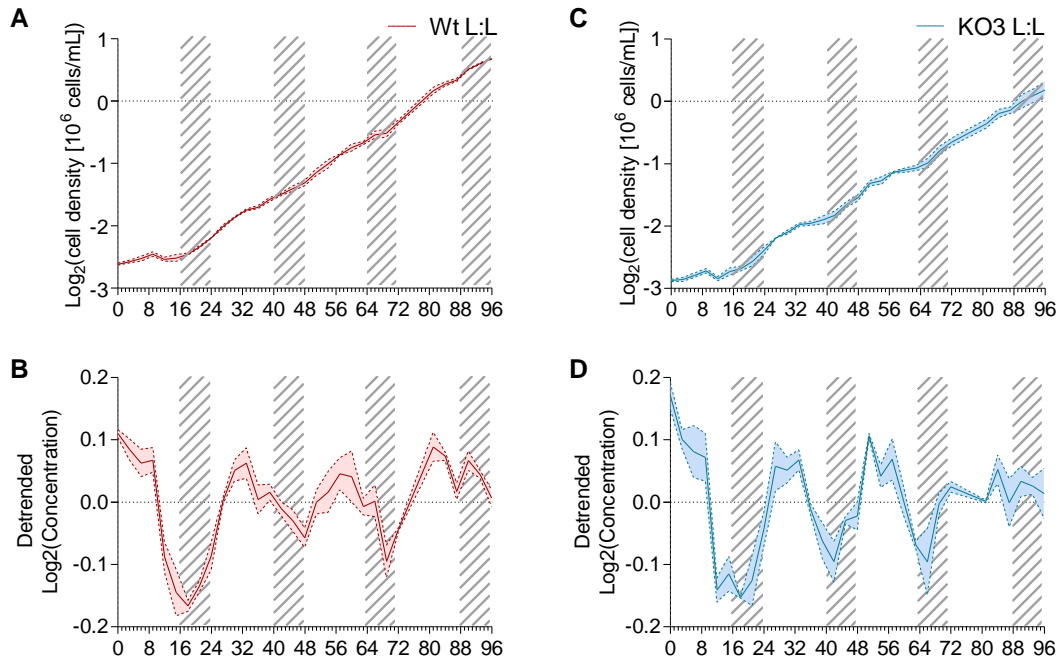


Figure S4. Time-resolved analysis of growth in free-run cultures.

Characterisation of growth and cellular fluorescence in Wt and KO3 cells entrained under 16L:8D  $25\mu\text{mol photons m}^{-2} \text{s}^{-1}$  and released to L:L  $17\mu\text{mol photons m}^{-2} \text{s}^{-1}$ . Samples were collected every three hours starting from LL0. (A) Concentration of Wt cultures plotted as  $\text{Log}_2$  of cell density expressed as  $10^6 \text{ cells mL}^{-1}$ . (B) Residuals of the curve in panel (A) after baseline detrending. Panels (C, D) report the same parameters for KO3 cultures. Solid lines represent the average, coloured ribbons represent the SD (n=3). All replicates (both for Wt and KO3) are rhythmic according to the EPR test.

Gene	Accession	Name	Strand	gRNA sequence	3' PAM
APT	Phatr3_J6834	APTg1	Rv	AAGCGTGGAAATGCCTTTGAA	GGG
		APTg3	Fw	CCTGGGTCCACCAATTGCC	TGG
RITMO1	Phatr3_J44962	gHLH1	Rv	TCAAGATTCGCGAAAGCAGG	CGG
		gHLH2	Fw	ATGCCGAGTGGGGCTAGAAA	CGG
		gHLH3	Fw	ATACAGTACATTGGTTACGG	TGG

Table S1. List of the sgRNAs used for CRISPR-Cas9 mutagenesis of the *RITMO1*.

Target gene, sgRNA name, target strand, gRNA sequence and the associated protospacer adjacent motif (PAM) are reported.

Wt divisions per day	Mean	s.e.m.
<b>16L:8D (25 <math>\mu\text{mol}\cdot\text{m}^{-2}\cdot\text{s}^{-1}</math>)</b>	0.97	0.02
<b>16L:8D (75 <math>\mu\text{mol}\cdot\text{m}^{-2}\cdot\text{s}^{-1}</math>)</b>	1.49	0.04
<b>12L:12D (25 <math>\mu\text{mol}\cdot\text{m}^{-2}\cdot\text{s}^{-1}</math>)</b>	1.05	0.05
<b>8L:16D (25 <math>\mu\text{mol}\cdot\text{m}^{-2}\cdot\text{s}^{-1}</math>)</b>	0.64	0.03
<b>8L:16D (50 <math>\mu\text{mol}\cdot\text{m}^{-2}\cdot\text{s}^{-1}</math>)</b>	1.02	0.01
<b>16L:8D (25 <math>\mu\text{mol}\cdot\text{m}^{-2}\cdot\text{s}^{-1}</math>) to D:D</b>	N.A.	N.A.
<b>16L:8D (25 <math>\mu\text{mol}\cdot\text{m}^{-2}\cdot\text{s}^{-1}</math>) to L:L (5 <math>\mu\text{mol}\cdot\text{m}^{-2}\cdot\text{s}^{-1}</math>)</b>	0.27	0.03
<b>16L:8D (25 <math>\mu\text{mol}\cdot\text{m}^{-2}\cdot\text{s}^{-1}</math>) to L:L (17 <math>\mu\text{mol}\cdot\text{m}^{-2}\cdot\text{s}^{-1}</math>)</b>	1.18	0.02
<b>16L:8D (25 <math>\mu\text{mol}\cdot\text{m}^{-2}\cdot\text{s}^{-1}</math>) to L:L (25 <math>\mu\text{mol}\cdot\text{m}^{-2}\cdot\text{s}^{-1}</math>)</b>	1.22	0.02
<b>16L:8D (75 <math>\mu\text{mol}\cdot\text{m}^{-2}\cdot\text{s}^{-1}</math>) to L:L (50 <math>\mu\text{mol}\cdot\text{m}^{-2}\cdot\text{s}^{-1}</math>)</b>	1.15	0.03
<b>16L:8D (75 <math>\mu\text{mol}\cdot\text{m}^{-2}\cdot\text{s}^{-1}</math>) to L:L (75 <math>\mu\text{mol}\cdot\text{m}^{-2}\cdot\text{s}^{-1}</math>)</b>	1.4	0.02

Table S2: Growth capacity of *P. tricornutum* Wt cells in the different conditions used throughout this study.

First column indicates the irradiation and photoperiodic conditions considered in the analyses. For each condition, the cell division/day was calculated in cells in exponential phase over the course of four days (n=3).

In the circadian experiments performed in cells preadapted to L:D cycles and then exposed either to darkness or light of different intensities, the data refers to the growth analysis in free running conditions, after the L:D to L:L shift.

LD	Wt		CTR			KO1			KO3			OE1		
	Mean	s.e.m	Mean	s.e.m	p value	Mean	s.e.m	p value	Mean	s.e.m	p value	Mean	s.e.m	p value
<b>16L:8D (25 <math>\mu\text{mol}^*\text{m}^{-2}\text{s}^{-1}</math>)</b>	4/4		3/3			3/3			3/3			3/3		
n =	4/4		3/3			3/3			3/3			3/3		
Phase	-2.27	0.39	-1.81	1.01	N.S.	-2.73	0.87	N.S.	-2.53	1.05	N.S.	-2.52	0.62	N.S.
R.A.E.	0.14	0.01	0.15	0.02	N.S.	0.18	0.01	N.S.	0.19	0.01	N.S.	0.19	0.00	N.S.
Amplitude	1.31	0.02	1.26	0.17	N.S.	1.26	0.10	N.S.	1.28	0.05	N.S.	0.94	0.02	**
Period	24.10	0.08	24.27	0.16	N.S.	24.08	0.06	N.S.	24.35	0.07	N.S.	24.27	0.14	N.S.
<b>16L:8D (75 <math>\mu\text{mol}^*\text{m}^{-2}\text{s}^{-1}</math>)</b>	4/4		3/3			3/3			3/3			3/3		
n =	4/4		3/3			3/3			3/3			3/3		
Phase	-1.07	0.54	-0.99	0.09	N.S.	0.21	0.50	N.S.	-0.45	0.80	N.S.	-2.88	1.65	N.S.
R.A.E.	0.26	0.03	0.31	0.03	N.S.	0.35	0.02	N.S.	0.29	0.02	N.S.	0.33	0.02	N.S.
Amplitude	0.78	0.08	0.68	0.09	N.S.	0.62	0.02	N.S.	0.58	0.04	N.S.	0.81	0.06	N.S.
Period	23.82	0.49	23.40	0.13	N.S.	23.00	0.24	N.S.	23.92	0.79	N.S.	25.54	0.98	N.S.
<b>12L:12D (25 <math>\mu\text{mol}^*\text{m}^{-2}\text{s}^{-1}</math>)</b>	4/4		3/3			3/3			3/3			3/3		
n =	4/4		3/3			3/3			3/3			3/3		
Phase	-1.35	0.51	-0.15	0.08	N.S.	-0.75	0.51	N.S.	-1.45	0.62	N.S.	-1.18	0.67	N.S.
R.A.E.	0.15	0.01	0.12	0.01	N.S.	0.15	0.03	N.S.	0.19	0.02	N.S.	0.14	0.01	N.S.
Amplitude	1.16	0.08	1.08	0.07	N.S.	1.09	0.03	N.S.	1.21	0.09	N.S.	0.93	0.05	N.S.
Period	24.47	0.19	23.84	0.16	N.S.	24.13	0.16	N.S.	25.08	0.60	N.S.	24.47	0.33	N.S.
<b>8L:16D (25 <math>\mu\text{mol}^*\text{m}^{-2}\text{s}^{-1}</math>)</b>	4/4		3/3			3/3			3/3			3/3		
n =	4/4		3/3			3/3			3/3			3/3		
Phase	2.47	0.13	3.28	0.48	N.S.	2.51	0.41	N.S.	1.68	0.19	N.S.	2.71	0.38	N.S.
R.A.E.	0.12	0.01	0.16	0.01	N.S.	0.17	0.02	N.S.	0.18	0.02	N.S.	0.13	0.00	N.S.
Amplitude	1.45	0.07	1.31	0.03	N.S.	1.28	0.10	N.S.	1.23	0.05	N.S.	1.10	0.03	**
Period	23.47	0.05	23.34	0.14	N.S.	23.60	0.23	N.S.	23.79	0.37	N.S.	23.79	0.16	N.S.
<b>8L:16D (50 <math>\mu\text{mol}^*\text{m}^{-2}\text{s}^{-1}</math>)</b>	3/3		3/3			3/3			3/3			3/3		
n =	3/3		3/3			3/3			3/3			3/3		
Phase	2.32	0.06	1.59	0.28	N.S.	2.68	0.17	N.S.	2.57	0.24	N.S.	3.27	0.38	N.S.
R.A.E.	0.19	0.03	0.22	0.01	N.S.	0.20	0.02	N.S.	0.24	0.03	N.S.	0.23	0.03	N.S.
Amplitude	1.40	0.07	1.40	0.09	N.S.	1.30	0.09	N.S.	1.23	0.09	N.S.	1.08	0.06	*
Period	23.75	0.22	24.40	0.24	N.S.	23.50	0.03	N.S.	24.22	0.12	N.S.	23.52	0.07	N.S.

Table S3. Characterisation of cellular fluorescence rhythmicity in Wt, CTR, KO1, KO3 and OE1 lines in L:D.

Calculated phases, amplitudes, relative amplitude errors and periods of the different lines grown in different L:D cycles, as indicated also in Fig. 3, panels (F-H). The fraction of rhythmic replicates/total of replicates is reported for each line in all conditions. P-values obtained via two tailed t- test against Wt are shown. N.S.: non significant, P>0.05.

L:L (17 $\mu\text{mol}^*\text{m}^{-2}\text{s}^{-1}$ )	Wt (10/10)		CTR (8/8)			KO1 (5/8)			KO3 (7/8)			OE1 (3/5)		
	Mean	s.e.m	Mean	s.e.m	p value	Mean	s.e.m	p value	Mean	s.e.m	p value	Mean	s.e.m	p value
Period	28.36	0.82	29.11	0.85	N.S.	24.21	0.91	*	21.97	0.82	***	27.03	1.73	N.S.
R.A.E.	0.31	0.05	0.20	0.03	N.S.	0.42	0.03	N.S.	0.46	0.03	N.S.	0.57	0.12	*
Amplitude	0.62	0.06	0.60	0.05	N.S.	0.41	0.04	*	0.34	0.02	**	0.28	0.04	**
Division/Day (n:3)	1.18	0.02	1.26	0.07	N.S.	1.18	0.03	N.S.	1.23	0.02	N.S.	1.23	0.06	N.S.
L:L (25 $\mu\text{mol}^*\text{m}^{-2}\text{s}^{-1}$ )	Wt (7/7)		CTR (6/6)			KO1 (4/6)			KO3 (5/6)			OE1 (2/6)		
Mean	s.e.m	Mean	s.e.m	p value	Mean	s.e.m	p value	Mean	s.e.m	p value	Mean	s.e.m	p value	
Period	28.54	0.62	28.99	0.71	N.S.	24.68	2.40	N.S.	27.31	1.54	N.S.	24.86	0.02	N.S.
R.A.E.	0.42	0.04	0.50	0.03	N.S.	0.68	0.05	**	0.48	0.04	N.S.	0.47	0.04	N.S.
Amplitude	0.47	0.01	0.42	0.04	N.S.	0.24	0.02	***	0.34	0.03	*	0.39	0.02	N.S.
Divisions/Day (n:3)	1.22	0.02	1.18	0.06	N.S.	1.16	0.01	N.S.	1.17	0.03	N.S.	1.14	0.09	N.S.

Table S4. Characterisation of cellular fluorescence rhythmicity in Wt, CTR, KO1, KO3 and OE1 lines in L:L.

Calculated periods, amplitudes and relative amplitude errors of the different lines after transition from 16L:8D 25  $\mu\text{mol}$  photons  $\text{m}^{-2} \text{s}^{-1}$  to L:L 15  $\mu\text{mol}$  photons  $\text{m}^{-2} \text{s}^{-1}$  or to L:L 25  $\mu\text{mol}$  photons  $\text{m}^{-2} \text{s}^{-1}$ . Average and s.e.m. values were calculated on the replicates considered rhythmic according to the EPR test. The fraction of rhythmic replicates/total of replicates is reported for each line in both conditions. Values correspond to what is shown in Fig.3, panels (N-P). P-values obtained via t- test against Wt are shown. N.S.: non significant, P>0.05.

Gene	Accession	Name	Strand	Sequence	Type
TBP	Phatr3_J10199	TBP_Fw	Fw	ACCGGAGTCAAGAGCACACAC	RT-qPCR
		TBP_Rv	Rv	CGGAATGCGCGTATACCAGT	RT-qPCR
RPS	Phatr3_J10847	RPS_Fw	Fw	CGAAGTCAACCAGGAACCAA	RT-qPCR
		RPS_Rv	Rv	GTGCAAGAGACCGGACATACC	RT-qPCR
RITMO1	Phatr3_J44962	RITMO1_total_Fw	Fw	ATTCTTGGTCCCACCCGGTA	RT-qPCR
		RITMO1_total_Rv	Rv	ACGCCACATTGAAAAACCGAG	RT-qPCR
		RITMO1_endogenous_Fw	Fw	TTATGTCTTTCGGCGACGGG	RT-qPCR
		RITMO1_endogenous_Rv	Rv	AGCAACGAATGCATGCAAGG	RT-qPCR
		RITMO1_allele1_seq_Fw	Fw	TCACCATCAGCAAGGGAAG	sequencing
		RITMO1_allele2_seq_Fw	Fw	TCCCATCACCATCAGCAAC	sequencing
		RITMO1_allele1_seq_Rv	Rv	GAACCGTAGCGATTGTCTT	sequencing
RITMO1_allele2_seq_Rv	Rv	GAACCGTAGCGATTTTCTG	sequencing		
bHLH1b	Phatr3_J44963	bHLH1b_Fw	Fw	CAAAAGCAGCCAACGACGAA	RT-qPCR
		bHLH1b_Rv	Rv	GATATGAGACCCGACCGCTG	RT-qPCR
bHLH3	Phatr3_J42586	bHLH3_Fw	Fw	CACTCTCATCATGCGGGAAT	RT-qPCR
		bHLH3_Rv	Rv	GCGCGTTGTCTTCTCTATC	RT-qPCR
bZIP7	Phatr3_J48800	bZIP7_Fw	Fw	CCTTATTGATATTTCAAGATTTCAAGG	RT-qPCR
		bZIP7_Rv	Rv	GTTTCGGAACCTGCATAGGA	RT-qPCR
Aureochrome 1a	Phatr3_J49116	Aureochrome1a_Fw	Fw	ATGTCCGAACAGCAAAAGGT	RT-qPCR
		Aureochrome1a_Rv	Rv	CTGGAGGGATTCCAACAAGA	RT-qPCR
Cpf1	Phatr3_J27429	Cpf1_Fw	Fw	CCAATTGTTGACCACAAGTTGG	RT-qPCR
		Cpf1_Rv	Rv	CGATTCTTTGCACTTTCTGTTAG	RT-qPCR
CYCP6	Phatr3_J6231	CYCP6_Fw	Fw	AGGTGCTTGCTGCTGTTC	RT-qPCR
		CYCP6_Rv	Rv	ACGAGGCATACTTGTGAATCC	RT-qPCR
dsCYC2	Phatr3_J34956	dsCYC2_Fw	Fw	CTATCATCGCACTCGTCATCAAC	RT-qPCR
		dsCYC2_Rv	Rv	TGTCCACCAAAGCCTCCAAC	RT-qPCR
CYCB1	Phatr3_J46095	CYCB1_Fw	Fw	TCCTGGTCCGCTACTTCAAAG	RT-qPCR
		CYCB1_Rv	Rv	GCTGGCTGGGAAGATAACGC	RT-qPCR
FtsZ	Phatr3_J42361	FtsZ_Fw	Fw	GTGATTTTCGGGGCTTTGGT	RT-qPCR
		FtsZ_Rv	Rv	TTCATTTCTGTTGCGGTCC	RT-qPCR
POR2	Phatr3_J13001	POR2_Fw	Fw	CCTGGTTGCATTGCCGAATC	RT-qPCR
		POR2_Rv	Rv	TCTCCAACGTATCCTCCCGT	RT-qPCR

Table S5. List of the oligonucleotides used in this work.

Target gene, name, pairing strand, sequence and use of the oligonucleotides used in this work. Sequencing primers for *RITMO1* are allele specific.



# Chapter II.d:

## *bHLH1b* as a candidate partner of *RITMO1* in diatom circadian clock

Contributions:  
Alessandro Manzotti, Andrés Ritter, Jean-Pierre Bouly, Angela Falciatore

Keywords: endogenous oscillators, circadian, protein-protein interaction, Yeast two Hybrid, cellular fluorescence rhythmicity

I was fully responsible for the sequence characterization of *bHLH1b* KO mutants, cellular fluorescence rhythmicity analysis and I contributed to the realization and analysis of the Yeast two Hybrid assay

# Abstract

In eukaryotes, the mechanisms responsible for generating endogenous biological rhythms of gene expression require the action of multiple molecular players involved in the positive and negative branches of a transcriptional-translational feedback loop. In the case of the circadian clock of diatoms, to date only the bHLH-PAS transcription factor RITMO1 has been identified as a component of the circadian clock of the model species *Phaeodactylum tricorutum*. The characterization of the timekeeper of these unicellular algae consequently necessitates the identification of the partners that interact with RITMO1 in the generation of cellular rhythms. In the case of *P. tricorutum*, a first candidate is the protein bHLH1b, also belonging to the bHLH-PAS family encoded by a gene located near the *RITMO1* locus and sharing with it a non-overlapping head-to-head arrangement. By means of a Yeast two Hybrid assay strategy we were able to demonstrate that bHLH1b and RITMO1 physically interact via their bHLH domain in yeast cells, suggesting their co-implication in the *P. tricorutum* clock. Also, KO lines for bHLH1b show an alteration in the rhythmicity of cellular fluorescence, with in particular a shortening of the oscillation period when released in continuous light. These results, similar to those already observed in RITMO1 mutants, confirm the involvement of bHLH1b in the diatom timekeeper and pave the way for further decryption of its architecture.



Figure 1. Genomic arrangement of *RITMO1* and *bHLH1b* loci

Schematic representation of the genomic arrangement of the loci of *RITMO1* (Phatr3\_J44962, position chr5:806,933-808,518 reverse strand) and *bHLH1b* (Phatr3\_J44963, position chr5: 809,453-811,854 forward strand) on the chromosome 5 of *P. tricornutum*. Exons are represented as black boxes, the introns as white boxes. The head-to-head orientation of the two genes is highlighted by the directional arrows.

## Introduction

The functional and molecular analyses reported in the previous two chapters clearly demonstrate an implication of the bHLH-PAS protein RITMO1 in the regulation of circadian rhythmicity in *P. tricornutum*. Its activity as a transcription factor still needs to be determined but given the strong deregulation of rhythmic gene expression in KO mutants, an implication of RITMO1 at the level of a TTFL-like core clock is plausible. However, a transcriptional-feedback system typical of endogenous timekeepers requires the implication of at least a minimal oscillator involving one transcription factor as the positive element and one factor as the negative element of the loop. Such a minimal oscillator can be found in the green unicellular alga *Ostreococcus tauri* (Corellou et al., 2009; Morant et al., 2010). An alternative possibility is that RITMO1 interacts with other proteins to form multiprotein complexes in the realization of its regulatory function, as in the case of more complex clocks found for example in animals or plants (Creux and Harmer, 2019; Peschel and Helfrich-Förster, 2011). The search for other proteins involved in the regulation of cellular rhythmicity in *P. tricornutum* is therefore essential for a complete dissection of the clock of this diatom.

A candidate-gene approach was performed to find potential partners of RITMO1. In order to select different candidates, we first focused on transcription factors with a strong daily or circadian

regulation and tested them via a Yeast two Hybrid approach with RITMO 1 as bait. In particular, a second *P. tricornutum* bHLH-PAS transcription factor, bHLH1b (Phatr3\_J44963) represents a prominent prime target for decrypting the *P. tricornutum* clock. The gene encoding this protein is in fact located adjacent to *RITMO1* on *P. tricornutum* chromosome 5. The two genes are arranged in a nonoverlapping 'head-to-head' orientation (Fig.1). The start codons of the two genes are located about 1,000bp apart and the 5' upstream sequences of RITMO1 and bHLH1b therefore overlap, suggesting a possible co-regulation of their expression. The two transcription factors both exhibit rhythmic and coordinated expression in light and dark cycles, showing a maximum transcription peak that anticipates the onset of darkness regardless of the photoperiod of growth (Annunziata et al., 2019). In addition, as reported in chapter II.c, *bHLH1b* expression is regulated in a circadian way, with a persistence of its oscillations after transition to continuous light. Also, *bHLH1b* transcription is affected in continuous light in both RITMO1a KO and OE lines, further stressing its circadian regulation. As described before, bHLH-PAS transcription factors homodimerize or heterodimerize in order to recognise and bind their target DNA sequences (Jones, 2004), the possibility that these two proteins cooperate in generating a negative transcriptional/translational feedback loop as partners of a heterodimer is therefore plausible. The results reported in the



following paragraph represent the first functional characterisation of bHLH1b protein and hint for its plausible co-

implication in the regulation of *P. tricornutum* circadian clock with RITMO1.

# Materials and methods

## Yeast two Hybrid (Y2H) Assay

Y2H assays were carried out according to previously published protocols (Cuéllar et al., 2013). Coding sequences of target genes were cloned from ecotype Pt1 cDNA via Gateway recombination into the pGADT7 and pGBKT7 yeast destination vectors (Clontech). Gene IDs and primers used for cloning are reported in Table 1. The pGADT7 (Prey) vector allows the expression of the protein of interest fused N-terminally to the Activation Domain of the yeast GAL4 transcription factor, while the pGBKT7 (bait) vector fuses the protein to the GAL4 DNA Binding Domain. Transcription was constitutively driven by the yeast *ADHI* promoter in both vectors. *LEU2* and *TRP1* auxotrophic markers were used for yeast selection pGADT7 and pGBKT7 respectively. Prey and bait vectors were co-transformed in *S. cerevisiae* strain PJ69-4 (*trp1-901*, *leu2-3*, *ura3-52* and *his3-200*) following (Cuéllar et al., 2013). Positive transformants were selected by auxotrophy on selective plates of Complete Supplement Mixture medium *-leu-trp* (CSM-LW). Positive bait-prey interaction was assessed by growth on CSM *-leu-trp-his* (CSM-LWH). In case of interaction between bait and prey hybrid proteins, the reconstitution of the GAL4 transcription factor drives the expression of the *HIS3* reporter under the control of the UAS promoter, allowing the growth in selective media lacking *his*. Baits were tested for autoactivation of the *HIS3* reporter by co-transforming the bait vector construct and an empty prey. Three technical replicates were realized for each prey-bait combination.

## Culture and irradiation conditions

Transgenic and control lines of *P. tricornutum* used for bHLH1b characterization share a Pt1 8.6; CCMP2561 genomic background. Cell cultures were

grown in batch culture in F/2 Guillard media (Guillard, 1975). Before performing experiments, cells were pre-adapted for two weeks to 16L:8D at 25  $\mu\text{mol photons m}^{-2} \text{s}^{-1}$ . Final refresh of culture was performed 3 days before the release to free-run conditions (17  $\mu\text{mol photons m}^{-2} \text{s}^{-1}$ ) to ensure minimal perturbation of physiology due to culture refreshment. For all experiments the temperature was set constant to 18°C and illumination was performed with white light (Bridgelux BXRV-DR-1830H-3000-A-13 LEDs). Change in light intensity upon transfer to L:L was performed at the moment of dark to continuous light transition.

## CRISPR/Cas9 Mutagenesis

*bHLH1b* KO mutants were generated following (Nymark et al., 2016) by biolistic bombardment transformation of a pKS diaCAS9\_sgRNA vector (Addgene ID: 74923). This vector contains a hSpCAS9 gene designed using the *P. tricornutum* codon usage and under the control of LHCF2 promoter and LHCF1 terminator sequences, plus a guide RNA sequence under the control of the *P. tricornutum* U6 snRNA promoter and U6 terminator. The adapters for targeting the bHLH1b gene were generated by annealing complementary oligos with TCGA and AAAC overhangs and cloned via BsaI digestion at the 5' -end of the guide RNA region (Nymark et al., 2016). Two sequences for bHLH1b adapters (named gHLH4 and gHLH5, Fig.3A) were designed via CRISPOR web tool (Concordet and Haeussler, 2018) and cloned in two independent pKS diaCAS9\_sgRNA. Target sequences of sgRNA are reported in Table 2 The two CRISPR/CAS9-sgRNA vectors were co-transformed with the pAF3 plasmid (Falciatore et al., 1999) containing the Sh ble gene conferring resistance to phleomycin. Full

Gene	Accession	Name	Strand	Sequence	Type
RITMO1	Phatr3_J4496	FL_bHLH1a_GW_FW	Fw	GGGGACAAGTTTGTACAAAAAAGCAGGCTCCATGAATAAGCCAGGACAGCGG	Full length Gateway Cloning
		bHLH1a_GW_RV_bHLHd	Rv	GGGGACCACTTTGTACAAGAAAGCTGGGTCTCAGTCTTCGGGTGTCGGGTTCTG	bHLH domain Gateway Cloning
		bHLH1a_GW_FW_PASd	Rv	GGGGACAAGTTTGTACAAAAAAGCAGGCTCCATGGAAACTCTAGTTTTTTGTCCG	PAS domain Gateway Cloning
		FL_bHLH1a_GW_RV	Rv	GGGGACCACTTTGTACAAGAAAGCTGGGTCTCACAGCTTCGCTGCATCGT	Full length Gateway Cloning
		FL_bHLH1b_GW_FW	Fw	GGGGACAAGTTTGTACAAAAAAGCAGGCTCCATGAATTCCTTAAGCGCAGCGG	Full length Gateway Cloning
bHLH1b	Phatr3_J44963	bHLH1b_GW_RV_bHLHd	Rv	GGGGACCACTTTGTACAAGAAAGCTGGGTCTCAGACCAATCGCTTTCGCTTCGA	bHLH domain Gateway Cloning
		FL_bHLH1b_GW_RV	Rv	GGGGACCACTTTGTACAAGAAAGCTGGGTCTCAACAGTAGTCGTGACTACCTTCA	Full length Gateway Cloning
		bHLH1b_sequencing_Rv	Fw	CCAATGTTACAGTTCCCT	sequencing
CPF1	Phatr2_27429	bHLH1b_sequencing_Fw	Rv	CACTCTTTGTCTTCTTCACT	sequencing
		FL_CPF1_GW_FW	Fw	GGGGACAAGTTTGTACAAAAAAGCAGGCTCCATGGCTAAATCGGAAGAGAAA	Full length Gateway Cloning
bZIP7	Phatr3_J4800	FL_CPF1_GW_RV	Rv	GGGGACCACTTTGTACAAGAAAGCTGGGTCTCAGTTGCGACGTTGTCGCTTTGGT	Full length Gateway Cloning
		FL_bZIP7_GW_FW	Fw	GGGGACAAGTTTGTACAAAAAAGCAGGCTCCATGCGTAATCAAGGATTAGAGGCAT	Full length Gateway Cloning
		FL_bZIP7_GW_RV	Rv	GGGGACCACTTTGTACAAGAAAGCTGGGTCTCAGGCGGTTCCATTGAGCCCATCA	Full length Gateway Cloning

Table 1. List of the oligonucleotides used in this work.

Target gene, name, pairing strand, sequence and use of the oligonucleotides used in this work.

Target gene	Accession	gRNA name	Strand	SEQUENCE	3' PAM
bHLH1b	Phatr3_J44963	bHLHg4	Fw	AGCGCATCACAAACCGAAGCT	TGG
		bHLHg5	Fw	GGAGCTACGAGAGGTTCTGA	CGG

Table 2. sgRNA used for bHLH1b KOs generation

List of the sgRNA used for CRISPR-Cas9 mutagenesis. Target gene, sgRNA name, target strand, gRNA sequence and the associated protospacer adjacent motif (PAM) are reported.

length sequence of the bHLH1b gene was amplified by PCR on the phleomycin-resistant colonies obtained (primers reported in Table 2). PCR fragments were purified from agarose gel with QIAquick Gel Extraction Kit (QIAGEN) and analyzed via Sanger sequencing using bHLH1b specific primers reported in Table 1 in order to retrieve biallelic mutants.

## Flow cytometry and fluorescence rhythmicity analysis

Cellular fluorescence rhythmicity assays were performed using a MACSQuant Analyser flow cytometer (Miltenyi Biotec). B3-A parameter (488 nm excitation, 655-730 nm detection) was used to track chlorophyll fluorescence (Annunziata et al., 2019). 30.000 events were analyzed per each time point per culture replicate and median B3-A value was used for following rhythmicity analysis. Culture samples were collected every 2 hours via a BVP standard ISM444 peristaltic pump

(Ismatec) controlled by a FC204 fraction collector (Gilson). Cells were stored at 4°C in the dark for at least 2 hours to a maximum of 24 hours previous to flow cytometry. The analysis of B3-A fluorescence dataset rhythmicity was performed using the BioDare2 webtool (<https://biodare2.ed.ac.uk/>, (Zielinski et al., 2014)). For graphical representation, data traces were baseline detrended, normalized to the maximum value and aligned to the mean values. Data traces were first analyzed using the Enright Periodogram (EPR) algorithm, which was used as an arrhythmicity test (Zielinski et al., 2014). Period, amplitude and RAE were calculated via Fast Fourier nonlinear least square algorithm (FFT-NLLS), within a period range of 18 and 34 hours. At least three full oscillations were considered for the analysis. Statistical differences in rhythmicity parameters among lines were evaluated via One-way analysis of variance against Wt with Bonferroni post-test correction.

# Results

## bHLH1b and RITMO1 physically interact via their bHLH fold

In order to investigate the regulation network in which RITMO1 is involved, we performed a series of Y2H assays aimed to identify interacting proteins potentially involved in *P. tricornutum* clock machinery. A first round of analysis was carried out by assessing the possible autoactivation of RITMO1 protein in a Y2H system. Autoactivation experiments are aimed to assess whether the protein fused to the GAL4 BD is able to recruit the transcription machinery and express *HIS3* on its own without a prey hybrid (Cuéllar et al., 2013). As shown in Fig.4A, RITMO1 is able to autonomously recruit the transcription machinery and to induce the expression of *HIS3* reporter. The autoinduction of RITMO1 in the yeast model made it impossible to perform a broad-spectrum screen of its possible protein interactors. Nevertheless, we decided to test the possible interaction of RITMO1 with a restricted set of proteins of interest: bHLH1b, BZIP7 and CPF1. bHLH1b and bZIP7 are transcription factor belonging to bHLH-PAS and the basic-leucine zipper (bZIP) family respectively which have a temporal expression profile similar to that of RITMO1 (Annunziata et al., 2019). CPF1 (cryptochrome photolyase family 1) was chosen for Y2H analysis since it was shown to repress the activity of CLOCK:BMAL1-induced reporter genes in a heterologous mammalian cell system (COS7 cell line from *Cercopithecus aethiops*), thus phenocopying the function of the endogenous animal cryptochrome (CRY, Coesel et al., 2009). Since mammalian CRY is known to physically bind the bHLH-PAS protein BMAL-1 (Tamaru et al., 2015), we wanted to assess whether CPF1 can display similar

dimerization properties with RITMO1 and/or bHLH1b.

Coding sequences of the four proteins were fused both to the BD (bait) and the AD (prey) of GAL4, for a total of eight constructs. First, the bait hybrids of bHLH1b, bZIP7 and CPF1 were tested for autoactivation by co-transforming them with empty pGADT7 plasmid. None of the other baits showed the same autoactivation outcome showed by RITMO1, thus excluding that the remaining proteins under investigation can activate gene expression on their own. As an additional negative control, the four prey hybrids were co-transformed with empty pGBKT7 (Fig.2A). None of these controls gave rise to colonies on the CSM-LWH selective medium.

bHLH1b, bZIP7 and CPF1 bait hybrids were subsequently co-transformed with RITMO1 prey in order to test their possible physical interaction in yeast cells (Fig. 2B). In addition, the bHLH1b bait hybrid was also co-transformed with the bHLH1b prey hybrid to test homodimerization. This round of analysis demonstrated the interaction between RITMO1 and its paralogous bHLH1b and the homo-dimerization of bHLH1b, confirmed by the growth on selective CSM-LWH media (Fig.2B). None of the colonies bearing other combinations of preys and baits grew on selective plates, excluding other interactions, at least in the yeast model.

Finally, to refine our understanding of the mutual interaction between RITMO1 and bHLH1b, a set of Y2H was carried out by splitting RITMO1 gene in its bHLH and PAS coding sequences and cloning them into pGADT7 and pGBKT7. Similar construction was performed with the bHLH fold of bHLH1b (Fig. 2C). First, the bait hybrids of bHLH and PAS domains of RITMO1 were

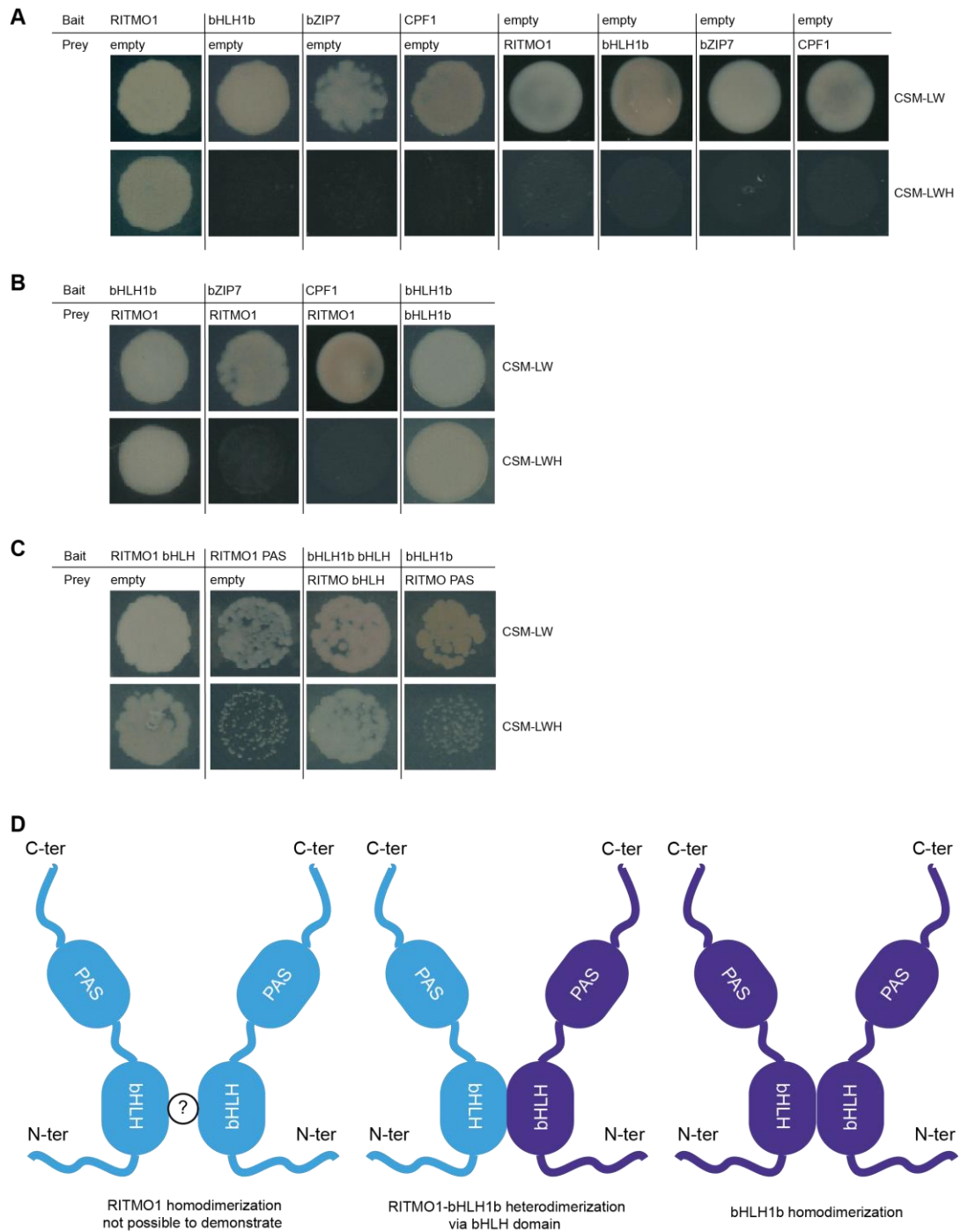


Figure 2. Results of the Yeast two Hybrid assay (Y2H)

(A) Results of the autoactivation test of the RITMO1, bHLH1b, bZIP7 and CPF1 full-length proteins cloned into bait and prey vectors. (B) Results of the Y2H interactions between the selected proteins co-transformed in yeast cells in different combinations of bait and prey hybrids. (C) Autoactivation tests of the RITMO1 bHLH and PAS folds in bait vector and analysis of the interaction between RITMO1 and bHLH1b bHLH and PAS folds. Top photos refer to cells grown in control medium (CSM-LW), bottom photos refer to cells grown in selective medium (CSM-LWH). (D) Schematic representation of the results of the Y2H assays showing the dimerization of bHLH1b with RITMO1 via the bHLH fold and the homodimerization of bHLH1b. The possible homodimerization of RITMO1 could not be assessed due to autoactivation of *His3* reported by RITMO1 bait constructs

co-transformed with the empty pGADT7 to assess which of the two regions is responsible for autoactivation (Fig.2C). Growth on selective media was observed only in yeast bearing the bHLH fold bait, thus hinting that this domain is accountable for recruiting the transcription machinery in yeast cells. Co-transformation of bHLH1b-bHLH bait hybrid with RITMO1-bHLH prey hybrid was also performed as well as full length bHLH1b bait with RITMO1 PAS prey hybrids co-transformation. Results indicate that RITMO1 and bHLH1b interact via their bHLH regions, which are known to represent the primary dimerization surface of bHLH-PAS family members (Kewley et al., 2004) (Fig.2C). A schematic summary of the interactions emerged in the Y2H assay is reported in Fig.2D.

## Generation of bHLH1b KO mutants

Following the results of the Y2H analysis, CRISPR/Cas9 mutagenesis of

*bHLH1b* locus was performed to test the obliteration of this protein on cellular rhythmicity (Fig.3). The transformation of *P. tricornutum* cells with the pKS diaCAS9\_sgRNA vector lead to the generation of two biallelic KO lines for bHLH1b (named KO 1b#1 and KO 1b#2 respectively) identified by Sanger sequencing. Sequencing analysis of the *bHLH1b* locus highlighted a 85 bp insertion at the level of gHLH5 target region in the allele 2 of KO 1b#1, a 128 bp deletion in allele 1 of KO 1b#2 and a 848 bp deletion in allele 2 (Fig. 3B and Fig.4). All mutagenic events induce a frameshift mutation that disrupts downstream protein sequence. Allele 1 of KO 1b#1 was impossible to amplify via PCR and was not found in Sanger sequencing chromatograms, suggesting that large insertions or deletions were induced by CRISPR/Cas9 mutagenesis. This phenomenon is defined as Loss of Heterozygosity and is not uncommon in CRISPR/Cas9 targeted mutagenesis (Serif et al., 2018).

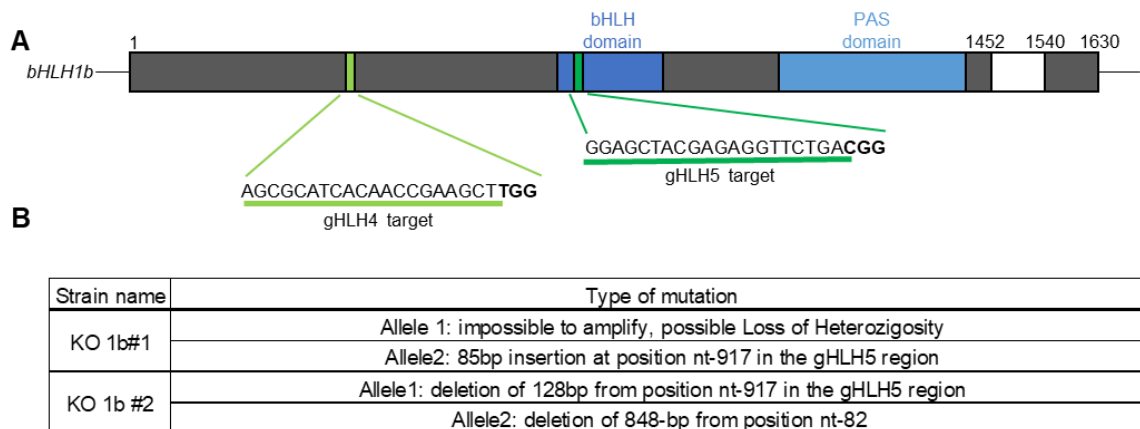


Figure 3. Generation of bHLH1b KO mutants

(A) Schema of the *bHLH1b* locus with the sgRNA target sites highlighted. Blue and light blue boxes represent the relative location of the bHLH and PAS domains respectively. Light and dark green boxes highlight the localisation of the target sequences (underlined) of the three gRNAs used for bHLH1b CRISPR-Cas9 mutagenesis. Letters in bold represent the protospacer adjacent motif associated with each target site. (B) Description of the mutations induced on each allele of the *bHLH1b* locus on the two KO mutants as identified by Sanger sequencing.

A

Reference sequence (1): Wt\_Allele\_1  
Identities normalised by reference length.  
Colored by: identity

```

cov pid 1 [
1 Wt_Allele_1 100.0% 100.0%
2 K02_Allele_1 91.7% 91.7%
1 1 ATGAATCTTTAAGCGCAGCGGCTGCAGAAAGGGCCAGTATGGCAGCTCGCTCAAAACGCTAGCTACAGGAAGCGGAGCACACACGCGTGGTTCGCTCTCCAGCCTTGAT
ATGAATCTTTAAGCGCAGCGGCTGCAGAAAGGGCCAGTATGGCAGCTCGCTCAAAACGCTAGCTACAGGAAGCGGAGCACACACGCGTGGTTCGCTCTCCAGCCTTGAT

cov pid 121
1 Wt_Allele_1 100.0% 100.0%
2 K02_Allele_1 91.7% 91.7%
1 121 ACGAAGGCGATGAAAATTTACAGAGGGACATCAGAAGTCGCGATATCGCTCTGGAGTGAATTCGCTGTAACACGGTAACTGCTCAAAAGCTTCAACGATTTATATCGCAG
ACGAAGGCGATGAAAATTTACAGAGGGACATCAGAAGTCGCGATATCGCTCTGGAGTGAATTCGCTGTAACACGGTAACTGCTCAAAAGCTTCAACGATTTATATCGCAG

cov pid 241
1 Wt_Allele_1 100.0% 100.0%
2 K02_Allele_1 91.7% 91.7%
1 241 ATGCAGCAGCACCCTGTACCTCAGCATCCAAAGCAACAGGAGCATCAATAGTCAACAAAGGTCACTCAACAAAGTCTTTGGCAGCAAGCTTGCAGACACTCGCTGGAGTACTTTT
ATGCAGCAGCACCCTGTACCTCAGCATCCAAAGCAACAGGAGCATCAATAGTCAACAAAGGTCACTCAACAAAGTCTTTGGCAGCAAGCTTGCAGACACTCGCTGGAGTACTTTT

cov pid 361
1 Wt_Allele_1 100.0% 100.0%
2 K02_Allele_1 91.7% 91.7%
1 361 CCTATGCTACGACGACCTGGCAGACGAATGGGCAACCATGTATGCCAATGTTCCAGTTCCTTAGTGCTATGCAACAAATTCAGTCAATACATTCGGTTCCTGGAAACAGGAAT
CCTATGCTACGACGACCTGGCAGACGAATGGGCAACCATGTATGCCAATGTTCCAGTTCCTTAGTGCTATGCAACAAATTCAGTCAATACATTCGGTTCCTGGAAACAGGAAT

cov pid 481
1 Wt_Allele_1 100.0% 100.0%
2 K02_Allele_1 91.7% 91.7%
1 481 AGCGATTTAACGGCGGGGGGGCTGCTGCTGAGTGCAGTCAACAATGTTGTTTCAGCAGCCGCAACCGCACTATACACATGCAAGGTCCAGCCACGGTCTGCTTAACCGGTT
AGCGATTTAACGGCGGGGGGGCTGCTGCTGAGTGCAGTCAACAATGTTGTTTCAGCAGCCGCAACCGCACTATACACATGCAAGGTCCAGCCACGGTCTGCTTAACCGGTT

gHLH4
cov pid 601
1 Wt_Allele_1 100.0% 100.0%
2 K02_Allele_1 91.7% 91.7%
1 601 CAAACGGGAAGCGATCAACCGAAGCTTGGTCCAGTACCCGTAACCAAGAAAGCAAGGCAATACGAAAAGTATACACAGGAAGTGAAGGCAAGAGCTCAGAAAGTTGAACCA
CAAACGGGAAGCGATCAACCGAAGCTTGGTCCAGTACCCGTAACCAAGAAAGCAAGGCAATACGAAAAGTATACACAGGAAGTGAAGGCAAGAGCTCAGAAAGTTGAACCA

cov pid 721
1 Wt_Allele_1 100.0% 100.0%
2 K02_Allele_1 91.7% 91.7%
1 721 TCTGTGTGCTTTCTCCAGTTACATTTCCAGGGACTCTTCTCAAAGCAGCCAAACGAGGCTCTTTTCATGGCTCAGAAAGACCCCGATTGGGCAAGATGACCCCGCGAGGCT
TCTGTGTGCTTTCTCCAGTTACATTTCCAGGGACTCTTCTCAAAGCAGCCAAACGAGGCTCTTTTCATGGCTCAGAAAGACCCCGATTGGGCAAGATGACCCCGCGAGGCT

cov pid 841
1 Wt_Allele_1 100.0% 100.0%
2 K02_Allele_1 91.7% 91.7%
1 841 CGTCGACATGAGCGAAATAGAGGGAGCAACAGCGGTCGGTCTCATATCGAACAGATCAAGGAGCTACGAGAGTTCTCAGAGGTTCAAAATATCTTTCAAACCAACAAAGTTTCC
CGTCGACATGAGCGAAATAGAGGGAGCAACAGCGGTCGGTCTCATATCGAACAGATCAAGGAGCTACGAGAGTTCTCAGAGGTTCAAAATATCTTTCAAACCAACAAAGTTTCC

gHLH5
cov pid 961
1 Wt_Allele_1 100.0% 100.0%
2 K02_Allele_1 91.7% 91.7%
1 961 ATCTTGTCTCTGTAGTGACTACATCAATCAATGCAAGCCAGAGCCATCGTGGACTCAGAACATCAAAACTGGCGGACACTTTCGAGAAGCAAGCGATTGTTGCTCAACGGG
ATCTTGTCTCTGTAGTGACTACATCAATCAATGCAAGCCAGAGCCATCGTGGACTCAGAACATCAAAACTGGCGGACACTTTCGAGAAGCAAGCGATTGTTGCTCAACGGG

cov pid 1081
1 Wt_Allele_1 100.0% 100.0%
2 K02_Allele_1 91.7% 91.7%
1 1081 TTAACCTGAAGAAGCAAGAGTCCATGCTCCACTTCCGACGAGCCGCAAGTGGCTCTTTGCTACAGGAATTTGACTACCGTGTGTTTCAATCATGTCCATTGCTCATG
TTAACCTGAAGAAGCAAGAGTCCATGCTCCACTTCCGACGAGCCGCAAGTGGCTCTTTGCTACAGGAATTTGACTACCGTGTGTTTCAATCATGTCCATTGCTCATG

cov pid 1201
1 Wt_Allele_1 100.0% 100.0%
2 K02_Allele_1 91.7% 91.7%
1 1201 GGGGTGGCTTCTGTGGCAGGAAGTATCGGCTCGCAAGCTCTTTCGAATCTGTTGGGCTAAATAGGACCGGGTCGACAGCAGAGTTTTTGTGTATTCGGAAACATCAA
GGGTGGCTTCTGTGGCAGGAAGTATCGGCTCGCAAGCTCTTTCGAATCTGTTGGGCTAAATAGGACCGGGTCGACAGCAGAGTTTTTGTGTATTCGGAAACATCAA

cov pid 1321
1 Wt_Allele_1 100.0% 100.0%
2 K02_Allele_1 91.7% 91.7%
1 1321 GATATATTGACGCCATGGCAGACCTGCTAAACGCTCAAGTGTGTCAGTGAACAGGGGAAGGAGTCTGATGAAGGAAGAACATTTGTGTACTGGTGTGGCAGGTAGTGTCTTGG
GATATATTGACGCCATGGCAGACCTGCTAAACGCTCAAGTGTGTCAGTGAACAGGGGAAGGAGTCTGATGAAGGAAGAACATTTGTGTACTGGTGTGGCAGGTAGTGTCTTGG

cov pid 1441
1 Wt_Allele_1 100.0% 100.0%
2 K02_Allele_1 91.7% 91.7%
1 1441 CGATCTCAACGGCTAATATCAACATCAGCTGACTAGTCTTTCGAAAGGAGGCAAGTTTTTGGTTCCTCAGCTGGAAGTGTACAGCTACTGTTAG
CGATCTCAACGGCTAATATCAACATCAGCTGACTAGTCTTTCGAAAGGAGGCAAGTTTTTGGTTCCTCAGCTGGAAGTGTACAGCTACTGTTAG

```

B

Reference sequence (1): Wt\_Allele\_2  
Identities normalised by reference length.  
Colored by: identity

```

cov pid 1 [
1 Wt_Allele_2 100.0% 100.0%
2 K01_Allele_2 100.0% 100.0%
3 K02_Allele_2 40.6% 40.6%
1 1 ATGAATCTTTAAGCGCAGCGGCTGCAGAAAGGGCCAGTATGGCAGCTCGCTCAAAACGCTAGCTACAGGAAGCGGAGCACACACGCGTGGTTCGCTCTCCAGCCTTGAT
ATGAATCTTTAAGCGCAGCGGCTGCAGAAAGGGCCAGTATGGCAGCTCGCTCAAAACGCTAGCTACAGGAAGCGGAGCACACACGCGTGGTTCGCTCTCCAGCCTTGAT

cov pid 121
1 Wt_Allele_2 100.0% 100.0%
2 K01_Allele_2 100.0% 100.0%
3 K02_Allele_2 40.6% 40.6%
1 121 ACGAAGGCGATGAAAATTTACAGAGGGACATCAGAAGTCGCGATATCGCTCTGGAGTGAATTCGCTGTAACACGGTAACTGCTCAAAAGCTTCAACGATTTATATCGCAG
ACGAAGGCGATGAAAATTTACAGAGGGACATCAGAAGTCGCGATATCGCTCTGGAGTGAATTCGCTGTAACACGGTAACTGCTCAAAAGCTTCAACGATTTATATCGCAG

cov pid 241
1 Wt_Allele_2 100.0% 100.0%
2 K01_Allele_2 100.0% 100.0%
3 K02_Allele_2 40.6% 40.6%
1 241 ATGCAGCAGCACCCTGTACCTCAGCATCCAAAGCAACAGGAGCATCAATAGTCAACAAAGGTCACTCAACAAAGTCTTTGGCAGCAAGCTTGCAGACACTCGCTGGAGTACTTTT
ATGCAGCAGCACCCTGTACCTCAGCATCCAAAGCAACAGGAGCATCAATAGTCAACAAAGGTCACTCAACAAAGTCTTTGGCAGCAAGCTTGCAGACACTCGCTGGAGTACTTTT

cov pid 361
1 Wt_Allele_2 100.0% 100.0%
2 K01_Allele_2 100.0% 100.0%
3 K02_Allele_2 40.6% 40.6%
1 361 CCTATGCTACGACGACCTGGCAGACGAATGGGCAACCATGTATGCCAATGTTCCAGTTCCTTAGTGCTATGCAACAAATTCAGTCAATACATTCGGTTCCTGGAAACAGGAAT
CCTATGCTACGACGACCTGGCAGACGAATGGGCAACCATGTATGCCAATGTTCCAGTTCCTTAGTGCTATGCAACAAATTCAGTCAATACATTCGGTTCCTGGAAACAGGAAT

cov pid 481
1 Wt_Allele_2 100.0% 100.0%
2 K01_Allele_2 100.0% 100.0%
3 K02_Allele_2 40.6% 40.6%
1 481 AGCGATTTAACGGCGGGGGGGCTGCTGCTGAGTGCAGTCAACAATGTTGTTTCAGCAGCCGCAACCGCACTATACACATGCAAGGTCCAGCCACGGTCTGCTTAACCGGTT
AGCGATTTAACGGCGGGGGGGCTGCTGCTGAGTGCAGTCAACAATGTTGTTTCAGCAGCCGCAACCGCACTATACACATGCAAGGTCCAGCCACGGTCTGCTTAACCGGTT

gHLH4
cov pid 601
1 Wt_Allele_2 100.0% 100.0%
2 K01_Allele_2 100.0% 100.0%
3 K02_Allele_2 40.6% 40.6%
1 601 CAAACGGGAAGCGATCAACCGAAGCTTGGTCCAGTACCCGTAACCAAGAAAGCAAGGCAATACGAAAAGTATACACAGGAAGTGAAGGCAAGAGCTCAGAAAGTTGAACCA
CAAACGGGAAGCGATCAACCGAAGCTTGGTCCAGTACCCGTAACCAAGAAAGCAAGGCAATACGAAAAGTATACACAGGAAGTGAAGGCAAGAGCTCAGAAAGTTGAACCA

cov pid 721
1 Wt_Allele_2 100.0% 100.0%
2 K01_Allele_2 100.0% 100.0%
3 K02_Allele_2 40.6% 40.6%
1 721 TCTGTGTGCTTTCTCCAGTTACATTTCCAGGGACTCTTCTCAAAGCAGCCAAACGAGGCTCTTTTCATGGCTCAGAAAGACCCCGATTGGGCAAGATGACCCCGCGAGGCT
TCTGTGTGCTTTCTCCAGTTACATTTCCAGGGACTCTTCTCAAAGCAGCCAAACGAGGCTCTTTTCATGGCTCAGAAAGACCCCGATTGGGCAAGATGACCCCGCGAGGCT

cov pid 841
1 Wt_Allele_2 100.0% 100.0%
2 K01_Allele_2 100.0% 100.0%
3 K02_Allele_2 40.6% 40.6%
1 841 CGTCGACATGAGCGAAATAGAGGGAGCAACAGCGGTCGGTCTCATATCGAACAGATCAAGGAGCTACGAGAGTTCTCAGAGGTTCAAAATATCTTTCAAACCAACAAAGTTTCC
CGTCGACATGAGCGAAATAGAGGGAGCAACAGCGGTCGGTCTCATATCGAACAGATCAAGGAGCTACGAGAGTTCTCAGAGGTTCAAAATATCTTTCAAACCAACAAAGTTTCC

gHLH5
cov pid 961
1 Wt_Allele_2 100.0% 100.0%
2 K01_Allele_2 100.0% 100.0%
3 K02_Allele_2 40.6% 40.6%
1 961 ATCTTGTCTCTGTAGTGACTACATCAATCAATGCAAGCCAGAGCCATCGTGGACTCAGAACATCAAAACTGGCGGACACTTTCGAGAAGCAAGCGATTGTTGCTCAACGGG
ATCTTGTCTCTGTAGTGACTACATCAATCAATGCAAGCCAGAGCCATCGTGGACTCAGAACATCAAAACTGGCGGACACTTTCGAGAAGCAAGCGATTGTTGCTCAACGGG

cov pid 1081
1 Wt_Allele_2 100.0% 100.0%
2 K01_Allele_2 100.0% 100.0%
3 K02_Allele_2 40.6% 40.6%
1 1081 TGAAGCCAGAGCCATCATGCTGGACTCAGAACATCAAAACTGGCGGACACTTTCGAGAAGCAAGCGATTGGTCAACCAAGGTTAACTAGTGAAGAGCAAAAGTGCATGCTTC
TGAAGCCAGAGCCATCATGCTGGACTCAGAACATCAAAACTGGCGGACACTTTCGAGAAGCAAGCGATTGGTCAACCAAGGTTAACTAGTGAAGAGCAAAAGTGCATGCTTC

cov pid 1201
1 Wt_Allele_2 100.0% 100.0%
2 K01_Allele_2 100.0% 100.0%
3 K02_Allele_2 40.6% 40.6%
1 1201 CACTTTCGACGAGCCGCAAGTGGCTGCTTTTTCGCAAGGAATGACTACCGTCTGTTTCAATCAITTCATATGCAATGGGGTGGCTTATGGCAGGAAGAAATACGGTCT
CACTTTCGACGAGCCGCAAGTGGCTGCTTTTTCGCAAGGAATGACTACCGTCTGTTTCAATCAITTCATATGCAATGGGGTGGCTTATGGCAGGAAGAAATACGGTCT
CACTTTCGACGAGCCGCAAGTGGCTGCTTTTTCGCAAGGAATGACTACCGTCTGTTTCAATCAITTCATATGCAATGGGGTGGCTTATGGCAGGAAGAAATACGGTCT

cov pid 1321
1 Wt_Allele_2 100.0% 100.0%
2 K01_Allele_2 100.0% 100.0%
3 K02_Allele_2 40.6% 40.6%
1 1321 GCACAGCTCTTGAATCTTTTGGGCTAAATAGGACCGGGCTGCACAGAGAGTTTTTGGTGTATTCGGAAATCAAGAAATATTTGACCTACGAGCTGCTTAAAC
GCACAGCTCTTGAATCTTTTGGGCTAAATAGGACCGGGCTGCACAGAGAGTTTTTGGTGTATTCGGAAATCAAGAAATATTTGACCTACGAGCTGCTTAAAC
GCACAGCTCTTGAATCTTTTGGGCTAAATAGGACCGGGCTGCACAGAGAGTTTTTGGTGTATTCGGAAATCAAGAAATATTTGACCTACGAGCTGCTTAAAC

cov pid 1441
1 Wt_Allele_2 100.0% 100.0%
2 K01_Allele_2 100.0% 100.0%
3 K02_Allele_2 40.6% 40.6%
1 1441 CGCTCAAGTGTGGCAGTGAACAGGGGAAGGGGCTGAGTAAAGGAAGAACATTTGTTGCTAGTGGTGGCAGGAGTGTGCTTTCGATCTCAACGGCTAATATTAACATCACCGTGA
GCTCAAGTGTGGCAGTGAACAGGGGAAGGGGCTGAGTAAAGGAAGAACATTTGTTGCTAGTGGTGGCAGGAGTGTGCTTTCGATCTCAACGGCTAATATTAACATCACCGTGA
GCTCAAGTGTGGCAGTGAACAGGGGAAGGGGCTGAGTAAAGGAAGAACATTTGTTGCTAGTGGTGGCAGGAGTGTGCTTTCGATCTCAACGGCTAATATTAACATCACCGTGA

cov pid 1561
1 Wt_Allele_2 100.0% 100.0%
2 K01_Allele_2 100.0% 100.0%
3 K02_Allele_2 40.6% 40.6%
1 1561 CTAGTCTTCAACGGAGGCAAGTTTTTGGTTCCTCAGCTGCTGAAGTGTACAGCTACTGTTAG
CTAGTCTTCAACGGAGGCAAGTTTTTGGTTCCTCAGCTGCTGAAGTGTACAGCTACTGTTAG
CTAGTCTTCAACGGAGGCAAGTTTTTGGTTCCTCAGCTGCTGAAGTGTACAGCTACTGTTAG

```



## Figure 4. Characterisation of bHLH1b KO mutants

Previous page: (A) Sequence alignment of bHLH1b allele 1 in Pt1 Wt strain and KO 1b#2. Allele 1 of KO 1b#1 was not possible to amplify, possibly due to Loss of Heterozygosity (B) Sequence alignment of RITMO1 allele 2 in Pt1 Wt strain and RITMO1 and KO 1b#1 KO 1b#2. Sequence alignments were generated via EBI Clustal Omega webtool and visualized via Mview tool. Bases are colored by identity to the Wt reference sequence. gHLH4 and gHLH5 sgRNA target sites are highlighted in light and dark green respectively.

### bHLH1b mutations affect free-run fluorescence oscillations

KO 1b#1 and #2 lines were characterized by flow cytometry in order to assess possible alteration of cellular rhythmicity, as previously done for the RITMO1 mutants. Transgenic cultures were pre-adapted in a 16L:8D photoperiod ( $25 \mu\text{mol photons m}^{-2} \text{s}^{-1}$ ) and subsequently released under constant light at  $17 \mu\text{mol photons m}^{-2} \text{s}^{-1}$ , choosing the experimental setting already optimized in Chapter II.c. As reported in Fig.4, all replicates of bHLH1b KOs were shown to maintain a rhythmicity in fluorescence oscillations in free-run condition. Nevertheless, both KO mutants show a shortening of the oscillation period when

compared to Wt lines, although to a minor extent to what was previously shown on RITMO1 KO mutants. Free run period is indeed equal to  $27.13 \pm 0.62$  and  $27.33 \pm 0.44$  hours in KO 1b#1 and KO 1b#2 respectively, versus the  $29.62 \pm 0.63$  period shown by Wt replicates in the same experiments (Fig.5 and Table 3). In distinct experiments with the same experimental set up, RITMO1 KO1 and KO3 showed a period of  $24.21 \pm 0.91$  and  $21.97 \pm 0.82$  (mean  $\pm$  s.e.m.) respectively, as reported in Chapter II.c. In addition, amplitude and R.A.E. of free run oscillations in bHLH1b KO lines show no alteration when compared to Wt line (Fig.5 and Table 3), differently to what was observed in RITMO1 mutants.

16L:8D ( $25 \mu\text{mol m}^{-2} \text{s}^{-1}$ ) to L:L ( $17 \mu\text{mol m}^{-2} \text{s}^{-1}$ )	Wt (6/6)		KO 1b#1 (10/10)			KO 1b#2 (10/10)		
	Mean	s.e.m	Mean	s.e.m	p value	Mean	s.e.m	p value
Period	29.62	0.6348	27.15	0.6163	0.02	27.33	0.4353	0.0084
R.A.E.	0.36	0.04733	0.423	0.04626	N.S.	0.391	0.04086	N.S.
Amplitude	0.7117	0.04764	0.754	0.05177	N.S.	0.752	0.03747	N.S.

Table 3. Characterisation of cellular fluorescence rhythmicity of bHLH1b mutants in L:L

Calculated periods, relative amplitude errors and amplitudes of the Wt, KO 1b#1 and KO 1b#2 lines after transition from 16L:8D  $25 \mu\text{mol m}^{-2} \text{s}^{-1}$  to L:L  $17 \mu\text{mol m}^{-2} \text{s}^{-1}$ . Average and s.e.m. values were calculated on the replicates considered rhythmic according to the EPR test. The fraction of rhythmic replicates/total of replicates is reported and correspond to the whole set of replicates. Values correspond to what is shown in Fig., panels (A-C). P-values obtained via One-way analysis of variance against Wt with Bonferroni post-test correction are shown. N.S.: non significant,  $P > 0.05$

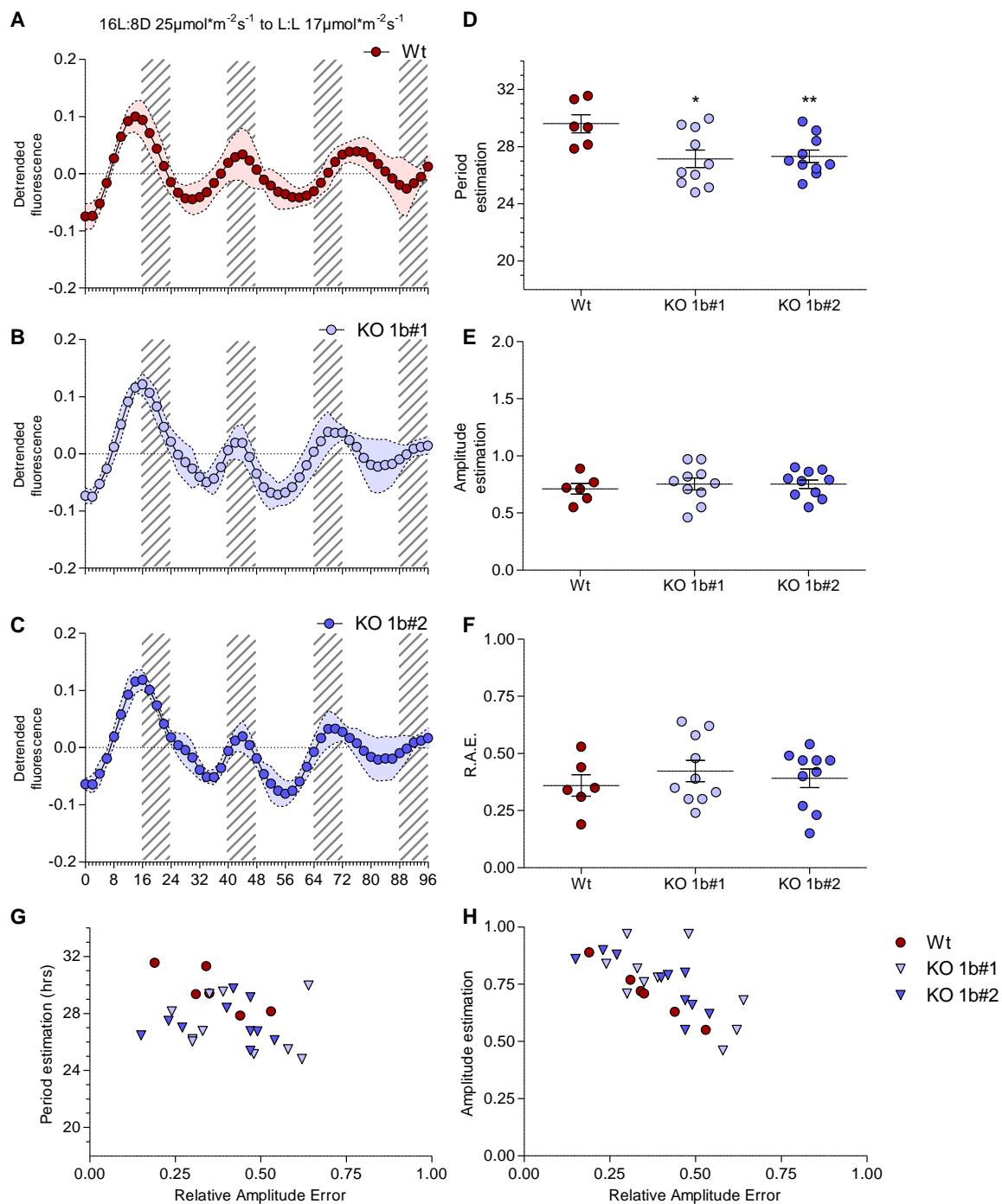


Figure 5. Effects of bHLH1b mutation on cellular fluorescence

(A-C) Oscillations of cellular red fluorescence (B3-A parameter) in Wt, KO 1b#1 and KO 1b#2 after transition from 16L:8D  $25\mu\text{mol}\cdot\text{m}^{-2}\cdot\text{s}^{-1}$  to L:L  $17\mu\text{mol}\cdot\text{m}^{-2}\cdot\text{s}^{-1}$  ( $n=6$  for Wt,  $n=10$  for KO lines). Dots represent mean B3-A values, coloured dashed lines represent SD. (D-F) Period (D), amplitude (E) and R.A.E. (F) estimations of B3-A fluorescence traces represented in panels A-C (mean  $\pm$ s.e.m., \* $P<0.05$ , \*\* $P<0.01$ , One-way analysis of variance against Wt with Bonferroni post-test correction). (G) Plot of period versus R.A.E. estimates and (H) plot of amplitude versus R.A.E. estimates of the replicates represented in panels A-C.

# Conclusions

Although preliminary, the results presented here suggest a possible complication of bHLH1b in the regulation of the circadian clock of *P. tricornutum* together with RITMO1. The data obtained through a limited range of Y2H analyses allowed us to demonstrate a direct physical interaction between RITMO1 and bHLH1b, an interaction that is achieved through their bHLH fold. Similarly, it was possible to highlight the homodimerization of bHLH1b, while homodimerization of RITMO1 was not possible to assess due to the autoactivation of the *His3* reporter in *S. cerevisiae* cells transformed with the RITMO1-bait hybrid. In parallel, no direct protein-protein association in the yeast model was observed between RITMO1 and other proteins presenting a similar rhythmic expression profile in *P. tricornutum*, the transcription factor bZIP7 and the photoreceptor CPF1. It is crucial to consider that the results obtained do not exclude that post-translational modifications (e.g. acetylation or phosphorylation of amino acid residues) may be required for the interaction of RITMO1 with CPF1 and bZIP7, since the Y2H setup does not allow to control the post-translational modifications of the protein under study. In mammals, CRY interaction with BMAL1 via the bHLH fold is enhanced by post translational modifications of BMAL1, specifically CK2 $\alpha$ -mediated phosphorylation and CLOCK-mediated acetylation (Tamaru et al., 2015). The homodimerization of RITMO1 remains an open possibility which could not be assessed in this experiment due to the autoactivation of the RITMO1-bait hybrid. Cellular fluorescence data obtained by flow cytometer analysis confirm a statistically significant alteration in the rhythmicity of bHLH1b KO mutants released in free running, with a shortening of the period, of about 2h compared to Wt. In contrast to the KO mutants of RITMO1 the quality of the oscillations is not altered (chapter II.c), as demonstrated by the fact that

the R.A.E. values are comparable between mutants and Wt and by the fact that the totality of the replicates analyzed passed the EPR test of rhythmicity (Zielinski et al., 2014). The presence of such differences in the phenotype of mutants for partially redundant clock proteins (as RITMO1 and bHLH1b are, plausibly) is not uncommon. An example is given by mutants of the MYB proteins CCA1 and LHY in *Arabidopsis thaliana*, both of which exhibit a shortening of the free-running period relative to Wt, albeit of different magnitude (Alabadi et al., 2002; Mizoguchi et al., 2002). The data accumulated to date do not allow advanced hypotheses as to why RITMO1 mutants exhibit a more pronounced phenotype than KOs for bHLH1b. An analysis of rhythmic free-run gene expression profiles in bHLH1 KOs (such as that reported for RITMO1 mutants in Chapter II.c) is essential to verify the presence of similar phenotypes in these lines. This analysis is currently in planning. One possibility is that the RITMO1-bHLH1b dimer and the bHLH1b-bHLH1b homodimer play a different and not perfectly complementary role in the regulation of gene transcription in *P. tricornutum*, as may be the case for the possible RITMO1-RITMO1 homodimer. This could happen by a recognition of different DNA target sites by the different dimers. Further investigations are needed to test this hypothesis. A future in-depth analysis of the interaction partners of RITMO1 and bHLH1b, e.g. by co-immunoprecipitation assay (Lin and Lai, 2017), will allow to elucidate the interactome of these proteins and to identify new potential components of the endogenous clock of *P. tricornutum*. Generation of RITMO1 KO lines complemented with an exogenous version of the protein modified with HA and fluorescent protein tags is currently underway. These lines will allow the realization of immunoprecipitation assays with commercial antibodies directed against the tag associated with the protein, thus allowing the identification of RITMO1 interactors. The

same lines will also provide the material for ChIP-Seq analysis for the characterization of DNA binding sites recognized by the protein. Similar complemented lines are also planned for bHLH1b KOs.

The generation of RITMO1 and bHLH1b double mutants is also planned in

order to attest the effect of double obliteration on the rhythmicity of this alga. In case the role is partially redundant, such co-mutation is expected to induce a major disruption of cellular rhythmicity, larger than those observed in single mutants (Alabadi et al., 2002; Mizoguchi et al., 2002).

# Bibliography

- Alabadi, D., Yanovsky, M.J., Más, P., Harmer, S.L., Kay, S.A., 2002. Critical Role for CCA1 and LHY in Maintaining Circadian Rhythmicity in Arabidopsis. *Curr. Biol.* 12, 757–761. [https://doi.org/10.1016/S0960-9822\(02\)00815-1](https://doi.org/10.1016/S0960-9822(02)00815-1)
- Annunziata, R., Ritter, A., Fortunato, A.E., Manzotti, A., Cheminant-Navarro, S., Agier, N., Huysman, M.J.J., Winge, P., Bones, A.M., Bouget, F.-Y., Cosentino Lagomarsino, M., Bouly, J.-P., Falciatore, A., 2019. bHLH-PAS protein RITMO1 regulates diel biological rhythms in the marine diatom *Phaeodactylum tricornutum*. *Proc. Natl. Acad. Sci.* 116, 13137–13142. <https://doi.org/10.1073/pnas.1819660116>
- Coesel, S., Mangogna, M., Ishikawa, T., Heijde, M., Rogato, A., Finazzi, G., Todo, T., Bowler, C., Falciatore, A., 2009. Diatom PtCPF1 is a new cryptochrome/photolyase family member with DNA repair and transcription regulation activity. *EMBO Rep.* 10, 655–661. <https://doi.org/10.1038/embor.2009.59>
- Concordet, J.-P., Haeussler, M., 2018. CRISPOR: intuitive guide selection for CRISPR/Cas9 genome editing experiments and screens. *Nucleic Acids Res.* 46, W242–W245. <https://doi.org/10.1093/nar/gky354>
- Corellou, F., Schwartz, C., Motta, J.-P., Djouani-Tahri, E.B., Sanchez, F., Bouget, F.-Y., 2009. Clocks in the Green Lineage: Comparative Functional Analysis of the Circadian Architecture of the Picoeukaryote *Ostreococcus*. *Plant Cell* 21, 3436–3449. <https://doi.org/10.1105/tpc.109.068825>
- Creux, N., Harmer, S., 2019. Circadian Rhythms in Plants. *Cold Spring Harb. Perspect. Biol.* 11, a034611. <https://doi.org/10.1101/cshperspect.a034611>
- Cuéllar, A.P., Pauwels, L., De Clercq, R., Goossens, A., 2013. Yeast Two-Hybrid Analysis of Jasmonate Signaling Proteins, in: Goossens, A., Pauwels, L. (Eds.), *Jasmonate Signaling, Methods in Molecular Biology*. Humana Press, Totowa, NJ, pp. 173–185. [https://doi.org/10.1007/978-1-62703-414-2\\_14](https://doi.org/10.1007/978-1-62703-414-2_14)
- Falciatore, A., Casotti, R., Leblanc, C., Abrescia, C., Bowler, C., 1999. Transformation of Nonselectable Reporter Genes in Marine Diatoms. *Mar. Biotechnol.* 1, 239–251. <https://doi.org/10.1007/PL00011773>
- Guillard, R.R.L., 1975. Culture of Phytoplankton for Feeding Marine Invertebrates., *Cultures of Marine invertebrate Animals*.
- Jones, S., 2004. An overview of the basic helix-loop-helix proteins. *Genome Biol.* 6. <https://doi.org/10.1186/gb-2004-5-6-226>
- Kewley, R.J., Whitelaw, M.L., Chapman-Smith, A., 2004. The mammalian basic helix-loop-helix/PAS family of transcriptional regulators. *Int. J. Biochem. Cell Biol.* 36, 189–204. [https://doi.org/10.1016/S1357-2725\(03\)00211-5](https://doi.org/10.1016/S1357-2725(03)00211-5)
- Lin, J.-S., Lai, E.-M., 2017. Protein-Protein Interactions: Co-Immunoprecipitation, in: Journet, L., Cascales, E. (Eds.), *Bacterial Protein Secretion Systems, Methods in Molecular Biology*. Springer New York, New York, NY, pp. 211–219. [https://doi.org/10.1007/978-1-4939-7033-9\\_17](https://doi.org/10.1007/978-1-4939-7033-9_17)
- Mizoguchi, T., Wheatley, K., Hanzawa, Y., Wright, L., Mizoguchi, M., Song, H.-R., Carré, I.A., Coupland, G., 2002. LHY and CCA1 Are Partially Redundant Genes Required to Maintain Circadian Rhythms in Arabidopsis. *Dev. Cell* 2, 629–641. [https://doi.org/10.1016/S1534-5807\(02\)00170-3](https://doi.org/10.1016/S1534-5807(02)00170-3)

- Morant, P.-E., Thommen, Q., Pfeuty, B., Vandermoere, C., Corellou, F., Bouget, F.-Y., Lefranc, M., 2010. A robust two-gene oscillator at the core of *Ostreococcus tauri* circadian clock. *Chaos Interdiscip. J. Nonlinear Sci.* 20, 045108. <https://doi.org/10.1063/1.3530118>
- Nymark, M., Sharma, A.K., Sparstad, T., Bones, A.M., Winge, P., 2016. A CRISPR/Cas9 system adapted for gene editing in marine algae. *Sci. Rep.* 6, 24951. <https://doi.org/10.1038/srep24951>
- Peschel, N., Helfrich-Förster, C., 2011. Setting the clock - by nature: Circadian rhythm in the fruitfly *Drosophila melanogaster*. *FEBS Lett.* 585, 1435-1442. <https://doi.org/10.1016/j.febslet.2011.02.028>
- Serif, M., Dubois, G., Finoux, A.-L., Teste, M.-A., Jallet, D., Daboussi, F., 2018. One-step generation of multiple gene knock-outs in the diatom *Phaeodactylum tricorutum* by DNA-free genome editing. *Nat. Commun.* 9, 3924. <https://doi.org/10.1038/s41467-018-06378-9>
- Tamaru, T., Hattori, M., Honda, K., Nakahata, Y., Sassone-Corsi, P., van der Horst, G.T.J., Ozawa, T., Takamatsu, K., 2015. CRY Drives Cyclic CK2-Mediated BMAL1 Phosphorylation to Control the Mammalian Circadian Clock. *PLOS Biol.* 13, e1002293. <https://doi.org/10.1371/journal.pbio.1002293>
- Zielinski, T., Moore, A., Troup, E., Halliday, K.J., Millar, A.J., 2014. Strengths and Limitations of Period Estimation Methods for Circadian Data. *PLOS ONE* 9, e96462. <https://doi.org/10.1371/journal.pone.0096462>



*L'altezza è profondità, la luce inaccessa è abisso, la chiarezza è tenebra, il magno è parvo, il  
distinto è confuso, la lite è amicizia, l'individuo è dividuo, l'immenso è atomo.*

adapted from Giordano Bruno - Epistole italiane





# Chapter III:

## bHLH2 is a light-intensity dependent modulator of photosynthesis and growth in the marine diatom *Phaeodactylum tricorutum*

Contributions:

Alessandro Manzotti, Soizic Cheminant-Navarro, Antonio Emidio Fortunato, Andres Ritter, Alessandra Bellan, Marianne Jaubert, Benjamin Bailleul, Tomas Morosinotto, Jean-Pierre Bouly, Angela Falciatore

Keywords: photosynthesis, plastid physiology, plastid retrograde signaling, light stress, chlorophyll fluorescence

In this project I designed and realized all the physiological characterization of photosynthetic parameters in RNAi transgenic lines grown in liquid medium, as well as the analysis of gene expression and growth.

In a parallel line of research, I led along the characterization of the diatom circadian clock, my PhD work identified bHLH2, another bHLH-PAS putative transcription factor, as a possible modulator of plastid physiology in *P. tricornutum*. This research integrated a project of the EMBRC-France (European Marine Biological Resource Centre) network, which was already in progress when I joined the laboratory for my Ph.D. program. More specifically, the project aimed to identify new diatom strains showing novel traits of interest (*e.g.*, altered photosynthesis and biomass productivity), by using a Transcription Factor (TF)-based genetic engineering strategy. TFs are master regulators of gene expression and excellent candidates both for fundamental research approaches and for applied research. The foundation for this project was a collection of transgenic lines with a deregulated expression of each of the 220 TFs of *P. tricornutum*, which has been generated in the laboratory using the RNA interference strategy (RNAi) by Soizic Cheminant Navarro (Navarro et al., in preparation). Established by the host laboratory in 2009 (De Riso et al., 2009), RNAi has been widely used by the diatom community before the advent of the genome-editing era. Aim of the TF-based genetic engineering strategy was to widely affect genetic regulation of diatoms, likely accelerating the discovery of new regulators and new phenotypes. This approach appeared particularly suitable for *P. tricornutum* considering that forward genetic screens (random insertion or chemical mutagens) are not feasible in this species presenting a diploid genome and lack of sexual cycle.

# Abstract

Accounting for more than 40% of marine primary production, diatoms represent one of the most prominent phytoplankton groups in the Oceans. Despite their ecological relevance, the knowledge on the regulation of diatom photosynthesis and on the genetic control of its plasticity is still very limited. To identify the unknown molecular regulators underlying these processes, we applied a transcription factor genetic engineering approach to the diatom model species *Phaeodactylum tricorutum* and generated a collection of bHLH transcription factor knock-down transgenic lines via RNA interference. Phenotyping by non-invasive imaging techniques based on measurements of chlorophyll fluorescence changes lead to the identification of the bHLH-PAS protein bHLH2 as a candidate regulator of diatom chloroplast activity. Lines bearing a *bHLH2*RNAi construct show a light intensity-dependent reduction of PSII maximal quantum yield and maximal thylakoid Electron Transfer Rate. Remarkably, this light-intensity conditional phenotype also translates in a reduced growth capacity of *P. tricorutum* following transition from low to high light conditions. Gene expression analysis of *bHLH2* showed a diurnal regulation of its expression, with a strong, plastid-signals mediated downregulation of *bHLH2* transcripts following dark to light transition. These results indicate the existence of a strong regulatory cross-talk between plastids and nucleus for the optimization of diatom growth capacity under changing lights. bHLH2 represents the first example of bHLH-PAS transcription factor characterized as a light-intensity dependent modulator of photosynthesis and growth and it represents an ideal entry point for further dissection of the gene regulatory network controlling these critical responses in diatoms.

# Introduction

Although diatoms represent one of the most abundant taxa of marine microalgae and a major actor of carbon biogeochemical cycles at the global level, the regulation of gene expression involved in their photosynthetic physiology is still largely uncharacterized. The proper functioning of photosynthetic metabolism and its dynamic adaptation to environmental stimuli require fine-tuning of gene expression. The complex evolutionary processes that led to the acquisition of the plastid by diatoms make the study of this regulatory process particularly complex. As secondary endosymbionts of the red plastid lineage, diatom chloroplasts are distinct from the green lineage ones and therefore, direct extrapolation on the regulation of photosynthetic processes from higher plants and chlorophytes is not always applicable or relevant (see Chapter I, paragraphs 3.a and 3.b). In recent years, particular genomic features and metabolic pathways have been identified in these algae by genomic analysis. Initial regulators of light stress mechanisms have been also identified by targeted modulation of the expression of specific proteins such as the LHGXs (Bailleul et al., 2010; Buck et al., 2019; Giovagnetti et al., 2022) However, information on the regulation of diatom photosynthesis and the genetic control of its plasticity remain still very limited. As already presented in Chapter I, approximately 15% of the entire proteome in diatoms is represented by genes targeted to the plastid or otherwise derived from the endosymbionts that gave rise to the plastid (Moustafa et al., 2009). A large part of these genes have been transferred into the nuclear genome of the host, so that only a reduced fraction of genes remain in the plastid genome (130 in the case of *P. tricornutum*, Oudot-Le Secq et al., 2007). The alteration of cellular processes by means of targeted deregulation of specific enzymes has already been proven as a potentially effective system to study diatom physiology and metabolism (Daboussi et al.,

2014; Levitan et al., 2015). A valid alternative that may allow a wide-ranging description of the regulatory mechanisms of plastid physiology is offered by transcriptional engineering, *i.e.* the deregulation of transcription factors (TFs, Bajhaiya et al., 2017). TFs are master regulators of gene expression and represent perfect candidates for obtaining a profound alteration of processes of interest through a single, pinpoint mutation. Hence TF engineering represents a powerful strategy to identify novel regulators of diatom biology (Bajhaiya et al., 2017; Huang and Daboussi, 2017). In a TF engineering approach, the modulations of TFs expression by RNA-mediated interference is a valid alternative to gene knock-out since a complete loss of TF gene function could lead to a highly noxious phenotype in the case of factors controlling vital processes for the cells. Differently, a partial deregulation of gene expression is expected to lead to less destructive phenotypes but still sufficient to characterize the physiological alterations. This kind of strategy is feasible in *P. tricornutum* since RNAi is an already established techniques (De Riso et al., 2009; Siaux et al., 2007). Hence, deregulation of gene expression via RNAi can allow the relatively straightforward generation of a multitude of mutants for different genes and favour a characterization of their phenotypic alterations. Following this principle, I performed a characterization of the photosynthetic physiology of a set of transgenic lines presenting an antisense construct aimed at silencing genes encoding bHLH proteins. The aim was to evaluate their possible involvement in the regulation of plastid activity and, in parallel, further analyze the proteins involved in the circadian clock of *P. tricornutum*. To this end, I have implemented a variety of biophysics techniques that rely on chlorophyll fluorescence as a reporter of photosynthetic

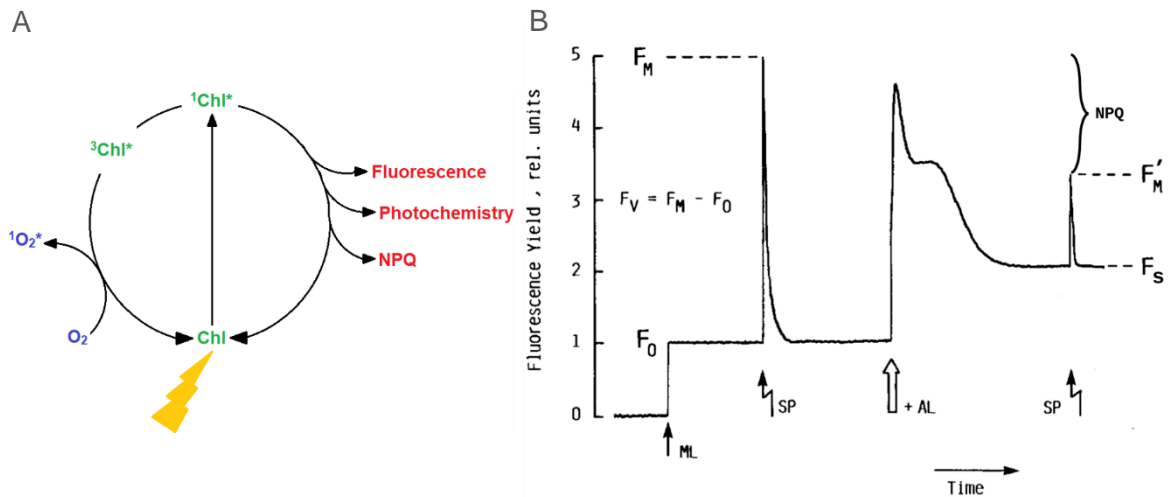


Figure 1. Principles of chlorophyll fluorescence analysis of PSII activity

A) When chlorophyll absorbs light it gets excited to its singlet-electron excitation state ( $^1\text{Chl}^*$ ), which tends to quickly get back to its basal condition in a time span of few ps. To return to its ground energy state chlorophyll can: emit light (as fluorescence), dissipate heat via photoprotective processes or fuel the photosynthetic machinery (photochemistry process).  $^1\text{Chl}^*$  can also decay to a triplet excitation state ( $^3\text{Chl}^*$ ), which in turn is able to generate singlet oxygen ( $^1\text{O}_2^*$ ). B) Sequence of a typical chlorophyll fluorescence trace. Cells are adapted to dark so to allow full opening of PSII centres and oxidation of their downstream electron acceptors. A measuring light (ML) is switched to measure basal fluorescence ( $F_0$ ) with no induction of photochemistry. Application of a saturating light pulse (SP) allows measurement of maximum fluorescence of the dark-adapted chlorophyll ( $F_M$ ). The variable fluorescence ( $F_V$ ) is equal to  $F_M - F_0$ . A light able to drive photosynthesis (AL) is switched on causing a rapid increase in fluorescence. After a period of time another SP is applied, allowing to measure the maximum fluorescence in the light ( $F_M'$ ). The level of stationary fluorescence when  $F_M'$  is measured is named  $F_S$ . Maximal fluorescence variation ( $F_M - F_M'$ ) represent the contribution of non-photochemical quenching (NPQ). Adapted from van Kooten 1990.

processes. The following section is devoted to introducing the principles of these techniques.

## Analysis of photosynthesis via chlorophyll fluorescence

The techniques used for studying photosynthetic and photoprotective capacity are based on the analysis of chlorophyll fluorescence. When excited by a photon, a *special pair* of chlorophyll molecules switch to a singlet-electron excitation state ( $^1\text{Chl}^*$ ), which is highly energetic and tends to quickly get back to its basal condition (in a time span of a few picoseconds). The relaxation process can occur in three ways: by transferring the excited electron to other components of the photosynthetic machinery (photochemical quenching), by fluorescence emission or by heat energy dissipation via the Non

Photochemical Quenching processes (Müller et al., 2001). These three processes are mutually-exclusive, so that an increase in the efficiency in one of the three leads to a decrease in the others (Fig.1). Measuring the fluorescence emitted by chlorophyll can be then a useful strategy to quantify the yield of photosynthesis and heat dissipation (Maxwell and Johnson, 2000; van Kooten and Snel, 1990). At room temperature, the observable fluorescence basically derives only from the chlorophyll special pairs of the Photosystem II, PSII. Under room temperature conditions, in fact, electron-acceptance reactions by molecules downstream of the PSI are relatively constant and occur at high efficiency and speed. Specifically, the de-excitation of the special pair of PSI by electron transfer to

downstream acceptors occurs at a rate greater than by fluorescence or non-photochemical dissipation, which are negligible. The analysis of chlorophyll fluorescence consequently allows to obtain a picture of the functionality of the PSII, but also the condition of other electron transport within the cell and the global efficiency of the electron transfer and redox processes downstream of it.

For evaluating the efficiency of PSII to absorb incoming photons and funnel their energy into photochemical processes (maximal PSII quantum yield, or  $\Phi_{\text{PSIImax}}$ ), a short adaptation of cells in the dark (in the range of a few minutes) is used. This treatment leads to the full reduction of the non-irradiated special pairs of PSII, and the oxidation of their downstream electron acceptors mobile plastoquinones (PQs), hence setting them in a state ready for charge separation. PSII reaction centers which are fully reduced and ready to cease their electrons to downstream acceptors are commonly defined “open”. Dark-adapted PSII are hence irradiated with a detection light (or ML, measuring light) that is sufficient to excite basal fluorescence of chlorophyll ( $F_0$ ) but too feeble to induce changes in photochemical electron transfer. Cells are then subjected to a brief and intense saturating pulse (SP) of actinic light (*i.e.* light capable of exciting photochemistry, AL) that causes the full oxidation of PSII reaction centers and the consequent reduction of electron acceptor PQ. If the SP is short enough, Non-Photochemical Quenching processes cannot take place. Also, due to the slow kinetics of electron transfer from PQs to downstream acceptors, if the SP is short enough no photochemistry can occur either and all the absorbed energy is released by fluorescence. The saturating pulse therefore leads to complete “closure” of the PSII pool and subsequent induction of maximal fluorescence ( $F_m$ ). Being  $F_m$  the highest amount of fluorescence of dark adapted PSII, the difference between  $F_m$  and  $F_0$  is equal to the variable fluorescence ( $F_v$ ).  $F_v/F_m$

represents the proportion of photons that activate the thylakoid electron transfer chain in absence of NPQ and that are not released as basal fluorescence. In other words,  $F_v/F_m$  is equal to the maximal quantum yield of PSII ( $\Phi_{\text{PSIImax}}$ ).  $\Phi_{\text{PSIImax}}$  gives information about the overall performance of the photosynthetic apparatus and of the downstream metabolism consuming ATP and redox potential produced by it (Maxwell and Johnson, 2000; van Kooten and Snel, 1990).

When cells are irradiated with continuous actinic light, the electron acceptors of PSII are quickly reduced, leading to an increase of chlorophyll fluorescence (Kautsky effect, (Kautsky, 1960; Maxwell and Johnson, 2000)). Fluorescence then decreases over a time scale of a few minutes. This progressive decline in fluorescence is due to the initiation of electron transfer along the thylakoid chain. When light pressure is sufficiently high to grant a saturation of electron transport chain, this decline is also associated with an increase in NPQ efficiency, whose magnitude depends on the actinic light intensity. When the stationary fluorescence reaches a steady state ( $F_s$ ), a SP is applied to calculate the emission of maximal fluorescence in presence of light ( $F_m'$ ). Under this condition,  $(F_m' - F_s)/F_m'$  represents the fraction of energy used for photosynthesis under illumination, *i.e.* the photochemical quantum yield of PSII in the light, or  $\Phi_{\text{PSII}}$ . The fraction  $(F_m - F_m')/F_m'$  is then equal to the energy dissipated via NPQ reactions (Müller et al., 2001). It is important to remember that part of the reduction in maximal fluorescence observed in light is attributable to either by energy-dependent heat dissipation (qE), or inactivation of PSII centers due to photodegradation of the D1 protein, a phenomenon that represents the photoinhibitory (qI) component of NPQ. While the qE component of NPQ reverses with rapid kinetics once light stress is interrupted, the replacement of damaged D1 subunits by photoinhibition, which is necessary for the reversion of the qI

component, requires a time lag of several minutes to several hours.

Since the parameter  $\Phi_{PSII}$  represents by definition the efficiency of conversion of light energy in photochemical process, the number of electrons flowing along the thylakoid chain for a given amount of time will be proportional to the product between  $\Phi_{PSII}$  and the light intensity ( $I$ , expressed as a number of photons reaching a given surface for a unit of time). This product is also named relative Electron Transfer Rate, as already shown in chapter II.c.

It is important to stress that the chlorophyll fluorescence parameters described above refer only to PSII. As this complex is only the first of the thylakoid chain, an alteration in the activity of any of the downstream electron transport components can impact its physiology and alter its quantum yield. A slowdown in the activity of one of the plastid's redox players (*e.g.* due to a mutation or reduction in expression) will lead to an accumulation of electrons upstream of it, an

over-reduction of the complexes preceding it and, consequently, a decrease in the quantum yield of PSII. Therefore, analysis of chlorophyll fluorescence at ambient temperature is a powerful tool for obtaining information about the overall activity of photosynthesis, but it does not allow for the precise localization of any bottlenecks.

In the case of an altered quantum yield of PSII, several strategies can be applied to better localize the perturbation. One of these consists in quantifying the oxidoreductive state of PSI. If the bottleneck in the transfer of electrons occurs upstream of PSI (*e.g.* at the level of cytochrome b6f), at the same light intensity the amount of electrons that will reach the PSI per unit time will be lower and therefore PSI itself will be over-oxidized compared to normal (Fig.2A). Conversely, if the defect is located downstream, the PSI will give up less quickly than normal the electrons it receives and will be consequently over-reduced. This is the case in the presence of perturbations of the Calvin Benson Bassham Cycle, the first consumer of

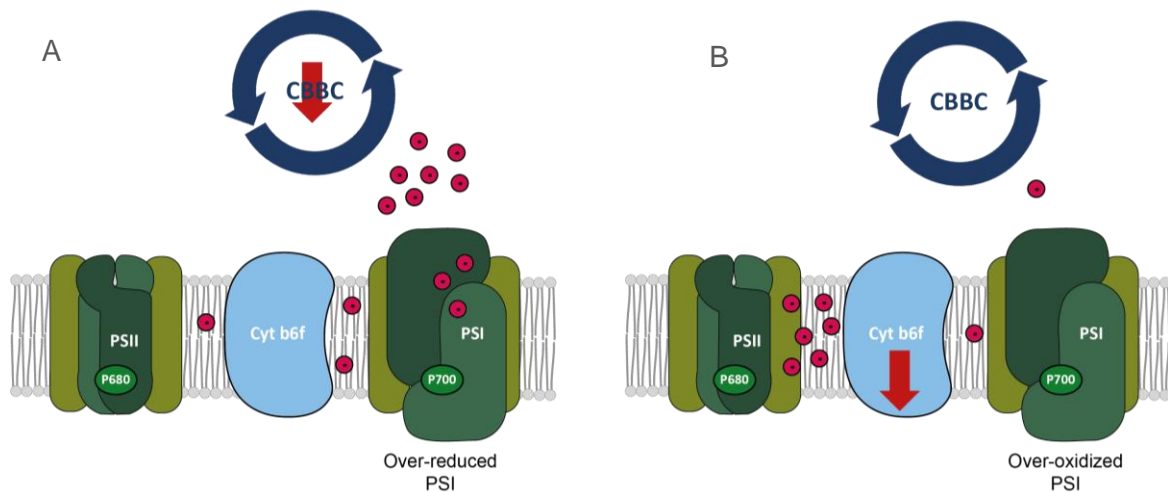


Figure 2. Use of P700 redox state to localize perturbations in the plastid electron transfer chain

Graphical representations of two possible scenarios of altered plastid electron transfer chain. A) depicts a situation where the bottleneck in the transfer of electron is placed downstream of PSI, specifically at the level of the CBBC. Due to the lowered capacity of the CBBC to consume the redox potential generated by PSI (NADPH), the photosystem will be limited on its electron acceptor side resulting in an over-reduction. B) depicts a situation where the bottleneck in the transfer of electron is placed upstream of PSI, in this example at the level of the cytochrome b6f. The impaired income of electron to the donor side of PSI will result in an over oxidation of the photosystem. The relative level of reduction of PSI can be determined exploiting its absorbance at 705nm, dependent on the redox state, hence allowing a finer localisation of electron transfer defects.



the reductive potential generated by the thylakoid (Fig.2B). To evaluate the redox state of PSI, it is possible to exploit the spectral properties of this complex, in particular its variable absorbance at 700 nm, absorbance that increases with increasing reduction level.

The possibility of large-scale characterization of the photosynthetic capacity of a high number of cell lines is a useful tool for the identification of regulators of plastid activity. Such a screening strategy has been developed on a variety of unicellular algae (Niyogi et al., 1997; Ozaki et al., 2007) and, recently, also on the *Eustigmatophyceae* (*Stramenopila*) *Nannochloropsis gaditana* (Perin et al., 2015). Large-scale screenings of this kind can be applied for a forward genetics strategy, in order to identify mutants of photosynthetic capacity generated by random mutagenesis and subsequently determine the gene associated with these alterations. Equally, large-scale screenings can be also applied to a reverse genetics strategy, for testing whether one or more genes of interest, obliterated by targeted mutagenesis, influence plastid activity. In addition, such analysis allows a measurement of PSII activity in a non-invasive way. As seen, the chlorophyll fluorescence of PSII provides an overview of the global activity

of the electron transfer chain and the metabolic processes that depend on them downstream. Consequently, its analysis is an extremely useful tool for a preliminary identification of lines mutated in genes involved in any of the various photosynthesis-dependent physiological processes.

As reported below, through the application of a set of these biophysical techniques I was able to pursue a characterization of alterations in photosynthetic physiology in cell lines containing a bHLH-PAS bHLH2 protein silencing construct. Although not yet conclusive due to the difficulty of obtaining a stable and significant reduction of bHLH2 expression in these lines, these analyses seem to suggest that this protein may play a role in the regulation of plastid activity in *P. tricornutum*. If the results are confirmed on KO lines for bHLH2 (analyses are currently in progress), this would be a first characterization of a bHLH-PAS protein as a modulator of photosynthesis. Given the absence of proteins with a similar architecture in *Archaeplastida*, this could open new perspectives on the study of regulation of plastid activity in secondary endosymbionts.

# Methods

## Generation of bHLH RNAi lines

The selection of genes encoding for putative bHLH family transcription factors was performed following the initial prediction reported in (Rayko et al., 2010) and re-annotation on the new version of *P. tricornutum* genome (“Phaeodactylum\_tricornutum - Ensembl Genomes 52,”). The list of the seven identified genes is shown in Table 1 along with their associated Phatr3 accession numbers. Transgenic and control lines of *P. tricornutum* used for bHLH2 have a Pt1 8.6; CCMP2561 genomic background. Lines targeted for gene silencing were generated following the protocol reported in (De Riso et al., 2009). Diatom cells were transformed by biolistic

bombardment (Falciatore et al., 1999) with a linear construct containing an anti-sense fragment of the target genes transcriptionally fused downstream of a *Sh ble* cassette conferring resistance to phleomycin (pKS-Sh ble-FA vector, (De Riso et al., 2009; Siaut et al., 2007)). Anti-sense fragments targeting sequences (~200bp) specific to each bHLH (coding sequence or transcribed regulatory UTR regions) were generated via PCR using the primers listed in Table 1 and cloned in the pKS-Sh ble-FA vector via EcoRI and StuI digestion. The expression of the *Sh ble* - antisense sequence construct was regulated via the constitutive *HA* promoter and the *FcpA* terminator. After transformation, transgenic lines expressing the antisense fragments were selected and maintained on F/2 media (Guillard, 1975) added with 1% agarose, in the presence of the selective phleomycin antibiotic.

Target gene	Accession	Primer name	5' to 3' sequence	Pairing length
bHLH1a (RITMO1)	Phatr3_J44962	bHLH1a_3	TCCCAGCCAAAGTCGAGGTAGCTCGCCTTTGCTCAATATTCAACCATC	23
		bHLH1a_4	ACGGCGGCCACGGGTCCGAGGCCTGAAGTGTACAGCCACGTTGGTA	22
bHLH1b	Phatr3_J44963	bHLH1b_3	TCCCAGCCAAAGTCGAGGTAGCTCGCACGTGAAGAGCTAATGAATGC	22
		bHLH1b_4	ACGGCGGCCACGGGTCCGAGGCCTTGAAGTTGCTTTTGATTCTT	22
bHLH2	Phatr3_J54435	bHLH2_3	TCCCAGCCAAAGTCGAGGTAGCTCGGTTCCAGCCAGCTATCGAGCTAT	22
		bHLH2_4	ACGGCGGCCACGGGTCCGAGGCCTAATATCAGTACGGTCCCCATT	22
bHLH3	Phatr3_J42586	bHLH3_3	TCCCAGCCAAAGTCGAGGTAGCTCGATGAGACAAGCCACAACAATGATAG	25
		bHLH3_4	ACGGCGGCCACGGGTCCGAGGCCTGCTAGTGATTTAGTGCGACTGTCTC	25
bHLH4	Phatr3_J31578	bHLH4_3	TCCCAGCCAAAGTCGAGGTAGCTCGACCATTTTCGGGAGGTAACAAT	22
		bHLH4_4	ACGGCGGCCACGGGTCCGAGGCCTCCGAATAATATGGAACGGAATG	22
bHLH5	Phatr3_J43365	bHLH5_3	TCCCAGCCAAAGTCGAGGTAGCTCGATGGGTCGATTTCTCAATGAAC	22
		bHLH5_4	ACGGCGGCCACGGGTCCGAGGCCTGTTGGTGATACGCACTTTCTGA	22
bHLH6	Phatr3_J48817	bHLH6_3	TCCCAGCCAAAGTCGAGGTAGCTCGACTTCCGTCGAAGAGATTGAG	22
		bHLH6_4	ACGGCGGCCACGGGTCCGAGGCCTGTGACTGTGCGTGAGGTAGTGT	22

Table. 1 Primers used for the construction of the RNAi cassettes

The table reports the primers used for amplifying the anti-sense sequences used for targeting *bHLH* genes following de Riso et al., 2009. Common names and Phatr3 accessions are reported for each targeted gene. Red and green letters highlight the common sequences of forward and reverse primers respectively used for cloning in the pKS-Sh ble-FA vector following de Riso et al., 2009. Black letters refer to the target specific sequence of the primers.

## On plate colony screening

Pre-screening of lines containing a construct for RNAi of each bHLH gene was performed by adapting to *P. tricornutum* the procedure developed on the alga *Nannochloropsis gaditana* by (Perin et al., 2015). Briefly, lines transformed with RNAi constructs and exhibiting phleomycin

resistance were grown in liquid culture and maintained under exponential growth phase. Following optical density analysis at 750nm, aliquots of the different cultures were diluted to equalize their optical density to OD=0.2 and equal volumes were spotted onto plates of F/2 (Guillard, 1975) supplemented with 1% agarose. Colonies were subsequently grown under continuous light at an irradiation intensity of 30  $\mu\text{mol photons m}^{-2} \text{s}^{-1}$ . The effect

of insertion of transformation cassettes was analyzed by taking into account two parameters. First, colony growth capacity was calculated by checking the change in basal chlorophyll fluorescence in cells adapted for 20 minutes in the dark ( $F_0$ ) and normalized for colony surface area. The variation of  $F_0$ /surface was followed over five days from the time of spotting on plate. Second, the maximum quantum yield of Photosystem II (PSII) was calculated by testing the ratio of the difference between chlorophyll fluorescence following exposure to a light-saturating pulse ( $F_m$ ) minus the basal fluorescence of dark-adapted cells ( $F_0$ ) divided by  $F_m$  (Maxwell and Johnson, 2000). This parameter allows us to obtain a rapid estimate of the maximum photosynthetic capacity over a large number of colonies. *In vivo* fluorescence analysis on colonies was performed using a FluorCam FC 800 video-imaging apparatus (Photon Systems Instruments), which allows a normalization of fluorescence signal over the surface of the colony.

## Liquid culture and irradiation conditions

Cells were grown in batch culture in F/2 Guillard media. Liquid cultures were grown and maintained at 18°C in a Standard Growth Chamber SGC120 (Weiss Gallenkamp™). Illumination was performed with white light Master TL90 36W/950 neon lamps (Philips™). Experiments were performed in constant light, if not specified otherwise. Cell concentrations were measured using a Z2 Coulter Particle Count and Size Analyser (Beckman Coulter). Minimal and maximal size thresholds were set to 3 µm and 11 µm. Growth rates were calculated in exponential phase of growth over four days and expressed as the average number of divisions per day over the experiment. The formula used is  $division\ per\ day = \frac{\ln(c_4) - \ln(c_0)}{(4 * \ln(2))}$ , where  $c_0$  and  $c_4$  represent the culture concentrations at day 0

and day 4. For experiments involving treatment with 3-(3,4-dichlorophenyl)-1,1-dimethylurea (DCMU), cultures in exponential growth phase were dark adapted for 50 hours and transferred to 30 µmol photons  $m^{-2}s^{-1}$  for 4 hours in presence of a 1000X dilution of DCMU ethanol solution (final concentration of 2µM). DCMU was added 10 minutes before the transfer to light in order to ensure its full penetration in the cells. Control replicates were treated with an equal amount of pure ethanol to exclude solvent dependent effects on photosynthesis.

## ΦPSII analysis via chlorophyll fluorescence in liquid cultures

All fluorescence analyses were performed on cultures grown in liquid F/2 media and sampled during exponential growth. To measure PSII maximal quantum yield, 10ml of biological replicate cultures (~ $10^6$  cells  $ml^{-1}$ ) were centrifuged at 2500 rpm for 15 minutes to be concentrated ten times in their own supernatant. Concentrated cells were adapted to dim light for 20 minutes to induce complete relaxation of PSII reaction centers. Fluorescence analysis was conducted using a Paradigme Camera Speedzen system (Beambio). Measuring light and actinic saturating flash were provided by blue and green LEDs, respectively. Saturating flash corresponded to 250ms of 2,000 µmol photons  $m^{-2}s^{-1}$ . Chlorophyll fluorescence was detected through a low-pass filter at wavelength >700 nm. Experiments demanding the analysis of ΦPSII upon light irradiation were performed with an in-house spectrofluorometer allowing irradiation of the samples in the analysis chamber and using green LEDs for both detection and saturating pulses. qE calculations presented in Fig.10C were realized considering cells at the end of the relaxation kinetics as completely relaxed (qE=0). qE was therefore calculated as equal to  $(F_m' - F_m)/F_m$ , where  $F_m$  is the maximal

fluorescence induced by the last saturating pulse.

## relative Electron Transfer Rate

Three biological replicates were adapted to continuous light (30  $\mu\text{mol photons m}^{-2} \text{s}^{-1}$  or 200  $\mu\text{mol photons m}^{-2} \text{s}^{-1}$ ). Analysis was performed on cultures in the exponential growth phase (1 to  $2 \times 10^6$  cells  $\text{ml}^{-1}$ ). Concentrated cultures were left under dim light in order to allow full relaxation of PSII before analysis. Samples were then exposed to increasing intensity steps of actinic light to obtain the saturation light curves. Each light step lasted at least five minutes until full adaptation of the photosynthetic apparatus to the irradiation level. Illumination was performed with green LED lights. At the end of each light step, chlorophyll fluorescence was measured with a blue light measuring pulse and a 250 ms green light saturating pulse was used to induce PSII maximal fluorescence in the light ( $F_m'$ ). Fluorescence of light adapted PSII ( $F_s$ ) was measured just prior to saturating light application. PSII quantum yield  $\Phi_{\text{PSII}}$  was calculated as  $(F_m' - F_s) / F_m'$  (Maxwell and Johnson, 2000). For each light step, the relative Electron Transfer Rate through the photosynthetic chain (rETR) was calculated as  $\Phi_{\text{PSII}} \times \text{Light intensity}$ . The light saturation curve resulting from plotting rETR as a function of light intensity was fitted to a double exponential decay function following (Platt et al., 1980; Ralph and Gademann, 2005). Fitting was performed via Origin software version 9.1 to the function 
$$\text{ETR} = \text{ETR}_{\text{max}} * \left(1 - e^{(-\alpha E / \text{ETR}_{\text{max}})}\right) * \left(e^{(-\beta E / \text{ETR}_{\text{max}})}\right)$$

## Evaluation of PSI redox state

The redox state of the PSI donor was calculated as the difference between the absorption kinetic at 705 nm similarly to (Long et al., 2021). Analysis was performed on cells adapted to continuous 5  $\mu\text{mol photons m}^{-2} \text{s}^{-1}$  for two weeks and after one day of exposure

to 200  $\mu\text{mol photons m}^{-2} \text{s}^{-1}$ . Properties of PSI were calculated from the measurements of the absorption changes in the dark and in the light-adapted condition. PSI redox state was estimated upon increasing light intensity steps to which samples were adapted for 20 minutes to assure stationary activity of photosynthetic chain. Absorption changes at 735 nm were also calculated to eliminate spectral contributions due to diffusion and other thylakoid complexes. As a control of the maximal possible oxidation state of PSI, cells were treated with a saturating dose of DCMU and subject to a saturating pulse of light to obtain the  $P_{\text{max}}$  value. All data were normalized to  $P_{\text{max}} - P_0$  (full oxidation - maximal reduction states). Analysis was performed on a Joliot-type spectrophotometer (JTS-10, Biologic, Grenoble, France).

## Lincomycin treatment

Photoinhibition analysis via lincomycin treatment was performed following Lavaud et al., 2016. Cultures were preadapted in continuous light at 5  $\mu\text{mol photons m}^{-2} \text{s}^{-1}$  for two weeks. Three biological replicates were treated with a saturating dose of inhibitor (500  $\mu\text{g ml}^{-1}$ ) and left 10 minutes under low light ( $\ll 5 \mu\text{mol photons m}^{-2} \text{s}^{-1}$ ) to allow full penetration of the compound. Cultures were subsequently exposed to 500  $\mu\text{mol photons m}^{-2} \text{s}^{-1}$  for sixty minutes to induce photoinhibition of D1 protein and then moved to 10  $\mu\text{mol photons m}^{-2} \text{s}^{-1}$  to allow relaxation of the residual non photodamaged PSII centers. Cultures aliquots were sampled periodically to determine  $\Phi_{\text{PSII}}$  using the in-house spectrofluorometer.

## RNA extraction and RT-qPCR analysis

For RNA purification,  $10^8$  cells from exponential growth cultures ( $\sim 10^6$  cells  $\text{ml}^{-1}$ ) were filtered onto Whatman filter 589/2. Filters were then washed with 25 mL of PBS

IX, cut in two to have technical replicates, flash frozen in liquid nitrogen and stored at -80°C. RNA was extracted with TriPure Isolation Reagent (Roche) following the protocol provided by the company and further purified by an ammonium acetate precipitation. RNA purity and integrity were checked on samples by the 260nm/230nm and 260nm/280nm OD ratios and by gel electrophoresis. 500ng of RNA were retro-transcribed via an oligo-dT and random primers mix using the QuantiTect Reverse Transcription Kit (Quiagen). For RT-qPCR,

ribosomal protein small subunit 30S (RPS) and TATA box Binding Protein (TBP) were used as reference genes (Siaut et al., 2007). For each sample, geometric mean of Ct was used as reference to evaluate the expression of genes of interest via the  $\Delta\Delta C_t$  Livak method (Livak and Schmittgen, 2001). Expression data was normalized against the average Wt expression value. All RT-qPCR analyses were performed on two biological replicates obtained in distinct experiments. TBP, RPS and bHLH2 primers used for RT-qPCR analysis are listed in Table 2.

Target gene	Accession	Primer name	Strand	Sequence	Type
TBP	Phatr3_J10199	TBP_Fw	Fw	ACCGGAGTCAAGAGCACACAC	RT-qPCR
		TBP_Rv	Rv	CGGAATGCGCGTATACCAGT	RT-qPCR
RPS	Phatr3_J10847	RPS_Fw	Fw	CGAAGTCAACCAGGAAACCAA	RT-qPCR
		RPS_Rv	Rv	GTGCAAGAGACCGGACATACC	RT-qPCR
RITMO1	Phatr3_J44962	RITMO1_total_Fw	Fw	ATTCTTGGTCCCACCCGGTA	RT-qPCR
		RITMO1_total_Rv	Rv	ACGCCACATTGAAAACCGAG	RT-qPCR
bHLH2	Phatr3_J54435	bHLH2_Fw	Fw	GCAAGGGAAGGGCTCAAAG	RT-qPCR
		bHLH2_Rv	Rv	GCTGCTGGAGAATGCGAATG	RT-qPCR
		bHLH2_Seq	Fw	CAAGGCGCTCATCAGTTCTC	sequencing

Table 2. List of the oligonucleotides used in this work.

Target gene, name, pairing strand, sequence and use of the oligonucleotides used in this work.

## Subcellular localization prediction

bHLH2 protein sequence was scanned with multiple online tools for subcellular localization prediction. HECTAR (Gschloessl et al., 2008) and ASAFind (Gruber et al., 2015) tools were used to search for the heterokont specific signal peptide and ASAFAP plastid localisation sequences (Kilian and Kroth, 2004). DeepLoc (Almagro Armenteros et al., 2017), NucPred (Bramciari et al., 2007), WoLF PSORT (Horton et al., 2007), LOCALISER (Sperschneider et al., 2017), SeqNLS (Lin and Hu, 2013) and NLStradamus (Nguyen Ba et al., 2009) were used for additional subcellular localisation

prediction and to search for Nuclear Localization amino acid Sequence (NLS).

## Generation of bHLH2 Knock-Out (KO) strains

*bHLH2* KO mutants were generated by biolistic delivery of the CRISPR/Cas9 ribonucleoproteins according to (Serif et al., 2018). Selection of transformed lines with the riboprotein complex was accomplished by co-targeting the APT gene (Phatr3\_J6834) to induce resistance to 2-fluoroadenine (2-FA). Wt cells were co-transformed with a total of 4 sgRNA, two for each gene (Table 3). 2-FA resistant lines were screened via Sanger sequencing (primer reported in Table 2).

Target gene	Accession	gRNA name	Strand	Sequence	3' PAM
APT	Phatr3_J6834	APTg1	Rv	AAGCGTGAATGCCTTTGAA	GGG
		APTg3	Fw	CCTGGGTCCACCAATTGCC	TGG
bHLH2	Phatr3_J54435	Guide_bHLH2_59	Rv	TACGTTAAGCGTAAGTGTGT	CGG
		Guide_bHLH2_135	Fw	GATAGCGGGAGCTCGAACCG	CGG

Table 3. gRNAs used for *bHLH2* KOs generation

List of the sgRNA used for CRISPR-Cas9 mutagenesis. Target gene, sgRNA name, target strand, gRNA sequence and the associated protospacer adjacent motif (PAM) are reported.

# Results and Discussion

## Generation of RNAi transgenic lines targeting bHLH genes

Perin et al., 2015, recently developed a protocol for screening photosynthesis mutants based on chlorophyll fluorescence in the *eustigmatophyceae* *Nannochloropsis gaditana*. This protocol represents the first application of such screening on algae of the *Stramenopila* group. The screening was performed on cultures grown on solid medium, with the advantage of allowing the analysis of several strains in parallel in a more compact set up than would be provided by an analysis of cultures in liquid. In order to generate colonies with a sufficiently large surface (and hence a sufficiently large signal) to allow fluorescence analysis, small amounts of liquid culture were spotted on agar plates. The possibility to characterize multiple cell lines at once also allows a direct comparison of chlorophyll fluorescence in the same experiment, hence uniforming results. To date, such a screening strategy has not yet been proposed for the study of diatoms. To test the applicability of this screening strategy to *P. tricornutum*, model used for the study of photosynthetic processes in diatoms, a characterization of a collection of transgenic lines containing a construct for RNA interference of the bHLH transcription factors of this alga was performed. The choice was motivated by the number of transcription factors belonging to this family (seven in total, shown in Table 1), thus allowing a preliminary evaluation of the screening method on a reduced number of target genes. A total of 159 phleomycin-resistant transgenic lines containing bHLH gene-specific RNAi constructs were generated, distributed among

the various bHLH factors as shown in Table 2. For each bHLH gene, one single RNAi antisense construct was used. The on-plate characterization of these lines was performed in collaboration with the laboratory of Plant Biology at the University of Padua, Italy where the screening strategy was originally developed on *N. gaditana* (Perin et al., 2015). Fig.3 shows an example of the fluorescence profiles of Wt lines and RNAi lines. The results of chlorophyll fluorescence analysis for the study of growth capacity and maximum PSII quantum yield of the mutant lines grown on agar plates are summarized in Table 4. The on-plate analysis was performed on plates without antibiotic. This exploratory plate screening revealed a relevant number of clones (between 10 and 20%) exhibiting alteration in growth or photosynthetic capacity compared with Wt lines for four of the bHLH genes. These included the three bHLH-PAS genes among which bHLH2 presented the highest percentage of altered lines at the level of on plate growth (20%, equal to 5 lines out of the 25 present). Cultures on agar does not represent the natural condition for *P. tricornutum* growth and consequently the physiological alterations observed may be independent of transformation with RNAi constructs. Therefore, a similar analysis of

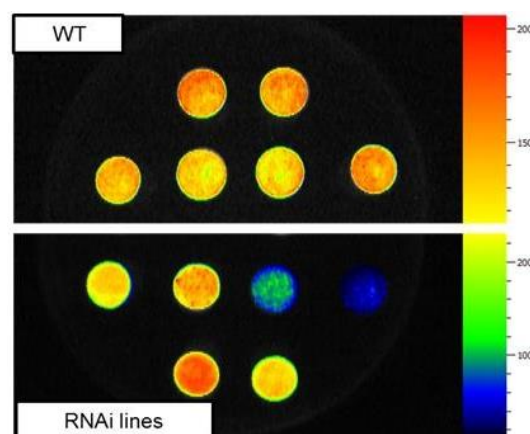


Figure 3. Screening on plate based on chlorophyll fluorescence

Representative  $F_0$  fluorescence results for *Wt* (top) and RNAi strains (bottom), spotted on plate at the same cellular concentration and analysed after 5 days of growth. Fluorescence signals are detected with a FluorCam FC 800 video-imaging apparatus (Photon Systems Instruments, Brno, Czech Republic).

		Number of clones	Clones affected in growth	Clones affected in Fv/Fm	% of clones affected
bHLH1a	Phatr3_J44962	22	2	0	9
bHLH1b	Phatr3_J44963	36	3	2	14
bHLH2	Phatr3_J54435	25	5	0	20
bHLH3	Phatr3_J42586	37	1	0	3
bHLH4	Phatr3_J31578	7	0	0	0
bHLH5	Phatr3_J43365	1	0	0	0
bHLH6	Phatr3_J48817	31	2	2	13

Table 4. Summary results of on plate screening.

The table reports the number of *P. tricornutum* phleomycin resistant clones obtained after transformation with RNAi constructs for each of the *bHLH* genes. A total of 159 resistant colonies were analysed. The number of colonies showing a significant reduction of growth (calculated as the variation of Fo/surface over five days) and of PSII maximal quantum yield Fv/Fm is reported, as well as the percentage of lines showing a phenotypic alteration for each gene.

maximum photosynthetic capacity on agar-grown cultures was performed on 208 independent transformation control lines containing only phleomycin resistance. As presented in Fig.4, these lines exhibit high scatter in Fv/Fm values, suggesting that the level of noise associated with chlorophyll fluorescence measurements on *P. tricornutum* cultures grown on solid medium makes identification of mutant lines difficult. Given that on-plate analysis were performed in absence of antibiotics, such a level of noisiness of photosynthetic parameters can be due either to the transformation process or to the growth on agar medium.

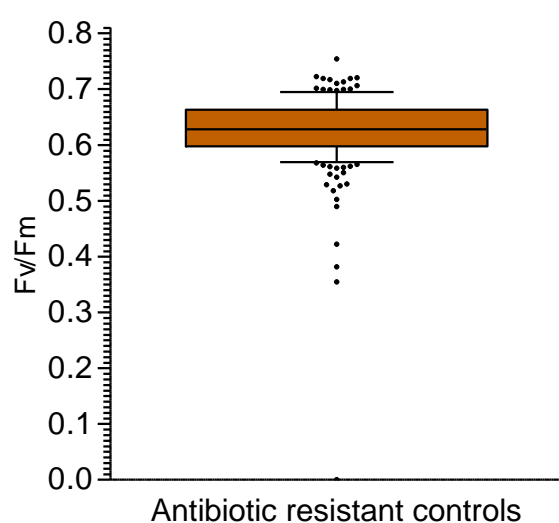


Figure 4. On plate screening of phleomycin resistant control

Fv/Fm of 208 independent phleomycin resistant control lines grown on plate. Box plot reports the first, second and third quartile. Whiskers represent the 10<sup>th</sup> and 90<sup>th</sup> percentiles. Black dots report the values of cultures above and below 10<sup>th</sup> and 90<sup>th</sup> percentiles. Mean and s.d. values for the 208 samples are equal to 0.634 and 0.130 respectively.

To verify whether similar alterations are also found under optimal growth conditions for *P. tricornutum* and to eliminate false positives, subsequent characterization of photosynthetic parameters was repeated on a limited set of independent RNAi lines grown in liquid medium. Given the interest in the laboratory in bHLH-PAS family proteins, these additional investigations were conducted on transgenic lines containing constructs for RITMO1, bHLH1b, and bHLH2 RNAi.

### *bHLH2* RNAi lines are affected in photosynthetic capacity in a light intensity dependent way

Characterization of the photosynthetic capacity of lines containing antisense constructs for bHLH-PAS proteins was performed in cells grown under continuous light, in continuity with the growth conditions used for plate colonies. In order to increase the detectability of any alteration of the photosynthetic capacity in the transgenic lines, the irradiation intensity was in this case increased to 200  $\mu\text{mol photons m}^{-2} \text{s}^{-1}$ . This light intensity is not to be considered stressful for Wt cells of *P. tricornutum* with unaltered

non-photochemical quenching (Lavaud and Goss, 2014; Lepetit et al., 2013; Taddei et al., 2016). However, this intensity is strong enough to saturate photosynthetic activity and would hence sensitize for eventual defects. A transgenic line transformed only with the phleomycin resistance cassette and hereafter named Resistance Control RC1 was used to exclude possible effects of the biolistic transformation and antibiotic resistance on photosynthetic physiology. Maximum quantum yield of PSII, Fv/Fm, was used as an indicator of the overall photosynthetic capacity of the lines under study. This analysis revealed that none of the lines containing the antisense construct targeting for *RITMO1* or for *bHLH1b* present a significant reduction in Fv/Fm compared with the Wt line or the control for phleomycin resistance (Fig.5A). Analysis of a subset of *RITMO1* RNAi lines reveals a reduction in the expression of this gene, suggesting that deregulation of its transcription levels does not bring alterations in maximal photosynthetic activity (Fig.5B). In contrast, three of the four lines presenting the antisense construct targeted against *bHLH2* (KD2.1, KD2.3, KD2.4) showed a significant reduction in the maximal quantum yield of PSII, ranging from 14% to 21% reduction compared with control lines (Fig.5A).

An alteration of photosynthetic efficiency as the one described can be expected to impact cellular growth and,

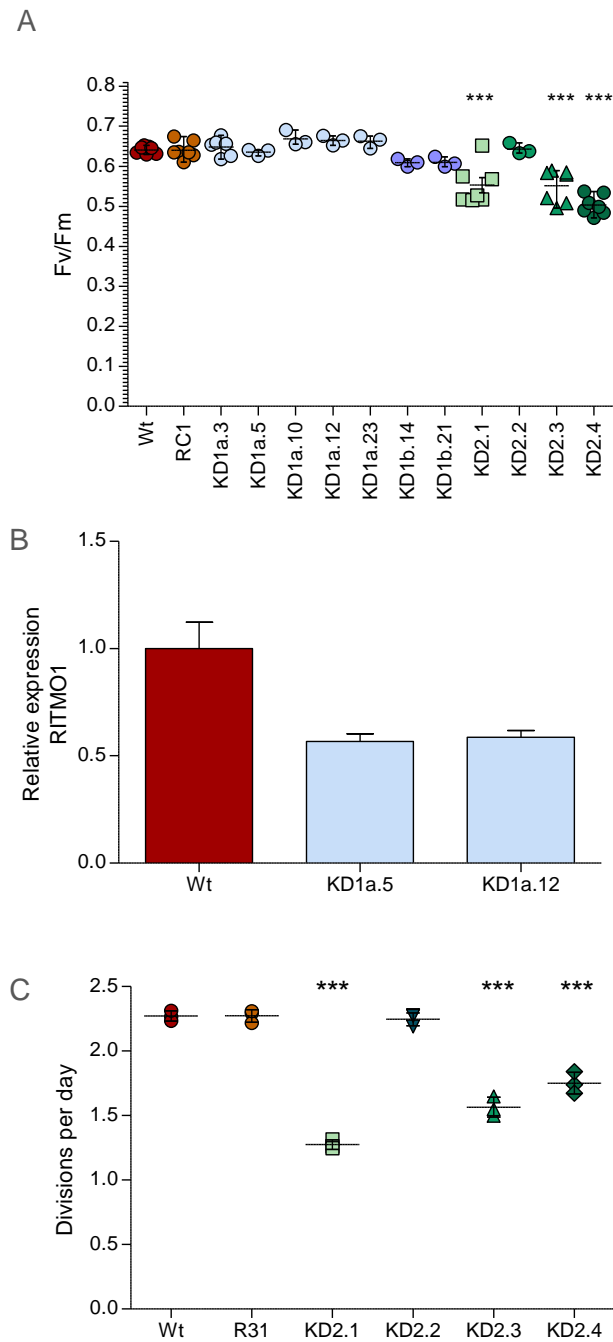


**Figure 5. bHLH2 lines are affected in photosynthesis and growth**

A) Wt, RC1 cells and transgenic lines containing RNAi constructs targeting the three different bHLH-PAS genes of *P. tricornutum* were grown under continuous 200  $\mu\text{mol photons m}^{-2} \text{s}^{-1}$  to test possible alterations of PSII maximal quantum yield (Fv/Fm). KD1a: RNAi lines for *RITMO1*; KD1b: RNAi lines for *bHLH1b*; KD2: RNAi lines for *bHLH2* ( $n \geq 3$ , mean  $\pm$  s.e.m., P-values obtained via One-way analysis of variance against Wt with Bonferroni post-test correction are shown as \*\*\* $P < 0.001$ ). B) Expression of RITMO1 KD1a.5 and KD1.12 RNAi lines ( $n=2$ , mean  $\pm$  s.e.m.). Cells were grown under 12L:12D at 30  $\mu\text{mol photons m}^{-2} \text{s}^{-1}$  and collected at ZT7. Expression values are normalized to the mean expression of Wt strain. C) Effect of bHLH2 RNAi construct on growth under 200  $\mu\text{mol photons m}^{-2} \text{s}^{-1}$ . Growth capacity of Wt, RC1 and bHLH2 RNAi lines grown under continuous 200  $\mu\text{mol photons m}^{-2} \text{s}^{-1}$ . Growth capacity was calculated on exponential growth cultures and is expressed as average number of divisions per day over four days. ( $n=3$ , mean  $\pm$  s.e.m., P-values obtained via One-way analysis of variance against Wt with Bonferroni post-test correction are shown as \*\*\* $P < 0.001$ )

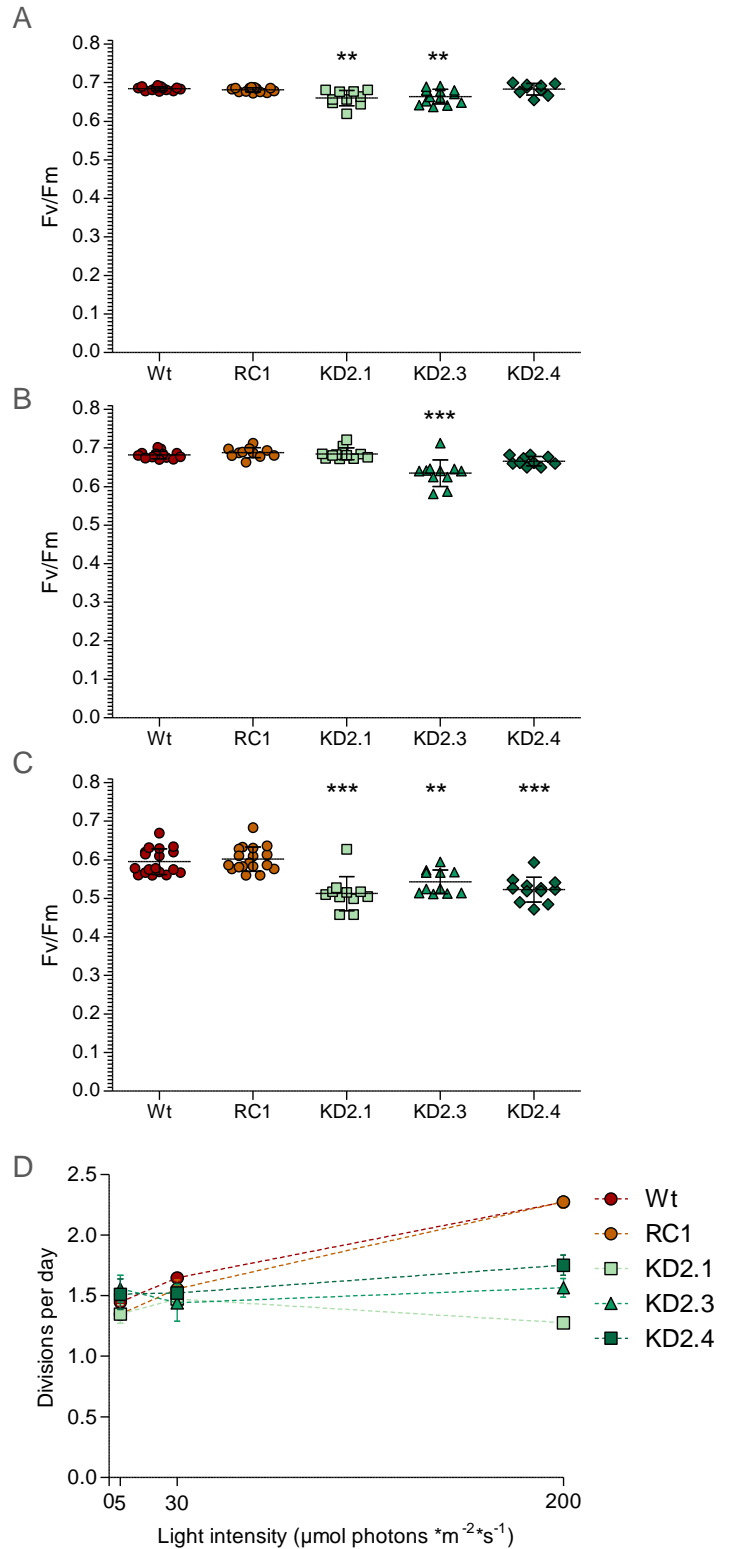


Figure 6. Effects of light intensity on Fv/Fm and growth in *bHLH2* RNAi lines

Wt, RC1, KD2.1 KD2.3 and KD2.4 lines were grown in liquid media under continuous 5  $\mu\text{mol photons m}^{-2} \text{s}^{-1}$  (A), 30  $\mu\text{mol photons m}^{-2} \text{s}^{-1}$  (B) or 200  $\mu\text{mol photons m}^{-2} \text{s}^{-1}$  (C) to test PSII maximal quantum yield (Fv/Fm).  $n \geq 10$ , mean  $\pm$  s.e.m., P-values obtained via t One-way analysis of variance against Wt with Bonferroni post-test correction are shown as \*\* $P < 0.01$ , \*\*\* $P < 0.001$ ). D) Growth capacity of Wt, RC1, KD2.1 KD2.3 and KD2.4 RNAi lines grown under continuous the light conditions of panels A-C. Growth capacity was calculated on exponential growth cultures and is expressed as average number of divisions per day over four days ( $n=3$ , mean  $\pm$  s.e.m.).

consequently, the growth capacity of these RNAi cultures. In order to verify this hypothesis, the growth rate of Wt, RC1 control cells and *bHLH2* RNAi lines adapted to continuous light 200  $\mu\text{mol photons m}^{-2} \text{s}^{-1}$  was determined. In a manner comparable to that shown at the maximal quantum yield level of PSII, the KD2.1 KD2.3 and KD2.4 lines are characterized by a significant reduction in growth capacity under these conditions, thus confirming the expected correlation between the reduction of photosynthetic efficiency and growth capacity (Fig.5C). Given the results above, we hence decided to characterize the photosynthetic alterations of the KD2.1 KD2.3 and KD2.4 lines at higher light intensity (400  $\mu\text{mol photons m}^{-2} \text{s}^{-1}$ ) assuming to potentially accentuate the observed phenotypes by imposing a stronger pressure on the thylakoid apparatus. Notably, when transferred to these irradiation conditions, the three transgenic lines showed a total growth arrest, thus making any characterization of photosynthetic capacity impossible.

Such a result suggests that the observed phenotype can be light intensity dependent, with an increase of perturbation of photosynthetic capacity under increasing photon fluency. To test this hypothesis and given the effects observed at 400  $\mu\text{mol photons m}^{-2} \text{s}^{-1}$ , it was decided to test whether the phenotype of the KD2.1 KD2.3 and KD2.4 lines is also visible at lower irradiances, specifically at 5 and 30  $\mu\text{mol photons m}^{-2} \text{s}^{-1}$ . At both intensities, growth capacity and maximal quantum yield of PSII were tested. *bHLH2* RNAi lines KD2.1 KD2.3 and KD2.4 showed a minor reduction in maximal PSII quantum yield when grown under low light in



comparison to the control lines, but these differences became progressively more pronounced when cells were adapted to higher light irradiation (30 and 200  $\mu\text{mol photons s}^{-1} \text{m}^{-2}$  Fig.,6A-C) confirming the light intensity dependent alteration in maximal yield of PSII.

In parallel, growth analysis highlighted that although control lines show a rise in growth speed as light irradiation (and consequently the energy available to power cell metabolism) increases, *bHLH2* RNAi manifest a saturation of growth rate capacity under low light irradiation (Fig.6D) and do not show a similar increase of growth capacity at higher light fluencies. Indeed, Wild-type and RC1 cells went from one and a half division per day at 5  $\mu\text{mol photons s}^{-1} \text{m}^{-2}$  to two and a half divisions per day at 200  $\mu\text{mol photons s}^{-1} \text{m}^{-2}$  (Fig.6D), while mutants impaired to increase their growth rate in response to light intensity and stayed at one and a half division per day even under higher light intensity.

### Effects of antisense RNAi on *bHLH2* transcription

In order to verify the effects of the antisense RNAi construct on the transcription of *bHLH2*, an analysis of the expression of this gene was performed on the KD2.1 KD2.3 and KD2.4 lines grown at the three light intensities of the physiological characterization of photosynthesis in the previous paragraph. As shown in (Fig.7A-C) the expression of *bHLH2* was not significantly altered in any of the three KD lines at 5  $\mu\text{mol photons m}^{-2} \text{s}^{-1}$  and 30  $\mu\text{mol photons m}^{-2} \text{s}^{-1}$ . At 200  $\mu\text{mol photons m}^{-2} \text{s}^{-1}$ , lines KD2.1 and KD2.3 showed a slight but not statistically significant reduction in *bHLH2* transcript content, whereas only KD2.4 manifested a major and significant

reduction (approximately 50% compared to Wt). Overall, this data suggests that although the RNAi construct may lead to a perturbation of the *bHLH2* expression, especially at higher light irradiance under study, no correlation between the phenotypes observed at the level of photosynthetic activity and this deregulation could be globally identified. It is important to note that it has been suggested the existence of two silencing mechanisms in *P. tricomutum*, one based on repression of transcription and

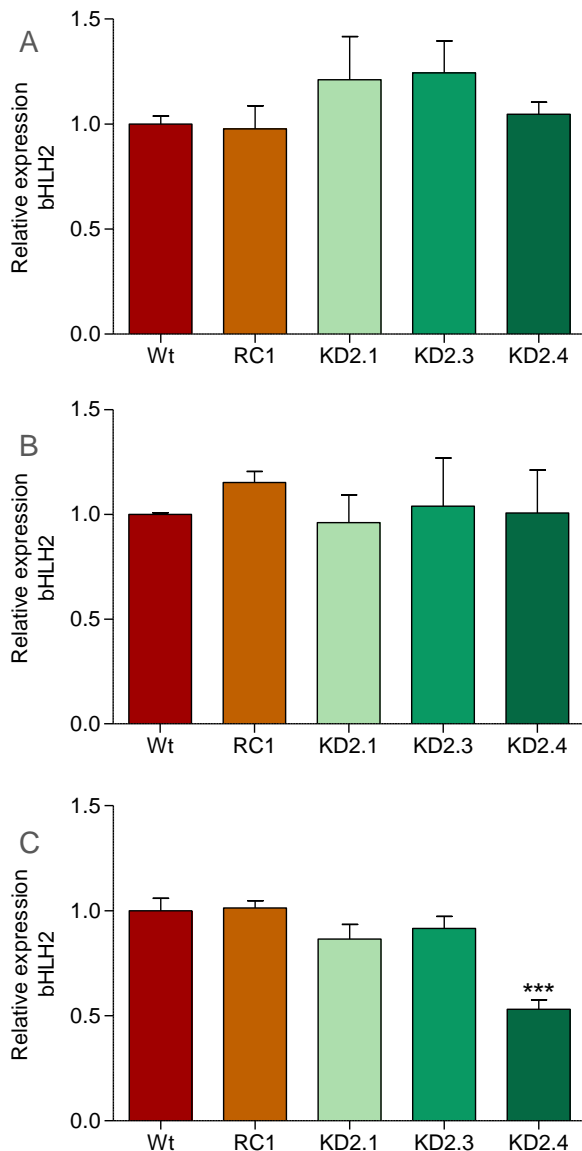


**Figure 7. Gene expression of *bHLH2* under the different continuous light irradiations**  
 Expression of *bHLH2* in Wt, RC1, KD2.1 KD2.3 and KD2.4 RNAi lines grown under continuous light at 5  $\mu\text{mol photons m}^{-2} \text{s}^{-1}$  (A n=3, mean  $\pm$  s.e.m.), 30  $\mu\text{mol photons m}^{-2} \text{s}^{-1}$  (B n=4, mean  $\pm$  s.e.m.) or 200  $\mu\text{mol photons m}^{-2} \text{s}^{-1}$  (C, n=3, mean  $\pm$  s.e.m.). Expression values are normalized to the mean expression of Wt strain. P-values obtained via One-way analysis of variance against Wt with Bonferroni post-test correction are shown as \*\*\*P<0.001).

a second based on translational inhibition (De Riso et al., 2009). A reduction in the content of the target protein can therefore occur where there is no visible reduction in the content of the mRNA encoding it (De Riso et al., 2009). On this basis, an in-depth photosynthetic characterization of the KD2.1 KD2.3 and KD2.4 lines was carried out to dissect in detail their alterations at the physiological level. An extensive molecular analysis of *bHLH2* expression patterns was also conducted in parallel and is reported in the paragraphs at the end of the chapter.

### *bHLH2* RNAi lines show a deficit in electron transfer at the thylakoid chain level

In order to characterize in detail the physiology of the KD2.1 KD2.3 and KD2.4 lines, I performed an analysis of their relative electron transport rate (rETR) in cells adapted under 30  $\mu\text{mol photons s}^{-1} \text{m}^{-2}$  and 200  $\mu\text{mol photons s}^{-1} \text{m}^{-2}$ . This parameter represents the rate of electron transport along the thylakoid redox chain as a function of increasing light intensity and it consequently gives an estimate of the efficiency of the photosynthetic apparatus to convert the incident photon flux into downstream chemical energy. As reported in Fig.8A, *bHLH2* RNAi lines adapted under continuous light at 30  $\mu\text{mol photons s}^{-1} \text{m}^{-2}$  showed a similar rETR profile to that of the control lines. Equally, they did not exhibit an alteration of rETR<sub>max</sub> (maximum electron flux along the thylakoid chain under saturating light) and of the E<sub>k</sub> value, which indicates the light intensity at which such saturation of photosynthetic activity theoretically occurs (Table 5). In the case of cells adapted to continuous light at 200  $\mu\text{mol photons s}^{-1} \text{m}^{-2}$ , KD2.1 KD2.3 and KD2.4 lines showed an altered rETR profile compared to control lines, with a lower rETR<sub>max</sub> as well as a saturation of electron transport at lower light values than controls (Fig.8C, Fig.8D and Table 5). In other words, the mutant lines are unable

to adequately exploit the totality of the incident light and consequently cannot sustain a photosynthetic metabolism comparable to that of the controls. In association with the analysis of growth reported in Fig.6D, this phenotype suggests that a bottleneck at the level of thylakoid electron transport results in a metabolic impairment that prevents the cells from sustaining a normal growth under increasing light conditions.

To further characterize this phenotype, the activity of Photosystem I was also tested on cultures grown under the same conditions. This measure was performed by means of a PSI differential absorbance spectroscopy analysis. A preliminary analysis showed that, when exposed to high light, the *bHLH2* KD2.3 RNAi cells present a more oxidized PSI than the control, indicating a deficit in the rate of electrons reaching this Photosystem, while no difference is observed under low light adapted cells (Fig.8E and Fig.8F). This finding suggests that the anomalies of the mutants are located between PSII and PSI. On the contrary, a higher level of reduction of PSI would have suggested a diminished activity of the metabolism downstream of PSI such, *e.g.* at the level of the Calvin-Benson-Bassham cycle. These analyses remain preliminary at this time and will need to be repeated on the remaining transgenic lines to confirm this observation.

### Response of photosynthesis upon transition to high light is affected in *bHLH2* RNAi lines

The light intensity-dependent alterations in photosynthesis described so far have been obtained in cells adapted in continuous light. The lack of a phenotype at the level of cells grown under weak irradiation may have two reasons: alterations in plastid physiology only occur

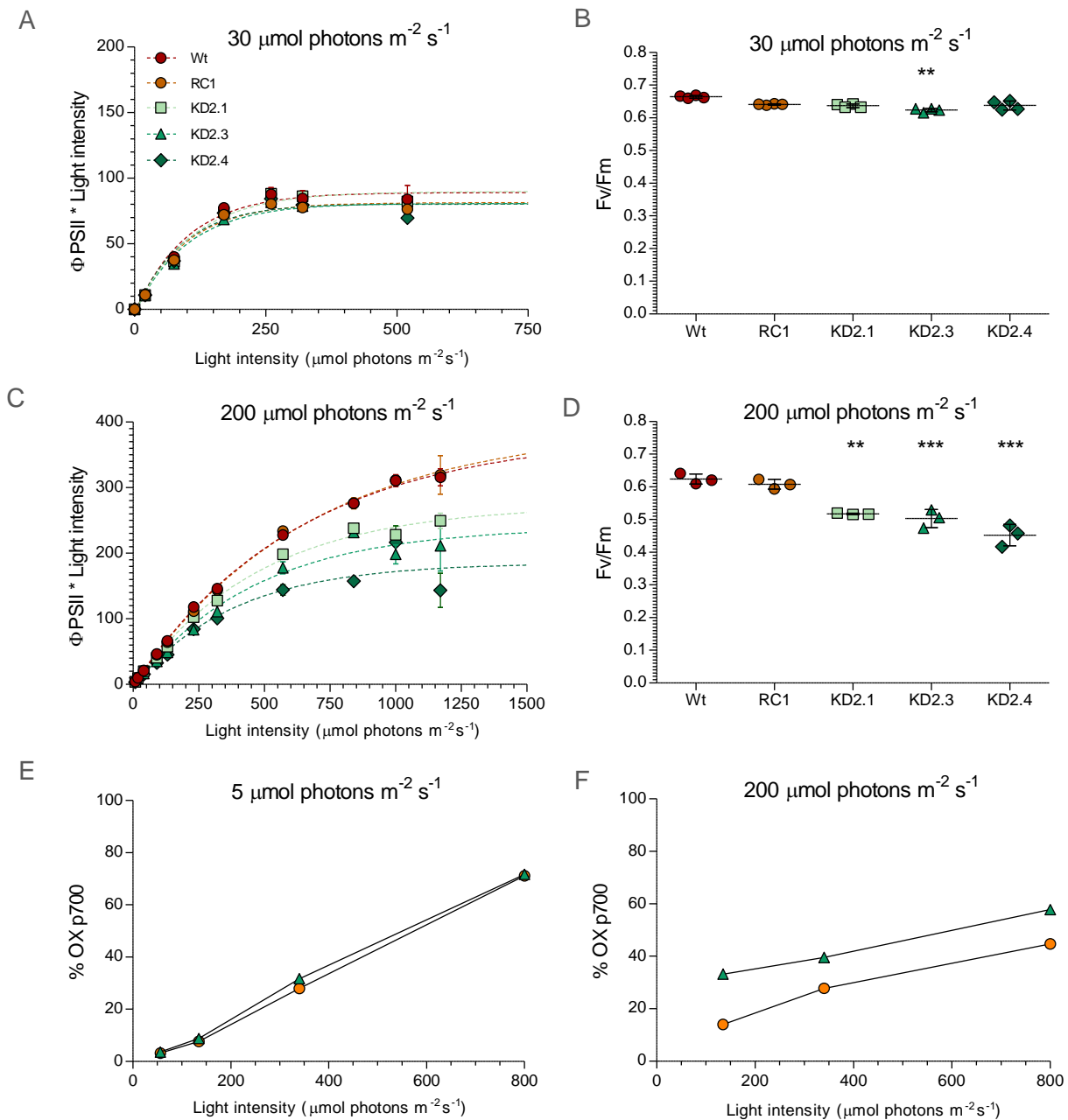


**Figure 8. bHLH2 RNAi lines show a defect in electron transfer located upstream of PSI**

A-D) Wt, RC1, KD2.1, KD2.3 and KD2.4 RNAi lines were grown under continuous light at  $30 \mu\text{mol photons m}^{-2}\text{s}^{-1}$  (A and B,  $n=4$ , mean  $\pm$  s.e.m.) or  $200 \mu\text{mol photons m}^{-2}\text{s}^{-1}$  (C and D,  $n=3$ , mean  $\pm$  s.e.m.). Panels A and C show the mean reETR of the five lines under increasing light intensities after sampling from the growth conditions. Dashed lines represent the double exponential decay fitting to the raw data. Panels B and D report the maximal PSII quantum yield of the replicates of panels A and C at the moment of the analysis. P-values obtained via One-way analysis of variance against Wt with Bonferroni post-test correction are shown as \*\* $P < 0.01$ , \*\*\* $P < 0.001$ ). E-F) PSI is over-oxidised in bHLH2 RNAi line exposed to high light. Representative results of the analysis of PSI redox state performed by differential absorbance analysis at 705nm in control line RC1 and bHLH2 RNAi line KD2.3. Cells grown under  $5 \mu\text{mol photons m}^{-2}\text{s}^{-1}$  (E) or exposed to  $200 \mu\text{mol photons m}^{-2}\text{s}^{-1}$  for one day (F) were used for the analysis. Graphs report the percentage of oxidised PSI under increasing light intensity steps, normalized to the maximal oxidation observed upon treatment with a saturating dose of DCMU that inhibits electron flow downstream of PSII. Higher oxidation of PSI in KD2.3 exposed to  $200 \mu\text{mol photons m}^{-2}\text{s}^{-1}$  locates the defect in electron flow upstream of PSI.

	Wt	RC1	KD2.1	KD2.3	KD2.4
30 $\mu\text{mol photons}$					
rETRmax	89.8 $\pm$ 3	81.9 $\pm$ 2	90.3 $\pm$ 3	81.2 $\pm$ 3	80.6 $\pm$ 4
Ek	106 $\pm$ 4	101 $\pm$ 4	114 $\pm$ 5	106 $\pm$ 6	94 $\pm$ 7
200 $\mu\text{mol photons}$					
rETRmax	386 $\pm$ 5	398 $\pm$ 7	277 $\pm$ 6	247 $\pm$ 10	188 $\pm$ 11
Ek	653 $\pm$ 18	690 $\pm$ 23	496 $\pm$ 23	501 $\pm$ 48	405 $\pm$ 60

under higher photon fluences, whereas at weak irradiations the physiological state is effectively unaltered; a second possibility is that the physiological state of the plastid is affected independently of the growth light intensity and that phenotypes at the level of photosynthetic performance is detected only when the light flux is high enough to be stressful for transgenic strains. In order to clarify this point and to test whether the ability of *bHLH2* RNAi cells to respond to high light is also altered when grown in low light, Wt, RC1, KD2.1, KD2.3 and KD2.4 cultures adapted to 5  $\mu\text{mol photons s}^{-1} \text{m}^{-2}$  were transfected at 200  $\mu\text{mol photons s}^{-1} \text{m}^{-2}$ . Aliquots of the cultures were sampled at 5 and after 20, 60 and 240 minutes from the beginning of the light treatment to characterize their PSII maximal quantum yield. As shown in Fig9, Wt and RC1 lines show a partial reduction of this parameter following the transition, in accordance with what previously observed in (Lavaud et al., 2016) under similar conditions. This reduction reflects the changes in photosynthetic capacity triggered by irradiation change and can be attributed to the establishment of NPQ phenomena functional to dissipate excess radiant energy, including a photo-damage phenomenon of the D1 protein, a photosensitive component of PSII (Campbell and Tyystjärvi, 2012). Compared to control lines, *bHLH2* RNAi

Table 5. Summary results of the RLC analysis

Maximal rETR and light of saturation of the photosynthetic apparatus (Ek) calculated on the curves reported in Fig9 A and C via the Platt equation. n=3, mean  $\pm$  s.e.m.

lines are characterized by an increased sensitivity to transitions from weak to strong light, showing a more pronounced reduction of photosynthetic capacity already in the four hours following light transition (Fig.9A). These results are further matched by the growth curves obtained on cells grown at 5  $\mu\text{mol photons s}^{-1} \text{m}^{-2}$  and transferred to 200  $\mu\text{mol photons s}^{-1} \text{m}^{-2}$  presented in Fig.9B. As shown, *bHLH2* RNAi lines exhibit a major perturbation of growth rate already after the

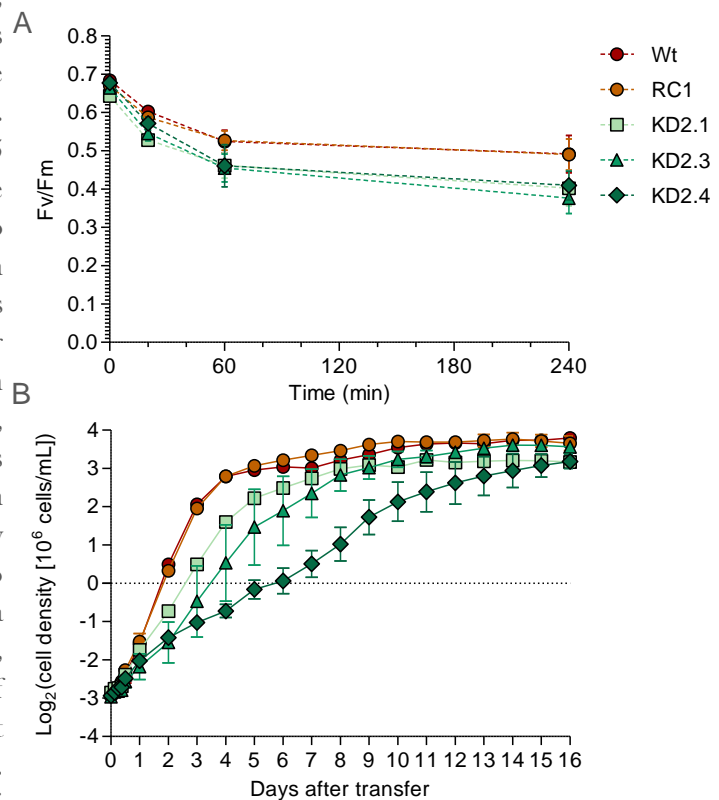


Figure 9. Response to light intensity transition is affected in *bHLH2* RNAi lines

A) Wt, RC1, KD2.1, KD2.3 and KD2.4 RNAi lines were grown under continuous light at 5  $\mu\text{mol photons m}^{-2} \text{s}^{-1}$  and subsequently exposed to 200  $\mu\text{mol photons m}^{-2} \text{s}^{-1}$  for four hours to assess response of PSII maximal quantum yield. Samples were collected before transition (T0) and after 20, 60 and 240 minutes after exposure to high light and their Fv/Fm was evaluated after full relaxation of PSII centers (N=4, mean  $\pm$  s.e.m.). B) Growth profiles of Wt, RC1, KD2.1, KD2.3 lines grown under 5  $\mu\text{mol photons m}^{-2} \text{s}^{-1}$  and subsequently exposed to 200  $\mu\text{mol photons m}^{-2} \text{s}^{-1}$  on day 0 (N=3, mean  $\pm$  s.e.m.).

time of transition to high light and never recover a growth rate comparable to that of controls over the course of the analysis. Overall, these data indicate that plastid physiology is potentially altered already in cells adapted to weak light irradiances in the *bHLH2* RNAi lines and that such perturbations do not build up progressively during the exposition to higher light. An alternative explanation would be that the perturbation of plastid physiology emerges with a quick kinetics upon irradiation with strong light (in the time of few minutes), while cells are still not affected under low light. Our experimental set up does not allow us to discriminate between these two possible scenarios.

### *bHLH2* RNAi lines are not affected in response to photoinhibition

The alterations in photosynthetic activity shown in the previous paragraphs can be caused by increased sensitivity to photoinhibition phenomena, *i.e.* the reduction of photosynthetic efficiency due to light induced damage of D1. To verify this possibility, the *bHLH2* RNAi lines under study grown under  $5 \mu\text{mol photons s}^{-1} \text{m}^{-2}$  were subject to a treatment with  $500 \mu\text{g ml}^{-1}$  of lincomycin, an inhibitor of plastid protein translation (Lavaud et al., 2016), and moved to  $500 \mu\text{mol photons s}^{-1} \text{m}^{-2}$  for inducing photo degradation of D1. Such a treatment allows to highlight the loss of PSII quantum yield in a condition where the damaged D1 cannot be

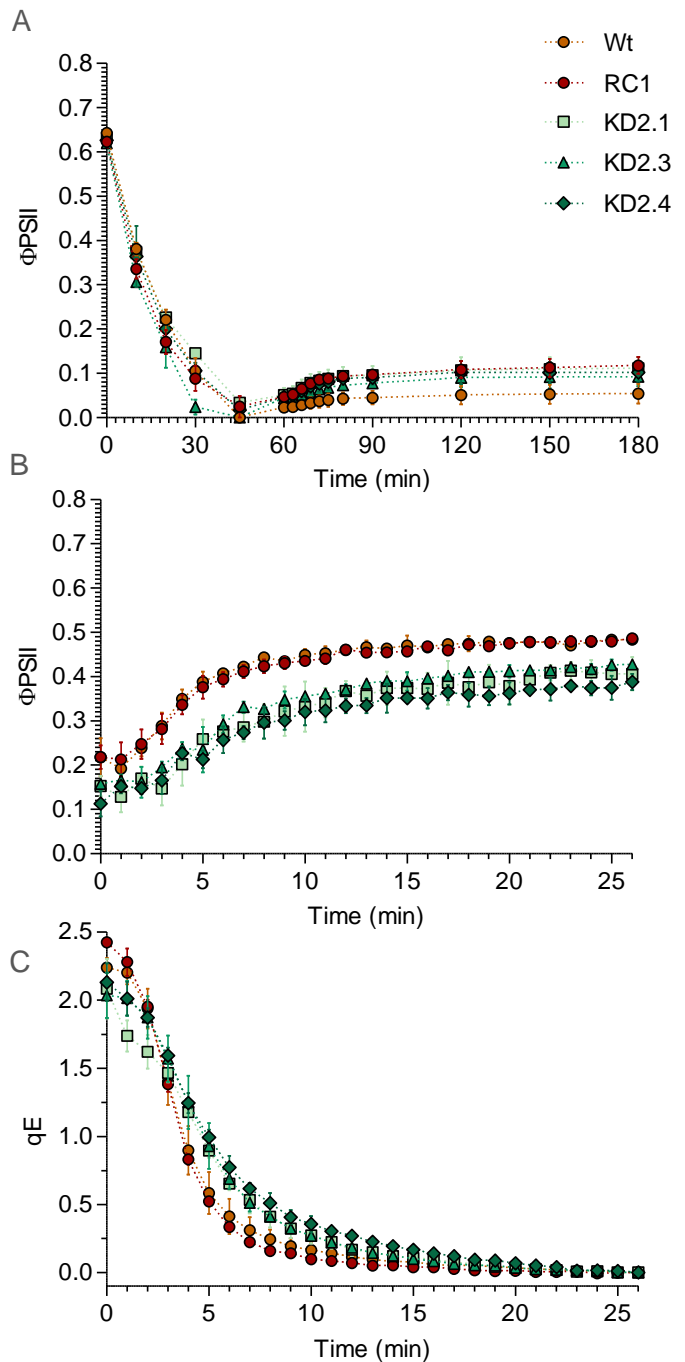


Figure 10. *bHLH2* RNAi lines are not affected in photoinhibition.

A) Wt, RC1, KD2.1 KD2.3 and KD2.4 RNAi lines were grown under continuous light at  $5 \mu\text{mol photons m}^{-2} \text{s}^{-1}$  and subsequently exposed to  $500 \mu\text{mol photons m}^{-2} \text{s}^{-1}$  for one hour in presence of  $500 \mu\text{g ml}^{-1}$  of lincomycin to assess sensitivity to photoinhibition of D1 protein when plastid translation is inhibited. After high light treatment cells were transferred for 2 hours under  $10 \mu\text{mol photons m}^{-2} \text{s}^{-1}$  to grant full relaxation of NPQ processes. PSII quantum yield under light irradiation  $\Phi_{PSII}$  is reported in the graph ( $n=3$ , mean  $\pm$  s.e.m.). B)  $\Phi_{PSII}$  relaxation of Wt, RC1, KD2.1 KD2.3 and KD2.4 RNAi lines grown under continuous light at  $200 \mu\text{mol photons m}^{-2} \text{s}^{-1}$  and subsequently exposed to  $5 \mu\text{mol photons m}^{-2} \text{s}^{-1}$  to induce relaxation of PSII reaction centers under non saturating light irradiation ( $n=3$ , mean  $\pm$  s.e.m.). C)  $qE$  component of NPQ in the same samples reported in panel A. NPQ values were calculated considering the cells at the end of the kinetics ( $t=26$  minutes) as completely relaxed.  $qE$  values at time  $t$  were hence calculated as  $(Fm'_t - Fm'_{26}) / Fm'_{26}$ .

replaced by newly synthesized subunits, hence making the photodamage of D1 itself the only factor involved in the kinetics of quantum efficiency reduction. As shown in Fig.10A, no difference emerged between control lines and mutants, hence excluding an increased sensitivity to photodamage under deregulation of *bHLH2* gene. An alternative explanation for the impaired maximum photosynthetic capacity of the mutants is that it is not the sensitivity of PSII to photodegradation that is altered, but rather the ability of the cells to replace degraded proteins, *i.e.* an alteration in protein resynthesis at the plastid level that causes an unbalance between the degradation of D1 subunits (that occurs at a normal rate) and its substitution with neo synthesized subunits. This hypothesis is supported by the fact that cultures grown under continuous light at 200  $\mu\text{mol photons s}^{-1} \text{m}^{-2}$  show a slower recovery of photosynthetic activity than controls once moved to non-stressful low light (5  $\mu\text{mol photons s}^{-1} \text{m}^{-2}$ ) (Fig.10B) Analysis of qE component of NPQ of the same cells upon relaxation (Fig.10C), highlights that *bHLH2* RNAi strains manifest a maximal NPQ at 200  $\mu\text{mol photons s}^{-1} \text{m}^{-2}$  (time zero) comparable to control strains. qE shows a slower relaxation in *bHLH2* RNAi lines in the first minutes after the transition to non-stressful light, but this difference still does not account for the impairment in  $\Phi\text{PSII}$  shown by transgenic lines after 25minutes from transition.

## Photosynthetic activity represses *bHLH2* expression

Available transcriptomic data of *P. tricornutum* cells exposed to different light conditions (Chauton et al., 2013; Matthijs et al., 2016; Nymark et al., 2013; Smith et al., 2016; Valle et al., 2014) show that *bHLH2* expression is strongly regulated by light cues. Its transcription is induced after a few hours in the dark and repressed following the dark to light switch. This pattern is independent of the photoperiod used for growing the cultures and

of the light colour and shows no anticipation of dark to light transitions, differently from what is observed for *RITMO1* and *bHLH1b* (Fig.11) This data suggests that inhibition of *bHLH2* transcription by light can be related to the activity of the plastid. Plastid development and gene expression are tightly regulated by nuclear encoded factors, a process called anterograde control (Eberhard et al., 2008). However, the plastid itself is in turn capable of transmitting information about its functional state to the nucleus to regulate expression of Photosynthesis Associated Nuclear Genes (PhANGs:). This signalling system originating in the plastids is referred to as retrograde signalling (Eberhard et al., 2008; Kleine et al., 2009). In diatoms, one of the main markers of photosynthetic activity to be involved in retrograde signalling is the redox state of plastoquinones (PQs see Chapter I, section I.3.a), similarly to what occurs in primary endosymbiotic phototrophs (Kleine et al., 2009; Lepetit et al., 2013). In *P. tricornutum*, the redox state of PQs has been shown to regulate the expression of a number of PhANGs (Lepetit et al., 2013; Taddei et al., 2016). To test the hypothesis that *bHLH2* transcription is controlled by this process, qRT-PCR analysis of *bHLH2* expression was performed on Wt cells adapted in the dark for 50 hours and then transferred back to light in the presence and in the absence of DCMU (3-(3,4-dichlorophenyl)-1,1-dimethylurea).

DCMU acts as a competitor of the mobile plastoquinone as electron acceptor on the donor side of PSII and induces the arrest of the linear electron flow along the thylakoid (Kyle, 1985; Metz et al., 1986; Trebst, 2007). As reported in Fig.12A, control replicates show a drastic reduction of *bHLH2* expression upon illumination, with *bHLH2* transcript being ten times less expressed relative to dark after one hour of light exposure and remaining constant to this expression level after 4 hours, but still detectable. In cells treated with DCMU the repression of *bHLH2*, although still present, is strongly slowed down. This result is

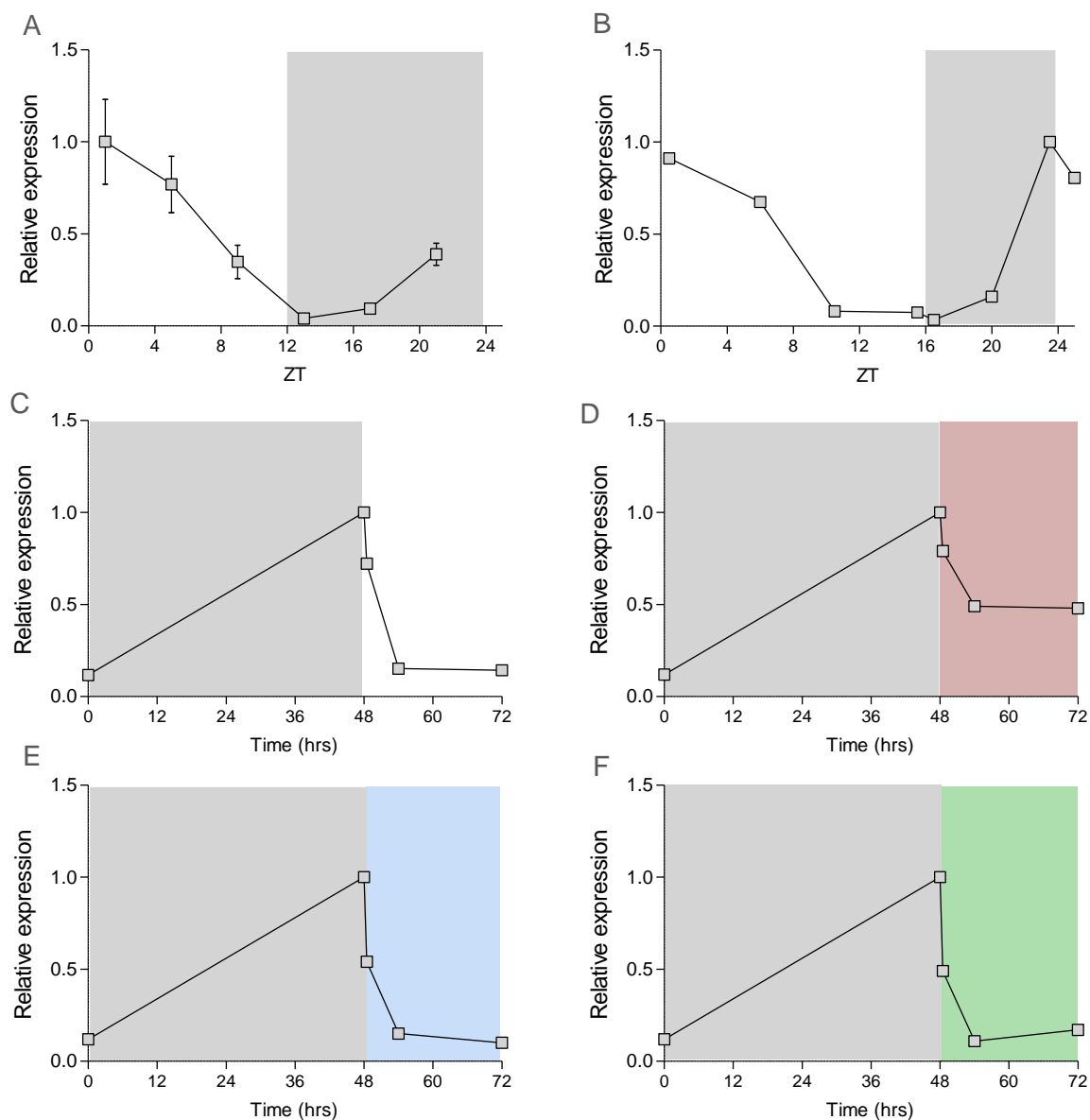


Figure 11. Expression profiles of *bHLH2* from publicly available transcriptomic data

Expression profiles of *bHLH2* under different illumination conditions as retrieved from different publicly available transcriptomic datasets. A) 12L :12D grown cells from Smith et al. 2014. High iron concentration was chosen as a representative study case from the article. *bHLH2* expression profiles did not appear to be altered by different iron concentrations (data not shown). B) Cells grown under 16L:8D from Chauton et al. 2013. Cells treated with 48h dark and exposed to white (C, from Nymark et al. 2013) red, blue or green light (D-F, from Valle et al. 2014). Expression values were normalized to the maximal expression of *bHLH2* during the course of the time course. Grey boxes indicate dark exposure, white boxes indicate exposure to white light, while red, blue and green boxes refer to exposure to different light colours. Further information on light quality and intensity can be found in the relative papers.



comparable to what is shown by other light-inhibited PhANGs such as the one encoding for the LHCX4 antenna (Taddei et al., 2016). The fact that inhibition of photosynthetic activity significantly slows down the repression of *bHLH2* expression demonstrates that its transcriptional regulation in the light depends on the activity of the electron transport chain. These results corroborate the existence of a regulatory cross-talk between plastids and nucleus for the optimization of diatom growth capacity under changing lights, a process in which *bHLH2* appears to play a relevant role. To note, *bHLH2* protein was not predicted to be targeted to the plastid by HECTAR and ASAFind localization tools, while all other tools used (see Materials and methods) identified a NLS in *bHLH2* sequence. Given its possible function as a bHLH-PAS transcription factor, we can speculate that *bHLH2* can act as a relevant regulator of PhANGs expression in response to light inputs and, consequently, in photoacclimation. Still, further characterization of *bHLH2* target genes is needed to deepen this hypothesis.

Given the information on dark transcription of *bHLH2*, we tested the effect of the antisense construct against *bHLH2* in the absence of light. To do so, the Wt, RC1, KD2.1, KD2.3, and KD2.4 lines were grown in a 12L:12D photoperiod and harvested at the end of the dark phase, when Wt expression levels are expected to be highest (Chauton et al., 2013; Smith et al., 2016). In a second analysis, the five lines pre-adapted in continuous light were exposed to 24 hr of darkness and sampled for RNA extraction to

verify the effect of prolonged dark treatment on *bHLH2* RNAi lines. As shown in Fig.12B and Fig.12C, the results obtained do not allow to demonstrate any major alteration in the expression level of *bHLH2* under these conditions compared to Wt, thus making it inconvenient to continue the analysis of photosynthetic physiology under these conditions. Indeed, a correlation between any

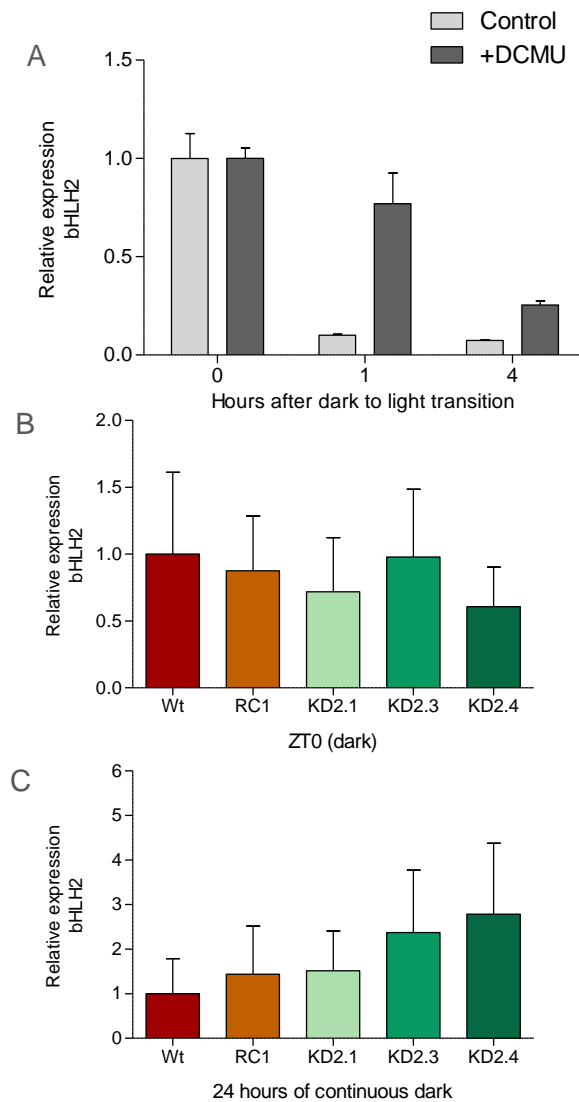


Figure 12. *bHLH2* expression in the dark

A) Wt cells were left in the dark for 50 hours to induce maximal expression of *bHLH2* gene before being exposed to light ( $30 \mu\text{mol photons m}^{-2} \text{s}^{-1}$ ) in presence or absence of  $2 \mu\text{M}$  of DCMU. Cells were collected just before exposure to light and after 1 and 4 hours from exposure to extract RNA and determine *bHLH2* expression. Expression values are normalized to the mean expression of Wt strain.  $n=3$ , mean  $\pm$  s.e.m. B) Expression of *bHLH2* in Wt, RC1, KD2.1, KD2.3 and KD2.4 RNAi lines grown under 12L:12D and collected at ZT0 before transition to light. C) Expression of *bHLH2* in Wt, RC1, KD2.1, KD2.3 and KD2.4 RNAi lines grown under continuous  $5 \mu\text{mol photons m}^{-2} \text{s}^{-1}$  and transitioned for 24 hours under dark before being collected for RNA extraction. Expression values are normalized to the mean expression of Wt strain.  $n=2$ , mean  $\pm$  s.e.m.

phenotypes in plastid physiology with the level of *bHLH2* messenger RNA is currently not possible. In the absence of antibodies to check for possible alterations of bHLH2 at the protein level, we decided to generate Knock-Out lines to confirm the correlation of the phenotypes seen so far with a role of bHLH2 in chloroplast regulation. Preliminary results are reported in the following paragraph.

### Preliminary characterization of bHLH2 KO mutants

KO mutants for *bHLH2* gene were generated in the laboratory by Marianne Jaubert. These mutants were generated to allow bHLH2 characterization in more detail in a controllable and stable genetic background. The mutagenesis of *bHLH2* was performed by proteolistic transformation of a CRISPR/Cas9 system in a manner similar to that performed for the mutagenesis of RITMO1 reported in Chapter II.c. By Sanger sequencing it was possible to identify two independent lines presenting a biallelic mutation at the *bHLH2* locus, henceforth

called RNP1 and RNP2 (for RiboNucleoProtein bombardment KO1 and 2). Sequencing was performed using a non-allele-specific primer to ensure early identification of biallelic mutants. The resulting chromatograms reported in Fig.13 demonstrate that RNP1 mutant presents a 67bp deletion in both alleles at the nt-65 position, implying a double cut of the Guide\_bHLH2\_59 and Guide\_bHLH2\_135 sgRNA target sites (Fig.14). The RNP2 mutant exhibits a chromatogram compatible with a 67bp deletion in one allele (as in RNP1) and a 2bp deletion in the second allele at the nt-65 position, at the level of the Guide\_bHLH2\_59 target site (Fig.13 and Fig.14). In all cases, the mutations induce a frameshift that causes a disruption of the downstream amino acid sequence. A more detailed characterization of the *bHLH2* gene by allele-specific sequencing is currently underway to precisely characterize the effect of the mutation on the two *bHLH2* alleles in the RNP2 mutant and determine the resulting sequences. An additional colony resistant to 2-FA but not targeted for *bHLH2* locus mutagenesis was chosen as control (CTR line).

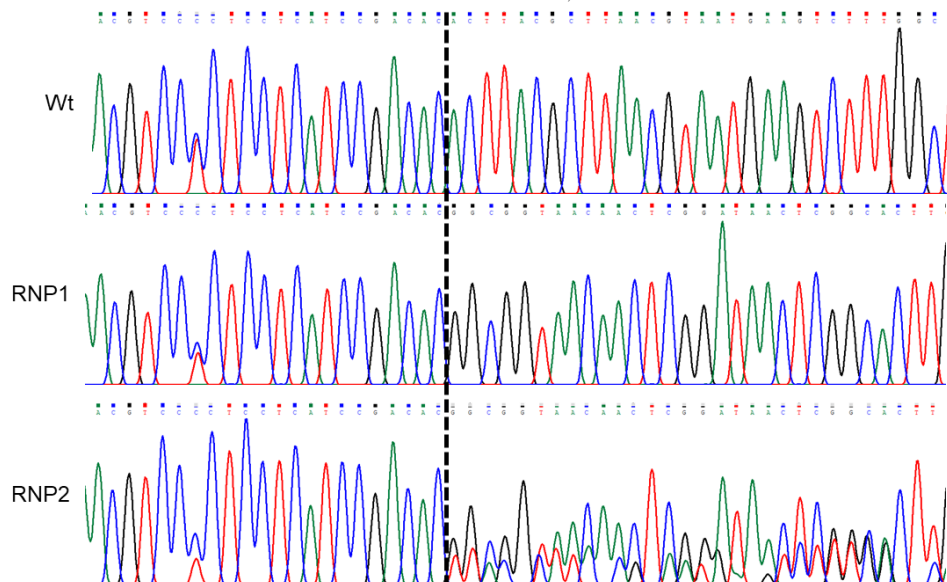


Figure 13. Mutants on *bHLH2* gene induced by CRISPR/Cas9

Chromatographic traces obtained by Sanger sequencing of the *bHLH2* locus in Wt, RNP1 and RNP2 lines. Dashed line highlights the nt-65 position where mutations occurred in both alleles in both RNP1 and RNP2 lines. RNP1 mutant show an identical 62 bp deletion starting from nt-65 position, leading to a single chromatographic trace downstream of the mutation site. RNP2 mutant show a 62 bp deletion in one of the two allele starting at nt-65 and a 2bp (AC) deletion in the second allele at the same position.

Reference sequence (1): Mt  
 Identities normalised by reference length.  
 Colored by: identity

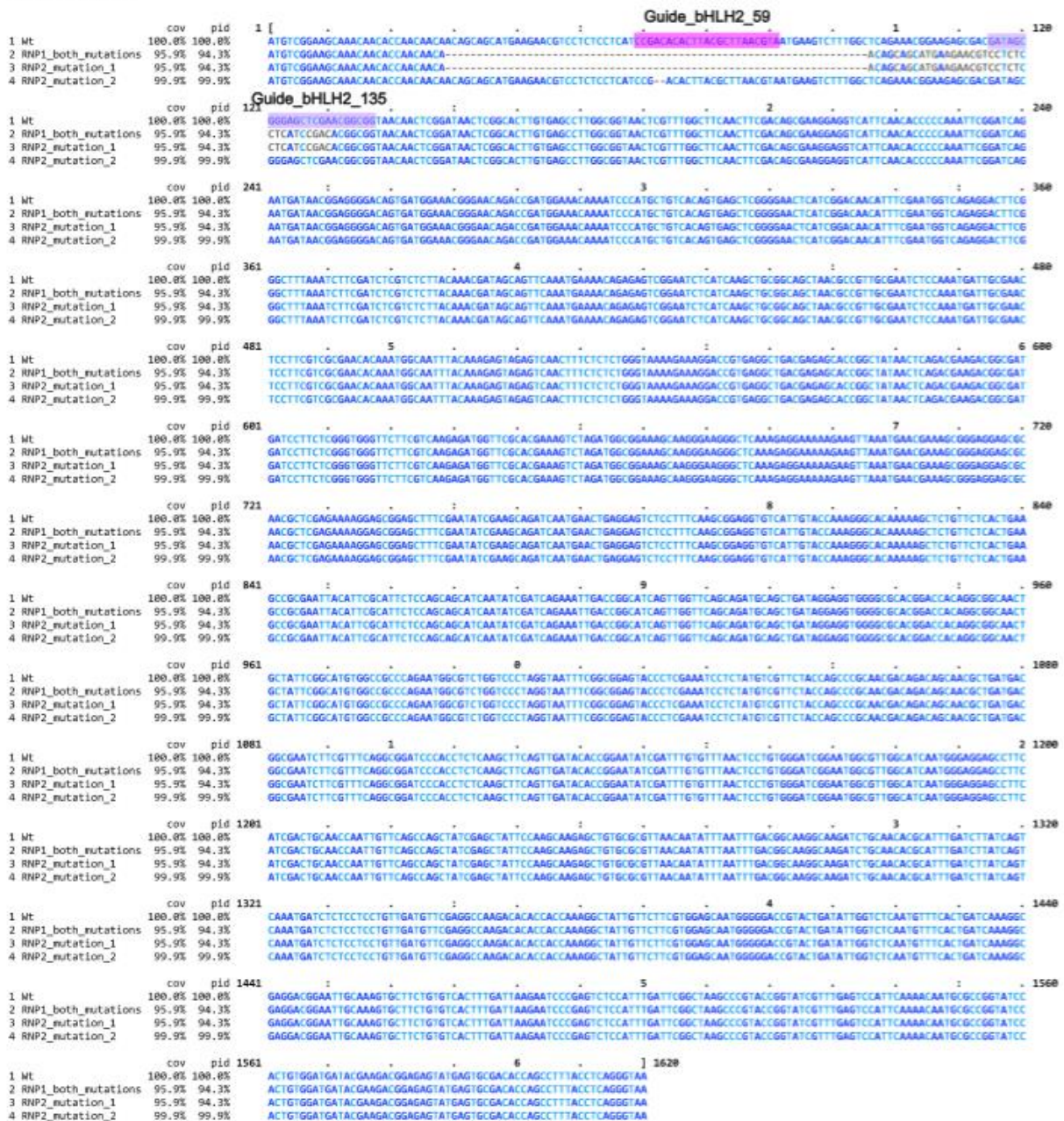


Figure 14. Sequence alignment of the KO mutants for the *bHLH2* gene.

Alignment of the reference coding sequence in Pt1 Wt strain with that of the *bHLH2* KOs RNP1 and RNP2. The alignments were generated via EBI Clustal Omega webtool and visualized via Mview. Bases are colored by identity to the Wt reference sequence. sgRNA Guide\_bHLH2\_59 and Guide\_bHLH2\_135 target sites are highlighted in dark and light purple respectively. Reference coding sequence of *bHLH2* was retrieved from EnsemblProtist web page

Currently, physiological characterization of KO mutants of *bHLH2* has been initiated in order to determine the precise role of this gene in the regulation of plastid activity and to verify a possible consistency of the phenotypes of these lines with that shown by RNAi lines. A first analysis was performed to verify if these lines present a response to the transition from weak light conditions,  $5 \mu\text{mol photons s}^{-1} \text{m}^{-2}$ , to  $200 \mu\text{mol photons s}^{-1} \text{m}^{-2}$  similar to that shown by the KD2.1 KD2.3 and KD2.4 lines. As preliminary, the results shown in Fig.15 demonstrate that the KO *bHLH2* mutants exhibit a response to such light transitions similar to that shown by the RNAi lines and, likewise, a more prominent reduction in the quantum yield of PSII than the control lines. A full range of analyses comparable to those performed for RNAi mutants is currently planned to elucidate the function of *bHLH2*. Similarly, special attention will be paid to verify the responses of KO lines in the transitions from dark to light, which is currently not probed in RNAi transgenic lines and which, from what has been reported in the previous paragraphs, represents one of the conditions under which the role of this protein should emerge more strongly.

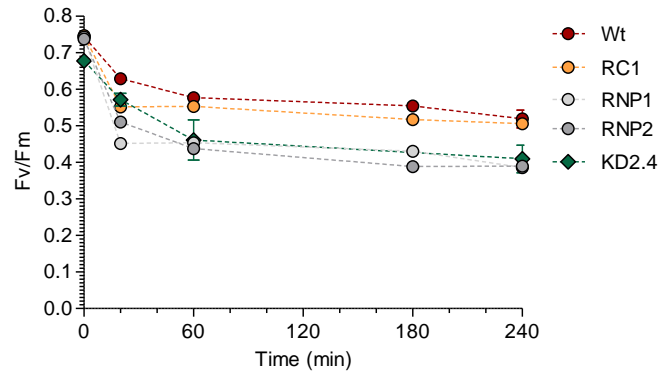


Figure 15. Response to light intensity transition in *bHLH2* KO lines

Wt, CTR, RNP1 and RNP2 lines were grown under continuous light at  $5 \mu\text{mol photons m}^{-2} \text{s}^{-1}$  and subsequently exposed to  $200 \mu\text{mol photons m}^{-2} \text{s}^{-1}$  for four hours to assess response of PSII maximal quantum yield. Samples were collected before transition (T0) and after 20, 60, 180 and 240 minutes after exposure to high light and their Fv/Fm was evaluated after full relaxation of PSII centers (N=2, mean  $\pm$  s.e.m.). The results for KD2.4 RNAi line showed in Fig.10 A are overlaid to allow the comparison between RNAi and KO lines



# Conclusion

The line of work here presented has allowed on the one hand a preliminary evaluation of an on-plate screening method for the identification of transgenic lines altered at the level of photosynthetic physiology. A large-scale phenotypic screening strategy had never been tested on diatoms, and the development and refinement of such a protocol would be a useful tool for the search for photosynthesis mutants in these algae. The results generated on transgenic lines presenting a construct for RNA silencing gave mixed results. A relatively high percentage of lines demonstrated phenotypic alterations at the level of growth or quantum yield of photosynthesis in plate-grown cells, for which confirmation in liquid was possible for the *bHLH2* line. These limitations may be attributed in part to the fact that growth on solid medium is not physiologically optimal for *P. tricornutum*, as demonstrated by the variability in photosynthetic capacity shown by multiple independent control lines only containing the resistance cassette for phleomycin antibiotic. While these preliminary tests have demonstrated the possible limitations of a plate screen in *P. tricornutum*, they also provide useful information that can serve to refine this technique in the future to make it eventually applicable.

Secondly, the results reported here on the *bHLH2*RNAi lines are consistent with an implication of this protein in managing the dynamic response of the plastid to light changes and irradiation exposures capable of affecting PSII stability. Physiological perturbations of *bHLH2*RNAi lines converge toward the description of *bHLH2* as a regulator of *P. tricornutum* plastid physiology, possibly via the modulation of PSII repair and plastid protein resynthesis. Given that predictions of cellular localization indicate that bHLH2 is targeted to the nucleus and not to the plastid, regulation of photosynthetic

activity likely passes through regulation of nuclear genes subsequently targeted to the thylakoid. What these genes are and the more general structure of the regulatory gene network managed by bHLH2 remain unexplored. The light intensity dependence of the observed phenotypes is probably attributable to the fact that the role of *bHLH2* is particularly important under conditions of light stress, where an impairment of the repair of photosynthetic complexes is more relevant in the face of more rapid photodegradation. Involvement in such a function is consistent with the expression profiles shown by the *bHLH2* gene in Wt lines, which is repressed by the activity of the photosynthetic apparatus and maximized following dark exposure. A similar type of regulation agrees with a role for bHLH2 in the response to transitions from dark to light, where the photosynthetic apparatus must be more ready to respond to a sudden change in received irradiance. bHLH2 could also act as a negative regulator of proteins implied in the photosynthetic processes and its repression in the light by plastid signalling could be necessary for a fine modulation of chloroplast activity during variable light stress conditions.

At present, it has not been possible to characterize in detail the photosynthetic properties of *bHLH2*RNAi lines during these dark-to-light transitions also because of the lack of a clear deregulation profile of gene expression in these lines under these conditions, which would impede to properly correlate possible phenotypes with the mRNA level itself. Although this lack of alteration of transcript levels has already been observed in other RNAi lines for other genes (Lavaud et al., 2012), this aspect has prevented us from proposing a clear correlation between *bHLH2* expression levels and the observed phenotypes. For this reason, the newly generated KO lines will represent an extremely useful tool to verify the results obtained on RNAi lines and to subsequently delineate more precisely the effects of

obliteration of this gene during dark-to-light transitions, in which bHLH2 likely plays its role. Should the KO lines lead to confirmation of the above data, bHLH2 would result as the first example of a bHLH-PAS protein implicated in the regulation of photosynthetic processes. This family of transcription factors is in fact absent in primary endosymbiont phototrophs and therefore probably originates from the heterotrophic ancestor from which *Stramenopila* emerged. This would underline how the regulation of chloroplast activity in

secondary endosymbionts is not based only on the action of genes from the endosymbiont but has also co-opted genes already present in the host before the symbiosis. Such a discovery would therefore open up new questions and new lines of study on the complex evolution of the regulation of photosynthesis in *Stramenopila* and other secondary endosymbionts.

# Bibliography

- Almagro Armenteros, J.J., Sønderby, C.K., Sønderby, S.K., Nielsen, H., Winther, O., 2017. DeepLoc: prediction of protein subcellular localization using deep learning. *Bioinformatics* 33, 3387–3395. <https://doi.org/10.1093/bioinformatics/btx431>
- Bailleul, B., Rogato, A., de Martino, A., Coesel, S., Cardol, P., Bowler, C., Falciatore, A., Finazzi, G., 2010. An atypical member of the light-harvesting complex stress-related protein family modulates diatom responses to light. *Proc. Natl. Acad. Sci.* 107, 18214–18219. <https://doi.org/10.1073/pnas.1007703107>
- Bajhaiya, A.K., Ziche Moreira, J., Pittman, J.K., 2017. Transcriptional Engineering of Microalgae: Prospects for High-Value Chemicals. *Trends Biotechnol.* 35, 95–99. <https://doi.org/10.1016/j.tibtech.2016.06.001>
- Brameier, M., Krings, A., MacCallum, R.M., 2007. NucPred Predicting nuclear localization of proteins. *Bioinformatics* 23, 1159–1160. <https://doi.org/10.1093/bioinformatics/btm066>
- Buck, J.M., Sherman, J., Bártulos, C.R., Serif, M., Halder, M., Henkel, J., Falciatore, A., Lavaud, J., Gorbunov, M.Y., Kroth, P.G., Falkowski, P.G., Lepetit, B., 2019. Lhcx proteins provide photoprotection via thermal dissipation of absorbed light in the diatom *Phaeodactylum tricorutum*. *Nat. Commun.* 10, 4167. <https://doi.org/10.1038/s41467-019-12043-6>
- Campbell, D.A., Tyystjärvi, E., 2012. Parameterization of photosystem II photoinactivation and repair. *Biochim. Biophys. Acta BBA - Bioenerg.* 1817, 258–265. <https://doi.org/10.1016/j.bbabi.2011.04.010>
- Chauton, M.S., Winge, P., Brembu, T., Vadstein, O., Bones, A.M., 2013. Gene Regulation of Carbon Fixation, Storage, and Utilization in the Diatom *Phaeodactylum tricorutum* Acclimated to Light/Dark Cycles. *Plant Physiol.* 161, 1034–1048. <https://doi.org/10.1104/pp.112.206177>
- Daboussi, F., Leduc, S., Maréchal, A., Dubois, G., Guyot, V., Perez-Michaut, C., Amato, A., Falciatore, A., Juillerat, A., Beurdeley, M., Voytas, D.F., Cavarec, L., Duchateau, P., 2014. Genome engineering empowers the diatom *Phaeodactylum tricorutum* for biotechnology. *Nat. Commun.* 5, 3831. <https://doi.org/10.1038/ncomms4831>
- De Riso, V., Raniello, R., Maumus, F., Rogato, A., Bowler, C., Falciatore, A., 2009. Gene silencing in the marine diatom *Phaeodactylum tricorutum*. *Nucleic Acids Res.* 37, e96–e96. <https://doi.org/10.1093/nar/gkp448>
- Eberhard, S., Finazzi, G., Wollman, F.-A., 2008. The Dynamics of Photosynthesis. *Annu. Rev. Genet.* 42, 463–515. <https://doi.org/10.1146/annurev.genet.42.110807.091452>
- Falciatore, A., Casotti, R., Leblanc, C., Abrescia, C., Bowler, C., 1999. Transformation of Nonselectable Reporter Genes in Marine Diatoms. *Mar. Biotechnol.* 1, 239–251. <https://doi.org/10.1007/PL00011773>
- Giordano, B., *Epistole italiane. Epistole italiane. Epistole italiane.*
- Giovagnetti, V., Jaubert, M., Shukla, M.K., Ungerer, P., Bouly, J.-P., Falciatore, A., Ruban, A.V., 2022. Biochemical and molecular properties of LHCX1, the essential regulator of dynamic photoprotection in diatoms. *Plant Physiol.* 188, 509–525. <https://doi.org/10.1093/plphys/kiab425>
- Gruber, A., Roca, G., Kroth, P.G., Armbrust, E.V., Mock, T., 2015. Plastid proteome prediction for diatoms and other algae with secondary plastids of the red lineage. *Plant J.* 81, 519–528. <https://doi.org/10.1111/tpj.12734>

- Gschloessl, B., Guermeur, Y., Cock, J.M., 2008. HECTAR: A method to predict subcellular targeting in heterokonts. *BMC Bioinformatics* 9, 393. <https://doi.org/10.1186/1471-2105-9-393>
- Guillard, R.R.L., 1975. Culture of Phytoplankton for Feeding Marine Invertebrates., *Cultures of Marine invertebrate Animals*.
- Horton, P., Park, K.-J., Obayashi, T., Fujita, N., Harada, H., Adams-Collier, C.J., Nakai, K., 2007. WoLF PSORT: protein localization predictor. *Nucleic Acids Res.* 35, W585–W587. <https://doi.org/10.1093/nar/gkm259>
- Huang, W., Daboussi, F., 2017. Genetic and metabolic engineering in diatoms. *Philos. Trans. R. Soc. B Biol. Sci.* 372, 20160411. <https://doi.org/10.1098/rstb.2016.0411>
- Kautsky, H., 1960. Chlorophyll-fluorescenz und Kohlenassimilation. XIII. Mitteilung. Die Fluorescenzkurve und die Photochemie der Pflanze. *Biochem Z* 332, 277–292.
- Kilian, O., Kroth, P.G., 2004. Identification and characterization of a new conserved motif within the presequence of proteins targeted into complex diatom plastids: Protein targeting into diatom plastids. *Plant J.* 41, 175–183. <https://doi.org/10.1111/j.1365-3113X.2004.02294.x>
- Kleine, T., Voigt, C., Leister, D., 2009. Plastid signalling to the nucleus: messengers still lost in the mists? *Trends Genet.* 25, 185–192. <https://doi.org/10.1016/j.tig.2009.02.004>
- Kyle, D.J., 1985. THE 32000 DALTON Q<sub>B</sub> PROTEIN OF PHOTOSYSTEM II. *Photochem. Photobiol.* 41, 107–116. <https://doi.org/10.1111/j.1751-1097.1985.tb03456.x>
- Lavaud, J., Goss, R., 2014. The Peculiar Features of Non-Photochemical Fluorescence Quenching in Diatoms and Brown Algae, in: Demmig-Adams, B., Garab, G., Adams III, W., Govindjee (Eds.), *Non-Photochemical Quenching and Energy Dissipation in Plants, Algae and Cyanobacteria, Advances in Photosynthesis and Respiration*. Springer Netherlands, Dordrecht, pp. 421–443. [https://doi.org/10.1007/978-94-017-9032-1\\_20](https://doi.org/10.1007/978-94-017-9032-1_20)
- Lavaud, J., Materna, A.C., Sturm, S., Vugrinec, S., Kroth, P.G., 2012. Silencing of the Violaxanthin De-Epoxidase Gene in the Diatom *Phaeodactylum tricorutum* Reduces Diatoxanthin Synthesis and Non-Photochemical Quenching. *PLoS ONE* 7, e36806. <https://doi.org/10.1371/journal.pone.0036806>
- Lavaud, J., Six, C., Campbell, D.A., 2016. Photosystem II repair in marine diatoms with contrasting photophysiology. *Photosynth. Res.* 127, 189–199. <https://doi.org/10.1007/s11120-015-0172-3>
- Lepetit, B., Sturm, S., Rogato, A., Gruber, A., Sachse, M., Falciatore, A., Kroth, P.G., Lavaud, J., 2013. High Light Acclimation in the Secondary Plastids Containing Diatom *Phaeodactylum tricorutum* is Triggered by the Redox State of the Plastoquinone Pool. *Plant Physiol.* 161, 853–865. <https://doi.org/10.1104/pp.112.207811>
- Levitan, O., Dinamarca, J., Zelzion, E., Lun, D.S., Guerra, L.T., Kim, M.K., Kim, J., Van Mooy, B.A.S., Bhattacharya, D., Falkowski, P.G., 2015. Remodeling of intermediate metabolism in the diatom *Phaeodactylum tricorutum* under nitrogen stress. *Proc. Natl. Acad. Sci.* 112, 412–417. <https://doi.org/10.1073/pnas.1419818112>
- Lin, J., Hu, J., 2013. SeqNLS: Nuclear Localization Signal Prediction Based on Frequent Pattern Mining and Linear Motif Scoring. *PLoS ONE* 8, e76864. <https://doi.org/10.1371/journal.pone.0076864>
- Livak, K.J., Schmittgen, T.D., 2001. Analysis of relative gene expression data using real-time quantitative PCR and the 2<sup>-</sup>ΔΔCT method.pdf. *METHODS* 25, 402–408.
- Long, M., Peltekis, A., González-Fernández, C., Hégaret, H., Bailleul, B., 2021. Allelochemicals of *Alexandrium minutum*: Kinetics of membrane disruption and photosynthesis inhibition in a co-occurring diatom. *Harmful Algae* 103, 101997. <https://doi.org/10.1016/j.hal.2021.101997>
- Matthijs, M., Fabris, M., Broos, S., Vyverman, W., Goossens, A., 2016. Profiling of the Early Nitrogen Stress Response in the Diatom *Phaeodactylum tricorutum* Reveals a Novel Family



- of RING-Domain Transcription Factors. *Plant Physiol.* 170, 489–498. <https://doi.org/10.1104/pp.15.01300>
- Maxwell, K., Johnson, G.N., 2000. Chlorophyll fluorescence—a practical guide. *J. Exp. Bot.* 51, 659–668.
- Metz, J.G., Pakrasi, H.B., Seibert, M., Arntzer, C.J., 1986. Evidence for a dual function of the herbicide-binding D1 protein in photosystem II. *FEBS Lett.* 205, 269–274. [https://doi.org/10.1016/0014-5793\(86\)80911-5](https://doi.org/10.1016/0014-5793(86)80911-5)
- Moustafa, A., Beszteri, B., Maier, U.G., Bowler, C., Valentin, K., Bhattacharya, D., 2009. Genomic Footprints of a Cryptic Plastid Endosymbiosis in Diatoms. *Science* 324, 1724–1726. <https://doi.org/10.1126/science.1172983>
- Müller, P., Li, X.-P., Niyogi, K.K., 2001. Non-Photochemical Quenching. A Response to Excess Light Energy. *Plant Physiol.* 125, 1558–1566. <https://doi.org/10.1104/pp.125.4.1558>
- Nguyen Ba, A.N., Pogoutse, A., Provart, N., Moses, A.M., 2009. NLStradamus: a simple Hidden Markov Model for nuclear localization signal prediction. *BMC Bioinformatics* 10, 202. <https://doi.org/10.1186/1471-2105-10-202>
- Niyogi, K.K., Bjorkman, O., Grossman, A.R., 1997. Chlamydomonas Xanthophyll Cycle Mutants Identified by Video Imaging of Chlorophyll Fluorescence Quenching. *Plant Cell* 9, 1369–1380. <https://doi.org/10.1104/pp.125.4.1558>
- Nymark, M., Valle, K.C., Hancke, K., Winge, P., Andresen, K., Johnsen, G., Bones, A.M., Brembu, T., 2013. Molecular and Photosynthetic Responses to Prolonged Darkness and Subsequent Acclimation to Re-Illumination in the Diatom *Phaeodactylum tricorutum*. *PLoS ONE* 8, e58722. <https://doi.org/10.1371/journal.pone.0058722>
- Oudot-Le Secq, M.-P., Grimwood, J., Shapiro, H., Armbrust, E.V., Bowler, C., Green, B.R., 2007. Chloroplast genomes of the diatoms *Phaeodactylum tricorutum* and *Thalassiosira pseudonana*: comparison with other plastid genomes of the red lineage. *Mol. Genet. Genomics* 277, 427–439. <https://doi.org/10.1007/s00438-006-0199-4>
- Ozaki, H., Ikeuchi, M., Ogawa, T., Fukuzawa, H., Sonoike, K., 2007. Large-Scale Analysis of Chlorophyll Fluorescence Kinetics in *Synechocystis* sp. PCC 6803: Identification of the Factors Involved in the Modulation of Photosystem Stoichiometry. *Plant Cell Physiol.* 48, 451–458. <https://doi.org/10.1093/pcp/pcm015>
- Perin, G., Bellan, A., Segalla, A., Meneghesso, A., Alboresi, A., Morosinotto, T., 2015. Generation of random mutants to improve light-use efficiency of *Nannochloropsis gaditana* cultures for biofuel production. *Biotechnol. Biofuels* 8, 161. <https://doi.org/10.1186/s13068-015-0337-5>
- Phaeodactylum tricorutum* - Ensembl Genomes 52 [WWW Document], n.d. URL [http://protists.ensembl.org/Phaeodactylum\\_tricorutum/Info/Index](http://protists.ensembl.org/Phaeodactylum_tricorutum/Info/Index) (accessed 3.3.22).
- Platt, T., Gallegos, C.L., Harrison, W.G., 1980. Photoinhibition of photosynthesis in natural assemblages of marine phytoplankton. *J. Mar. Res.* 38, 9. <https://doi.org/10.1093/pasj/57.2.341>
- Ralph, P.J., Gademann, R., 2005. Rapid light curves: A powerful tool to assess photosynthetic activity. *Aquat. Bot.* 82, 222–237. <https://doi.org/10.1016/j.aquabot.2005.02.006>
- Rayko, E., Maumus, F., Maheswari, U., Jabbari, K., Bowler, C., 2010. Transcription factor families inferred from genome sequences of photosynthetic stramenopiles. *New Phytol.* 188, 52–66. <https://doi.org/10.1111/j.1469-8137.2010.03371.x>
- Serif, M., Dubois, G., Finoux, A.-L., Teste, M.-A., Jallet, D., Daboussi, F., 2018. One-step generation of multiple gene knock-outs in the diatom *Phaeodactylum tricorutum* by DNA-free genome editing. *Nat. Commun.* 9, 3924. <https://doi.org/10.1038/s41467-018-06378-9>

- Siaut, M., Heijde, M., Mangogna, M., Montsant, A., Coesel, S., Allen, A., Manfredonia, A., Falciatore, A., Bowler, C., 2007. Molecular toolbox for studying diatom biology in *Phaeodactylum tricorutum*. *Gene* 406, 23–35. <https://doi.org/10.1016/j.gene.2007.05.022>
- Smith, S.R., Gillard, J.T.F., Kustka, A.B., McCrow, J.P., Badger, J.H., Zheng, H., New, A.M., Dupont, C.L., Obata, T., Fernie, A.R., Allen, A.E., 2016. Transcriptional Orchestration of the Global Cellular Response of a Model Pennate Diatom to Diel Light Cycling under Iron Limitation. *PLOS Genet.* 12, e1006490. <https://doi.org/10.1371/journal.pgen.1006490>
- Sperschneider, J., Catanzariti, A.-M., DeBoer, K., Petre, B., Gardiner, D.M., Singh, K.B., Dodds, P.N., Taylor, J.M., 2017. LOCALIZER: subcellular localization prediction of both plant and effector proteins in the plant cell. *Sci. Rep.* 7, 44598. <https://doi.org/10.1038/srep44598>
- Taddei, L., Stella, G.R., Rogato, A., Bailleul, B., Fortunato, A.E., Annunziata, R., Sanges, R., Thaler, M., Lepetit, B., Lavaud, J., Jaubert, M., Finazzi, G., Bouly, J.-P., Falciatore, A., 2016. Multisignal control of expression of the LHCX protein family in the marine diatom *Phaeodactylum tricorutum*. *J. Exp. Bot.* 67, 3939–3951. <https://doi.org/10.1093/jxb/erw198>
- Trebst, A., 2007. Inhibitors in the functional dissection of the photosynthetic electron transport system. *Photosynth. Res.* 92, 217–224. <https://doi.org/10.1007/s11120-007-9213-x>
- Valle, K.C., Nymark, M., Aamot, I., Hancke, K., Winge, P., Andresen, K., Johnsen, G., Brembu, T., Bones, A.M., 2014. System responses to equal doses of photosynthetically usable radiation of blue, Green, and red light in the marine diatom *Phaeodactylum tricorutum*. *PLoS ONE* 9, 1–37. <https://doi.org/10.1371/journal.pone.0114211>
- van Kooten, O., Snel, J.F.H., 1990. The use of chlorophyll fluorescence nomenclature in plant stress physiology. *Photosynth. Res.* 25, 147–150. <https://doi.org/10.1007/BF00033156>



# Chapter IV:

Conclusions  
and  
perspectives

In spite of diatom ecological relevance, very little is known on the basic regulatory processes controlling gene expression in these organisms. *In silico* predictions of transcription factors have already been carried out in various diatom species (Rayko et al., 2010). However, a functional characterization of these elements is largely missing so far, with the exception of few studies (Matthijs et al., 2017, 2016). Likewise, the specific binding sites of diatom TFs, their interaction in gene regulatory networks (GRN) and the mechanisms behind the precise temporal regulation of gene expression are mostly undetermined. Furthermore, this kind of information cannot be easily extrapolated by comparative genomic analysis considering the divergence of diatom genomes in respect to other established plant and animal model systems (Blaby-Haas and Merchant, 2019; Keeling, 2013). With the work presented here, I contributed to address these questions by partaking in the functional characterization of three putative transcription factors of the model diatom *P. tricornutum*, named bHLH1a (also known as RITMO1), bHLH1b and bHLH2. The common elements shared by these proteins are the presence in their structure of a bHLH and a PAS domains (Rayko et al., 2010). Notably, before being identified in *Stramenopila*, transcription factors containing both bHLH and PAS were thought to be a peculiarity of metazoans. The work currently carried out therefore represents the first effort ever made to study this family of proteins in a photosynthetic organism.

Specifically, the main body of my thesis work focused on studying the role of bHLH1a in regulating the biological rhythmicity of *P. tricornutum*. At the time I began my research work in the lab, the study of the molecular regulators that control the internal clock of diatoms was still lacking in literature. The totality of studies carried out on rhythmic processes in these algae had previously focused on the analysis of

physiological and metabolic processes, such as migration in sediments in the case of benthic intertidal diatoms or metabolic processes associated with photosynthesis (Brand, 1982; Happey-Wood and Jones, 1988; Palmer et al., 1964; Palmer and Round, 1967). An in-depth overview of these studies and similar works on other marine algae is provided in Chapter I and Chapter II.a. However, these studies were very few and, although they had begun to provide initial indications that diatoms possess an endogenous oscillator capable of maintaining free-running biological rhythmicity, no study had ever addressed the regulators underlying these phenomena. Understanding how the molecular life of diatoms is synchronized with environmental rhythms is, however, essential both from an ecological point of view and more generally to be able to make the most of these organisms in basic research. For this reason, before my arrival, the host laboratory had already conducted a preliminary search for transcription factors that present the typical features of the components of a transcriptional clock and that could therefore represent good candidate components of such a system. These works led to identify bHLH1a as a first candidate and to demonstrate how its deregulation leads to an alteration of gene expression rhythmicity in *P. tricornutum*, the reason why this protein has been renamed RITMO1. In this early work, reported in Chapter II.b, one of my roles was to characterize how overexpression of this protein influences the expression of a number of target genes under light-dark cycles. Additional steps were still needed to prove RITMO1 function as a regulator of cellular rhythmicity. Indeed, once a possible molecular clock component has been identified, it is critical to implement a thorough characterization of how its mutation or deregulation impacts cellular rhythms. One of the most commonly exploited strategies for this purpose is to transform the organism under study with a luciferase placed under the control of a rhythmic promoter and to follow

its expression by imaging its bioluminescence. Such a protocol is the basis of major work on clock characterization in organisms such as *Arabidopsis thaliana* (Millar et al., 1995), *Chlamydomonas reinhardtii* (Matsuo et al., 2008), *Ostreococcus tauri* (Corellou et al., 2009) or, more recently, *Nannochloropsis* spp. (Poliner et al., 2019). To date, however, attempts to obtain similar transformed lines to follow *in vivo* luciferase activity have been successful only using strong constitutive promoters for the expression of luciferase (Seo et al., 2015), but have never been reproduced with promoters of rhythmic genes. Thus, it became necessary to develop alternative techniques to be able to follow the cellular rhythmicity in these algae effectively and with minimal human intervention. The possibility to follow long time courses with a non-labor-intensive set up enormously facilitated the characterization of possible clock mutants. One of the first important results of my work was thus to optimize the strategy based on the analysis of cellular fluorescence via flow cytometry. This system showed to be an efficient and straightforward method to collect and study large amounts of data for prolonged circadian experiments, all requiring minimal human intervention for the sampling process. Globally, chlorophyll-related fluorescence clearly emerged as a useful tool for studying daily rhythmicity in *P. tricornutum* and became the backbone of the characterisation of the clock presented in Chapters II.b, II.c and II.d.

This technique also allows fluorescence to be used as a proxy for cell division (Chapter II.b and II.c) and had me demonstrate how *P. tricornutum* adapts its division to the growth photoperiod, setting the timing of division based on the length of light periods as reported in Chapter II.c. I was also able to show that rhythmic cellular fluorescence persists following release into continuous light, indicating that cellular fluorescence, as well as likely cell cycle regulation, are controlled by an endogenous

clock. In unicellular organisms that exhibit a growth rate close to one division per day, such persistence of a circadian rhythmicity of cell division can be attributed to a simple persistence of this daily division rate following release into continuous light, without it actually being regulated by an endogenous pacemaker. In such a case, one would expect that in continuous light the doubling time and the free run period of cell division (or, in this case, fluorescence oscillations) should coincide perfectly. As reported in Chapter II.c the persistence of cellular fluorescence however has a free running period of 29h in continuous light even when the doubling time is less than 24h. This might imply that the internal circadian clock rhythmically defines the time when cells have the opportunity to divide, both in the presence of dark light cycles and after release into continuous light. Importantly, when light gets too high, the persistence of rhythms is lost, possibly because the metabolic inputs play a role in making the oscillations of the clock visible. On the contrary, when light is too low, oscillations are equally lost, simply because rhythms cannot be present if cells are not dividing. Such a regulation of the circadian phase in which cell division is "allowed" has already been observed in the past for unicellular algae with an infradian doubling periodicity, both eukaryotic (*e.g.* *Chlamydomonas reinhardtii*, (Goto and Johnson, 1995), *Euglena gracilis*, (Carré and Edmunds, 1993) or *Ostreococcus tauri*, (Moulager et al., 2007) and prokaryotic cyanobacteria (see Mori et al., 1996). Although the data collected so far point in this direction, at the moment it is not yet possible to definitively conclude whether indeed the endogenous clock of *P. tricornutum* guarantees such a gating of cell division. In order to obtain a conclusive answer, the next analysis that will be important to perform in this direction is a phase response curve of cell division as a function of transitions from dark to light, similar to what has already been done in *C. reinhardtii* (Goto and Johnson, 1995) or in *O. tauri* (Moulager et al., 2007).

Unfortunately, due to a lack of time it has not yet been possible for me to perform this test, but this analysis will address if under specific conditions the timing of cell division in *P. tricornutum* is dependent on clock control and not on a simple metabolic response to light exposure.

However, cellular fluorescence analysis was the kickstarter for the characterization of the *P. tricornutum* clock and is the tool that allowed us to demonstrate how RITMO1 is directly implicated in the regulation of cellular rhythmicity. Analysis of over-expressing lines before (Chapter II.b) and KO lines after (Chapter II.c) for this protein allowed me to confirm how its perturbation radically alters the persistence of fluorescence oscillations in free run. Once these data were obtained, it was then possible to further characterize the rhythmic physiology in these cell lines with more targeted techniques.

In particular, one of the most important results of my thesis was the demonstration that perturbation of RITMO1 expression almost completely disrupts the rhythms of gene expression in cells released in free run. Although several papers had already probed the rhythmicity of gene expression in *P. tricornutum* cells subjected to different rhythms of light and dark (Chauton et al., 2013; Smith et al., 2016), at the beginning of my Ph.D. it was still unexplored whether such gene expression oscillations could persist following release in continuous light. With my work I not only demonstrated the existence of such persistence, but I was also able to show how RITMO1 plays a crucial role in this phenomenon. This reflects the function of RITMO1 as a transcription factor. In addition, the generalized deregulation of gene transcription rhythmicity observed implies that RITMO1 regulates cellular rhythmicity over a broad spectrum, not solely controlling cellular fluorescence, thus favoring its place at the heart of the endogenous regulator. At the

moment, the results obtained have been limited to a reduced set of genes selected and analyzed by real time qRT-PCR, but the generalized alteration of transcription profiles observed indicate that this deregulation is to be referred to cellular gene rhythmicity in a broad sense. In addition, these analyses allowed to determine the optimal conditions to conduct a genome-wide transcriptomic study that will attest the effect of the mutation of RITMO1 on the global transcriptome. Such an analysis is being planned and will involve sampling of Wt and KO lines at time points comparable to those used for the experiments in Chapter II.c.

Another important result was the observation of how the rhythmic photosynthetic activity of *P. tricornutum*, is also affected by RITMO1 mutagenesis, while in Wt lines it maintains a periodicity following free-run release, as reported in Chapter II.c. These results demonstrate the importance, also in diatoms, of controlling the timing of plastid activity, a crucial factor to better exploit ambient light in a natural context. It will be interesting, in the future, to conduct more in-depth molecular and biophysical analyses to determine which step(s) of photosynthetic metabolism are actually regulated by the transcriptional clock in which RITMO1 is involved. In plants, it has been widely demonstrated that the clock regulates plastid metabolism through the cyclic expression of genes involved in both light-dependent and biochemical phases of photosynthesis such as the Calvin Benson Bassham cycle (Espinoza et al., 2010; Farré and Weise, 2012; Filichkin et al., 2011).

In plants, the circadian clock has also been shown to be involved in the modulation of the cyclic expression of thioredoxins f and m, fundamental redox-dependent regulators of Calvin Benson Bassham cycle activity, to the point of being considered among the possible central mediators of the interaction between clock and metabolism (Barajas-

López et al., 2011). These enzymes are ubiquitous in all organisms and diatoms possess several copies of them, some of which are targeted in the plastid (Weber et al., 2009). It will be relevant to verify if a similar regulation of gene expression is conserved in *P. tricornutum* and at which level the mutation of RITMO1 alters its profile. An additional interesting aspect of the results obtained is that, in the wild-type line, oscillations at the level of photosynthetic activity as well as gene expression seem to present a period close to 24 hours in free running light. On the contrary, the oscillations of cellular fluorescence present a period of about 28-29 hours in the same conditions as shown in chapter II.c. The analyses carried out so far do not allow to calculate precisely the free running period of these two other clock outputs, as they could be conducted only over a day and a half for technical limitations. If future analyses confirm them, these observations could indicate that a different level of control to the circadian clock influences fluorescence oscillations and, potentially, cell division.

More in general, studies on the rhythmic regulation of metabolism in diatoms are still at their beginnings, but some studies allow us to advance some initial hypotheses. It has already been observed, in fact, that as in plants also in *P. tricornutum* the genes associated with the tricarboxylic acids (TCA) cycle have an important rhythmic regulation (Matthijs et al., 2017). Remarkably, it has been observed that a transcription factor of the bZIP family, bZIP14, is involved in the regulation of carbon metabolism via the TCA cycle and that it also shows a cyclic expression (Matthijs et al., 2017). Under Light-Dark cycles, this protein is expressed at the end of the day and peaks its expression after dusk, so that its regulation has been proposed to be modulated by the endogenous oscillator (Matthijs et al., 2017). It is therefore plausible that the regulation of metabolism via the circadian clock has a key node in the cycle of

tricarboxylic acids. The importance of probing the links between circadian clock and carbon metabolism is also marked by the fact that bZIP14 and RITMO1 appear to be the transcription factors most induced in response to nitrogen deprivation (Matthijs et al., 2017), a condition in which the TCA cycle is itself upregulated. At present, we have not yet been able to explore this subject, but it will certainly be relevant in the future.

Overall, from what has been observed, it is clear that RITMO1 is the first identified component of the endogenous diatom clock. However, it is fundamental to consider that in transcriptional clock systems proteins play a key role in gene expression regulation in physical interaction networks, with protein complexes assembled during the daily cycle and acting in coordination to activate or repress transcription (Creux and Harmer, 2019; Takahashi, 2017; Wijnen and Young, 2006). With my work I hence contributed to expand our comprehension on the molecular clock of diatoms by starting the identification of RITMO1 partners. As presented in Chapter II.d, I used a Yeast two Hybrid approach to demonstrate how RITMO1 can interact with its paralogous protein bHLH1b through their bHLH fold thus adding a new piece to the puzzle of *P. tricornutum* timekeeper. The implication of this second bHLH-PAS protein in the clock system was further confirmed by the generation of KO mutants for this protein which showed a deregulation of fluorescence persistence in free run similar to that presented by mutants lacking RITMO1. However, the phenotypes manifested by bHLH1b KO mutants appeared to be weaker than in RITMO1 mutants, possibly implying that these two proteins have non completely superposing functions. As reported in Chapter II.b and II.c, the perturbation of *RITMO1* expression led to an alteration of *bHLH1b* transcription, meaning that these two proteins control their own expression, possibly via their heterodimer. This phenomenon is logical



considering the feedback loop structure of clock machinery. It will be relevant in future to verify to what extent the obliteration of bHLH1b leads to similar deregulation of its RITMO1 counterpart.

The identification of bHLH1b as a partner of RITMO1 clearly represents only the first step toward the delineation of the *P. tricornutum* clock structure. It is plausible that proteins that physically interact with these two TFs to regulate their activity are numerous, and their identification represents a strategy for the future discovery of novel components of the endogenous clock. As seen in Chapter II.d, RITMO1 is capable of autonomously recruiting the transcriptional machinery in *Saccharomyces cerevisiae* and thereby inducing expression of the *His3* reporter. This makes a screening strategy for yeast two hybrids of RITMO1 partners inapplicable. Furthermore, although Y2H strategies have already been exploited in the past on other organisms for characterizing the interactome of transcription factors (e.g. (Gunther et al., 2000; Mitsuda et al., 2010), this technique is limited by the fact that it's really labor intensive and the fact that the interactions are observed in a yeast model and not *in vivo* in the species under study. Indeed, analysis of protein interactions would be limited by the impossibility to control post translational modifications, which can play a relevant role in determining dimerization properties, as already discussed in Chapter II.d. For this reason, alternative *in vivo* proteomics methods will be used for this purpose. Specifically, it is planned to perform a co-immunoprecipitation analysis to define which other proteins physically interact with these two transcription factors. To this end, KO mutants of RITMO1 have been complemented by transformation with an exogenous copy of the gene modified with an HA tag and, in independent lines, with fluorescent protein tags. These complemented lines will be used to efficiently precipitate RITMO1 and its interaction partners by commercial antibodies directed

against the tag, all in a genetic background deprived of the endogenous copy of the gene. The same lines are also currently being analyzed to see if the exogenous copy of RITMO1 restores proper cellular rhythmicity. Such confirmation would further confirm the involvement of RITMO1 in the *P. tricornutum* clock. Similarly, it is planned to perform complemented transgenic lines and similar analysis also in bHLH1b mutants, so as to conduct in parallel the characterization of the two transcription factors.

The fact that RITMO1 and bHLH1b mutants both exhibit a free-run period shortening outlines their possible partial redundancy in the generation of endogenous rhythms in *P. tricornutum*. The same is given by the fact that the two genes coding for these proteins share their 5' regulatory regions, suggesting likely co-modulation of gene expression by other transcriptional regulators. Which are these regulators, however, still remains an unanswered question. Recent transcriptomics data generated on aureochrome 1a KO mutants show that the expression of RITMO1 and bHLH1b is strongly induced upon exposure to blue light, in a response profoundly altered by the mutation of the photoreceptor (Mann et al., 2020). This suggests that the two proteins are likely implied in the regulatory network involving aureochrome 1a. Whether this occurs directly or indirectly remains to be defined. The picture is made even more complex to delineate because of the large number of genes whose expression is impacted by the aureochrome 1a mutation, suggesting that the response to blue light mediated by this photoreceptor is fundamental to the physiology of *P. tricornutum* beyond the regulation of the circadian clock (Mann et al., 2020). For this, the laboratory is currently collaborating with Peter Kroth's research group, Konstanz University, to probe this point. Specifically, a Yeast one Hybrid assay is being used to test whether aureochrome 1a recognizes the

promoter sequences of RITMO1 and bHLH1b, as well as other genes possibly involved in the clock network. Such a setup will give in the near future an answer to this question. Protein binding microarrays, Chromatin Immunoprecipitation and Yeast one hybrid techniques could also be used to identify the binding sites of RITMO1 and bHLH1b transcription factors. This set of data would shed a light on their targets, helping to outline the GRN they are involved in.

Returning to the possible overlapping role of RITMO1 and bHLH1b, similar partial redundancy of factors involved in the clock mechanisms have already been widely demonstrated and studied in other organisms, most notably in land plants. CCA1 and LHY or the Pseudo Response Regulators 7 and 9 are the best-described cases of paralogous proteins that exhibit similar co-implication in the core of the endogenous oscillator (Alabadi et al., 2002; Farré et al., 2005; Mizoguchi et al., 2002; Salomé and McClung, 2005). Similar to what I observed in KO mutants of RITMO1 and bHLH1b, single gene KOs for these genes also manifest only partial alteration of free-running rhythmicity, whereas dual CCA1-LHY (Alabadi et al., 2002; Mizoguchi et al., 2002) or PRR7-PRR9 (Farré et al., 2005; Salomé and McClung, 2005) mutagenesis is required to achieve large clock disruption and possibly arrhythmicity. At present, a similar characterization has not yet been conducted in *P. tricornutum*, but mutagenesis techniques for CRISPR/Cas9 are now well mastered within the laboratory and KO mutant lines for both these genes will make the generation of double mutants straightforward.

Although the redundancy of function of RITMO1 and its paralogue bHLH1b is likely, it remains possible that these two proteins have a set of gene targets that are not totally overlapping and may therefore present a different regulatory role. Indeed, as seen, I was able to demonstrate not only

heterodimerization of RITMO1 with bHLH1b, but also homodimerization of the latter. The homodimerization of RITMO1 is also possible, although it was not possible to demonstrate it for the moment because of the self-activation phenomenon shown by this protein. The possibility that the different dimers show a different preference for DNA binding sites remains open, although this remains purely speculative. Also, the results obtained on the model species *P. tricornutum* also allow for a broader understanding of the entire diatom family. Indeed, the fact that genes homologous to RITMO1 and bHLH1b have been found in other diatoms (Bilcke et al., 2021) allows us to assume that their function is potentially conserved in other species. The search for functional homologues of RITMO1 and bHLH1b in other diatoms will necessarily pass through a careful analysis of the daily transcription of these proteins, so as to look for those that present profiles compatible with the components of an oscillator. First studies in this sense are beginning to emerge, as in the case of a recent work on *Seminavis robusta* that identified multiple candidate functional homologues for these proteins with similar expression profiles (Bilcke et al., 2021).

To conclude this overview on the characterization of the diatom pacemaker, it is important to emphasize that there are still numerous aspects that need to be explored to fully dissect its functioning. It will be interesting to characterize the clock response to light of different colors, an analysis that will be useful to determine which photoreceptor(s) are involved in the entrainment via the input pathways. This study can be conducted with two alternative strategies. On the one hand, it will be possible to test which colors can entrain the clock and ensure persistence of oscillations after free run release. The cellular fluorescence results reported in Chapter II.b have already shown that Wt cells are capable of maintaining proper cellular fluorescence oscillation when released in free-running blue

light, but in these experiments the cells were initially entrained in white light during light-dark cycles. To determine precisely which wavelengths affect the input pathways and which do not, it will be necessary to perform analyses using monochromatic light already. In a second strategy, dissection of input pathways could be accomplished by analyzing endogenous rhythmicity in lines mutated for different photoreceptors. The laboratory has already developed KO lines for phytochrome and equally possesses KO lines for the different aureochromes of *P. tricornutum*. These transgenic lines will allow a rapid evaluation of the role of these proteins by using the techniques already applied on RITMO1 and bHLH1b mutants. Similar analyses may also be performed on mutants of other *P. tricornutum* photoreceptors (e.g. CPF1) currently under development. Through the analysis of gene expression presented in Chapter II.c I have already highlighted how these proteins are involved in the regulatory network managed by RITMO1 and it will therefore be necessary to verify how they, in turn, are able to influence the activity of the clock.

Also, during my thesis work it was not possible for me to verify the temperature compensation properties of the oscillator of *P. tricornutum*. The maintenance of the correct periodicity of endogenous rhythms under a wide range of temperatures is, as presented in the introduction, Chapter I.4.a, one of the fundamental characteristics of the clock. This property has already been recently analyzed in *Nannochloropsis spp.*, also belonging to the *Stramenopila*, where the rhythmicity of gene expression persists as expected over a wide range of temperatures (Poliner et al., 2019). A complete clock dissection of *P. tricornutum* will require similar analyses.

Also, the techniques and knowledge gained so far pave the way for the study of the ecological role of the clock in diatoms. As reported in Chapter II.c, *P. tricornutum* is

capable of synchronizing its cellular fluorescence rhythms in different photoperiods. Correct response to different light-dark cycles is a key factor for seasonal adaptation of cellular physiology. However, the analyses conducted so far have been carried out on only one ecotype of *P. tricornutum*, *Pt1*, originating from temperate regions (Blackpool, UK, 54°N). A comparative analysis of cellular rhythmicity in different ecotypes from different latitudes, already available in the laboratory, will permit to highlight possible geographical adaptations to the seasonal photoperiods observed in different environments. The characterization of ecogeographic adaptations of the clock at the level is a subject that is gaining increasing interest in the field of chronobiology, in animal as well as in plant, e.g. see (Beauchamp et al., 2018; Greenham et al., 2017). Moreover, diatoms are cosmopolitan algae found at all latitudes and are the dominant form of phytoplankton in the poles. In these regions, the extreme variations of photoperiod during the year open many questions about the possible role and functioning of a circadian clock and it will be therefore relevant if and how the endogenous rhythmicity is maintained in diatoms under these conditions. As reported in Chapter II.b, homologs of RITMO1 and bHLH1b are found in several diatom species. Expanding the functional study of its role in other species with different geographic origins and lifestyles will help to elucidate the properties of the timekeeper in these algae.

Still, the use of the homologs of RITMO1 and bHLH1b as entry points for the potential study of circadian rhythms in other diatom species will have to be conducted with caution. Indeed, as shown extensively in Chapter III, the functions of the bHLH-PAS family members are not limited to the regulation of endogenous rhythmicity. The second important result of my thesis work was in fact to characterize a set of transgenic lines containing a construct for RNA mediated

silencing of the third member of the bHLH-PAS family of *P. tricornutum*, bHLH2. These lines exhibit a strong perturbation of photosynthetic activity. Similar alterations of photosynthesis were not found in RNAi lines in which silencing is directed toward the other two bHLH-PAS proteins, indicating that the phenotypes are specific to bHLH2. Thus, by further characterizing these transgenic lines, I was able to show that anti-bHLH2 antisense results in reduced electron transfer rates at the thylakoid level, with a defect that differential absorbance spectroscopy analysis suggests to be localized upstream of the PSI. The perturbations of the photosynthetic apparatus shown by these lines appear to be dependent on the intensity of light irradiation and lead to a defect in growth rate as light intensity increases. The main limitation of this work is that it has been so far impossible to demonstrate a significant and homogeneous reduction of the bHLH2 transcript level in RNAi transgenic lines, which prevents to date to definitively correlate the observed phenotypes to this protein. Therefore, the KO lines deprived of bHLH2 and described at the end of Chapter III will represent the important tool to confirm these results and definitively define bHLH2 as a modulator of photosynthetic activity. However, it will be important to determine whether complete obliteration of the activity of this protein is lethal under high light growth conditions or following dark to bright light transitions. As seen, *bHLH2* RNAi lines could not be grown under irradiation more intense than 200  $\mu\text{mol photons m}^{-2}\text{s}^{-1}$ . If the effects of KO are even more intense, this could lead to lower tolerance by the mutants of strong light levels. All of this will obviously need to be verified. Such a confirmation, would be of primary relevance for understanding chloroplast regulation in diatoms and this for multiple reasons. First, as already seen in Chapter I, Paragraphs I.3.a and I.3.b, the study of photosynthetic activity in these algae has focused essentially on proteins that are directly implicated in photochemical processes and

thylakoid photoprotection mechanisms. Although there are still many questions to be solved, an important amount of information has in fact been acquired, for example, on LHCX proteins and their implication in non-photochemical quenching (Bailleul et al., 2010; Taddei et al., 2016), on the structure and spatial distribution of antenna complexes (Flori et al., 2017, 2016; Wang et al., 2019) or on the control of carbon fixation at the level of the Calvin Benson Bassham cycle (Matsuda et al., 2017; Tsuji et al., 2017). What are the gene regulatory networks underlying this modulation of plastid activity remains an almost unexplored field. Therefore, bHLH2 would represent one of the first cases of diatom transcription factors directly involved in these processes and would thus provide a crucial entry point for the dissection of such networks.

Secondly, this protein presents an expression profile totally distinct from that shown by RITMO1 and bHLH1b and that allows us to exclude that it is predominantly controlled by the endogenous oscillator. bHLH2 shows in fact an expression that responds directly to light exposure and does not present an anticipation of transitions from light to dark or from dark to light. As I demonstrated in my analyses of dark-adapted cells subsequently treated with DCMU, bHLH2 expression is inhibited by the action of the photosynthetic apparatus in a retrograde signaling mechanism already observed in other *P. tricornutum* nuclear genes and probably mediated by the oxidoreductive state of the thylakoid plastoquinone pool (Lepetit et al., 2013; Taddei et al., 2016). For this, bHLH2 also represents an important starting point to dissect how these retrograde signaling mechanisms mechanically influence nuclear activity in diatoms. Although this is merely a speculation for the moment, given its expression profile inhibited by light and its function as a candidate transcription factor, bHLH2 could indeed represent a key link in this process and potentially be a central

element in this communication between the two cellular compartments. For the same reason, it will be of great interest to test whether homologs of bHLH2 in other diatoms exhibit the same expression profile and, potentially, the same function. The regulation of cell physiology in the dark and its preparation for re-exposure to light is of utmost importance for these algae. As mentioned above, diatoms are abundant in Polar Regions, where they are exposed to prolonged darkness for months during polar nights. Understanding how they regulate their plastid activity upon dark to light transitions may shed light on their ecological success.

As a final point, these results open new questions on the evolution of photosynthesis regulation in diatoms and, more generally, in secondary endosymbionts. Indeed, if the bHLH-PAS proteins of diatoms originated from the heterotrophic ancestor and not from the algae that gave rise to their plastid, the function of bHLH2 would imply

that these organisms have co-opted genes originally not involved in photosynthesis for the control of the chloroplast, in a complex process of evolution of gene regulation. Whether bHLH2 is an isolated case or just an example of a larger such process is an open question. As already described for circadian oscillator proteins, KO mutants of bHLH2 may also be used for genome-wide transcriptomics, chromatin immunoprecipitation and protein co-immunoprecipitation analysis, so to identify the genes whose expression is affected by its obliteration and its binding partner proteins.

Overall, the work done opened a window on bHLH-PAS containing proteins never examined before in diatoms, which have been demonstrated to be involved in the control of two processes of crucial importance for the life of these organisms and their ecological success in the environment.

# Bibliography

- Alabadi, D., Yanovsky, M.J., Más, P., Harmer, S.L., Kay, S.A., 2002. Critical Role for CCA1 and LHY in Maintaining Circadian Rhythmicity in Arabidopsis. *Curr. Biol.* 12, 757–761. [https://doi.org/10.1016/S0960-9822\(02\)00815-1](https://doi.org/10.1016/S0960-9822(02)00815-1)
- Bailleul, B., Rogato, A., de Martino, A., Coesel, S., Cardol, P., Bowler, C., Falciatore, A., Finazzi, G., 2010. An atypical member of the light-harvesting complex stress-related protein family modulates diatom responses to light. *Proc. Natl. Acad. Sci.* 107, 18214–18219. <https://doi.org/10.1073/pnas.1007703107>
- Barajas-López, J. de D., Serrato, A.J., Cazalis, R., Meyer, Y., Chueca, A., Reichheld, J.P., Sahrawy, M., 2011. Circadian regulation of chloroplastic f and m thioredoxins through control of the CCA1 transcription factor. *J. Exp. Bot.* 62, 2039–2051. <https://doi.org/10.1093/jxb/erq394>
- Beauchamp, M., Bertolini, E., Deppisch, P., Steubing, J., Menegazzi, P., Helfrich-Förster, C., 2018. Closely Related Fruit Fly Species Living at Different Latitudes Diverge in Their Circadian Clock Anatomy and Rhythmic Behavior. *J. Biol. Rhythms* 33, 602–613. <https://doi.org/10.1177/0748730418798096>
- Bilcke, G., Osuna-Cruz, C.M., Silva, M.S., Poulsen, N., Bulankova, P., Vyverman, W., Veylder, L.D., Vandepoele, K., 2021. Diurnal transcript profiling of the diatom *Seminavis robusta* reveals adaptations to a benthic lifestyle. *Plant J.* 107. <https://doi.org/10.1111/tpj.15291>
- Blaby-Haas, C.E., Merchant, S.S., 2019. Comparative and Functional Algal Genomics. *Annu. Rev. Plant Biol.* 70, 605–638. <https://doi.org/10.1146/annurev-arplant-050718-095841>
- Brand, L.E., 1982. Persistent diel rhythms in the chlorophyll fluorescence of marine phytoplankton species. *Mar. Biol.* 69, 253–262. <https://doi.org/10.1007/BF00397491>
- Carré, I.A., Edmunds, L.N., 1993. Oscillator control of cell division in *Euglena*: cyclic AMP oscillations mediate the phasing of the cell division cycle by the circadian clock. *J. Cell Sci.* 104, 11. <https://doi.org/10.1242/jcs.104.4.1163>
- Chauton, M.S., Winge, P., Brembu, T., Vadstein, O., Bones, A.M., 2013. Gene Regulation of Carbon Fixation, Storage, and Utilization in the Diatom *Phaeodactylum tricornutum* Acclimated to Light/Dark Cycles. *Plant Physiol.* 161, 1034–1048. <https://doi.org/10.1104/pp.112.206177>
- Corellou, F., Schwartz, C., Motta, J.-P., Djouani-Tahri, E.B., Sanchez, F., Bouget, F.-Y., 2009. Clocks in the Green Lineage: Comparative Functional Analysis of the Circadian Architecture of the Picoeukaryote *Ostreococcus*. *Plant Cell* 21, 3436–3449. <https://doi.org/10.1105/tpc.109.068825>
- Creux, N., Harmer, S., 2019. Circadian Rhythms in Plants. *Cold Spring Harb. Perspect. Biol.* 11, a034611. <https://doi.org/10.1101/cshperspect.a034611>
- Espinoza, C., Degenkolbe, T., Caldana, C., Zuther, E., Leisse, A., Willmitzer, L., Hinch, D.K., Hannah, M.A., 2010. Interaction with Diurnal and Circadian Regulation Results in Dynamic Metabolic and Transcriptional Changes during Cold Acclimation in Arabidopsis. *PLoS ONE* 5, e14101. <https://doi.org/10.1371/journal.pone.0014101>
- Farré, E.M., Harmer, S.L., Harmon, F.G., Yanovsky, M.J., Kay, S.A., 2005. Overlapping and Distinct Roles of PRR7 and PRR9 in the Arabidopsis Circadian Clock. *Curr. Biol.* 15, 47–54. <https://doi.org/10.1016/j.cub.2004.12.067>
- Farré, E.M., Weise, S.E., 2012. The interactions between the circadian clock and primary metabolism. *Curr. Opin. Plant Biol.* 15, 293–300. <https://doi.org/10.1016/j.pbi.2012.01.013>
- Filichkin, S.A., Breton, G., Priest, H.D., Dharmawardhana, P., Jaiswal, P., Fox, S.E., Michael, T.P., Chory, J., Kay, S.A., Mockler, T.C., 2011. Global Profiling of Rice and Poplar Transcriptomes Highlights Key Conserved Circadian-Controlled Pathways and cis-Regulatory Modules. *PLoS ONE* 6, e16907. <https://doi.org/10.1371/journal.pone.0016907>
- Flori, S., Jouneau, P.-H., Bailleul, B., Gallet, B., Estrozi, L.F., Moriscot, C., Bastien, O., Eicke, S., Schober, A., Bártulos, C.R., Maréchal, E., Kroth, P.G., Petroustos, D., Zeeman, S., Breyton, C., Schoehn, G., Falconet, D., Finazzi, G., 2017. Plastid thylakoid architecture optimizes photosynthesis in diatoms. *Nat. Commun.* 8, 15885. <https://doi.org/10.1038/ncomms15885>

- Flori, S., Jouneau, P.-H., Finazzi, G., Maréchal, E., Falconet, D., 2016. Ultrastructure of the Periplastidial Compartment of the Diatom *Phaeodactylum tricorutum*. *Protist* 167, 254–267. <https://doi.org/10.1016/j.protis.2016.04.001>
- Goto, K., Johnson, C.H., 1995. Is the cell division cycle gated by a circadian clock? The case of *Chlamydomonas reinhardtii*. *J. Cell Biol.* 129, 1061–1069. <https://doi.org/10.1083/jcb.129.4.1061>
- Greenham, K., Lou, P., Puzey, J.R., Kumar, G., Arnevik, C., Farid, H., Willis, J.H., McClung, C.R., 2017. Geographic Variation of Plant Circadian Clock Function in Natural and Agricultural Settings. *J. Biol. Rhythms* 32, 26–34. <https://doi.org/10.1177/0748730416679307>
- Gunther, M., Laithier, M., Brison, O., 2000. A set of proteins interacting with transcription factor Sp1 identified in a two-hybrid screening. *Mol. Cell. Biochem.* 210, 12. <https://doi.org/10.1023/A:1007177623283>
- Happy-Wood, C.M., Jones, P., 1988. Rhythms of vertical migration and motility in intertidal benthic diatoms with particular reference to *Pleurosigma angulatum*. *Diatom Res.* 3, 83–93. <http://dx.doi.org/10.1080/0269249X.1988.9705018>
- Keeling, P.J., 2013. The Number, Speed, and Impact of Plastid Endosymbioses in Eukaryotic Evolution. *Annu. Rev. Plant Biol.* 64, 583–607. <https://doi.org/10.1146/annurev-arplant-050312-120144>
- Lepetit, B., Sturm, S., Rogato, A., Gruber, A., Sachse, M., Falciatore, A., Kroth, P.G., Lavaud, J., 2013. High Light Acclimation in the Secondary Plastids Containing Diatom *Phaeodactylum tricorutum* is Triggered by the Redox State of the Plastoquinone Pool. *Plant Physiol.* 161, 853–865. <https://doi.org/10.1104/pp.112.207811>
- Mann, M., Serif, M., Wrobel, T., Eisenhut, M., Madhuri, S., Flachbart, S., Weber, A.P.M., Lepetit, B., Wilhelm, C., Kroth, P.G., 2020. The Aureochrome Photoreceptor PtAUREO1a Is a Highly Effective Blue Light Switch in Diatoms. *iScience* 23, 101730. <https://doi.org/10.1016/j.isci.2020.101730>
- Matsuda, Y., Hopkinson, B.M., Nakajima, K., Dupont, C.L., Tsuji, Y., 2017. Mechanisms of carbon dioxide acquisition and CO<sub>2</sub> sensing in marine diatoms: a gateway to carbon metabolism. *Philos. Trans. R. Soc. B Biol. Sci.* 372, 20160403. <https://doi.org/10.1098/rstb.2016.0403>
- Matsuo, T., Okamoto, K., Onai, K., Niwa, Y., Shimogawara, K., Ishiura, M., 2008. A systematic forward genetic analysis identified components of the *Chlamydomonas* circadian system. *Genes Dev.* 22, 918–930. <https://doi.org/10.1101/gad.1650408>
- Matthijs, M., Fabris, M., Broos, S., Vyverman, W., Goossens, A., 2016. Profiling of the Early Nitrogen Stress Response in the Diatom *Phaeodactylum tricorutum* Reveals a Novel Family of RING-Domain Transcription Factors. *Plant Physiol.* 170, 489–498. <https://doi.org/10.1104/pp.15.01300>
- Matthijs, M., Fabris, M., Obata, T., Foubert, I., Franco-Zorrilla, J.M., Solano, R., Fernie, A.R., Vyverman, W., Goossens, A., 2017. The transcription factor bZIP14 regulates the TCA cycle in the diatom *Phaeodactylum tricorutum*. *EMBO J.* 36, 1559–1576. <https://doi.org/10.15252/embj.201696392>
- Millar, A.J., Carré, I.A., Strayer, C.A., Chua, N.-H., Kay, S.A., 1995. Circadian Clock Mutants in *Arabidopsis* Identified by Luciferase Imaging. *Science* 267, 1161–1163. <https://doi.org/10.1126/science.7855595>
- Mitsuda, N., Ikeda, M., Takada, S., Takiguchi, Y., Kondou, Y., Yoshizumi, T., Fujita, M., Shinozaki, K., Matsui, M., Ohme-Takagi, M., 2010. Efficient Yeast One-/Two-Hybrid Screening Using a Library Composed Only of Transcription Factors in *Arabidopsis thaliana*. *Plant Cell Physiol.* 51, 2145–2151. <https://doi.org/10.1093/pcp/pcq161>
- Mizoguchi, T., Wheatley, K., Hanzawa, Y., Wright, L., Mizoguchi, M., Song, H.-R., Carré, I.A., Coupland, G., 2002. LHY and CCA1 Are Partially Redundant Genes Required to Maintain Circadian Rhythms in *Arabidopsis*. *Dev. Cell* 2, 629–641. [https://doi.org/10.1016/S1534-5807\(02\)00170-3](https://doi.org/10.1016/S1534-5807(02)00170-3)
- Mori, T., Binder, B., Johnson, C.H., 1996. Circadian gating of cell division in cyanobacteria growing with average doubling times of less than 24 hours. *Proc. Natl. Acad. Sci.* 93, 10183–10188. <https://doi.org/10.1073/pnas.93.19.10183>

- Moulager, M., Monnier, A., Jesson, B., Bouvet, R., Mosser, J., Schwartz, C., Garnier, L., Corellou, F., Bouget, F.-Y., 2007. Light-Dependent Regulation of Cell Division in *Ostreococcus*: Evidence for a Major Transcriptional Input. *Plant Physiol.* 144, 1360-1369. <https://doi.org/10.1104/pp.107.096149>
- Palmer, J.D., Livingston, L., Zusy, Fr.D., 1964. A Persistent Diurnal Rhythm in Photosynthetic Capacity. *Nature* 203, 1087-1088. <https://doi.org/10.1038/2031087a0>
- Palmer, J.D., Round, F.E., 1967. PERSISTENT, VERTICAL-MIGRATION RHYTHMS IN BENTHIC MICROFLORA. VI. THE TIDAL AND DIURNAL NATURE OF THE RHYTHM IN THE DIATOM HANTZSCHIA VIRGATA. *Biol. Bull.* 132, 44-55. <https://doi.org/10.2307/1539877>
- Poliner, E., Cummings, C., Newton, L., Farré, E.M., 2019. Identification of circadian rhythms in *Nannochloropsis* species using bioluminescence reporter lines. *Plant J.* 99, 112-127. <https://doi.org/10.1111/tpj.14314>
- Rayko, E., Maumus, F., Maheswari, U., Jabbari, K., Bowler, C., 2010. Transcription factor families inferred from genome sequences of photosynthetic stramenopiles. *New Phytol.* 188, 52-66. <https://doi.org/10.1111/j.1469-8137.2010.03371.x>
- Salomé, P.A., McClung, C.R., 2005. PSEUDO-RESPONSE REGULATOR 7 and 9 Are Partially Redundant Genes Essential for the Temperature Responsiveness of the Arabidopsis Circadian Clock. *Plant Cell* 17, 791-803. <https://doi.org/10.1105/tpc.104.029504>
- Seo, S., Jeon, H., Hwang, S., Jin, E., Chang, K.S., 2015. Development of a new constitutive expression system for the transformation of the diatom *Phaeodactylum tricornutum*. *Algal Res.* 11, 50-54. <https://doi.org/10.1016/j.algal.2015.05.012>
- Smith, S.R., Gillard, J.T.F., Kustka, A.B., McCrow, J.P., Badger, J.H., Zheng, H., New, A.M., Dupont, C.L., Obata, T., Fernie, A.R., Allen, A.E., 2016. Transcriptional Orchestration of the Global Cellular Response of a Model Pennate Diatom to Diel Light Cycling under Iron Limitation. *PLOS Genet.* 12, e1006490. <https://doi.org/10.1371/journal.pgen.1006490>
- Taddei, L., Stella, G.R., Rogato, A., Bailleul, B., Fortunato, A.E., Annunziata, R., Sanges, R., Thaler, M., Lepetit, B., Lavaud, J., Jaubert, M., Finazzi, G., Bouly, J.-P., Falciatore, A., 2016. Multisignal control of expression of the LHCX protein family in the marine diatom *Phaeodactylum tricornutum*. *J. Exp. Bot.* 67, 3939-3951. <https://doi.org/10.1093/jxb/erw198>
- Takahashi, J.S., 2017. Transcriptional architecture of the mammalian circadian clock. *Nat. Rev. Genet.* 18, 164-179. <https://doi.org/10.1038/nrg.2016.150>
- Tsuji, Y., Nakajima, K., Matsuda, Y., 2017. Molecular aspects of the biophysical CO<sub>2</sub>-concentrating mechanism and its regulation in marine diatoms. *J. Exp. Bot.* 68, 3763-3772. <https://doi.org/10.1093/jxb/erx173>
- Wang, W., Yu, L.-J., Xu, C., Tomizaki, T., Zhao, S., Umena, Y., Chen, X., Qin, X., Xin, Y., Suga, M., Han, G., Kuang, T., Shen, J.-R., 2019. Structural basis for blue-green light harvesting and energy dissipation in diatoms. *Science* 363, eaav0365. <https://doi.org/10.1126/science.aav0365>
- Weber, T., Gruber, A., Kroth, P.G., 2009. The Presence and Localization of Thioredoxins in Diatoms, Unicellular Algae of Secondary Endosymbiotic Origin. *Mol. Plant* 2, 468-477. <https://doi.org/10.1093/mp/ssp010>
- Wijnen, H., Young, M.W., 2006. Interplay of Circadian Clocks and Metabolic Rhythms. *Annu. Rev. Genet.* 40, 409-448. <https://doi.org/10.1146/annurev.genet.40.110405.090603>









## Alessandro MANZOTTI

### Curriculum vitae

#### Personal informations

Name	Alessandro Manzotti
Date of birth	03/06/1994
E-mail	<a href="mailto:alessandro.manzotti@protonmail.com">alessandro.manzotti@protonmail.com</a>
Phones	+33(0)766334971 +39 340 7955 601
Address	15, rue Fernand Enguehard Bagneux, 92220
Professional references	Angela Falciatore (Ph.D. director, <a href="mailto:falciatore@ibpc.fr">falciatore@ibpc.fr</a> ), Jean-Pierre Bouly (Ph.D. co-director, <a href="mailto:jean-pierre.bouly@upmc.fr">jean-pierre.bouly@upmc.fr</a> )

---

#### Work experiences

Ph.D. research candidate (2018-2022)	Ph.D. project in molecular and cell biology at the Institut de Biologie Physico Chimique – UMR7141 (Ecole Doctorale Complexité du Vivant ED515, Sorbonne Université). Project title : “ <i>Response to light stimuli in the marine diatom Phaeodactylum tricornutum: Involvement of bHLH/PAS proteins in the circadian clock and plastid physiology</i> ”
Teaching (2019-2021)	Sorbonne Université – Campus Pierre et Marie Curie – Teaching experience in biochemistry and molecular biology

---

#### Studies

University	<b>Ph.D</b> Ongoing Sorbonne Université
Date	<b>Master</b> Juin 2018
Title	Double degree master program in Molecular Biology and Genetics -
University	Università degli Studi di PADOVA (Italie) et Université Paris Diderot Paris VII
Evaluation	110/110 <i>cum laude</i>
Date	<b>Bachelor</b> 26/09/2016
University	Università degli Studi di PADOVA
Title	Biologia molecolare (Biologie Moléculaire)
Evaluation	110/110 <i>cum laude</i>

---

#### Trainings

- > Statistics course in « R » - Ecole Doctorale du MNHN (30 hrs)
  - > Course « Multidimensional data analysis in R » - Agro Campus Ouest (25 hrs)
  - > Course « Scientific integrity for researchers » - Université de Bordeaux (15 hrs)
  - > Summer school « Climate action for sustainable development » - Radboud University, Nijmegen (Netherlands) (1 week, full time)
  - > Course « Biodiversity and global changes », Université Virtuelle Environnement et Développement Durable (12hrs)
  - > Course « Pedagogy and teaching in Biology for University » - Sorbonne Université (11hrs)
-

---

## Publications

### Published :

- Rossella Annunziata, Andrés Ritter, Antonio Emidio Fortunato, **Alessandro Manzotti**, Soizic Cheminant-Navarro, Nicolas Agier, Marie J.J. Huysman, Per Winge, Atle M. Bones, François-Yves Bouget, Marco Cosentino Lagomarsino, Jean-Pierre Bouly, and Angela Falciatore ; **bHLH-PAS protein RITMO1 regulates diel biological rhythms in the marine diatom *Phaeodactylum tricorutum***. PNAS 116 (26) 13137-1314, 2019. doi : <https://doi.org/10.1073/pnas.1819660116>

### Submitted

- Sören Häfker\*, Gabriele Andreatta\*, **Alessandro Manzotti\***, Angela Falciatore, Florian Raible and Kristin Tessmar-Raible. **Rhythms and clocks in marine organisms**, Submitted to Annual Reviews of Marine Science at the end of February 2022.

\*: co-first authors

### In preparation :

- **Alessandro Manzotti**, Raphael Monteil, Antoine Hoguein, Soizic Cheminant-Navarro, Denis Jallet, Francois-Yves Bouget, Fayza Daboussi, Marianne Jaubert, Jean-Pierre Bouly & Angela Falciatore\*  
**Physiological rhythms in the marine diatom *Phaeodactylum tricorutum* are regulated by the circadian clock transcriptional regulator RITMO1**, in preparation, to be submitted in April 2022
- **Alessandro Manzotti**, Soizic Cheminant-Navarro, Marianne Jaubert, Antonio Emidio Fortunato, Andres Ritter Alessandra Bellan, Tomas Morosinotto, Jean-Pierre Bouly & Angela Falciatore, **bHLH2 is a light-intensity dependent modulator of photosynthesis and growth in the marine diatom *Phaeodactylum tricorutum***, in preparation

---

## Languages

English	C2
French	DALF C1
Italian	Mother tongue

---

## Informatics and programming

GraphPad Prism	Excellent
Zotero	Excellent
Adobe Photoshop + Lightroom	Excellent
Adobe Illustrator	Really good
InkScape	Good
R	Discrete

---

## Distinctions

Scholarship awarded to the best university students of the city of Novara by the Nobile Collegio Caccia di Novara (2013-2018)  
Gold medal for merit from the Nobile Collegio Caccia di Novara (2018)

---

## Additional activities

### Students representative

Università degli Studi di Padova (2013 - 2017)

Member of the Student Council as a representative of the students of the School of Biology

### Popularization of science

Coordination, organization and implementation of the conference cycle for scientific dissemination "L'ombra di Galileo" at the University of Padua (2014-2017).

# Abstract

## Response to light stimuli in the marine diatom *Phaeodactylum tricorutum*: Involvement of bHLH-PAS proteins in the circadian clock and plastid physiology

Diatoms are eukaryotic microalgae that represent one of the most successful groups of phytoplankton. Despite their ecological relevance, little information is available on the regulatory mechanisms controlling gene expression in these algae. Through the use of the model marine diatom *Phaeodactylum tricorutum*, the work presented highlighted the role of bHLH-PAS family transcription factors in the regulation of two critically important light-dependent processes. On the one hand, it was shown how the bHLH1a protein, later renamed RITMO1, is involved in the modulation of endogenous rhythmicity regulated by light-dark cycles. Overexpression and knock-out mutation of this gene led to a disruption of daily cellular fluorescence oscillations, photosynthetic activity, and gene expression under constant light condition, identifying RITMO1 as the first characterized component of the diatom circadian clock. It was also shown that a paralogous transcription factor, bHLH1b, dimerizes with RITMO1 and a mutation of this protein led to similar disruptions of cellular fluorescence rhythmicity, indicating its co-implication in the endogenous timekeeper. In parallel, the third *P. tricorutum* bHLH-PAS protein, bHLH2, has been shown to be involved in the modulation of photosynthetic activity in a light intensity-dependent mechanism not controlled by the endogenous clock. Cell lines presenting a construct for RNA interference against bHLH2 showed reduced electron flow at the level of the thylakoid photosynthetic chain and a subsequent deficit in growth. It has been shown that the expression of this protein is controlled by a retrograde signalling pathway, thus highlighting a crosstalk between nucleus and plastid. This study represented the first characterization of bHLH-PAS proteins in a photosynthetic organism.

Keywords: diatoms, *Phaeodactylum tricorutum*, light, circadian clock, photosynthesis, bHLH-PAS proteins

# Résumé

## Réponse aux stimuli lumineux chez la diatomée marine *Phaeodactylum tricorutum* : implication des protéines bHLH-PAS dans l'horloge circadienne et la physiologie du plaste

Les diatomées sont des microalgues eucaryotes qui représentent l'un des groupes de phytoplancton les plus répandus. Malgré leur importance écologique, peu d'informations sont disponibles sur les mécanismes de régulation contrôlant l'expression des gènes chez ces algues. En utilisant la diatomée marine modèle *Phaeodactylum tricorutum*, les travaux présentés ont mis en évidence le rôle des facteurs de transcription de la famille bHLH-PAS dans la régulation de deux processus critiques dépendant de la lumière. D'une part, il a été montré qu'une protéine bHLH1a, renommée RITMO1, est impliquée dans la modulation de la rythmicité endogène régulée par les cycles lumière-obscurité. La surexpression et la mutation KO de cette protéine conduisent à une perturbation des oscillations journalières de la fluorescence cellulaire, de l'activité photosynthétique et de l'expression génique en condition de lumière continue, l'identifiant comme le premier composant caractérisé de l'horloge circadienne des diatomées. Il a également été montré que RITMO1 dimérise avec son paralogue bHLH1b et que la mutation de cet autre facteur de transcription mène à des perturbations similaires de la rythmicité de la fluorescence cellulaire, indiquant sa co-implication dans l'horloge endogène. En parallèle, il a été démontré qu'un troisième facteur de transcription de type bHLH-PAS, bHLH2, est impliqué dans la modulation de l'activité photosynthétique dans un mécanisme dépendant de l'intensité lumineuse et non contrôlé par l'horloge endogène. Les lignées cellulaires transformées avec des ARN interférents contre bHLH2 montrent un flux d'électrons réduit au niveau de la chaîne photosynthétique thylakoïdale et un déficit de croissance subséquent. L'expression de cette protéine s'est avérée dépendre d'un système de signalisation rétrograde, mettant ainsi en évidence une communication croisée entre le noyau et le plaste. Cette étude représente la première caractérisation des protéines bHLH-PAS dans un organisme photosynthétique.

Mots-clés : diatomées, *Phaeodactylum tricorutum*, lumière, horloge circadienne, photosynthèse, protéines bHLH-PAS.